Human skin and mucosa, majorly constituted of keratinocytes, are the most exposed cells to the impact with electromagnetic radiation.
Keratinocytes are so an ideal model to analyse the biological effects of non ionising electromagnetic field, because they are the first cells to which the energy associated to the radiation, will directly be transferred.
HaCaT are epithelial cell line, ideal to understand if a physical agent such as electric field exposure (7 Hz) can interfere with cell morphology, biochemistry and modulate keratinocytes differentiation.
Our results indicate that two ours exposure daily to 7 Hz electric field could be responsible to a different morphological and cytoskeletal assept on HaCaT, together with the increase in involucrin expression, suggesting that EMF takes such cells at an upper differentiation level.
This data strongly support the efficacy of 7 Hz therapy for the treatment of skin deseases as well as a co adjuvant in the therapy of undifferentiated deseasaes.

MATERIALS AND METHODS

Cell Cultures

Cells were grown in Serum Free Medium (GIBCO Laboratories, Scotland) supplemented with antibiotics (110 IU /ml of penicillin and 100 μg/ml of streptomycin) at 37 ± 0.3 °C, 5% CO_2, and sub-cultivated once a week at a 1:3 ratio.

Exposure System.

The flask containing cells were placed between two electrode and exposed twice daily for 1 hours to a 7 Hz electric field at 100mV in a cells incubator under controlled condition (37 °C and 5% CO_2).
As a control experiment other sample of the same cells was placed in the cell incubator with no field, in the same conditions of the exposed one.
No differences were detected between control and sham cells.

Immunofluorescence Assay

HaCaT cells were cultured in SFM medium, starting at a concentration of 6 X 10^5/ml. Exposed cells were cultivated in the same conditions in the exposure system at 7 Hz electric field for 72 hours. Cells were washed, air dried, fixed in paraformaldeide 4% in PBS for 15 minutes and tested by indirect immunofluorescence for the presence of involucrin, β catenin. Antibody against involucrin (Sigma) was used at 1:100 dilution, anti β catenin (Calbiochem) at a 1:500 dilution. After 45 minutes incubation in primary antibody, the slides were washed three times with PBS, dried and stained with fluorescein –isothiocyanate-conjugated goat antiserum to human immunoglobulin G (Amersham) at a dilution of 1:200. After further incubation for 45 minutes the slides were washed and examined by fluorescence microscopy. Four different sets of experiments were performed.

Electrophoresis

SDS-polyacrylamide gel electrophoresis (SDS-Page) was carried out according to Laemmli, 1970 . After 72 hours exposure to electromagnetic fields, equal amount of cell proteins from control and exposed cells , measured by Lowry test, were loaded for each line, after lysis in sample buffer. The samples were boiled for 5 minutes . Electrophoresis was carried on 7.5% SDS polyacrilamide gel at 30 mA for about 2 hours. Gel was subsequently transferred on nitrocellulose membrane (Biorad) at 200 mA for 3 hours, and membrane, after blocking in 3% not dried fat milk for 1 hours at room temperature, was incubated with EGF receptor antibody (Sigma) at a dilution of 1:100 as suggested by manufacturer and revealed by ECL (Amersham).
Three different sets of experiments were performed.

RESULTS

Indirect Immunofluorescence microscopy of modulation of Involucrin, and β-Catenin expression after exposure at 7 Hz electric field

The effect of EMF exposure on HaCaT cell expression of differentiation (Involucrin) and adhesion (βCatenin) markers is respectively reported in Tab and Fig. 1.
Exposed HaCaT cells showed an apparent increase in cells becoming positive to involucrin expression after field exposure compared to control cells. The increase in Involucrin positivity can suggests that 7 Hz HaCaT exposed cells were driven to an upper differentiation level.
As reported for the involucrin experiment also βCatenin seems to be more evident in cells after fiels exposure. The amount of cells positive to β Catenin and involucrine by indirect immunofluorescence is reported in Tab.1

The increase in β Catenin positivity in 7 Hz electric field exposed HaCaT cells, indicates a major cellular adhesion capacity compared to control cells.
Western blot analysis of both involucrin and β Catenin after 7 Hz exposure is reported in Fig. 1. The amount in both proteins seems to be affected by the treatment with the electric field.

DISCUSSION

In the last two decades, reports of biological effects of low-energy EMF have been increasing (Adey 1993, Pilla 1992, Hinsenkamp 1997). Particularly debated is the question of the epidemiological evidence (14) of adverse effects of an extremely low frequency magnetic field (ELF) generated by 50-60 Hz high voltage power transmission lines, video display terminals, electric blankets and other home appliances, which raise the possibility of deleterious health effects (Adey 1981) from exposure to radio frequency (Tenforde 1995) or low frequency fields (Savitz 1987). A valid objection is that field intensity is many orders of magnitude below the noise threshold so that selective, cooperative, or amplifying mechanisms must be postulated. There also problems of reproducibility of reported effects. The therapeutic potential of ELF can be seen in the proven efficacy of low-energy, pulsed magnetic fields in non-union bone fracture healing (Weaver 1990), confirming that under certain conditions non-ionising electromagnetic energy can influence physiological processes in organisms (Kaiser 1988). Physiological paradigms for ELF effects are required. Clues may be found in the mechanisms by which ELF interacts with cultured cells under controlled laboratory conditions and by correlating in vivo evidence with in vitro data (Glaser 1992). Low frequency magnetic fields at 50 or 60 Hz are also reported to stimulate nerve regeneration (Phillips 1992) or alter gene transcription. They may also play a synergic role in cellular processes that are already activated, such as cell proliferation (Walleczeck 1992). The role of Ca^{2+} in the transduction of these effects has been suggested, and indirect evidence of its involvement has been shown (Karabachtsian 1994).
In our work we analysed the effect of 7Hz ELF therapy on human epithelial cell line (HaCaT). Epithelial cells are an interesting model to study the biological effect of the interaction with non-ionising radiations, are not shielded by any other stratum of cells in the impact with electromagnetic radiation, and so they are totally available to the field.
Human keratinocytes cells are also a very good model to investigate the epithelial switch between proliferation and differentiation (Medema 1994).
The effect of 7 Hz exposure on HaCaT cells by ultra microscopy (data not shown), at cells confluency showed a modified morphological aspect: they are bigger and more elongated than controls. Exposed cells lost filopodia, and show a higher number of lamellipodia, specialized structures for cell-cell contact. The augment of cell-cell contact junctions , is also supported by the different distribution in β-Catenin as reported in and Tab.1.
β-Catenin is a protein implicated in cell-cell-adhesion, binding cytoplasmic domain of cadherin, and in signal transduction (Szabo 2001, Vasioukin 2001).
Cell adhesion molecules and their association with actin cytoskeleton play an important role not only in the maintenance of tissue integrity, but also in proliferation and differentiation .
Exposure to the field also causes rearranging of actin filaments (data not shown), leading to an increase in actin expression and in formation of stress fibres that cross parallel to the elongated cells.
Since modification of cellular growth rate and gap junction number with the consequent cytoskeleton rearrangement are implicated in cells transformation (Hsu 2000) we analysed the expression of involucrin as a differentiation marker of keratinocytes (Batta 2000). In human epidermis, involucrin is first observed in the cytoplasm of spinous and granular layer cells. In transition cells, it is equally distributed between the cytoplasm and the nascent corneified envelope, while in the corneocytes it is largely corneified envelope associated. In our experiments involucrin and epecially β catenin expression in the exposed cells, is increased compared to control. (Fig .1). Since involucrin is a keratinization-associated molecules our observation may suggest that the exposed cells are at an upper differentiation level than controls..
This is a very important point suggesting a possible application of electrotherapy in the therapy of skin proliferative diseases. It would be very interesting, for example, to analyse the possibility of using electrotherapy as non invasive chemoterapic agent. Other authors have just reported therapeutical effects of electromagnetic radiation for clinical aims (Basset 1993, Leszczynski 2001, Pletnev 2000).
In summary, 7Hz electric field induces an alteration of growth and differentiation pattern on HaCaT cells. The modification of morphology, cytoskeletal assept, and expression of adhesion and differentiation markers confirm our previous data that exposed cells are at an upper differentiation level.
Our results strongly suggests the possibility to use physical agents such as electric or electromagnetic field, in support to chemiotherapy to fight epithelial proliferation diseases, as well as all the deseases in which cells are characterized to a lower differentiation state

LEGENDS

Tab.1 7 Hz Electric Field modulation of Involucrin and β Catenin by Indirect Immunofluorescence Microscopy.

Tab 1 shows modulation of involucrin and β Catenin expression in control and exposed cells.

Experiment is representative of cells at 72 hours growth and exposure.

Figure 1. Western Blotting of β Catenin and Involucrin

In the first (left) lane: proteins extracted by control cells, in the second (right) lane: proteins extracted by 7 Hz, exposed cells. The amount of proteins inoculated is the same for control and exposed samples, quantitated by Lowry test.

REFERENCES

Adey W.R: Tissue interaction with non-ionizing electromagnetic field. Physiological Review, 61: 435-514, 1981.

Adey W.R: Biological effects of electromagnetic fields. J Cell Biochem 51(4): 410-6, 1993.

Barnes P.S.: Effect of electromagnetic field on the rate of chemical reactions. Biophysics, 41: 801-808, 1996.

Basset C.A.L: Beneficial effects of electromagnetic fields. Journal of Cellular Biochemistry, 51: 387-393, 1993.

Batta K., Rugg E.L., Wilson N.J., West N., Goodyear H., Lane E.B., Gratian M., Dopping-Hepenstal P., Moss C., Eady R.A. A keratin 14 'knockout' mutation in recessive epidermolysis bullosa simplex resulting in less severe disease. Br J Dermatol, 143(3): 621-7, 2000.

Chiabrera A., Nicolini C., Schwan H.P.: Interactions between electromagnetic fields and cells. In Chiabrera eds, Plenum, New York, 1985.

Dominey A.M., Wang X.J., King L. jr, Nanney L.B., Gagne T.A., Sellheyer H., Bundman D.S., Longley M.A., Rothnangel J.A., Greenhalg D.A., et al. Targeted over expression of transforming growth factor alpha in the epidermis of transgenic mice elicits hyperplasia, hyperkeratosis, and spontaneous, squamous papillomas. Cell Growth Differ., 4: 1071-1082, 1993.

Fukunaga M., Oka M., Ichihashi M., Yamamoto T., Matsuzaki H., Kikkawa U. UV-Induced Tyrosine Phosphorylation of PKC delta and Promotion of Apoptosis in the HaCaT Cell Line. Biochem, Biophys, Res, Commun., 30; 289(2):573-9, 2001.

Glaser R.: Current concepts of the interaction of of weak electromagnetic fields with cells. Bioelectrochem. Bioener., 27: 255-268, 1992.

Hinsenkamp M., Jercinovic A., De Graef Ch., Wilaert F., Heenen M. Effects of low frequency pulsed electrical current on keratinocytes in vitro. Bioelectromagnetics, 18 : 250-254, 1997.

Hsu M., Andl T., Li G., Meinkoth J.L., Herlyn M. Cadherin repertoire determines partner-specific gap junctional communication during melanoma progression. J Cell Sci, 113 (pt9): 1535-42, 2000.

Kaiser F. Theory of non-linear excitation. In : Frolich H. et al. (eds). Biological coherence and response to external stimuli. Springer Heidelberg Germany, 25-48, 1988.

Karabakhtsian R., Bronde N., Shalts N., Kochlatyi S., Goodman R., Henderson A.S. : Calcium is necessary in the cell response to EM fields. FEBS Lett., 301: 53-59, 1994.

John C.F., Morris K., Jordan B.R., Thomas B., A-H-Mackerness S:
Ultraviolet-B exposure leads to up-regulation of senescence-associated genes in Arabidopsis thaliana. J. Exp. Bot., 52(359):1367-73, 2001.

Jost M., Kari C., Rodeck U. The EGF receptor-an essential regulator of multiple epidermal functions: Eur J Dematol., 10: 505-510, 2000.

Laemmli U.K.: Cleavage of structural proteins during the assembly of the head bacteriophage T4. Nature, 227: 680-685, 1970.

Alberto Foletti M.D. Mario Ledda , Emanuela Rosola , Antonella Lisi, Enrico D' Emilia , Settimio Grimaldi

Liburdy R.P.: Calcium signalling in lymphocytes and ELF fields: evidence for an electric field metric and a site of interaction involving calcium ion channels. FEBS Lett., 301(1): 53-59, 1992.
Leszczynski D., Pitsillides C.M., Pastila R.K., Rox Anderson R., Lin C.P: Laser-beam-triggered microcavitation: a novel method for selective cell
destruction. Radiat. Res., 156(4):399-407, 2001.

Medema J.P., Sark M.W., Backendorf C., Bos J.L. Calcium inhibits epidermal growth factor-induced activation of p21ras in human primary keratinocytes. Mol Cell Biol, 14(11): 7078-85, 1994.
Pilla A.A., Markov M.S: Bioeffects of weak electromagnetic fields. Rev Environ Health, 10(3-4): 155-69, 1992.
Phillips J.L., Haggren W., Thomas W.J., Jones T.I., Adey W: Magnetic field-induced changes in specific gene transcription. Biochimica Biophysica Acta, 1132: 140-144, 1992.
Peus D., Hamacher L., Pittelkow M.R. EGF-receptor tyrosine kinase inhibition induces keratinocytes growth arrest and terminal differentiation. J.Invest. Derm., 109: 751-756, 1997.

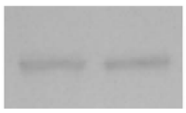
Pletnev S.D.: The use of millimeter band electromagnetic waves in clinical oncology. Crit. Rev. Biomed. Eng., 28(3-4): 573-87, 2000.
Rusovan A. and Kanje M. Magnetic fields stimulate peripheral nerve regeneration hypophyctiomia rats. Neuroreport 3 (12) : 1039-1041, 1992.
Savitz D.A., Pearce N., Poole C. Update on methodological issues in the epidemiology of electromagnetic fields and cancer. Epidemiological Rewievs,. 15: 558-566, 1987.

Szabo I., Rojavin M.A., Rogers T.J., Ziskin M.C. Reactions of keratinocytes to in vitro millimeter wave exposure. Bioelectromagnetics, 22: 358-364, 2001.
Tenforde T.S: Interaction of extremely low frequency electric and magnetic fields with humans. In C. Polk, E. Postow Eds: "Handbook of biological effects of electromagnetic fields". 2nd Ed., CRC Press, Boca Raton, 185-230, 1995.
Vasioukhin V., Bauer C., Degenstein L., Wise B., Fuchs E. Hyperproliferation and defects in epithelial polarity upon conditional ablation of alpha-catenin in skin. Cell, 23: 104 (4): 605-617, 2001.
Weaver J.C., Astumian R.D. The response of living cells on very weak electric fiels: the thermal noise limit. Science, 247:459-462, 1990.
Walleczeck J: Electromagnetic field effect on cells of the immune system: the role of calcium signalling. Faseb Journal, 6 : 3177-3185, 1992.
Zhadin M.N.: Review of russian literature on biological action of DC and low-frequency AC magnetic fields. Bioelectromagnetics, 22(1): 27-45, 2001.

Aknowledgements
Specially thanks for the realisation of this work is due to Italian Medical Society for Bio-Physical Information Therapy.

Fig.1

Involucrin



β catenin



Table 1. % HaCaT cells increasing Involucrin and β Catenin Immunofluorescence positivity after 7 Hz electric treatment

	% Positive Cells
Involucrin	**8 ± 1**
β Catenin	**10 ± 1**

– **±S.D**

STATIC MAGNETS AND PC6 CELLS: DIFFERENTIATION AND PROLIFERATION

Amanda B. Spence and Betty F. Sisken

Dept. of Biological Sciences and Center for Biomedical Engineering, University of Kentucky, Lexington, KY 40506

The objective of this study was to assess the effects of static magnetic fields on proliferation and differentiation of PC6 cells. Proliferation was measured by counting the number of cells in four different quadrants of each well in a 6-well plate after 2 days of incubation. Differentiation was assessed in the same wells by measuring the percentage of cells with neurites (cell extensions) growing from the cell bodies.

We used two Tectonic ceramic magnets (800 Gauss surface field strength, 4 cm in diameter) one under a well at each end of the plate and exposed the cells for three hours /day for each of 2 days . Culture plates were placed directly on the surface of the two magnets. Nerve growth factor (NGF) in phosphate buffered saline (PBS) or PBS alone was added to the cultures; the final concentration of NGF tested was 10 and 20 ng/ml.

A significant effect on differentiation ($p=0.0215$) was found when comparing cultures treated with either concentration of NGF and cultures treated with PBS. The presence of a static magnetic field had no additive effect with the NGF nor did it have any effect alone. Growth, in terms of number of cells, was not affected by the magnetic field + PBS, NGF alone, or NGF + magnetic field.

We also asked the question whether the magnetic fields had any direct effect on the culture media alone or with the addition of PBS or NGF. Therefore, the culture media (+PBS or +NGF) was exposed to the magnetic fields for 3 hours and then the PC 6 cells were added. After 2 days of incubation the results demonstrated that the fields did not affect NGF action since cell differentiation was still increased to the same extent over PBS controls, and no differences were found in growth (proliferation) assessments.

These results are can be compared and contrasted to those found when we tested
2 Hz pulsed electromagnetic fields (PEMF) on PC6 cells, where neurite outgrowth was inhibited (Shah et al, 2001) and with 15 Hz PEMF where differentiation of dissociated sensory neurons was inhibited (Webb et al, 1994). In contrast, we described a stimulation of neurite outgrowth from explants of chick sensory ganglia (Sisken et al, 2000) using the same 800 gauss static magnetic field + NGF. The mechanisms underlying these effects are not known, but may involve magnetic field regulation of NGF activity. Since this dose of magnetic fields may be outside the biological window for single cells, future studie will be run in which the magnetic fields are reduced in strength.

EFFECTS OF GSM-900 JAMMER'S ELECTROMAGNETIC FIELD ON HUMAN ELECTROENCEPHALOGRAM

R. MASKANI

DEPARTMENT OF MEDICAL PHYSICS, TARBIAT MODARES UNIVERSITY, TEHRAN, IRAN

maskany@modares.ac.ir

S.M.P. FIROOZABADI

DEPARTMENT OF MEDICAL PHYSICS, TARBIAT MODARES UNIVERSITY, TEHRAN, IRAN

pourmir@modares.ac.ir

B. JALALIAN

SHAHRUD CAMPUS OF ISLAMIC AZAD UNIVERSITY, SHAHRUD, IRAN

jalalianbabak@hotmail.com

Abstract

Widespread use of mobile phones and the necessity for restriction of it in some places have increased the growth of mobile phone jammer (MPJ). The MPJ produces an electromagnetic field (EMF) that blocks the mobile phone communications. It generates noisy signals at a frequency in order of the mobile phone. People, who exposed to the MPJ field, usually are unaware about its effects on their health. So, at this study the influences of mobile phone jammer's exposures on human electroencephalogram (EEG) are evaluated experimentally.

Thirty healthy participants attended two sessions, one week apart. In experimental and sham session, before exposure, 19 Channels EEG signal was recorded with closed eyes. In experimental session, they exposed to the MPJ's EMF for twenty minutes. In sham session, MPJ was turned off. Then, in two sessions, EEG signal was recorded twenty minutes after beginning of each session. The follow-up EEG signal was recorded at fortieth minutes. Then, power spectrum of EEG signals was calculated using Matlab toolbox.

The analysis of results showed that area under power spectrum curve off EEG signals in some channels has changed between sham and exposure session. The frequency parameters of EEG signals have been changed due to the MPJ exposures, especially in the alpha and theta band of frequency domain. We concluded that this radiofrequency exposure could affect the participant's awareness

Keywords*:* Electromagnetic Field, Mobile Phone Jammer, GSM 900MHz, EEG

Introduction

Widespread use of mobile phones and the necessity for restriction of it in some places have increased the growth of mobile phone jammer (MPJ). The MPJ produces an electromagnetic field (EMF) that blocks the mobile phone communications. GSM use 900MHz EMF as a carrier for communications. But MPJs generate noisy signals at a frequency in order of the mobile phone. Therefore in study of MPJ's effects we can refer to researches of mobile phone effects. Should be noted that MPJs just used for produce noise and may be have other deferent frequencies that defer between company's products and their noise production methods.

The first cell phone jammer was marketed in 1998 after Goldshtein. MPJs are used in some places that mobile phone usage is forbidden such as exams or in places that quite is necessary, for example banks, mosques, churches, theaters and meetings. Furthermore People may be resident long time near MPJ, for example in offices or prisons. Operation of these devices is illegal or very limited in some countries and discussions about its usage continue [1]. These discussions are on two subjects; MPJs usage limits mobile benefits essentially in emergency situations, and probable health hazard of MPJ's EMF [2].

On the other hand, some people that think mobile phone ring and their families and friend's irregular call is ruining their rest and Security and has contrast with their relationship with another people, interest to use low power MPJs and try to make this a manner [3].

People, who exposed to the MPJ field, usually are unaware about its effects on their health. So it's necessary to validate the effect of MPJ on human health.

Generally EMF effects can be divided in to thermal and non-thermal effects. More Standards are based on released heat from EMF that SAR (specific energy absorption rate) is famous standard. But in order weak Electric field that emitted from mobile phone and MPJs non-thermal effects is more probable [4].

Non-thermal effects of EMF that often has been considered are effect on carcinogenic processes, tumor growth, etc. until now Scientific can't find any exact relationship between Mobile phone or MPJ usage and human physiology and pathology. Among researches effect on brain and nervous system has been considered, specially.

Some of probable effects of EMF on nervous system are effect on function of neural membrane, calcium efflux, neuronal excitability, neurotransmitter systems, thermoregulatory behavior, Motor activity, auditory responses, learning and memory, blood–brain barrier and finally effect on brain activity such as EEG and ERP [5].

EEG is an immediate reflection of change in function of nervous system that make it considerable. The effect of EMF on brain activity has been studied later in number of experiments. Studies often report EMF exposure of mobile phone increase spectral power of resting EEG, especially in alpha band [6,7,8,9,10,11,12] but in another research didn't observe such changes [13,14,15].

In some experiment spectral power of Sleep EEG increased due to EMF exposure of mobile phone [10,16,17,18,19,20,21,22] and in another studies didn't result these effects [23,24,25,26].

About effects of mobile phone exposure on EPs some researches have been done. Some of this research report changes in measured parameters [7,9,26,27,28,29,30,31,32] and in another studies can't observed any changes [33,34,35,36].

At this study the influences of mobile phone jammer’s exposures on human resting electroencephalogram (EEG) are evaluated experimentally.

Materials and methods

Subjects

Thirty healthy males aged between 18 and 27 years participate in the study. Participants often had university degrees and easily have been described about purpose and procedures of the study. Before participate in experiment any participant was introduced with experimental tools and situation.

Participant were asked about any nerves illness and difficulties such as long term headache, sleep disorder etc. also in first session of experiment an EEG with clinical order has been recorded and a neural specialist reviewed this record and finally sample with neural difficulty has been forgave from experiment and invited for more clinical exam. During the experiment two peoples were invited for clinical difficulty investigating exams.

Before first session participants have been noted that had sufficient sleep and didn't use sleepy and neural drugs. Before experiment any participant wrote an informed consent that contained detail of study.

Procedure

Participants attended two sessions, one week apart, for experimental and sham session. In each session participant seat on a comfortable armchair and an expert technician placed the electrodes on his head. Before exposure, 19 Channels EEG signal was recorded with closed eyes. In experimental session, they exposed to the MPJ EMF for twenty minutes from right side. In sham session, MPJ was turned off and participants were unaware that MPJs was on or off. In two sessions, EEG signal was recorded twenty minutes after beginning of each session. The follow-up EEG signal was recorded at fortieth minutes. The experimental protocol is shown in table 1.

Table 1: experimental protocol

Session	30 s EEG Recording	20 min being near the MPJ	30 s EEG Recording	20 min after Second record	30 s EEG Recording
First	Background	ON Exposure / OFF	After	Follow-up time	Follow-up
Second		OFF Exposure / ON			

EMF exposure

GSM 900 use 890-960 MHz EMF as a carrier for communications. This wide band divided to two bands, uplink band 890-915 MHz, and downlink band 935-960 MHz. downlink is the transmission path from a Base Station to the Cell Phone. Uplink is the transmission path from a mobile station to the base station [37].

MPJs emit EMF similar to downlink (935-960 MHz) but with ramp modulation, which block mobile communications around itself. MPJs emit EMF similar to carrier of GSM, but in a stable frequency band and with constant power for a long time. These make MPJ a suitable EMF generator for our study.

EMF emitter that has been used in our study was MPJ 101 (Moje Nasr Gostar co.) that emits noisy 935-960 MHz EMF with power of 1 W and can block GSM900 communications in a 15 meters circle. Fig 1

Frequency of EMF that emitted form MPJ 101 was tested with a Spectrum Analyzer (TR4131) that has correct frequency band



Fig 1: MPJ 101

MPJ 101 has an 8 cm, quarter wavelength antenna. Participants sat approximately 50 cm apart the MPJ. It can be assumed that participants placed in far field of antenna. Therefore power density on volunteer head can be estimated:

$$\frac{I}{S} = \frac{I}{4\pi r^2} = \frac{1}{4\pi(0.5)^2}\left(\frac{W}{m^2}\right) = 0.32\ Wm^{-2}$$

Public standard level for power spectrum that ICNIRP determined in 935 MHz is 4.68 Wm^{-2}. It can be seen that power spectrum is smaller than standard level.

Data acquisition

EEG was recorded using a 19 Channels EEG recording system (sholeh danesh co.). It has an 8-bit A/D card and its sampling rate is 250 Hz. 19 Ag-AgCl Saline Pad Electrodes placed on participant's head using 10-20 system and fixed with a head cap strap. Two earlobe electrodes were hanged to ears with ear clip as reference and recording was performed with monopole montage.

Data acquisition, Preview and primary analysis performed using SD-C24 EEG software that install on recording PC. Default mode of recording system that performed for clinical application has a 35 Hz low pass

and a 1 Hz high pass filter. We were using this mode for clinical exam of participants that has been said before. For experimental record a 70 Hz low pass and a 0.3 Hz high pass filter were used.

More than 30 s EEG with closed eye was recorded in any record (background, after and follow-up) that has been said before.

Data analyzes

Recording data was saved in special file format. This primary format has been converted to a data array with Matlab software format (MathWorks, Inc. version 7) that can be analyzed in Matlab toolboxes. The MAT file after convert has been reviewed with eeglab4.515 toolbox [38] and compared with printed records to validate conversion program.

Recorded EEG was reviewed with eeglab4.515 toolbox and in any record (background, after and follow-up), 10 without movement artifact 1 s windows have been selected.

Frequency analysis has been done in the Matlab. FFT (Fast Fourier Transform) was performed on each 1 s data to calculate power spectrum. Because frequency contents of normal adult lie between 0.1-40Hz [39] in power spectrum calculation we abandoned upper than 45 Hz contents. We also abandoned frequency content lower than 1Hz because our frequency resolution in power spectrum calculation. Then Relative Power Spectrum (RPS) has been calculated as below.

RPS= Area under Power Spectrum curve of any rhythm / Total area under Power Spectrum curve

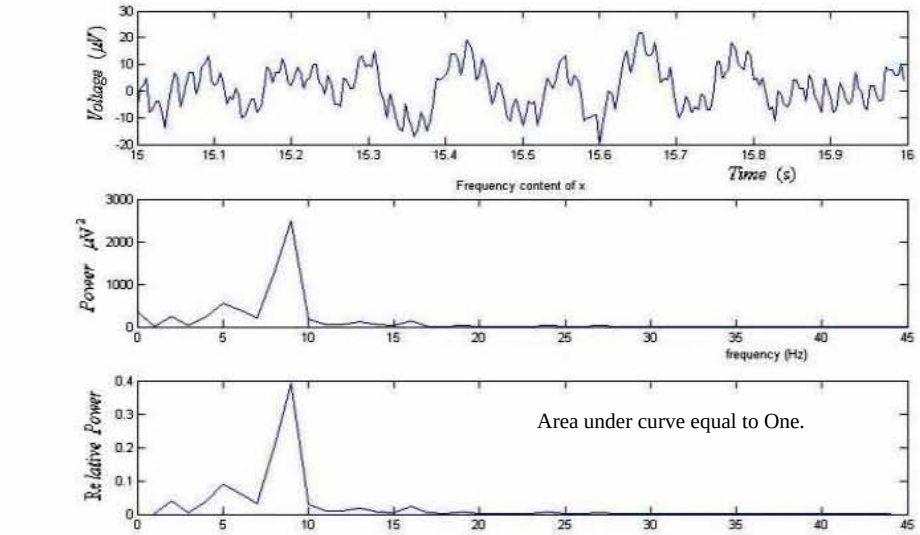


Fig 2: Original EEG wave ,Voltage as a function of time (first), Power Spectrum (second) and RPS (third)

Then power spectrum has been averaged in 10 second. For evaluation of changes in EEG rhythms, RPS has been summed in each rhythm. EEG rhythms have been determined as shown below

Delta	δ	1-3 Hz	Beta	β	14-35 Hz
Theta	θ	4-7 Hz	Gamma	γ	36-45 Hz
Alpha	α	8-13 Hz			

Essentially EEG RPS may change as a function of time during each session. For finding any effect of EMF exposure, recording data during the real exposure with that recorded in sham session should be compared. In each session, Growth Ratio (GR) from background to after, from after to follow-up and from background to follow-up records were calculated as below.

GR=(after RPS-background RPS)/background RPS …

Therefore we could compare between two sessions with three GRs.

Statistical analyses

Statistical analyses were performed with SPSS (SPSS Inc. version 11.5.) software Paired T-test was performed for GR of RPS between two sessions. Differences were considered statistically significant at $P< 0.05$. Paired T-test was performed for each 19 electrodes in all rhythms separately.

For Paired T-test the data should be normal. Therefore normality of data was checked in One-Sample Kolmogorov-Smirnov Test. If normality test failed nonparametric test (Wilcoxon signed rank test) would use.

Additionally for evaluation the inherent changes of EEG rhythms due to time, Repeated measures have been performed on background, after and follow-up records in each session separately. Mauchly's Test of Sphericity Were performed before Repeated measures tests. If Mauchly's Test of Sphericity failed, other methods (Greenhouse-Geisser, Huynh-Feldt and Lower-bound) would perform.

Result

Repeated measures of data showed changes in EEG rhythm due to time especially in Theta and Alpha rhythms. Analyze of differences showed significant changes in GR from background RPS to after, between two sessions in some electrode and in some rhythms. As be shown in Table 2. Positive sign in the table shows increase in RPS change in those rhythm and negative sign show decrease in it. It seems that immediately after exposure the natural changes of EEG rhythms were modified. Slow brain potentials increased due to exposure. Analyze of GR from follow-up to after record also showed more differences between sham and experimental sessions as shown in Table 3. Comparing sham and experimental records showed decrease in GR in Theta rhythms. Result of comparing GR from follow-up to background record showed less change in two sessions(Table 4).

Discussion

Our result showed RPS of slow brain potential increased immediately after exposure in some electrode, it is inconsistent with result of more experiment that have reported increase in alpha rhythm due to exposure. It may be result of large widespread data in upper rhythms that unable us to see significant differences.

Comparing GR from follow-up to after record in sham and experimental records showed decrease in natural changes in Theta rhythms.

Results showed increase in GR from background to after record and decrease from after to follow-up record in Theta rhythm due to EMF exposure that is reasonable.

Analogizing GR from background to follow-up record in two sessions showed partially increase in beta rhythm that perhaps it happens accidentally.

In our study the frequency parameters of EEG signals have been changed due to the MPJ exposures, especially in the alpha and theta band of frequency domain. We concluded that this radiofrequency exposure could affect the frequency content of EEG and participant's awareness.

Table 2- changes in RPS from background to after records due to EMF exposure

Location	Delta 1-3 Hz	Theta 4-7 Hz	Alpha 8-13 Hz
C3			-
Cz		+	
F7	+		-
Fp2		+	
Fz		+	
P3	+		
T3	+		-
T5	+		

.

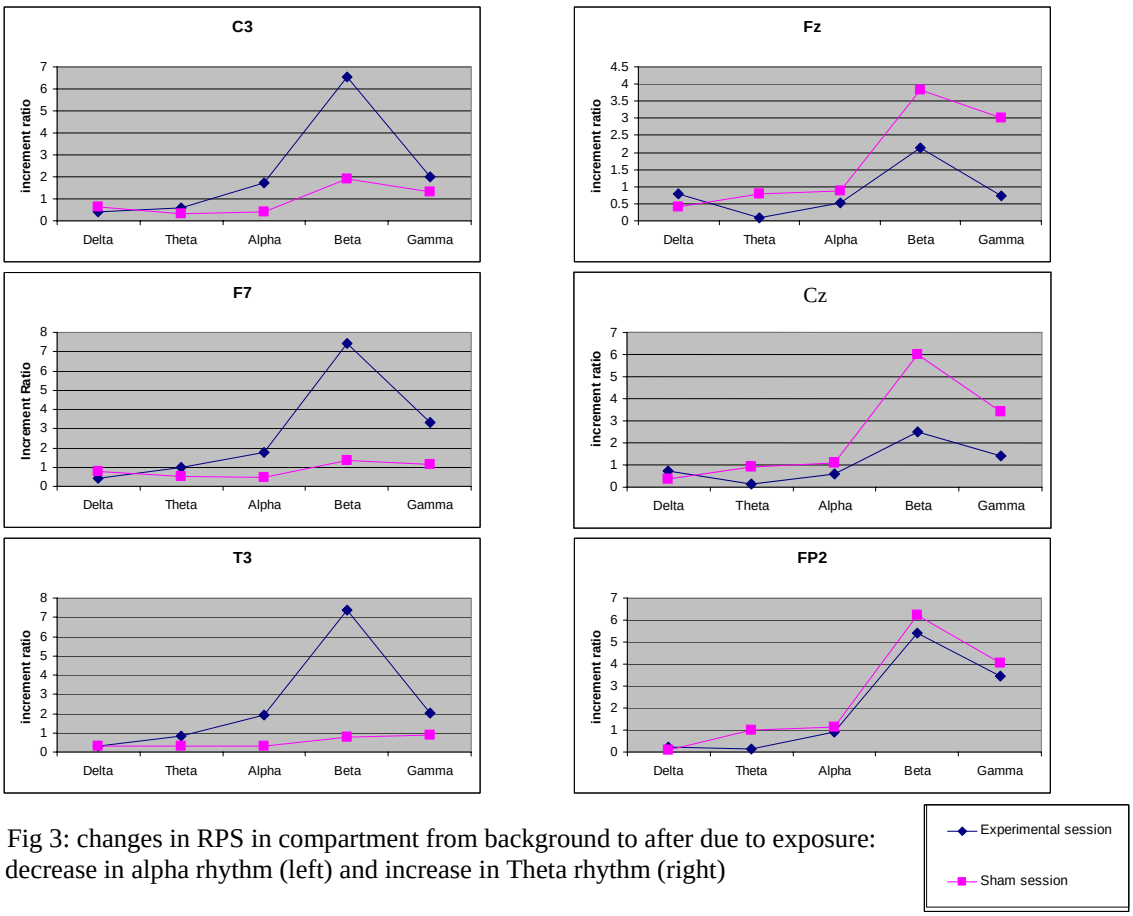


Fig 3: changes in RPS in compartment from background to after due to exposure: decrease in alpha rhythm (left) and increase in Theta rhythm (right)

Table 3- Changes in RPS from after to follow-up records due to EMF exposure.

Location	Delta 1-3 Hz	Theta 4-7 Hz	Alpha 8-13 Hz
C3		-	
CZ		-	
Fp1			+
Fp2		-	
Fz		-	
O1		-	
O2		-	
Pz		-	
T3			+

Table 4- Changes in RPS between from background to follow-up records due to EMF exposure.

Location	Delta 1-3 Hz	Theta 4-7 Hz	Alpha 8-13 Hz
C3	+	-	
F8	+		
O1	+		
P3	+	-	

References

[1] James Careless, Canada phones face legalized jammers, Wireless Week; Mar 26, 2001; 7, 13; ProQuest Telecommunications, pg. 71
[2] Australian Communications Authority (ACA) Report, mobile phone jammers, July 2003
[3] Limor Fried, Social Defense Mechanisms: Tools for Reclaiming Our Personal Space, thesis, Department of Electrical Engineering and Computer Science, Massachusetts Institute of Technology, January 2005
[4] IEGMP Independent Expert Group on Mobile Phones. Mobile phones and health. 2000, ISBN 0-8591-450-1, http://www.iegmp.org.uk.
[5] EMF international project, http://www10.who.int/peh-emf/emfstudies/database.cfm
[6] Reiser H-P, Dimpfel W, Schober F. The influence of electromagnetic fields on human brain activity. Eur J Med Res 1995;1:27–32.
[7] Thuroczy G, Kellenyi L., Faludy B., Lenard L, effects of mobile gsm radiotelephone exposure on the auditory brainstem response (ABR), Neurobiology, Vol. 7, Pg. 79 - 81, 1999
[8] Lebedeva N. N., cellular phone electromagnetic field effects on bioelectric activity of human brain, Crit Rev Biomed Eng, Vol. 28, Pg. 323 - 337, 2000
[9] Croft R. J., Chandler J. S., Burgess A. P., Barry R. J., Williams J. D., Clarke A. R., Acute mobile phone operation affects neural function in humans, J Altern Complement Med., Vol. 8, Pg. 427 - 435, 2002.
[10] Hamblin D. L., Wood A. W. Effects of mobile phone emissions on human brain activity and sleep variables, Int. J. Radiat. Biol., Vol. 78, Pg. 659 - 669, 2002.
[11] D'Costa H., Trueman G., Tang L., Abdel-rahman U., Abdel-rahman W., Cosic I., Human brain wave activity during exposure to radiofrequency field emissions from mobile phones, Australian Physical and Engineering Sciences in Medicine, Vol. 26, Pg. 162 - 167, 2003.
[12] G. Curcio, M. Ferrara, F. Moroni, G. D'Inzeo, M. Bertini, L. De Gennaro, Is the brain influenced by a phone call? An EEG study of resting wakefulness, Neuroscience Research 53 (2005) 265–270
[13] Roschke J, Mann K. No short term effects of digital mobile radio telephone on the awake human electroencephalogram. Bioelectromagnetics 1997;18:172–176.
[14] Kim Y. S, Characteristics of eeg and aep in human volunteers exposed to RF, Korean Journal of Environmental Health Society, Vol. 24, Pg. 58 - 65, 1998.
[15] Hietanen M, Kovala T, Hamalainen AM. Human brain activity during exposure to radiofrequency fields emitted by cellular phones. Scand J Work Environ Health 2000;26(2):87–92.
[16] Mann K, Ro¨schke J. Effects of pulsed high-frequency electromagnetic fields on human sleep. Neuropsychobiology 1996;33:41–7.
[17] Borbely A, Huber R, Graf T, Fuchs B, Gallman E, Achermann P. Pulsed high-frequency electromagnetic fields affects human sleep and sleep electroencephalogram. Neurosci Lett 1999;275:207–10.
[18] Huber R., Graf T., Cote K. A., Wittmann L., Gallmann E., et al, Exposure to pulsed high-frequency electromagnetic field during waking affects human sleep EEG NeuroReport, Vol. 11, Pg. 3321 - 3325, 2000
[19] Lebedeva, N.N.; Sulimov, A.V.; Sulimova, O.P.; Korotkovskaya, T.I.; Gailus, T. Investigation of brain potentials in sleeping humans exposed to the electromagnetic field of mobile phones. Biomedical Engineering 2001; 29(1):125-133
[20] Huber R., Treyer V., Borbely A. A., Schuderer J., Gottselig J. M., et al ., Electromagnetic fields, such as those from mobile phones, alter regional cerebral blood flow and sleep and waking, J. Sleep Res., Vol. 11, Pg. 289 - 295, 2002
[21] Huber R., Schuderer J., Graf T., Borbely A. A., Kuster N., Achermann P., Radio frequency electromagnetic field exposure in humans: estimation of sar distribution in the brain, effects on sleep and heart rate, Bioelectromagnetics, Vol. 24, Pg. 262 - 276, 2003.
[22] Mann K., Roschke J., Sleep under exposure to high-frequency electromagnetic fields, Sleep Medicine Reviews, Vol. 8, Pg. 95 - 107, 2004.
[23] Wagner P, Roschke J, Mann K, Hiller W, Frank C. Human sleep EEG under the influence of pulsed radiofrequency electromagnetic fields: a polysomnographic study using standardised conditions. Bioelectromagnetics 1998;19:199–202.
[24] de Seze R., Effects of radio cellular telephones on human sleep, J. Sleep Research, Vol. 9(Suppl 1), Pg. 18 - , 2000.
[25] Wagner P, Roschke J, Mann K, Fell J, Hiller W, Frank C, Grozinger M. Human sleep EEG under the influence of pulsed radio frequency electromagnetic fields. Neuropsychobiology 2000;42:207–212.
[26] Jech R, Sonka K, Ruzicka E, Nebuzelsky A, Bohm J, Juklyckova M, Nevsymalova S. Electromagnetic field of mobile phones affects visual event related potential in patients with narcolepsy. Bioelectromagnetics, 2001;22:519–28.
[27] Freude G, Ullsperger P, Eggert S, Ruppe I. Effects of microwaves emitted by cellular telephones on human slow brain potentials. Bioelectromagnetics 1998;19:384–7.

[28] Krause C. M., Sillanmäki L., Koivisto M., Häggqvist A., Saarela C., et al., Effects of electromagnetic field emitted by cellular phones on the eeg during a memory task, NeuroReport, Vol. 11, Pg. 761 - 764, 2000.
[29] Krause C. M., Sillanmaki L., Koivisto M., Haggqvist A., Saarela C., Revonsuo A., effects of electromagnetic fields emitted by cellular phones on the electroencephalogram during a visual working memory task, Int. J. Radiat. Biol., Vol. 76, Pg. 1650 - 1667, 2000.
[30] Freude G, Ullsperger P, Eggert S, Ruppe I. Microwaves emitted by cellular telephones affect human slow brain potentials. Eur J App Physiol 2000; 81:18–27.
[31] Hamblin D. L., Wood A. W., Croft R. J., Stough C., Examining the effects of electromagnetic fields emitted by gsm mobile phones on human event-related potentials and performance during an auditory task, Clinical Neurophysiology, Vol. 115, Pg. 171 - 178, 2004.
[32] Maby E., Jeannes R. L., Faucon G., Liegeois-Chauvel C., de Seze R., Effects of gsm signals on auditory evoked responses Bioelectromagnetics, , Pg. - , 2005
[33] Urban P, Lukas E, Roth Z Does acute exposure to the electromagnetic field emitted by a mobile hone influence visual evoked potentials? a pilot study. Cent Eur J Pub Health 1998;6:288–90.
[34] Krause C. M., Haarala C., Sillanmaki L., Koivisto M., Hamalainen H., et al. , Effects of electromagnetic field emitted by cellular phones on the eeg during an auditory memory task - a double blind replication study, Bioelectromagnetics, , Vol. 25, 2004, Pages: 33-40
[35] Arai N., Enomoto H., Okabe S., Yuasa K., Kamimura Y., Ugawa G., Thirty minutes mobile phone use has no short-term adverse effects on central auditory pathways, Clinical Neurophysiol., Vol. 114, Pg. 1390 - 1394, 2003.
[36] Oysu C, Topak M, Celik O, Yilmaz HB, Sahin AA., Effects of the acute exposure to the electromagnetic field of mobile phones on human auditory brainstem responses, Eur Arch Oto-Rhino-Laryngology, , 262(10):839-43,2005.
[37] Wikipedia, http://en.wikipedia.org/wiki/Main_Page
[38] http://sccn.ucsd.edu/eeglab, Swartz Center for computational Neuroscience, University of California, San Diego.
[39] Ernest Niedermeyer, The Normal EEG of Waking Adult, Electroencephalography Basic Principle, Clinical Applications and Related Fields. Second edition, P 97-117, 1987

WAVELET ANALYSIS OF THE EFFECT OF A 900MHZ ELECTROMAGNETIC FIELD ON EVENT RELATED POTENTIALS OF EEG SIGNALS.

NANOU ELENA[1], PAPAGEORGIOU CHARALAMBOS[2, 3], HOUNTALA CHRISSANTHI[1], MAGANIOTI ARGIRO[1], TSIAFAKIS VASILEIOS[1], KAPARELIOTIS EVANGELOS[1], SOLDATOS KONSTANTINOS[2], RABAVILAS ANDREAS[3] CAPSALIS CHRISTOS[1]

[1] NATIONAL TECHNICAL UNIVERSITY OF ATHENS, DEPARTMENT OF ELECTRICAL ENGINEERING, DIVISION OF INFORMATION TRANSMISSION SYSTEMS AND MATERIAL TECHNOLOGY, GREECE

9 IROON POLYTECNEIOY STR., ATHENS, GREECE, 15773, Tel: ++30210-7722574, Fax: ++30210-7723520, email:enanou@mail.ntua.gr

[2] DEPARTMENT OF PSYCHIATRY, EGINITION HOSPITAL, UNIVERSITY OF ATHENS, GREECE
email: cpapage@eginitio.uoa.gr

[3] UNIVERSITY MENTAL HEALTH RESEARCH INSTITUTE, ATHENS, GREECE.

Abstract

Wavelet analysis has proven a useful tool for time-frequency analysis of EEG and Event Related Potential (ERP) signals. Moreover the effect of electromagnetic fields (EMFs) on brain activity is an important issue that requires further investigation.

The present study focused on the temporal analysis of the early components of ERPs stimulated by sounds of different frequencies (low=500 Hz and high=3000Hz), using wavelets. The ERPs were recorded at 16 scalp electrodes during a working memory test with and without electromagnetic radiation (900 MHz). The sample included 10 women and 9 men. Temporal comparisons were made between the energies, averaged at the time intervals before and after the P50 amplitude peak (30-80 msec after warning stimulus onset).

Results showed that the maximum energy variability was observed for the α-band at the C4 electrode. In the absence of radiation men exhibited a significant increase after the P50 peak of the energy for the low frequency stimulus, while women exhibited this significant increase for the high frequency stimulus. Conversely the presence of radiation seemed to suppress this energy increase for both sexes with the exception of women for the low tone.

Introduction

Since the advent of GSM-based cellular phone networks general concerns have been raised regarding potential health effects of high frequency electromagnetic fields (EMF). The close proximity of a mobile phone to the user's head leads to the absorption of part of the EMF energy in the head and the brain [1]. This is especially important in view of the observation that the shape of the head is oval, with a short axis of 15 – 17 cm in length, which is half the wavelength of the 900MHz transmission signals of the cellular phones. Consequently, the head may serve as a lossy resonator absorbing much of the energy emitted by cellular phones [2]. The above considerations necessitate the study of the possible effects of EMF on brain and behavior [3].

Analysis of EEG signals proved a useful and appropriate approach in measuring the level and spatial distribution of cortical activation during cognitive task performance. Several reports provide evidence that the exposure to EMFs increases the cortical activity as it is reflected in the increase of spectral power in the alpha band of the EEG signal. [4, 5, 6, 7]. However, there are reports which do not confirm these results [8].

The event-related brain potentials (ERPs) consist of a series of positive and negative peaks of the brain signals occurring at a fixed time relative to an event. These component peaks are studied with the assumption that they index meaningful aspects of cognitive processing [9]. Specifically the earlier components of the ERPs (0 – 100 msec after stimulus) are thought to represent the activity of the sensory pathways that transmit the signal generated at peripheral receptors to central processing systems.

There have been several studies of mobile phone emissions on the brain activity using the sensory components of ERPs methodology with various results [10, 11, 12, 13, 14 and 15]. It should be noted that the early components are 'modality specific', that is they are influenced primarily by the stimulus parameters such as intensity and frequency [16].Our team recently found that the MP-EMF affect the patterns of the auditory P50 component of ERPs (generally 30-80 msec post-stimulus)[17]. In particular the amplitude of P50 evoked by low frequency stimuli at Fp1 and O1 electrode is statistically significant increased in the presence of MP-EMFs. In contrast the exposure to MP-EMFs revealed statistically significant decrease of the amplitude of P50 evoked by high frequency stimuli, at Fp1 electrode as compared to themselves without MP-EMF exposure. These findings have been conceived as evidence that the MP-EMF emitted by mobile phone affect pre-attentive information processing reflected by the synchronized responses of the thalamocortical system of the P50 component of ERPs. [18, 19]

Moreover, having in mind that EEG and ERP data sets are nonstationary a useful tool to analyze these signals in both time and frequency domain is the Wavelet Analysis. Many studies have used wavelets in order to explore EEG and ERP waveform structure. Rosso and Figliola [20] used the wavelet transformation at generalized epileptic tonic/clonic EEG signals and showed that the Relative Wavelet Energy describes accurately the epileptic recruitment rhythm. Samar et al. applied wavelets at data collected from a sample consisted of controls and alcoholics in order to compare ERP values at different frequency levels [21]. They found significant group differences at the theta band at the span of P300 and also at the alpha band for the P100-N100-P200-N200. However, up to our knowledge, there are no studies specifically examining the effect of EMFs on ERPs using wavelets.

On the other hand the gender-dependent brain function is a subject under research. In a study about sex differences in resting EEG activity it was reported that EEG power for females was greater than the EEG power for males, with significant differences observed for delta, theta and beta bands, but not for the alpha band [22]. These findings concur with the results of a study of Briere et al. where women were found to have higher EEG power values at the central, parietal and left temporal electrodes [23]. Only one study has so far investigated EEG gender-related differences under exposure to mobile phone EMFs [24]. The subjects' EEG was recorded during the anticipatory period of performance on an auditory Wechsler test for 500 ms, either under real (900 MHz CW with a mean power at 0.64 W) or sham exposure. The amount of baseline EEG spectral energy of males was greater than that of females, while EMF exposure decreased the EEG energy of males and increased that of females. The above findings indicate that it is necessary to examine the possible impact of EMFs on brain activity separately for males and females in order to avoid the confounding effects of gender.

In summing up, cortical activation during the early components of the ERP signal is thought to be gender, modality and frequency specific. In view of the above considerations, the wavelet analysis of energy changes at the time intervals before and after the P50 could be of value in identifying possible pathophysiological alterations evoked by EMFs. Thus, the present study was designed to determine the time dependence of the effect of EMF exposure on the energy of early components of ERP during a working memory test.

Methods

Participants

Nineteen healthy individuals (9 men and 10 women, mean age = 23.3 ± 2.23 years, mean education = 16.9 ± 1.82 years) participated in the experiment. The male and female subgroups were homogeneous with regards to age and educational level. All participants were right-handed and had no history of any hearing problem. Informed consent was obtained from all subjects.

Experimental setup and Measurement Procedure

The subjects were evaluated with the digit span Wechsler Auditory test [25]. A warning stimulus of either high "(3000 Hz)" or low frequency "(500 Hz)" was presented through earphones to the subjects, who were asked to memorize the numbers that followed. The warning stimulus lasted 100msec. A one second interval followed the onset of the warning stimulus and then the numbers to be memorized were presented by a male voice. At the end of the number sequence presentation, the same signal tone was repeated. If the frequency of the signal tone was low the subjects had to recall the numbers in the same order as that presented, else, if the frequency was high, the subjects had to recall the numbers in the opposite order. Before any ERPs' recording, practice trials were administered until the subjects could clearly discriminate the warning stimuli (tones). After completion of the above-mentioned process, i.e. the practice trials, a rest period of five minutes followed, before the recording of the ERPs.

The experimental setup included a Faraday room, which screened any electromagnetic interference that could affect the measurements. The subjects sat in an anatomical chair and a certified dipole antenna was fixed near their right ear. The dipole's model was ELECTRO-METRICS EM6924 and the antenna factor was 27.4dB/m at 900MHz. Care was taken so that the distance between telephone and ear (about 20 cm) was constant during the whole session. The antenna was driven by a signal generator, which could be switched on or off. In the on mode the antenna emitted a 900 MHz electromagnetic field with mean power at 64 mWatt. [24] The signal was not modulated. The field strength was 3V/m at the point where the subjects' head was standing.

ERPs were recorded during 1.1 sec between the onset of the warning stimulus and the onset of the first administered number. The electrophysiological signals were recorded with Ag/AgCl electrodes. Electrode resistance was kept constantly below 5 kΩ. EEG activity was recorded from 15 scalp electrodes based on the International 10-20 system of Electroencephalography [26], referred to both earlobes. An electrode placed on the subject's forehead served as ground. The bandwidth of the amplifiers was set at 0.05 Hz to 35Hz. During the administration of stimuli, the subjects had their eyes closed in order to minimize eye movements and blinks. Eye movements were recorded through electro-oculogram (EOG) and recordings with EEG higher than 75mV were rejected. Warning stimuli, as well as learning material, i.e. the numbers to recall, were presented binaurally via earphones at an intensity of 65dB sound pressure level. The earphones did not have metal components in order to avoid EMF concentration.The evoked biopotential signal was submitted to an analogue-to-digital conversion, at a sampling rate of 1 KHz. Each recording session consisted of 52 repetitions of the trial.

The subjects performed the task twice, with (on mode) and without (off mode) radiation, with an interval of two weeks between the measurements. The order in which the subject was exposed at the EMF (exposure at the first or second visit) was random.

Because the P50 component is included in the array of early-endogenous ERPs components, which normally are modality specific, the ERPs induced by the two modal stimuli were averaged separately [16]. In particular, two varieties of P50 waveforms were obtained, one (low P50) evoked by the low frequency modality (26 trials) for each lead in all subjects and another (high P50) evoked by the high frequency modality (26 trials) for each lead in all subjects .

Wavelet Analysis

The Discrete Waveform Transform (DWT) was applied at the collected ERP data. The DWT analyzes the signal at different frequency bands with different resolutions by decomposing the signal into a coarse approximation and detail information. DWT employs two sets of functions, called scaling functions and wavelet functions, which are associated with low pass and high pass filters, respectively. The decomposition of the signal into different frequency bands is simply obtained by successive high pass and low pass filtering of the time domain signal. The original signal is first passed through a half band high pass filter and a low pass filter. After the filtering, half of the samples can be eliminated according to the Nyquist's rule, since now the highest frequency of the signal is half of this before filtering. The signal can therefore be subsampled by 2, simply by

discarding every other sample. This constitutes one level of decomposition. The "mother" wavelet function that was used to our analysis was Daubechies 1 (db1) and the levels of decomposition were seven.

This decomposition halves the time resolution since only half the number of samples now characterizes the entire signal. However, this operation doubles the frequency resolution, since the frequency band of the signal now spans only half the previous frequency band, effectively reducing the uncertainty in the frequency by half. At every level, the filtering and subsampling will result in half the number of samples (and hence half the time resolution) and half the frequency band spanned (and hence doubles the frequency resolution). The ERP data of the experiment consisted of 1000 values for each channel for each person after the averaging. In order to obtain high frequency resolution in δ band, the 1000 value sample was artificially subsampled. That is, the average of each 8 successive measurements of the signal was calculated the and consequently, 125 values were formed to which the Wavelet transform (WT) was applied.

The second step of the analysis was the reconstruction of the signal (or in our case the reconstruction of the details of the signal), that is how its components can be assembled back into the original signal without loss of information. The details of the signal at each level j are given by the function

$$D_j(t) = \sum_{k \in Z} C_{j,k} \psi_{j,k}(t)$$

where $\psi_{j,k}$ is the mother wavelet and $C_{j,k}$ are the wavelet coefficients which were calculated at the previous step. The wavelet coefficients $C_{j,k}$ can be interpreted as the local residual error between successive signal approximations at scales j-1 and j. $D_j(t)$ is the residual signal at scale j. It contains the information of the signal at frequencies $2^{j-1}f_s \leq |f| \leq 2^j f_s$.

Then the energy at each resolution level j=1,…,7 and at each instant, was calculated. This is the energy of the reconstructed detail signal:

$$E_j(t) = | D_j(t) |^2$$

The energies of the last three levels ($E_5(t)$,$E_6(t)$, $E_7(t)$) were summed up so that the sum stands for the energy at the time domain of the delta band (frequency 1-4 Hz). Each one of the remaining four levels with descending order represents the energy of the basic EEG rhythms theta, alpha, beta and gamma respectively.

The total energy at each time was calculated as follows:

$$E_{tot}(t) = \sum_{j=1}^{N} E_j(t)$$

The accuracy of the results was confirmed by comparing them with those derived from previous analysis with the FFT [24].

Finally the energy at each band was evaluated on a temporal basis. This means that the energies, were averaged at the time intervals before and after the P50 amplitude peak (30-80 msec after warning stimulus onset) and comparisons were made between these energies (before – after P50).

Statistical analysis

The parameter under consideration is the energy calculated with the Wavelet Transform. Preliminary statistical analysis was carried out independently for each modality (high, low) and for each frequency band (delta, theta, alpha, beta and gamma). The energies at the 15 leads were subjected to three way MANOVA with radiation (on – off), gender (male – female) and time interval (before – after the P50 peak) as the three independent factors. When the MANOVA procedure revealed statistical significance, the energies before and after the P50 peak were subjected to multiple pairwise comparisons for each lead, gender and radiation condition independently. Statistical significance was set at the 0.05 level.

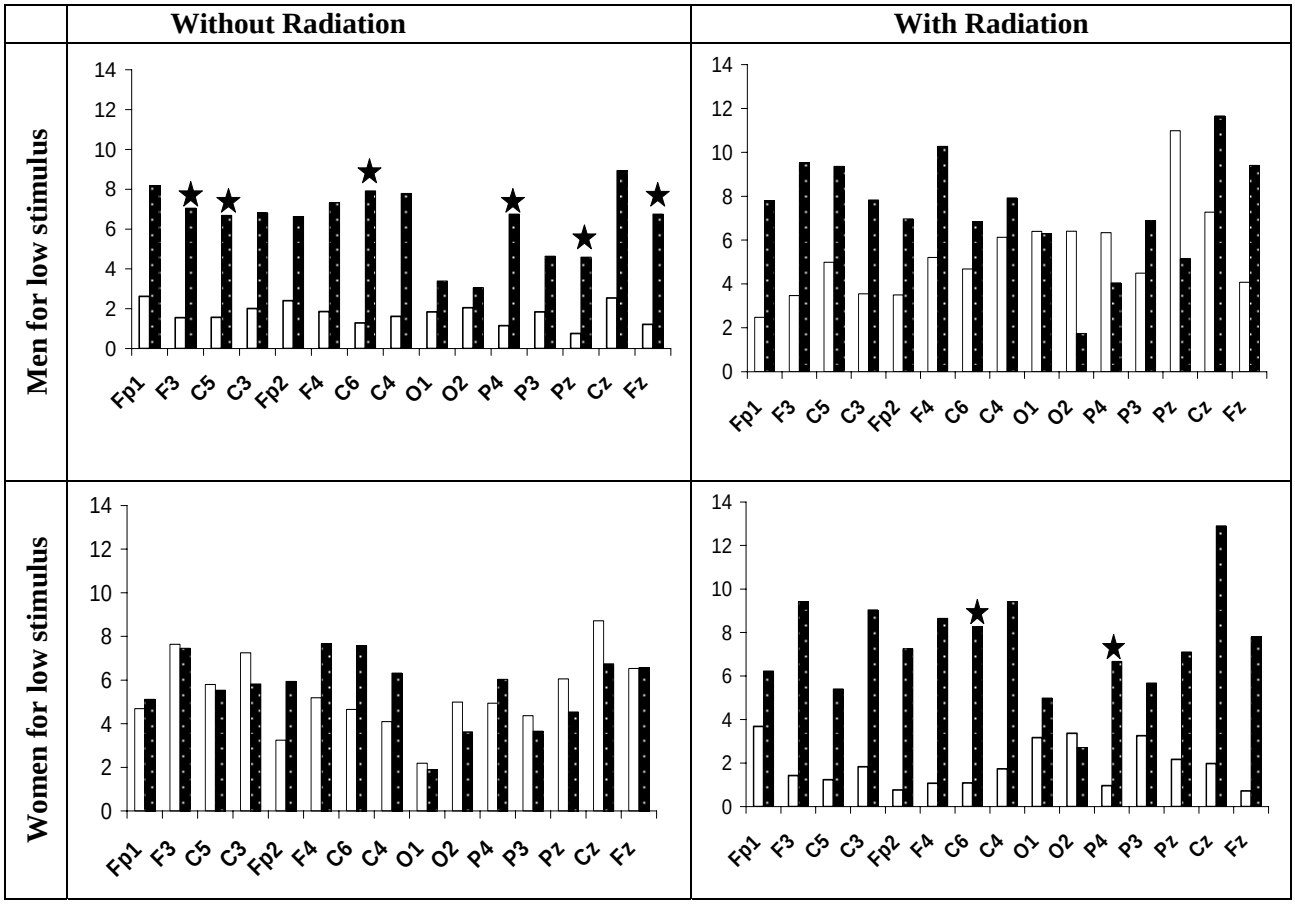
Results

The MANOVA procedure revealed that significant energy differences were found only at the alpha frequency band. Figure 1 displays the energies before and after the P50 component and Table 1 displays the energy differences after – before the P50 component for tones, genders and EMF conditions. . In Figure 1 asterisks indicate the electrodes for which the energy differences are statistically significant. It seems that these temporal energy differences are mostly positive and highly dependent on the interaction among modality, gender and EMF. In the absence of radiation men witnessed a significant increase of the energy of the alpha frequency band

for the low stimulus at electrodes F3,C5,C6,P3,Pz and Fz, while women evidenced the same increase for the high stimulus at electrodes F3,Fp2,F4,C6 and C4. The presence of radiation seems to suppress this temporal energy increase with the exception of women for the low tone at electrodes C6 and P4.

Electrodes	Energy (Joule) Differences after – before P50 for *low* stimulus				Energy (Joule) Differences after – before P50 for *high* stimulus			
	Male		Female		Male		Female	
	EMF Off	EMF On	EMF Off	EMF On	EMF Off	EMF On	EMF Off	EMF On
Fp1	5.56	5.32	0.43	2.55	-3.35	2.45	0.83	2.33
F3	**5.49**	6.07	-0.18	7.98	-6.22	6.78	**5.57**	-5.88
C5	**5.12**	4.37	-0.26	4.17	0.88	3.23	3.28	-4.3
C3	4.8	4.28	-1.43	7.21	-1.05	2.64	3.69	-4.01
Fp2	4.23	3.46	2.7	6.48	-4.05	2.16	**4.09**	-1.92
F4	5.46	5.06	2.49	7.58	-0.94	4.65	**7.37**	-3.43
C6	**6.63**	2.16	2.91	**7.18**	-1.02	3.29	**6.14**	-0.7
C4	6.17	1.79	2.22	7.68	-3.2	5.79	**6.58**	-1.42
O1	1.55	-0.11	-0.29	1.82	-4.98	-1.55	1.05	2.88
O2	1	-4.66	-1.37	-0.66	-4.53	-1.05	1.43	-1.31
P4	**5.6**	-2.3	1.09	**5.71**	-2.96	0.81	4.41	5.52
P3	2.79	2.39	-0.71	2.42	-4.56	1.68	3.03	-2.69
Pz	**3.83**	-5.84	-1.52	4.94	-7.2	3.07	6.15	-4.67
Cz	6.39	4.38	-1.97	10.93	-3.98	7.66	4.22	-6.59
Fz	**5.54**	5.33	0.05	7.08	-3.54	4.28	3.95	0.85

Table 1. Energy differences after – before the P50 component for tones, genders and EMF conditions.



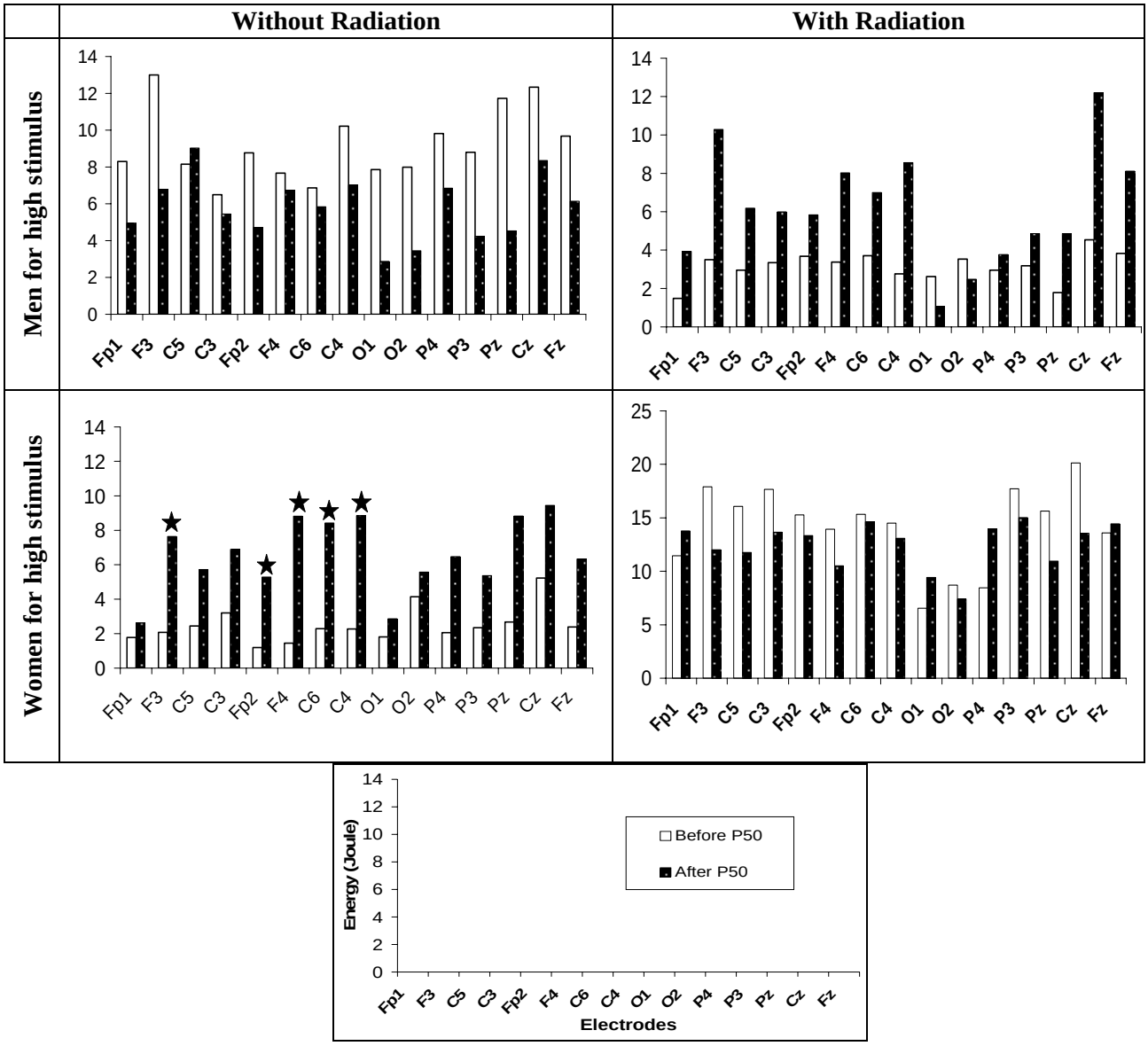


Figure 1. Energies before and after the P50 component for tones, genders and EMF conditions.

Discussion

The main objective of this study was the investigation of the influence of EMF on the sensory components of ERPs (within, 100msec after warning stimulus onset) elicited during a WM task. In order to retain both time and frequency domain information of ERPs we used the Wavelet analysis. Utilizing the two key aspects of Wavelet analysis-its multiresolution nature and its adaptivity to nonstationarity in ERP data elicited during a WM task- temporal comparisons between the energies, averaged at the time intervals before and after the P50 amplitude peak (30-80 msec after warning stimulus onset) were made.

The most robust findings were observed in alpha-frequency band activities. In particular in the absence of radiation, comparing the energies of the alpha frequency band before and after the P50 component, men exhibited a significant increase for the low stimulus at electrodes F3,C5,C6,P3,Pz and Fz, while women evidenced the same increase for the high stimulus at electrodes F3,Fp2,F4,C6 and C4. The importance of the obtained results may be explained, considering the activation of 'alpha system', using the so called conventional ways of EEG variables (power-, amplitudes-, network connection measures and phase delays). When a subject is stimulated (e.g. auditory stimulus) the flow of information is accompanied by alpha enhancement involving structures in the auditory pathways (e.g. reticular formation, medial geniculate nucleus, thalamus, hippocampus and the auditory cortex). [27]

Neurophysiological studies underscore that the alpha-band of evoked potentials is strongly correlated

with sensory function (e.g. thalamo-cortical circuits associated with working memory and probably with long – term memory engrams) [28]. It was also suggested that the alpha-band activity reflects a cortical –deactivation (the augmentation of attention-demanding mental activity is associated with decrease of alpha rhythm) [29]. In the light of these theories, the stimulus-related increase of the energy (before and after the P50), mostly for the alpha activity, which was found here, could though speculative, point to the possibility that the underlying neural networks of pre-attentive operation needs to be deactivated (relaxed) when the process of attention is ongoing. Conventionally the waveform of P50 which (as noted earlier) reflects pre-attentive operations is followed by the N100 waveform which represents the process of attention [16].

A second striking finding was the effect of gender on the patterns of energy changes within the time-window of the sensory components of ERPs for the alpha frequency. Gender has been shown to influence a variety of electrophysiological measures. However, the factors that mediate gender-related electrophysiological differences are not well understood. One possible mechanism which has been postulated is that steroid hormones estrogens and testosterone might be related to the neural oscillations associated with thalamocorical circuits which underlie alpha band activity [30]. Within this context, in order to understand better the observed gender-related differences concerning the two warning stimuli (high- vs low-warning tone) which evoked the measured ERPs, it seems reasonable to keep in mind that the auditory pathways from cochlear nucleus to the auditory cortex exhibit tonotopic organization during the ontogenesis.[31] In the light of these theoretical assumptions , it could be speculated that males and females have different neural networks activities involved in the transfer of information in thalamo-cortical circuits. This is in line with neurophysiological studies indicating that during the adolence in males the volume of white matter increases faster than in females. [32]

Moreover, the observed increase of the energy, before - after the P50 amplitude peak, points to an increased cortical activation as a direct consequence of EMF exposure. Such an effect may be due either to the psychophysic effect of the EMF exposure on brain tissue and/ or to its neurophysiological consequences (e.g. influence on blood brain barrier and/or thermal alterations). In relation to the neurophysiological point of view recent studies provide evidence, indicating the involvement of blood brain barrier (BBB) permeability, in the effect of mobile phones on the brain [33]. For instance it has been shown that EMF radiation has the potency to significantly open the BBB in a way that not only small but also large molecules, including toxic ones, can pass the BBB producing neuronal damage in the cortex, hippocampus and basal ganglia of rats exposed to EMF radiation for two (2) hours [34, 35]. On the other hand the EMF radiation is associated with enhancement of the temperature of the underlying tissues of the brain. It has been reported local heating (estimated to $0.11^{O}C$ rise in brain) due to radiation of EMF [36]. Interestingly, psychophysiological and neurophysiological studies have provided a direct relationship between alpha EEG activity regarding both thermal stimulations of the brain and changes of BBB. For example EEG coherence in alpha band significantly decreased in human subjects during tonic thermal stimulation [37]. Within this context, a brain imaging study by Korn et al., 2005 [38] using single photon emission computed tomography (SPECT) and addressing to both cortical- and BBB function in patients with postconcussion syndrome found significantly lower power in the alpha band compared with matched controls in conjunction with BBB disruption. Therefore, the changes described regarding the alpha EEG activity would seem to indicate adverse effects of EMF upon brain operation, which possibly may be mediated through the thermal and BBB alterations induced by EMF radiation.

In summary, the present study is an attempt to find sensory ERPs correlates associated with possible effects on human brain after exposure to EMFs. In order to retain both time and frequency domain information of ERPs we used the Wavelet analysis. Temporal comparisons between the energies, averaged at the time intervals before and after the P50 amplitude peak (30-80 msec after warning stimulus onset) were made. It was found that only for the alpha band the energy was mostly increased and this change is highly dependent on the interaction among modality, gender and EMF exposure.

Acknowledgements

The authors would like to thank Mr. M.Kyprianou, Scientific Investigator, Athens, Greece, for his professional support on the statistical analysis of the experimental results.

References

[1] F. Schönborn, M. Burkhardt, N. Kuster, Differences in energy absorption between heads of adults and children in the near field of sources. Health Phys. 74 (1998) 160-168.

[2] Z. Weinberger, E. D. Richter, Cellular telephones and effects on the brain: The head as an antenna and brain tissue as a radio receiver, Med. Hypotheses 59(2002) 703-705.

[3] R. Westerman, B. Hocking, Diseases of modern living: neurological changes associated with mobile phones and radiofrequency radiation in humans, Neurosci. Lett. 361 (2004) 13-16.

[4] H. Reiser, W Dimpfel, F Schober, The influence of electromagnetic fields on human brain activity, Eur J Med Res. 1995 Oct 16;1(1):27-32.

[5] R Huber, V Treyer, AA Borbely, J Schuderer, JM Gottselig, HP Landolt, E Werth, T Berthold, N Kuster, A Buck, P Achermann, Electromagnetic fields, such as those from mobile phones, alter regional cerebral blood flow and sleep and waking EEG. J Sleep Res. 2002 Dec;11(4):289-95.

[6] RJ Croft, JS Chandler, AP Burgess, RJ Barry, JD Williams, AR Clarke, Acute mobile phone operation affects neural function in humans. Clin Neurophysiol. 2002 Oct;113(10):1623-32.

[7] Curcio G, Ferrara M, Moroni F, D'Inzeo G, Bertini M, De Gennaro L. Is the brain influenced by a phone call? An EEG study of resting wakefulness. Neurosci Res. 2005 Nov;53(3):265-70. Epub 2005 Aug 15.

[8] J Roschke and K Mann, No short-term effects of digital mobile radiotelephone on the awake human electroencephalogram. Bioelectromagnetics 1997; 18:172–176.

[9] N Yeung, R Bogacz, B Clay Holroyd,, JD Cohen, eds. Psychophysiology, Blackwell Publishing Inc. Printed in the USA. 41 (2004), 822–832.

[10] C. Eulitz, P. Ullsperger, G. Freude, T. Elbert, Mobile phones modulate response brain activity, Neuroreport 9 (1998) 3229-3232.

[11] G. Freude, P. Ullsperger, S. Eggert, I. Ruppe, Effects of microwaves emitted by cellular phones on human slow brain potentials, Bioelectromagnetics, 19 (1998)384-387.

[12] W. A. Preece, G.Iwi, A. Davies-Smith, K. Wesnes, S. Butler, E. Lim, A. Varey, Effect of a 915-MHz simulated mobile phone signal on cognitive function in man. Int J Radiat Biol. 75 (1999) 447-456.

[13] M. Koivisto, A. Revonsuo, C. Krause, C. Haarala, L. Sillanmaki, M. Laine, H. Hamalainen, Effects of 902 MHz electromagnetic field emitted by cellular telephones on response times in humans. Neuroreport 11 (2000) 413-415.

[14] M. Koivisto, M.C. Krause, A.Revonsuo, M. Laine, H. Hamalainen, The effects of electromagnetic field emitted by GSM phones on working memory. Neuroreport 11 (2000) 1641-1643.

[15] M.C. Krause, L. Sillanmaki, M. Koivisto, A. Haggqvist, C. Saarela et al. Effects of electromagnetic fields emitted by cellular phones on the electroencephalogram during a visual working memory task. Int J Radiat Biol. 76 (2000) 1659-1667.

[16] M.Fabiani, G. Gratton, M. Coles, Event-related potentials: methods, theory, and applications. In: Cacioppo J, Tassinary L, Bernston G, eds. Handbook of psychophysiology. Cambridge University Press, New York, 2000, pp53–84.

[17] Papageorgiou C., Nanou D., Tsiafakis V., Kapareliotis E., Kontoangelos K., Capsalis C, Rabavilas A., Soldatos C.Acute mobile phone effects on pre-attentive operation, Neuroscience Letters 2006 (Paper in press).

[18] A.B.Clementz, D.L. Blumenfeld, S. Cobb, The gamma band response may account for poor P50 suppression in schizophrenia. Neuroreport. 8(18) (1997)3889-3893.

[19] G. Zouridakis, N.N. Boutros, H.B. Jansen, A fuzzy clustering approach to study the auditory P50 component in schizophrenia. Psychiat. Res. 69 (1997) 169-181.

[20] Rosso O.A., Figliola A. Order/disorder in brain electrical activity, Revista Mexicana de Fisica 50(2) (2004) 149-155.

[21] Samar V.J., Begleiter H., Chapa J.O., Raghuveer M.R., Orlando M., Chorlian D., Matched Meyer neural wavelets for clinical and experimental analysis of auditory and visual evoked potentials, 1996,In G. Ramponi, G.I. Sicuranza, S. Carrato and S.Marsi(Eds.), Signal processing: VII. Theories and applications, Proceedings of EUSIPCO-96(pp. 387-390). Trieste: Edizioni LINT.

[22] Horita M, Takizawa Y, Wada Y, Futamata H, Hashimoto T. Sex differences in EEG background activity: a study with quantitative analysis in normal adults. Rinsho Byori 43(2): 177-80, 1995Feb.

[23] Briere ME, Forest G, Chouinard S, Godbout R. *Evening and morning EEG differences between young men and women adults*. Brain Cogn 53(2): 145-8, 2003 Nov.

[24] C. Papageorgiou, E. Nanou, V. G. Tsiafakis, C. Capsalis, A. D. Rabavilas, Gender related differences on the EEG during a simulated mobile phone signal, Neuroreport, 15 (2004) 2557-2560.

[25] D. Wechsler, Manual for the Wechsler adult intelligence scale. New York: Psychological Corporation, 1955.

[26] H. Jasper, The ten-twenty electrode system of the international federation. Electroencephalogr Clin Neurophysiol. 10 (1958) 371–375.

[27] Basar E.Memory as the "whole brain work": a large-scale model based on "oscillations in super-synergy".Int J Psychophysiol. 2005;58(2-3):199-226.

[28] Basar E, Basar-Eroglu C, Karakas S, Schurmann M.Gamma, alpha, delta, and theta oscillations govern cognitive processes.Int J Psychophysiol. 2001;39(2-3):241-8.

[29] Laufs H, Kleinschmidt A, Beyerle A, Eger E, Salek-Haddadi A, Preibisch C, Krakow K. 2003. EEG-correlated fMRI of human alpha activity. Neuroimage 19:1463-1476.

[30] Carozzo S, Fornaro S, Garbarino S, Saturno M, Sannita WG.From neuroscience to application in neuropharmacology: A generation of progress in electrophysiology.Clin EEG Neurosci. 2006 Apr;37(2):121-34. Review.

[31] Romand R. Modification of tonotopic representation in the auditory system during development. Prog Neurobiol. 1997 ;51(1):1-17.

[32] De Bellis MD, Keshavan MS, Beers SR, Hall J, Frustaci K, Masalehdan A, Noll J, Boring AM.Sex differences in brain maturation during childhood and adolescence.Cereb Cortex. 2001 Jun;11(6):552-7.

[33] Hossmann KA and Hermann DM. Effects of electromagnetic radiation of mobile phones on the central nervous system. Bioelectromagnetics 2003;24:49–62.

[34] Persson BR, Salford LG, Brun A, Eberhardt JL, Malmgren L. Increased permeability of the blood-brain barrier induced by magnetic and electromagnetic fields. Ann N Y Acad Sci. 1992 Mar 31;649:356-8. No abstract available.

[35] Salford LG, Brun AE, Eberhardt JL, Malmgren L, Persson BR. Nerve cell damage in mammalian brain after exposure to microwaves from GSM mobile phones. Environ Health Perspect. 2003 Jun;111(7):881-3;

[36]Van Leeuwen GM, Lagendijk JJ, Van Leersum BJ, Zwamborn AP, Hornsleth SN, Kotte AN. Calculation of change in brain temperatures due to exposure to a mobile phone. Phys Med Biol. 1999 Oct;44(10):2367-79.

[37] Huber MT, Bartling J, Pachur D, Woikowsky-Biedau SV, Lautenbacher S.EEG responses to tonic heat pain.Exp Brain Res. 2006;173(1):14-24.

[38] Korn A, Golan H, Melamed I, Pascual-Marqui R, Friedman A. Focal cortical dysfunction and blood-brain barrier disruption in patients with Postconcussion syndrome. J Clin Neurophysiol. 2005 Jan-Feb; 22(1):1-9.

MODULATED MICROWAVE EFFECT ON DEPRESSION

MAIE BACHMANN[1], HIIE HINRIKUS[1], KAIRE AADAMSOO[2], ÜLLE VÕHMA[2], JEKATERINA RUBLJOVA[1], ANNA SUHHOVA[1], JAANUS LASS[1], JEVGENI RIIPULK[1]

[1]Biomedical Engineering Centre, Tallinn University of Technology

Address: 5 Ehitajate Rd, EE19086 Tallinn, Estonia

[2]Clinic of Psychiatry, North Estonia Regional Hospital,

Address: 19 J.Sütiste Rd, EE13419 Tallinn , Estonia

Abstract

The preliminary experiments were carried out on the group of depression patients (women, 18 subjects) and comparison group of healthy volunteers exposed during 30 min to 450 MHz microwave radiation modulated with 1000 Hz frequency. The field power density at the scalp was 0.9 mW/cm^2. As a subjective criteria of depression mood, the Brief Affect Scale (BAS) and Visual Analogue Scale (VAS) before and after each exposure procedure was used. Parallel a ratio of the EEG power in symmetric EEG channels of the different brain hemispheres FP1/ FP2, T3/T4, P3/P4 and O1/O2 was evaluated. Statistical analysis of these parameters for individuals with post-hoc Bonferroni correction was applied.

The BAS revealed mood improvement after exposure for majority of depressive subjects (11) and no changes for others (7). The VAS detected significant improvement in subjective mood score after exposure. The EEG analysis showed the biggest difference in symmetry between hemispheres in temporal area. Average values are higher in higher EEG rhythms. The difference was significant in 3 cases of exposed and in 5 cases of sham recordings. Significant results in sham condition indicate that the parameter selected as a measure is not very steady among depressive patients. This makes difficult to detect the effect caused by the EMF exposure.

Keywords: EMF effect, depression, Brief Affect Scale, EEG analysis, symmetry of brain hemispheres.

.

Introduction

Clinical treatment approaches for depression disorder utilize primarily pharmacologic agents, antipsychotic and antidepressant drugs, that sometimes are of limited efficacy and may have objectionable side effects. ECT is usually effective as a treatment for depressive disorder, but it involves general anesthesia and some degree of memory loss, and its effects can be transient. Repetitive transcranial magnetic stimulation (rTMS), initially developed to test gross central nervous system function, more recently has been applied with some success in the treatment of depression [1–3]. The success of rTMS in the treatment of depression has been varied and has been described in a recent review as "often statistically significant (but) below the threshold of clinical usefulness" [1]. rTMS treatment can be unpleasant, with some patients declining participation due to scalp pain induced by the apparatus [4]. There is also a small risk of seizure [5].

Recent report has suggested mood improvement in patients with bipolar disorder immediately after they underwent an echo-planar magnetic resonance spectroscopic imaging (EPMRSI) procedure that can be performed within clinical MR system limits [6]. The mood states of subjects in an ongoing EP-MRSI study of bipolar disorder were assessed by using the Brief Affect Scale, a structured mood rating scale, immediately before and after an EP-MRSI session. The characteristics of the electric fields generated by the EP-MRSI scan were analyzed. Mood improvement was reported by 23 of 30 bipolar disorder subjects who received the actual EP-MRSI examination, by three of 10 bipolar disorder subjects who received sham EP-MRSI, and by four of 14 healthy comparison subjects who received actual EP-MRSI. Significant differences in mood improvement were found between the bipolar disorder subjects who received actual EP-MRSI and those who received sham EP-MRSI. The electric fields generated by the EP-MRSI scan were smaller (0.7 V/m) than fields used in repetitive transcranial magnetic stimulation (rTMS) treatment of depression (1–500 V/m) and also extended uniformly throughout the head, unlike the highly nonuniform fields used in rTMS. The EP-MRSI waveform, a 1-kHz train of monophasic trapezoidal gradient pulses, differed from that used in rTMS. These preliminary data suggest that the EP-MRSI scan induces electric fields that are associated with reported mood improvement in subjects with bipolar disorder. The findings are similar to those for rTMS depression treatments, although the waveform used in EP-MRSI differs from that used in rTMS.

The findings reported above allowed expecting EMF effect on depression at the field power density much lower than used in TMS. In our previous studies the effect of the modulated 450 MHz microwave radiation on human EEG has been detected at the EMF level 0.16 mW/cm^2, lower than the recommended health protection limit [7-10]. In majority of modulation frequencies and EEG rhythms the exposure increases the EEG energy level and variability. Has such stimulation any effect on depression?

The aim of this study is to investigate the effect of modulated microwave exposure to the state of depression. In the study we tested the hypothesis that the modulated with 1000 Hz frequency 450 MHz EMF has an effect on subjects with depressive disorder. Distinction of reactions to microwave exposure will be performed by 1) clinical rating utilising psychiatric tests 2) EEG analysis.

Method and equipment

Subjects

The experiments were carried out on two groups of volunteers: a group of patients with major depressive disorder and a group of healthy comparison subjects. The group of subjects consisted of 18 persons, mean age 39 years, standard deviation 10 years.

The study was conducted in accordance with the Declaration of Helsinki and has formally approved by the local Medical Research Ethics Committee. All risks, benefits and possible adverse events associated with EMF study participation were explained to subjects, who provided written informed consent before entering the study.

Subjects with major depressive disorder were selected from hospital inpatient unit. Subjects with non-psychotic major depressive disorder as defined by ICD-10 criteria and determined by 17-item Hamilton Depression Rating Scale (HAM-D) score more than 14 were eligible. The average HAMD score for the group was 21 (SD 3.3). Subjects were without antidepressant treatment, only regular (same dosage for more than 3 weeks) benzodiazepine use was allowed. Concomitant treatments for current general medical conditions were permitted on the basis of clinical judgment (patients receiving medication with known CNS side effects were not eligible).

All the subjects passed two experimental procedures - with exposure and sham. During each test session, the succession of exposure-sham was randomly assigned. Only one experimental EEG recording was performed for a subject during a day between time interval 9 a.m. to noon. The subjects were not informed of their exposure, however, they were aware of the possibility of being exposed.

Subjects were asked to evaluate Becks Depression Inventory (BDI) and Visual Analogue Scale (VAS) before and after each EMF procedure (both exposure and sham). Subjects were also asked to evaluate Brief Affect Scale (BAS) after each EMF procedure.

Microwave exposure

The 450 MHz microwave radiation was generated by the Rhode & Swartz (Germany) signal generator model SML02. The RF signal was 100% amplitude modulated by the pulse modulator SML-B3 at 1000 Hz requency (duty cycle 50%). The generator signal was amplified with the Dage Corporation (USA) power amplifier model MSD-2597601 and additional laboratory amplifier (Miteq-Eesti, Estonia). The generator and amplifier were carefully shielded and located in the laboratory room. The 10W EMF output power was guided by a coaxial to the quarter-wave antenna NMT450 RA3206 by Allgon Mobile Communication AB, Sweden, located at 10 cm from skin from the left side of the head.

The spatial distribution of the microwave power density was measured by the Fieldmeter C.A 43 Chauvin Arnoux (France) field strength meter. The calibration curves of the field power density dependence on the distance from the radiating antenna were obtained from these measurements performed in the real condition of the experiment. During the experiments, the stability of the microwave level was monitored by the IC Engineering (USA) Digi Field C field strength meter. Estimated by the measured calibration curves, the field power density at the skin from the left side of the head was 0.9 mW/cm^2. The spatial distribution of the field density around the head and upper torso was not uniform: Digi Field C field strength meter indicated maximum level of 0.9±0.1 mW/cm^2 at the left side of the head, minimum level of 0.14±0.05 mW/cm^2 at the right side of the head and 0.45±0.05 mW/cm^2 above the head. Measured field power density was 0.8±0.15 mW/cm^2 at 10 cm distant from the left ear, near and the left shoulder and 0.17±0.05 mW/cm^2 near the right shoulder. The SAR value, calculated based on the maximum field power density, is 2 W/kg.

Experimental procedure and EEG recording equipment

The study consisted of two experimental procedures identical for all subjects. The first protocol included continuous EEG recording during 30 minutes. The 450 MHz 1000 Hz modulated microwave exposure is switched on during all recording. The second protocol is the same except that the microwave exposure is switched off.

The experimenter and the subjects were in the same laboratory room during the experiments. The room was dark but no other special conditions were provided. The subjects were lying in a relaxed position, eyes closed and ears blocked during the experiments.

The Cadwell Easy II EEG measurement equipment was used for the EEG recordings The EEG was recorded using 32 electrodes, which were placed on the subject's head according to the international 10-20-electrode position classification system. The channels for analysis were chosen to cover the entire head: frontal - FP1, FP2; parietal P5, P4, temporal - T3, T4; occipital O1, O2 and the reference electrode Cz). The EEG recordings were stored on a computer with a 400 Hz sampling frequency. The recorded EEG signals were observed by an experienced neurologist. The artifacts were detected by visual inspection. The recordings containing multiple artifacts were removed and the recording was repeated.

Afterwards, off-line data processing was executed. The energies of the five basic EEG rhythm frequencies (delta, theta, alpha, beta and beta2) were extracted from the total EEG signal (0.5 - 48 Hz) by filtering.

Clinical evaluations

Each subject completed the Visual Analogue Scale (VAS) and the Brief Affect Scale (BAS) based on their subjective feeling and symptoms before and/or after every experimental procedure.

Visual Analogue Scale (VAS) was introduced for subject self-evaluation of mood. VAS is 100-millimeter line with one end matching mood "very bad" and second end matching as "very good". Subject has to determine visually her mood on the day of evaluation marking this on the line. In our study subjects evaluated VAS on the day before and the day after EMS procedure (both exposure and sham). This allows to determine immediate effect as scale can be to be applied every day. The lengths of the lines from beginning up to the marker were manually measured afterwards (results from 0 to 100 are possible). The lower numeric results in VAS show more depressive mood. VAS was introduced to determine immediate effect of EMS, as HAMD and BDI are designed for longer period (minimum 1 week).

The Brief Affect Scale was applied to the study after the experimental protocols. The subjects were asked to fill out the form and answer how much, if any, their feeling had improved or worsened since the time before experimental protocol. The subjects provided their responses on a 7-point scale, as follows: 3, very much improved; 2, much improved; 1, minimally improved; 0, no change; –1, minimally worse; –2, much worse; and –3, very much worse. These numerically ranked responses were grouped into the categories of improved (3 to 1), same (0), and worse (–1 to –3) for statistical treatment. This grouping is referred to as the Brief Affect Scale ratings.

The two-tailed paired Student t-test was used to estimate differences between exposed and sham exposed results for depressive and healthy subjects. All *p* values lower than 0.05 were considered as significant.

EEG analysis

The dynamics of the EEG energy of the theta (4-8 Hz), alpha (8-13 Hz), beta1 (13-20 Hz) and beta2 (20-40 Hz) rhythms frequencies was analyzed.

Assymmetry between left and right brain hemisphare EEG channels was selected as a measure for estimation of the effect. The ratio of the power spectral density of the signals for the symmetric channels FP2/FP1, T4/T3, P4/P3, O2/O1 from right and left hemispheres was calculated and analysed.

The power spectral density (PSD) was estimated by means of Welch's averaged periodogram method. The signal was divided into overlapping sections (50%), with the length of 2048 points and windowed by the Hanning window. Afterwards, the power on the theta, alpha, or beta band W_{mn} was computed for each subject (indexed by $n \in [1,18]$) and hemisphere (indexed by $m=1,2$) as the area under the spectrum for the corresponding frequency band (integral of the band).

The relative misbalances of the PSD in symmetric channels were selected for further analysis. Finally, parameter *A* for a subject was calculated as follows:

$$A=(W_{1n} / W_{2n} -1)*100\ \%,$$

where W_{1n} and W_{2n} were the power spectral densities of the right and left symmetric channel respectively.

The average values and standard deviations of parameter *A* for different EEG channels pairs for the individual subjects and for the whole group were calculated.

Statistical analysis was performed for the differences between exposed and sham exposed recordings. For sham recordings, normal physiological processes determine the asymmetry between hemispheres and the standard deviation σ for the parameter *A* was calculated.

According to the "zero hypothesis", the EEG recordings of subjects under microwave exposure cannot be distinguished from sham signals. Thus, the "zero hypothesis" implies that and $\left\langle \left(W_1 - W_2\right)^2 \right\rangle = \left\langle \left(\tilde{W}_1 - \tilde{W}_2\right)^2 \right\rangle$. Consequently, if the "zero hypothesis" is true, the quantity $x = \left(W_{1n} - W_{2n}\right)^2 \sigma^{-2}$ is a *f*-distributed random quantity, the cumulative distribution of which is routinely designated as $F_{1,15}(x)$; the indices 1 and 18 stand for the numbers of the degrees of freedom.

Accordingly, the ratio of the computed power difference to the standard deviation (calculated on the basis of sham signals) of the differences can be used as a quantitative measure, showing how well the "zero hypothesis" is satisfied, respective *p*-values are obtained by means of the cumulative *f*-distribution:

$$p = F_{1,15}\left[\left(W_{1n} - W_{2n}\right)^2 \sigma^{-2}\right].$$

Post-hoc mean comparisons were tested by Bonferroni approach with a 0.05 confidence level.

Signal processing and calculation of parameters were performed in the LabVIEW and MatLab programming and signal processing environment.

Results

The results of psychiatric tests are presented in Table 1. Most of the depressive subjects reported improvement of her mood after exposure (11). This number is less for sham procedure (7). Numbers of the subjects with no changes of mood is less for exposed subjects (7) and higher for sham subjects (10). Only one subject reported worsening of her mood during sham procedure.

The changes in mood during procedure are quite well reflected in score of the BAS test: average score for exposed procedure is 0.81 and sham procedure 0.62.

VAS test revealed significant change between scores before (average 33.3) and after (average 40.2) for exposed subjects and no significant change for sham exposed subjects.

These results are in good agreement with the study [6], where mainly the Brief Affect Scale was used for evaluation of the mood improvement in bipolar depression. Anyway, such results may be caused by the factors different from EMF as inconveniences related to MRI equipment or EEG cap.

Table 1. Data of the Brief Affect Scale (BAS) and Visual Analogue Scale (VAS) tests for depressive subjects

	Total number of subjects	Sub. Reporting improvement	Sub. Reporting worsening	Sub. Reporting no change	BAS		VAS			
							Before		After	
					Mean for group	SD	Mean for group	SD	Mean for group	SD
Depression subjects exposed	18	11	0	7	0.81	0.75	33.34	17.97	40.21	25.18
							p=0.04			
Depression subjects sham exposed	18	7	1	10	0.62	1.20	35.68	19.46	40.29	21.21
							p=0.25			

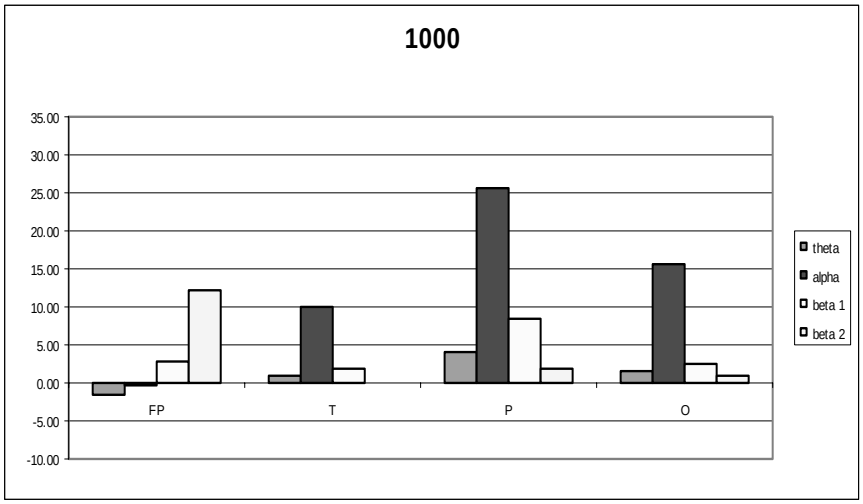
Data of the EEG analysis are presented in Figures 1 and 2. Figure 1 presents the average values of *A* for different frequency bands, for control group in sham (1a) and EMF condition (1b). As can be seen, those values behave quite similarly. The biggest difference seems to be in frontal region. However, trends in different channels are the same in sham and EMF condition.

As expected, for control group, there were no significant results in the ratio of the computed power difference to the standard deviation of differences (calculated on the basis of sham signals) in the case of sham recordings nor recordings under the influence of EMF.

Figure 2 presents the average values of A for different frequency bands, for depressive group in sham (2a) and EMF condition (2b). The results are not as similar between two EMF conditions as they were in control group. The biggest difference occurs in temporal area. Average values are higher in higher EEG rhythms, however having opposite signs. Beta rhythms are more influenced also in frontal area. Trends in other brain regions are mostly the same in sham and EMF conditions.

In the case of EMF recordings of depressed patients, the ratio of the computed power difference to the standard deviation of differences (calculated on the basis of sham signals) was significant in 3 cases, and in the case of sham recordings in 5 cases. Significant results in sham condition indicate that parameter *A* is not very steady among depressive patients. This makes difficult to detect which deviation of the parameter is caused by EMF.

1a)



1b)

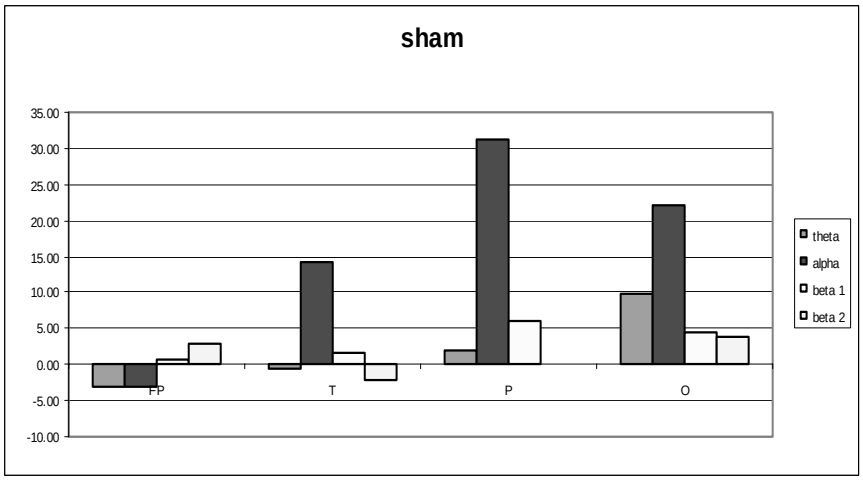
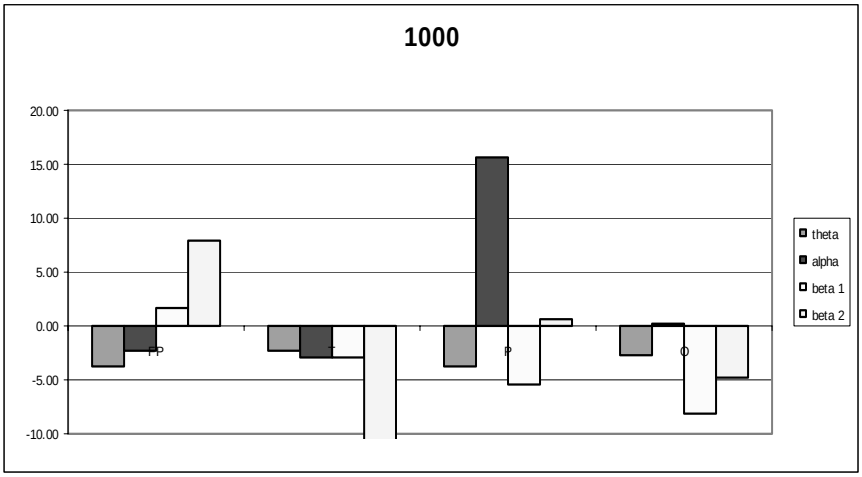


Figure 1. The average asymmetry of hemispheres (average values of *A*) for different EEG rhythms for control group in EMF (1a) and sham (1b) condition.

To investigate the behaviour of parameter *A* with depression, the depressive patients' sham recordings were compared with the sham recordings of the control group.

Now, the ratio of the computed power difference to the standard deviation of differences (calculated on the basis of sham signals) for control group sham recordings was zero and depressive group sham recordings had 7 significant results. The influence was highest in frontal theta rhythm 16.7% and the depression slightly influenced also the beta1 and beta2 rhythms in frontal and temporal region (5.6%).

2a)



2b)

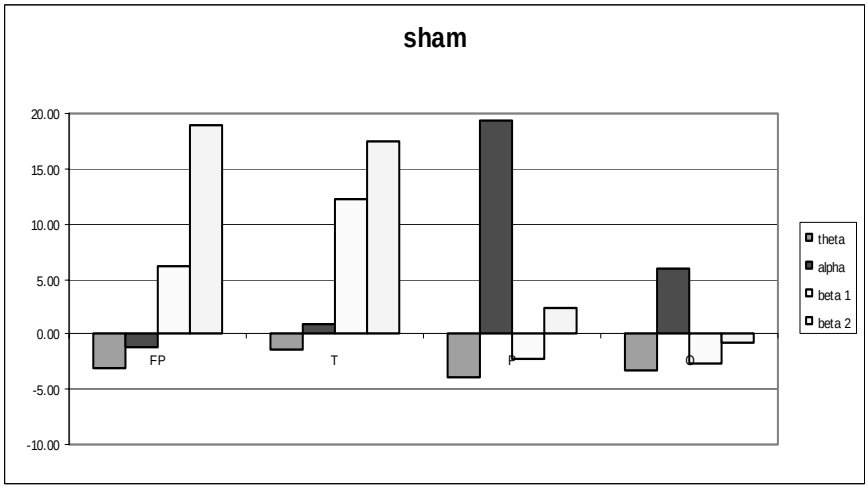


Figure 2. The average asymmetry of hemispheres (average values of *A*) for different EEG rhythms for the group of patients with major depressive disorder in EMF (2a) and sham (2b) condition.

Summary

The BAS revealed mood improvement after microwave exposure for majority of depressive subjects (11) and no changes for others (7). The VAS detected significant improvement in subjective mood score after exposure. These results support the recent promising research where mood improvement in bipolar depression by low-frequency magnetic field has been reported [6].

The EEG analysis based on evaluation of symmetry between brain hemispheres detected the biggest difference related to EMF exposure in temporal area. Average values are higher in higher EEG rhythms. But the difference related to EMF was significant in 3 cases, and in the case of sham recordings in 5 cases. Significant results in sham condition indicate that the parameter selected as measure is not very steady among depressive patients and makes difficult to detect which deviation of the parameter is caused by EMF exposure.

The preliminary results are promising and the further investigation should be aimed to finding a better measure for EEG analysis and performing experiments on larger number of subjects.

Acknowledgement

This study has been supported by the Estonian Science Foundation grant No 6632.

References

1. Wassermann EM, Lisanby SH: Therapeutic application of repetitive transcranial magnetic stimulation: a review. Clin Neurophysiol 2001, **112**:1367–1377.
2. McNamara B, Ray JL, Arthurs OJ, Boniface S: Transcranial magnetic stimulation for depression and other psychiatric disorders. Psychol Med 2001, **31**:1141–1146.
3. Lisanby SH: Focal brain stimulation with repetitive transcranial magnetic stimulation (rTMS): implications for the neural circuitry of depression. Psychol Med 2003; **33**:7–13.
4. George MS, Nahas Z, Molloy M, Speer AM, Oliver NC, Li XB, Arana GW, Risch SC, Ballenger JC: A controlled trial of daily left prefrontal cortex TMS for treating depression. Biol Psychiatry, 2000; **48**:962–970.
5. Wassermann EM: Risk and safety of repetitive transcranial magnetic stimulation: report and suggested guidelines from the International Workshop on the Safety of Repetitive Transcranial Magnetic Stimulation, June 5–7, 1996. Electroencephalogr Clin Neurophysiol 1998; *108*:1–16.
6. Rohan M, Parow A, Stoll AL, Demopolus C, Friedman S, Dager S, Hennen J, Cohen BM, Renshaw PF, 2004. Low-field magnetic stimulation in bipolar depression using an MRI-based stimulator. Am J Psychiatry; **161**: 93-98.
7. Hinrikus, H., Parts, M., Lass, J., Tuulik, V. Changes in Human EEG Caused by Low Level Modulated Microwave Stimulation. Bioelectromagnetics . 2004, **25**: 431-440.
8. Bachmann, M., Kalda, J., Lass, J., Tuulik, V., Sakki, M., Hinrikus, H. Non-linear analysis of the electroencephalogram for detecting effects of low-level electromagnetic fields. Medical & Biological Engineering & Computing, 2005, **43**:142-149.
9. Lass, J., Hinrikus, H., Bachmann, M., Tuulik, V. Microwave radiation has modulation frequency dependent stimulating effect on human EEG rhythms. Proceedings of the 26th Annual International Conference of the IEEE EMBS San Francisco, USA, 2004, 4225-4228.
10. Bachmann, M., Säkki, M., Kalda, J., Lass, J., Tuulik, V., Hinrikus, H. (2005): Effect of 450 MHz microwave modulated with 217 Hz on human EEG in rest. The Environmentalist, 2005, **25**: 65-171.

EFFECTS OF THE STATIC MAGNETIC FIELD GENERATED BY 0.5 T MRI UNIT ON TNF-α RELEASE OF HUMAN PBMC FROM PATIENTS WITH RHEUMATOID ARTHRITIS.

ANTONIO LO CASTO[1], CARMELA LA MENDOLA[2], SERGIO SALERNO[1], GIUSEPPE MAMONE[1], NADIA CACCAMO[2], ROBERTO LAGALLA[1]

[1] Sezione di Scienze radiologiche - Dipartimento di Biotecnologie mediche e Medicina legale - Università degli Studi di Palermo
[2]Dipartimento di Biopatologia - Università degli Studi di Palermo

Abstract
The aim of this study was to investigate the effects of a 0.5 T static magnetic field (SMF) of a MRI clinical unit on TNF-α release from peripheral blood mononuclear cells (PBMC) obtained from patients with rheumatoid arthritis (RA). These patients didn't take biological drugs, as receptor TNF-α or anti-TNF-α monoclonal antibodies, at the time of collecting samples. PBMC were isolated and cultured in complete medium and split into 2 groups of samples, one to be exposed and the other one as control. After 2 hrs of exposure to the SMF at 37°C, cells were stimulated or non stimulated with a mitogen, and incubated for 48 hrs. After the incubation the supernatants were collected and assayed by ELISA technique for TNF-α production. The results demonstrated a significant decrease of TNF-α release in PBMC of patients with RA exposed to 0.5 T SMF. RA is a multisystem disorder. It predominantly causes inflammation in synovial joints and tendon sheaths and results in suppressed erythropoiesis, but can also lead to serositis, alveolitis, ocular scleritis, subcutaneous nodules and hepatosplenomegaly. The positive clinical response to drug therapy with TNF-α-neutralizing agents shows that the inflammation is largely TNF-α dependent, at least in the synovium.

Introduction
Static magnetic field (SMF) produces different bioeffects on cells of the human immune system. A strong SMF is commonly employed by magnetic resonance devices in clinical practice to obtain tomographic images of the whole body (MRI, magnetic resonance imaging). Immune system cells represent a well known and sensitive model for the study of magnetic field bioeffects [1-3]. We have previously demonstrated that the SMF generated by a 0.5 T superconducting MRI clinical unit causes *in vitro* alteration on cytokine release in human peripheral blood mononuclear cells (PBMC) from healthy volunteers [1, 3]. Among these cytokines, it was observed a decreased release of TNF-α in exposed cells [4, 5]. TNF-α is a regulator of the immune response, playing an important role in several inflammatory conditions, such as rheumatoid arthritis (RA) [6, 7]. Some papers have dealt the effects of electromagnetic fields (emf) as a potential therapy in the treatment of arthritis [8, 9]. The aim of this study was to investigate the effects of a 0.5 T SMF of a MRI clinical unit on TNF-α release from PBMC obtained from patients with rheumatoid arthritis (RA).

Materials and methods
PBMC of 4 patients affected by RA and that didn't take biological drugs, as receptor TNF-α or anti-TNF-α monoclonal antibodies, at the time of collecting samples, were used for the experiment. PBMC were isolated from heparinized blood by centrifugation on Ficoll-Hypaque (Pharmacia, Uppsala, Sweden). Cells were maintained in RPMI-1640 (Gibco, Grand Island, NY) supplemented with 10% heat-inactivated pooled human AB^+ serum, 2 mM L-glutamine, 20 mM HEPES, 100 U/ml penicillin, 100 μg/ml streptomycin, 5 x 10^{-5} M 2-mercaptoethanol and 150 IU/ ml rIL-2. PBMC were split into two groups of samples, one to be exposed and the other one as control to be kept under isothermal conditions for the whole time of the experiment. After 2 hrs of exposure to the SMF, cells were stimulated with a mitogen, lypopolisaccaride (LPS), employed at a 0.5 μg/ml suboptimal concentration. After 48 hrs of culture supernatants were collected and stored at –70° C until tested. TNF-α content was assessed using immunoenzymatic methods. The commercial enzyme-linked immunosorbent assay (ELISA) was reagent set human TNF-α (EUROCLONE, Devon, UK). A superconducting MRI unit (Vectra; GE Medical Systems, Milwaukee, WI, USA) commonly employed for clinical examinations was the source of the 0.5 T SMF. A specific device for keeping the cell samples at 37° C was used; it was constituted

by a thermostated water bath in which a plexiglass tube holder, with the tubes containing cell samples, was placed before its introduction within the gantry of the MRI unit.

Results

After 48 hrs of *in vitro* culture, a significant decrease of TNF-α release was observed in PBMC of 4 patients affected by RA exposed for 2 hrs to a 0.5 T SMF, stimulated or not stimulated with LPS, in comparison with sham-exposed cells (Fig. 1).

Discussion

It has been previously observed that exposure of human PBMC from healthy volunteers for 2 hrs at 37 °C to the 0.5 T SMF of a MRI clinical unit caused a decreased release of cytokines in exposed cell [1, 3]. It was also demonstrated a decreased release of TNF-α in human macrophages under the same condition of exposure [4]. A related decrease of intracellular free calcium -whose compartimentalization through cell membrane is a part of the cell response mechanism to magnetic fields and inhibits activation of immune system cells- was also found in the exposed macrophages [5]. In this study the effects of a 0.5 T SMF of a MRI clinical unit on TNF-α release from PBMC obtained from patients with RA was evaluated. RA is a chronic inflammatory disease affecting 1% of the population [6]. TNF−α is a cytokine that promotes the inflammation and its associated with fever and signs (pain, tenderness, and swelling) in several inflammatory conditions, including RA [6, 7]. Some drugs have been introduced that, blocking the action of TNF-α, reduce the signs and symptoms of inflammation and stops the progression of joint damage [10]. Moreover, TNF−α is now recognized as a critical cytokine orchestrating differentiation and proliferation, as well as the ability to induce cell death [6]. TNF−α has been implicated as the causative agent in a number of pathologies, including cachexia, septic shock, rheumatoid arthritis, autoimmunity, and induction of HIV expression. Activated T cells, macrophages, and other non-lymphoid cells produce TNF−α. In RA, the antibodies (IgM) produced react with connective tissue components such as collagen and proteoglycans as well as with determinants in the Fc region of IgG and form IgG–IgM complexes, which get deposited in the joints and activate complement cascade [11]. This mechanism leads to erosion of cartilage and bone. The existing treatments available for RA cannot be considered as curative or definitive therapy. Hence, alternative and safe therapy regulating signaling pathways is absolutely essential. There is an increasing interest in the therapeutic use of emfs in arthritis, stimulated in large part by recent advances in alternative and complementary medicine [8, 9]. In this paper, after 48 hrs of *in vitro* culture, a significant decrease of TNF-α release was observed in PBMC of patients affected by RA exposed for 2 hrs to the 0.5 T SMF of a MRI clinical unit. Although these preliminary results, obtained from PBMC of only 4 patients affected by RA, need to be confirmed on wider population, this work may supply a key to the comprehension of mechanisms responsible of the therapeutic effects of emfs in arthritis. Interesting perspectives in the use of emfs as an adjuvant or alternative form of therapy in arthritis may furthermore develop.

References

1. Salerno S, Lo Casto A, Caccamo N, D'Anna C, De Maria M, Lagalla R, Scola L, Cardinale AE. Static magnetic fields generated by a 0.5 T MRI unit affects in vitro expression of activation markers and interleukin release in human peripheral blood mononuclear cells (PBMC). Int J Radiat Biol 1999; 75:457-63.
2. Aldinucci C, Garcia Blanco J, Palmi M, Sgaragli G, Benocci A., Meini A, Pessina F, Rossi C, Bonechi C, Pessina GP. The effect of strong static magnetic fields on lymphocytes. Bioelectromagnetics 2003; 24:109-117.
3. Salerno S, La Mendola C, Lo Casto A, Mamone G, Caccamo N, Cardinale AE, Salerno A. Reversible effect of MR and ELF magnetic fields (0.5 T and 0.5 mT) on human lymphocyte activation patterns. Int J Radiat Biol 2006; 82:77-85.
4. Lo Casto A, La Mendola C, Salerno S, Mamone G, Caccamo N, De Maria M. Effects of the static magnetic field generated by 0.5 T MRI unit on the release of TNF-α from human monocytes. Proceedings Biological effects of EMFs, 7-11 October, Rhodes, Greece, 2002: 363-366.
5. Lo Casto A, La Mendola C, Salerno S, Mamone M, Caccamo N, Lagalla R. Effects of the static magnetic field generated by 0.5 T MRI unit on intracellular calcium concentration and TNF-α release of human macrophages. Proceedings Biological effects of EMFs – 3rd International Workshop, 4-8 October, Kos, Greece, 2004: 70-73.
6. Beutler B. TNF in pathophysiology: biosynthetic regulation. J Invest Dermatol 1990; 95:81S–84S.
7. Kunkel SL, Spengler M, Kwon G, May MA, Remick DG. Production and regulation of tumor necrosis factor alpha. A cellular and molecular analisys. Methods Achiev Exp Pathol 1988; 13: 240-249.
8. Kumar VS, Kumar DA, Kalaivani K, Gangadharan AC, Raju KV, Thejomoorthy P, Manohar BM, Puvanakrishnan R. Optimization of pulsed electromagnetic field therapy for management of arthritis in rats. Bioelectromagnetics 2005; 26:431-9.
9. Fischer G, Pelka RB, Barovic J. Adjuvant treatment of knee osteoarthritis with weak pulsing magnetic fields. Results of a placebo-controlled trial prospective clinical trial. Z Orthop Ihre Grenzgeb. 2005; 143:544-50.

10. Iannone F, Trotta F, Montecucco C, Giacomelli R, Galeazzi M, Matucci-Cerinic M, Ferri C, Cutolo M, Bambara LM, Triolo G, Ferraccioli G, Valentini G, Lapadula G. Etanercept maintains the clinical benefit achieved by infliximab in patients with rheumatoid arthritis who discontinued infliximab due to side effects. Ann Rheum Dis. 2006 Jul 12; [Epub ahead of print].
11. Kohl J, Gessner JE. On the role of complement and Fc gammareceptors in the arthus reaction. Mol Immunol 1999; 36:893-903.

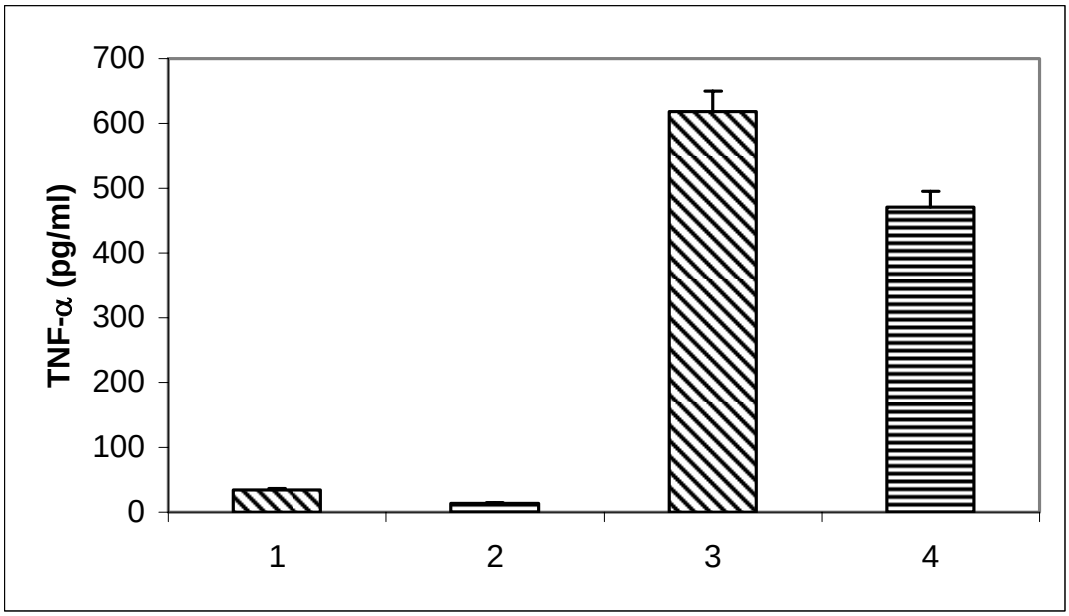


Fig.1. Release of TNF-α by human PBMC exposed to a 0.5 T SMF
Legends:

1. Sham exposed PBMC after 48 h of culture in complete medium.
2. SMF exposed PBMC after 48 h of culture in complete medium.
3. Sham exposed PBMC stimulated with mitogen (LPS) after 48 h of culture in complete medium.
4. SMF exposed PBMC stimulated with mitogen (LPS) after 48 h of culture in complete medium.

Overview of ISO TC215 Technical Report #21730: "Health informatics - Use of mobile wireless communication and computing technology in healthcare facilities - Recommendations for electromagnetic compatibility with medical devices

Joseph J Morrissey

Motorola Labs, 8000 West Sunrise Blvd, Ft. Lauderdale, FL 33322

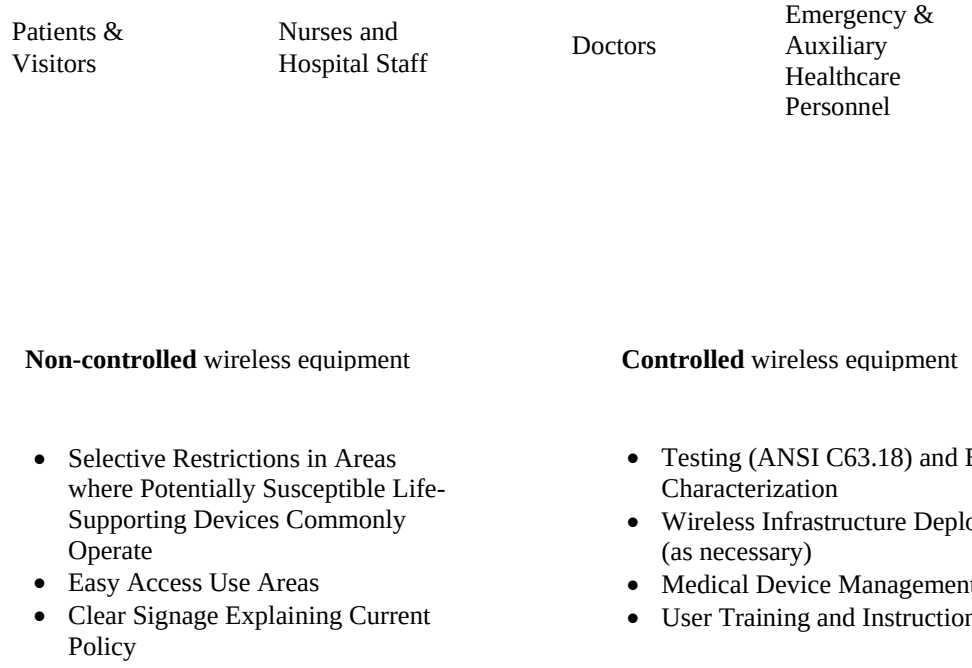
Abstract: Worldwide, healthcare facilities are recognizing the need to incorporate new technology and provide better point-of-care information to improve healthcare delivery, while reducing medical errors. Computing technologies, electronic medical record systems, and seamless access to information using wireless communication can offer significant advancements to healthcare communication and health informatics exchange. Such wireless technologies include the use of mobile phones, handheld computers / PDAs, WiFi / 802.11.x local area networks, personal area networks including 802.15.1 (Bluetooth) / 802.15.4 (Zigbee) / WiMedia / UWB Alliance (UWB), two-way pagers, radios, etc. In addition, visitors and patients are also finding use of personal mobile phones and other wireless devices increasingly valuable, especially in times of crisis. Previously, no uniform international guideline existed for the appropriate deployment, use, and management of mobile wireless communication and computing technology within healthcare facilities to mitigate potential electromagnetic interference (EMI) with medical devices. At one extreme, overly-restrictive policies in some healthcare facilities may inadvertently act as obstacles to the deployment of beneficial technology. At the other extreme, unmanaged use of mobile wireless handsets in healthcare facilities can place patients at risk. An equally important factor in this issue is that healthcare organizations throughout the world have a variety of different resources, needs, concerns, and RF environments that may not all be addressed by implementation of a single prescriptive management strategy. The current Technical Report offers balanced guidance to allow diverse healthcare organizations realize the benefits of mobile wireless technology while also providing necessary and sufficient safeguards against undesired and unintended risks of EMI.

Introduction: The non-controlled/unmanaged use of mobile wireless equipment by individuals visiting or working in healthcare facilities has steadily increased, regardless of existing healthcare policy. However, published reports suggest that the level of risk for accidental EMI events from government and other non-profit health agency sources appears to be relatively small, although underreporting of such events may be substantial. Anecdotal observations of suspected EMI events or incidents with ECG and EEG machines, apnoea monitors, ventilators and radiant warmers, infusion pumps, wheelchairs, and other devices have been reported or referred to in a number of publications [1]-[15]. Ad hoc test studies [16]-[28] have confirmed that EM interference effects can be caused by certain wireless transmitters in susceptible medical devices, although this generally requires specific conditions (transmission at higher power levels, close proximity, for extended periods of time) that may not be common during normal use.

Although the recently approved second edition of the IEC International Standard 60601-1-2 specifies general immunity levels of 3 V/m for medical equipment and systems that are not life-supporting and 10 V/m for life-supporting medical equipment and systems, manufacturers in the US and many other countries are allowed to justify lower levels and there is no consistent international regulation enforcing this standard. Many mobile wireless handsets exceed the 3 and 10 V/m limits when operating at maximum power and in close proximity. Further, older medical devices still in use may not have been constructed or tested to the same EM immunity level. Despite the potentially serious level of risk due to unmanaged mobile wireless handset use, most mobile wireless equipment might be allowed to operate, even where potentially susceptible medical devices are used, if comprehensive management procedures are implemented.

Recommendations: The following recommendations are intended to help the healthcare facility achieve a reasonable assurance of EMC with their medical devices while allowing for the deployment of wireless RF technology. These recommendations are built on the foundations from the AAMI TIR 18-1997, recommendations from the AMA Council on Scientific Affairs, the American Society for Healthcare Engineers,

and several other publications and reports. In general, the healthcare facility should create a management, testing, procurement, and education program and policies addressing electromagnetic compatibility with active medical devices and the deployment of wireless technology. Because of the wide range of wireless technology involved, there are specific recommendations dealing with both the wireless emitters that are controlled or managed by the healthcare facility and wireless emitters that are not easily controlled by the facility (e.g., patient or visitor PDAs, computers, or cellular telephones). The following flow chart illustrates basic steps outlined in the specific recommendations to develop a facility strategy allowing wireless equipment to operate without unnecessary restrictions while at the same time sufficiently managing and mitigating potential EMI issues.



Important recommendations are made equally to Medical Device Manufacturers, Healthcare facilities, and Wireless Equipment Manufacturers.

Risk management of medical devices is covered in ISO 14971. All medical devices (including systems of medical devices such as would be formed with wired or wireless communication devices) should meet that standard and be managed to take into account compliance with ISO 14971 over the life cycle of the device.
For Medical Device Manufacturers, they should continue to meet and exceed current IEC 60601-1-2 [33] listed electromagnetic immunity levels in the design of new medical equipment. Medical devices that are not directly covered by this technical report should also be designed, manufactured, and deployed using the appropriate consensus standards with respect to EMC. (e.g., active implanted devices [55], in vitro diagnostics [56]). It is expected that medical devices will increasingly operate in environments where emissions from mobile RF/wireless transmitters are increasingly common.

For Healthcare facilities, they should manage wireless equipment within their facility in accordance with the following guidelines, and neither unduly limit the use of otherwise beneficial technology or ignore the potential for EMI issues. Similar recommendations electromagnetic compatibility with medical devices should also be directly incorporated into corporate policies, strategic plans, and / or governance models.
For Wireless Equipment Manufacturers, they should have full understanding of the potential EMI issues that can arise in worse case scenarios with medical devices as well as other wireless equipment, and deploy their equipment and systems appropriately in accordance with the following recommendations.

Responsibility within healthcare facilities
Within the healthcare facility, clinical/biomedical engineers or other appropriate technical personnel (e.g., spectrum management, IT, telecom, and building services) should be the focal point for EMC, EMI mitigation, and EMC/EMI education and training. Qualifications are not specified in this document, although consideration should be given to appropriate education, expertise, and experience of the responsible individuals

Inventory within healthcare facilities
The medical device inventory within a healthcare facility should be managed to the extent possible and practical to ensure compatibility with the ever-increasing RF environment.
a) In the purchase of new medical devices by healthcare facilities, every effort should be made to ensure the equipment meets (and exceeds if possible) minimum EMC immunity requirements set out by IEC 60601-1-2:2001 or other appropriate medical device EMC standard. Older equipment found to be particularly susceptible to EMI caused by mobile wireless transmitters should be phased out as is possible and practical within the healthcare facility budget.

b) While significant modifications to medical devices should not be made by healthcare facilities, certain simple precautions can be taken to reduce the risk of EMI caused by mobile wireless transmitters. EMI susceptibility in all medical devices can be reduced by positioning cables, sensors, and electrical accessories in such a way as to increase the distance between these components and RF transmitters operating in the area. Life-supporting medical devices or those known or suspected of being susceptible to EMI can be positioned away from high traffic areas or adjoining rooms where mobile wireless equipment may be in routine operation.

Testing within healthcare facilities
The **IEEE / ANSI C63.18** protocol is recommended for comprehensive ad hoc, on site testing of all mobile wireless equipment that might be used in the healthcare facility by doctors, staff, visitors, or patients. However, it is fully understood that exhaustive testing is rarely feasible, and different needs, resources, and personnel constraints of the healthcare facility may dictate widely different approaches. General recommendations regarding EMC testing are as follows:

a) Testing should be performed, whenever possible and practical, on selected medical devices in the equipment inventory that are considered to have life supporting functions (i.e., according to the prioritization recommendations of ANSI C63.18) using one of the mobile handsets as a test transmitter (see ANSI C63.18 for details on the test protocol).

b) Testing should take special consideration of older medical devices, life-supporting medical devices, and any device where EMI is suspected. Testing can be extended to other medical devices where feasible and practical (see ANSI C63.18 for details on a recommended prioritization).

c) Periodic testing should be performed on a regular schedule (e.g., once per year), and especially after changes such as the introduction of new communication devices, new medical equipment, or significant repositioning on a regular basis

d) If comprehensive testing of mobile wireless equipment is not possible, focused testing on mobile wireless equipment routinely operating within the healthcare facility that can transmit at higher power (e.g., two-way radios, mobile / cellular phones) may be most appropriate (see section 3, Table 1, and Annex A sections 4 and 5 for more detailed information about the frequency and RF output power for several types of wireless equipment). If testing of mobile wireless equipment is not possible at all, some information may be obtained by communicating with larger healthcare facilities that have performed prior testing or from ad hoc EMI testing databases found on the internet (one such ad hoc EMI testing database is currently being developed in cooperation with ASHE, although as of this revision it is not yet operational).

e) Assistance with obtaining transmitter equipment, setting the equipment in test mode for constant output at maximum power, and performing ad hoc testing can often be requested from mobile wireless equipment manufacturers and/or network providers.

f) Consideration may be given to have testing performed by an independent third party, in conjunction with the healthcare organization's clinical engineering group. The involvement of a third party may facilitate a consistent

and impartial evaluation of EMI issues and proposed management strategies, and more importantly may offer an independent analysis in cases where a further level of indemnity for the healthcare facility, equipment manufacturer, and/or network service provider is desired.

g) Medical devices found in ad hoc testing to be susceptible to EMI should be replaced whenever feasible and practical with more electromagnetically compatible devices, e.g. those compliant with new IEC 60601-1-2:2001 and other relevant immunity requirements. However, it should be noted that medical devices meeting 60601-1-2 can still be susceptible to emissions from mobile wireless equipment such as mobile / cellular phones at close range where the electromagnetic fields exceed the immunity testing levels specified in this standard.

h) Results from ad-hoc testing tend to be variable, due to variability in RF source power, medical-device differences, and test-site differences. It is important to understand that the primary function of ad-hoc testing is to identify unreasonably-susceptible medical devices so that they can be managed appropriately, not act as a quantitative assessment of their susceptibility.

Controlled use within healthcare facilities
For controlled mobile wireless equipment to be used by doctors and healthcare organization staff under managed conditions, it is recommended that necessary and sufficient procedures be implemented to identify, characterize, and mitigate potential EMI problems.

a) The **IEEE / ANSI C63.18** recommended practice (as outlined above) is the suggested test protocol for rapid ad hoc, on-site RF EMI testing for EMI identification and characterization.

1) Testing should be performed using the mobile wireless handsets to be used in the controlled system as a test transmitter. If multiple in-house systems are to be deployed, testing should be performed with each different RF signal. If new in-house systems are deployed, each different RF signal should be tested. Different EMI effects can be caused by different RF signals.

2) Ad hoc testing should be an ongoing effort, with a record of EMI test results kept including characterization of new medical device acquisitions and investigation / verification of reported EMI incidents, making any necessary adjustments to policy.

3) Periodic testing should be performed on a regular schedule (e.g., once per year), and especially after changes such as the introduction of new communication devices, new medical equipment, or significant repositioning on a regular basis.

4) Given the qualitative nature of the ANSI C63.18 ad hoc testing, even if no significant EMI issues are identified, nominal management policies including recommended minimum separation distances may still be prudent.

b) For mobile handsets that transmit at a constant output power, having no dynamic power control (e.g., standard two-way radios, family radios, two-way pagers, 802.11 systems), EMC management should involve ensuring adequate separation from identified susceptible medical devices. In the case of radio transmitters with relatively high constant power output (1 W or more), this may require significant separation distances and possibly necessitate their restriction from certain areas of the healthcare facility. In the case of pagers with extremely short burst transmissions or IEEE 802.11 a/b/g / Local Area Network or IEEE 802.15 / Bluetooth / Zigbee / IEEE 802.15.3a PAN equipment (see table 1 for more information about these) with relatively low constant power output (~10 milliwatts), the risk of EMI may be significantly less than for equipment such as two-way radios. Testing is still recommended whenever possible, although it is understood that it may reveal little susceptibility and the feasibility and practicality of all testing must be considered and prioritized.

c) If mobile wireless transmitters are dynamically power controlled (e.g., mobile / cellular phones, PDAs operating on wide area networks), EMC management should involve network characterization, design, and in-building engineering to supplement the wide area network as necessary to insure handsets are directed to transmit at RF power levels sufficient to minimize EMI issues. The existence of numerous shielding and reflecting objects in a healthcare facility may create areas with variations in downlink signal coverage, some of which could lead to significant intermittent changes in transmit power of the handsets causing them to deviate from their normal output power. Such areas should be characterized (by measuring existing signal strength with the mobile wireless handset set to a "trace" mode – this can often be done by the network service provider) and managed appropriately.

d) Medical device management procedures may include identification through labelling, repositioning or other means to reduce exposure to the wireless emissions, or replacing particularly susceptible devices with newer model units. Because of medical device regulations, modifications to a medical device should only be made by the device manufacturer.

e) User guidelines can be provided as an additional layer of management directing healthcare staff to maintain a predetermined and practical separation distance between their mobile wireless handsets and potentially susceptible medical devices (between 25 cm and 2 meters).

f) The AAMI TIR 18 is recommended for additional details on medical device management and EMC/EMI guidelines.

g) Testing of specific fixed-infrastructure components such as local electrical circuits and circuit breakers can be considered for testing if failure could represent a significant hazard, and if testing can be performed without placing the facility at risk.

h) Healthcare facilities should actively manage spectrum usage (e.g, maintain a list of all controlled-use RF sources indicating where they are authorized to operate, as well as the maximal number of such units permitted within each area or zone).

i) Wireless security issues (which are outside of the scope of this document) must be properly considered, otherwise patient safety may be threatened if the informatics system becomes compromised or incapacitated

Non-Controlled use within healthcare facilities
For non-controlled mobile wireless equipment that may be brought randomly into the healthcare facility by visitors, patients, or staff and transmit a variety of different signals at different output power levels:
a) Separate EMC/EMI management policies than those listed for controlled mobile wireless handsets should be applied. While ad hoc testing and management solutions are always encouraged whenever possible, this may not be practical for every wireless system.

1) While certain mobile handsets may be able to operate compatibly throughout a healthcare facility environment, other mobile handsets may have greater potential to cause EMI events due to local differences in output power or signal type. As the number of handsets continues to increase and new models reduce size, internalize antennas, and combine technologies (i.e.; mobile phone / pager / PDA device / local area IEEE 802.11a/b/g / personal area IEEE 802.15.1 / UWB / IEEE 802.15.4, etc), it is becoming increasingly difficult to differentiate between RF transmitter types based upon visual appearance alone. Further confounders include the growing number of wireless headsets and accessories that relocate the actual RF transmitter to a pocket or purse, keeping them from obvious view even when in use. An increasing number of mobile wireless handsets can transmit multiple signal types, including data transmission that may use different bursting technologies (i.e., GPRS, WAP). Wireless laptop cards and PDAs may operate on either wide area (mobile phone-type) or local (IEEE 802.11.x - type) networks with different carrier frequencies, signal types, and power output. Ultimately, it may be impossible to enforce any policy that differentiates between different non-controlled mobile wireless handset types with regard to their use in the healthcare facility based upon visual appearance. For this reason, all non-controlled mobile wireless handsets should be treated with the same management / restrictions regardless of whether or not they appear to be the same as controlled handsets.

2) Restrictive policies might involve requesting that individuals not use their personal mobile wireless handsets in areas of the facility where potentially susceptible medical devices are used. This should involve requesting by appropriate signage or some other reliable mechanism that non-controlled mobile wireless equipment is turned off before entering areas where potentially susceptible life-supporting medical devices are commonly operating, as even well-intentioned individuals may feel compelled to receive and respond to incoming calls or messages.

3) Implementation and enforcement of restrictive policies should be facilitated by signs, especially in areas where potentially susceptible medical devices are commonly located, to make patients and visitors aware of the existing healthcare facility policy. Compliance with existing policy can be facilitated by defining numerous areas with easy access where the use of wireless handsets by patients, visitors, and staff is unlikely to interfere with medical devices.

4) Any restrictive policy should be balanced between an informed assessment of EMI risk and the increasing need among patients, visitors, and healthcare facility staff for mobile wireless communication and computing. In the extreme, healthcare facilities could ban the use of all non-controlled mobile wireless handsets altogether, although such measures are likely to be excessive from an EMI management perspective (58) and not responsive to the growing needs of individuals for direct access to mobile wireless communication, especially in times of emergency and crisis.

b) While instructing patients and visitors to maintain a minimum separation distance between their personal mobile wireless handsets and medical devices might theoretically act as a safeguard against EMI events, such a recommendation may be impractical in many facility areas, and further be exceedingly difficult to monitor and enforce. Such minimum separation requirements are not recommended as a primary management strategy. However, the minimum separation distances determined from ad hoc testing can be used as an added layer of management in areas where potentially susceptible life-supporting medical devices are commonly operating.

RF emissions from network sources

a) RF emissions from in-building system network antennas (WAN microcells or repeaters, LAN access points) are most appropriately managed by locating them in a place where separation distance mitigates medical device EMI effects, such as the roof of corridors and rooms.

b) RF emissions from base station sites physically located on healthcare facility roof-top or building structures should conform to existing national radio regulations to limit emissions directly into the supporting building structure.

Medical devices within healthcare facilities

a) Although outside the current scope of this recommendation, the placement and operation of RF-emitting medical devices within the healthcare environment is an area that should be carefully considered. There are many types of medical devices that generate and use electromagnetic energy for their medical function. For example, Electric scalpels (e.g. high frequency electrosurgical equipment) often generate RF and microwave fields for cauterization purposes, physio-diathermy units may emit 915, 433, 2450 MHz or other frequencies for deep tissue heating (36), and ultrasound machines may radiate up to their operating frequency of ~ 3 - 20 MHz. The healthcare facility should exercise caution in where and how these types of emitters are used in the vicinity of other potentially susceptible medical devices.

b) Electromagnetic type security and inventory systems such as metal detectors, anti-systems, and RFID emit signals that may disrupt potentially susceptible medical devices. The policies and practices of the healthcare facility should address this equipment. For example, RFID tags used in the healthcare environment may be passive emitters, activated by inductive processes when brought into proximity of RFID readers. However, the readers may emit high field strength magnetic fields and should be included as a transmitter in ad hoc testing and in EMC/EMI management policies. The recently published ASTM F 2401-04 “Standard Procedures for Security Checkpoint Metal Detector Screening of Persons with Medical Devices” provides useful information [57]

c) For medical devices used outside the healthcare facility in a domiciliary setting, such as dialysis equipment, blood glucose analyser, infusion pumps, etc, instruction should be provided to patients advising them to maintain at least 1 meter of separation distance between the medical device and mobile wireless equipment while it is in operation.

References:

1) Segal B et al (2001) Risk of Patient Injury due to Electromagnetic Interference Malfunctions: Estimation and Minimization. Proc 2001 IEEE International Symposium on Electromagnetic Compatibility, p. p. 1308-1312.

2) ECRI "Cellular Telephones and Radio Transmitters—Interference with Clinical Equipment". Health Devices 1993 Aug-Sep;22[8-9]:416-8

3) ECRI "Electromagnetic Interference and Medical Devices: An Update on the Use of Cellular Telephones and Radio Transmitters in Healthcare Facilities". Health Devices Feb-Mar 1996;25(7):263

4) Segal B et al (1994) The Health Canada Medical Devices Bureau Roundtable Discussion on Electromagnetic Compatibility in Healthcare. Biomedical Instrumentation Technol 29:350-354

5) Bassen H.I., Ruggera, P.S., O'Bryan, E.R., Casamento, J.P., Silberberg, J.L. (1992) Medical Device RF Susceptibility - Research and Proposed Standards for Infant Apnea Monitors. EMC Technology Magazine Expo '92 International Conference on Electromagnetic Compatibility Technical Record, pp. 256-260

6) Sykes, S., ed. Forum on Electromagnetic Compatibility. FDA/AAMI Conference Report (proceedings available from the Association for the Advancement of Medical Instrumentation, Arlington, Virginia), May 1995 (ISBN 1-57020-054-8).

7) Silberberg JL (1993) Performance Degradation of Electronic Medical Devices Due To Electromagnetic Interference. Compliance Engineering 10:25-39

8) ECRI (2001) Wireless communication devices and electromagnetic interference. ECRI's updated recommendations. Health Devices (2001) Nov;30(11):403-9

9) Silbert PL (1994) J. Polysomnographic Technology 10:20-22

10) AAMI TIR 18 (1997) Guidance on Electromagnetic Compatibility of Medical Devices for Clinical/Biomedical Engineers. Part 1: Radiated Radio Frequency Electromagnetic Energy

11) Paperman WD et al (August 1994) Electromagnetic Interference: Causes and Concerns in the Health Care Environment, Healthcare Facilities Management Series, Number 055110, AHA/ASHE.

12) David Y et al (June 1997) EMC: How to Manage the Challenge, Healthcare Facilities Management Series, Number 055144, AHA/ASHE.

13) MDA Bulletin (MDA DB 9702, MDA SN2001 (06): http://www.medical-devices.gov.uk/sn2001(06).htm March 1997

14) MDA update (MDA SN 2001(06): http://www.medical-devices.gov.uk/mda/mdawebsitev2.nsf/webvwSearchResults/37CE5B0D2F6E45C900256A99005B8734?OPEN

15) Silberberg JL (2001) Achieving Medical Device EMC: The Role Of Regulations, Standards, Guidelines, and Publications. Proc 2001 IEEE International Symposium on Electromagnetic Compatibility, p. p. 1298-1307.

16) Irnich et al (1999) Mobile Phones In Hospitals. Biomed Instrum Technol 33:28-34

17) Morrissey et al, Characterization of Electromagnetic Interference of Medical Devices in the Hospital Due To Cell Phones. Health Physics (2002) 82:45-51

18) Barbaro Electromagnetic Interference by GSM Cellular Phones and UHF Radios with Intensive Care and Operating Room Ventilators. Biomedical Instrumentation & Tech (2000) 34:361-369

19) Handa Electromagnetic Interference on Medical Equipment by Low Power Mobile Telecommunication Systems. IEEE Trans Electromagnetic Compatibility (2000) 42:470-475

20) Sibakov and Hietanen Safe Use of Mobile Phones in Hospitals. Health Physics (2000) 79(suppl):S77-S84

21) Bassen HI, Moore HJ, Ruggera PS. Cellular Phone Interference Testing of Implantable Cardiac Defibrillators In Vitro. Pacing Clin Electrophysiol. 1998 Sep;21(9):1709-15.

22) Davis D, Segal B, Pavlasek T. Can Minimum Separation Criteria Ensure Electromagnetic Compatibility in Hospitals? An Experimental Study. Biomed Instrum Technol. 1999 Sep-Oct;33(5):411-6.

23) Sibakov and Hietanen VTT Technical Bulletin (ESPOO 1998)

24) Rice (2000) 2.4 GHz RF LAN EMI in Medical Devices. J. Clin Engineering (Sep/Oct 2000) 260-264

25) Turcott & Witters Biomed Instrum Technol (1998) A Practical Technique for Assessing EMI in the Clinical Setting: Ad Hoc Testing. May-Jun;32(3):241-52

26) Tri et al, Cellular Phone Interference with External Cardiopulmonary Monitoring Devices. Mayo Clinic Procedings (2001) 76:11-15

27) Aki W et al (2002) Influence of Electromagnetic Waves on Portable Electronic Instruments in Medicine [Japanese]. Nippon Hoshasen Gimutsu Gakkai Zasshi [Japanese] 58:948-956

28) Medicine and Health Products Regulatory Agency: http://www.medical-devices.gov.uk/mda/mdawebsitev2.nsf?Open

ELECTROMAGNETIC COMPATIBILITY BETWEEN WiFi ACCESS POINT AND EEG SIGNALS.

KAPARELIOTIS EVANGELOS[1], NANOU ELENA[1], TSIAFAKIS VASILEIOS[1], SOTIRIOU APOSTOLOS[1], PRAGIATIS LAZAROS[1], CAPSALIS CHRISTOS[1]

[1] NATIONAL TECHNICAL UNIVERSITY OF ATHENS, DEPARTMENT OF ELECTRICAL ENGINEERING, DIVISION OF INFORMATION TRANSMISSION SYSTEMS AND MATERIAL TECHNOLOGY, GREECE

9 IROON POLYTECNEIOY STR., ATHENS ,GREECE, 15773, Tel: ++30210-7722574, Fax: ++30210-7723520, email:enanou@mail.ntua.gr

Abstract

In the current work, we study the EMC problem that involves the usage of an electroencefalographer in an environment with electromagnetic radiation produced by a WiFi access point.

The experimental setup was situated in an anechoic chamber so that no electromagnetic interference would affect the measurements. The amplifier room, outside the anechoic room, situated the other part of the experimental apparatus. 32 electrodes entered a low-pass filter placed at the boundary wall of the Faraday screen room. The signal was amplified, before entering a 32-bit analog to digital converter. The recording frequency was at 1 kHz.

The wireless access point operated at the typical frequency band of 2.4 – 2.4835 GHz and the maximum EIRP allowed in Europe that is 100mW. The distance of the access point to the electroencephalographer was 10cm. Two sets of measurements were performed. One with measuring the noise of the system and the other with the WiFi transmitter switched on.

The results showed that there was no interference of the WiFi Access point to the measured signals. This is of great importance because of the great expansion of wireless technology.

Introduction

Since the early 1990s, reports of medical device failure from electromagnetic interference have increased [1, 2]. This is due to several factors. The number of electronically controlled medical devices has burgeoned in hospitals and other medical facilities. The modern instruments are often more sensitive to electromagnetic interference (EMI) because they incorporate low power integrated electronic circuitry that can be much more sensitive to electromagnetic fields than their electrical and electromechanical predecessors. Digital wireless communications systems often utilize pulsed amplitude modulation, a type of modulation that can enhance the potential for EMI.

The European Union has gotten much of attention with regard to the regulation of electromagnetic compatibility (EMC) and medical electronics. Today, most medical EMC regulations originate within the International Electro technical Commission (IEC). The standard EN60601-1-2 [5] defines limits for emissions and levels of immunity and was updated to encompass the frequencies used by mobile phones and other communication technologies such as wireless local area networks (WLAN). The IEC standard states that electronic medical equipment must operate normally in electric field intensity of 3 V/m and at a 10 V/m threshold for life – sustaining equipment.

The Electroencephalograph (EEG) is a recording equipment of brain signals with typical voltage of 100 μV and frequency range (EEG bands) 0.5 Hz up to several hundreds Hz. The EEG is connected directly to the patient in order to detect these small physiological signals which are then amplified. The EEG is known to be very sensitive to EMI due to the fact that the pulsed RF signals maybe demodulated by non-linear elements in amplifier circuits. [Robinson 2003]. Morrisey et al. reported distortion of EEG bands throughout the 0-70 Hz range during full power exposure to CDMA and GSM signals for both frequencies of 1.800 and 1900 MHz at distances of between 0.25 to 0.5 m.[Morrisey 2002].

Wireless Local Area Networks (WLANs) in a hospital typically consist of multiple antenna sites (known as base stations) interspersed throughout the hospital building that connect to a central “hub” or “router” unit. This latter unit connects the WLAN with the wired hospital network. WLANs transmit and receive signals with various handheld devices (or laptop computers, etc) as these devices roam throughout the coverage net work in the building. WLANs typically use the 802.11 standards that operate on frequencies around 2.45 GHz and 5.8 GHz. The handheld devices are not power controlled, but transmit at a very low constant power (on the order of 1-10 milliwatts) as they are designed to never be very far away from the nearest network node. As a consequence, the likelihood of electromagnetic interference of W LANs with critical and life support medical equipment is very small, since they transmit at power levels t hat are well below the IEC recommended levels. The WLAN base stations transmit at a higher power level (typically around 500 mW), which increases the chances for electromagnetic interference. Research by [13] revealed that peak values of such base stations often exceed the critical 10V/m field strength value.

Taking into account the above considerations, in our current work, we study the EMC status that involves the usage of an electroencefalograph in an environment infested with electromagnetic radiation produced by a WiFi Access Point. The purpose is to observe the effects of the WiFi signal on the EEG signal.

Materials and Methods

The experimental setup (Fig 1) was situated in a Faraday chamber so that no electromagnetic interference would affect the measurements. A head phantom was placed in the chamber and the signals were recorded from thirty two electrodes (Fp1, Fp2, Fpz, AFz, F2, F3, F4, F7, F8, FC1, FC2, FC5, FC6, C2, C3, C4, A1, A2, CP1, CP2, CP5, CP6, P3, P4, Pz, T3, T4, T5, T6, O1, O2,Oz) with a surface of Ag/ AgCl, which were placed on the scalp of the model-head. The electrodes were positioned according to the International 10-20 system of electroencephalography [8]. The measured magnitude was the voltage at the edges of a 2 kΩ resistance placed between each electrode and a common ground. The total electrode impedances were below 5 kΩ. The amplifier room, outside the Faraday room, situated the other part of the experimental apparatus. The electrodes entered a low-pass filter placed at the boundary wall of the Faraday screen room. The filter cut frequencies over 35 Hz so that the signal of the power supply network which is at 50 Hz would not interfere with the signal. The signal was amplified by a Braintronics DIFF/ISO-1032 amplifier, before entering a 32- bit analogue to digital converter (NI SCB-68) which has a GPIB output. The digitized signal comprises an input for a Data Acquisition Card (32 bit NI 6035E DAQ Card). The PC with the DAQ Card ran a LabView program for the recording of the signals, which can be monitored by an on-screen graphical representation. The recording frequency was at 1

kHz. Another PC, connected with the one described above, ran a program which triggered the other PC to save the brain signals whenever the user wanted .The recording time was 1.5 sec so the saved signal consisted of 1500 values. The total task consisted of 55 repetitions.

The WiFi Access Point was placed in the Faraday room and made a link with a laptop that was inside the room. The WiFi signal was radiated by a dual dipole antenna,, with 20dBm power and QPSK modulation. The Access Point was placed at a distance of 1m from the head.

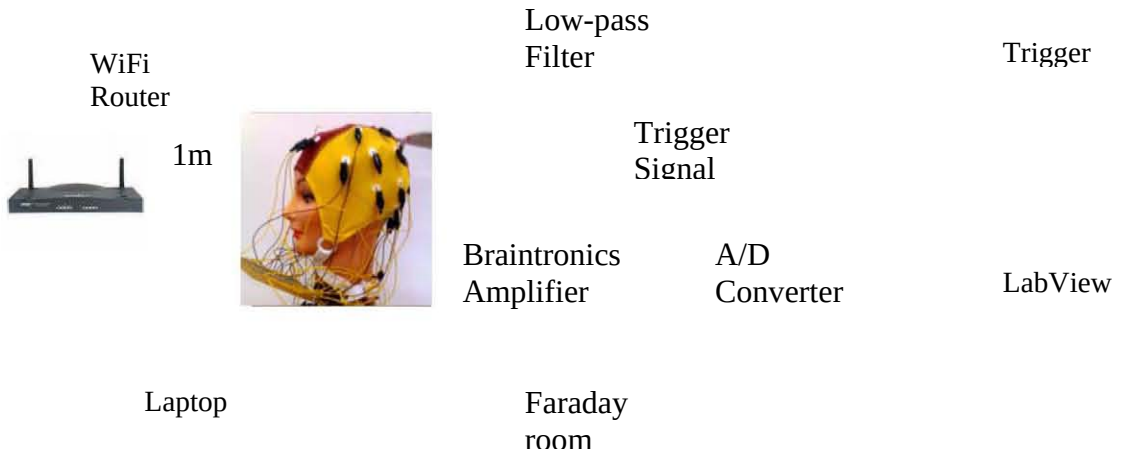


Figure1. Experimental Setup

The experimental procedure was done twice. The first time the WiFi Access Point was off and practically the noise of the device was measured and the second time the WiFi was functioning.

Regarding the collected data analysis, in order to optimize the signal to noise ratio (SNR) the grand average across the 55 repetitions for each channel was calculated according to the following equation:

$$\overline{V}_t = \frac{1}{55} * \sum_{j=1}^{55} V_{jt}$$

Where Vjt is the value that results after the subtraction of the amplification and the average referencing and corresponds at the time t of the trial j. This SNR optimization procedure is considered a standard practice when it comes to brain signal measurements, which are generally considered to be quite noisy. (Roth et al., 1995, pp.805-910)

The final data for analysis for each EMF condition consisted of 1500 amplitude values for each electrode, expressed in μVolts corresponding to the 1500 msec of the time period as described above.

For each electrode, the following magnitudes were also calculated:

- the energy E of the recorded signals ($E=V_t^2$)
- the amplitude in the frequency domain by using the Fourier Transform (FFT).

Data analysis

The differences between the values of the energy at the two EMF conditions were calculated for each of the thirty two leads. The data were also compared to real EEG recordings at certain representative electrodes. The mean values and the standard deviations of the final data were calculated for each group (WiFi Off, WiFi On, EEG) at these electrodes.

Results

The data analysis revealed that the maximum difference between the values of the signal energies for each EMF was 0.7 Joules with the exception of T5 electrode, which is a small value if compared with the energy values. Figure 1 is quite helpful in explaining this fact. The white bars denote the calculated energy in the absence of the WiFi signal while the black bars denote the signal energy in the presence of the WiFi signal.

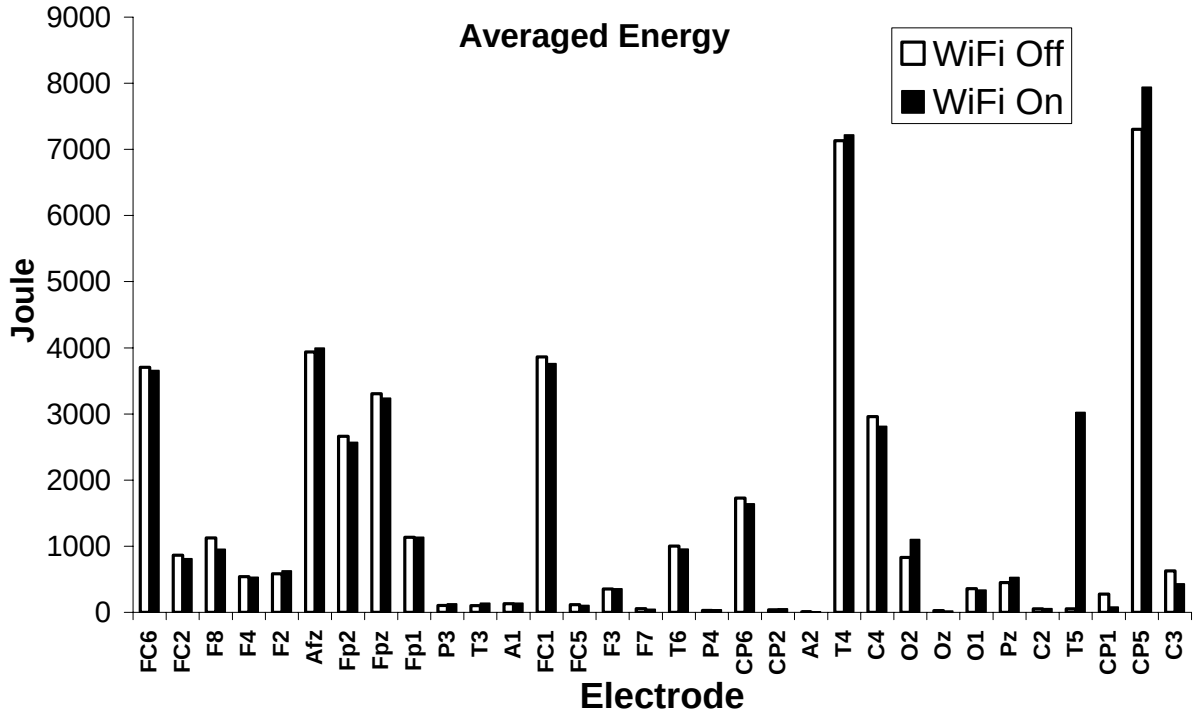


Figure 2. Averaged Energy at each electrode and each radiation condition. . The white bars denote the calculated energy in the absence of the WiFi signal while the black bars denote the signal energy in the presence of the WiFi signal.

Table 1 shows the mean values and the standard deviations at some representative electrodes, of the three groups of data at different conditions: absence of WiFi Signal, presence of the WiFi signal and EEG recordings. It is notable that the mean values and the standard deviations for the first two cases (WiFi Off, WiFi On) are very similar. The comparison of these values to the respective values of the data that come from human measurements reveals great variation.

	Mean Values			SD		
Electrode	**WiFi Off (Noise)**	**WIFi On**	**Human**	**WiFi Off (Noise)**	**WiFi**	**Human**
F4	-0.59	-0.59	-0.27	0.08	0.10	2.58
Fz	-0.62	-0.64	-1.37	0.09	0.11	2.91
Fp2	1.33	1.30	-1.61	0.11	0.11	3.14
Fp1	-0.86	-0.86	-1.37	0.09	0.12	3.45
P3	0.25	0.28	2.65	0.08	0.10	3.01
F3	0.48	0.48	-0.52	0.09	0.09	2.74
P4	-0.06	-0.12	2.33	0.12	0.11	2.89
C4	-1.40	-1.36	0.95	0.14	0.12	3.00
O2	-0.74	-0.73	2.97	0.09	0.45	2.89
O1	-0.48	-0.46	1.52	0.09	0.11	2.05
Pz	0.54	0.58	2.87	0.12	0.12	3.54
C3	-0.63	-0.52	2.02	0.14	0.14	3.35

Table1. Mean values and standard deviations for three conditions (WiFi Off, WiFi On, EEG) at a number of electrodes

Figure 3 is a representative diagram of the grand averaged amplitudes during a recording period for the three experimental conditions at the electrode O1. The diagram helps in realising the considerable variation of the EEG data .

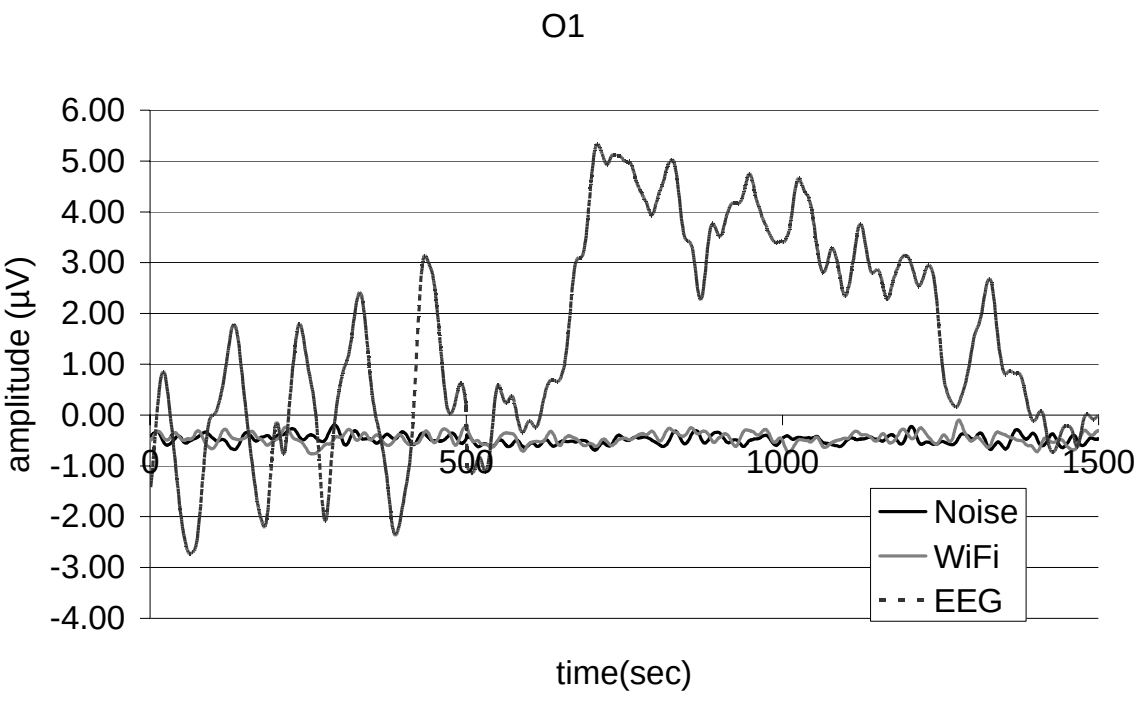


Figure 3. Grand averaged amplitudes for the three experimental conditions at the electrode O1

Discussion

From the data analysis and the results which aroused, there is no evidence that a WiFi signal at a distance of 1m from EEG electrodes causes interference at the EEG recordings. WiFi is a low power protocol that has flexible power settings and can be deployed in various conditions in order to ensure that all radiation is well within the limits set even by the most strict hospital authority. Other tests [14] indicate that not only WiFi shows no interference to medical equipment but has the edge when compared to other wireless technologies. Wireless communication is a promising opportunity for future medical systems in the hospital. Today's wireless standards with moderate output power represents no real danger for the operation of medical equipment [14] and seems to be suitable for medical environment even with several wireless devices used simultaneously. The various applications that hospitals can create through the use of WiFi in a quick and cost effective fashion have been the subject of many a discussions, wireless patient monitoring in steady state [15] or in IC units or in OR units [14,16] is an application of great importance that will greatly improve the working conditions of the staff but moreover it will make the care of patients more efficient. Even though the results indicate that there is more tests are no interference between EEG and WiFi we need to investigate further in order to verify the suitability and assure the reliability of WiFi communication in medical equipment of any sort.

References

1. Silberberg JL: Performance degradation of electronic medical devices due to electromagnetic interference. Compliance Eng 10(5):25-39, 1993.

2. Joyner K, Anderson V, Wood M: Interference and energy deposition rates from digital mobile phones. In: Abstracts Annual Meeting of the Bioelectromagnetics Society 16:67-68, 1994

3. Silberberg JL: Medical device electromagnetic interference issues, problem reports, standards, and recommendations. In: Proc Health Canada Medical Devices Bureau Round-Table Discussion on Electromagnetic Compatibility in Health Care, Ottawa, Canada, pp. 11-20, 1994.

4. Segal B, Skulic B, Liu-Hinz C, Retfalvi S, Lorange M, Pavlasek T: Preliminary study of critical-care medical device susceptibility to portable radiofrequency sources. In: Proc Annual Meeting and Exposition of the Association for the Advancement of Medical Instrumentation 13:83, 1995.

5. International Electrotechnical Commission, "IEC 60601-1-2, Medical Electrical Equipment Part 1: General Requirements for Safety, Amendment No. 2. Collateral Standard: Electromagnetic Compatibility—Requirements and Tests," 1st ed., Geneva, 1993.

6. Barbaro V, Bartolini P, Militello C, Altamura G, Ammirati F, Santini M: Do European GSM mobile phones pose a potential risk to pacemaker patients: Invitro observations. PACE 18(6):1218- 1224, 1995.

7. Joyner, K., Wood, M., Burwood, E., Allison, D., Strange, R: Interference to Hearing Aids by the New Digital Mobile Telephone System, Global System for Mobile (GSM) Communications Standard. National Acoustic Laboratories, Australian Hearing Services, Sydney Australia, 1993.

8. Jasper H. The ten-twenty electrode system of the international federation. Electroencephalogr Clin Neurophysiol, 1958

9. S Kirk, "Designing Medical Equipment for Electromagnetic Compatibility," Medical Device Technology 3, no. 4 (1992): 42-49.

10. D Davis, B Segal, and T Pavlasek, "Can Minimum Separation Ensure Electromagnetic Compatibility in Hospitals? An Experimental Study," Biomedical Instrumentation and Technology/Association for the Advancement of Medical Instrumentation 33, no. 5 (1999): 411- 416.

11. S Kirk, "Solving Electromagnetic Problems in Medical Equipment," Medical Device Technology 3, no. 1 (1992): 27-30

12. Roth, W.T., Ford, J.M., Pfefferbaum, A. and Elbert, T.R. Methodological issues in event-related potential and magnetic field studies. Chapter 78 in Psychopharmacology: The Fourth Generation of

Progress, F.E. Bloom and D.J. Kupfer (Eds.), pp. 895-910. New York, NY: Raven Press, 1995

13. Rice, WP 2.4 GHz RF WLAN EMI in medical devices. J. Clin. Engineering(Sept/Oct) 2000: 260-264

14. Jan Olav Høgetveit, Ilangko Balasingham, Karl Øyri, Øystein Jensen The 3rd European Medical and Biological Engineering Conference: Introducing Multiple Wireless Connections To The Operating Room, Interference Or Not?

15. WLAN-based, indoor medical residents positioning system Ke Yu; Chen, J.; Refai, H.H.;Wireless and Optical Communications Networks, 2005. WOCN 2005. Second IFIP International Conference on 6-8 March 2005 Page(s):556 - 560 Digital Object Identifier 10.1109/WOCN.2005.1436088

16. Patient's data browsing in wireless LAN in TELEMEDIK Kundu, S.; Mukherjee, J.; Majumdar, A.K.; Personal Wireless Communications, 2005. ICPWC 2005. 2005 IEEE International Conference on 23-25 Jan. 2005 Page(s):272 - 275 Digital Object Identifier 10.1109/ICPWC.2005.1431347

LACK OF PROMOTING EFFECTS OF CHRONIC EXPOSURE TO 1.95-GHZ W-CDMA SIGNALS FOR MIT-2000 CELLULAR SYSTEM ON DEVELOPMENT OF N-ETHYLNITROSOUREA-INDUCED CENTRAL NERVOUS SYSTEM TUMORS IN F344 RATS

TOMOYUKI SHIRAI[1*], TOSHIO ICHIHARA[2], KANAKO WAKE[3], SO-ICHI WATANABE[3], YUKIO YAMANAKA[3], MAYUMI KAWABE[2], MASAO TAKI[4], OSAMU FUJIWARA[5], JIANQING WANG[6], SATORU TAKAHASHI[1]AND SEIKO TAMANO[2]

[1]DEPARTMENT OF EXPERIMENTAL PATHOLOGY AND TUMOR BIOLOGY, NAGOYA CITY UNIVERSITY GRADUATE SCHOOL OF MEDICAL SCIENCES, NAGOYA 467-8601, JAPAN.E-mail: tshirai@med.nagoya-cu.ac.jp
[2]DIMS INSTITUTE OF MEDICAL SCIENCE, INC, ICHINOMIYA, AICHI, JAPAN
[3]COMMUNICATIONS RESEARCH LABORATORY, TOKYO, JAPAN
[4]DEPARTMENT OF ELECTRICAL AND ELECTRONIC ENGINEERING, TOKYO METROPOLITAN UNIVERSITY, TOKYO, JAPAN
[5]DEPARTMENT OF ELECTRICAL AND COMPUTER ENGINEERING, NAGOYA INSTITUTE OF TECHNOLOGY, NAGOYA, JAPAN
[6]DEPARTMENT OF COMPUTER SCIENCE AND ENGINEERING, NAGOYA INSTITUTE OF TECHNOLOGY, NAGOYA, JAPAN

ABSTRACT

The present study was performed to evaluate effects of a 2-year exposure to an electromagnetic near-field (EMF) equivalent to that generated by cellular phones on tumor development in the central nervous system (CNS) of rats which were born from ENU-treated F344 mother rats. A total of 500 pups were divided into 5 groups, each composed of 50 males and 50 females. A 1.95 GHz W-CDMA signal for IMT-2000, was used for the exposure of the rat head starting from 5 weeks of age, 90 min a day, 5 days a week, for 104 weeks. Brain average specific absorption rate (SAR) was designed to be 0.67 and 2.0 W/kg for low and high exposures, respectively. Whole-body average SAR was less than 0.4 W/kg. The incidence and number of brain tumors in female rats exposed to 1.95 GHz EMF had a tendency to be increased but there was no statistical significance. Overall, no increase in their incidences or numbers per group, either in the males or females, was detected in the EMF-exposed groups. Thus, under the present experimental conditions, 1.95 GHz W-CDMA signal for IMT-2000 exposure to the heads of rats for a 2-year period did not accelerate or affect ENU-initiated brain tumorigenesis.

INTRODUCTION

Since there is serious concern that exposure to an electromagnetic field (EMF) due to cellular phones is associated with an increase risk of disease such as brain dysfunction and/or brain tumor development, many epidemiological and experimental research studies to explore this possibility. However, none of epidemiological studies revealed a clear association between exposure to EMF and development of brain tumors. Furthermore, none-of 5 long-term (2-year period) animal experiments which had been performed demonstrated the presence of association of exposure to time-division multiple access (TDMA) or frequency-modulated signals with tumor development in the central nervous system of rats. Recently we also conducted a 2-year EMF exposure experiment in an ENU-exposed rat model with a 1.439-GHz TDMA signal for the Personal Digital Cellular (PDC), Japanese standard cellular system at brain average specific absorption rates (SARs) of 0.67 and 2.0 W/kg for low and high exposures. The results disclosed no inter-group differences in body weights, food

consumption, or survival rates and no increase in the brain and spinal tumor incidences or numbers per group, either in males or females of the EMF-exposed groups [Shirai, et al. 2005].

Recently the International Telecommunication Union (ITU) has introduced the new mobile telecommunication system, i.e., International Mobile Telecommunication 2000 (IMT-2000) which has also been named the 3rd generation (3G). The wide-band code division multiple access (W-CDMA) is also termed the Universal Mobile Telecommunication System (UMTS) in the EU. The first IMT-2000 service was started in Japan in 2001. This service, the freedom of mobile multimedia access (FOMA) by NTT DoCoMo, uses W-CDMA signals and the 1.95 GHz region for up-links and the 2.14 GHz region for down links. The number of subscribers to the W-CDMA system in Japan was about 28 million in April 2006 while that to the TDMA systems was about 41 million. Because the number of W-CDMA users is rapidly increasing, this type of signal will probably become the most major digital signal for the Japanese general public in near future.

Therefore, the present study was designed as a first long-term investigation of effects of chronic exposure to 1.95-GHz W-CDMA signals for MIT-2000 cellular system on development of ENU-induced CNS tumors in F344 rats. It was conducted in compliance with the Good Laboratory Practice (GLP) Standards of the Japanese Ministry of Health and Welfare Ordinance No, 21. This is the first experimental result on a long-term effects of MIT-2000 cellular system on development of central nervous system tumors.

MATERIALS AND METHODS

A total of 100 pregnant F344 rats were purchased from Charles River Japan (Atsugi, Kanagawa Japan) and given a single intravenous administration of ENU on gestational day 18. ENU (Nacalai Tesque Tokyo, Japan) was dissolved in physiological saline for this purpose and injected into the tail vein at a dose of 4 mg/ml/kg body weight. ENU-exposed pups of both sexes were allocated to 4 groups, each composed of 50 females and 50 males. Pups (50 males and 50 females) from mothers that received the vehicle instead of ENU served as complete controls. Dummy animals were used to cover any vacancy in EMF exposure boxes due to interim death to maintain the exposure conditions unchanged. All animals were allowed free access to pelleted diet and drinking water.

The rats in Groups 1 to 5 were exposed to EMF; Group 1 was a complete control without any treatment. Group 2 received ENU alone and was kept in cages throughout the experiment. Group 3 was given ENU set in exposure boxes in the same manner as in Groups 4 and 5 but with no actual exposure to EMF (sham exposure group). Groups 4 and 5, given ENU, then were exposed to EMF at low (SAR: 0.67 W/kg) and high (SAR: 2.0 W/kg) levels, respectively.

The exposure box was 90 x 90 x 60 cm. Ten rats fixed individually in plastic tubes were set on disk-shaped plates like a carousel with the nose pointing to the center. Each plate was 65 cm in diameter, with adjustable height supported by a center hollow cylinder pole. A resonant monopole antenna for 1.95 GHz was set from the ceiling of the exposure box in order to fit in the center of the disk-shaped plate. The distance between the antenna and each rat nose was set at 30 mm.

A 1.95-GHz W-CDMA signal from Cellular Phones for MIT-2000 Cellular system was applied. Long-term intermittent exposure to the heads of the rats (90 min a day, 5 days a week, Monday through Friday) was started at 5 weeks of age and continued for 104 weeks. All exposures including sham exposure were controlled with the assistance of a computer system. If the number of rats became less than 10 in an exposure box due to loss through mortality, dummy rats were used to maintain the symmetrical arrangement of animals and the scheduled specific absorption rate (SAR) of EMF exposure.

SAR distributions in rats were evaluated by numerical dosimetry with the Finite Difference Time Domain method (FDTD). Brain average SAR was set at levels, 0.67 and 2.0 W/kg, respectively. Whole-body average SAR averaged over the 2-year experimental period was limited within lower level which cannot cause any thermal effects; the highest whole-body averaged SAR was 0.464 W/kg which is much lower than 4 W/kg, the threshold for thermal effects.

All surviving animals after the 104 week-exposure to EMF were killed under light anesthesia with ethyl ether and aorta blood was collected from all rats for hematology analysis, before a complete autopsy was performed. Organ weights were measured for the brain, heart, liver, kidney, spleen, pituitary gland, adrenal glands, testes and ovaries. All organs including the CNS and macroscopically observable lesions were fixed in 10% buffered formalin routinely processed for embedding in paraffin and sections (4 m thickness) were stained with H & E for histological examination. Rats that died or became moribund during the experiment were also autopsied.

RESULTS

There were no significant differences in growth rates between rats receiving maternal ENU and untreated controls (Group 1) in either males or females. Restraint of rats in the plastic holders in the exposure

boxes itself suppressed growth, particularly in the males, but this suppression was not exacerbated by actual EMF exposure. No significant inter-group differences in survival rates were observed in either sex. No clear increase in death rates with EMF exposure was observed in males or females. There were no significant differences in food consumption among groups throughout the experiment in either the females or the males. There were no inter-group differences in the relative organ weights of the brain, heart, liver, kidney, spleen pituitary gland, adrenal glands and testes or ovaries.

In this study, one CNS tumor was also observed in a female not receiving ENU. The lesions were astrocytomas, oligodendrogliomas, mixed gliomas, ependymomas, meningiomas, granular cell tumors and malignant reticulosis. The major type was the astrocytoma. The incidences of brain tumors in the females ranged from 2 to 22% and the numbers of rats ranged from 1 to 11. The incidences and numbers of brain tumors were very similar in males and females. While values in female rats exposed to 1.95-GHz W-CDMA signals for IMT-2000 had a tendency to be increased, this was no statistical significant. Spinal cord tumors were sporadically found in the males but not the females. There were no statistically significant differences in CNS tumors in males among the groups given ENU. Thus, the data for both sexes indicate that EMF does not accelerate ENU-initiated CNS tumor development.

Besides CNS tumors, sporadic tumors were noted in other organs/tissues. Among these tumors, skin fibromas and large granular lymphocytic leukemia were less frequent in the EMF exposed males and there was a statistical significance between sham exposed and the high dose EMF group at $p<0.05$.

DISCUSSION

In the literature, there are conflicting epidemiological data regarding the risk of EMF exposure for brain tumor development; some demonstrating very small association between workers in electrical industry and in the US Air Force population and brain tumors. However, there are five recent epidemiological studies that did not demonstrate any association between cellular telephone use and brain tumor risk.

With such conflicting epidemiological data, long-term animal experiments are essential for scientific evaluation of the risk of EMF with reference to brain tumor development. Four animal studies specifically targeting this question had already been performed prior to the present work. Neither 2-year animal bioassays with digital nor frequency-modulated signals found any detrimental effects of EMF exposure after intrauterine administration of ENU. A similar experiment with Sprague-Dawley rats carried out by others resulted in no initiation or promotion of brain tumors by any of the RF fields tested. Our group also previously conducted a long-term exposure animal experiment with intrauterine treatment with ENU for brain tumor initiation and we concluded that exposure to 1.439-GHz TDMA signal for 1.5 h/day, 5 days for 2-year period, did not accelerate ENU-initiated CNS tumor development in rats.

The present experimental design with 1.95GHz W-CDMA signals for IMT-2000 cellular system was also planned by the Committee of the Study on Human Exposure to EMF in Japan established in 1997 with the aim of scientifically clarifying any effects of radio waves from mobile telephone terminals on the human body. The whole body average SAR was limited as far as possible in order to avoid significant thermal stress and was less than 0.464 W/Kg. In the present experiment, there were no statistically significant inter-group differences in the incidences of CNS tumors in either males or females initiated with ENU although there was a tendency of slight increase in brain tumor development in the females exposed to EMF. No increase in spinal tumor development by EMF exposure was observed in either sex. Furthermore, development of tumors in organs other than CNS was not enhanced. Thus, it can be stated that the present data demonstrate that 1.95-GHz W-CDMA signals for IMT-2000 Japanese cellular system at a brain average SAR of 0.67 or 2.0W/kg for 2 years do not possess promotion potential for ENU-initiated CNS tumor development in either sex of F344 rats. In our previous study with 1.439 GHz TDMA signal, the incidences of pituitary tumor in both sexes received ENU showed a tendency for increase, but were clearly suppressed by 2.0 W/kg EMF, with statistical significance in males. However, such increase by ENU and suppression by EMF were not evident in the present study. Since the increase of pituitary tumor development in EMU-treated animals was concluded to be within the wide range of background data, the present data for pituitary tumor incidence seem reasonable.

In conclusion, the present large scale 2-year exposure experiment to 1.95GHz W-CDMA signals for IMT-2000 cellular system demonstrated that EMF at brain average SAR of 0.67 or 2.0W/kg does not promote ENU-induced rat brain carcinogenesis, providing additional evidence in support of no association between EMF and brain tumor risk in man.

Acknowledgement

This work was supported by a Grant from the Ministry of Internal Affairs and Communications, Japan

ORDER CHANGES IN CELL MEMBRANE INDUCED BY APPLIED ELECTROMAGNETIC FIELD

E. KOVACS[1], T. SAVOPOL[1], D. MARTIN[2], N. IACOB[2], M. MOISESCU [1]

[1]Biophysics and Cell Biotechnology Dept., « Carol Davila » Medical University, P.O. Box 35-43, 050461 Bucharest, Romania,
[2]National Institute for Lasers, Plasma and Radiation Physics

Abstract

Changes in membrane order are known to alter the function of integral proteins. Consequently, microwave induced changes of membrane lipid order may have physiological implications. The detailed biophysical mechanisms for these effects are not currently available and experiments on in vitro models are expected to offer the keys to understanding the nature of microwaves non-thermal and windowed effects.
We studied the changes in membrane fluidity (fluorescence depolarization) and generalized polarization of human platelets extracted from freshly donated blood, induced by irradiation with 2.45 GHz microwaves, CW at 24 mW incident power, SAR 10 W/kg. The experimental arrangement consisted mainly in a 2.45 GHz generator of adjustable output power in the range of 0 – 30 mW and a modified conventional coaxial probe used for two functions: as impedance matching device and as microwave (MW) irradiating antenna. Irradiation of samples during fluorescence anisotropy and generalized polarization records was made by introducing the antenna into the fluorometric cuvette. Changes of the same membrane parameters of a liposome suspension irradiated by microwaves was performed in order to have as reference a simple lipid bilayer, consisting of a single type of lipids.
Studies of membrane phase-transition temperature and other physical and chemical parameters lead to the conclusion that the liposome and platelet membranes, whose isothermal electric susceptibility is dramatically increased around phase-transition temperature, undergo order changes by interacting with oscillating electromagnetic field; these are reflected in the observed shift of the phase transition temperature of the microwave exposed liposomes comparatively to the sham exposed samples as well as in the higher values of generalized polarization (GP) of the cell/liposome membrane.
Membrane dipolar components such as polar amino acid side chains and cell membrane associated bound water which undergo orientation resulting in rotational motions with an associated time constant similar to the wave number of the impressed oscillating electromagnetic field, are the most probable targets which trigger the observed membrane order changes.

Introduction

Decades of experimental and theoretical research stay behind the attempts to reveal and account for the observed biological effects of RF and microwaves. Despite the investment of creativity, funds and hard work, few sound statements and facts concerning the specific interaction of microwaves with living structures/cells are available.
In our work, we choose simple phenomena and biological models in the attempt to dissociate the specific microwave interaction with the substrate from the non-specific thermal effect; the assumption is that while a great part of incident microwaves energy is dissipated as heat, the other part is absorbed resonantly by specific structures accounting for non-thermal "biological effects".
Two phenomena were chosen to analyse the specific interaction mechanisms.
1/The changes of *lipid packing* in *membrane bilayer* potentially induced by microwaves and formally reflected in a fluorescent marker mobility and in critical events accompanying the phase transition of the lipid bilayer. These changes would shift the temperature dependence curves and phase transition temperature in irradiated versus control samples as shown by fluorescence depolarization recordings.
2/ The change in *generalized membrane polarizability* induced by microwave application which must be reflected in fluorescent emission of Laurdan – a fluorescent dye, sensitive to polarization of hydrophilic environment within the lipid bilayer.

Method and results

Fluorescence depolarization

Fluorescence depolarization measurements of a membrane fluorescent marker (TMA-DPH in our case) provide information about the rigidity of lipid tails packing around the site of marker insertion. As higher is fluorescence anisotropy (r) as less fluid may be considered the membrane in the region of marker insertion (in case of TMA-DPH, below the polar heads in the outer lipid layer). A lipid bilayer is characterized by a specific phase – transition temperature, when it switches from a gel-like organization (lipid packing) to a liquid-crystalline organization, when lipid packing is looser (more fluid). The degree of looseness of lipid packing is critical for many membrane functions which rely on protein conformational changes within or across the membrane. It is considered that subtle conformational changes of proteins which occur along the signal transduction pathways may be hindered under low level microwave irradiation although no plausible physical mechanism for explaining this effect is yet available.

Here we use a simple model of lipid bilayer, *the liposome membrane*, to check if lipid packing is influenced by microwave irradiation. The fluorescence marker used is a TMA-DPH molecule.

1-[4-(trimethylammonium)phenyl]-1,3,5-hexatriene (TMA-DPH)

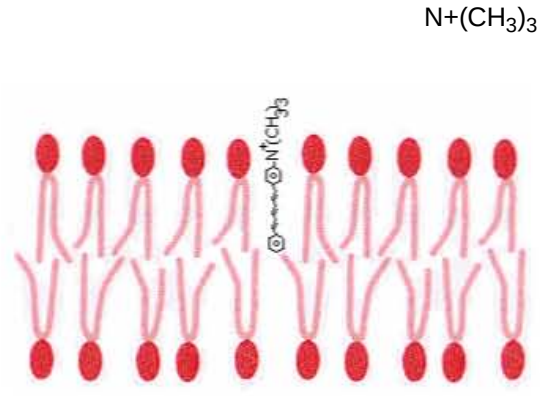


Fig. 1 The insertion of the fluorescent probe (TMA- DPH) in the lipid bilayer

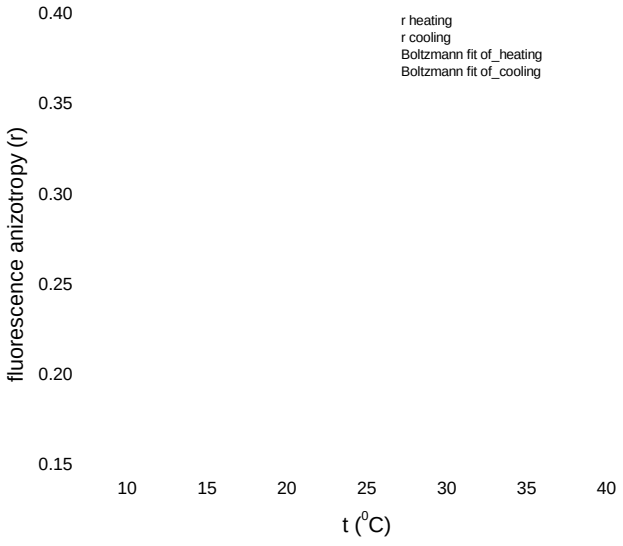


Fig.2 Fluorescence anisotropy of 1,2-dimyristoyl-sn-glycero-3-phosphocholine (DMPC) liposomes recorded versus temperature increase (red squares) and temperature decrease (black squares). The sigmoid fit of the experimental curves indicate a phase transition around 23 ^{o}C.

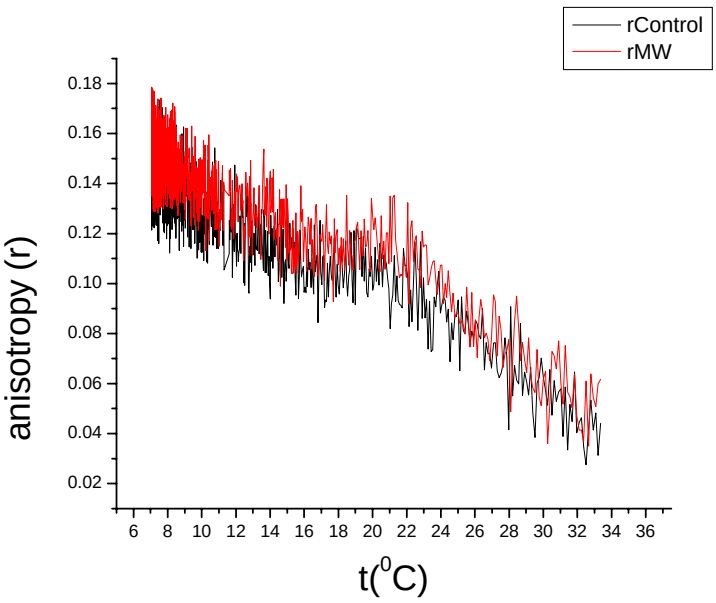


Fig.3 Fluorescence anisotropy of 1,2-dimyristoyl-sn-glycero-3-phosphocholine (DMPC) liposomes recorded versus temperature increase induced by thermostate (black) and microwave heating (red).

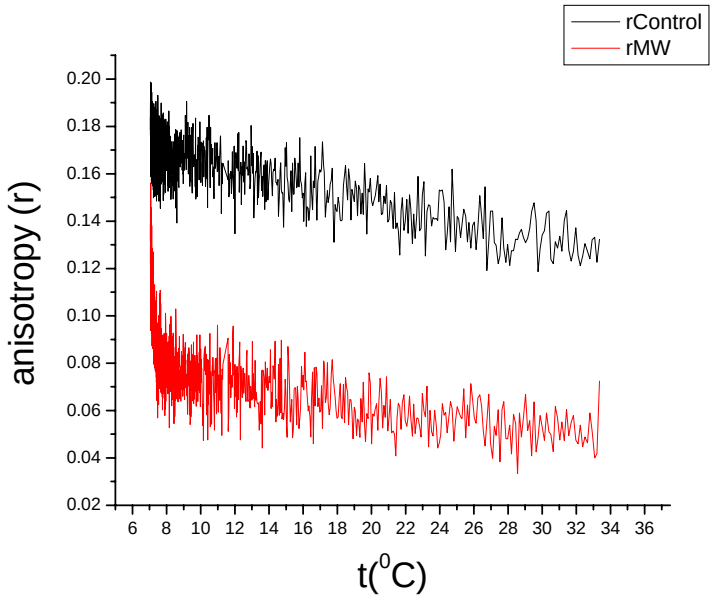
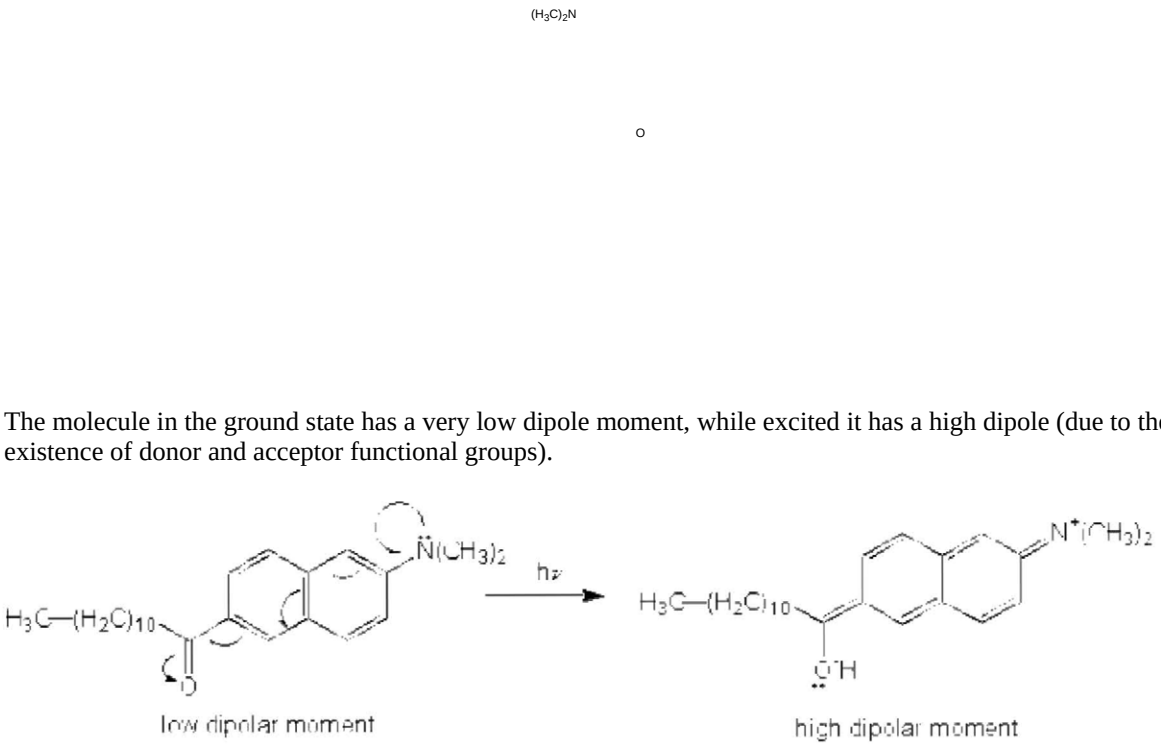


Fig.4 Fluorescence anisotropy of human platelet membranes vs. temperature increase at thermostate (black) and microwave (red) heating

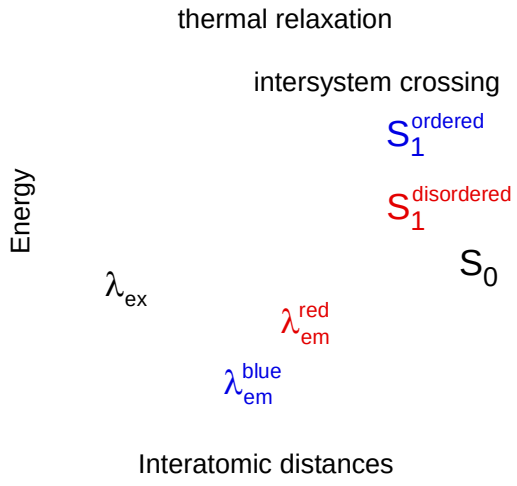
Generalized polarization (GP)

Laurdan (6-dodecanoyl-2-(dimethylamino)-naphthalene) is a fluorescent dye which spontaneously incorporates into phospholipid membranes due to its long hydrophobic tail, as shown in the scheme below:



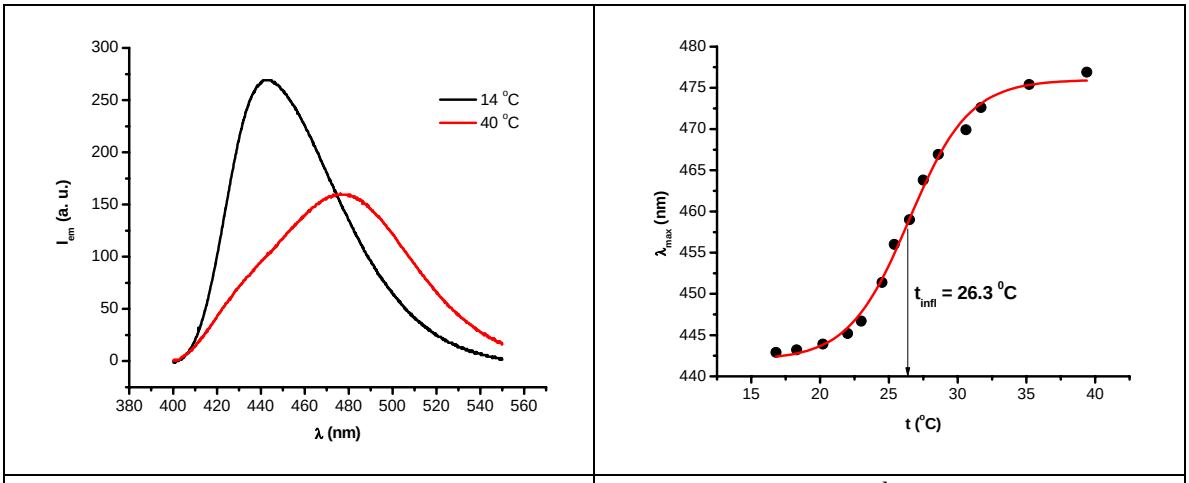
The molecule in the ground state has a very low dipole moment, while excited it has a high dipole (due to the existence of donor and acceptor functional groups).

When the membrane contains dipolar molecules (e.g. water), these molecules will strongly interact with the excited form of Laurdan, shifting its emission spectrum toward lower energies (higher wavelengths), because part of the excitation energy is dissipated in the reorientation process. This phenomenon is illustrated in the diagram bellow:



In MW fields, the permanent dipoles of water are supposed to align along the electric field lines. This “ordering” phenomenon of the molecules inside the membrane will hinder the energy transfer process between the excited molecules of Laurdan and the surrounding water molecules, compared with the same process in a non-irradiated sample. Thus, when heating a sample, the profiles of the plots representing the emission maxima position vs. temperature, will depend on the heating procedure (“thermal” or by MW irradiation).

In the case of simple membranes, containing one single component, like liposomes, the plot of λ_{max} vs. temperature has an S-shaped aspect, showing a quite sharp inflexion point corresponding to the phase transition temperature of the phospholipid used for liposomes preparation.



a b

Fig.5 Modification of emission spectra of Laurdan in 1,2-dimyristoyl-sn-glycero-3-phosphocholine (DMPC) liposomes, induced by "thermal" heating. a) Aspect of emission spectra at two extreme temperatures (14 and 40 °C); b) Shift of the emission maxima as a function of temperature.

As concerns the generalized polarization, it depends on the temperature in the same S-shaped way as the emission maxima, but in a less well defined manner, presenting the inflexion point at approximately the same temperature:

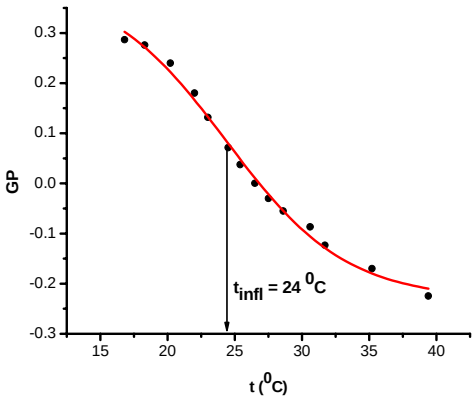


Fig.6 The temperature dependence of generalized polarization. The difference between the values of the inflexion point as determined by GP and λ_{max} lays within the standard error of the two computation methods

When the same heating is performed by applying MW, the corresponding plot looks like:

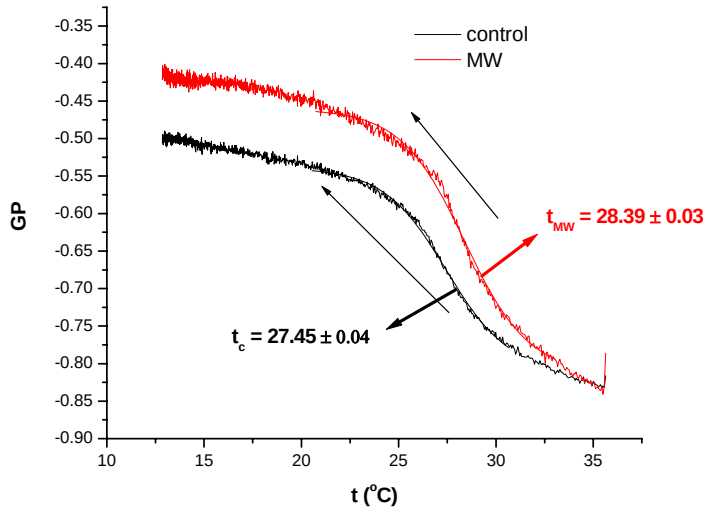


Fig.7 General polarization of DMPC liposome suspension cooled in the presence (red curve) and the absence (black curve) microwave irradiation (SAR 10mW/g).

Containing cholesterol and many other lipidic or non-lipidic components, many cell membranes do not elicit a clear critical temperature of phase transition, the different phases coexisting in various proportions. In the figure below, the record of GP at warming and cooling of platelets suspension in the absence of MW irradiation is shown.

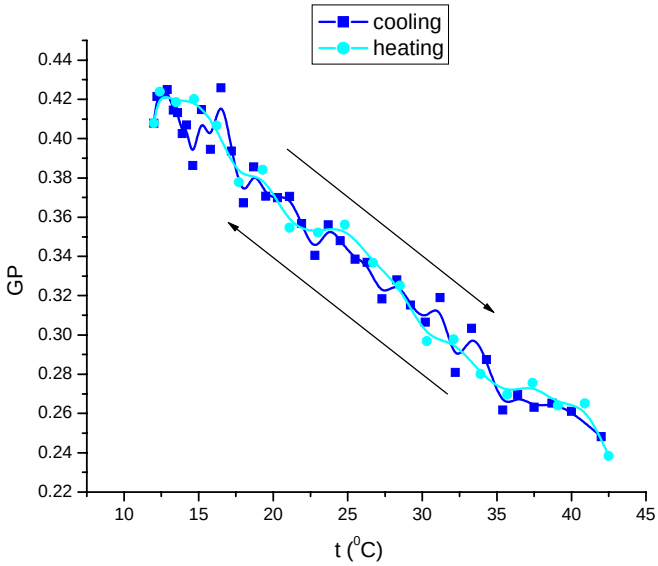


Fig.8 General polarization of human platelets suspension in HBBS buffer as evaluated by Laurdan fluorescence. No obvious inflection point (phase transition temperature) can be noticed.

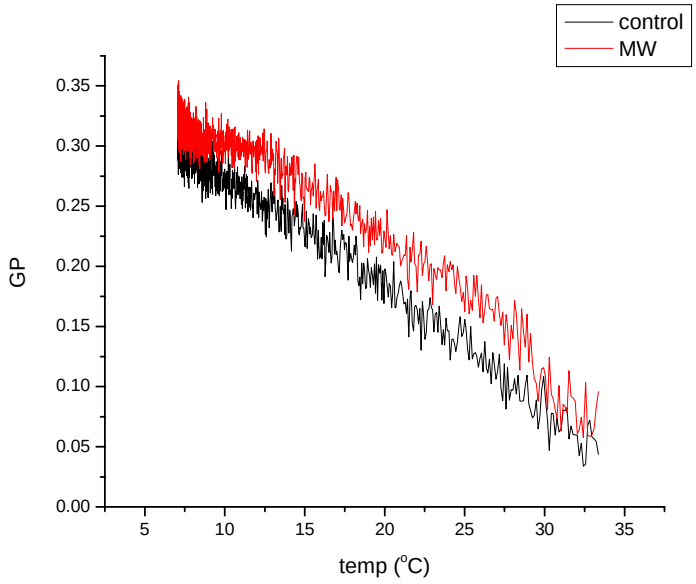
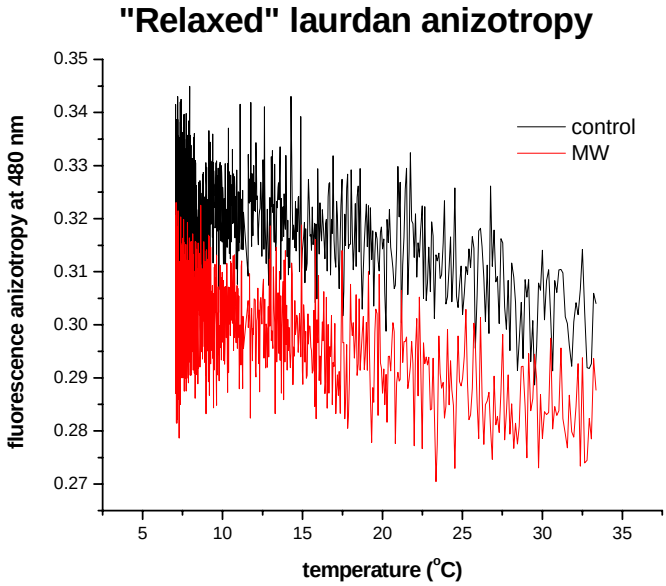


Fig.9 Generalized polarization of human platelets suspension in HBBS buffer as evaluated by Laurdan fluorescence. Higher GP of irradiated sample (red) show a predominance of non-relaxed Laurdan population



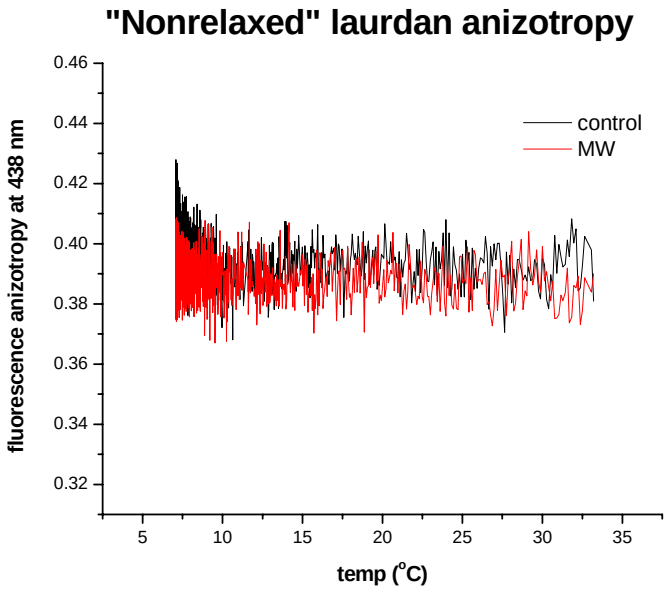


Fig.10 Fluorescence depolarization platelets membranes labelled by Laurdan, recorded at a/ λ_{em48o} and b/λ_{em438} nm

Discussion

The higher values of generalized polarization in irradiated lipid vesicles as well as in platelets reflect formally an increase in population of non-relaxed Laurdan molecules which cannot orient locally the polar, hydrophilic molecules (water). We could expect this, since water molecules are already oriented by microwave field, contributing to a more rigid, gel-like lattice at low temperatures (see figure 7). This is also why the phase – transition temperature is higher in irradiated liposome sample. As system pass to a liquid-crystal phase (above T_c), the difference between the two samples vanishes since thermal motion oppose the dipole orienting effect of the field.

The same effect can be observed in recording the fluorescence anisotropy based on emission of relaxed and nonrelaxed laurdan molecules. Under microwave irradiation the anisotropy of relaxed Laurdan emission is lower comparatively to that of the non-relaxed Laurdan due to the greater mobility of the fluorescent marker in the lipid environment when it cannot strongly orient the neighboring dipoles (water, aminoacids) already oriented in the direction of the applied field.

In case of TMA-DPH fluorescence measurements the local mobility of lipid tails packed within the membrane bilayer is followed up. While in case of model liposome membrane no dramatic effect of irradiation was observed (fig.3), in case of platelet membrane a pronounced loosening (decrease of fluorescence anisotropy) of lipid packing is noticed (fig.4) similar to that recorded when using Laurdan (fig.10).

Conclusion

Based on evidence of the effects of radiofrequency fields in different biological endpoints, it has been suggested (Adey 1993), that co-operative interactions on the surface of cell membranes may allow weak fields to influence cellular processes through signal amplification and transduction processes.

At frequency used in our measurements (2.45 GHz), the basic interaction mechanism is the rotation of molecules in which positive and negative charges are separated in space (polar molecules). The most common such molecule in biological matter is water. Polar molecules tend to align themselves with the electric field and, as this oscillates, they tend to follow these oscillations. In this process energy is dissipated in the form of heat.

To discuss on *long lasting* effects of microwave application on a living system is only meaningful in terms of interference with signal pathways and this is, most probable, the specific “nonthermal” effect of microwaves although, as mentioned above, it may be accompanied by system heating.

An example of (interfacial) membrane polarity modulating the binding of signal molecules is the case of protein kinase C (PKC). This enzyme plays an important role in signal transduction. It is an amphitropic enzyme, existing in both aqueous and membrane phases. Binding of PKC to membranes increases its activity against most substrates. Membrane interfacial properties affect both the binding of the enzyme to a membrane as well as the activity of the enzyme in the membrane-bound state (Giorgione et al., 1998).

Our experiments provide the evidence that in simple bilayer systems (liposomes) as well as in a living cell membrane there is a change in local order of lipid packing (membrane fluidity) and polar molecules orientation induced by microwave irradiation. These changes are consistent with many reported cellular effects of microwaves and provide a meaningful biophysical mechanism for them.

References

Adang D., Remacle C., Vander Vorst A., *Long-term and low-thermal biological effects of microwaves, WIT Transactions on Biomedicine and Health, Vol 9, © 2005 WIT Press, www.witpress.com, ISSN 1743-3525 (on-line)*

Adey, W.R. *Biological effects of electromagnetic fields.* J. Cellular Biochem. 51. (1993) 410-416.

Adey, W.R. *Electromagnetics in biology and medicine In: H. Matsumoto ed. Modern Science* (1993) Oxford Univ. Press 227-245.

Ambrosini A., Zolese G., Balercia G., Bertoli E., Arnaldi G., Mantero F., *Laurdan* fluorescence: a simple method to evaluate sperm plasma membrane alterations*, Fertility and Sterility, 76, (2001) 501-505

CSIRO - *BIOLOGICAL EFFECTS AND SAFETY OF EMR* , June 1994

De Vequi-Suplicy C., Benatti C., Lamy T., *Laurdan in Fluid Bilayers- Position and Structural Sensitivity,* Journal of Fluorescence, 16(2006), 431-439

Epand R., Kraayenhof R., *Fluorescent probes used to monitor membrane interfacial polarity*, Chemistry and Physics of Lipids, 101 (1999) 57–64

Giorgione J., Kraayenhof R., Epand R.,*Interfacial membrane properties modulate protein kinase C activation: role of the position of acyl chain unsaturation*, Biochemistry 37 (1998) 10956-10960

Lee-Gou Chong P., Sugar I., *Fluorescence studies of lipid regular distribution in Membranes,* Chemistry and Physics of Lipids, 116 (2002) 153–175

Liburdy R, Vanek PJr., *Microwaves and the cell membrane. II. Temperature, plasma, and oxygen mediate microwave-induced membrane permeability in the erythrocyte,* Radiat Res.102 (1985) 190-205

Parasassi T., KrasnowskaE., Bagatolli L., Gratton E., *Laurdan and Prodan as Polarity – Sensitive Fluorescent Membrane Probes*, Jornalof Fluorescence, 8 (1998) 365-373

Zubiri D., Domecq A., Bernik D., *Phase behavior of phosphatidylglycerol bilayers as a function of buffer composition: fluorescence studies using Laurdan probe,* Colloids and Surfaces B: Biointerfaces 13 (1999) 13–28

The Use of Electromagnetic Noise as a Universal Inhibition Factor for the Mitigation of Biological Effects from Exposure to Electromagnetic Fields

Miguel Penafiel

Vitreous State Laboratory
The Catholic University of America
Washington, DC
USA

Running Title: Inhibition of bio-effects with ELF noise

Please send correspondence to:

Miguel Penafiel
Vitreous State Laboratory
Catholic University
Hannan Hall, Room 410
Washington, DC 20064
USA

Telephone: 202-319-5335
FAX: 202-319-4469
Email: Penafiel@vsl.cua.edu

Abstract

Numerous studies have reported biological effects from exposure to electromagnetic fields both in the ELF and RF ranges, but there is a lack of consensus about the validity of observed effects. In part this is due to replication difficulties. At the core of this issue is the fact that observed effects, while significant, can be of a subtle nature and can be easily masked by equally subtle changes in experimental conditions. The result is that effects that are observed in one experimental setting may not be observed in another seemingly equivalent setting. An alternate approach to verify the validity of observed effects that overcomes the difficulties associated with attempting to duplicate experimental conditions is to intentionally use an inhibition factor to demonstrate that observed effects can be elicited or negated at will. Our own research and that of others supports the notion that a universal inhibition factor is ELF electromagnetic noise. The superposition of ELF noise to inhibit biological effects elicited by exposure to electromagnetic fields has been found to be effective in all instances tested. Inhibited effects include: changes in enzymatic activity, changes in hormone levels, changes in oncogene transcript levels, alterations in gap junction intercellular communication, increases in DNA breaks, activation of stress proteins, increases in cell proliferation, teratogenic effects, and memory effects. The superposition of ELF noise has been shown to be equally effective in blocking ELF and RF induced effects. A physical understanding of how EM noise acts to block EMF induced effects can be formulated in terms of a detection process of the EM stimulus

analogous to the detection of chemical gradients in bacterial chemotaxis. This theory hypothesizes a temporal sensing mechanism involving two characteristic time constants: τ_a, the "averaging" time (~0.05s), and τ_m, the "memory" time (~5s). To elicit a full response a stimulus of constant intensity over τ_a must be applied for a time period greater than τ_m. The superposition of EM noise effectively inhibits the response by destroying amplitude uniformity of the EM stimulus over the required time scale.

Key words: ELF noise, temporal sensing, inhibition factor

Introduction

As far back as the 1980's reports about so-called nonthermal biological effects of exposure to weak electromagnetic fields (EMFs) were being widely circulated (Luben et al. 1982). These reports created a great deal of controversy as they went against the then commonly held belief that electromagnetic exposure could be of biological consequence only when the energy transfer was sufficient to produce measurable increases in temperature. Today, more than 25 years later and after hundreds of studies the controversy still remains. But the source of the controversy is not that biological effects from exposure to nonthermal fields have not been observed, but rather that biological mechanisms that explain the observed phenomena are still not well understood and cannot be easily explained, leading some to believe that effects are not plausible in spite of the evidence (Adair 1991, 2003).

All life on earth has evolved in the presence of environmental factors that include a broad spectrum of electromagnetic radiation. Much of this radiation is from natural sources that have been an essentially constant part of the environment in recorded time. But the technological leap that has taken place over the last 75 years or so has substantially increased the background radiation. This increase is particularly evident in the Extremely Low Frequency (ELF) range due to the ever-expanding electric power distribution grid, and in the Radio Frequency (RF) range due to the exponential growth of telecommunication networks. The increased exposure to man-made fields has fuelled the interest in understanding biological interactions, not only as a means to gain scientific knowledge, but also to assist in the setting of regulatory guidelines for exposure to such fields.

The issue of regulatory guidelines is most relevant in connection with the use of the ubiquitous cellular phone. Present guidelines, which coincide with practical limitations for the deployment of these devices, are based on the assumption that only effects accompanied by strong thermal interactions are likely. Yet there are hundreds of studies that show effects from nonthermal exposure (Adair 2003). Most of the observed effects are of a subtle nature and are therefore susceptible to numerous factors that make replication difficult. In part due to replication difficulties, some have suggested that all of the studies that show effects are somehow flawed (Adair 2003). The alternative is that there are as yet not clearly defined biological mechanisms that have escaped scientific understanding. Of course, the lack of a full understanding does not make observed effects invalid. Such is the case, for instance, with EMF-mediated bone fracture repair, which is clinically effective but still not well understood (Aaron et al. 2004).

Published studies that have reported biological effects from exposure to weak ELF and RF fields are too many to mention individually. Effects in the ELF range include changes in enzymatic activity (Litovitz et al.1997), teratogenic effects (Farrell et al. 1997), changes in gene expression (Lin et al. 1994), stress response effects (Lin et al.1997, DiCarlo et al. 2002), and DNA damage effects (Lai and Singh 1997). RF effects include changes in enzymatic activity (Penafiel et al. 1997), memory effects (Lai et al. 1994, Wang and Lai 2000), and DNA damage effects (Lai and Singh 1996). There are also a number of experiments that show similar effects for both ELF and RF exposure indicating that common biochemical pathways may be involved in the response. These effects include changes in enzymatic activity (Penafiel et al. 1997), memory effects on rats (Lai et al. 1994, 1998) and effects on chromatin conformation (Belyaev et al. 2005).

While the evidence for biological effects from exposure to weak EMFs is extensive, it is important to point that a number of experiments have also reported null effects. Many of these are experiments that have attempted to replicate previously reported results (Desta el al. 1999, Cosquer et al. 2005). Such null effects bring into question either the validity of reported effects or the accuracy of replication conditions (Krause et al. 2004). The issue of replication was also evident in our own laboratory while studying teratogenic effects from ELF EMF exposure of chick embryos. Statistically significant effects were observed in some experimental campaigns but not in others even though experimental conditions appeared to be the same. The discrepancy in the results was eventually tracked down to a change in the chick progenitor flock. The unknown factor causing the variability in results was apparently a genetic factor (DiCarlo and Litovitz 1999).

The ability to examine experimental data to look for unknown factors usually requires that a large number of experiments be performed. More often than not this is not possible. The issue of experimental validity when exact replication is difficult to achieve can be best addressed using a suitable inhibition factor, if such a factor can be found. We have previously demonstrated in a number of instances, that in the case of exposure to weak ELF and RF EMFs, the inhibition factor is ELF electromagnetic noise (e.g.,Litovitz et al. 1993, 1994, 1997b). The purpose of this paper is to show that the inhibiting ability of ELF noise covers a wide range of biological effects thereby suggesting that it might be a universal inhibition factor for EM induced biological effects.

Temporal characteristics of a bio-effecting stimulus

One of the issues concerning the general acceptance of experimental results that show effects from exposure to weak electromagnetic field is one of plausibility based on accepted demonstrable mechanisms. By one argument, weak EMFs do not carry sufficient energy to cause biologically significant interactions in the presence of local thermally driven electromagnetic noise. Calculations based on general physical properties of biological matter, which do not account for biological complexity, do indeed appear to demonstrate that local noise considerations make such interactions unlikely (Adair 1991, 2003). For interactions within the cellular membrane the magnitude of the local electromagnetic noise, thus calculated, is of the order of 500 V/m, which is many orders of magnitude larger than induced fields within humans from background ELF EMFs (< 0.001 V/m). Yet undisputable effects associated with research on bone fracture repair, which appears to be rooted in membrane bound interactions, have been observed with induced electric fields of 0.1V/m or even less (Luben et al. 1982). This evidence suggests that thermal noise considerations are not sufficient to render certain effects implausible.

If we accept that certain bio-effecting interactions are possible, notwithstanding thermal noise considerations, then it is of interest to find alternate approaches to determine the viability of such interactions. Clearly, EMFs affect biological material at an elemental level, but beyond the obvious primary interaction the biological response is determined by the signal processing characteristics of the living biological entity. These characteristics are an inherent property of the living system defined by a complex transfer function, which if known, would predict what signals are filtered out and what signals are passed through. An important consideration in this simple model is how stimulating signal varies as a function of time.

The biological response to an environmental stimulus is a multi-step process involving a series of chained biochemical reactions characterized by varying rate constants, which form what is referred to as a signalling cascade. The net response results from the interplay of the biochemical events in the signalling cascade. This process, which incorporates the functions of signal detection and discrimination and control of the endogenous cellular reply, is referred to as signal transduction. A model system for the study of signal transduction is that of bacterial chemotaxis. This model involves two time-dependent processes that together constitute a rudimentary memory system. One is a fast process, occurring on a time scale of the order of 0.04s, which performs the function of measuring the concentration of chemotactant molecules through binding of these molecules to surface receptors. The other is a slower process, taking place on a time scale of the order of 5s, which performs a comparison function by modification of the receptors when no changes in chemotactant concentration are detected. This is a process of temporal sensing through which the bacterium makes continuous measurements of chemotactant concentration, compares successive measurements, and responds to the difference between them.

A model analogous to that of bacterial chemotaxis can describe the biological response to weak EMF exposure (Litovitz et al 1997a). The parameters of this model were determined in studies of the effect of EMF stimulation on ODC activity. A constantly applied 60 Hz EMF stimulus yielded a consistent doubling of the ODC activity. Changes in the ODC response were first examined by introducing zero-field gaps of varying duration in the exposure signal. It was determined that the magnitude of the response decreased as the frequency of the gaps increased. The full response was elicited when a field of constant intensity was applied, without interruption, for a minimum of 10s. The characteristic time associated with the response to this gapped stimulus was found to be 5s and was termed the memory time, $\tau_{m.}$. Knowing the requirements to elicit a full response, zero-field gaps were introduced periodically at 1s intervals for much shorter intervals that were increased until the response was negated. The magnitude of the response was found to decrease with increasing gap duration. No response was obtained when the gap duration was 100ms. The characteristic time constant associated with the response to this second gapped stimulus was found to be 0.05s and was termed the averaging time, τ_a. In essence these results showed that the ODC response to EMF stimulation involved two processes with rudimentary memory. Continuous measurements averaged over a time τ_a are compared successively. The response is elicited when a constant measurement persists over a time greater than $\tau_{m.}$

The use of ELF noise to negate electromagnetic effects

The similarities of the temporal characteristics of the response to EMF exposure, as determined for the ODC model, with those of bacterial chemotaxis suggests that this may be a more general model applicable to the response to weak environmental stimuli. Furthermore, the requirement that certain temporal characteristics must be met to elicit a response suggests that strategies to alter the temporal characteristics of a stimulus could be devices for the purpose of negating the response. Such a scheme might be useful, for instance, for the mitigation of unwanted effects from EMF exposure.

The simplest strategy to alter the temporal parameters of an EMF stimulus is by the superposition of another EMF stimulus whose temporal characteristics do not meet the requirements to elicit a response. One such signal is ELF magnetic noise. Using the temporal sensing model with $\tau_a = 0.05$s and $\tau_m = 5$s, it can be shown a noise signal with bandwidth in the biologically active frequency range below 100 Hz will not elicit a response. The superposition of a noise EMF stimulus over an existing stimulus results in a new stimulus which is noisy itself and is the sum of the local stimulus s(t) and the superimposed noise n(t). In order to fully negate the response n(t)/s(t) must be greater than or equal to 1.

Measurements with the ODC model confirmed that the superposition of ELF noise could indeed negate the response (Litovitz 1994, 1997b). Other studies in our laboratory demonstrated that noise could also be used to inhibit teratogenic effects and effects on the stress response in chick embryos (Litovitz 1993, DiCarlo 1998, 1999b, 2000, 2002, Shallom 2002). Furthermore, it was also found that ELF noise could inhibit biological effects induced by mild mechanical vibration (DiCarlo 2002). Considered together this evidence makes a strong case for the argument that the inhibiting effect of ELF noise may be universal to weak stimuli.

Experiments carried out in other laboratories have also demonstrated the efficacy of ELF noise to inhibit both ELF and RF effects. Table 1 shows a list of published results that show the range of effects negated by the superposition of ELF noise. In the ELF domain effects elicited with field intensities between 1uT and 400 uT have been blocked. In the RF domain effects from exposure to fields of the order of 1 to 3 W/kg have been negated. The lower intensity cases represent situations in which the viability of effects might be called into question based on thermal noise consideration. The thermal noise issue can still be a possible argument against viability in the higher intensity cases, but it is a less convincing argument particularly since equivalent field intensities have been demonstrated to be bio-effecting in bone growth stimulation studies (Luben et al 1982). The results of Table 1 show that the outcome of the observed response can be manipulated through the use of another stimulating agent of the same type as the bio-effecting agent, thereby lending credibility to the existence of such effects.

Table 1: Biological effects inhibited by the superposition of ELF noise			
Model	*Exposure field*	*Effect inhibited*	*Reference*
Chick embryos	4 uT, 60 Hz sine	Two-fold increase/shift in ODC activity	Farrell et al. 1993
Chick embryos	1 uT peak, 100 Hz pulsed	Two-fold increase in developmental abnormalities	Litovitz et al. 1993
L929 cells	10 uT, 60 Hz sine	Two-fold increase in ODC activity	Mullins et al. 1993
L929 cells	10 uT, 60 Hz	Two-fold increase in ODC activity	Litovitz et al 1994
HL60 cells	6.7 uT, 60 Hz sine	40 % increase in c-myc transcript	Lin et al. 1995
Chick embryos	4 uT, 60 Hz sine	40 % reduction in the activity of 5'-nucleotidase	Martin et al. 1995
AMA cells	5uT, 50Hz sine	15% increase in cell proliferation	Rasmark et al. 1996
PC12 cells	8 uT, 60 Hz sine	15% decrease in intracellular dopamine	Opler et al 1997
L929 cells	835 MHz amplitude modulated, 2.5 W/Kg	40-100% increase in ODC activity	Litovitz et al. 1997
Chick embryos	4 uT to 10 uT, 60 Hz sine	Two-fold enhancement of survival of chick embryos in anoxic conditions by EM pre-conditioning	DiCarlo et al. 1999
Chick embryo	8 uT, 60 Hz sine 915 MHz CW, 1.7 W/kg repeated	27% decrease in HSP70 levels consistent with decreased cyto-protection	DiCarlo et al. 2002
Chick embryo	915 MHz CW, 1.75 or 2.5 W/Kg	Increase in HSP70 by preconditioning consistent with increased survival after hypoxia	Shallom et al. 2002
NIH3T3 cells	0.4 mT 50Hz	40% suppression in gap junction intercellular communication	Zeng et al 2002
Rats	2.45 GHz CW, 1.2 W/Kg	35% learning deficit	Lai 2004
NIH3T3 cells	0.2 mT 50Hz	50% co-suppression in gap junction intercellular communication with phorbol ester	Gao et al 2004
NIH3T3 cells	0.4 mT, 0.2 mT, 50Hz	30% suppression in gap junction intercellular communication	Zeng et al 2006

Discussion

In spite of hundreds of published results that claim the existence of biological effects from exposure to weak ELF and RF EMFs using a broad range of end points, there is still a great deal of uncertainty about whether these effects are real. Part of the problem is that effects have often been difficult to replicate and proposed biological mechanisms have not been substantiated and thus often remain speculative. But even when effects are generally accepted, a full understanding of the underlying biological mechanisms can still be lacking. Such is the case, for instance, in the case of EMF induced bone growth stimulation (Aaron et al. 2004).

Stimulation of living biological entities by weak exogenous stimuli involve signal transduction processes which often include signal integration and amplification. A model proposed in bacterial chemotaxis, which may apply to many other weak signal detection situations, assumes the existence of long-range cooperative interactions between receptors as a means to achieve signal amplification (Sourjik and Berg 2004). Other processes that could result in further signal amplification and discrimination are communication interactions between cells through gap junction channels. Direct cell to cell communication, evident in organized tissues and even in cell cultures as demonstrated by contact growth inhibition, is critical to bone-forming cells (Lecanda et al 1998). Biological effects could result from the disruption of any of the signalling pathways of the signal transduction process.

The biochemical basis for the interaction of EMFs with living entities is not clear. It is possible that the primary site of interaction is at the cellular membrane via modulation of receptor binding. If this were the case, a myriad

of downstream signalling pathways could be affected leading to observable effects. But the ability of noise to inhibit many of these effects provides a common link that sheds some light about the nature of the response. It is generally accepted that at a fundamental level the extent of the electromagnetic interaction is proportional to the intensity of the stimulus. As the intensity level increases direct heat dissipation resulting in measureable increases in temperature could be a consequence of the exposure. At such levels the superposition of a signal of equivalent intensity would only result in further heating. But at exposure levels for which heating is not an issue, such as the experiments listed in Table 1, the inhibiting ability of superimposed ELF noise indicates that these interactions are a signalling events with common temporal sensing characteristics. This also suggests that while the effects of EMF exposure may be evident in a multitude of observable parameters, it is possible that such responses might share a few key common biochemical pathways. The shared common pathways would be those that establish the signal averaging time, τ_a, and the memory time, τ_m of the temporal sensing process.

The evidence shown in Table 1 is suggestive of a general effect that may be universally applicable. This inductive conclusion would be difficult to prove for all cases. However, the fact that ELF noise inhibition has been effective in all instances in which it has been examined adds to the weight of the evidence supporting this argument.

Conclusions

A review of experimental results on the use of the superposition of ELF noise for the inhibition of effects induced by exposure to weak EMFs shows the efficacy of this technique to negate observed effects. These results apply to a broad range of end points and over a wide range of signal intensities suggesting that a common factor is at play. This common factor is likely to be a temporal sensing process characterized by two common rate constants. The broad scope of inhibited effects also suggests the applicability of the temporal sensing hypothesis as a general signal transduction mechanism for the interaction of EMFs with living systems.

Two general conclusions can be drawn from the foregoing review which shows that the superposition of ELF noise is an effective inhibiting factor in bioelectromagnetic effects: 1) the use of ELF noise in a pseudo-sham exposure condition would be beneficial in determining whether observed effects are attributable to EMF exposure, and 2) the superposition of ELF noise would be effective as a prophylactic means to inhibit unwanted biological effects in situations where exposure is unavoidable.

References

Aaron RK, Boyan BD, Ciombor DM, Schuartz Z, Simon BJ. 2004. Stimulation of growth factor synthesis by electric and electromagnetic fields. Clin. Orthop. Relat. Res. 419:30-37.

Adair RK. 1991. Constraints on biological effects of weak extremely low frequency electromagnetic fields. Phys. Rev. A 43:1049-1048.

Adair RK. 2003. Biophysical limits on athermal effects of RF and microwave radiation, Bioelectromagnetics 24(1):39-48.

Belyaev IY, Hillert L, Protopopova M, Tamm C, Malmgrem LO, Person BR, Selivanova G, Harms-Ringdahl M. 2005. 915 MHz Microwaves and 50 Hz Magnetic field affect chromatic conformation and 53BP1 foci in human lymphocytes from hypersensitive and healthy persons. Bioelectromagnetics 26:173-184.

Cosquer B, Kuster N, Cassel JC. 2005. Whole-body exposure to 2.45 GHz electromagnetic fields does not alter 12-arm radial-maze with reduced access to spatial cues in rats. Behav Brain Res. 161:331-334.

Desta AB, Owen RD, Cress LW. 1999. Ornithine decarboxylase activity in developing chick embryos after exposure to 60-hertz magnetic fields. Biochem Biophys Res. Comm. 265:211-213.

DiCarlo AL, Farrell JM, Litovitz TA. 1998. A simple experiment to study electromagnetic field effects: Protection induced by short-term exposures to 60 Hz magnetic fields. Bioelectromagnetics 19:498-500.

DiCarlo AL, Litovitz TA. 1999a. Is genetics the unrecognized confounding factor in bioelectromagnetics? Flock-dependence of field-induced anoxia protection in chick embryos. Bioelectrochem Bioenerg. 48:209-215.

DiCarlo AL, Farrell JM, Litovitz TA. 1999b. Myocardial protection conferred by electromagnetic fields. Circulation. 99:813-816.

DiCarlo AL, Mullins JM, Litovitz TA. 2000. Electromagnetic field-induced protection of chick embryos against hypoxia exhibits characteristics of temporal sensing. Bioelectrochemistry 52:17-21.

DiCarlo A, White N, Guo F, Garrett P, Litovitz T. 2002. Chronic electromagnetic field exposure decreases HSP70 levels and lowers cytoprotection. J. Cell. Biochem. 84:447-454.

Farrell JM, Barber M, Doinov P, Krause D, Litovitz TA. 1993. Superposition of a temporally incoherent magnetic field suppresses the change in ornithine decarboxylase activity in developing chick embryos

induced by a 60 Hz sinusoidal field. In: Blank M, ed. Electricity and Magnetism in Biology and Medicine. San Francisco, USA: San Francisco Press.
Farrell JM, Litovitz TL, Penafiel LM, Montrose CJ, Doinov P, Barber M, Brown KM, Litovitz TA. 1997. The Effect of Pulsed and Sinusoidal Magnetic Fields on the Morphology of Developing Chick Embryos, Bioelectromagnetics 18:431-438.
Gao XW, Xu ZP, Huo YN, Jiang H, Fu YT, Lu DQ, Zeng QL. 2004. [Noise magnetic fields block co-supression effect induced by power frequency magnetic field and phorbol ester]. Zhonghua Yu Fang Yi Xue Za Zhi 38:11-13.
Krause CM, Haarala C, Sillanmaki L, Koivisto M, Alanko K, Revonsuo A, Laine M, Hamalainen H. 2004. Effects of electromagnetic field emitted by cellular phones on the EEG during an auditory memory task: a double blind replication study. Bioelectromagnetics 25:33-40.
Lai H, Horita A, Guy AW. 1994. Microwave irradiation affects radial-arm maze performance in the rat. Bioelectromagnetics 15:95-104.
Lai H, Singh HP. 1996. Single- and double-strand DNA breaks in rat brain cells after acute exposure to radiofrequency electromagnetic radiation, Int J Radiat Biol. 69:513-21.
Lai H, Singh HP. 1997. Acute exposure to a 60 Hz magnetic field increases DNA strand breaks in rat brain cells, Bioelectromagnetics 18:156-65.
Lai H, Carino MA, Ushijima I. 1998. Acute exposure to a 60 Hz magnetic field affects rats' water-maze performance. Bioelectromagnetics 19:117-122.
Lai H. 2004. Interaction of microwaves and a temporally incoherent magnetic field on spatial learning in the rat. Physiology and Behavior 82:785-789.
Lecanda F, Towler DA, Ziambaras K, Cheng SL, Koval M, Steinberg TH, Civitelli R. 1998. Gap junctional communikcation modulates gene expression in osteoblastic cells. Mol. Biol. Cell. 9:2249-2258.
Lin H, Goodman R, Shirley-Henderson A. 1994. Specific region of the c-myc promoter is responsive to electric and magnetic fields, J Cell Biochem 54:281-8.
Lin H, Goodman R. 1995. Electric and magnetic noise blocks the 60 Hz magnetic field enhancement of steady state c-myc transcript levels in human leukemia cells. Bioelectrochem. Bioenerg. 36:33-37.
Lin H, Opler M, Head M, Blank M, Goodman R. 1997. Electromagnetic field exposure induces rapid, transitory heat shock factor activation in human cells, J Cell Biochem 66:482-488.
Litovitz TA, Montrose CJ, Doinov P, Brown KM, Barber M.1993. Superimposing spatially coherent electromagnetic noise inhibits field-induced abnormalities in developing chick embryos. Bioelectromagnetics.15:105-113.
Litovitz TA, Krause D, Penafiel M, Elson EC, Mullins JM. 1993. The Role of Coherence Time in the Effect of Microwaves on Ornithine Decarboxylase Activity, Bioelectromagnetics 14:395-403.
Litovitz TA, Krause D, Montrose CJ, Mullins JM. 1994. Temporally incoherent magnetic fields mitigate the response of biological systems to temporally coherent magnetic fields. Bioelectromagnetics 15:399-409.
Litovitz TA, Penafiel M, Krause D, Zhang D, Mullins JM. 1997a. The role of temporal sensing in bioelectromagnetic effects. Bioelectromagnetics 18:388-395.
Litovitz TA, Penafiel LM, Farrel JM, Krause D, Meister R, Mullins JM. 1997b. Bioeffects induced by exposure to microwaves are mitigated by superposition of ELF noise. Bioelectromagnetics 18:422-430.
Luben RA, Cain CD, Chen MC, Rosen DM, Adey WR. 1982. Effects of electromagnetic stimuli on bone and bone cells in vitro: Inhibition of responses to parathyroid hormone by low-energy low-frequency fields, Proc. Natl. Acad. Sci. USA 79:4180-4184.
Martin AH, Moses GC. 1995. Effectiveness of noise in blocking electromagnetic effects on enzyme activity in the chick embryo. Biochem. Mol. Biol. Int. 36:87-94.
Mullins JM, Krause D, Litovitz TA. 1993. Simultaneous application of a spatially coherent noise field blocks response of cell cultures to a 60 Hz electromagnetic field. In: Blank M, ed. Electricity and Magnetism in Biology and Medicine. San Francisco, USA: San Francisco Press.
Opler M, Rukenstein A, Cote L, Goodman R. 1997. Reduced dopamine levels in PC12 cells exposed to low frequency electromagnetic fields. Bioelectrochem. Bioenerg. 42:235-239.
Penafiel LM, Litovitz TA, Krause D, Mullins JM. 1997. Role of Modulation on the Effect of Microwaves on Ornithine Decarboxylase Activity in L929 Cells. Bioelectromagnetics 18:132-141.
Raskmark P, Kwee S. 1996.The minimizing effect of electromagnetic noise on the changes in cell proliferation caused by ELF magnetic fields. Bioelectrochem. Bioenerg. 40:193-196.
Shallom JM, DiCarlo AL, Ko D, Penafiel LM, Nakai A, Litovitz TA. 2002. Microwave exposure induces Hsp70 and confers protection against hypoxia in chick embryos. J. Cell. Biochem. 86:490-496.
Skyberg K, Hansteen IL, Vistnes AI. 2001. Chromosomal aberrations in lymphocytes of employees in transformer and generator production exposed to electromagnetic fields and mineral oil. Bioelectromagnetics 22:150-160.

Sourjik V and Berg HC. 2004. Functional interactions between receptors in bacterial chemotaxis. Nature 428:437-441.

Wang B, Lai H. 2000. Acute exposure to pulsed 2450-MHz Microwaves Affects water-maze performance of rats. Bioelectromagnetics 21:52-56.

Zeng QL, Chiang H, Fu YT, Lu DQ, Xu ZP. 2002. [Electromagnetic noise blocks the gap-junctional suppression induced by 50 Hz magnetic field], Zhonghua Lao Dong Wei Sheng Zhi Ye Bing Za Zhi 20:243-245.

Zeng QL, Ke XQ, Gao XW, Fu YT, Lu DQ, Chiang H, Xu ZP. 2006. Noise magnetic fields abolish the gap junction intercellular communication suppression induced by 50 Hz magnetic fields, Bioelectromagnetics 27:1-6.

ELF and RF/MW Electric fields as bioeffectors: a much needed new direction in bioelectromagnetics?

ROGER COGHILL

For several decades now Western research attention in bioelectromagnetics has largely centred on the magnetic component of the electromagnetic wave. In their original 1979 paper, which some argue heralded much of the subsequent scientific interest, Wertheimer and Leeper concluded that the elevated incidence of childhood cancer near pole-mounted transformers in Denver was probably due to the magnetic field. Their conclusion was based on preceding research, which had reported magnetic field sensitivities of some animals and fishes. Savitz et al. later attempted to include electric field measurements in their replication of the Denver study, but abandoned their effort through an inability to address the topic of chronic exposure. It may have escaped the notice of both authors that pole mounted transfoirmers inevitably generate large electric fields in converting the primary to the secondary induced voltage. Moreover, electric fields (unlike magnetic) are present wherever there is connection to the main supply, so the electric component was actually an equal candidate for Wertheimer and Leeper's speculations.
The world's power utilities have also favoured magnetic field research, comforted by the recognition that few homes will experience the 0.4uT commonly used as a cut point in epidemiological studies to define relative risk. The popular EmDEX probes (designed for EPRI) indeed do not even permit the user to collect electric field data without elaborate engineering modification.

Eastern bloc countries do not share this view, arguing that mankind has always had evolutionary experience of magnetic fields, in that we all live on the large magnet of the Earth.: and if anything new has occurred on the planet since the advent of electricity then it is the alternating electric field, for which there is no evolutionary counterpart (Shandala et al, 1988). The search for a mechanism of interaction incorporating the magnetic field only has proven inconclusive to date despite the evidence of many non thermal effects. It might therefore be more fruitful to reappraise the role of the electric component.

Out of eight published domestic epidemiological studies of the electric field only three took proper measurements, and these together offer strong support for the electric field at the nocturnal bedplace as the active parameter (see Table 1). The remaining five used spot or portable probes, or room centre measurements which do not adequately characterise bedplace exposure (see Table 2). The three pertinent studies show a consistent dose response pattern indicating that chronic exposure to ELF electric fields above 20V/m are hazardous to child health.

Table 1: Bedplace ELF electric field exposure in childhood cancer homes

Study	Exposure measures	**Odds ratio (OR) or relative risk (RR)**	95CI%
Coghill, Steward et al, 1996	12 hours TWA, bedplace only	**4.69**	1.17-27.0
Dockerty, Elwood et al, 1997	24 hours TWA, bedroom and one other room	**2.3**	0.4 – 12.7
Skinner Mee et al., 2002	Spot, 48 hours apart, bedplace and one other room	**1.42**	0.88-2.27

Table 2: Residential ELF electric field studies with poor characterisation

Study	Year	Deficiency
Savitz, Wachtel et al, *	1988	room centres only
Green et al,	1999	daytime personal monitor
McBride, Gallagher et al.,	1999	48hrs personal monitor
Tynes and Haldorse	1997	room corner nearest HT line
London, Thomas et al,	1991	spot measurements only

- abandoned a third way through the collection

Our laboratory has recently reported that ELF electric fields at levels commonly seen near powerlines and domestic electric appliances can create nitrites in aerated distilled water to a concentration reported by other studies to cause ill health. The effect is robust over many experiments. This simple physico-chemical effect (paralleling the effect in respiring organisms largely composed of aqueous solutions) may explain the thirty year old mystery of how such weak fields can cause ill health in the absence of heating.

Other studies show that many of the disorders associated with chronic ELF EM field exposure are also associated with excess nitrites found in the patients biological fluids. In childhood leukaemia for example the nitrite level is four times normal in serum and two orders of magnitude higher than normal in the CSF.

An appraisal of the literature as presented in this paper offers the conclusion that more research attention should be paid to electric fields and this in turn may lead to new standard setting which recognises at last the importance of non-thermal effects.

EFFECT OF LOW POWER MILLIMETER WAVES IRRADIATION ON $C_{12}EO_5/^2H_2O$ MEMBRANE MODEL: A ^{2}H-NMR SPECTROSCOPY INVESTIGATION.

LUIGI FILIPPELLI, AMERIGO BENEDUCI, GIUSEPPE CHIDICHIMO.

CHEMISTRY DEPARTMENT, UNIVERSITY OF CALABRIA, 87036 ARCAVACATA DI RENDE (CS), ITALY

CORRESPONDING AUTHORS: - l.filippelli@unical.it , beneduci@unical.it

Abstract

The influence of low power millimeter wave (MMW) irradiation in the 53.57-78.33 GHz frequency range, on water molecules of a model membrane has been investigated by Deuterium Nuclear Magnetic Resonance (^{2}H-NMR) Spectroscopy. The quadrupole splitting (Δ) of deuterated water within the lamellar mesophase of the $C_{12}EO_5/^2H_2O$ binary system has been measured, at 25°C constant temperature. It has been found that continuos wave (wide band 53.57-78.33 GHz) irradiation of the above membrane model system produces, a significant increase of the quadrupole splitting of deuterated water molecules. The observed variation of the Δ for heavy water is opposite with respect to a temperature increase and it depends on the level of hydration of the lamellar sample: in samples with an higher water content, MMW irradiation produced a larger Δ increase. The observed effect was totally reversible. In few hours the splitting came back to the initial value. We propose an explanation in terms of variation of the free/bound water population ratio and calculate the change in the Gibbs free energy of the system after the irradiation treatment. The interaction model membrane-MMW, might involve the structures that liquid water can adopt by using hydrogen bonds.

Short running title: millimeter wave effect on membrane hydration
Key words: membrane hydration; low power millimeter waves; ^{2}H-NMR spectroscopy

Introduction

The interaction between low power millimeter waves (power density below 1 mW/cm^2) and biological systems, concern either the effects induced by this radiation on the systems, or the basic mechanisms of interaction.

In 1968 Webb and Dodds observed the inhibitory effect of MMW on the growth of the *E. Coli* bacterium [Webb, 1968]. Afterwards H.D. Devyatkov [Devyatkov, 1974, 1981, 1983] and other Russian scientists [Sevastyanova, 1974, 1981] observed the influence of such radiation on various biological systems. Interesting studies on the growth of Saccaromices cerevisiae were performed by Grundler and Keilmann [Grundler, 1977, 1978, 1983]. A review of the most important results, in which some physical-chemical aspects of the MMW-biological systems interaction are also reported, is due to Pachomov et al. [Pachomov, 1998]. The effects observed on MMW irradiated cell systems go from cell growth variations, to changes in DNA morphology [Brill, 1993]. Ionic membrane transport alterations were also reported [Brovkovich, 1991, Geletyuk, 1995, Kataew AA, 1993].Since 2002, we have shown that low power (<10 mW/cm^2) electromagnetic radiation, in the millimeter wavelength range (3.84-5.78 mm), could be used as a physical mean in order to influence the proliferative behavior of several cultured cells [Chidichimo, 2002]. It should be highlighted that the proliferation rate of the investigated tumoral systems was inhibited by MMW in certain exposure conditions, whereas that of the healthy cell systems was not. Moreover, we have also shown that the frequency of the radiation and the irradiation time [Beneduci, 2005a] influence the observed effects. Besides the effect on cell proliferation, significant morphological alterations were observed on human melanoma, breast carcinoma and erythromyeloid leukemia cells [Beneduci, 2005a,b, Beneduci, 2006].

Until now however, there is not a generally accepted point of view on the biophysical mechanism of interaction between millimeter radiation and biological systems. Besides thermal effects that occur at high powers (>10 mW/cm^2), it was hypothized that the MMW-biosystems interaction could involve resonant nonthermal mechanisms at very low powers [Fröhlich, 1968, 1977, 1980, 1983, 1986a, b, Kaiser, 1988, Sinizin, 1998;]. Data on the dielectric properties of water [Ellison, 1996] and of biological systems [Schwan, 1983, Grant, 1984] agree on the fact that water is the only molecular system, able to directly interact with electromagnetic waves in the millimeter range above 1 GHz [Beneduci, 2006].

However, besides the direct field effect on water dipoles, any biological effects could be explained only if the electromagnetic field affects the reaction sensitivity of some cellular processes, that is crucially determined by the reaction moments [Neumann,2000].

The absorption of microwave radiation by water molecules may induce changes in the equilibrium free water/bound water involved in several cellular processes in which a chemical control is exerted [Neumann,2000]. Water plays also crucial roles in proton transfer reactions and in transport processes through narrow channels or pores in which water molecules assume particular interfacial orientations [Neumann,2000]. The millimeter radiation could affects the orientational dynamics of water molecules in such systems, causing several bio-effects.

The above considerations and the morpho-functional alterations of the membrane observed on some *in vitro* cultured tumoral cells after MMW irradiation [Chidichimo 2002, Beneduci 2005b, Beneduci, 2006, Szabo 2006, Chen 2004], brought us to begin the study of the MMW-membrane interaction.

The present work therefore, deals with some aspects of the physico-chemical mechanisms that occur when a model membrane system interacts with the millmeter waves.

All the biological membranes exist because of the intermolecular forces occurring between the components of the system (hydrophobic interactions, dipole-dipole, ion-dipole, hydrogen bonds network) . The water molecules interacting with the polar head groups of the anfiphilic molecules by non-bonding forces are in chemical equilibrium with those ones that constitute the bulk water and are the so called “free water” molecules. A general reaction step that summarizes such type of chemical process occurring at the polar interface of a double layer is the following:

$$S(H_2O)_r + nH_2O \xleftrightarrow{K_{eq}} S(H_2O)_{r+1} + (n-1)H_2O \qquad (1)$$

where $S(H_2O)_r$ is the amphiphilic molecule that binds r water molecules and being in thermodynamic equilibrium with the species $S(H_2O)_{r+1}$ that bind r+1 water molecules, $(n-1)H_2O$ being the free water molecules. The model membrane system investigated in the present work was the penta(oxyethylene)n-dodecylether/water lamellar lyotropic-liquid crystal system, which has been extensively studied in the past [Mitchell, 1983, Dimitrova et al., 1996,]. Such binary system was conveniently adopted by us because it easily forms double layer of lamellar structures (like biomembranes), at room temperature in a relatively wide range of compositions.

If a model membrane is made by using heavy water (^2H_2O) instead of ordinary water (H_2O), one can record a deuterium NMR spectrum which will be the result of a superposition of spectral doublets whose peak separation (in Hz) depends on the orientation of the double layer (lamella) with respect to the NMR static magnetic field [Pake 1948]. When the plane of the lamella is oriented parallel to the static magnetic field, the peak separation is called quadrupole splitting, Δ.

In the case under study, the $C_{12}EO_5/^2H_2O$ system, Δ is proportional to the total fraction of water molecules bound to the polar head group of the surfactant, p_b, and to an average order parameter S_b that brings information about the local motion of the O-D bonds in heavy water:

$$\Delta = \frac{3}{4}\nu_q p_b S_b \qquad (2)$$

where, ν_q is the quadrupole coupling constant. The equilibrium reaction that concern the hydration process of the surfactant molecules in the lamellar structures, could be written in the general form (3) [Mitchell et al., 1983], where S_f are the free surfactant molecules, W_f the free water molecules, $S_b(W_b)_r$ are the complexes formed by a surfactant molecule and r water molecules and K_b is the thermodynamic equilibrium constant.

$$S_f + rW_f \xleftrightarrow{K_b} S_b(W_b)_r \qquad (3)$$

It is clear that any cause affecting the free/bound water equilibrium must reflects a change in the value of the quadrupole splitting that can be conveniently measured by the ^{2}H-NMR technique [Mitchell et al., 1983].

Materials and methods

Deuterium NMR spectra were recorded on a 300 MSL Bruker spectrophotometer operating at 46.053 MHz deuterium resonance frequency, using a 10 mm tunable probe. To record the spectra, samples were introduced in a 10 mm NMR tube. Each spectrum is the Fourier transform of a FID obtained integrating 400 scans, with a 1 sec repetition time. Each scan is a quadrupolar echo pulse sequence, with a 9 µs 90° pulse and a 88 µs delay time. Sample temperature was constantly maintained at 25°C by the spectrophotometer variable temperature controller VT 1000.

Chemicals

Normaldodecylpentaoxyhetylene ether ($C_{12}EO_5$) was purchased from Sigma-Aldrich (99% purity) and deuterated water from Cambridge Isotope Laboratories, Inc. (99.9% purity). Both chemicals were used without

further purification. Lamellar lyotropic liquid crystal samples, $C_{12}EO_5/^2H_2O$, were prepared by weight adding the right amount of heavy water to the surfactant placed in a 5 mm NMR tube. The mixtures were then warmed up and vortex stirred to achieve homogeneity . Three samples were prepared containing 30% (sample A),25% (sample B) and 20% (sample C) by weight D_2O. A 4 mm glass bar was introduced inside a 5 mm NMR tube to obtain a thin layer (0.5 mm) of lamellar phase (fig.1). Samples were then sealed and stored at 25°C for about three days.

Experimental MMW facilities and sample irradiation

The MMW radiating apparatus AMFIT 32 (made in Russia by the UWOM company of Nizhnj Novgorod), was used as radiation source. It is a microwave noise generator diode, able to supply a 53.57-78.33 GHz frequency band at a global mean power density < 1μWatt. Samples were placed at the end of the conical antenna of the instrument and were irradiated for 7 hours. Temperature was strictly controlled and maintained at 25 °C along the experiment. Samples were weighted after the irradiation treatments to check for evaporation of water but weights remained constant.

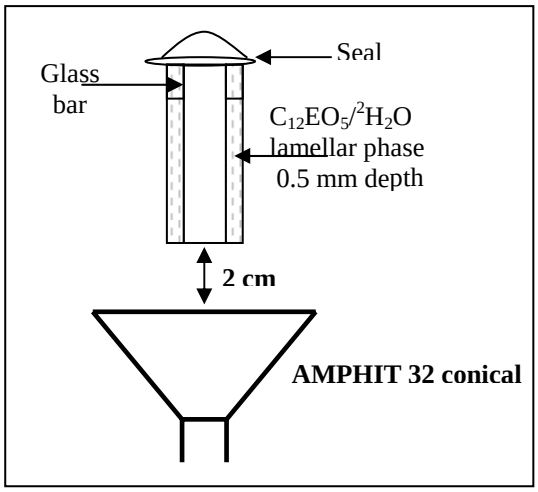


Fig. 1. Schematic representation of the lamellar sample and of the irradiation geometry (not in scale).

Results

Stability of the system under constant temperature condition

Prior to perform any irradiation experiment, the stability of the lamellar samples was tested under 25°C constant temperature condition. In fig. 2, the variation (%) of the quadrupole splitting is showed for a time course of 4 days, in the case of the sample A. It could be noted that Δ resulted very stable showing only restricted oscillations of the order of ± 0.25% (N=96), around the equilibrium Δ value. These random variations could be attributed to small fluctuations of the temperature of the thermostated chamber (probe). Analogous behaviour was observed for the other samples B and C (data not shown).

Quadrupole splitting behavior of heavy water under MMW irradiation

Typical ^{2}H-NMR spectra recorded before and after three irradiation treatments, were reported in fig.3 **A**, **B** for sample **A** and **B**. Significant increases of 5.3±1.0% (N=3) and 2.6±0.5% (N=3) of the quadrupole splitting of heavy water, were observed in the irradiated samples **A** and **B** respectively. A negligible perturbation of the Δ, was also observed in the irradiated sample **C** (data not shown).

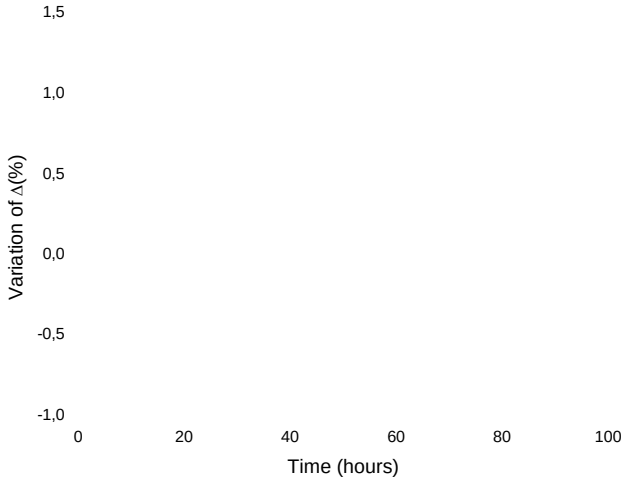


Fig. 2. Sample A before irradiation. Quadrupole splitting variation of ^2H_2O as a function of time (T=25°C). Spectra were recorded along 4 days with 1 hour steps. The sample is very stable.

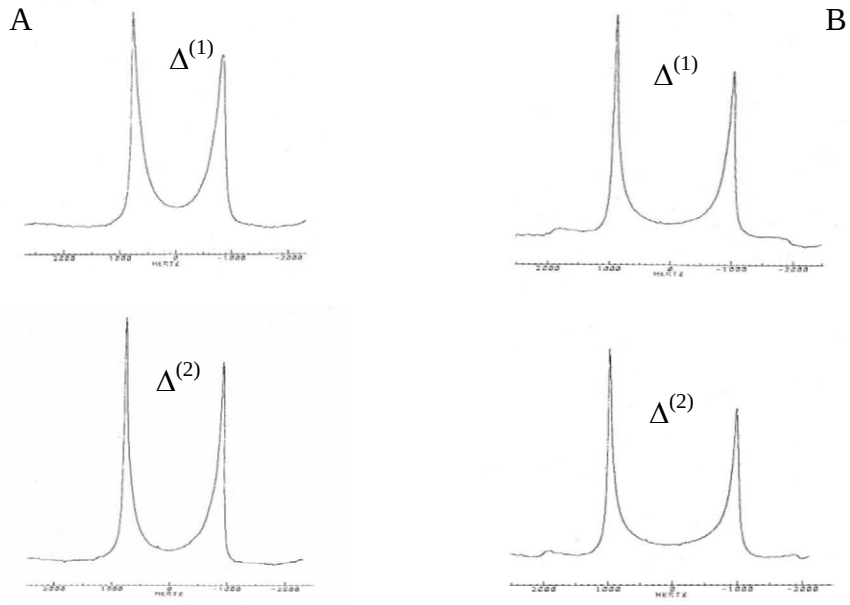


Fig 3. ^2H_2O-NMR spectra of the investigated samples. The Δ of heavy water in sample A ($\Delta^{(1)}$=1608 Hz) gained 80 Hz after the irradiation ($\Delta^{(2)}$=1688 Hz). The increase of the Δ for the sample B was 45 Hz ($\Delta^{(2)}$=1918 Hz; $\Delta^{(2)}$=1963 Hz).

The observed variations are very far from those which could be induced by thermal fluctuations. Actually, from control sample data, we have seen that thermal fluctuations (of less than 1 degree) caused statistical random variations of the quadrupole splitting about the equilibrium value at 25°C, which were not larger than 4 Hz (0.25%).

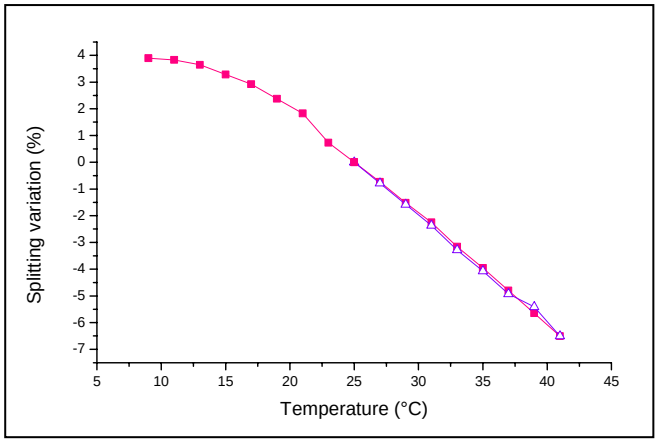


Fig. 4. Sample A.Variation of the splitting value in percentage as a function of temperature. The point zero on the ordinates corresponds to 25 °C.

^2H_2O quadrupole splitting temperature dependance

In fig.4 the variation of the quadrupole splitting of heavy water relative to sample **A** was shown as a function of temperature, in the range 9°C – 41°C. The thermal process, from 9°C to 41°C, is reversible (see upfacing triangle in fig. 4). At this point, two fundamental findings have to be underlined: 1) to produce a 6% increase in Δ in such a system (sample **A**), equal to that observed under MMW irradiation, it was necessary to reduce the temperature of the system of about 15°C. 2) MMW irradiation produced an increase of Δ while a temperature increase produced a Δ decrease. This temperature dependence was similar for the other two samples (**B** and **C**), as previously reported [Rendall K, 1984].

MMW irradiation increases membrane hydration

In view of equation (2), the quadrupole splitting (Δ) can change only if p_b and/or S_b changes. Summarizing the results, the variation of the quadrupole splitting of D_2O contained in the irradiated model membranes, increases as the percentage of heavy water within the samples increases. Going from the less hydrated (C) to the more hydrated system (A) the free water dispersed between the surfactant lamellae gradually increase. Hence a crucial parameter influencing the variation of Δ after MMW irradiation, must be the amount of free water present in the system. More precisely, we observed that the effects produced on the quadrupole splitting of heavy water by the MMW irradiation increases as the free water/ bound water (p_b) ratio increases. A variation of only the order parameter S_b cannot explain the observed trend. Indeed, such a parameter reflects the local orientational order of the bound water. Thus the value of S_b depends on the mobility of water molecules linked to the surfactant polar heads. If the MMW irradiation had acted on this physical property of the system, the variation of Δ should not depend on the sample composition. Thus, we interpreted our experimental findings, identifying a primary interaction occurring between the millimeter radiation and the free water of the membrane system that strongly absorbs the MMW. As first order effect, consequence of such direct interaction, is the shift of the thermodynamic equilibrium (3) towards right. Hence, the membrane resulted more hydrated (greater *pb* values) after the MMW irradiation treatment, than the equilibrium initial condition. Such fundamental perturbation was observed as a quadrupole splitting increase. In thermodynamic terms, this means that the Gibbs free energy variation relative to the process (3), expressed by equation (4) is shifted towards more negative values (more favoured thermodynamic process) by millimeter wave irradiation.

$$\Delta G = G_{W_b} - G_{W_f} \tag{4}$$

The first term (G_{Wb}) of eq.4 is the Gibbs free energy of a mole of bound water molecules. Its value depends on local thermodynamic properties of water molecules bound to the polar heads of the surfactant, that are not susceptible to change under irradiation. Then, $G_{Wb,}$ does not change. Hence we can write equation (5)

$$G_{W_b}^{(1)} = G_{W_b}^{(2)} \tag{5}$$

where the superscript (1) and (2) refer to the state of the system before and after MMW irradiation, respectively.

Variation of the Gibbs free energy of the system under MMW Irradiation

We derived the change in the Gibbs free energy variation of the system produced by MMW (ΔG_{MW}). Using equation (4), the equality (5), and defining the states of the system before and after irradiation by the superscript (1) and (2) respectively, we can write the following equations:

$$\Delta G^{(1)} = G_{W_b}^{(1)} - G_{Wf}^{(1)} = -RT \ln K_b^{(1)} \quad (6)$$

$$\Delta G^{(2)} = G_{W_b}^{(2)} - G_{Wf}^{(2)} = -RT \ln K_b^{(2)} \quad (7)$$

We can express thus, the quantity ΔG_{MW} as the difference between the Gibbs free energy variation relative to equilibrium (3) before and after irradiation:

$$\Delta G_{MW} = \Delta G^{(2)} - \Delta G^{(1)} = -[G_{W_f}^{(2)} - G_{W_f}^{(1)}] \quad (8)$$

Equation (8) tells us that energetic changes of the state of the system, produced by MMW irradiation, are due to changes, opposite in sign, in the energetic state of free water present in the system.
We can correlate the quantity ΔG_{MW} with the thermodynamic equilibrium constant K_b relative to process (3) before and after MMW irradiation:

$$\Delta G_{MW} = -RT \ln \frac{K_b^{(2)}}{K_b^{(1)}} \quad (9)$$

In table 1, quadrupole splitting experimental values and calculated thermodynamic data relative to systems **A**, **B**, and **C** were collected.
The p_b values were determined by means of equation (2) and using the S_b value as reported by Mitchell et.al . The increase of the Gibbs free energy of free water, produced on the systems after irradiation, is greatest for sample **A** (+2882 J/mol). Consequently, equilibrium (3) is shifted towards the water-surfactant complex ($K_b^{(2)}$ 3.2 fold greater than $K_b^{(1)}$ after irradiation). This effect is less pronounced in system **B** (+834 J/mol; $K_b^{(2)}$ 1.4 fold greater than $K_b^{(1)}$ after irradiation). No net increase was observed in system **C**.

Table 1

State of the System	Δ (KHz)	p_b	S_b	$K_b^{(2)} / K_b^{(1)}$	ΔG_{MW} (J)	$C_{12}EO_5/^2H_2O$ %(w/w)
1	1.608	0.51	0.0146	3.2	-2882	70
2	1.688	0.54				
1	1.918	0.61		1.4	-834	75
2	1.963	0.63				
1	1.946	0.62		≈1	0	80
2	1.956	0.63				

Table 1. Experimental and calculated data of the parameters characterizing the lamellar system. Low power MMW irradiation induces an increase of the fraction of water molecules bound to the surfactant. See text above for details.

Summary
The quadrupole splitting of deuterated water of a $C_{12}EO_5/^2H_2O$ membrane model was measured by ^{2}H-NMR spectroscopy. By irradiating the model membranes utilizing low power millimeter waves (wide band 53.57-78.33 GHz, continous wave), we modified (increase) the splitting value of the heavy water. This cannot be explained in terms of solely provided heat. In fact, raising temperature produces an opposite behaviour of the monitored parameter (splitting decrease). Weighting the samples after millimeter waves exposure, allowed us to be sure that water did not evaporate. We also found that the effect is completely reversible after few hours. Furthermore, the most hydrated samples were more sensitive to the irradiation treatment. Making some assumptions we propose that the MMW interact primarly with the free water trapped between the layers of the system, inducing the water molecules to bound the surfactant. Literature data and studies we are carrying out on the dielectric constant of both normal and deuterated water (data to be published), strongly indicate that water is the primary absober of the millimeter wavelengths and the obtained dielectric data are different for the two kind of water at the same frequencies. Works in progress are clearly indicating that very likely the structures that water can adopt by means of hydrogen bond network play a central role in the observed effects; phospholipid model and in vitro cultured cells, respond to some specific frequencies rather than others.

Acknowledgements
This work was supported by Fondazione CARICAL, Lega Italiana per la Lotta Contro i Tumori Sezione Cosenza and Regione Calabria (POR 2000/2006, misura 3.16, progetto PROSICA)

References

Beneduci A et al. 2005a. Frequency and irradiation time-dependant antiproliferative effect of low-power millimeter waves on RPMI 7932 human melanoma cell line, Anticancer Research 25:1023-1028.

Beneduci A et al. 2005b. Transmission electron microscopy study of the effects produced by wide-band low-power millimeter waves on MCF-7 human breast cancer cells in culture, Anticancer Research 25:1009-1014.

Beneduci A et al. 2006. Antiproliferative effect of millimeter radiation on human erythromyeloid leukemia cell line K562 in culture: ultrastructural-and metabolic-induced changes, *Bioelectrochemistry* (2006), doi:10.1016/j.bioelechem.2006.07.008.

Brill G et al. 1993. Effect of low level extremely high frequency radiation on the genetic activity of polytene chromosomes of Chironomus plumosus. Fizicheskaia Meditzina 3:69.

Brovkovich VM et al. 1991. Action of millimeter-range electromagnetic radiation on the Ca^{++} pump of sarcoplasmic reticulum. Radiobiologia 31: 268.

Chen Q et. al. 2004. Millimeter wave exposure reverses TPA suppression of gap junction intercellular communication in HaCaT human keratinicytes. Bioelectromagnetics 25:1-4.

Chidichimo G et al. 2002. Selective inhibition of tumoral cells growth by low power millimeter waves. Anticancer Research 22:1681-1688.

Devyatkov ND et al. 1974. Sov. Phis-Usp. 16, 4: 568-579.

Devyatkov ND. 1981. Non thermal effects of millilmeter wave irradiation. In: Devyatkov ND, editor. Use of Low Intensity Millimeter Radiation in Biology and Medicine. Moscow: Inst Radiotech Electrotech Moscow. Acad. Sci USSR (in Russian).

Devyatkov ND. 1983. Non thermal effects of millilmeter wave irradiation. In: Devyatkov ND, editor. Use of Low Intensity Millimeter Radiation in Biology and Medicine. Moscow: Inst Radiotech Electrotech Moscow. Acad. Sci USSR (in Russian).

Dimitrova GT. 1996. Investigation into phase behavior of nonionic ethoxylated surfactanst using ^{2}H NMR spectroscopy. Langmuir 12:315-318.

Ellison WJ. 1996. Water : A dielectric reference. Journal of Molecular Liquids 68:171-279.

Fröhlich H. 1968. Long range coherence and energy stored in biological systems. Int J Quantum Chemistry 2:641-649.

Fröhlich H. 1970. Long range coherence and the action of enzymes. Nature 228:1093.

Fröhlich H. 1980. The biological effects of microwaves and related questions In: Marton L ed. Advances in electronics and electron physics. Academic Press, New York, pp. 53:85-152.

Fröhlich H. 1983. Evidence for coherent excitation in biological system Int. J. Quantum Chem 23:1589-1595.

Fröhlich H. 1986. Coherent action of enzymes. In: R. Welch ed. The fluctuating enzymes. John Wiley, New York, pp. 421-449.

Fröhlich H. 1986. Coherent excitation in biological systems. In: F. Gutmann, H. Keyser, eds. Modern bioelectrochemistry Plenum, New York, pp 241-261.

Geletyuk VI et al. 1995. Dual effects of microwaves on single Ca^{++} activated K^{+} channels in cultured Kidney cells *Vero*. FEBS Lett 359:85-88.

Grant EH. 1983. Molecular interpretation of the dielectric behavior of biological materials. In: Grandolfo M, Michaelson SM and Rindi A eds. Biological Effects and Dosimetry of Nonionizing Radiation, NATO Advanced Study Institutes Series. Series A, Life Sciences; v. 49, Plenum Press New York and London pp 179-194.

Grundler W, Keilmann F. 1977. Resonant growth rate response of yeast cells irradiated by weak microwaves. Phys Lett 62A:463-466.

Grundler W, Keilmann F. 1978. Nonthermal effects of millimiter microwaves on yeast growth. Z Naturforsch 33c:15-22.

Grundler W, Keilmann F. 1983. Sharp resonances in yeast growth prove non-thermal sensitivity to microwaves. Phys. Rew. Lett 51:1214-1216.

Kaiser F. 1988. Theory of Non-Linear Excitations In: H. Fröhlich ed. Biological Coherence and Response to External Stimuli, Springer-Verlag pp 25-48.

Kataew AA et al. 1993. Frequency-dependent effects of the electromagnetic millimeter waves on the ion current in the cell membrane of Nitellopsis obtusa: non thermal action. Biofizika 38:446-462.

Mitchell DJ et al. 1983. Phase behavior of polyixyethylene surfactants with water J. Chem. Soc., Faraday Trans 19:975-1000.

Neumann E 2000. Digression on chemical electromagnetic field effects in membrane signal transduction–cooperativity paradigm of the acetylcholine receptor, Bioelectrochemistry 52: 43-49.
Pake GE. 1948. J Chem Phys 16:327.
Pakhomov G. 1998. Current state and implication of research on biological effects of millimeter waves: a review of the literature. Bioelectromagnetics 19:393-413.
Rendall K and Tiddy GJT. 1984. Interaction of water and oxyethylene group in lyotropic liquid crystalline phases of poly(oxyethylene)n-dodecyl ether surfactants studied by ^{2}H Nuclear Magnetic Resonance spectroscopy. J Chem Soc Faraday Trans 80:3339-3357.
Schwan HP. 1983. Dielectric properties of biological tissue and cells at RF-and MW-frequencies. In: Grandolfo M, Michaelson SM and Rindi A eds. Biological Effects and Dosimetry of Nonionizing Radiation, NATO Advanced Study Institutes Series. Series A, Life Sciences; v. 49, Plenum Press New York and London pp 179-194.
Sevastyanova LA, Vilenskaya RL. 1974. A study of the effect of millimeter-band microwaves on the bone marrow of mice. Sov. Phis-Usp (Engl Transl) 16:570.
Sevastyanova LA, Vilenskaya RL. 1981. Specific influence of millimeter waves on biological objects. In: Devyatkov ND, editor. Non thermal effects of millilmeter wave irradiation. Moscow: Inst Radiotech Electrotech Moscow. Acad. Sci USSR (in Russian) pp 86-113.
Sinizin NI. 1998. The special role of the Millimeter waves-aqueous medium interaction in nature. Biomedicina Radiotecnika 5:5-23 (in Russian).
Szabo I et. al. 2006. Millimeter wave induced reversibile externalization of phosphatidylserine molecules in cells exposed in vitro. Bioelectromagnetics 27:233-244.
Tanaka H. 1998. Simple physical explanation of the unusual thermodynamic behavior of liquid water Phys Rev Lett 80:5750-5753.
Tanaka H. 2000. The two state model of water. J Chem Phys 112:799-809.
Tanaka H. 2000. Thermodynamic anomaly and polyamorphism of water. Europhys Lett 50(3):340-346.
Webbs SJ, Dodds D. 1968. Inhibition of bacterial cell growth by 136gc microwaves. Nature 218: 374-375.

BIOLOGICAL COMPLEXITY AND MAGNETIC-FIELD SENSITIVITY

PIETRO VOLPE AND TAMILLA EREMENKO

AREA OF BIOPHYSICS
OF THE DEPARTMENT OF BIOLOGY,
UNIVERSITY OF ROME "TOR VERGATA", ROME, ITALY
(volpe@bio.uniroma2.it)

Abstract. This contribution points to the mechanisms of zero-frequency (DC) and oscillating (AC) magnetic field (MF) bioeffects. The survey pays particular attention to the action of artificial MFs not only at the ionic, molecular or macromolecular levels, but also at the levels of *in vitro* cycling cells, *in situ* functioning tissues or organs and total bodies. The significance of crucial findings concerning the MF-dependence of cell proliferation *vs*. cell death, extent of necrosis *vs*. apoptosis and cell membrane fluidity is judged by comparing the results obtained in a solenoid (SLD), where an MF can be added to the geomagnetic field (GMF), with those obtained in a magnetically shielded room (MSR), where the MFs can be partially attenuated or null. This comparative criterion is required because the differences detected in the experimental samples against the controls are often rather small *per se*, as observed in estimating the MF-dependence of expression of single genes or of the rates of total DNA replication, RNA transcription and protein translation. The analysis also considers the MF-dependence of the interactions between host eukaryotic cells and infecting bacteria. In the framework of studies on the origin and adaptation of life on Earth, theoretical insights paving the way to elucidate the mechanism(s) of MF-interaction with biostructures and biosystems of different orders of organization are considered.

Introduction

Since life on Earth originated in natural MFs, while a large part of the living matter became subjected to artificial MFs only in the XXth Century, a question concerning the adaptation of organisms to these new unexpected fields emerged. For instance, would an animal maintain the normal ontogenesis in an artificial MF characterized by an amplitude much greater than that in which it evolved?

In recent years, the number of reports posing this question has increased. In particular, the epidemiological aspect was debated with emphasis since the negative effects of extremely low frequency (ELF) MFs generated by 50 Hz high voltage power transmission lines, video screens, electric blankets or other home appliances, was forcibly denounced as time went by [1]. The belief that the field intensity was rationally fixed below a risk threshold functioned as objection to the alarm. However, the available data were contradictory [2]. On the one hand, a benefit from the low-energy pulsed MFs in non-union bone fracture healing and in cell regeneration was reported [3]. On the other, the influence of MFs at 50-60 Hz exerted on the nervous system [1] induced preoccupation.

In any case, the MFs showed a distinct influence on cell proliferation (Figs. 1 and 2) [4] and on the role of the calcium ions in the transduction of this influence [5-10]. In particular, it was reported that a 22 μT MF at 60 Hz modulated the calcium influx [8]. The MF-dependence of the state of the cell membrane was studied through microscopy [11] and cytofluorimetry [12]. The influence of 1-10 μT MFs at 50 Hz on the membrane conductivity and permeability was taken into account [11]. A study was performed on the effects of very weak MFs (10^{-6} to 10^{-5} T) on chicken embryogenesis [13]. The results of this investigation were confirmed in some laboratory conditions [14] and contradicted in others [15,16].

The divergences encountered in the literature with respect to the MF-dependence of certain biological structures and functions are not due only to the differences of equipment facilities or experimental accuracy, but rather to the adequacy of proposed methodological approaches. In addition, there is still a largely recognized lack of theoretical analysis to explain the mechanisms which underlie the interactions between the MFs and the various cellular targets. Thus, the main aim of this report is to draw the attention on the efforts that have been made to define the basic physical laws describing MF-biosensitivity.

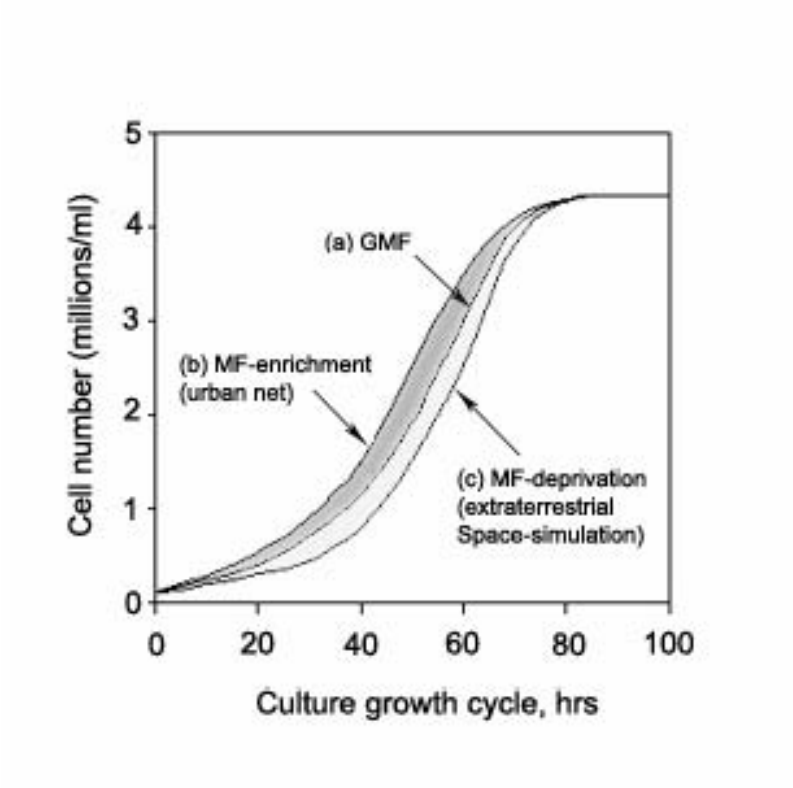


Fig. 1. *Acceleration and deceleration of cell proliferation after addition or subtraction of MFs* [4]. Cultures of *Friend erythroleukemia* cells were left to grow in parallel for about 100 hrs: (a) under the control 45 μT DC of the Earth's MF, (b) in an LSD where 70 μT at 50 Hz were added to the 45 μT DC of the Earth's MF and (c) in a MSR where the highly attenuated field essentially reflected the residual 20 nT DC of the Earth's MF and the 2.5 pT AC of the power line MF (in the MSR the 45 μT DC of the Earth's MF was attenuated 2500 times at 0.0 Hz because the AC shielding factor was estimated to be about 2500 for frequencies between 0.001 and 10000 Hz, while the applied AC MF was 30000-40000 times smaller at 50 Hz). The results represent the mean of five experiments for (b) *vs*. (a) and three experiments for (c) *vs*. (a). The Student's paired *t* test showed *P* values of 0.02 for both (b) *vs*. (a) and (c) *vs*. (a).

Is the question of the mechanisms of magnetic-field bioeffects still open?

Following the well known contributions of several laboratories which attracted the attention of the scientific community on the possible involvement in MF bioeffects of resonance at the cyclotron frequency under the combined influence of DC and AC MFs [17-20], Blanchard and Blackman [21] tried to enrich the Magnetobiology with a theory based on an ion parametric resonance model.

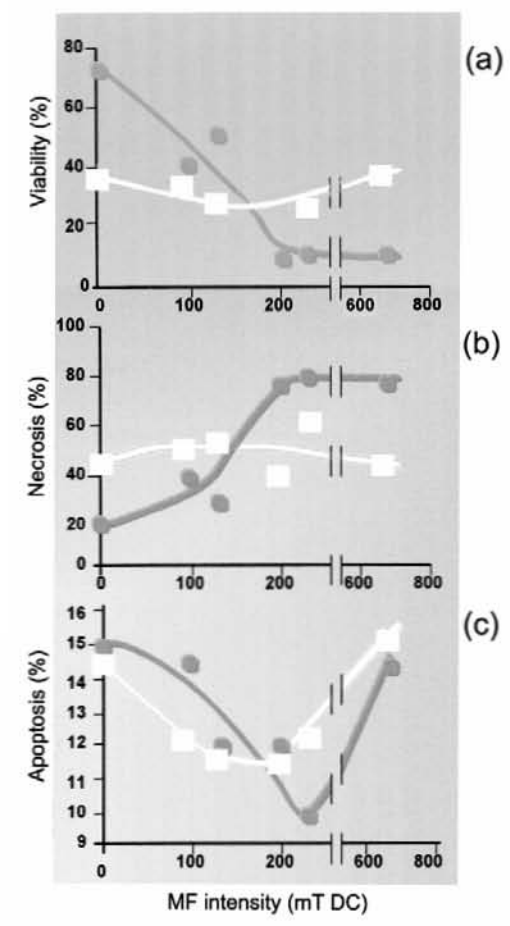


Fig. 2. *Dependence of the human macrophage viability, necrosis and apoptosis, in the absence and in the presence of mycobacterial infection, upon static MFs* [39,40]. Macrophages (MDMs), separated from PMB cells attached for 1 hr to the bottom of a flask, were subdivided, using dishes, into a number of equal samples each consisting of $1 \cdot 10^6$ MDMs in 1.5 ml of RPMI-1640 medium. Five samples were maintained for 5 days under DC MFs of various intensity, while a control sample was kept in the absence of any MF. At the end of the fifth day of exposure, each sample was washed twice with PBS, while the MDMs were detached from their dish, treated with PI and analyzed cytofluorimetrically. A parallel set of samples (each also consisting of $1 \cdot 10^6$ MDMs in 1.5 ml of RPMI-1640 medium), after a 5-day permanence in culture without MF, was infected with *Mycobacterium tuberculosis* (MTB) and maintained for another 2 days under the same MFs of various intensity (a control MTB-infected MDM sample was kept for 2 days in the absence of any MF). At the end of the second day of exposure, each MTB-infected MDM sample was washed twice with PBS, detached from the dish bottom, treated with PI and analyzed cytofluorimetrically. (**a**) Viability of the uninfected MDMs *vs*. that of the MTB-infected MDMs; (**b**) necrosis of the uninfected MDMs *vs*. that of the MTB-infected MDMs; (**c**) apoptosis of the uninfected MDMs *vs*. that of the MTB-infected MDMs. (λ-λ) Uninfected MDMs; (ρ–ρ) MTB-infected MDMs. The values represent the mean of three experiments, each performed in triplicate. The Student's paired *t* test showed *P* values of 0.04 for (a), 0.01 for (b) and 0.05 for (c).

Anyway, from a unifying physico-chemical point of view and despite the list of MF bioeffects reported earlier, the research is still unable to provide a proper explanation. For this reason, it is convenient to re-

consider, in detail, other contributions which could make the efforts more circumstantiated and allow a comprehensive theory of the MF bioeffects.

Long ago, it was suggested that the rise of a ponderomotive force caused in a biostructure by non-uniform static MFs could lie on the basis of the magnetotropism of plants, where the "paramagnetic cells" representing a minor biomass, would be forced towards a point of maximal field while the "diamagnetic cells" representing a major biomass would be forced towards the opposite direction. Studying the interaction of the neuromembrane ionic channels with the spreading action potential, Volobuev and Coworkers [22] proposed that "external" MFs interact with hypothetical "internal" MFs created by the ionic channels and nodes of Ranvier. This could explain the decrease observed in the speed of propagation of the action potentials in static MFs. Another study by Agulova and her Colleagues [23], concerning the behaviour of non-equilibrium systems in low-frequency/low-intensity MFs, distinguished the direct perception of the MF by biomolecular structures from the signalling role of the MF through the central nervous system.

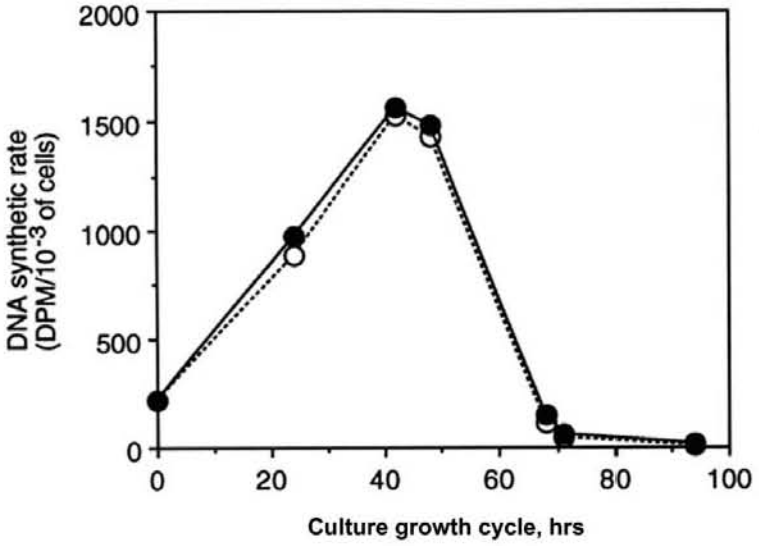


Fig. 3. *Stability of the rates of DNA replication in Friend erythroleukemia cells after their long exposure to an AC MF* [42]. The cells were pre-exposed to 70 μT at 50 Hz plus 45 μT DC of the Earth's MF for 318 days, during which they were necessarily reinoculated into a fresh medium twice per week (during each reinoculum, the cells remained in the absence of irradiation for 20 min). Then, two samples were inoculated at a density of $0.3 \cdot 10^6$ cells/ml and followed during their culture growth cycle. At intervals of 24 hrs, $2 \cdot 10^6$ cells were incubated in 2 ml of the same medium in which they grew (containing ten per cent foetal calf serum) with 2 μCi of [^{3}H]thymidine (86.1 Ci/mmol). The incubation lasted 50 min at 37 ^{o}C under shaking, in the absence of 5% CO_2 in air. The labelled cells were washed three times with PBS (without Ca^{2+} and Mg^{2+}), harvested and treated with 1 ml of 10% TCA at 4 ^{o}C for 1 hr. The TCA-precipitable material was loaded through a 0.45 μm Millipore filter and washed twice: first, with 15 ml of cold 5% TCA and, second, with 5 ml of 70% ethanol. The yielded sediment was dried at 20 ^{o}C and introduced into 10 ml of Ultima Gold scintillation liquid to measure its radioactivity. (μ-μ) Cell proliferation outside the SLD under the sole 45 μT DC of the Earth's MF; (λ-λ) cell proliferation inside the SLD under 70 μT at 50 Hz plus 45 μT DC of the Earth's MF. The experiments were repeated three times. The Student's paired *t* test showed *P* values of 0.06.

They noted an influence of the GMF variations on the precipitation and agglutination reactions in aqueous solutions and on the Piccardi test [24]. Kislovsky [25], in an attempt to explain the biovariations caused by GMF perturbations, suggested the occurrence of dissipative clathrate structures in the aqueous medium and on its borders in non-equilibrium conditions. The length of conservation of these structures was taken as an example

of near-critical phenomena that are close to the temperature of phase transitions of the second kind: liquid-liquid. In such a case, the phase transitions would be at the lower critical temperatures of stratification of the aqueous solutions, when the elements of short-range order inherent in clathrate structures are abolished.

Zhvirblis [26], being interested in the influence of solar activity on the biosphere, paid attention to the correlation of some medico-biological tests with the index of GMF perturbation, in which sector boundaries of the interplanetary MF, associated with the solar wind, were taken as zero. This study revealed that the direction along the phase trajectory contour changed when the Earth crossed the sector boundary. Vladimirsky and Temurjants [27,28], on the basis of the fact that the Piccardi test was sensitive to the polarity of a radial component of the interplanetary MF, supposed that this sensitivity could be due to the geomagnetic micropulsations in the range from 0.007 to 0.1 Hz. Therefore, they presented a list of principles concerning the influence of weak ("non-thermal") and ultraweak ("natural") AC MFs on inorganic and biological systems.

In contrast with the opinion of Binhi [29] who considered the nuclear magnetic resonance as impossible in biological magnetoreception, this list re-encouraged the idea of a possible role of nuclear magnetic resonance in the GMF variations. Hence, Lednev and Coworkers [30] suggested that the calcium-binding proteins constitute the place of primary action of combined MFs. In their opinion, these proteins cause a splitting of energetic levels of the calcium ion oscillation in the protein (*Zeman effect*) while the width of the splitting is equivalent to the cyclotron frequency of calcium and the applied DC MF. On this basis, the parametric resonance was thought as a mechanism for increasing ionic energy. Moreover, the same Authors proposed that DC, AC and combined DC+AC MFs can change the polarization degree, while the biological effects of the MFs can be induced by the same polarization degree of the calcium ion oscillation.

Binhi and Coworkers [31-33] studied the mechanism of the magnetosensitive ion binding by proteins, under the influence of external AC MFs, in the framework of an idealized quantum model. It turned out that the dissociation probability of an ion-protein complex depends on frequency and amplitude. This was shown to be a consequence of the interference of angular modes of the ion wave function.

Moreover, attention was drawn on the problem of the dielectric response of some biological tissues [34] (in relation with the orientation, in a DC MF [35], of ions, molecules and cells), while Zhadin [36] investigated the thermal oscillations of the calcium ion in a calcium-binding protein, under the influence of combined DC+AC MFs. From the study it emerged that the DC MF causes the Larmor procession of ion oscillations. Since the cyclotron frequency is twice the Larmor frequency, this led to the suggestion that the phenomenon could serve as a basis for increasing the kinetic energy of the calcium ion due to parametric resonance. In harmony with this suggestion, an AC electric field perpendicular to a DC MF (or an AC MF parallel to a DC MF) was expected to increase the ionic energy while a maximal effect was expected at the cyclotron frequency of an AC MF.

Zhadin [36] tried to solve equations of motion of the ion in a macromolecule under the influence of the MFs, considering the damping effects and the influence of particles surrounding this ion. In contrast with Lednev and Coworkers [30] and Blanchard and Blackman [21], he showed that the possibility of parametric resonance is not credible for the AC MF frequencies, being many orders of magnitude lower than the natural frequency of an ion in a macromolecule. Indeed, resonance-like phenomena were found to be induced by the influence of a DC MF alone and by a combined DC and AC MFs without any parametric resonance. Zhadin [36] estimated that the MFs may cause changes in energy of the ionic thermal motion which, in turn, would be sufficient to trigger variations in the conformational state of a macromolecule.

Does the MF-effect depend upon the complexity of given biostructures or biosystems?

The debate was focused on the theoretical basis of the MF-action on macromolecules (Fig. 3): on the one hand, it was suggested that weak extremely low-frequency MFs affect intracellular DNA directly, since the MFs must exert a force of the order of $I_{DNA} = 1.6 \cdot 10^{-13}$ A on the currents that flow in the DNA [37]; on the other, it was claimed that this conclusion is not in agreement with physical principles, since the force on the current carrying strands generated for example by a MF, B = 5 μT, would be extremely weak, i. e. equal to $F = BI_{DNA} = 8 \cdot 10^{-19}$ N/m [38]. In other words, a motion of a 1 mm long strand through a distance equal to that of the strand diameter of 2 nm represents an energy of $1.6 \cdot 10^{-33}$ J or $3.7 \cdot 10^{-13}$ kT (hence, the energy transfer from the action of the MF on the strand would be negligible compared to the energy of thermal agitation).

Whatever the conclusion of the debate will be, several years ago we suggested that, at variance with the influence of a weak AC MF on cell-cycle kinetics [4] and cell membrane fluidity [12], this field is insufficient to exert an appreciable influence on macromolecular biosynthesis [41]. This was also in harmony with recent studies concerning, on the one side, the genome stability *vs*. deprivation or enrichment of the GMF [42] and, on the other, the gene expression in a Space-simulating magnetically shielded environment [43].

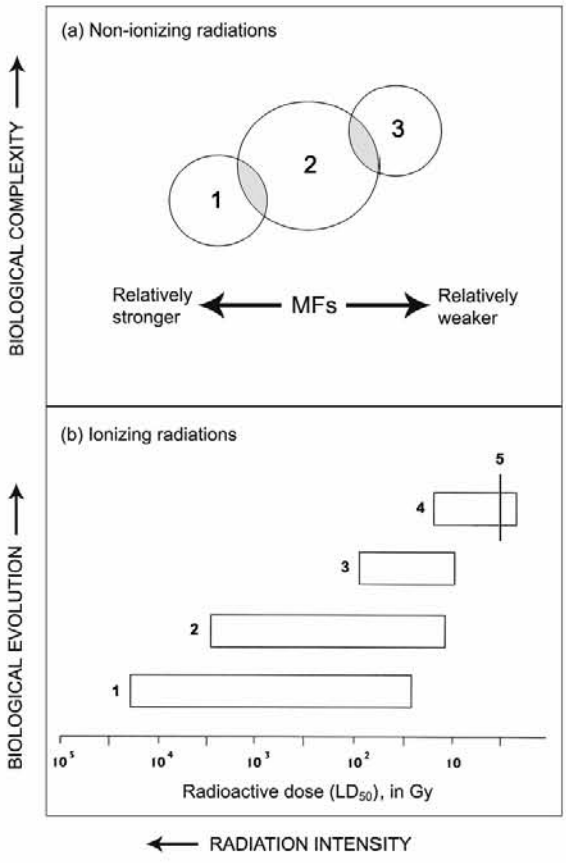


Fig. 4. *MF-sensitivity as a function of complexity of the irradiated biological target*. (**a**) Orders of organization of biostructures or biosystems invested by non-ionizing radiations: 1. molecules and macromolecules; 2. biostructures; 3. biosystems. The size of the areas reflects the results of 100 experiments, estimated from the literature, performed by using DC MFs for about 30% and AC MFs for about 70%. (**b**) Evolution of biosensitivity to ionizing radiations [85]: 1. bacterial cells; 2. plants; 3. animals with cold blood; 4. animals with warm blood; 5. Man.

Therefore, the state of the art suggests that the mechanism or the mechanisms which underlie the interactions of the MFs with the biostructures and biosystems (Fig. 4) are still an open question [44]. In this respect, it was suggested that the approach towards the non-equilibrium thermodynamics of the systems under electromagnetic (EM) waves was of primary importance [45].

It still remains to be explained why pulsed EM fields can be more active biologically than continuous ones [46]. This acquires interest in connection with the fact that an alternative basic mechanism of MF bioeffects could be the forced-vibration of all the free ions in proximity of a cell plasma membrane caused by an external AC field. The model proposed by Del Moral and Coworkers [47] explaining the bioelectric activity of single

unit neurons under DC and ELF MFs, based on the strong anisotropy of diamagnetic susceptibility of membrane phospholipids acting cooperatively (superdiamagnetism), would also seem to deserve special attention.

Remarks on the order of organization of a biological target

The observations concerning the MF-dependence of the volume of a whole cell or its nucleus [4,48] were supported by those regarding the MF-dependence of the electrokinetic properties of nuclei in human buccal epithelial cells [49]. Other studies were devoted to the analysis of the so-called "electromagnetic man" *vs*. the magnetic resonance tomography [50] and of the effect of MFs on synchronization of mammalian cell permeabilization *vs*. the MF-dependence of gene delivery [51].

From a methodological point of view, attempts were made to employ the programmed chrono-potentiometry as a tool to study electroporation and resealing of pores in bilayer lipid membranes [52] while an eu-wide initiative, to characterize the biological effects of an electromagnetic field (EMF) on human and mouse cell lines by gene expression, was taken [53].

There is a consensus about the effect of MFs on cell-cycle kinetics. In fact, the changes of FL cell-cycle kinetics, following the addition or deprivation of MFs (Figs. 1 and 2a,b) [4], were consistent with the alteration of the onset of S-phase observed after a 50 Hz MF exposure of normal human fibroblasts [54] and with variation of cell-cycle kinetics and colony forming ability after exposure of budding yeast to 50 Hz magnetic radiation [55]. This was shown to influence, in turn, the change in growth and differentiation of PC6 cells exposed to pulsed EMFs [56].

Although the question about the influence of MFs on the development of programmed cell death remains in many respects open (Fig. 2c), especially in terms of the correlation of ion homeostasis and apoptosis [57], investigations strikingly suggested that the MF causes an inhibition of apoptosis [58]. In fact, Annexin V was shown to counteract apoptosis by inducing calcium influx in human lymphocytic T cells [59] while it was demonstrated that by using the patch clamp technique there is an effect of MF exposure on the calcium channel currents [60]. It was also suggested that membrane dielectric changes may indicate induced apoptosis in HL-60 cells [61]. In any case, there was no question about the influence of the MFs on apoptosis: a transient suppression of X-ray-induced apoptosis by exposure to power frequency MFs in MCF-7 cells was evidenced [62], a change in the rate of DNA repair due to apoptosis mediated by MF exposure was detected [63], an exposure of a neuroblastoma cell line to 50 Hz MFs definitely caused changes in the apoptotic rate [64].

Here follows a list of the harmful AC bioeffects investigated at various levels.

At the morphological level, developmental changes in *Drosophila melanogaster* following exposure to alternating EMFs were observed [65] while effects of permanent MF on wing size parameters of the same insect were found [66].

At the cellular level, there were some effects of extremely low frequency EMFs on mammalian follicle development [67]. ELF EMFs as well as heat shock proved to increase microvescicle motility in astrocytes [68]. In addition, it was observed that both sedimentation and aggregation of erythrocytes were MF-dependent [69].

At the macromolecular level, while stability of the DNA replication reaction to MFs was observed (Fig. 3), electric relaxation processes were shown in lipid-bilayers after exposure to weak magnetic pulses [70]. In the framework of the studies on genotoxicity of radiofrequency signals, the occurrence of DNA damage in cultured human blood cells was seen [71] while there were clear cytogenetic effects of 900 MHz microwaves on human lymphocytes [72]. Also, there were an increase in X-ray-induced gene mutations by exposure to AC MFs in NF-kappa B-inhibited cells and an increase in hypoxanthine-guanine phosphoribosyl transferase gene mutations by exposure to electric fields [73]. ELF-pulsed MFs modulated gene expression in myocardial cells [74] while an effect of UV B radiation and 100 Hz EMFs on DNA synthesis of Jurkat cells was detected [75]. As for protein macromolecules, there was an influence of the high ELF MFs on DNA and RNA polymerases *in vitro* and on a cell-free mismatch repair [76].

At the molecular level, effects of exposure to weak radiofrequency fields on acethylcholine release in hippocampus of freely moving rats were revealed [77]. Effects of 60 Hz MF on the immune system in wistar rats was denounced [78]. Also, at the level of ionic events, factors distorting cytosolic calcium measurements in Jurkat cells during exposure to ELF MFs were revealed [79] while there was a calcium spiking in ROS 17/2.8 cells exposed to ELF EMF [80].

The hypothesis suggesting that the rescue of damaged cells may be the mechanism explaining why MFs, which are not mutagenic *per se*, are often able to increase mutation and tumor frequencies [58], is being considered in a number of laboratories. As a matter of fact, there seems to be a general consensus on MFs which may be indeed correlated with cancer [81]. Effects of a 50 Hz MF exposure were also observed on tumor experimental models [82]. The correlation of the MF action with cancer must also be added to the general concern about the harmful effect of MFs on human health.

Summary

Both old [1-16] and new [83] contributions continue to recognize, on the one hand, that the mechanisms of the MF-bioeffects are not yet understood [84] and, on the other, pave the way towards the assumption of an inverse correlation between the degree of MF-sensitivity and the order of complexity of the biological target (Fig. 4a). Such a hypothesis, by analogy, could be judged in the framework of the known inverse correlation existing between the intensity of the ionizing radiation and the evolutionary state of the species (Fig. 4b) [85]. In other words, although both AC and DC MFs do not cause electron movements inside the atom, their final action might depend on peculiar ontological and phylogenetic features of biodiversity. This idea emerged particularly from the comparison of the interactions between the MFs and the living matter at the molecular, tissue and total-body levels [84]. In fact, at variance with cell-cycle kinetics and cell membrane molecular dynamics, which unequivocally depend upon low-frequency/low-intensity MFs [4,12], the single molecular reactions, as some of those occurring in gene expression, react to these fields to a lesser extent [41-43]. An interest of the differential response to MFs, evolving as a function of the biological complexity, would also appear if one correlated Markov's "biological windows" [86] with the heterogeneous MF-sensitivity established for the various cell-cycle stages [4,54] and, thus, for the whole cell proliferation process.

Acknowledgements

This study was supported by the University of Rome "Tor vergata" and a MIUR-CNR-ENEA Project.

References

[1] A. F. Lawrence and W. R. Adey. Non linear wave mechanisms in interactions between excitable tissue and electromagnetic fields. *Neurol. Res.* 4, 115-53 (1982).

[2] A. Lacy-Hulbert, J. C. Metcalfe and R. Hesket. Biological responses to electromagnetic fields. *FASEB J.* 12, 395-420 (1998).

[3] C. A. Basset. Beneficial effects of electromagnetic fields. *J. Cell. Biochem.* 51, 387-393 (1993).

[4] T. Eremenko, C. Esposito, A. Pasquarelli, E. Pasquali and P. Volpe. Cell-cycle kinetics of *Friend erythroleukemia* cells in a magnetically shielded room and in a low-frequency/low-intensity magnetic field. *Bioelectromagnetics* 18, 58-66 (1997).

[5] M. Blank. The surface compartment model: a theory of ion transport focused on ionic processes in the electric double layers at membrane protein surface. *Biochim. Biophys. Acta* 906, 277-294 (1987).

[6] J. Walleczeck. Electromagnetic field effect on cells of the immune system: the role of calcium signaling. *FASEB J.* 6, 3177-3185 (1992).

[7] R. Glaser. Current concepts of the interaction of weak electromagnetic fields with cells. *Bioelectrochem. Bioenerg.* 27, 255-268 (1992).

[8] R. P. Liburdy. Calcium signaling in lymphocytes and ELF fields. Evidence for an electric field metric and a site of interaction involving the calcium ion channel. *FEBS Lett.* 301, 53-59 (1992).

[9] R. Karabakhtsian, N. Broude, N. Shalts, S. Kochlatyi, R. Goodman and A. Henderson. Ca^{2+} is necessary in the cell response to EM fields. *FEBS Lett.* 349, 1-6 (1994).

[10] F. S. Barnes. Effect of electromagnetic fields on the rate of chemical reactions. *Biophysics* 41, 801-808 (1996).

[11] S. Paradisi, G. Donelli, M. T. Santini, E. Straface and W. Marloni. A 50 Hz magnetic field induces structural and biophysical changes in membranes. *Bioelectromagnetics* 14**,** 247-255 (1993).

[12] P. Volpe, T. Parasassi, C. Esposito, G. Ravagnan, A. M. Giusti, A. Pasquarelli and T. Eremenko. Cell membrane lipid molecular dynamics in a solenoid *vs*. a magnetically shielded room. *Bioelectromagnetics* 19, 107-111 (1998).

[13] J. M. Delgado, J. Leal, L. Moneagudo and G. Gracia. Embryological changes induced by weak ELF EMF. *J. Anat.* 134, 533-551 (1982).

[14] A. H. Martin. Development of chicken embryos following exposure to 60 Hz MF with differing waveforms. *Bioelectromagnetics* 13, 223-230 (1992).

[15] S. Maffeo, M. Miller and E. Carstensen. Lack of effect of weak low-frequency EMF on chick embryogenesis. *J. Anat.* 139, 613-618 (1984).

[16] B. F. Sisken, I. Fowler, C. Mayaud, J. Ryaby and A. Pilla. Pulsed EMF and normal chick development. *J. Bioelectr*. 5, 25-34 (1986).

[17] A. R. Liboff. Geomagnetic cyclotron resonance in living cells. *J. Biol. Phys.* 9, 99-100 (1985).

[18] B. R. McLeod and A. R. Liboff. Cyclotron resonance in cell membranes: the theory of the mechanism. In "*Mechanistic Approaches to Interactions of Electric and Electromagnetic Fields with Living Systems"* (M. Blank and E. Findl, eds.), Plenum Press, New York, pp. 97-108 (1987).

[19] A. Chiabrera, B. Bianco, J. J. Kaufman and A. A. Pilla. Quantum dynamics of ions in molecular crevices under electromagnetic exposure. In "*Electromagnetics in Biology and Medicine*" (C. T. Brighton and S. R. Pollak, eds.), San Francisco Press, San Francisco, pp. 21-26 (1991).

[20] D. T. Edmunds. Larmor procession as a mechanism for the detection of static and alternating magnetic fields. *Bioelectrochem. Bioenerg* 30, 3-12 (1993).

[21] J. P. Blanchard and C. F. Blackman. Clarification and application of an ion parametric resonance model for magnetic field interactions with biological systems. *Bioelectromagnetics* 15, 217-238 (1994).

[22] A. N. Volobuev, B. N. Zhukov, A. U. Bakhito, E. L. Ovcinnikov and I. A. Trufanov. Influence of constant magnetic field and laser emission on neurophysiological processes. *Biofizika* 38, 372-377 (1993).

[23] L. P. Agulova, A. M. Opalinskaja and V. C. Kirjanov. Specific features of reactions of different objects sensitive to change in cosmophysical factors and action of weak electromagnetic fields. In "*Problems of Cosmic Biology*" (M. N. Gnevishev, ed.), Nauka, Leningrad, Vol. 65, pp. 160-181 (1989).

[24] G. Piccardi. The Chemical Basis of Medical Climatology, Springer, New York (1962).

[25] L. D. Kislovsky. Reaction of biological system to weak low-frequency electromagnetic fields adequate for it. In *"Problems of Cosmic Biology*" (A. M. Ugolev, ed.), Nauka, Moscow, Vol. 43, pp. 148-166 (1982).

[26] V. E. Zhvirblis. On reproducibility of heliobiological experiments. In "*Problems of Cosmic Biology*" (M. N. Gnevishev, ed.), Nauka, Leningrad, Vol. 65, pp. 145-160 (1989).

[27] B. M. Vladimirsky. Biological rhythms and the solar activity. In "*Problems of Cosmic Biology*" (V. N. Chernigovsky, ed.), Nauka, Moscow, Vol. 41, pp. 289-315 (1980).

[28] B. M. Vladimirsky and N. A. Temurjants. Nuclear magnetic resonance of weak electromagnetic field action on biological, physical and chemical systems. *Biofizika* 38, 372-377 (1996).

[29] V. N. Binhi. Nuclear spins in primary mechanisms of biomagnetic effects. *Biofizika* 40, 671-685 (1995).

[30] V. V. Lednev, N. A. Belova, I. K. Srebnitskaja, E. N. Iljasova, Z. N. Rozhdesvenskaja, A. A. Klimov, N. A. Belova and K. P. Tiras. Magnetic parametric resonance in biosystems: experimental verification of the theoretical predictions with the use of regenerating planarians *Dugestia tigrina* as a test system. *Biofizika* 41, 815-825 (1996).

[31] V. N. Binhi, Y. D. Alipov and I. Y. Belyaev. Effect of static magnetic field on *E. coli* cells and individual rotations of ion-protein complexes. *Bioelectromagnetics* 2001, 22, 79-86.

[32] V. N. Binhi. On the model ion channel-electrical solenoid. *Biofizika* 40, 549-550 (1995).

[33] V. N. Binhi. Mechanism of magnetosensitive ion binding by some proteins. *Biofizika* 42, 338-342 (1997).

[34] A. El-Lakkani. Dielectric response of some biological tissues. *Bioelectromagnetics* 22, 272-279 (2001).

[35] R. Emura, N. Ashida, T. Higashi and T. Takeuchi. Orientation of bull sperms in static magnetic fields. *Bioelectromagnetics* 22, 60-65 (2001).

[36] M. N. Zhadin. Action of magnetic fields on the ion motion in a macromolecule: theoretical analysis. *Biophyzika* 41, 832-850 (1996).

[37] M. Blank and R. Goodman. Do electromagnetic fields interact directly with DNA? *Bioelectromagnetics* 18, 111-115 (1997).

[38] R. K. Adair. Extremely low frequency electromagnetic fields do not interact directly with DNA. *Bioelectromagnetics* 19, 136-137 (1998).

[39] F. Mariani, G. Cappelli, T. Eremenko and P. Volpe. Influence of static magnetic fields on cell viability, necrosis and apoptosis. *J. Biol. Res*. 77, 71-84 (2001).

[40] P. Volpe, G. Cappelli, F. Mariani, A. Serafino and T. Eremenko. Macrophage sensitivity to static magnetic fields. In "*Biological Effects of EMFs*" (P. Kostarakis, ed.), University of Ioannina and NCSR Demokritos Publishers, Rhodes, Vol. 1, pp. 374-381 (2002).

[41] T. Eremenko, C. Esposito, P. Iacovacci, E. Tartaglini and P. Volpe. Regulation of macromolecular biosynthesis in growing erythroleukemia cells exposed to a magnetic field. In "*Annual Review of Research on Biological Effects of Electric and Magnetic fields*" (D. Wisecup, ed.), San Diego, A15, pp. 1-2 (1992).

[42] P. Volpe and T. Eremenko. Genome stability *vs*. deprivation or enrichment of the geomagnetic field. *The Environmentalist* 25, 72-82 (2005).

[43] P. Volpe and T. Eremenko. Gene expression in a Space-simulating magnetically shielded environment. *The Environmentalist* 25, 83-92 (2005).

[44] C. M. Cook, A. W. Thomas and F. S. Prato. Human electrophysiological and cognitive effects of exposure to ELF magnetic and ELF modulated RF and microwave fields: a review of recent studies. *Bioelectromagnetics* 23, 144-157 (2002).

[45] Y. P. Chukova. The general laws of biological effects of optical electromagnetic fields. In "*Biological Effects of EMFs*" (P. Kostarakis, ed.), University of Ioannina and NCSR Demokritos Publishers, Rhodes, Vol. I, pp. 318--326 (2002).

[46] D. J. Panagopoulos, N. Messini, A. Karabarbounis, A. L. Filippetis and I. H. Margaritis. A mechanism for action of oscillating electric fields on cells. *Biochem. Biophys. Res. Commun.* 272, 634-640 (2000).

[47] A. Del Moral, M. J. Azanza, A. C. Calvo and R. N. Perez-Bruzon. Cooperative diamagnetism and Ca^{2+} liberation of plasma membrane molecules explains the neuron responses to applied static and extremely low frequency magnetic fields. In "*Biological Effects of EMFs*" (P. Kostarakis, ed.), University of Ioannina and NCSR Demokritos Publishers, Rhodes, Vol. 1, pp. 298-308 (2002).

[48] S. Grimaldi, D. Pozzi, M. Santoro, A. Lisi, E. Pasquali, A. Serafino, L Giuliani, M. Vignati, T. Eremenko and P. Volpe. Magnetic field is affecting biophysical and morphological properties of mammalian cells. In "*2nd Workshop on Biostructures and Biosystems*" (Italian Society of Biophysics, ed.), SIB Publishers, Portonovo, Abstr., C, 25 (1997).

[49] Y. G. Shokorbatov, V. G. Shakhbazov and A. O. Rudenko. Modification of electrokinetic properties of nuclei in human buccal epithelial cells by electric fields. *Bioelectromagnetics* 22, 106-111 (2001).

[50] F. Bistolfi. Electromagnetic man and magnetic resonance tomography: Update on the biological effects and new paths of research. *Riv. Neuroradiol*. 14, 63-82 (2001).

[51] M. Golzo, J. Teissie and M. P. Rols. Cell synchronization effect on mammalian cell permeabilization and gene delivery by electric field. *Biochem. Biophys. Acta* 1563, 23-28 (2002).

[52] S. Koronkievicz, S. Kalinowsky and K. Bryl. Programmable chronopotentiometry as a tool for the study of electroporation and resealing of pores in bilayer lipid membranes. *Biochem. Biophys. Acta* 1561, 222-229 (2002).

[53] C. Maercker, J. Czyf, A. M. Wobus, W. Huber, A. Poustka, S. Ivancsits, H. W. Ruediger, O. Jhan, E. Diem, J. Schuderer, N. Kuster, D. Fornasari, F. Clementi, K. Schlatterer, R. Tauber, R. Fitzner, J. Reivenen, F. Aldokofer and D. Leszczynski. An eu-wide initiative to characterize the biological effects of EMF on human and mouse cell lines by gene expression profiling. In "*Biological Effects of EMFs*" (P. Kostarakis, ed.), University of Ioannina and NCSR Demokritos Publishers, Rhodes, Vol. II, pp. 588-594 (2002).

[54] N. A. Cridland, R. G. E. Haylock and R. D. Saunders. 50 Hz magnetic field exposure alters onset of S-phase in normal human fibroblasts. *Bioelectromagnetics* 20, 446-452 (1999).

[55] A. Markkanen, J. Juutilainen, S. Lang, J. Pelkonen, T. Rytomaa and J. Naarala. Effects of 50 Hz magnetic field on cell-cycle kinetics and the colony forming ability of budding yeast exposed to ultraviolet radiation. *Bioelectromagnetics* 22, 345-350 (2001).

[56] J. P. Shah, P. Midkiff, P. C. Brandt and B. F. Sisken. Growth and differentiation of PC6 cells: the effects of pulsed electromagnetic fields (PEMF). *Bioelectromagnetics* 22, 267-271 (2001).

[57] S. P. Yu, L. M. T. Canzoniero and D. W. Choi. Ion homeostasis and apoptosis. *Curr. Opin. Cell Biol*. 13,405-411(2001

[58] C. Fanelli, S. Coppola, R. Barone, C. Colussi, G. Gualardi, P. Volpe and L. Ghibelli. Magnetic fields increase cell survival by inhibiting apoptosis via modulation of Ca^{2+} influx. *FASEB J*. 13, 95-102 (1999).

[59] C. Gidon-Jeangirard, E. Solito, A. Hofman, F. Russo-Marie, J. M. Freyssinet and M. C. Martinez. Annexin counteracts apoptosis while inducing Ca^{2+} influx in human lymphocytic T cells. *Biochem. Biophys. Res. Commun.* 265, 265-215 (1999).

[60] M. Obo, S. Konishi, Y. Otaka and S. Kitamura. Effect of magnetic field exposure on calcium channel currents using patch clamp technique. *Bioelectromagnetics* 23, 306-314 (2002).

[61] X. Wang, F. F. Becker and P. R. C. Gascoyne. Membrane dielectric changes indicate induced apoptosis in HL-60 cells more sensitively than surface phosphatidylserine expression or DNA fragmentation. *Biochem. Biophys. Acta* 1564, 412-420 (2002).

[62] G. R. Ding, T. Nakahara, R. R. Tian, Y. Guo and J. Miyakoshi. Transient suppression of X-ray-induced apoptosis by exposure to power frequency magnetic fields in MCF-7 cells. *Biochem. Biophys. Res. Commun.* 286, 953-957 (2001).

[63] J. G. Robinson, A. R. Pendieton, K. O. Manson, B. K. Murray and K. L. O'neill. Decreased DNA repair rates and protein from heat induced apoptosis mediated by electromagnetic field exposure. *Bioelectromagnetics* 23, 106-112 (2002).

[64] A. Negroni, M. C. Pirozzoli, G. A. Lovisolo, L. Mosiello, C. Laconi and C. Marino. Exposure to 50 Hz magnetic fields of a neuroblastoma cell line: effects on apoptosis. In "*Biological Effects of EMFs*" (P. Kostarakis, ed.), University of Ioannina and NCSR Demokritos Publishers, Rhodes, Vol. II, pp. 865--868 (2002).

[65] G. Mirabolghasemi and M. Azarnia. Developmental changes in *Drosophila melanogaster* following exposure to alternating electromagnetic fields. *Bioelectromagnetics* 23, 416-420 (2002).

[66] M. Stamenkovich-Radak, I. Kitanovic, Z. Prolic, I. Tomisic, B. Stoijkovic and M. Andjelkovic. Effects of permanent magnetic field on wing size parameters in *Drosophila melanogaster*. *Bioelectromagnetics* 22, 365-369 (2001).

[67] S. Cecconi, G. Gualtieri, A. Di Bartolomeo, G. Troiani, M. G. Cifone and R. Canipari. Evaluation of the effects of extremely low frequency electromagnetic fields on mammalian follicle development. *Hum. Reprod.* 15, 2319-2325 (2000).

[68] F. Golfert, A.Hoter, M. Thrummler, H. Bauer and R. H. W. Funk. Extremely low frequency electromagnetic fields and heat shock can increase microvesicle motility in astrocytes. *Bioelectromagnetics* 22, 71-78 (2001).

[69] M. Lino and Y. Okuda. Osmolality dependence of erhythrocyte sedimentation and aggregation in strong magnetic field. *Bioelectromagnetics* 22, 46-52 (2001).

[70] A. Pazur. Electric relaxation processes in lipid-bilayers after exposure to weak magnetic pulses. *Zeitschr. Natur. J. Biosci.* 56, 831-837 (2001).

[71] R. R. Tice, G. G. Hook, M. Donner, D. I. McRee and A. W. Guy. Genotoxicity of radiofrequency signals: I. investigation of DNA damage and micronuclei induction in cultured human blood cells. *Bioelectromagnetics* 23, 113-126 (2002).

[72] A. Maes, M. Collier and L. Vershaeve. Cytogenetic effects of 900 MHz (GSM) microwaves on human lymphocytes. *Bioelectromagnetics* 22, 91-96 (2001).

[73] G. R. Ding, K. Wake, M. Taki and J. Miyakoshi. Increase in hypoxanthine-guanine phosphoribosyl transferase gene mutations by exposure to electric field. *Life Sci.* 68, 1041-1046 (2001).

[74] C. Ventura, M. Maioli, G. Pintus, G. Gottardi and F. Bersani. Elf-pulsed magnetic fields modulate opioid peptide gene expression in myocardial cells. *Cardiov. Res*. 45, 1054-1064 (2000).

[75] G. Nindi, E. F. Hughes, M. T. Johnson, D. N. Vesper and W. X. Balcavage. Effect of ultraviolet B radiation and 100 Hz electromagnetic fields on proliferation and DNA synthesis of Jurkat cells. *Bioelectromagnetics* 23, 455-463 (2002).

[76] S. Herada, S. Yamada, O. Kuramela, Y. Gunji, M. Kawasaki, T. Miyakawa, H. Yonekura, S. Sakurai; K. Bessho, R. Hosono and H. Yamamoto. Effects of high ELF magnetic fields on enzyme-catalyzed DNA and RNA synthesis *in vitro* and on a cell-free mismatch repair. *Bioelectromagnetics* 22, 260-268 (2001).

[77] G. Testylier, L. Tonduli, R. Malablau and J. C. Debouzy. Effects of exposure to low level radiofrequency fields on acethylcholine release in hippocampus of freely moving rats. *Bioelectromagnetics* 23, 249-255 (2002).

[78] A. C. T. De Lucia, C. W. S. F. Anselmo, I. M. Oliveira, M. B. Filho and M. T. J. De Almeida Catanho. Effects of 60 Hz electric and magnetic field on the immune system in the wistar rats. In "*Biological Effects of EMFs*" (P. Kostarakis, ed.), University of Ioannina and NCSR Demokritos Publishers, Rhodes, Vol. II, pp. 837--845 (2002).

[79] C. R. McCreary, A. W. Thomas and F. S. Prato. Factors confounding cytosolic calcium measurements in Jurkat E6.1 cells during exposure to ELF magnetic fields. *Bioelectromagnetics* 23, 315-328 (2002).

[80] R. Shahidain, R. D. Mullins and J. E. Sisken. Calcium spiking and baseline calcium levels in ROS 17/2.8 cells exposed to extremely low frequency electromagnetic fields (ELF EMF). *Internat. J. Rad. Biol.* 77, 241-248 (2001).

[81] C. E. Minder and D. H. Pfluger. Minder and Pfluger respond to "Electromagnetic fields and cancer in railway workers" by Savitz. *Amer. J. Epidemiol*. 153, 839-840 (2001).

[82] P. Galloni and C. Marino. Effects of 50 Hz magnetic field exposure on tumor experimental models. *Bioelectromagnetics* 21, 608-614 (2000).

[83] A. Morelli, S. Ravera, I. Panfoli and I. M. Pepe. Effects of extremely low frequency electromagnetic fields on membrane-associated enzymes. *Arch. Biochem. Biophys*. 441, 191-198 (2005).

[84] P. Volpe. Interactions of zero-frequency and oscillating magnetic fields with biostructures and biosystems. *Photochem. Photobiol. Sci.* 2, 637-648 (2003).

[85] P. Volpe. Introduzione alla Biofisica delle Radiazioni. Unesco Office Publishers, Venice, pp. 1-256 (1999).

[86] M. S. Markov. Myosin phosphorylation - a plausible toole for studying "biological windows". In "*Biological Effects of EMFs*" (P. Kostarakis, ed.), University of Ioannina and NCSR Demokritos Publishers, Kos, Vol. I, pp. 1-9 (2004).

MODELS OF NEURONE DYNAMICS: SPONTANEOUS AND UNDER ELF ALTERNATING MAGNETIC FIELD

A. DEL MORAL(*), MARÍA J. AZANZA(+) AND R. N. PÉREZ-BRUZÓN(+)

(*) LABORATORIO DE MAGNETISMO DE SÓLIDOS, DEPARTAMENTO DE FÍSICA DE MATERIA CONDENSADA AND ICMA, UNIVERSIDAD DE ZARAGOZA AND CSIC, 50009 ZARAGOZA, SPAIN.
(+) LABORATORIO DE MAGNETOBIOLOGÍA, DEPARTAMENTO DE ANATOMÍA E HISTOLOGÍA HUMANAS, FACULTAD DE MEDICINA, UNIVERSIDAD DE ZARAGOZA, 50009 ZARAGOZA, SPAIN.

Abstract

We report about a developed model of single neurone dynamics from where we calculate the effects of low frequency (ELF) magnetic field (MF) upon single neurones and simple neurone networks. Calculations are based on the membrane phospholipids (PP) superdiamagnetism and Ca^{2+} coulomb explosion model and on an extension of the Hodgkin & Huxley (HH) equation under MF. *Integration* of HH equation, under AC MF application, by assuming the membrane as a Kirchoff electrical knot, and within the relaxation-time, τ approximation for the HH n(t), m(t) and h(t) characteristic conductance functions have been performed, obtaining the theoretical time dependence of membrane voltage for hyperpolarization (H) and depolarization (D) processes, so allowing a determination of K^+, τ_K, and Na^+, τ_{Na} relaxation times. Calculated frequency spectra of single bioelectric impulse H and D voltages are *lorentzians*, as experimentally observed in single unit neurones of mollusc *Helix aspersa*. On the other hand a model which explains the *frequency window effect* (FWE) in neural tissue is developed, explaining Bawin & Adey's first FWE observation in chicken brain and also our observations of FWE in mollusc *Helix aspersa*, both respectively showing *lorentzian* dependencies for Ca^{2+} efflux, $\phi(f_M)$ and bioelectric frequency $f(f_M)$ with AC MF frequency, f_M i.e a resonance when spontaneous $f_0 = f_M$.

1.- Introduction.-

In the bioelectric activity of neural tissue, either spontaneous or under applied magnetic field (MF) there appear two issues: the generation and structure of the bioelectric impulse and the frequency of it, to which we should add the sinusoidal or alternating (AC) MF induced firing correlation observed between neurones or *AC-MF-synchronization effect* (1). The generation of the impulse, after the refractory time, is one of the main problems of neurone physiology, during which the ATP-Na/K pumps operate. The process by which the impulse starts it is thought to be the result of small sub-threshold voltages sum up to a threshold voltage, V_S where the depolarization (D) process starts, with the entrance of Na^+ ions to the cell, through voltage activated Na^+-channels. We are not going to treat here this problem, but about the time shape of the impulse once it is formed, dividing it in D and hyperpolarization (H, due the sorting out of K^+ ions through delayed rectifier voltage-operated K^+-channels). The MF effect on electrogenic pumps, which promote the entrance of $3\,K^+$ ions against the sorting out of $2\ Na^+$ ions, making the membrane going to the resting potential, was already considered elsewhere (2), so completing the full scenario. The MF effect on the refractory process is the decrease of impulse D amplitude. All those impulse parts we will see are explained by the *integration* of the Huxley & Hodgkin (HH) equation (3), supplemented by the MF produced Ca^{2+} current, that has been done by assuming the membrane as a Kirchoff *electric knot*, instead of as a parallel conductances network as done so far (4). Regarding to the second issue, the neuron impulse frequency, *f* strongly changes with the MF intensity, B and in the case of AC MF with the RMS field intensity, $B_{eff} = B_0/\sqrt{2}$ (B_0 is the AC MF amplitude) and also with the AC MF frequency, f_M. With all those models we have conformed a full picture of the single unit neurone bioelectric behaviour, either for spontaneous regime or under AC MF, this of extremely low frequencies (ELF).

2.- Superdiamagnetism (SD) and Ca^{2+} coulomb explosion (CE) model under AC magnetic fields.-

The explanation of above effects will be based on the membrane phospholipid (PP) *superdiamagnetism* (SD) and Ca^{2+} *coulomb explosion* (CE) model (5, 6). This model has been widely tested in single neurones and simple neurone networks under static and ELF MF respectively, where in the latter the MF also induces a *synchronized* bioelectric activity within those networks (1, 7). The model contemplates three ingredients: i) the anisotropy of the diamagnetic susceptibility tensor components, $\tilde{\chi}$ (< 0) of the long PP "rods", or difference $\Delta\chi = \chi_{\parallel} - \chi_{\perp}$, between the directions parallel ($\parallel$) and perpendicular ($\perp$) to the PP axis; ii) the well proved cluster formation in the membrane liquid crystal of *correlated* PP long axes through their electric quadrupolar moments, $\tilde{Q}_i$ interaction, of pair (i, j) correlation function $C_Q = \tilde{Q}_i\tilde{Q}_j - \tilde{Q}_i\ \tilde{Q}_j$, by which the PPs cooperatively rotate out from the MF **B** axis (SD; PP electric dipolar moment is very weak). ... is the ensemble thermal average. The correlation length, ξ usually exceeds a single neurone, *via* the PPs of the interposed glia membranes between neurones, and through the gap junctions (8); iii) when the Ca^{2+} ions attached to their PP bilayer inner and outer binding sites (polar heads) happen to be nearest-neighbours (NN, in number N_{nn} per cluster face, with estimated $N_{nn} \cong 0.007\,N_c$, N_c being the PP number per cluster), and the NN PPs suffer opposite (with clearly 1/2 probability) magnetic torques $\boldsymbol{\tau}_m = \pm\mathbf{m}\,x\,\mathbf{B}$, the weak ionic bindings are broken by their mutual coulomb repulsion, of energy ε_{coul}. This produces a *simultaneous* detaching (coulomb explosion, *CE*) of Ca^{2+} pairs (see Fig.1 for a view of the mechanisms involved). Note that the Ca^{2+} water solvating and dielectric mem-

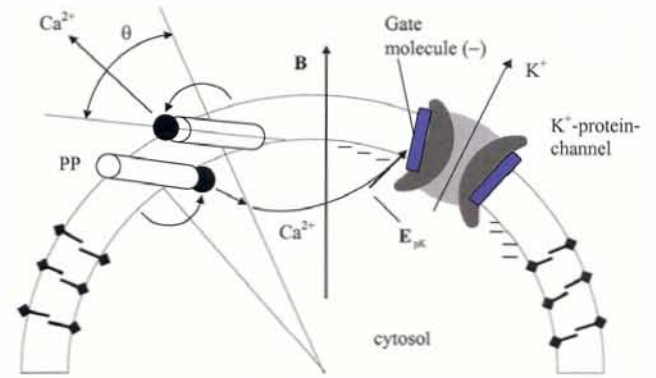


Fig.1.- Schematic view of the mechanisms involved in the SD-CE model. The circular shell represents the membrane neurone phospholipid (PP) bilayer. Two nearest-neighbour Ca^{2+}-charged phospholipids (rods) rotate under their assumed opposite magnetic torques, approaching the Ca^{2+} ions (black circles), attached to the PP negatively charged heads (lozenges). The ions become simultaneously detached from the membrane surfaces when their weak ionic bonds to the heads are broken due to Ca^{2+}-Ca^{2+} coulomb repulsion. Within the cytosol the Ca^{2+} ions diffuse towards the K^+-protein channels, which are opened when Ca^{2+} is captured by the "gate" molecule (calmodulin), giving rise to the K^+ outwards current (hyperpolarization).

brane negative electric images formation reduce the Ca^{2+} effective charge to only $q_{ef} \cong 0.025\ q_{Ca^{2+}}$, making the ionic bond energy, ε_{bind} rather weak. But since ε_{bind} is supplemented by the water-PP surface tension energy the bond becomes stable against *normal* to the surface thermal fluctuations (of energy $(1\ 2)k_BT \cong 8$ meV at r.t.) (5)**.** $\mathbf{m} = \tilde{\chi}\mathbf{H}$ is the field induced diamagnetic PP magnetic moment and it rotates out from **B** axis because $\chi_{\parallel} > \chi_{\perp}$, therefore alternatively approaching the NN Ca^{2+} charged PP heads (Fig.1). The PP magnetic energy is given by $\varepsilon_m = -(1\ 2\mu_0)B^2(\chi_{\perp} + \Delta\chi\cos^2\theta)V$, where θ is the angle formed by the PP axis with **B** and $\boldsymbol{\tau}_m = -(\partial\varepsilon_m\ \partial\theta)\hat{\boldsymbol{\theta}}$, which acts against the opposite coulomb repulsion torque, $\boldsymbol{\tau}_r = -(\partial\varepsilon_{coul}(\theta)\ \partial\theta)\hat{\boldsymbol{\theta}}$ (V is the PP volume). Under AC MF the scenario is the detaching from the cluster of gaussian bursts of Ca^{2+} ions for about half a MF cycle, since the magnetic torque is oscillatory, i.e. $\tau_m = (1\ 2\mu_0)B_0^2\,\Delta\chi\ \sin 2\theta(t)\ \sin^2\omega_M t$. The Ca^{2+} detaching occurs when $N_{nn}(\varepsilon_{coul}(\theta) - \varepsilon_{bind}) + N_c\varepsilon_m(\theta) \cong 0$, a condition that allows to weak MF to detach about 7 Ca^{2+} per 10^3 PP for large enough N_c (5, 6). Note that the small q_{eff}, the interposed membrane dielectric constant ($\in_r \cong 2.6$) and the final Ca^{2+}-Ca^{2+} approaching distance $d_f \cong 5.3$nm yield a small energy $\varepsilon_{coul}(\theta_f) = (1\ 4\pi \in_r \in_0)(q_{eff}^2\ \ d_f^2)$ at the coulomb explosion angle θ_f. The MF detaching process, which occurs within a spherical apex of 120º around **B**, produces a cytosol Ca^{2+} concentration about ten times the normal one and similar to the produced one in the D process (see (6) for greater detail).

The main result from the SD-CE model (5, 6) is the *field intensity dependence* of the neurone bioelectric frequency, $f(B_{eff},T)$. This frequency is controlled by chemistry mass action law between Ca^{2+} and membrane binder radical, R^- (sialic acid outside and phosphatidylserine inside), i.e. $[Ca^{2+}][R^-]=k(T,B_{eff})[CaR]$, where k is the kinetics constant. Thus $f \propto [R^-]$ becomes inversely proportional to the number of Ca^{2+} ions detached per cluster, $N^c_{Ca^{2+}} = N_{nn}\exp(-\Delta E_c\ k_B T)$, where $\Delta E_c(\theta)=-(N_c\varepsilon_m+N_{nn}\varepsilon_{coul})$ is the *dynamic* Peierls's energy barrier to be overcome by the Ca^{2+} ion in order for the PP to steadily rotate. Moreover under AC MF the H process (where the cytosol becomes more negative due the K^+ ions sorting out) is modified by the Ca^{2+} ions (in number of four) binding to the K^+ protein-channel (more specifically to the calmodulin "gate" molecule) and opening it due to the calmodulin electrical unfolding (9). Therefore it should be $f \propto 1\ N_{Ca^{2+}}$, to first order. Summing now $N^c_{Ca^{2+}}$ from all the PP clusters in membrane (s), the final result is that the neurone bioelectric frequency varies with RMS MF as (5, 6)

$$f(B_{eff},T)=f(0,T)\exp(-\alpha B^2_{eff}), \qquad [1]$$

where $f(0,T)\equiv f_0$ is the *spontaneous* frequency and the parameter $\alpha = N_c\ \chi_\perp\ V\ 2\mu_0 k_B T$, that encompasses the PP cluster physical properties and membrane temperature, T. As mentioned before for ELF AC MF (quasistatic) we have introduced in [1] the RMS B_{eff}, since magnetic energy density stored in the membrane is $B(t)^2\ 2\mu_0$, of time average $B^2_{eff}\ 2\mu_0$. Eq.[1] has been widely and firmly tested in single neurones of *Helix aspersa* for static (5) and ELF weak MF (1,11) and for T modification, by using standard microelectrode transmembrane voltage real time recording technique. In fact for weak ELF MF the observed *f* in *Helix* neurones follows a dependence $f(B_{eff})\cong f(0)(1-\alpha B^2_{eff})$, which precisely is the obtained one by performing a series expansion of [1] for $\alpha B^2_{eff} << 1$ (1). Regarding to *f* (T) dependence, preliminary observations in mapped *Helix* neurones F47 and F2 show that *f* first decreases with increasing T at fixed B_{eff}, in disagreement with eq.[1] (see Fig.2). The reason is that those neurones belong to the $\approx$ 26% of studied ones where *f increases* with increasing B_{eff} (6). The responsible mechanism is that the by MF detached Ca^{2+} ions depolarize the membrane, cytosol becoming more positive, so opening Na^+ and/or Ca^{2+} channels operated by voltage. Also D amplitude V_d *decreases*, the calculated variation in V_d being $\Delta V_d(B_{eff})=-(4\pi N_c)E_p\exp(+\alpha B^2_{eff})$, where E_p is the pump e.m.f. , due to opposite to PP protein pump rotation (since $\chi < \chi_\perp$), where PP partially cover the protein pump (2). Also observed are two transitions in the form of increasing *f* within a ΔT small interval, at $T_{f1}\approx 30^oC$ and $T_{f2}\approx 37^oC$, corresponding to phase transitions within the membrane liquid crystal. After second transition *f* decreases with T increase, now in agreement with [1], although temperature behaviour requires deeper investigation, and PP liquid crystal viscosity energy dissipation, $\varepsilon_v=-\eta_r(T)\theta(t)$ introduction in SD - CE model (η_r is the viscosity coefficient).

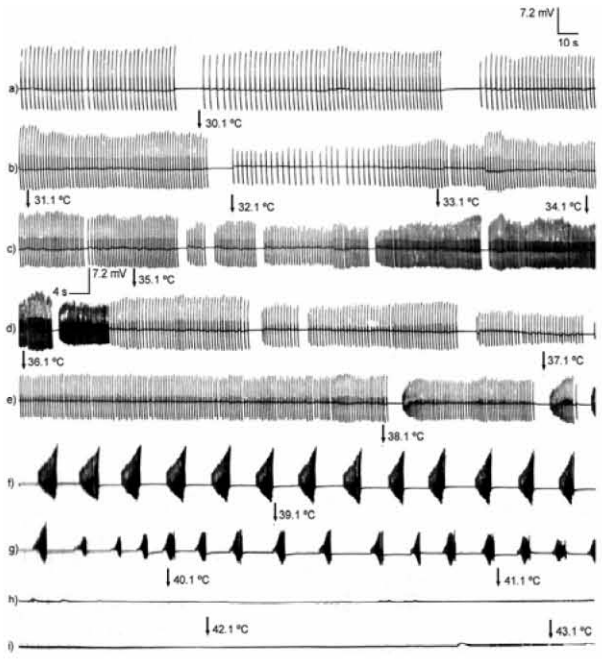


Fig.2.- Temperature effect for neurone F47 bioelectric activity. Transitions at 30ºC and 37ºC are observed.

3.- Biolectric impulse shape and frequency spectrum.-

The D and H main trams of bioelectric impulse (Fig.3) in neurones are controlled by the well known Hodgkin & Huxley equation (3). This equation has been usually referred to an equivalent electric circuit of in

parallel conductances, membrane capacitance, C_m and DC generators, the latter being the equilibrium Nersnt $Na^+$and K^+e.m.f., E_{Na} and E_K, due to the ions electrochemical gradients. Consideration of this network by meshes does not allow its solution, and we will consider the membrane as a knot where the currents concur

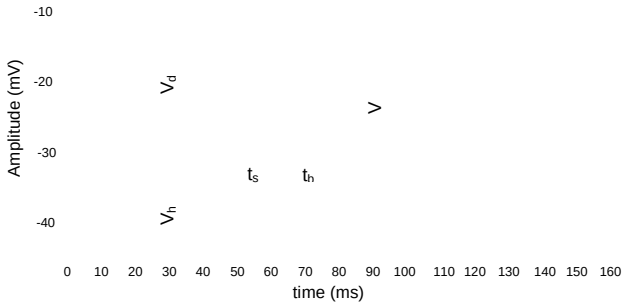


Fig.3.- Neurone V-14 impulse of *Helix* , with D, R and H trams.

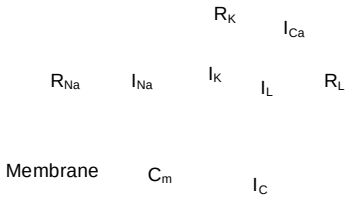


Fig.4.- Membrane equivalent Kirchoff electric knot.

(Fig.4). Therefore HH equation takes the knot law of charge conservation (no charge accumulation in membrane),

$$C_m(dV\ dt)+g_{Na}m(t)^3h(t)(V-E_{Na})+g_K n(t)^4(V-E_K)+g_L(V-V_L)-I_{Ca}(B_{eff},t)=0 \quad , \qquad [2]$$

where V is the transmembrane voltage, g_i (i =Na, K, L) the channels conductances. m and n are the HH channel excitatory and h inhibitory functions, of microscopic origin not yet well known, although the phenomenologically needed powers four, point out to four independent processes, acting for the opening (m, n) and closing (h) of corresponding channels. Leakage (L) channels and ligand operated ones are probably responsible for the setting of the threshold voltage, V_s but current through them is weak and here neglected. Finally, HH currents have been supplemented by the Ca^{2+}current produced by MF (*HH magnetic* (HHM) equation). We will solve eq.[2] in the *relaxation time, τ, approximation* for the HH functions, where e.g.

$$dn\ dt=-n(t)\ \tau_K \qquad [3]$$

where n(t) is assumed to be proportional to the number of K^+-channels which remain closed at time t. Integration of [3] taking t = 0 at the beginning of repolarization (R) plus H process, yields $n(t)=n_0\exp(-t\ \tau_K)$. Similarly taking t = 0 at the beginning of D process we obtain that function $m(t)=m_0\exp(-t\ \tau_{Na})$. Otherwise the inhibition function at D process follows the equation $dh\ dt=+h(t)\ \tau_{inh}$, of integral $h(t)=h_0\exp(+t\ \tau_{inh})$. We will now obtain the membrane voltage V(t) dependence, partitioning the impulse in the mentioned regimes.

Repolarization and hyperpolarization: these two processes follow one after other and it is well known that in the R+H process only K^+-channels are open and therefore [2] becomes, $C_m(dV\ dt)+g_K n(t)^4(V-E_K)-I_{Ca}(B_{eff},t)=0$, which integration after substitution of n(t) yields

$$V_K(t)=E_K+(E_{Na}-E_K)\exp\left[-(g_K n_0^4\tau_K\ \ 4C_m)(1-e^{-4t\ \tau_K})+\int_0^t dt'\ I_{Ca}(B_{eff},t')\ (V_K(t')-E_K)\right], \qquad [4]$$

which is an integral equation with kernel $I_{Ca}(B_{eff},t)$. We will show below (from [1] and [9]) that $I_{Ca}(B_{eff},t)=-(N(0)f(B_{eff}=0)q_{Ca}\ \ \tau_{Ca})\exp(-\alpha B_{eff}^2)\exp(-t\ \tau_{Ca})$, where N(0) is the initial Ca^{2+} ion number in a burst and τ_{Ca} the Ca^{2+} relaxation time (diffusion time in the cytoplasm) (t origin in [4] is taken at $V(t)=E_{Na}$, origin of R). For comparison with experimental results in single neurones, it is useful to work in frequency domain, ω, so that we will obtain the *frequency spectrum* of spontaneous impulse $V_K(t)$. Fourier transform of [4] exp[…] function is unknown, but for $t<\tau_K$ first exponential can be series expanded, so obtaining

$$V_K(t)\approx E_K+(E_{Na}-E_K)\left[1-(g_K n_0^4\tau_K\ \ 4C_m)(1-e^{-4t\ \tau_K})+\int_0^t dt'\ I_{Ca}(B_{eff},t')\ (V_K(t')-E_K)\right]. \qquad [5]$$

The ω spectrum of [5] *spontaneous* $V_K(t)$ ($I_{Ca} = 0$) is obtained by Fourier transforming $V_K(t)$ around a central frequency ω_0^*, characteristic of the impulse, yielding (except for a Dirac $\delta(\omega - \omega_0^*)$ artefact introduced by the exponential series cut-off)

$$V_{Na}(\omega) = A^* \Big/ \left[(\omega - \omega_0^*)^2 + (\Delta\omega/2)^2 \right] , \qquad [6]$$

where $A^* \equiv g_K n_0^4 \tau_K / 4C_m$ and $\Delta\omega/2 = 2\pi/\tau_K$ the HMHW, which provides τ_K. Therefore the impulse spectrum is the familiar *lorentzian* function, taking its maximum value at $\omega = \omega_0^*$. Eqs. [5] and [6] can be easily extended to the real situation of having different types of K^+-channels (up to seven in *Helix aspersa* (13)), but this extension is not suitable for comparison with the impulse because of the too large number of parameters involved.

Depolarization: this process follows after the refractory time and threshold voltage establishment, and since involved Na^+ channels are operated by voltage, inclusion of Ca^{2+} current sums only a term to $V_{Na}(t)$. But also retarded in time K^+ channels are opened, although being in small number during D tram their current can be neglected. The HHM relevant equation is then $C_m(dV/dt) + g_{Na} m(t)^3 h(t)(V - E_{Na}) - I_{Ca}(B_{eff}, t) = 0$, which in presence of MF yields another integral equation. Integration followed by the first exponential expansion as before yields

$$V_{Na}(t) \approx E_{Na} \left[1 - (g_{Na} m_0^3 h_0 \tau_{eff} / 3C_m) \exp(-t/\tau_{eff}) + \int_0^t dt' \, I_{Ca}(B_{eff}, t') \Big/ (V_{Na}(t') - E_{Na}) \right], \qquad [7]$$

where the relaxation time is given by $\tau_{eff}^{-1} = \tau_{Na}^{-1} - \tau_{inh}^{-1}/3$, since the inhibition and activation are independent processes. As before the ω-spectrum of spontaneous $V_{Na}(t)$ is lorentzian of $\Delta\omega/2 = 2\pi/\tau_{eff}$, and $A^* \equiv g_{Na} m_0^3 h_0 \tau_{eff} / 3C_m$. Extension to different kinds of Na^+-channels is not worthwhile because of above mentioned reason.

Comparison with experiments in single neurones: we will compare our HHM model with electrophysiological experiments performed on *Helix aspersa* single unit neurones, a good bench for present studies. Thus in Fig.5 we present the spontaneous ($B_{eff} = 0$) R+H potential time variation for two mapped neurones (14), fitted by the approximate solution [5], the agreement being reasonable, but where we do not reproduced the sigmoidal variation at the ends, due to the series cut-off in [4]. The more "accurate" used "sigmoidal" fit by $(1 - e^{-t/\tau_K})^4$ is also shown, but its basis is purely phenomenological. We took $E_K = -75\,mV$, $E_{Na} = +50\,mV$ (this e.m.f. rectified by the delayed K^+ channels), $g_K = 1.6 \times 10^{-7} m^{-2} \Omega^{-2}$ and $C_m = 4 \times 10^{-2} Fm^{-2}$, and from the fits we obtained the n_0 and τ_K values quoted in Table 1. Clearly we can not identify n_0 with the number of K-protein channels (KP), with a density of ≈ 7 KP/μm^2, which for a neurone of 100 μm diameter yields $\approx 2x10^4$ KP. In Fig.6 we show the frequency spectrum of a bioelectric impulse of neurone V19, together with the fitted theoretical one by eq. [6] , using the parameter values of Table 1 the agreement being excellent, the same happening for other neurones (not shown). Under applied AC MF we have observed that shape of the impulse becomes *unmodified*, which means that the solution of full integral eq.[4] is not needed. Integral eqs. [4] and [7] can be easily transformed into second order linear differential equations of well known solutions, not given here.

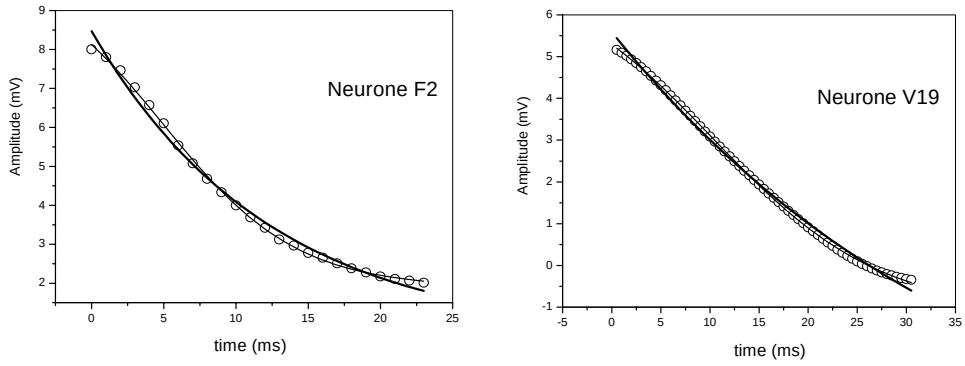


Fig.5.- Experimental (o) and model (thick line) R+H time variations for neurones F2 and V19; sigmoid (thin line).

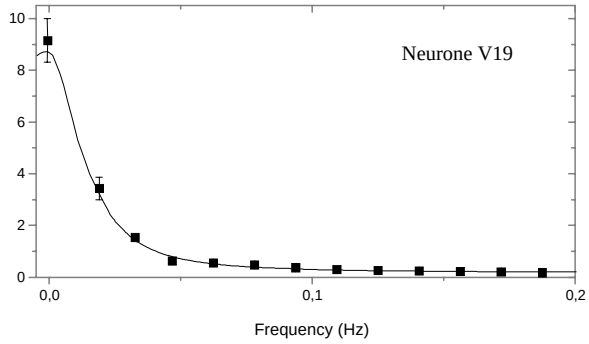


Fig.6.- Frequency spectrum of R+H tram impulse. Experiment (v) and model fit (full line).

Similarly in Figs. 7 we show the D voltages for the same neurones impulses, fitted by [7], using the above parameter values and $g_{Na} = 1.9 \times 10^{-7}\, m^{-2}\, \Omega^{-2}$, from the fits obtaining the values of $\left(m_0^3 h_0\right)^{1/4}$ and τ_{eff} quoted in Table 1. Values of $\left(m_0^3 h_0\right)^{1/4}$ are larger than n_0 ones, and same above consideration apply to them. Also sodium τ_{eff} are larger than τ_K, although in the impulse times $t_S < t_b$ because $V_{Na}(t)$ is interrupted at the smaller (abs.value) E_{Na} than E_K for $V_K(t)$. In Fig.8 is shown the frequency spectrum of $V_{Na}(t)$ for neurone V-19, and the fit by the corresponding lorentzian. D voltage is unmodified by applied AC MF and again solving of R+D equation under MF with I_{Ca} term is not needed.

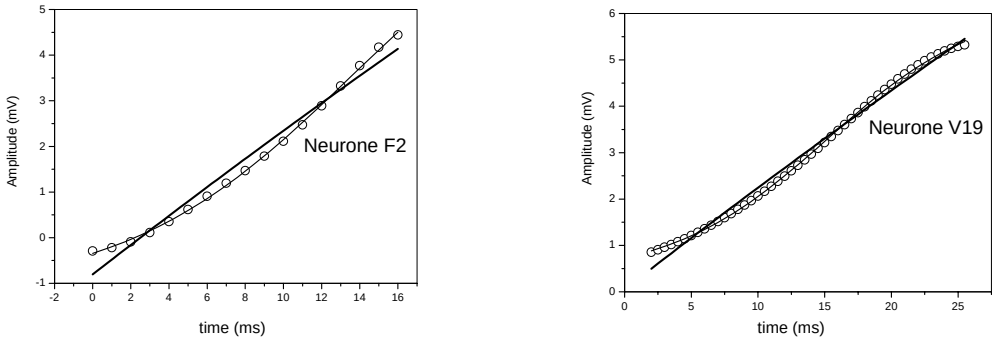


Fig. 7.- Ibidem Fig.5 for the depolarisation (D) process; lines: thick, model fit; thin, sigmoid.

Overall our HHM model explains well the spontaneous time dependence of the bioelectric impulse and its frequency spectrum. Demonstration that AC MF produced voltage, V_{Ca} is negligible is a mathematical problem of HHM differential equation resolution as mentioned before. As we will see in Section 3, the main effect of $I_{Ca}(B_{eff}, t)$ is upon the neurone bioelectric *frequency*.

Table 1.- Initial values of n, m, and h HH functions and K^+ and Na^+ relaxation times.

Neurone	n_0	τ_K (ms)	$\left(m_0^3 h_0\right)^{1/4}$	τ_{eff} (ms)
F1	200	33.0	51	92.7
F2	188	49.4	45	149.9
V3	202	45.0	49	109.6
V14	272	12.4	58	57.0
V19	155	156.7	41	222.8

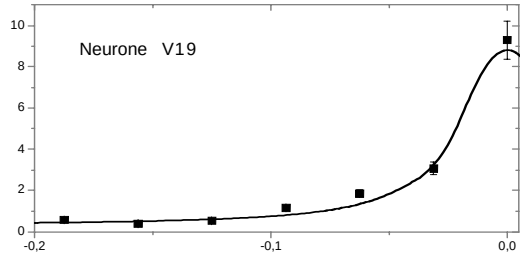


Fig.8.- Frequency spectrum (v) for impulse depolarization of neurone V-19. Line is the lorentzian fit, $L(f)$.

4.- Magnetic field frequency dependence of biolectric activity: frequency window effect.-

The experiments initiated in 1975 by Adey and co. (15) about the effects of ELF MF upon neural tissue are a breakthrough in the understanding of how AC ELF MF interacts with this tissue, apart from its *negligible* Joule heating. They prepared newborn chicken brain slices and embedded them in a physiological HCO_3^- water solution doped with radioactive $^{45}Ca^{2+}$ as marker. The tissue was then irradiated with a radiofrequency (RF) field of 147 MHz, *amplitude modulated* by an ELF MF (of amplitude 25 - 30 nT) in the interval 0.5 - 35 Hz, observing an increase of $^{45}Ca^{2+}$ efflux from the tissue. The experiments demonstrated two things: i) the RF (147 MHz) electromagnetic field (EMF) does *not* produce a measurable efflux increase; ii) a calcium efflux increase was observed for the tissue irradiated with the modulated wave, but only within an interval of about 5-25 Hz, so called *frequency window* effect (FWE) (see Fig.9). Recently we have found a FWE in *Helix aspersa* brain, irradiated with microwaves of 9.6 GHz amplitude modulated between 2-25 Hz. Since Ca^{2+} electrochemical gradient, E_{Ca} displaces these ions to the cell interior, the observed efflux was interpreted as Ca^{2+} liberation from the external membrane surface. FWE was afterwards found in many other kinds of cells and experimental conditions (see (6) for a review), in particular for the bioelectric *frequency, f* dependence with the applied ELF MF frequency, f_M in *Helix aspersa* single neurones (16). Our new observation is that the calcium efflux closely follows a *lorentzian* curve, written now in the normalized form,

$$\phi(\omega_M) = \phi(\omega_0)(\Delta\omega\ 2)^2\ \left[(\omega_M - \omega_0)^2 + (\Delta\omega\ 2)^2\right]\ , \qquad [8]$$

where ω_0 is the frequency at the maximum efflux $\phi(\omega_0)$. Effectively, in Fig.9 the continuous line is the fit by [8] to the experimental calcium efflux (v points), and where $f_0 = \omega_0\ 2\pi \cong 14$ Hz and $\Delta f = \Delta\omega\ 2\pi = 14.8$ Hz.

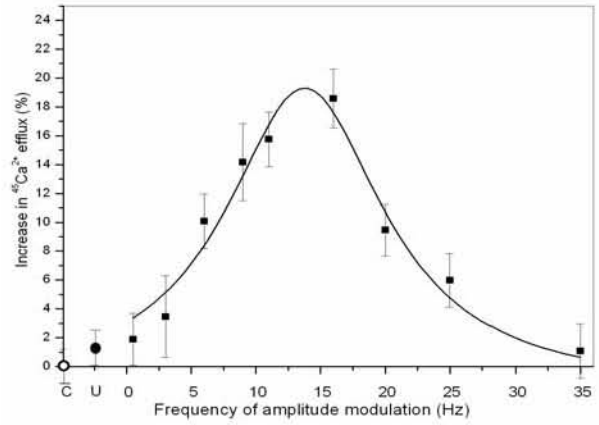


Fig.9.- The points (v) are the experimental $^{45}Ca^{2+}$ efflux increase from chicken brain under application of 147 MHz EMF carrier (intensity $0.8\,mW\ cm^2$), *amplitude modulated* by a MF of frequency, f_M between 0.5-35 Hz and $B_0 \cong 30$ nT (15). The curve is the theoretical lorentzian, fitted according to the model eq.[8] (symbols C (o) and U (λ) respectively correspond to control and unmodulated EM wave experiments).

The quantitative explanation of such a FWE, although profusely mentioned and discussed since then (6), has remained unknown. Although those workers considered that the electric field of the ELF EMF was the responsible for the effect, it seems now clear that it is the MF the responsible one (16). This conclusion also stems from our experiments performed upon single neurones of *Helix aspersa*, submitted to an AC MF, of amplitude $B_0 = 0.1\mu T$-1 mT in the range of 0.1 - 80 Hz. We observed for $\approx$ 56% of the neurones studied a *decrease* in their bioelectric frequency, *f* with the increase of MF frequency, f_M ($\omega_M = 2\pi f_M$), and that the frequency dependence $\omega(\omega_M)$ follows a *lorentzian* function as well, i.e. there appears a FWE too. Moreover in other experiments at the fixed frequency of 50 Hz and with variable amplitude AC MF, we found a *decrease* of the bioelectric frequency with field, of the form [1] for also about 56% of the neurones studied (1, 11**).**

The *lorentzian* frequency, f_M dependence either of the calcium efflux to the extra-cellular fluid from chicken neurones, $\phi(\omega_M)$ or the bioelectric frequency dependence $f(f_M)$ in *Helix aspersa* neurones suggest a common origin for the time dependence of the mechanism involved in the Ca^{2+} ions detaching from their binding sites and their final sequestration or capture. This dependence merely is that the amount of Ca^{2+} ions

either freed to the external or to the cytosol sides from the membrane *must* vary in the form

$$N(t) = N(0)\exp(-t/\tau_{Ca}) , \qquad [9]$$

for an applied ELF MF starting at t = 0. This is so *because the Fourier transform of a lorentzian function is an exponentially time decaying function* (i.e. a relaxation mechanism), with relaxation time $\tau_{Ca} = 2\,\Delta f$, as we have shown in Section 2. This is our main point in favour of a *resonance* effect for the FWE. The time τ_{Ca} is the one required for performing the process of Ca^{2+} liberation from membrane binders, mainly Ca^{2+} diffusion within the external or cytosol fluids and final Ca^{2+} sequestration either by a protein channel (or by other cytosol structures) or incoming to the radioactivity counter for the externally freed $^{45}Ca^{2+}$ ions. In their diffusion the Ca^{2+} ions traverse a RMS distance $\ell^2 \cong D\tau_{Ca}$, the one for a random walk, where *D* is the diffusion coefficient of the ion in the fluid (17). Therefore we come up with $N(t)$ obeying a dynamic equation of relaxation $dN/dt = -N/\tau_{Ca}$, as we would expect for a two states system (freed Ca^{2+} and bonded Ca^{2+} to its sites) in thermodynamic equilibrium, with Ca^{2+} decay between the two states. For the Ca^{2+} ions freed to the extra-cellular fluid they will end up fully thermalized and dissolved in it, increasing its concentration ($^{45}Ca^{2+}$ efflux in Adey & Bawin's experiment). For the Ca^{2+} ions liberated to cytosol, they will diffuse and finally will have a certain probability of being captured by a K^+-protein channel through the calmodulin attractive electric field, $\mathbf{E}_{pK}$ (see Fig.1).

We can quantitatively express the above considerations by Fourier transforming the observed lorentzian function $L(\omega_M)$, which represents either the efflux $\phi(\omega_M)$ or the bioelectric frequency $\omega(\omega_M)$ dependencies, around the neurone spontaneous frequency, ω_0, i.e.

$$N(t) = \int_{-\infty}^{+\infty} L(\omega_M)\,\omega(B_{eff}=0)\exp(-\alpha B_{ef}^2)\exp(-i(\omega_M-\omega_0)t)\,d\omega_M = \qquad [10]$$

$$\omega(B_{eff}=0)\exp(-\alpha B_{eff}^2)\int_{-\infty}^{+\infty} \frac{2(\Delta\omega\ 2)}{(\omega_M-\omega_0)^2+(\Delta\omega\ 2)^2}\exp(-i(\omega_M-\omega_0)t)\,d\omega_M = \omega(B_{eff}=0)\exp(-\alpha B_{eff}^2)\exp(-t\ \tau_{Ca}).$$

If we now call $N(0) = \omega(B_{eff}=0)\exp(-\alpha B_{eff}^2)$ to the initially (at t = 0) detached Ca^{2+} ion number within a burst, we end up with the Ca^{2+} relaxation [9] (note, in [10] $\omega(B_{eff}=0)$ is dimensionless). Since τ_{Ca} is related to $\Delta\omega\ 2$, which is experimentally accessible from the spectra $L(\omega_M)$, we can determine that time from experiment.

The central frequency ω_0 in [10] is assumed to be the spontaneous average bioelectric frequency, so that we obtain a *resonance* or maximum of calcium efflux when $\omega_M = \omega_0$. This resonance mechanism should not be confused with the unspecific stochastic resonance model one. This model is based also on a two-states system, but assuming a critical noise which is modulated by the AC driving agent and reaches a threshold value (18). A difficulty with this model is that the *physical* mechanism involved in the weak AC agent interaction with the system is neither specified nor quantified. Therefore it becomes of questionable application to the distribution of spontaneous bioelectric frequencies, $D(\omega_0)$ (density of frequencies) for the biological system (membrane), also *lorentzian* (setting $\omega_M = 0$ in [8] and [10]). In fact such a distribution has been clearly inferred from our experiments with *Helix* brain neurones, in the form of repetitive narrow bursts of higher frequency (Fig.10), localized in time when f_M is increased, and superposed to the main $f(f_M)$ lorentzian decrease below ω_0 (12).

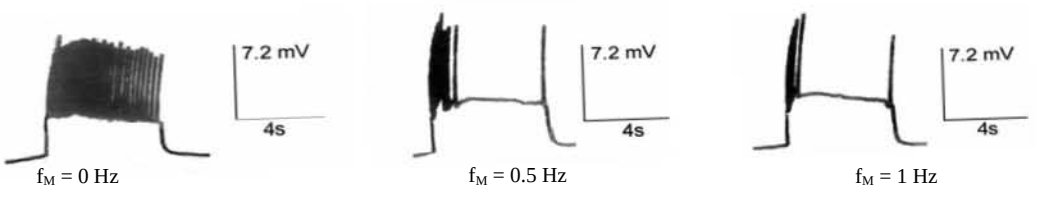


Fig.10.- Neuron D-5 spontaneous bursts of variable f.

In Fig.9 we show the excellent fit by [8] of the calcium efflux increase vs. f_M, and which means that our SD-CE and Ca^{2+} kinetics model gives a physical and quantitative explanation to the Adey & Bawin's FWE observation (15). According to our assumption chicken cerebral neurones average bioelectric frequency should be $f_0 \cong 14$ impulses/s, to some extent comparable with the mollusc neurones with $f_0 \approx 0.1-5$ impulses/s.

Similarly in Fig.11 we present, the bioelectric frequency *f* vs. f_M variation for *Helix aspersa* brain mapped neurones F1 and V14, under AC MF of B_0=1 mT. The fit of $f(f_M)$ by $L(\omega_M)$ is also rather good. Now, as above mentioned, the bioelectric activity is commanded by the AC MF Ca^{2+} ions internally detached towards the cytosol, which join the K^+-protein channels and open them, giving rise to the bioelectric impulse of K^+ ions sorting out. Therefore this mechanism should be also operative in the chicken brain bioelectric activity, and therefore both experiments reveal the Ca^{2+} simultaneous detaching from both surfaces of the membrane. Besides the determined Ca^{2+} relaxation times, τ_{Ca} are 135 ms (chicken brain) and between 93-365 ms for the studied neurones of *Helix aspersa*. An *ab-initio* calculation of the Ca^{2+} relaxation time, τ_{Ca} is difficult, if we consider the mentioned above kinetics involved. In fact a first principles calculation of the K^+ and Na^+ relaxation times in HH equations is still an open problem, relaxation times left as adjustable parameters as we did in section 2. However for τ_{Ca} if we estimate the mean diffusion length of Ca^{2+} in water, taking $D \approx 10^{-9}\ m^2 s^{-1}$, the typical diffusion coefficient for small molecules in water (18**)**, we obtain $\ell^2 \approx 30-60\ \mu m$, reasonable values for the studied neurones of average diameter $d \approx 100\ \mu m$ (1, 14).

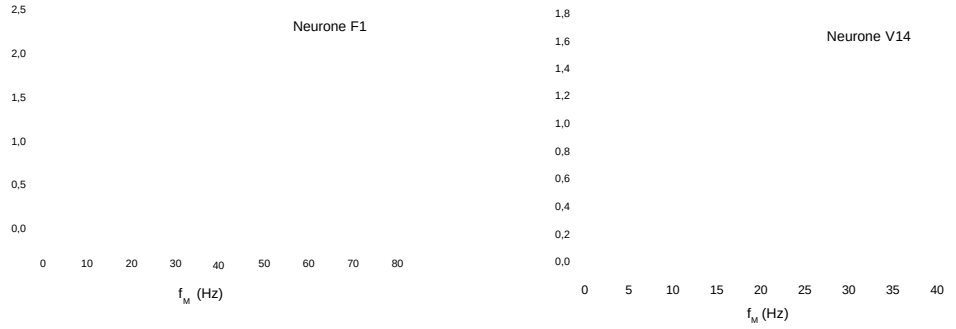


Fig.11.- Variation of bioelectric frequency, *f* with MF frequency, f_M. Experiment (λ); lines are lorentzian fits $L(f_M)$, with f_0=2.5, 2.0 Hz and Δf 2= 9.9, 2.7 Hz for neurones F1 and V14 respectively.

A final check of the SD-CE model suitability is the obtaining of the clusters PP numbers, N_c in *Helix aspersa* neurones. This can be done by determining the parameter α from the slopes of the above $f(B_0)$ mentioned plots from time synchronized neurone pairs under f_M = 50 Hz MF field. (1,7). In Fig.12 are shown such a plots for the pair V13-V23 of the visceral ganglion. Taking $\chi_\perp \cong -0.56\times10^{-7}$, determined in erythrocyte membranes by combined SQUID magnetometry ($\Delta\chi$) and electrophysiological experiments (5,19**)**, $V \approx 5\times10^{-28}\ m^3$**,** T≅293K and α values, obtained from the slopes, we respectively obtain $N_c \approx 4$ and 1 x10^{12} PP in a cluster. Considering that the numbers of PP in such a membranes, of average diameters 120 and 103 μm respectively, are $N_{pp} \approx$ 2 and 1.5 x10^{11} (1, 7**),** that numbers throw about $c = N_c\ N_{pp} \approx 42$ and 16 correlated neurones respectively, firing in *synchronized* way with the probe ones, i.e. forming "giant" PP clusters of linear extension $\approx 300\ \mu m$ (the visceral ganglion has a diameter of about 600 μm and *Helix* brain has $\approx 2\times10^4$ neurones) (14). Therefore neurones form correlated small networks under ELF weak MF. In the case of the chicken brain we do not dispose of data about the calcium efflux dependence with the modulating MF amplitude B_0 and that calculation is not possible.

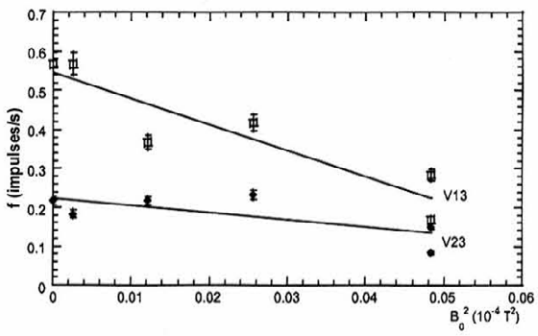


Fig.12.- Plots of the bioelectric frequency, *f* vs. B^2_{eff} (f_M = 50 Hz) for *Helix aspersa* neurone pair V23-V13 (14), showing *synchronization* under MF. From line slopes is determined the α parameter.

5.- Conclusions.-

We have integrated, by the first time to our knowledge, the Hodgkin & Huxley (HH) equation for the biolectric impulse, by considering the membrane as a Kirchoff *electric knot*. Integration has been performed

under applied AC MF, by partitioning the bioelectric impulse in its depolarization (D) and repolarization (R) plus hyperpolarization (H) regimes. For the spontaneous regimes we have obtained the time variations of the D and R+H voltages, in reasonable agreement with our experiments on single unit neurones of mollusc *Helix aspersa*. The HH characteristic functions n(t) and m(t) (excitatory) and h(t) (inhibitory) have been treated within the relaxation time,τ approximation, from the comparison with the bioelectric impulse obtaining τ_{Na} and τ_K, as well as the initial values of those functions. The calculated frequency spectrum of the impulse is *lorentzian*, in good agreement with experimental one, from the HMHW also determining τ_{Na} and τ_K. The cytosol Ca^{2+} ion current, produced by the SD and CE under AC MF has been calculated, although experimentally the *single* impulse is *not* modified by weak applied MF to *Helix aspersa* neurones. This means that MF produced extra-voltage, $V_{Ca}(t)$ is negligible, its numerical calculation value being deferred for further work.

On the other hand, we have shown that the hallmark Adey & Bawin's *frequency window effect* is a consequence of the phospholipids superdiamagnetism and Ca^{2+} coulomb explosion in the outer surface of the neurones, and that the effect is a *resonance* of *lorentzian* shape, when the MF frequency matches the neurone spontaneous frequency. In *Helix aspersa* single neurones, same mechanism is operating but now due to the Ca^{2+} liberation from the inner membrane surface towards the cytosol, so operating the K^+ channels. In both situations the *lorentzian* spectrum is a consequence of the exponentially decaying relaxation followed by the Ca^{2+} current, freed by the MF to the extra-cellular or cytosol fluids, ions suffering *diffusion* before capture. This diffusion mainly determines the lorentzian spectrum vs. applied MF frequency f_M.

Acknowledgements.

We acknowledge financial support of Fundación Humanismo y Ciencia (Madrid) and of Diputación General de Aragón (Zaragoza) under project B-43.

References

(1) Azanza M.J., Calvo A.C. and del Moral A. Evidence of synchronization of neurones activity of molluscan brain ganglia induced by alternating 50 Hz applied magnetic field. Electro-Magnetobiology. 21: 221-232, 2002.
(2) Azanza M.J., and del Moral A. Isolated neuron amplitude spike decrease under static magnetic fields. J. Magn. Magn. Mat. 157-158: 593-594, 1996.
(3) Hodgkin A. I. and Huxley A.F. A quantitative description of membrane current and its application to conduction and excitation in nerve. J.Physiol. 117: 500-544, 1952.
(4) Kandel E.R., Schwartz J.H. and Jessell T.M. *Principles of neural science*. McGraw Hill, New York, 2000.
(5) del Moral A., and Azanza M.J. Model for the effect of static magnetic field on neurons. J. Magn. Magn. Mat.114: 240-242, 1992.
(6) Azanza M.J., and del Moral A. Cell membrane biochemistry and neurobiological approach to biomagnetism. Prog. Neurobiol. 44: 517-601, 1994.
(7) Azanza M.J., Pérez-Bruzón R.N., Calvo A.C. and del Moral A. Elemental neuron network dynamics under applied sinusoidal magnetic fields. Bioelectromagnetics. 2005 Congress, pp. 312-314, Dublín, 2005.
(8) Azanza M.J., Pes N., Raso M., Pérez-Bruzón R.N., Junquera C., Pérez-Castejón C., Maestú C., Aisa J., Lahoz M., Martinez-Ciriano C., Vera-Gil A. and del Moral A. Characterization of connexins in *Helix aspersa* suboesophageal brain ganglia neurons and glia cells by immunocitochemistry, Histol. Histopathol., 2006, (in press).
(9) Babu Y.S., Sack J.S., Greenough T.J., Bugg C.E., Means A.R. and Cook W.J. Three-dimensional structure of calmodulin. Nature. 315: 37-40, 1985.
(10) Azanza M.J., and del Moral A. ELF-magnetic field induced effects on the bioelectric activity of single neurone cells. J. Magn. Magn. Mat. 177-181: 1451-1452, 1998.
(11) Azanza M.J. and del Moral, A. ELF-magnetic field induced effects on the bioelectric activity of single neuron cells. J. Magn. Magn. Mat. 177-181: 1451-1452, 1998.
(12) del Moral A., Pérez-Bruzón R.N. and Azanza M.J., to be published.
(13) Pérez-Castejón C., Junquera C., Pueyo A., Pérez-Bruzón R.N., Azanza M.J., Raso M., Pes N., Maestu C., Aisa J., Lahoz M., Martínez-Ciriano C., Vera-Gil A., and del Moral A. Charaterization of neuron membrane ionic protein channels involved in the responses to applied ELF-Magnetic fields observed in *Helix aspersa* brain ganglia neurons. Histol. Histopathol. Suppl.1: S134, 2005.
(14) Kerkut G.A., Lambert J.D.C., Gayton R., Loker J.E. and Walker R.J. Mapping of nerve cells in the ganglia of *Helix aspersa* neurons. Comp. Biochem. Physiol. 50A: 1-25, 1975.
(15) Bawin S.M., Sheppard A. and Adey W.R., Bioeletrochem. Bioenergetics. 5: 67, 1978.
(16) Pérez-Bruzón R.N., Azanza M.J and del Moral A. J. Magn. Magn. Mat. 272-276: 2424, 2004.
(17) See e.g. Nelson P., *Biological Physics, Energy, Information, Life*, Freeman, New York, 2004.
(18) See e.g. Wellens T., Shatokhin V. and Buchleitner A. Stochastic resonance. Rep. Prog. Phys. 67: 45, 2004.
(19) Azanza M.J., Blott B.H., del Moral A. and Peg M.T., Bioelectrochem. Bioenergetics. 30: 45,1993.

EFFECTS OF EXTREMELY LOW FREQUENCY ELECTROMAGNETIC FIELDS ON MEMBRANE-BOUND ENZYMES. AN OVERVIEW.

I.M.PEPE, S. RAVERA, D. CALZIA, I. PANFOLI, C. CUGNOLI and A. MORELLI

DEPARTMENT OF BIOLOGY, UNIVERSITY OF GENOA, VIALE BENEDETTO XV, 3 GENOVA, 16131 ITALY, e-mail: mario.pepe@unige.it.

Abstract

In order to give an interpretation at molecular level of the macroscopic effects produced by ELF-EMFs on biological systems, the activities of different enzymes were studied under exposure to electromagnetic fields of 75 Hz. The activities of cytosolic enzymes as well as those of integral or periferal membrane enzymes were not affected by the field exposure. Only the activities of some lipid-linked enzymes decreased approximately of about 54 % to 61 % with field amplitudes above different thresholds (from 0.66 to 1.35 mTesla). The decrease in enzymatic activity of the field-sensitive enzymes was independent of the time of permanence in the field and was completely reversible. When these enzymes were solubilized with Triton, no effect of the field was obtained on the enzymatic activity, suggesting the crucial role of the membrane, as well as the linkage to it, in determining the conditions for enzyme inactivation.

INTRODUCTION

The interactions between electromagnetic fields of extremely low frequency (ELF-EMFs) and biological systems have been widely investigated [Walleczek, 1995; Kaiser, 1996; Eremenko et al., 1997; Berg, 1999; Ivancsits et al., 2002;Volpe, 2003]. The problem concerning the mechanisms which can determine biological effects is not yet solved [Lawrence and Adey, 1982; Glaser, 1992; Basset, 1993; Barnes, 1996; Lacy -Hulbert et al., 1998; McCann et al.,1998; Weaver, 2002]. The related phenomena are still not clear, but their existence is certain at least in many specific cases. However, a generally accepted interaction model able to explain these phenomena is lacking. A contribution in this direction could be that of an interpretation at molecular level of the macroscopic effects produced by ELF- EMFs. Therefore, our attention was focused on the enzymatic activity which are known to be underlying many biological processes. The hypothesis that ELF EMFs could affect enzymes activities was tested on a number of soluble enzymes as well as on membrane-associated enzymes. Among cytosolic enzymes hexokinase, pyruvate kinase**,** glucose 6 phosphate dehydrogenase and adenylate kinase were chosen. The membrane-associated enzymes were: integral membrane proteins such as CaATPase, Na/K,ATPase, succinic dehydrogenase; periferal membrane proteins such as photoreceptor phosphodiesterase 6 (PDE); lipid-linked proteins such as alkaline phosphatase and acetylcholinesterase. Membrane-bound phosphoglycerate kinase was also assayed.

When exposed to ELF-EMFs of 75 Hz , the activities of soluble enzymes were not affected by the field, whilst those of four enzymes out of eight bound to membrane were lowered dramatically of about 54% to 61%. Moreover, the effects of the applied field on these enzymes vanished when they were mildly solubilized by Triton, suggesting that the membranes could have an important role for mediating the effect of the field on the enzymatic activity. In fact, interesting results involving biological membranes exposed to ELF electromagnetic fields has been already reported [Miller, 1991; Paradisi et al., 1993; Astumian et al., 1995; Baureus-Koch et al., 2003;]. In particular, measurements by fluorescent probes showed changes in lipid molecular dynamics of the cell membrane [Volpe et al., 1998], while electron microscope images of freeze-fractured membranes exposed to the field indicated a significant clustering of the distribution of the intramembrane proteins [Bersani et al., 1997]. The applied field could modify the membrane organization and structure by acting directly on the strong anisotropy of diamagnetic susceptibility of membrane phospholipids [Del Moral et al., 2002]. An interesting result on the effects of ELF EMFs on carbonic anhydrase entrapped in liposomes seems to exclude the role of the enzyme molecule in favour of the direct action of the field on charged lipids of the membrane [Ramundo-Orlando et al., 2000].

METHODS

Electromagnetic field production. EMFs were produced by an equipment (Biostim Igea, Modena, Italy) mainly used for clinical application and already described [De Mattei et al., 2003; Ravera et al., 2004]. The generator system supplies a square wave with a maximal applied tension of 180 V, a period of 13.3 ms (75 Hz of frequency), a duty cycle of 10%, to a couple of identical coils aligned on a central axis. Each coil, made up of 1000 turns of copper wire of 0.2 mm of diameter, had internal and external diameter of 72.5 mm and 82.5 mm respectively. As the current supplied by the equipment to the coils was not adjustable, different amplitudes of magnetic field were obtained by separating the two coils with different distances. Measurements of the magnetic field B maximal intensity with a gaussmeter showed that it was fairly constant midway between the coils, giving values of about 2.20 ± 0.08 mT when the distance between the coils was 12 cm and about 0.45 ± 0.02 mT at 29.6 cm distance. An error of 0.5 cm in determining the distance between the coils gave an error of 4% in the field measurements. The values of the field near the threshold (see Fig 1) were determined more accurately (sd of 1 % , n=10). Time course of the magnetic field as well as that of the induced electric field were measured as already described [De Mattei et al., 2003; Ravera et al., 2004], at the center of the distance between the two coils where the samples were always placed. Temperature variations of the order of magnitude of experimental error (± 0.1 ° C) were measured with a termocouple inside the sample in the presence of the applied field.

Enzymatic activities measurements.

Hexokinase activity assay. Hexokinase activity was measured in the presence or in the absence of the field for 1 min after glucose addition (200 mM final concentration) to the reaction mixture containing the purified enzyme. The reaction mixture contained 100 mM Tris–HCl pH 8, 8 mM $MgCl_2$, 1 mM ATP and 2 µl of Hexokinase (Cat n° 11 426 362 001, Roche), in final volume of 1 ml. Before and after 1 min of incubation 100 µl of the reaction mixture were withdrawn and added to 50 µl of 25% PCA. Each sample was centrifuged shortly at 14,000 rpm and then 100 µl of supernatant was withdrawn and neutralized with 50 µl K_2CO_3. The centrifugation was repeated to remove potassium perchlorate. Aliquots of 100 µl of each neutralized extract were used to assay Glucose-6-phosphate, monitoring NADPH formation by spectrophotometer (340 nm), according to Bergmeyer et al.[1983].

Pyruvate Kinase activity assa.y Pyruvate Kinase activity was measured in the presence or in the absence of the field for 1 min after phosphoenol-pyruvate (PEP) addition (0.6 mM final concentration) to the reaction mixture containing the purified enzyme. The reaction mixture contained 100 mM Tris–HCl pH 8, 8 mM $MgCl_2$, 5 mM ADP and 0.5 µl of Pyruvate Kinase (Cat n° P-1506, Sigma), in final volume of 1 ml. Before and after 1 min of incubation 100 µl of the reaction mixture were withdrawn and added to 50µl of 25% PCA. Each sample was centrifuged shortly at 14,000 rpm and then 100 µl of supernatant was withdrawn and neutralized with 50 µl K_2CO_3. The centrifugation was repeated to remove potassium perchlorate. Aliquots of 100 µl of each neutralized extract were used to assay Pyruvate, monitoring NAD^+ formation as already described [Bergmeyer et al., 1983].

Glucose 6 phosphate dehydrogenase (G6PD) activity assay. Glucose 6 phosphate dehydrogenase activity was measured in the presence or in the absence of the field for 1 min after glucose-6-phosphate addition (10 mM final concentration) to the reaction mixture containing the purified enzyme. The reaction mixture contained 100 mM Tris–HCl pH 8, 8 mM $MgCl_2$, 0.5 mM NADP and 0.25 µl of Glucose-6- phosphate dehydrogenase (Cat n° G-5760, Sigma), in final volume of 1 ml. Before and after 1 min of incubation 100 µl of the reaction mixture were withdrawn and added to 50 µl of pure Aceton. Each sample was centrifuged shortly at 14,000 rpm and then 100 µl of supernatant was withdrawn, added to 900 µl of water and immediately assayed to spectrophotometer (340 nm), to observe the NADPH formation.

All the other enzymatic activities presented in Table 1 were measured following the methods described in the Appendix

Protein concentration

Protein concentrations were determined using the Bradford method [1976].

RESULTS AND DISCUSSION

In order to measure the direct effects of ELF - EMFs on enzymatic activities, the enzymes were studied in purified state when available or in rough extracts from cell-free homogenates. Different length of exposure to the fields lasted from 1 min to 60 min. The effects on enzymatic activities were detectable only during the field exposure. No effects were measured immediately after the withdrawal of the field, suggesting a perfect

reversibility of the mechanism. Table 1 shows the activities of different enzymes exposed to ELF - EMFs of 75 Hz frequency and 3.0 mT magnetic field amplitude for 20 min. The activities of the cytosolic enzymes, that is: hexokinase, pyruvate kinase**,** glucose 6 phosphate dehydrogenase and adenylate kinase were not affected by the field exposure with a statistical significance of $P < 0.001$. Among membrane-associated enzymes instead: alkaline phosphatase, acetylcholinesterase from ghosts or from synaptosomes, phosphoglycerate kinase and membranous adenylate kinase, decreased their activities of about 54%, 60%, 58% 61% and 54% respectively, while either integral membrane enzymes such as CaATPase, Na/K,ATPase and succinic dehydrogenase, or periferal membrane enzymes such as photoreceptor PDE were insensitive to the applied field.

Table 1. Activities of different enzymes upon 20 min exposure to a field of 75 Hz and 3.0 mT.

Enzyme	Control sample	Sample + field
Hexokinase	47 ± 2 U/mg	47 ± 2 U/mg
Pyruvate Kinase	175 ± 10 U/mg	177 ± 10 U/mg
Glucose 6 phosphate dehydrogenase	75 ± 7 U/mg	73 ± 6 U/mg
Cytosolic adenylate kinase	385 ± 33 U/mg	390 ± 30 U/mg
Alkaline phosphatase	61 ± 2 U/mg	28 ± 1 U/mg
Acetylcholinesterase from ghosts	3.5 ± 0.1 U/mg	1.4 ± 0.1 U/mg
Acetylcholinesterase from synaptosomes	13.7 ± 0.2 U/mg	5.8 ± 0.1 U/mg
Phosphoglycerate kinase	0.465 ± 0.005 U/mg	0.18 ± 0.01 U/mg
membrane Adenylate kinase	177 ± 10 U/mg	81 ± 5 U/mg
CaATPase	21 ± 1 U/mg	20 ± 1 U/mg
Na/K,ATPase	78 ± 5 U/mg	80 ± 5 U/mg
Succinic dehydrogenase	100 ± 5 U/mg	101 ± 5 U/mg
rod outer segment PDE	50 ± 5 U/nmol of Rhodopsin	48 ± 5 U/nmol of Rhodopsin
Alkaline phosphatase in 0.1% Triton	58 ± 2 U/mg	56 ± 2 U/mg
Acetylcholinesterase from ghosts in 0.1% Triton	3.3 ± 0.2 U/mg	3.0 ± 0.2 U/mg
Acetylcholinesterase from synaptosomes in 0.1% Triton	15.1 ± 0.2 U/mg	14.5 ± 0.2 U/mg
Phosphoglycerate kinase in 0.1% Triton	0.43 ± 0.01 U/mg	0.43 ± 0.01 U/mg
membrane Adenylate kinase in 0.1% Triton	175 ± 10 U/mg	180 ± 10 U/mg

Each value represents the mean ± SD of five measurements. The enzymatic activity is expressed as Units/mg (nmoles of substrate transformed /min/ mg protein). The activity of each enzyme was measured for 1 min before the withdrawal of the field. The solubilization with Triton in itself did not affect the activity of alkaline phosphatase or acetylcholinesterase from blood cells but decreased of about 7.5 % the activity of phosphoglycerate kinase while enhanced of about 10% the activity of acetylcholinesterase from synaptosomes. Such activity differences are usually observed when membrane bound enzymes are solubilized in low concentration of a mild detergent [Helenius and Simons, 1975].

The activities of the field-sensitive enzymes were measured in function of the concentration of their substrates and the resulting Michaelis-Menten kinetics showed a behaviour of a pure noncompetitive inhibition where only V_{max} was affected by a field exposure. The Lineweaver-Burk plot of the data obtained for acetylcholinesterase from blood cell ghosts showed that K_M remained constant whereas V_{max} dropped of about 60% when exposed to the field.

The decrease of the enzymatic activities shown in Table 1 of the four enzymes was independent of the time of permanence in the field and appeared constant within the experimental errors under exposure lengths of 1 min to 60 min. In other words, the same decrease in the enzymatic activity was measured independently of the

exposure time, indicating that the effect of the field starts within the first min exposure and remains constant during all the the field permanence. The action of the field seems that to switch the enzyme to a state of a reduced activity which is immediately restored when the enzyme is removed from the field.

The decrease of the enzymatic activities was studied at different amplitudes of the applied field. Fig 1 shows that field amplitude of about 1.35 ± 0.05 mT or 0.80 ± 0.03 mT were the lowest value which produced a supra-threshold response respectively for alkaline phosphatase and acetylcholinesterase from blood cells. At field amplitudes under the thresholds the enzymatic activities were statistically indistinguishable from those of the controls. Similar data were found for the other two field-sensitive enzymes and the corresponding suprathreshold field values were 0.66 ± 0.02 mT or 0.85 ± 0.03 mT for phosphoglycerate kinase or acetylcholinesterase from synaptosomes respectively. The effect of the field on enzymatic activities seems independent of its amplitude above the threshold up to 2.2 mT as well as for the amplitude of 3.0 mT reported in Table 1.

Fig 1. Enzymatic activity of alkaline phosphatase (○) or acetylcholinesterase from ghosts (●) measured during 10 min exposure to 75 Hz magnetic field of different amplitudes. Each value represents the mean ± SD of five measurements.

When the same experiments were run on the field-sensitive enzymes solubilized by 0.1 % Triton, the results showed that the activities of the solubilized enzymes were not affected by the field (see the last five lines of Table 1) with a statistical significance of $P < 0.001$.

Changing of enzymatic activities due to exposure to ELF-EMFs have already been reported by different workers. However, the differences in the observed effects could be due to the wide variety of the experimental conditions used by the various authors. The choice of field frequency is crucial as the quantistic interaction of the electromagnetic wave with molecules can only operate through frequency windows. However, fields of 60 Hz frequency, close to 75 Hz used in our experiments, caused opposite and small effects on soluble enzymes [Zhang and Berg, 1992; Litovitz et al., 1991; Thumm et al., 1999; Harada et al., 2001]. Many reported changes of enzymatic activities in whole cells and tissues suggest that ELF-EMFs may stimulate a general response to electromagnetic stress. In the case of ornithine decarboxylase for instance, the enzymatic activity was enhanced approximately 1.5 to 4-fold when exposed to ELF- EMFs [Mullins et al., 1999]. However, in this case the experiments were run on entire fibroblasts cells and the exposure to 60 Hz field for 4 hours presumably did not affect the enzyme activity directely. The activity of another soluble enzyme such as enolase was found

decreased by 28% in *Escherichia coli* colture exposed for 30 min to a field of 60 Hz [Dutta et al., 1994]., In this case however, the enzymatic activity was assayed in cell extracts, after the withdrawl of the field, and its decrease maybe be due to stress effects induced by the field and not to a direct interaction of the field with the enzyme molecule.

Among integral membrane protein, Na/K,ATPase and cytochrome oxidase were found to increase its enzymatic activity by approximately 30 % and 40% respectively in experimental conditions similar to those described in this paper, under exposure to a pulsed magnetic field of 60 Hz with an amplitude of only 10 μT [Blank and Soo, 2001]. The frequency window for Na/K,ATPase was very sharp with a maximal change at 60 Hz while at 100 Hz the change in enzymatic activity was only 10%.

The results shown in Table 1 strongly suggest that the field action is mediated by the membrane organization and structure which is crucial in determining the conditions of the enzyme inactivation. However, the effect of the field on the membrane is not sufficient alone to explain the decrease in enzymatic activity: in the case of acetylcholinesterase, it was independent of the source of the membrane, as the activity decrease for the enzyme coming from blood cells (60 % ± 4%) was not statistically different from that prepared from synaptosomes (58 % ± 5 %).On the other hand, integral membrane enzymes such as Ca,ATPase and Na/K,ATPase or periferal membrane enzymes such as PDE were not affected by the field suggesting the importance of the linkage to the membrane. Alkaline phosphatase, acetylcholinesterase from blood cell or from synaptosomes and adenylate kinase from rod disk membranes are lipid-linked membrane enzymes: alkaline phosphatase as well as acetylcholinesterase are known to be anchored to the membrane through a glycosylphosphatidylinositol while adenylate kinase is presumably bound to rod disk membranes through a myristic fatty acid [Notari et al., 2003]. Instead, the kind of attachment to red blood cell membranes of the field-sensitive enzyme phosphoglycerate kinase is not yet known, although a covalent linkage to hydrophobic group such as myristylate has been suggested [Concepcion et al., 2001]. In a recent report [Caseli et al., 2005], the enzymatic activity of alkaline phosphatase incorporated into artificial phospholipid monolayers dropped of about 40 % following a lipid phase transition from liquid expanded to liquid condensed state, when surface pressure increased above 18 mN/m. Fluorescence microscopy revealed that above this pressure, proteins aggregated and formed clusters which would affect the substrate accessibility to the catalytic site and therefore decrease the enzymatic activity. It has also been reported that a pulsed field of 50 Hz is able to induce a decrease in lipid molecular dynamics of cell membranes [Volpe et al., 1998] and significant clustering of the distribution of the membrane proteins [Bersani et al., 1997]. Therefore, we can speculate that the field of 75 Hz would be able to induce a transition of the lipid bilayer to a more liquid ordered phase, as suggested by the sharp threshold behaviour shown in Fig 1, followed by the partition of the lipid-anchored enzymes in clusters with a subsequent activity decrease.

However, the results presented in this paper are important for the interpretation at molecular level of macroscopic effects produced by ELF- EMFs on biological systems. An example could be that of the clinical application of weak EMFs of 75 Hz frequency currently used to accelerate the healing of bone fractures. The molecular mechanisms underlying these empirical observations could originate from alkaline phosphatase inhibition by the pulsed field. As a matter of fact, alkaline phosphatase is commonly used as an osteoblast differentiation marker, although its role in bone formation is still controversial as it could be involved in the process of bone mineralization or in the organic matrix synthesis as well. However, a decrease in its activity was found in concomitance with an increase of the number of human bone cells in culture following dynamic strain [Kaspar et al., 2000].

Another example of field effect which needs a molecular interpretation comes from several studies that indicate that ELF-EMFs affect cell division timing and embryos development of many organisms [Delgado et al., 1982; Dixey and Rein, 1982; Koch et al., 1993]. In particular, the effects of low-intensity electromagnetic fields on the early development of the sea urchin *Paracentrotus lividus*. [Falugi et al., 1987] could be interpreted as due to acetylcholinesterase inhibition. A recent report on exposure of fertilized eggs of the sea urchin *Paracentrotus lividus* to an electromagnetic field of 75 Hz frequency, shows a dramatic loss of synchronization of the first cell cycle, with formation of anomalous embryos linked to irregular separation of chromatides during the mitotic events [Ravera et al., 2006.]. As acetylcholinesterase is thought to regulate the embryonic first developmental events of the sea urchin [Shmukler et al., 1998], its enzymatic activity was assayed in embryo homogenates and found it decreased by 48% when exposed to the same pulsed field. This enzymatic inactivation had a threshold of about 0.75 mTesla, the same field threshold found for the effect on the formation of anomalous embryos. The conclusion is that one of the main causes of the dramatic effects on the early development of the sea urchin by field exposure could be the accumulation of acetylcholine due to acetylcholinesterase inactivation. Moreover, the effects of accumulation of acetylcholine last presumably even after the removal of the field and the consequent reversible restoration of acetylcholinesterase activity. In other words, even though the effects of ELF-EMFs are likely transient, the consequences of the exposure may not be overlooked as they can be irreversible.

On the other hand, some field bioeffect could be positive. It was reported that cholinesterase inhibitors, such as methanesulfonyl fluoride, improve cognitive performance in patients with senile dementia of the Alzheimer type [Moss et al.,1999]. In this case, ELF-EMFs may be of some help for treatment of the desease as a mild tool without farmacological side effects.

Summary

The hypothesis that ELF EMFs could affect directly enzymes activities was tested on a number of soluble enzymes as well as on membrane-associated enzymes. Among cytosolic enzymes, hexokinase, pyruvate kinase**,** glucose 6 phosphate dehydrogenase and adenylate kinase were chosen; among integral membrane protein: CaATPase, Na/K,ATPase, succinic dehydrogenase; among periferal membrane proteins: photoreceptor phosphodiesterase 6 (PDE); among lipid-linked proteins: alkaline phosphatase, acetylcholinesterase and membranous adenylate kinase. Membrane-bound phosphoglycerate kinase was also assayed. When exposed to ELF-EMFs of 75 Hz , the activities of soluble enzymes as well as those of integral or periferal membrane enzymes were not affected by the field, whilst those of lipid-linked enzymes were lowered dramatically of about 54% to 61%. Moreover, the effects of the applied field on these enzymes vanished when they were mildly solubilized by Triton, suggesting that the membranes, as well as the protein linkage to them, could have an important role in mediating the effect of the field on the enzymatic activity.

REFERENCES

Astumian, R.D. Weaver, J.C. Adair,R.K. 1995 Rectification and signal averaging of weak electric fields by biological cells. *Proc.Natl.Acad.Sci.U.S.A.* 92(9): 3740-3743.

Barnes, F. S. 1996. Effect of electromagnetic fields on the rate of chemical reactions. *Biophysics*. 41: 801-808.

Basset, C. A. 1993. Beneficial effects of electromagnetic fields. *J. Cell. Biochem.* 51: 387-393.

Baureus-Koch,C.L. Sommarin,M. Persson,B.R. Salford,L.G. and Eberhardt,J.L. 2003 Interaction between weak low frequency magnetic fields and cell membranes. *Bioelectromagnetics.* 24(6): 395-402.

Berg, H. 1999. Problems of weak electromagnetic field effects in cell biology. *Bioelectrochem. Bioenerg*. 48: 355-360.

Bergmeyer H.U. Grassl M. Walter H-E, 1983, Enzymes, in: H.U. Bergmeyer (Ed.), Methods of enzymatic analysis vol 2, Verlag Chemie, Weinheim, pp. 126-281.

Bersani, F., Marinelli ,F., Ognibene, A., Matteucci, A., Cecchi,S., Squarzoni, F., and Maraldi, N.M. 1997. Intramembrane protein distribution in cell cultures is affected by 50 hz pulsed magnetic fields. *Bioelectromagnetics* 18: 463-469.

Blank, M. Soo, L. 2001. Optimal frequencies for magnetic acceleration of cytochrome oxidase and Na,K-ATPase reactions. *Bioelectrochemistry* 53: 171-174.

Bonner W. 1955. Succinic dehydrogenase, assay method. *Meth. Enzymol*. 1: 722-729.

Bradford M. 1976. A quantitative, semiquantitative and qualitative assay of protein, *Anal. Biochem.* 72: 248-256.

Caseli, L., Oliveira R. G., Masui D. C., M.Furriel R. P., Leone F. A., Maggio B., and Zaniquelli M.E.D. 2005, Effect of Molecular Surface Packing on the Enzymatic Activity Modulation of an Anchored Protein on Phospholipid Langmuir Monolayers. *Langmuir* 21:4090-4095.

Concepcion J. L., Adje´ C. A. Quinones W., Chevalier N., Dubourdieu M. and Michels P.A.M. 2001. The expression and intracellular distribution of phosphoglycerate kinase isoenzymes in *Trypanosoma cruzi. Molecular & Biochemical Parasitology* 118: 111–121.

Delgado, J. M. R., Leal, J., Monteagudo, J.L., Gracia, M.G.J. 1982, Embriological changes induced by weak extremely low frequency electromagnetic field. *J. Anat.* 134: 533-551.

Del Moral, A., Azanza, M. J., Calvo A. C., and Perez-Bruzon, R. N. 2002. Responses to applied static and extremely low frequency magnetic fields. *In* Biological Effects of EMFs. P. Kostarakis, editor. Demokritos Publishers, Rhodes. vol. 1, 298-308.

Dixey, R. and Rein, G. H. 1982, Noradrenaline Release Potentiated in a Clonal Nerve Cell Line by Low-Intensisty Pulsed Magnetic Fields. *Nature* 296: 253-255.

De Mattei M, Pasello M, Pellati A, Stabellini G, Massari L, Gemmati D and Caruso A. 2003. Effects of electromagnetic fields on proteoglycan metabolism of bovine articular cartilage explants. *Connective Tissue Research*. 44(3-4):154-159.

Dutta; S.K., Verma, M.; Blackman, C.F. 1994. Frequency-dependent alterations in enolase activity in Escherichia coli caused by exposure to electric and magnetic fields. *Bioelectromagnetics.* 15: 377-83.

Eremenko T., C. Esposito, A. Pasquarelli, E. Pasquali and P. Volpe. 1997. Cell-cycle kinetics of Friend erythroleukemia cells in a magnetically shielded room and in a low-frequency/low-intensity magnetic field. *Bioelectromagnetics.* 18: 58-66.

Falugi, C., Grattarola, M., Prestipino, G. 1987 Effects of low-intensity pulsed electromagnetic fields on the early development of *Paracentrotus lividus*. *Biophys. J.* 51: 999-1003.

Glaser, R. 1992. Current concepts of the interaction of weak electromagnetic fields with cells. *Bioelectrochem. Bioenerg.* 27: 255-268.

Harada S., Yamada S., Kuramata O., Gunji Y. Kawasaki M., Miyakawa T., Yonekura H., Sakurai S., Bessho K., Hosono R., Yamamoto H. 2001. Effects of high ELF magnetic fields on enzyme-catalyzed DNA and RNA synthesis in vitro and on a cell-free DNA mismatch repair. *Bioelectromagnetics* 22(4): 260-266.

Helenius, A., Simons K. 1975. Solubilization of membranes by detergents, *Biochim. Biophys. Acta* 415: 29-79.).

Ivancsits, S., Diem, E., Pilger, A., Rudiger, H., and Jahan, O. 2002. Induction of DNA strand breaks by intermittent exposure to extremely-low-frequency electromagnetic fields in human diploid fibroblasts. *Mutation Res*. 519: 1-13.

Kaiser, F. 1996. External signals and oscillation dynamics: biophysical aspects and modelling approaches for interactions of weak electromagnetic fields at the cellular level. *Bioelectrochem. Bioenerg*. 41: 3-18.

Kaspar D, Seidl W, Neidlinger-Wilke C and Claes L. 2000. In vitro effects of dynamic strain on the proliferative and metabolic activity of human osteoblasts. *J. Musculoskelet. Neuronal. Interact*. 1: 161-164.

Koch, W.E.,Koch, B.A., Martin, A.H. and Moses, G.C. 1993, Examination of development of cicken embryos following exposure to magnetic fields. *Comp. Biochem. Physiol., Comp. Physiol.* 105: 617-624.

Lacy-Hulbert, A., Metcalfe, J. C., and Hesket, R. 1998. Biological responses to electromagnetic fields. *FASEB J.* 12: 395-420

Lawrence, A. F., and Adey, W. R. 1982. Non linear wave mechanisms in interactions between excitable tissue and electromagnetic fields. *Neurol. Res.* 4: 115-53.

Litovitz, T.A., Krause, D.J., and Mullins, J.M. 1991. Effect of coherence time of the applied magnetic field on the enhancement of ornithine decarboxylase activity. *Biochem. Biophys. Res. Commun.* 178: 862–865)

Martin J.B. and Doty D.M. 1949, Determination of inorganic phosphate; modification of isobutyl alcohol procedure, *Anal. Chem.* 21: 965–967.

McCann, J., Dietrich, F., and Rafferty, C. 1998. The genotoxic potential of electric and magnetic fields: an update. *Mutation Res*. 411: 45-86.

Miller, D. L. 1991, Electric fields induced in chicken eggs by 60-Hz magnetic fields and the dosimetric importance of biological membranes. *Bioelectromagnetics.* 12(6): 349-360.

Moss D.E., Berlanga P.,. Hagan M.M, Sandoval H. and Ishida C. 1999, Methanesulfonyl fluoride: a double-blind, placebo-controlled study of safety and efficacy in the treatment of senile dementia of the Alzheimer type, *Alzheimer Dis. Assoc. Disord.* 1**3**: 20–25.

Mullins, J.M. Penafiel, L.M. Juutilainen, J. Litovitz, T.A. 1999 Dose-response of electromagnetic field-enhanced ornithine decarboxylase activity. *Biochemistry and Bioenergetics* 48(1): 193-199.

Notari L., Morelli A. and Pepe I.M. 2003. Studies on adenylate kinase isoform bound to disk membranes of rod outer segment of bovine retina. *Photochem. Photobiol. Sci*.2: 1299-1302.

Paradisi, S., Donelli, G., Santini, M. T., Straface E., and Marloni, W. 1993. A 50 Hz magnetic field induces structural and biophysical changes in membranes. *Bioelectromagnetics.* 14: 247-255.

Pontremoli S., Salamino F., Sparatore B., Melloni E., Morelli A., Benatti U., De Flora A. 1979, Isolation and partial characterization of three acidic proteinases in erythrocyte membranes, *Biochem. J.* 181: 559-568.

Ramundo-Orlando, A., Morbiducci, U., Mossa, G., D'Inzeo, G. 2000, Effects of low frequency, low amplitude magnetic fields on the permeability of cationic liposomes entrapping carbonic anhydrase *Bioelectromagnetics*, 21: 491-498.

Ravera S. Repaci E. Morelli A. Pepe I.M. Botter R. and Beruto D. 2004. Effects of extremely low frequency electromagnetic fields on the adenylate kinase activity of rod outer segment of bovine retina. *Bioelectromagnetics*. 25: 545-551.

Ravera, S. Falugi, C. Calzia, D. Pepe, I.M. Panfoli, I. Morelli, A. 2006 First cell cycles of sea urchin *Paracentrotus lividus* are dramatically impaired by exposure to extremely low frequency electromagnetic field. *Biology of Reproduction* (in press)

Rawls S.M., McGinty J.F., Terrian D.M. 1999, Presynaptic K-opioid and muscarinic receptors inhibit the calcium-dependent component of evoked glutamate release from striatal synaptosomes, *J. Neurochem.* 73: 1058-1065

Schnetkamp P.P. and F.J. Daemen. 1982 Isolation and characterization of osmotically sealed bovine rod outer segments. *Methods Enzymol*. 81: 110-116.

Shmukler, Y.B. and Buznikov, G.A. 1998, Functional Coupling of Neurotransitters with second messengers During Cleavage Divisions. Facts and Hypotheses. *Perspect. Developmental Neurobiol.* **5**, 469-480.

Smith, H.G., Stubbs G.W., and Litman, B.J. 1985. The isolation and purification of osmotically intact discs from retinal rod outer segments. *Exp.Eye Res*. 20: 211-217.

Thumm, S., Loschinger, M., Glock, S., Hammerle, H., and Rodemann, H.P.1999. Induction of cAMP-dependent protein kinase A activity in human skin fibroblasts and rat osteoblasts by extremely low-frequency electromagnetic fields. *Radiat. Environ. Biophys*.38: 195-199.

Volpe, P., Parasassi, T., Esposito, C., Ravagnan, G., Giusti, A. M., Pasquarelli, A., and Eremenko, T. 1998. Cell membrane lipid molecular dynamics in a solenoid *vs*. a magnetically shielded room. *Bioelectromagnetics.* 19: 107-111.

Volpe, P. 2003. Interactions of zero-frequency and oscillating magnetic fields with biostructures and biosystems. *Photochem. Photobiol. Sciences* 2: 637-648.

Walleczek, J. 1995. Electromagnetic fields: Biological interactions and mechanisms. *In* Advances in Chemistry Series vol. 250. Blank, M. editor., ACS, Washington, pp 396-404.

Weaver, J.C. 2002. Understanding conditions for which biological effects of nonionizing electromagnetic fields can be expected. *Bioelectrochem*. 56: 207-209

Zhang, L, and Berg, H. 1992. Electrostimulation of the dehydrogenase system of yeast by alternate current. *Bioelectrochem. Bioenerg*. 28: 341-353.

Appendix

Erythrocyte membranes (ghost) preparation Erythrocytes, completely free of leucocytes and platelets, were obtained following a method already reported [Pontremoli et al., 1979] with minor modifications, starting from 25 mls human blood treated with 1mg/ml EDTA to avoid coagulation. The sample was centrifuged at 3,500 rpm for 15 min at 4 °C and the pellet containing erythrocytes was collected and resuspended in 130 mM KCl and 20 mM Tris-HCl pH 7.4 (1:1 v/v) and centrifuged thrice at 3,500 rpm for 15 min. In order to obtain the erythrocytes membranes the last pellet was resuspended in hemolysis buffer (1:5 v/v) containing 1 mM EDTA-Na and 10 mM Tris-HCl pH 7.4 and centrifuged at 17,000 rpm for 40 min. The pellet containing erythrocyte membranes was resuspended in few mls of distilled water. Samples were stored at –80°C.

Synaptosomal preparation For synaptosomal preparation, the method published by Rawls [1999] was followed with minor modifications. For each preparation, six dorsal striata were removed from decapitated *Mus musculus* mouse and pooled in ice-cold 100 mM Tris buffer pH 7.4. The striata were transferred to 0.32 M unbuffered sucrose and manually disrupted in a glass homogenizer with a Teflon pestle. The homogenate was centrifuged at 3,000 *g* for 2 min. The supernatant was centrifuged at 14,000 *g* for 12 min. The soft pellet was resuspended in 0.32 M sucrose containing 10 mM N-tris(hydroxymethyl)-methyl-2-aminoethanesulfonic acid (TES, pH 7.4), and 4-ml aliquots were loaded onto discontinuous gradients consisting of three layers of Ficoll (Sigma) in sucrose (wt/vol ; 12%, 4 ml ; 9%, 1 ml ; 6%, 4 ml). The gradients were centrifuged at 62,483 *g* for 35 min. Synaptosomes were harvested from the 9% layer, diluted with 3 volumes of 10 m*M* TES buffer containing 140 m*M* NaCl, 5 m*M* KCl, 5 m*M* $NaHCO_3$, 1.2 mM Na_2HPO_4, 1 mM $MgCl_2$, and 10 mM glucose (pH 7.4), and centrifuged at 14,000 *g* for 12 min. Synaptosomes were resuspended in 0.5 ml of 10 mM TES buffer (pH 7.4). The preparation was divided into aliquots containing 0.8 mg of protein and centrifuged at 10,000 *g* for 2 min. Synaptosomes were overlaid with 200 µl of 0.25 M sucrose containing 5 mM TES (pH 7.4) and stored as pellets at –80°C.

Acetylcholinesterase activity Acetylcholinesterase activity was measured by using acetylthiocholine chloride (Sigma) as substrate and monitoring the thiocoline production as already described [Bergmeyer et al., 1983]. Synaptosomal (100 µg of protein) or erythrocyte membranes preparations (200 µg of protein) were added to a reaction mixture containing 0.4 mM acetylthiocholine in 50 mM phosphate buffer pH 7.2. The final volume of 1 ml was kept in the electromagnetic field 75 Hz, 2.5 mT. At different time intervals, aliquots of 100 µl were withdrawn and added to 50 µl of 25% PCA. Control samples were run in the same experimental conditions as above but in the absence of field. Each sample was centrifuged for 3min at 14,000 rpm and then 100 µl of supernatant was withdrawn and neutralized with 50 µl 2 M K_2CO_3. Centrifugation was repeated to remove potassium perchlorate. Aliquots of 100 µl of each neutralized extract were used for thiocoline assay by addind 0.5 mM DTNB in phosphate buffer pH 7.2 (1 ml final volume). Thiocoline reaction with DTNB gave thionitrobenzoate formation (ε_{405} = 1.33 mM^{-1} cm^{-1}) which was monitored spectrophotometrically by following the rise in absorbance.

Phosphoglycerate kinase activity Phosphoglycerate kinase activity was measured in red blood cell ghosts by following a method already described [Bergmeyer et al., 1983] with minor modifications. Ghosts (100 µg) were added to a solution containing 6.5mM glycerate-3-phosphate and 1.2mM ATP in 40 mM Tris HCl pH 8, 120 mM KCl, 10 mM $MgCl_2$. The final volume of 1 ml was kept in the electromagnetic field of 75 Hz and 2.5 mT.

At different time intervals, aliquots of 100 µls were withdrawn and added to 50 µl of 25% PCA. Control samples were run in the same experimental conditions as above but in the absence of the field.

Each sample was centrifuged for 3min at 14,000 rpm and then 100 µl of supernatant was withdrawn and neutralized with 50 µl 2 M K_2CO_3. Centrifugation was repeated to remove potassium perchlorate. Aliquots of 100 µl of each neutralized extract were used for the enzymatic assay by addind 2µl of glycerate–3-phosphate dehydrogenase, 0.2 mM NADH, 10 mM $MgCl_2$, 50mM Tris HCl buffer pH 8 (1 ml final volume). The corresponding NADH oxidation was monitored spectrophotometrically by following the decrease in absorbance at 340 nm (ε_{340} = 6.22 mM^{-1} cm^{-1}).

(Na, K)ATPase activity Plasma membrane Ca-ATPase activity was measured in erythrocyte membranes preparation through inorganic phosphate release. The standard reaction mixture contained 30 mM HEPES, pH 7.6, 140 mM KCl, 0.2 mM ouabain, 2 µg/ml CaATPase activity calmodulin, 2 mM ATP and 0.005 mM free Ca^{2+} (obtained with a Ca^{2+}-EGTA buffer; EGTA was 2mM). 2mM EGTA) in a final volume of 1 ml. Aliquots of erythrocyte membranes preparation (about 70 µg proteins) were added to the reaction mixture and incubated at room temperature for 20 min in the presence or in the absence of the field of 75 Hz and 2.5 mT. The final volume of 1 ml was kept in the electromagnetic field. At different time intervals, aliquots of 100 µls were withdrawn and added to 50 µl of 25% PCA. Each sample was centrifuged for 3min at 14,000 rpm and then 100 µl of supernatant was withdrawn and neutralized with 50 µl 2 M K_2CO_3. Centrifugation was repeated to remove potassium perchlorate. Control samples were run in the same experimental conditions as above but in the absence of field. The released inorganic phosphate was determined colorimetrically as described by Martin and Doty (1949). Blank subtraction was obtained by considering the amount of inorganic phosphate released by parallel samples incubated in the absence of Ca^{2+} and in the presence of 2 mM EGTA.

ATPase activity of erythrocyte membranes was assayed by the pyruvate kinase, lactate dehydrogenase system in which hydrolysis of ATP is coupled to the oxidation of NADH. ATP hydrolisis was measured in the presence or in the absence of the field for 20 min. An aliquot of 0.145 mg/ml erythrocyte membranes preparation was added to the reaction mixture containing 100 mM Tris–HCl pH 8, 2 mM $MgCl_2$, 150 mM NaCl, 50 mM KCl, 1 mM ATP. Aliquots of 100 µl of the reaction mixture were withdrawn and added to 50 µl of 25% PCA. Each sample was centrifuged shortly at 14,000 rpm and then 100 µl of supernatant was withdrawn and neutralized with 50 µl of 2M K_2CO_3. The centrifugation was repeated to remove potassium perchlorate. In order to measure the amount of ATP hydrolized, 100 µl aliquots of each neutralized extract were added to 1 ml final vol of reaction mixture containing 0.16 mM NADH, 1.5 mM phosphoenolpyruvate, 8 µg/ml pyruvate kinase, 8 µg/ml lactate dehydrogenase, 100 mM Tris–HCl pH 8.0; 5 mM $MgCl_2$. ATP hydrolysis coupled to oxidation of NADH was followed at 340 nm (ε_{340} for NADH=$6.22\times10^3 M^{-1}cm^{-1}$) in spectrophotometers. Ouabain-sensitive (Na^+,K^+)ATPase was determined as the difference between the enzyme activities in the presence and in the absence of 0.1 mM ouabain.

Microsome preparation Bovine liver was chopped and homogenized in 20 mM Tris-HCl pH 7.5 containing 0.25 M sucrose in a Potter apparatus. The homogenate was centrifuged for 10 min at 900 g. The supernatant was collected and centrifuged for 20 min at 20,000 g. The resulting supernatant containing cytosol and microsomes was collected and centrifuged at 100,000 g for 1 hr. The pellet containing microsomes was stored at –80°C.

Alkaline phosphatase activity Alkaline phosphatase activity was measured by using 4-nitrophenylphosphate (Sigma) as substrate and monitoring 4-nitrophenol formation as already described [Bergmeyer et al., 1983]. Microsomes from liver (100 µg of protein/ml) were added to a reaction mixture containing 4-nitrophenylphosphate (12 mM) 0.1 M glycine, 0.1 mM $ZnCl_2$, 1mM $MgCl_2$ (glycine buffer pH 10.5). The final volume of 1 ml was kept in the electromagnetic field for 20 min. At different time intervals, aliquots of 100 µls were withdrawn and added to 50 µl of 25% PCA. Control samples were run in the same experimental conditions as above but in the absence of field. Each sample was centrifuged 3 min at 14,000 rpm and then 100 µl of supernatant was withdrawn and neutralized with 50 µl 2 M K_2CO_3. Centrifugation was repeated to remove potassium perchlorate formed by the reaction between PCA and K_2CO_3. Aliquots of 100 µl of each neutralized extract were used for 4-nitrophenol assay by adding 0.1 M glycine buffer pH 10.5 (1 ml final volume) and measuring spectrophotometrically the increase in absorbance at 405 nm (ε = 1.85 $mmol^{-1}$ x cm^{-1}) which is proportional to the nitrophenol produced.

Mitochondria preparation Pieces of rat liver (3 g) were homogenated at ice temperature by Potter-Elvehjem system in 20 ml Buffer containing 0.25M Sucrose, 5 mM HEPES pH 7.2, 1mM EDTA. The liver homogenate was centrifuged for 10 min at 500g, at 4°C. After centrifugation, precipitate was discarded and supernatant was centrifuged again for 20 min at 20,000g. Then the pellet was collected and dissolved in 2 ml of homogenizing Buffer.

Succinic dehydrogenase activity Succinic dehydrogenase activity was assayed by the oxidation of succinic acid to fumaric acid coupled with $K_3Fe(CN)_6$ reduction, following the method of Bonner [1955] with minor modifications. The enzymatic activity was measured in the presence or in the absence of the field of 75 Hz and 2.5 mT for 20 min after addition of mitochondria preparation (0.1 mg of proteins) to 1 ml final volume of the

reaction mixture containing 100 mM Phosphate buffer pH 7.6, 70 mM Na succinate, 2 mM $K_3Fe(CN)_6$. At different time intervals, aliquots of 100 µls were withdrawn and the reaction was stopped with 0.25 ml Aceton. Then the samples were centrifuged for 3 min at 14,000 rpm, and supernatant was used for the succinic acid oxidation coupled to reduction of $K_3Fe(CN)_6$, which was followed spectrophotometrically at 400 nm (ε_{400} for $K_3Fe(CN)_6$ = 920 $M^{-1}cm^{-1}$).

Rod outer segments and disk membranes preparations In a typical experiment, rod outer segments (ROS) were isolated from 30 bovine retina in dim red light by following the method of Schnetkamp and Daemen [1982] by sucrose gradient centrifugation. Intact ROS were first washed in an isotonic medium containing 40 mM Tris-Maleate pH 7, 120 mM KCl and then centrifuged for 10 min at 1,500 g. Osmotically intact disks were obtained after bursting intact ROS for 3 h in 30 ml of 5% Ficoll (Sigma) in distilled water containing 5 mM DTT and 70 mg/ml leupeptin and then by collecting them in dim red light at the 5% Ficoll surface after centrifuging for 2 h at 25,000 rpm in a Beckman FW-27 rotor [Smith et al., 1985]. The disk membranes were washed in distilled water and centrifuged for 10 min at 1,500 g. The pellet (purified disk membrane preparation) was resuspended in the initial volume of distilled water and stored in the dark at - 80° C.

Rod disk phosphodiesterase activity cGMP Phosphodiesterase was assayed as follows. The reaction mixture contained 100 mM MOPS (pH 7.1), 140 mM KCl, 20 mM NaCl, 5 mM $MgCl_2$, 2mM GTP and 5 mM cGMP. The reaction was started by adding 50 µl of reaction mixture containing 4 µCi [8-^{3}H] cGMP (specific activity: 12.7 Ci/mmol) to 50 µl of purified disk membrane preparation previously bleached in the room light (final concentration: 1 – 2 mg/ml protein). The reaction was run in the presence or absence of ELF-EMF of 75 Hz and 2.5 mT, at room temperature and stopped after 1, 3, 5, 10 and 20 min by adding 5 µl of 100 mM EDTA to each 20 µl withdrawn sample and boiling for 2 min. After centrifuging, 10 µl of the supernatants were analysed by TLC on polyethyleneimine-cellulose developed in one dimension with 1M LiCl. 5'-GMP was added as internal standard. The separed spots corresponding to cGMP and 5'-GMP, visualized under UV light, were cut into scintillation vials, eluted in 0.5 ml of 0.7M MgCl2/1M TrisHCl pH 7.4 (10/2 v/v) , added to 3 ml of Instagel, left overnight and then counted in a LKB liquid scintillation counter.

LIPOSOME: A MODEL FOR PROBING THE INTERACTION OF ELECTROMAGNETIC FIELDS AND BIOSYSTEMS

ALFONSINA RAMUNDO-ORLANDO[a], GUGLIELMO D'INZEO[b], GIAN PIERO GALLERANO[c]

[a]INSTITUTE OF NEUROBIOLOGY AND MOLECULAR MEDICINE OF ITALIAN RESEARCH COUNCIL, VIA DEL FOSSO DEL CAVALIERE, 00133 ROME, ITALY; [b]DEPARTMENT OF ELECTRONIC ENGINEERING, UNIVERSITY 'LA SAPIENZA', VIA EUDOSSIANA, 18-00184 ROMA, ITALY; [c]UTS TECNOLOGIE FISICHE AVANZATE, ENEA-FRASCATI, VIA ENRICO FERMI 4, P.O. BOX 65, 00044 FRASCATI –ITALY.

Abstract

Liposomes are very useful model membrane systems: Although they are unable to mimic all the complexity of a cell membrane, they have a well-defined chemical composition, the capacity to arrange themselves in bilayers, selectivity to ionic species and molecules, and many other useful features. Interactions can take place between this model system and electromagnetic fields (EMFs) at different frequencies, from extremely low frequency up to microwave and THz range, so that, a comparative evaluation of the observed effects with different EMF components is allowed. In this context we used cationic Carbonic Anhydrase (CA)-loaded liposomes. The CA was entrapped into these liposomes and the hydrolysis rate of substrate p-nitrophenyl acetate (p-NPA) added in the bulk aqueous phase was adopted as the index of membrane permeability changes. In fact previous kinetic experiments showed a very self-diffusion rate of p-NPA across intact liposome bilayer. Observations reported by our group evidenced that combined 7 Hz sinusoidal (B_{acpeak} = 50μT) and parallel static (B_{dc} = 50μT) magnetic fields can induce permeability changes in these liposomes. Further, we reported on the effects of 2.45 GHz microwave exposure (6 mW/g) on the permeability of these cationic liposomes. Finally, we report on the effects of 130 GHz radiation modulated at low frequency of 5, 7 and 10 Hz on the permeability of these cationic liposomes. The enzyme activity, as function of increased diffusion of p-NPA, rises from 23% to 61% over 3 min of 130 GHz radiation modulated at 7 Hz, at incident intensity of 10.5 mW/cm^2, and a peak electric field of 2.6 kV/cm. The increase of the incident intensity up to 17 mW/cm^2 did not further increase the enzyme activity. This biological model demonstrates an extraordinary sensibility in revealing the influence of EMFs on the lipid bilayer permeability and allowed an interaction mechanism with an ELF magnetic field to be derived.

Introduction

When considering the action of electromagnetic fields (EMFs) on a biological system, the cell membrane is indicated by the most part of studies as the primary site of interaction [1]. Living organisms are made of cells bound by their membranes. They are self-assembly entities; each is organizing a particular combination of phospholipids in the form of a bilayer with other constituents (e.g. proteins) embedded in it. This lipid bilayer existing in all biomembranes is most unique; it serves not merely as a physical barrier but functions as a two-dimensional matrix for reactions. Also the lipid bilayer acts as a conduit for ion transport, as a framework for antigen-antibody binding, as bipolar electrode for redox reactions, and as a reactor for energy conversion (e.g. light to electric to chemical). Further, a modified lipid bilayer performs as a transducer for signal transduction (i.e., sensing), and numerous other functions as well. All these myriad activities require the ultra thin lipid bilayer. In particular, molecular systems that have been suggested to be candidates for direct modulation by

EMFs are the binding of extracellular ligands to the cell-surface receptor sites, and translocation of charged ionic species across the lipid bilayer. Both events lead to the activation of diverse biochemical pathways that transduce signals to internal sites within the cell [2].

In spite of the huge number of papers that have studied the biological effects of EMFs exposure on cell membrane, from an experimental and theoretical point of view [see reviews 3-6], we reckon to have a nearly complete knowledge by now only in the case of thermal effects. These are due to a sharp increase of temperature that can be systemic or localized. Such effects typically correspond to high power radiation. On the other hand, the complexity of the cell membrane we want to study the interaction with leads to hypothesize the possibility of more subtle specific or non-thermal effects. These are due to phenomena that have no dependence on the thermal energy deposited, or for which temperature is merely one of many significant parameters, and can occur even if the external EMF is weak. Research on these specific effects requires an experimental approach enabling to reduce the complexity of the systems involved.

The cell membrane acts as a gateway to the cell, 30% of all proteins within the body are membrane proteins and 60% of drug targets are membrane proteins. Despite its immense complexity, however, the functionality of the membrane is ultimately determined by its mechanical and electrical properties.

In order to reduce the complexity of this biological system, we suggest the use of membrane model so that physical, biochemical, and physiological processes may be isolated and analysed in molecular terms. Amongst these model systems, liposomes are very useful, although they are unable to mimic all the complexity of a cell membrane; they have a well-defined chemical composition, the capacity to arrange themselves in bilayers, selectivity to ionic species and molecules, and many other useful features [7-8]. Liposomes occur naturally and can be prepared artificially from natural or synthetic lipid molecules [9]. They can encapsulate or bind a variety of molecules, such as drug molecules, proteins, nucleotides and even plasmids, into or onto the membrane [10].

For more than 15 years our laboratory has been studying the possibility of the use of liposomes in an effort to clarify the mechanism of how EMFs exposure induce alterations of membrane permeability, focusing the attention mainly on the membrane phospholipidic components [11-14].

In this context cationic CA-loaded liposomes (Fig.1) revealed an extraordinary sensibility toward the EMFs induced-effects.

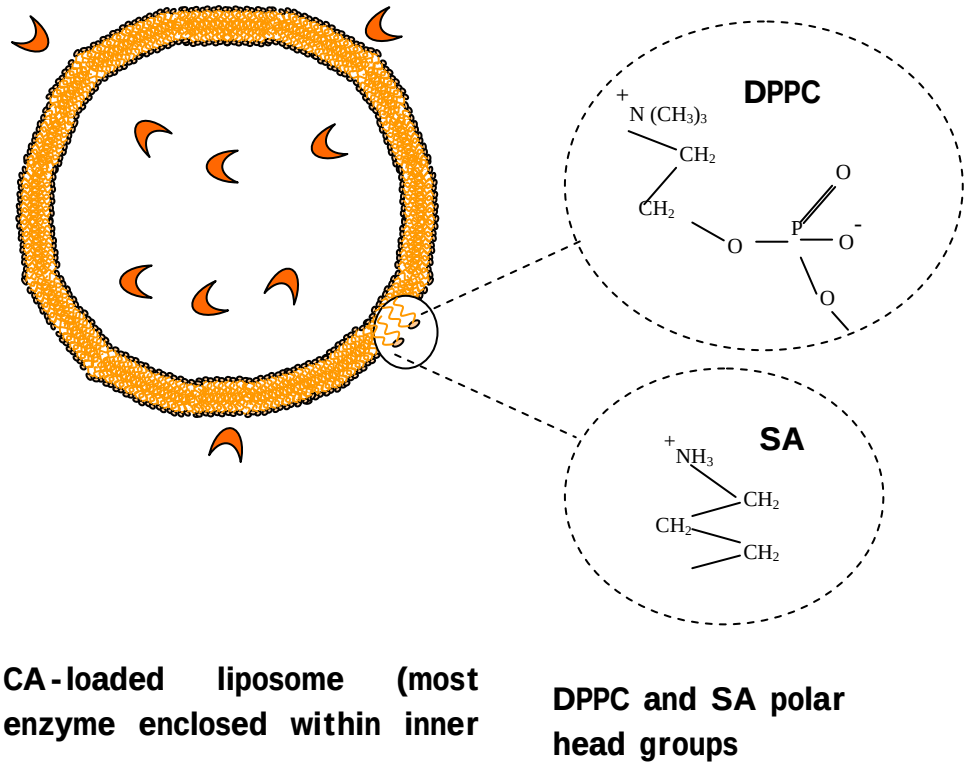


Fig. 1. Schematic representation of CA-loaded liposomes where the dipolar (e.g. DPPC) and unipolar (e.g. SA) chemical structures in the lipid bilayer are depicted.

They are formed by controlled dialysis of detergent (DIAL) and containing dipalmitoylphosphatidylcholine (DPPC), cholesterol (CHO), and the charged lipid stearylamine (SA). Because entrapping Carbonic Anhydrase (CA) these liposomes could be considered as a bioreactor. To follow any alteration due to EMFs exposure on the permeability of lipid membrane we add in the bulk aqueous phase the substrate p-nitrophenyl acetate (p-NPA) in great excess to have a steady-state condition limited only by the enzyme activity. Because the p-NPA cannot pass freely across the lipid bilayer, or with a very low self-diffusion, any enhancement of its hydrolysis rate can be assumed due to permeability change enabling the p-NPA to reach the enzyme into the inside of liposomes. We carry out kinetic measurements by monitoring the appearance of the product of p-NPA hydrolysis at its peak of absorbance at 400 nm in a Cary50 spectrophotomer. Typical recorded curves of change of absorbance at 400 nm against time (min) in the sham and exposed samples are shown in Fig. 2. The difference between the p-NPA hydrolysis rate in the exposed sample and the sham one is taken as an index of permeability changes due to the exposure. The temperature is always recorded during the entire exposure time.

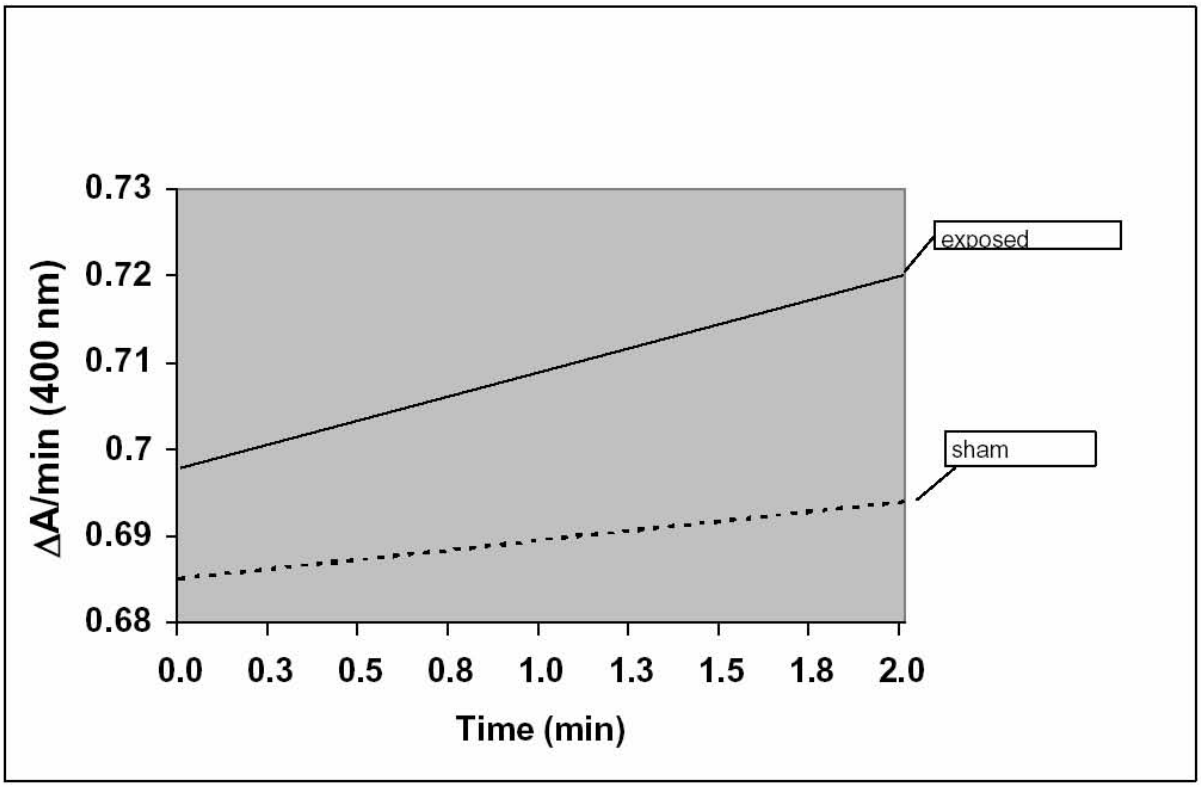


Fig. 2. Typical recorded curves of the p-NPA hydrolysis rate of CA-loaded liposomes during EMFs exposure are shown.

Typically, in these cationic liposomes, a non-zero p-NPA hydrolysis rate resulted in the sham samples (Fig. 2). Indeed, due to electrostatic interactions between the enzyme and the positive charge on the lipid membrane, a small fraction of enzyme is located on the surface of liposomes.

In order to normalize the kinetic data obtained with several liposome preparations used throughout our studies, we determine the total activity of CA (100%) released from each liposome preparations after their disruption with detergent (n-octyl-β-glucopiranoside). Then, the relative *p*-NPA hydrolysis rates in intact liposomes are expressed as percentage values (%), and calculate for every exposed and sham sample toward 100% of CA.

We speculated that the above experimental system, in contrast to living cells, was well defined and had

only a limited number of parameter, thus allowed to evaluate in a comparative way the biological effects induced by EMFs with different components. This idea was supported by the following findings.

We found that 2.45 GHz microwave radiation (6 mW/g) induced an increase of p-NPA hydrolysis rate from 41% ± 7 to 80% ± 11 in eight different CA-loaded liposome preparations [15]. An S-band exposure chamber, with a coax-waveguide transition bandwidth input 1.7-2.6 GHz, was used. The SAR of the samples was calculated by the experimental curve of the temperature increase inside a water-filled cuvette in absence of thermostatic control. We speculated that the net surface charge in the vesicles might be involved in the response of liposomes to MW field exposure, since the permeability effect could be dependent on electrostatic charge. This idea was supported by the finding that liposomes with higher net surface charge (i.e., DPPC:CHO:SA at 5:3:2 lipid ratio) showed an higher effect than ones with 6:3:1 ratio. We also found that the MW induced-effect on substrate permeation occurred well below (20°C) the phase-transition temperature of liposomes (≈ 40°C), in agreement with literature data [16-17]. It should be noted that liposomes exhibit phase transitions which can be triggered by (inter alias) changes in the total or average area of polar heads on the outer monolayer, these transitions has been proposed to induce changes in the membrane permeability which are analogous to microwave-induced permeability changes [18].

We used the same experimental approach in an effort to clarify the mechanism for how extremely low frequency (ELF) electromagnetic fields exposure influences the trans-membrane movement of free ions in cell membranes [19-21]. Such experimental evidences demonstrate a change in free calcium concentration between the extra- and the intracellular medium under the presence of an ELF magnetic field combined with a static magnetic field.

In this context, we investigated whether combined sinusoidal (AC) and static (DC) magnetic fields could affect the permeability of our cationic CA-loaded liposomes under well-controlled field exposure conditions. The magnetic field was generated by a series of perpendicular nested coils. Each set of coils controls the component direct along its axis. In the center of the apparatus a large isofield region (8 cm^3) with a field uniformity of 1% was obtained. The values of the three components of the magnetic field were generated and maintained by the feedback system [22]. We found that 7 Hz sinusoidal (Bacpeak = 50μT) and parallel static (Bdc = 50μT) magnetic fields exposure induced an increase in the hydrolysis rate of p-NPA in these liposomes [22]. We speculated that the positive charges of SA on the liposome surface might be responsible for the effect. This idea was supported by the findings that the effect was linear with the increase of SA concentration in the lipid mixture and nullified by neutralizing the positive charge of SA, upon going from pH 7.55 to 8.95 in the reaction medium. Moreover, the presence of CA partially located on the external surface of these liposomes would be expected to be a confounding factor in determining the primary target on the membrane for the interaction of the ELF magnetic field. Therefore we studied the influence of ELF magnetic field on the catalytic parameters of the CA. No structural change of the enzyme, as revealed by the K_m values, was found when CA was either free in solution or loaded in liposomes. Further a specific treatment of the liposomes with a protease able to remove the CA partially located on their surface did not indicate any role for the enzyme itself in the effect [23].

Based on these results an interaction model between the magnetic field and the polar structures embedded in the liposomes has been proposed [23]. The proposed model shows the possibility of inducing a precessional motion by applying suitable dynamic magnetic field. As a result, the charged structures (e.g. - $CH_2CH_2NH_3^+$ in SA) on the lipid membrane could move in a way such as to facilitate the passage of external substances right through the membrane [23-24].

The increasing interest in the THz (Tera-Hertz) region of the electromagnetic spectrum, extending from 100 GHz to 10 THz, in biomedical science [25-26], and the scarce knowledge about the biological effects of this THz region on living systems, suggested us to use our experimental approach in the context of the European Project THz-BRIDGE dealing specifically to investigations on diagnostic and potential genotoxic effects induced by THz radiation.

A series of experiments examining the effects of 130 GHz radiations, modulated at low frequency (5, 7 and 10 Hz) on membrane permeability were carried out. The THz radiation were conducted by using a Compact THz Free Electron Laser (FEL) providing coherent radiation at 130 GHz with a 10% relative bandwidth in the form of a "train" of micro pulses of about 50 ps duration each, with 330 ps spacing between adjacent pulses [27]. The overall duration of the train (macro pulse) is 4 μs. Macro pulses can be produced up to a maximum repetition frequency of 10 Hz.

We found that the THz exposure induces an increase of the p-NPA hydrolysis rate on CA-loaded liposomes in a dose-dependent manner. Indeed, by applying an incident power lower than 8 mW/cm^2 the effect was found only for modulation at 7 Hz. By increasing the field power the effect was also found at modulation of 5 and 10 Hz, though always much more less significant than at 7 Hz. We speculated that probably a temperature rise in the exposed sample rather than a modulation at a specific frequency might be responsible for the effect. Therefore, we studied exposure induced membrane changes on liposome at a different phase transition state by exchanging the DPPC with POPC in the lipid mixture. Further, we prepared the latter

liposome in a different manner avoiding the detergent dialysis, thus producing VET liposome populations with a higher diameter *vs.* DIAL ones. POPC liposomes, which are in fluid phase, showed that THz exposure does not induce any increase in liposome permeability, and that the temperature variations recorded in the samples during the exposure were negligible. Based on these results we excluded a thermal-based explanation for the effect.

Electrical double layers form at each side of the cell membrane, in equilibrium, this potential is of the order 100 mV ($E_{bilayer} \sim 10^7$ Vm^{-1}) when the net ion flux (mainly K^+, Na^+, Cl^-, Ca^{2+}) through the membrane is zero, and any disturbance of the membrane (e.g. by absorption of electromagnetic radiation in the membrane) can result in a change in the potential difference across the system. In the 130GHz experiments noted above, the peak electric field (E_{130GHz}) was two orders of magnitude lower than naturally developed across bilayers. Despite this comment, the influence of the electric field cannot be excluded for the effect of permeability change on lipid membrane, as the effects appear be pronounced only within a certain field range (Fig. 3). As living organisms are not adapted to this spectral range of radiation, and the possible resonance characteristics of its action, it may be possible that a relatively small influence causes a pronounced effect.

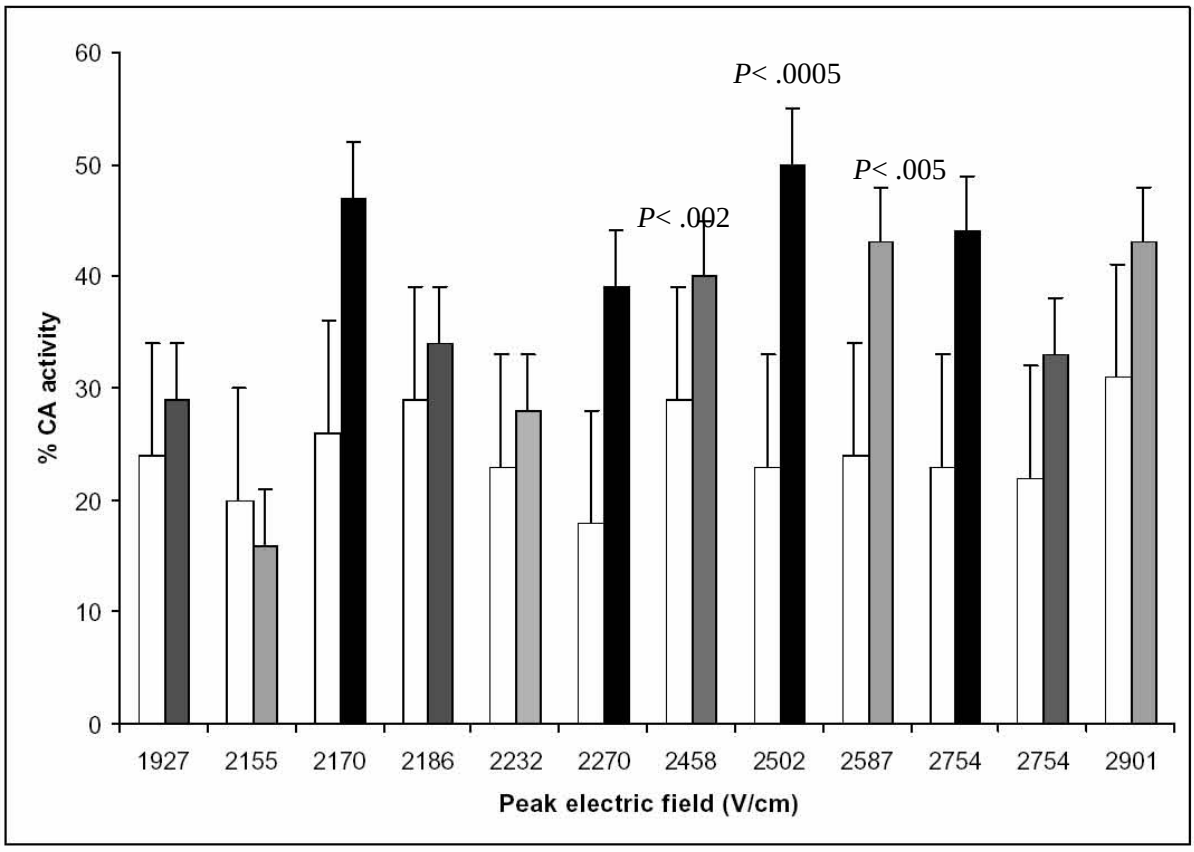


FIG. 3. Effect of 130 GHz radiation on CA reaction rate of DIAL liposomes. % CA reaction rates as a function of the peak electric field are shown for three different pulse repetition rates: 10 Hz (dark grey), 7 Hz (black) and 5 Hz (light grey), sham (white). Statistical significances are presented as P of unpaired two-tailed t-test at 95% confidence intervals.

Summary

The use of cationic liposomes entrapping an enzyme for the evaluation of permeability changes induced by EMFs on cell membrane has been proposed. This system allows comparative evaluation of the induced effects by exposure at different EMF components. Specifically, membrane components, with typical dipolar (e.g. phospholipids), or unipolar (e.g. cationic amines) structures, may be focused to study and find interpretation keys on the biointeraction phenomenon, under EMFs exposure conditions.

References

1. C. Polk, E. Postow. Biological Effects of Electromagnetic Fields. CRC Press, Boca Raton, 2nd Edition, 1996.

2. Rodbell, E. Signal transduction: evolution of an idea. *Biosci. Rep.* 15 :117-133, 1995.

3. Zhadin, M. N. Review of Russian literature on biological action of DC and low-frequency AC magnetic fields. *Bioelectromagnetics* 22:27-45, 2001.

4. Repacholi, M.H. Health risks from the use of mobile phones. *Toxicology Letters* 120:323-331, 2001.

5. Litvak, E. Foster, K.R., Repacholi, M.H. Health and safety implications of exposure to electromagnetic fields in the frequency range 300 Hz to 10 MHz. *Bioelectromagnetics* 23:68-82, 2002.

6. Fedorov, V.I., Popova, S.S., Pisarchik, A.N. Dynamic effects of submillimeter wave radiation on biological objects of various levels of organization. *Int. J. Infrared Millimetr Wave* 24:1235-1253, 2003.

7. Gregoriadis G. (Editor) Liposome Technology 2nd Edition Boca Raton CRC, 1993.

8. Walde P. Preparation of vesicles. Encyclopedia of Nanonoscience and Nanotechnology in: H.S. Nalwa (Ed.) American Scient. Publishers, vol. X, pp. 1-37, 2003.

9. Lasic, D. D. Liposomes: from physics to applications. *Trends in Biotechnology* 16:307-321, 1998.

10. Ramundo-Orlando, A., Serafino, A., Villalobo, A. Gap junction channels reconstituted in two closely apposed lipid bilayer. *Archives of Biochemistry and Biophysics* 436:128-135, 2005.

11. Ramundo-Orlando, A., Arcovito, C., Palombo, A., Serafino. A.L., and Mossa, G. Enzymatic kinetic change of Ascorbate Oxidase loaded into liposomes induced by microwave fields exposure. *Journal of Liposomes Research* 3(3): 717-724, 1993.

12. Ramundo-Orlando, A., Gensabella, R., and d'Inzeo, G. The enhancement of lipid peroxidation kinetics in phosphatidylcholine liposomes by microwave radiation. *Res. Commun. Biochem. Cell & Mol. Biology* 3, 233-250, 1999.

13. Ramundo-Orlando, A., Liberti, M., Mossa, G., and d'Inzeo, G: Effect of 2.45 GHz microwave fields on liposomes entrapping glycoenzyme ascorbate oxidase. Evidence for oligosaccharide side chains involvement. *Bioelectromagnetics* 25: 338-345, 2004.

14. Ramundo-Orlando, A., Serafino, A., Schiavo, R., Liberti, M., d'Inzeo, G. Permeability changes of connexin32 hemichannel reconstituted in liposomes induced by extremely low frequency, low amplitude magnetic fields. *BBA-Biomembranes* 1668(1): 33-40, 2005.

15. Ramundo-Orlando, A., Mossa, G., and d'Inzeo, G. Effect of microwave radiation on permeability of Carbonic Anhydrase loaded unilamellar liposomes. *Bioelectromagnetics* 15(4): 303-313, 1994

16. Liburdy R.P. Fingado, B. "Effects of MW fields on liposome permeability: Non-phase transition liposome vesicles" 12th Annual BEMS Meeting, San Antonio, Texas, 10-14 June, 1990

17. Saalman, E. Norden, B., Arvdsson, L., Hamnerius, Y., Hojevik, P. Connell, K.E., Kurucsev, T. Effect of 2.45 GHz microwave radiation on permeability of unilamellar liposomes to 5(6)-carboxyfluorescein. Evidence of non-thermal leakage. *Biochem. Biophys Acta* 1064:124-130, 1991.

18. Liburdy, R.P. Magin, R.L. Microwave stimulated drug release from liposomes. *Radiat. Res.* 103:266-275, 1985

19. Liboff, A.R. Cyclotron resonance in membrane transport. In Interaction between EMFs and cells". Chiabrera A.,Nicolini, C. and H.P. Schwan (eds), London, Plenum Press, pp. 281-296, 1985.

20. Liboff, A.R. Smith, S.D. and McLeod B.R. Experimental evidence forion cyclotron resonance mediation of membrane transport. In Mechanistic Approach to Interaction of Electric and EMFs with living systems, M. Blank and E. Findl (eds), New York, Plenum Press, pp.109-132, 1987.

21. Blackman C. F., Benabe, S.G., House, D.E. and Joines W.T. Effects of ELF(1-120 Hz) and modulated (50 Hz) RF fields on the efflux of calcium ions from brain tissue in vitro. *Bioelectromagnetics*, 6:1-11, 1985.

22. Ramundo-Orlando, A., Morbiducci, U., Mossa, G., and d'Inzeo, G. Effect of low-frequency, low-amplitude magntic fields on the permeability of cationic liposomes entrapping carbonic anhydrase.I. Evidence for charged lipid involvement. *Bioelectromagnetics* 21:491-498, 2000.

23. Ramundo-Orlando, A., Mattia, F., Palombo, A., and d'Inzeo, G. Effect of low-frequency, low-amplitude magntic fields on the permeability of cationic liposomes entrapping carbonic anhydrase.II. No evidence for surface enzyme involvement. *Bioelectromagnetics* 21: 499-507, 2000.

24. Cappelli, M. d'Inzeo, G. Apollonio, F. and Liberti, M. A possible mechanism explaining variation in membrane permeability under exposure to weak magnetic fields. Proceedings of 26th IEEE-EMBS Congress, 1-5 Sept. 2004.

25. Woodward R. 2004. Terahertz Technology in the Medical and Pharmaceutical Industry. *Preclinica* 2:328-335.

26. Woolard DL, Brown ER, Pepper M, Kemp M. 2005. Terahertz frequency sensing and imaging: a Time of reckoning future applications? Proceedings IEEE 93:1722-1743.

27. Gallerano GP, Doria A, Giovenale E, Renieri A. Compact free electron lasers: from Cerenkov to waveguide FELs. *Infr. Phys. Tech.* 40:16-20, 1999.

ELF MAGNETIC FIELDS AFFECT STEM CELL DIFFERENTIATION: RESULTS AND PERSPECTIVES

F. BERSANI*, C.VENTURA§, P.MESIRCA*, M. MAIOLI‡
*DEPARTMENT OF PHYSICS, UNIVERSITY OF BOLOGNA, ITALY
§INSTITUTE OF CARDIOLOGY, UNIVERSITY OF BOLOGNA, ITALY
‡DEPARTMENT OF BIOMEDICAL SCIENCES, UNIVERSITY OF SASSARI, ITALY

Abstract

The exposure of mouse embryonic stem (ES) cells to extremely low frequency magnetic fields (ELF-MFs) triggered the expression of GATA-4 and Nkx-2.5, acting as cardiac lineage-promoting genes in different animal species, including humans. ELF-MFs also enhanced prodynorphin gene expression, and the synthesis and secretion of dynorphin B, an endorphin playing a major role in cardiogenesis. These effects occurred at the transcriptional level and ultimately ensued into a remarkable increase in the yield of ES-derived cardiomyocytes. These results demonstrate the ability of ELF-MFs to modify the gene program of cardiac differentiation in ES cells without the aid of gene transfer technologies.

INTRODUCTION

Extremely low frequency Magnetic fields (ELF-MFs) have been shown to elicit behavioural changes in intact organisms (1) and affect proliferation and growth factor expression in cultured cells (2,3).
Nevertheless, only a few reports suggest that ELF-MFs may affect cell differentiation (4-6).

In the present study, we used murine embryonic stem (ES) cells as an in vitro model of cardiac differentiation and assessed whether ELF-MF (Fig. 1) may be involved in the activation of a gene program of cardiac lineage commitment

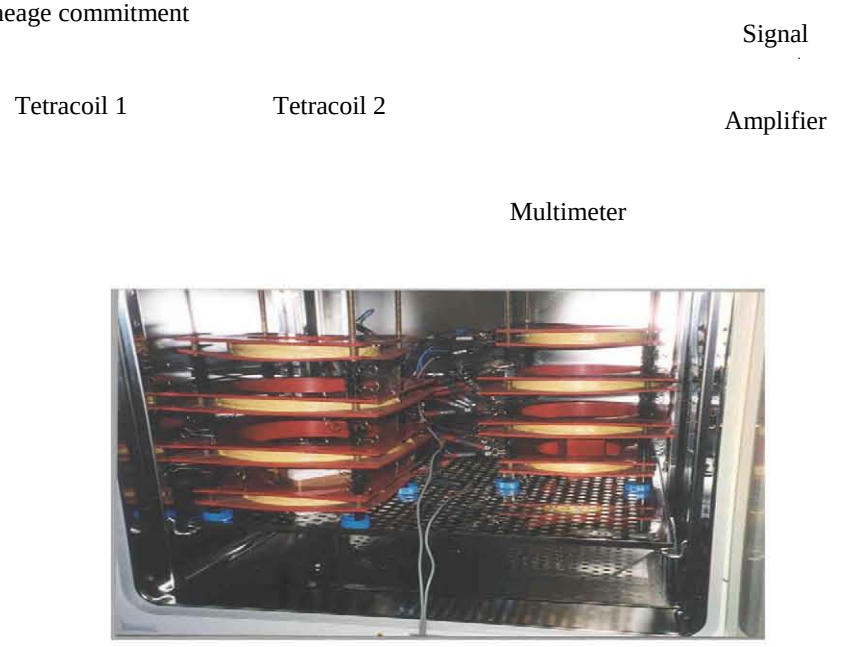


Figure 1

Exposure system and signal characteristics:

- signal generator: Beckman FG3A
- c.c. current amplifier (home made) for low resistive load
- multimeter: Fluke 85III

- two tetracoils, each composed of four coaxial coils, 40 (20+20) turns each, which were double-wrapped to obtain wound (active) or counter-wound (sham) configuration. The inner coils have radii of 10 cm, and the outer of 7 cm. With this configuration a very large region of magnetic field uniformity can be obtained.
- Signal: 50 Hz, sinusoidal, intensity 0.8 mT_{rms}
- The two tetracoils were placed inside the same incubator as shown in the picture.

ELF-MFs were applied to GTR1 ES cells, a derivative of R1 ES cells bearing the puromycin resistance gene driven by the cardiac specific MHC promoter (GTR1 cells were kindly provided by Dr. William L. Stanford, University of Toronto and Centre for Modeling Human Disease, Canada). ES cells were maintained in the undifferentiated state by culturing in KNOCKOUT D-MEM containing 15% FBS, supplemented with 1000 U/ml LIF (Leukemia Inhibitory Factor). To induce cardiac differentiation, cells were plated onto special plates (Costar ultra low attachment clusters), containing KNOCKOUT D-MEM, lacking supplemental LIF. After 2 days, the resulting embryoid bodies (EBs) were plated onto tissue culture dishes. When spontaneous contractile activity was noticed, puromycin (2µg/ml) was added to eliminate non-myocardial cells. After 2 days, puromycin selected cells were transferred to new tissue culture dishes. EBs, collected at several stages after plating, as well as puromycin-selected cells were processed for gene expression analyses. Following LIF removal and throughout puromycin selection, GTR1 cells were also exposed to a sinusoidal ELF-MF (50 Hz, 0.8 mT_{rms}). The analysis of mRNA expression was performed by RT-PCR technique.

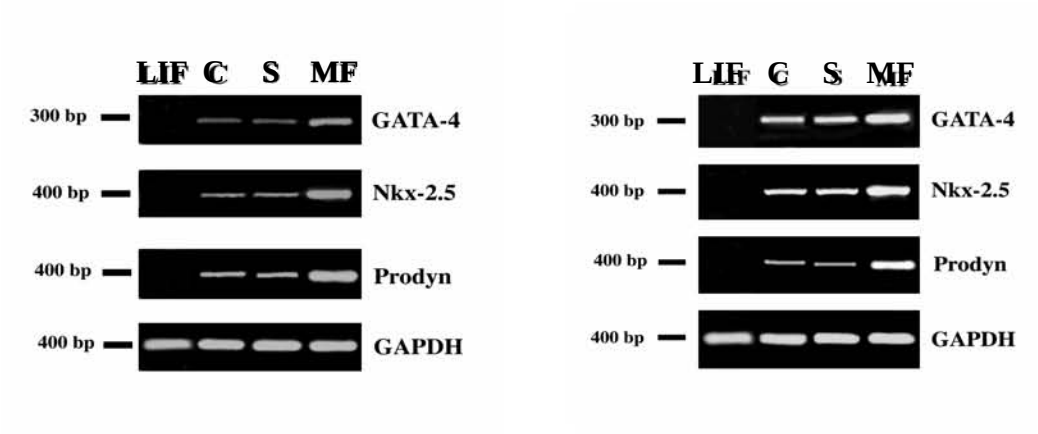


Figure 2

Effect of ELF-MFs on a cardiogenic transcriptional profile in embryoid bodies (left panel) and puromycin-selected cardiomyocytes (right panel). LIF, leukemia inhibitory factor; C, control; S, sham; MF, magnetic field; Prodyn, prodynorphin. GAPDH, (Glyceraldehide-3-phosphate dehydrogenase) was used as reference.

Exposure to ELF-MFs triggered the expression of GATA-4 and Nkx-2.5 mRNA in both EBs and puromycin-selected cardiomyocytes. Notably, these transcripts encode for a zinc finger-containing transcription factor and a homeodomain, that are both essential for cardiac lineage commitment in different animal species, including humans (7-9). Moreover, ELF-MF increased the expression of the prodynorphin gene, which encodes for the dynorphin family of endorphin peptides, previously shown to act as orchestrators of the transcription of both cardiogenic and cardiospecific genes in mouse ES cells (10,11). Consonant with our previous findings (12), the increase in prodynorphin mRNA was associated with an increase in the expression of dynorphin B, a bioactive end-product of the gene (not shown).

The attainment of a cardiac fate was inferred by the observation that ELF-MFs also elicited the expression of cardiac specific genes, including myosin light chain 2-V and alpha-myosin heavy chain, as shown in Fig. 3.
On the whole, the over-expression of both cardiogenic and cardiac-specific genes induced by ELF-MFs ensued in a remarkable increase in the yield of ES-derived spontaneously beating cardiomyocytes.

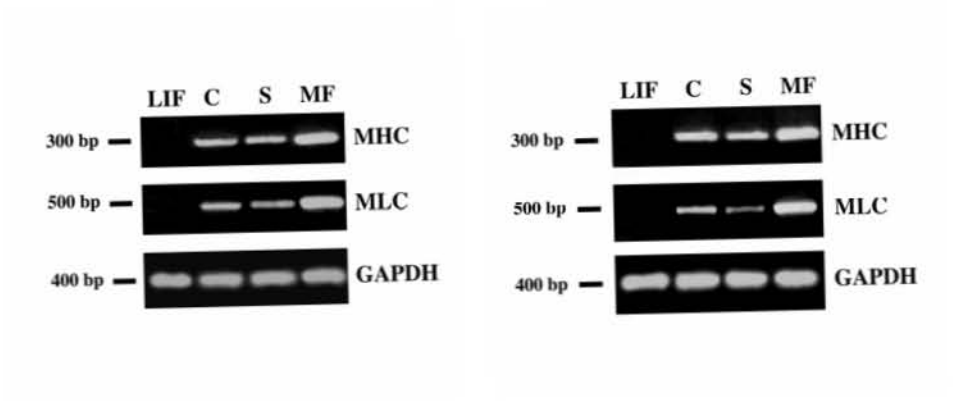


Figure 3
Effect of MF on the Expression of Cardiac Specific Genes.

Left panel, ELF-MF was applied from the time of LIF removal and EBs were collected after 3 days.
Right panel, ELF-MF was applied from the time of LIF removal throughout puromycin selection. Four days after puromycin addition, ES-derived cardiomyocytes were processed for gene expression analyses.
MHC, alpha-myosin heavy chain; MLC, myosin light chain-2V; C, control cells; S, Sham; MF, magnetic field.

To assess whether commitment to other cell lineages were recruited by ELF-MF, we investigated the expression of neurogenin-1, a gene involved in neuronal specification, and myoD, a transcript associated with skeletal myogenesis. While myoD was not affected by cell exposure, neurogenin-1 mRNA was only slightly increased in EBs (Fig. 4).

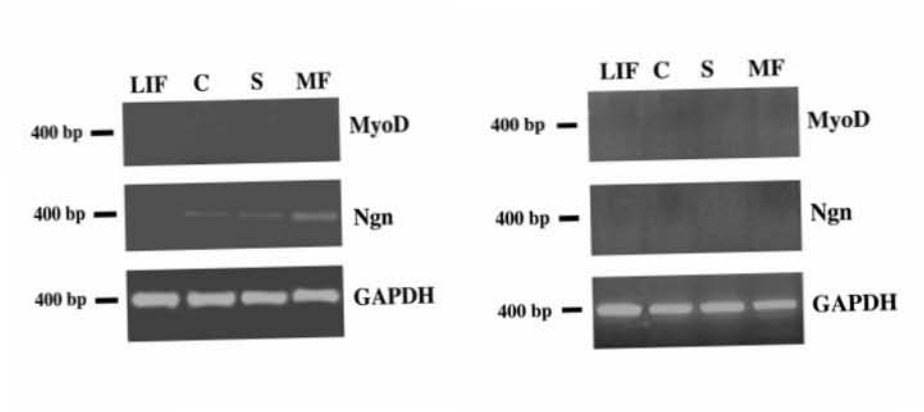


Figure 4
Effect of ELF-MF on the expression of genes promoting non-myocardial lineages.
Left Panel, ELF-MF was applied from the time of LIF removal and EBs were collected after 3 days.

Right panel, ELF-MF was applied from the time of LIF removal throughout puromycin selection. Four days after puromycin addition, ES-derived cardiomyocytes were processed for gene expression analyses. Ngn, neurogenin1, determination gene; C, control; S, Sham; MF, magnetic field.

Summary

The development of a model of *in vitro* cardiogenesis based on "gene trapping" selection of cardiomyocytes from pluripotent GTR1 cells provided a homogeneous and reproducible approach to assess the effect of MF on developmental decisions in ES cells.

In this model of cardiogenesis, MF elicited the expression of a gene program of cardiogenesis, along with the induction of cardiac-specific transcripts.

MF failed to activate skeletal myogenesis but slightly enhanced the expression of a vertebrate neural determination gene.

These results demonstrating the potential use of magnetic fields for modifying the gene program of cardiac differentiation in ES cells without the aid of gene transfer technologies may pave the way for novel approaches in tissue engineering and cell therapy. Within this context we are now planning to investigate whether ELF-MF with different physical characteristics (frequency, amplitude and wave shape) may influence cell lineage commitment even in human mesenchymal stem cells.

Acknowledgments

This work was supported by the European Project "Risk evaluation of potential environmental hazards from low-energy electromagnetic field exposure using sensitive in vitro methods" (REFLEX), by Ministero dell'Istruzione, dell'Università e della Ricerca (MIUR) 5% "Salvaguardia dell'uomo e dell'ambiente dalle emissioni elettromagnetiche," by MIUR Fondo Integrativo Speciale per la Ricerca – 2001, and by Ministero della Sanità (Attività di Ricerca Finalizzata – 2002).

References

1. Lai H, Carino MA, Horita A, Guy AW. Effects of a 60 Hz magnetic field on central cholinergic systems of the rat. *Bioelectromagnetics.* 1993;14:5–15.
2. Cossarizza A, Monti D, Bersani F, Cantini M, Cadossi R, Sacchi A, Franceschi C. Extremely low frequency pulsed electromagnetic fields increase cell proliferation in lymphocytes from young and aged subjects. *Biochem Biophys Res Commun.* 1989;160:692-8.
3. Cossarizza A, Angioni S, Petraglia F, Genazzani AR, Monti D, Capri M, Bersani F, Cadossi R, Franceschi C. Exposure to low-frequency pulsed electromagnetic fields increases interleukin-1 and interleukin-6 production by human peripheral blood mononuclear cells. *Exp Cell Res.* 1993; 204:385–7.
4. Diniz P, Shomura K, Soejima K, Ito G. Effects of pulsed electromagnetic field (PEMF) stimulation on bone tissue like formation are dependent on the maturation stages of the osteoblasts. *Bioelectromagnetics.* 2002;23:398-405.
5. Manni V, Lisi A, Rieti S, Serafino A, Ledda M, Giuliani L, Sacco D, D'Emilia E, Grimaldi S. Low electromagnetic field (50 Hz) induces differentiation on primary human oral keratinocytes (HOK). *Bioelectromagnetics.* 2004;25:118-26.
6. Lisi A, Ciotti MT, Ledda M, Pieri M, Zona C, Mercanti D, Rieti S, Giuliani L, Grimaldi S. Exposure to 50 Hz electromagnetic radiation promote early maturation and differentiation in newborn rat cerebellar granule neurons. *J Cell Physiol.* 2005;204:532-8.
7. Biben C, Harvey RP. Homeodomain factor Nkx-2.5 controls left/right asymmetric expression of bHLH gene eHand during heart development. *Genes Dev.* 1997;11:1357–69.
8. Lints TJ, Parsons LM, Hartley L, Lyons I, Harvey RP. Nkx-2.5: a novel murine homeobox gene expressed in early heart progenitor cells and their myogenic descendants. *Development.* 1993;119:419–31.
9. Benson DW, Silberbach GM, Kavanaugh-McHugh A, Cottrill C, Zhang Y, Riggs S, Smalls O, Johnson MC, Watson MS, Seidman JG, et al. Mutations in the cardiac transcription factor Nkx-2.5 affect diverse cardiac developmental pathways. *J Clin Invest.* 1999;104:1567–73.

10. Ventura C, Zinellu E, Maninchedda E, Fadda M, Maioli M. Protein kinase C signaling transduces endorphin-primed cardiogenesis in GTR1 embryonic stem cells. *Circ Res.* 2003;92:617–22.
11. Ventura, C., Zinellu, E., Maninchedda, E., and Maioli, M. Dynorphin B is an agonist of nuclear opioid receptors coupling nuclear protein kinase c activation to the transcription of cardiogenic genes in GTR1 embryonic stem cells. *Circ Res.* 2003;92:623–29.
12. Ventura C, Maioli M, Asara Y, Santoni D, Mesirca P, Remondini D, Bersani F. Turning on stem cell cardiogenesis with extremely low frequency magnetic fields. *FASEB J.* 2005;19:155-7.

EFFECTS OF GSM BASE STATION ELECTROMAGNETIC RADIATION ON OXIDATIVE STRESS IN RATS

ALI IHSAN YUREKLI, MSC
TUBITAK – UEKAE, P.K.74 GEBZE 41470 KOCAELI, TURKEY

MEHMED OZKAN, PROF.DR.
BOGAZICI UNIVERSITY, INSTITUTE OF BIOMEDICAL ENGINEERING
34342 BEBEK-ISTANBUL, TURKEY

TUNAYA KALKAN, PROF.DR.
ISTANBUL UNIVERSITY, CERRAHPASA MEDICAL FACULTY,
BIOPHYSICS DEPARTMENT, ISTANBUL, TURKEY

HALE SAYBASILI, ASSOC.PROF.DR.
BOGAZICI UNIVERSITY, INSTITUTE OF BIOMEDICAL ENGINEERING
34342 BEBEK-ISTANBUL, TURKEY

HANDAN TUNCEL, PHD
ISTANBUL UNIVERSITY, CERRAHPASA MEDICAL SCHOOL,
BIOPHYSICS DEPARTMENT, ISTANBUL, TURKEY

PINAR ATUKEREN, PHD
ISTANBUL UNIVERSITY, CERRAHPASA MEDICAL SCHOOL,
BIOCHEMISTRY DEPARTMENT, ISTANBUL, TURKEY

KORAY GUMUSTAS, PROF.DR.
ISTANBUL UNIVERSITY, CERRAHPASA MEDICAL SCHOOL,
BIOCHEMISTRY DEPARTMENT, ISTANBUL, TURKEY

SELIM SEKER, PROF.DR.
BOGAZICI UNV., FACULTY OF ENG., ELECTRICAL-ELECTRONICS ENG.
DEPARTMENT, 34342 BEBEK-İSTANBUL, TURKEY

Abstract:

The ever-increasing use of cellular phones and increasing number of associated base stations are becoming a widespread source of non-ionizing electromagnetic radiation.
In this study, we submit an animal study in a confined, well-controlled environment, with an intention to investigate effects of GSM Base Transceiver Station (BTS) EM radiation on oxidative stress and generation of free radical. During this study a group of young adult male Wistar albino rats was exposed to EM fields inside a test chamber, while another group was sham-exposed under the same conditions. Malondialdehyde (MDA) levels were assessed as a marker of lipid peroxidation and the activities of GSH and SOD were determined in order to evaluate antioxidant status in the blood samples of exposed rats.

MDA level was increased significantly ($p<0.0001$) for the experiment group when compared to the sham-exposed group. SOD activity was also increased for the experiment group, although less significantly ($p=0.019$), when compared to the sham-exposed group. GSH concentration decreased significantly ($p<0.0001$) for the experiment group when compared to the sham exposed group.
Our results indicate that exposure to EM fields at BTS frequencies may modulate the oxidative stress of free radicals by enhancing lipid peroxidation and reducing the concentration of GSH.
Keywords: Electromagnetic field, base transceiver station, antioxidants, oxidative stress, GTEM.

1. INTRODUCTION

The fast growing second generation mobile phone system, Global System for Mobile Communications (GSM), has become the world's largest mobile telecommunications system, with its one billion subscribers in over 200 countries [1]. Electromagnetic (EM) radiation produced by mobile phone and their base station antennas are in the 890 – 960 MHz frequency range for the GSM900 system. While mobile phones emit low power (2 Watts or less) EM fields in the 890 – 915 MHz range, the base station emissions are much higher in power and in the 935 – 960 MHz range. Since mobile phones are kept and used near the body, in particular near the head, emissions should be analyzed in the near field. On the other hand, base station radiation must be modeled with far field considerations. Another concern on base stations is the continuous emission of EM radiation. Therefore, residents who live close to base stations may have a bigger health concern than the casual users of the mobile phones.

There are a number of governmental and independent organizations working on the regulation of the EM radiation from mobile phones and their base stations. As a result useful guidelines and directives have been placed in act [2, 3]. These guidelines, however, focus on the SAR values, which addresses the energy deposition in the body in terms of heat. In May 2000, in IEGMP *Mobile Phones and Health* report [4], concerns were reaffirmed in the following statement, as: "…There is now scientific evidence, however, which suggests that there may be biological effects occurring at exposures below these guidelines…"

A relatively recent comprehensive survey on mobile phone health effects, published by NRPB (UK) [5], summarizes 26 reports from several countries. The survey concludes that although the possibility of low level EM field exposure causing adverse health effects remain "unproven", additional well targeted, high quality research will be valuable to explore the remaining uncertainties further.

One of the areas of interest by scientists in recent years is the EM radiation induced oxidative stress in biological systems. The issue was first studied for the extremely low frequency (ELF) range, particularly for the power-line frequency the magnetic fields [6, 7]. Some recent studies also address effects in radio frequency (RF) range, especially for the mobile telecommunications emissions [8, 9, 10, 11].

Free radical is a molecule or ion that has an unpaired electron in its outer orbit. Radical particles are unstable and are very reactive. Most common free radicals are produced from oxygen metabolism and are, thus, called as reactive oxygen species (ROS). Free radicals start chain reactions as the unpaired electron is transferred from one molecule to another. One known consequence of this kind of a chain reaction is the lipid peroxidation, where reactive radicals, such as NO_2^-, OH^- or $CCl_3O_2^-$, abstract an atom of hydrogen from poly-unsaturated fatty acid (PUFA) side chains in membranes or lipoproteins. This leaves an unpaired electron on carbon. The carbon radical reacts with oxygen and the resulting peroxyl radical attacks adjacent fatty acid side chains to generate new carbon radicals and so the chain reaction continues. The attack of one reactive free radical can oxidize multiple fatty acid side chains to lipid peroxides, damaging membrane proteins. This makes the membrane leaky and eventually causes complete membrane breakdown [12]. MDA is one of the end products of lipid peroxidation which is mostly used as an oxidative stress marker.

There are experimental evidences that oxidative stress and consequent free radical production are important causative factors in the pathology of several degenerative disorders; such as neurodegenerative diseases, carcinogenesis, atherosclerosis, hypertension and diabetic mellitus [13,14,15,16]. Oxidative stress refers to the cytotoxic consequences of oxygen radicals, such as superoxide anion ($O_2^{\cdot -}$), hydroxyl radical ($OH\cdot$) and hydrogen peroxide (H_2O_2), which are generated as byproducts of cellular aerobic metabolism. Oxygen radicals can attack DNA, proteins and lipid membranes, thus disturbing their physical function.

Fortunately, there are enzymatic systems to counterbalance the production of ROS. Superoxide dismutase (SOD), catalase (CAT) and glutathione peroxidase (GSH-Px) are enzymes responsible for

degradation of $O_2^{\cdot -}$. While SOD converts $O_2^{\cdot -}$ to H_2O_2, GSH-Px converts H_2O_2 to water and oxygen. GSH-Px uses H_2O_2 to oxidize reduced glutathione (GSH). Decreased activity of GSH-Px leads to accumulation of H_2O_2, which in the presence of iron and copper promotes the Fenton reaction to yield $OH^{\cdot}$. Hydroxyl radical is the most reactive form of oxygen radicals that can initiate a chain reaction to generate numerous toxic reactants. GSH-Px also participates in detoxification of lipid peroxyl radicals [17, 18].

In this article, we submit an animal study in a confined, well-controlled environment, with an intention to investigate effects of GSM Base Transceiver Station (BTS) EM radiation on oxidative stress and generation of free radical. During this study a group of young adult male Wistar albino rats was exposed to EM fields inside a test chamber, called Gigahertz Transverse Electromagnetic (GTEM) Cell, while another group was sham-exposed under the same conditions. Malondialdehyde (MDA) levels were assessed as a marker of lipid peroxidation and the activities of GSH and SOD were determined in order to evaluate antioxidant status in the blood samples of exposed rats.

2. METHODS

2.1 Exposure Environment

The test setup is a general purpose EM shielded chamber that is suitable to house laboratory animals. In this exposure environment electromagnetic radiation of specific energy, frequency and waveform can be applied. The main element of the setup (Figure 1) is a GTEM Cell [GTEM 1750, MEB, Germany], installed in Electromagnetic Compatibility (EMC) Laboratory of TUBITAK-UEKAE.

GTEM Cell is a radiated field generation and measurement device that has a single input/output port for EM immunity and emission test purposes. GTEM Cell, in essence, is a transmission line terminated with 50 Ω load. The asymmetrical inner conductor (called “septum”) is designed to match the impedance of a tapered, rectangular wave guide cross section. The outer surface of the GTEM Cell is made of metal sheets with an attenuation of around 60 dB at high frequency EM fields. Note that honeycomb waveguides are installed at the bottom of the GTEM Cell for ventilation purposes. Electric field level is directly proportional to the amplitude of the voltage applied to the input port and inversely proportional with the septum height. In order to obtain increased field level with constant input power, cages that contain the test subjects are designed and placed closer to the input port of the GTEM Cell for the purpose of biological effect studies as illustrated in Figure 2

Signal generators, are used to feed the input port of the GTEM cell in order to imitate the electromagnetic fields emitted from base transceiver stations. A properly selected signal generator [SMY01, Rohde&Schwarz, Germany] generates the 945 MHz carrier wave which is then pulse modulated at 217 Hz [using Stanford Research Systems DG535 Digital Delay/Pulse Generator, USA] in accordance with GSM specifications. Output of the signal generator is then connected to a 100W power amplifier [757LCB-CE, Kalmus, USA]. Power feed to the GTEM cell input is provided through a directional coupler. One port of the directional coupler is connected to a power meter [Rohde&Schwarz NRVS with thermal probe NRV-Z51] through which applied power level is monitored (Figure 1).

The rats are enclosed inside two “*metabolic cages*” which are placed adjacent to each other. These cages are designed so as to feed and water the rats and collect urine samples through its structure. The cages are composed of transparent Plexiglas material. It is thus assumed that the cages have minimal effect on the applied electric field. The rats are free to move inside a volume of 24 cm (W) x 34 cm (L) x 12.5 cm (H). The applied electric field is perpendicular to the plane on which the rats move; therefore each animal is exposed to the field without any obstruction caused by its “neighbors”.

2.2 SAR Calculation

It is necessary to make the dosimetric evaluation of an electromagnetic field exposure experiment in order to deduce meaningful results and compare various biological effects produced with different test setups. Dosimetric evaluation is performed, in general, in terms of Specific Absorption Rate, known as “SAR” in short. Since exposure from Base Transceiver Stations (BTS) is generally in the far field, whole-body average SAR is taken into consideration in this experiment. Whole-body average SAR is defined as the total energy, transferred to the body per unit time, divided by the total mass.

.

The Finite-Difference Time-Domain (FDTD) method implemented in a MATLAB program was used to compute the expected SAR values on the subjects in a simulation environment.

In order to validate the numerical model and MATLAB implementation of the FDTD technique, electric field levels were measured at 10 selected positions on an XY plane located at the middle of the Z axis and compared with those that were obtained by the FDTD technique. These points were selected such that they represent the position of the rats in metabolic cages during actual EM exposure. The simulation software was executed for three times for different input power levels. Electric field levels were also measured by an electric field meter [Acterna EMR-300 with Type 8 E-field probe, Germany], again at those specified input power levels. We found out that FDTD model closely simulates the actual exposure environment (less than 7% difference in the average electric field levels). Thus, the model is a good approximation of the real life measurements. Electric field measurement results also indicated that a fairly uniform electric field was applied to the test subjects in the exposure environment.

The test subject was, on the other hand, modeled roughly with an effort to maintain some details of its geometry. The rat, as a whole, was modeled using electrical properties at 945 MHz, calculated for average muscle tissue, corresponding to: ε =55.853462 and σ=0.985515. Rat muscle tissue density was taken as, ρ=1040 mg/cm^3. For the sake of simplicity, rat cages were not included in the model since they are transparent to electromagnetic radiation. Normalized SAR value for this exposure environment was found to be 0.90 mW/kg per input W. Thus, when this exposure setup is used for assessment of biological effects, we can compute the SAR values through the FDTD model easily once the GTEM input power level is given.

2.3 Electromagnetic Exposure

Calculations above show that in this test environment SAR values we can induce are well below the safety standards [3]. A set of exposure experiments was performed in two phases to investigate the biological effects of the electromagnetic fields at GSM BTS frequency. The first phase was the EM field exposure experiment and the second was the sham exposure (see Table 1). In each phase, the following procedure was applied:

The animals were obtained from the Experiment Animals Center of Istanbul University Cerrahpasa Medical School. For each of the two phases a set of 9 healthy, young adult male Wistar albino rats were used. The rats were cared for in accordance with the Guide for the Care and Use of Laboratory Animals [20]. The rats have been fed with standard pellet food and watered by tap water ad libitum. The rats have been weighted before, after and at each day of the experiment. Average weights of both groups before and after the experiment and their average food and water consumption are given in Table 2.

The subjects were placed inside two metabolic cages, 5 rats in one cage and 4 rats in the other. The cages were placed in the test volume inside the GTEM cell as shown in Figure 2. Radiofrequency EM field (3.67 W/m^2 power density) was applied onto the exposure group for the first phase, while there was no EM field exposure onto the sham group, in the second phase. We could only apply a low power level, which corresponds to a SAR value of 11.3 mW/kg, because of the time averaging of the applied peak power level in accordance with the GSM modulation of the carrier wave. The cages containing the rats were kept inside the GTEM Cell for 7 hours for a period of 8 days for each group.

2.4. Metabolite Gathering and Analysis

At the end of each phase, the animals were anesthetized. After exploration of the thorax, intracardiac blood was quickly obtained. The tubes containing the processed blood samples were stored at -24 ^{o}C until they were analyzed at the Cerrahpasa Medical School Biochemistry Laboratory. These samples were processed for measuring MDA, GSH and SOD levels. The materials collected were analyzed using a spectrophotometer [JASCO V-530 UV/VIS] according to standard laboratory procedures [21,22].

MDA level was determined in plasma using the principle of spectrophotometric determination of absorbance at 535 nm of colored complex which is formed by condensation of two molecules of thiobarbituric acid and one molecule of the material that it reacts with. For this purpose, 1 ml of a stock solution, which was prepared from trichloroacetic acid, thiobarbituric acid and hydrochloric acid, was added to 0.5 ml of plasma. After pippeting, tubes were closed and put inside a boiling water bath for 20 minutes. After cooling down, they were centrifuged at 2000 cycles/min for 10 minutes. Absorbance of the supernatant solution was read against the blind solution. MDA level is given in millimoles per liter (mM/L).

GSH concentration was determined in total blood by color reading at 412 nm of the solution that is formed by the reaction of free sulfhydryl compounds in the whole blood with 5,5'-Dithiobis (2-nitrobenzoic acid) (DTNB). Note that DTNB is a disulfide chromogen that is readily reduced by sulfhydryl compounds to an intensely yellow compound and the absorbance of the reduced compound is directly proportional to the GSH concentration. Cuverts were prepared for GSH calibrator, erythrocyte and precipitating agent. After incubating at room temperature for 5 minutes, the solutions were centrifuged at 3000 cycles/min for 10 minutes. Upper phase was extracted and phophate buffer, DTNB and distilled water were added. The color reading was performed at 412 nm against the blind solution in 4 minutes. Using glutathione standard curve did the calculation. GSH concentration was expressed in milligrams per gram hemoglobin (mg / g Hb).

The method of determination of SOD activity was based on the reduction of nitroblue tetrazolium by superoxide anions that were formed by xanthine/xanthine-oxidase system and then inhibition of superoxide anions by SOD. Reaction mixture used to determine the SOD activity in erithrocytes was prepared using xanthine, EDTA, nitroblue tetrazolium, Na_2CO_3 and bovin serum albumin at specified concentrations inside a 200 ml flask. Reaction mixture was set to a pH level of 10.2. Supernatant solution was prepared using chloroform letanal, erythrocyte and distilled water. This solution was centrifuged at 15000 cycles/min for 10 minutes. Test and blind solutions of 1.07 ml were incubated at 25 ^oC for 20 minutes.After adding 0.05 ml of $CuCl_2$ (8 mM/l) reaction was stopped. Note that the 50 % inhibition with respect to the blind inside the reaction tube corresponds to 1 unit of SOD activity. The units of SOD activity was determined by simple linear ratio. But it had to be further determined with respect to the hemoglobin concentration inside the solution, so the resultant SOD activity was formulated in terms of units per gram hemoglobin (or U / g Hb).

Hemoglobin concentration for GSH and SOD analysis was determined using Drabkin's reagent. 3 mL reagent was mixed with 1:20 hemolysate and kept in dark for 10 minutes. Absorbance at 540 nm was read against a blank of Drabkin's solution and hemolysate hemoglobin concentration was determined from a calibration curve.

Data was presented as means standard deviation. SPSS software package (SPSS for Windows release 11.50) was used for statistical analysis. The analysis results were evaluated based on Mann-Whitney U test statistics and a $p<0.05$ was considered significant.

3. RESULTS

Lipid peroxidation (MDA – malondialdehyde), GSH (reduced glutathione) and SOD (superoxide dismutase) analysis results are given in Figure 3, Figure 4 and Figure 5, respectively. Levels of all the three parameters of interest have been changed significantly under EM radiation effect. MDA level was increased significantly ($p<0.0001$) for the experiment group (10.20 ± 0.78 mM/L) when compared to the sham-exposed group (6.77 ± 0.60 mM/L). SOD activity was also increased for the experiment group (2.53 ± 0.87 Units / mg Hb), although less significantly ($p=0.019$), when compared to the sham-exposed group (1.79 ± 0.72 Units / mg Hb). GSH concentration, on the other hand, decreased significantly ($p<0.0001$) for the experiment group (7.84 ± 1.15 mg / g Hb) when compared to the sham exposed group (19.19 ± 1.64 mg / g Hb).

4. DISCUSSION AND CONCLUSION

A two-phase experiment was designed in order to investigate the effects of EM fields at GSM BTS transmitter frequencies. In the first phase, EM field at 945 MHz of 3.67 W/m^2 power density, which is calculated to produce a SAR value of 11.3 mW/kg, was applied on a group of 9 rats inside a GTEM Cell. In the second phase, the same number of rats was sham exposed under the same conditions. The duration was 7 hours/day for a period of 8 days, in each phase.

Biochemical analysis of blood samples indicate that the GSM BTS EM radiation exposed rats have higher concentration levels of MDA (malondialdehyde) and lower GSH (glutathione) concentrations when compared to the sham exposed group. This outcome is in agreement with the results of some previous studies. Dasdag et al. [9] studied the effects of mobile phone EM radiation on rat brain tissues, where rats are exposed to EM fields for 20 min/day for 30 days (SAR=0.52 W/kg). The MDA levels in rat brain tissues increased significantly after exposure. In another study by Ozguner et al. [11], renal impairment in rats was investigated under mobile phone radiation (SAR=0.016 W/kg). Rats were exposed 30 min/days for 90 days and the result was increase of renal tissue MDA, NO (nitric oxide) and urinary NAG (N-acetyl-β-D-glucosaminidase) levels

and significant decrease of tissue SOD, CAT (catalase) and GSH-Px (glutathione peroxidase) levels. Ilhan et al. [10] studied mobile phone induced oxidative stress in rat brain. Rats were exposed to mobile phone emissions (SAR=0.25 W/kg) for 1 hour/day for 7 days. MDA and NO levels were increased whereas GSH-Px and SOD activities were decreased significantly in rat brain tissue. Additionally, XO and ADA levels were also increased. Moreover, Moustapha et al. [24] have studied acute mobile phone exposure effects on human volunteers and found out that MDA level in plasma was increased and GSH-Px and SOD activities were decreased in human erythrocytes after 1h, 2h and 4h of exposure. No significant change was observed for CAT activity in this study.

However, some other studies in literature have concluded in no relation between EM field exposure and free radical activity. Irmak et al. [24] have shown that EM radiation from mobile phones applied 30 min/days for 7 days on rabbits had no significant effect on rabbit brain, suggesting that oxygen free radicals were not generated. But, they have observed a significant increase in serum SOD activity in the exposed group. In addition, Zmyslony et al. [8] have exposed rat lymphocytes in vitro to 930 MHz continuous wave (CW) radiation inside a GTEM Cell (SAR=1.5 W/kg). Five min and 15 min acute exposure resulted in no change in reactive oxygen species production in living cells. However, change was observed when lymphocytes were treated with $FeCl_2$ as a stimulating agent.

Some research studies relates oxidative stress to certain diseases. In a Parkinson's disease model SOD, CAT and GSH-Px activities were increased in striatum and ventral midbrain of mice [25]. In another Parkinson's disease model Thiffault et al. [26] showed an increase in SOD activity with no increase in GSH-Px activity in mice brain. Neuronal GSH deficiency and age dependent neurodegeneration were found to be related with the down regulation of excitatory amino acid transporters in mice [27].

According to our results, MDA level and SOD activity were increased, whereas GSH concentration was decreased in EM radiation exposed rats when compared to sham-exposed group. We think that decreased GSH concentration may be due to the higher consumption of GSH for scavenging the higher production of free radicals. The lower GSH concentration may have some relation to the increased SOD activity. Note that the endogenous GSH has a protective function in scavenging radicals and in molecular repair. However, such scavenging can set up a superoxide-dependent chain production of H_2O_2 and oxidized glutathione, which would oxidatively stress the cell. Therefore, the increased SOD activity may be a response to suppress the higher chain oxidation of GSH, or a response to balance the decreased GSH concentration.

Thus, the up regulated SOD activity converts $O_2^{\cdot-}$ to H_2O_2 and down regulated GSH concentration leads to the insufficient detoxification and accumulation of H_2O_2 in the system. H_2O_2 is known to be converted to hydroxyl radical in the presence of iron rapidly, which is the most damaging form of ROS. Note that the balance between GSH-Px and SOD appears to be important for the cellular resistance to oxidative stress [28].

In conclusion, our results indicate that exposure to EM fields at BTS frequencies may modulate the oxidative stress of free radicals by enhancing lipid peroxidation and reducing the concentration of GSH. It is highly probable that detoxification of lipid peroxyl radicals can not be accomplished in our system. We note that reactive oxygen species may have a probable role on adverse effects of EM fields at mobile telecommunication frequencies. The outcome of this study needs confirmation by repetitive laboratory studies, including higher dose and longer duration exposure, and theoretical mechanisms underlying this effect should also be addressed in future.

Acknowledgements:

The authors thank Mehmet YAZICI for his help on SAR calculation using FDTD method and Dr. Huseyin AKSU for his help on statistical evaluation.

The present work was supported by the Research Fund of Istanbul University. Project No: 859/16082006.

This research is sponsored by Bogazici University Research Fund, project number: 01HX102D.

References:

1. NRPB. Mobile Phones and Health 2004. National Radiation Protection Board Report. **2004** 15:5. UK. Available from: http://www.hpa.org.uk/radiation/publications/documents_of_nrpb/abstracts/absd15-5.htm

2. ICNIRP. Guidelines for limiting exposure to time-varying electric, magnetic and electromagnetic fields (up to 300 GHz). Health Physics **1998**, 74, 494-522.
3. CENELEC. EN 50360. Product standard to demonstrate the compliance of mobile phones with the basic restrictions related to human exposure to electromagnetic fields (300 MHz - 3 GHz). European Standards Organization. Directive 199/5/EC on Radio Equipment and Telecommunications Terminal Equipment and the mutual recognition of their conformity. **2001**.
4. IEGMP. Mobile Phones and Health. Report of Independent expert Group on Mobile Phones. National Radiation Protection Board Report. Oxon, UK. **2000**. Available from: http://www.iegmp.org.uk/report/text.htm.
5. Sienkiewicz ZJ, Kowalczyk CI.. A Summary of Recent Reports on Mobile Phones and Health (2000–2004). National Radiation Protection Board Publication. W65. UK. **2005**. Available from: http://www.hpa.org.uk/radiation/publications/w_series_reports/2005/nrpb_w65.htm
6. Brocklehurst B, McLauchlan KA.. Free radical mechanism for the effects of environmental electromagnetic fields on biological systems. Int J Radiat Bio **1996**, 69, 3-24.
7. Lacy-Hubert A, Metcalfe JC, Hesketh R. Biological responses to electromagnetic fields. FASEB Journal **1998**, 12, 395-420.
8. Zmyslony M, Politanski P, Rajkowska E, Szymczak W, Jajte J. Acute exposure to 930 MHz CW electromagnetic radiation in vitro affects reactive oxygen species level in rat lymphocytes treated by iron ions. Bioelectromagnetics **2004**, 25, 324-328.
9. Dasdag S, Akdag MZ, Aksen F, Bashan M, Buyukbayram H. Does 900 MHz GSM Mobile Phone Exposure Affect Rat Brain? Electromagnetic Biology and Medicine **2004**, 23, 201-214.
10. Ilhan A, Gurel A, Armutcu F, Kamisli S, Iraz M, Akyol O, Ozen S. Gingko biloba prevents mobile phone-induced oxidative stress in rat brain. Clinica Chemica Acta **2004**, 340, 153-162.
11. Ozguner F, Oktem F, Ayata A, Koyu A, Yilmaz HR. A novel antioxidant agent caffeic acid phenetyl ester prevents long-term mobile phone exposure-induced renal impairment in rat. Molecular and Cellular Biochemistry **2005**, 277, 73-80.
12. Anderson D. Antioxidant defences against reactive oxygen species causing genetic and other damage. Mutation Research **1995,** 350, 103-108.
13. Simonian NA, Coyle JT. Oxidative Stress in Neurodegenerative Diseases. Annu Rev Pharmacol Toxicol **1996**, 36, 83-106.
14. Turner RN. Free radicals and disease: the toxaemia hypothesis, Complementary Therapies in Medicine **1996**, 4, 43-47.
15. Mahboob M, Shireen KF, Atkinson A. Lipid peroxidation and antioxidant enzyme activity in different organs of mice exposed to low level of mercury. J Environ Sci Health B. **2001**, 36, 687-697.
16. Maritim AC, Sanders RA, Watkins JB 3rd. Diabetes, oxidative stress, and antioxidants: a review. J Biochem Mol Toxicol **2003**,17, 24-38.
17. Stadtman ER. The Role of Free Radical Mediation of Protein Oxidation in Aging and Disease. In Özben T (eds.): Free Radicals, Oxidative Stress, and Antioxidants). New York: Plenum Press, **1998**, 131-143.
18. Coyle JT, Puttfarcken P. Oxidative Stress, Glutamate and Neurodegenerative Disorders. Science **1993**, 262, 689-694.
19. Chou CK, Bassen H, Osepchuk J, Balzano Q, Petersen R, Meltz M, Cleveland R, Lin JC, Heynick L. Radiofrequency Electromagnetic Exposure: Tutorial Review on Experimental Dosimetry. Biolectromagnetics **1996**, 17, 195-208.
20. National Research Council. Guide for the Care and Use of Laboratory Animals, National Academy Press Washington, D.C. **1996**.
21. Burtis CA, Ashwood ER, Tietz NW. Tietz Textbook of Clinical Chemistry. W.B. Saunders Company. 3rd Ed. **1999**.
22. Yi Sun, Oberley LW, Ying Li,. A simple method for clinical assay of superoxide dismutase. Clinical Chemistry **1988** , 34, 497-500.
23. Moustapha YM, Moustapha RM, Belacy A, Abou-El-Ela SH, Ali FM. Effects of acute exposure to radiofrequency fields of cellular phoneson plasma lipid peroxide and antioxidase activities in human erythrocytes, Journal of Pharmaceutical and Biomedical Analysis **2001**, 26, 605-608.
24. Irmak K, Fadillioglu E, Gulec M, Erdogan H, Yagmurca M, Akyol O.Effects of electromagnetic radiation from a cellular telephone on the oxidant and antioxidant levels in rabbits. Cell Biochemistry and Function **2002**, 20, 279-283.
25. Cassarino DS, Fall CP, Swerdlow RH, Smith TS, Halvorsen EM, Miller SW, Parks JP, Parker WD, Bennett JP. Elevated Reactive Oxygen Species and Antioxidant Enzyme Activities in Animal and Cellular Models of Parkinson's Disease. Biochimica et Biophysica Acta **1997**, 1362, 77-86.
26. Thiffault C, Aumont N, Quirion R, Poirier J.Effect of MPTP and L-Deprenyl on Antioxidant Enzymes and Lipid Peroxidation Levels in Mouse Brain. J Neurochem **1995**, 65, 2725-2733.
27. Aoyama K, Suh SW, Hamby AM, Liu J, Chan WY, Chen Y, Swanson RA. Neuronal glutahione deficiency and age dependent neurodegeneration in the EAAC1 deficient mice. Nature Neurosci , **2005**, 9, 110-126.
28. Amstad P, Moret R, Cerutti P. Glutathione Peroxidase Compensates for the Hypersensitivity of Cu, Zn-Superoxide Dismutase Overproducers to Oxidant Stress. J Biol Chem **1994**, 269, 1606-1609.

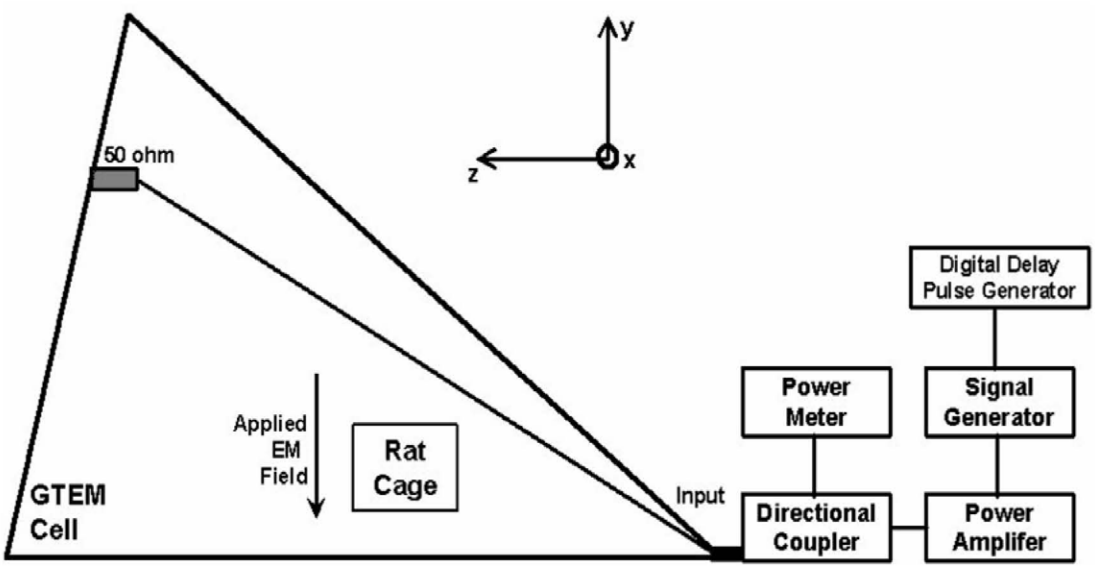


Figure 1. Electromagnetic field exposure setup.

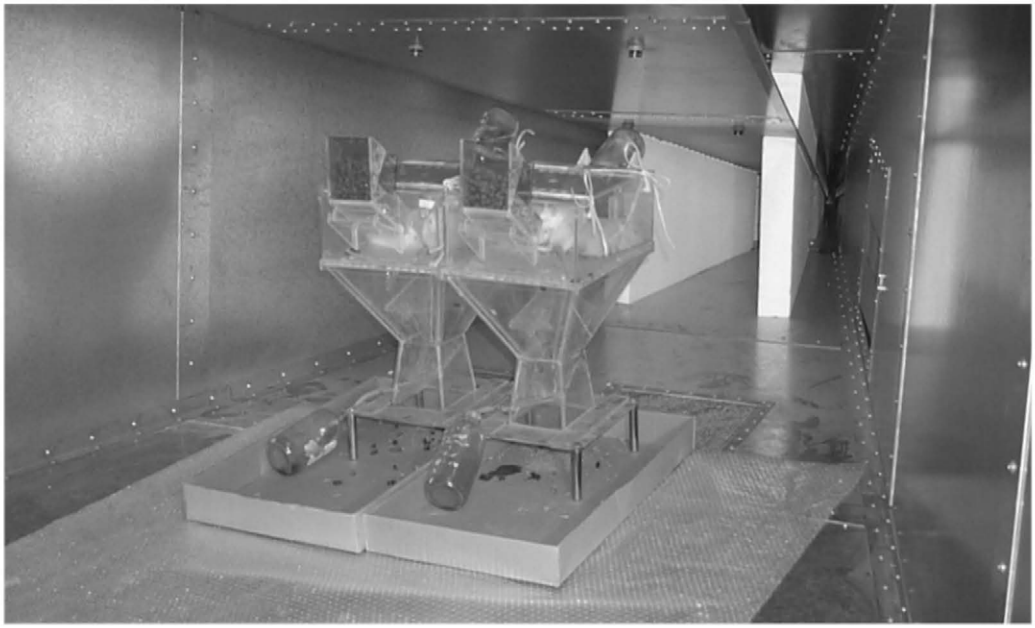


Figure 2. A group of rats contained in two metabolic cages inside GTEM Cell.

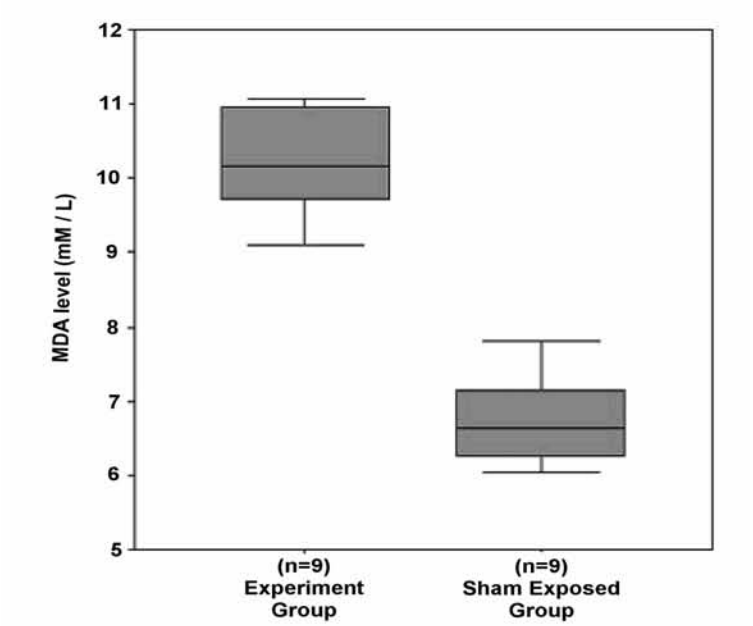


Figure 3. Effects of 945 MHz electromagnetic radiation on lipid peroxidation levels in rat blood samples (mean ± SD). $p<0.0001$ vs. sham according to Mann-Whitney U test.

Table 1. Exposure parameters.

Phase	# Rat	GTEM Input Power (W)	Applied E Field Level (V/m)	Power Density (W/m^2)	SAR (mW/kg)	Exposure Duration (days)	Effective Exposure Time (hours/day)	Time Spent in GTEM Cell (hours/day)
Experiment	9	12.5	37.2	3.67	11.3	8	7	7
Sham Exposure	9	-	-	-	-	8	-	7

.

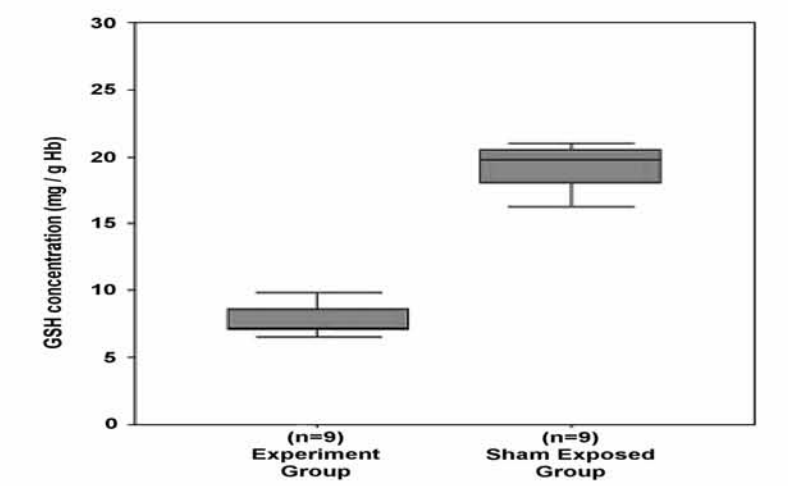


Figure 4. Effects of 945 MHz electromagnetic radiation on GSH concentration in rat blood samples (mean ± SD). $p<0.0001$ vs. sham according to Mann-Whitney U test.

Table 2. Average weights of the rats before and after the experiment and their average food and water consumption.

GROUPS	Initial Weights (g)	Weights After Exposure (g)	Average consumed food per day by single rat (g)	Average consumed water per day by single rat (ml)
Experiment	190 ± 40	220 ± 38	22	21
Sham Exposure	162 ± 43	191 ± 44	30	18

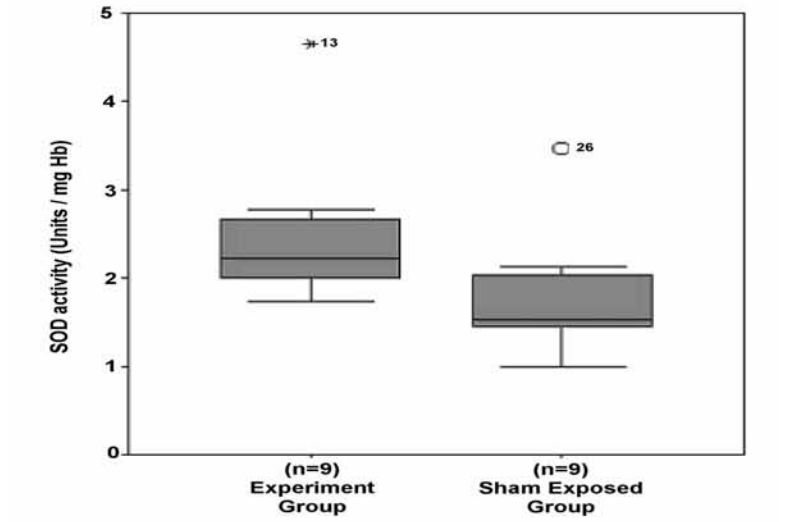


Figure 5. Effects of 945 MHz electromagnetic radiation on SOD activity in rat blood samples (mean ± SD). $p=0.019<0.05$ vs. sham according to Mann-Whitney U test.

THE PHYSIOLOGICAL BASIS FOR BASIC RESTRICTIONS IN EXTREMELY LOW FREQUENCY STANDARDS AND GUIDELINES

ANDREW W WOOD

BRAIN SCIENCES INSTITUTE, SWINBURNE UNIVERSITY OF TECHNOLOGY, HAWTHORN, VICTORIA 3122, AUSTRALIA

Abstract

In the range 0.1 – 3,000 Hz, there are significant disparities between basic restrictions in the ICNIRP guidelines and the IEEE (ICES) standard, even though in both these are derived from consideration of abnormal retinal responses (phosphenes) and peripheral nervous system stimulation. Considerable uncertainties exist in i) interpreting the available data ii) in determining the point at which bioeffects become health effects and iii) deciding on an appropriate margin for safety for occupational and general public exposure. The available data tend to be rather sparse outside the range 20 – 60 Hz.

Recent data from large-scale voxel models and from human volunteer and modeling studies of the effects of MRI switching field gradients permit some comparisons between external fields known to cause certain bio-effects and external fields estimated from basic restriction values. Some interpolation and extrapolation across the frequency range is possible. In particular, electric field limits, which were previously thought to be entirely determined by indirect effects (contact currents and micro-shock) should now, because of results from recent voxel-based modeling, be determined more by direct effects derived from basic restrictions.

The presentation will review the approach taken by a Working Group for the development of the Australian ELF Standard

Introduction

The Australian ELF Standard Working Group, from their first meeting, faced the dilemma of whether to follow the approach of ICNIRP (ICNIRP 1998) or of IEEE (IEEE 2002) in recommending basic restrictions for protection. For example, at power frequencies and for the general public, the former approach limits induced current density (J) to 2 $mA.m^{-2}$ (averaged over 1 cm^2 of tissue, perpendicular to current direction) and the latter limits induced electric field (E_{int}) to different limits in different parts of the body (averaged over a 0.5 cm line segment in the body). In the most sensitive value, the brain, the 50 Hz value is 14.7 V/m. Since the two quantities can be related via $J = \sigma E_{int}$, the two approaches can be made equivalent by taking $\sigma = 0.136$ S/m, which is not too different from the average value of 0.2 S/m often used as an average value for tissue conductivity. However, because of the different assumed frequency variation, the disparities become very large at non-power frequencies. For example, the difference at 750 Hz (assuming $\sigma = 0.136$ S/m) is 15-fold (with IEEE less conservative) and at 1 Hz, 10-fold (with IEEE more conservative at these lower frequencies). This forced the Working Group to re-examine the experimental data upon which these limits (and the associated reference levels) were derived. A number of important issues emerged, as follows:

Synaptic effects in the retina

A number of experimental reports are relevant to making estimates of the threshold tissue E_{int} for a measurable physiological response to occur. Most identify 20 Hz as the frequency for the lowest threshold. Eight studies involve the application of current to the retina (electro-phosphenes) and three the application of alternating magnetic fields (magneto-phosphenes). Considerable assumptions need to be made in each case to estimate tissue threshold, which range from 1 to over 600 mV/m. Although there is a large overlap, the electro-phosphene thresholds tend to be higher than the magneto-phosphene. The pooled value (assuming the two phenomena to be equivalent) is 56 mV/m (95% CI 2.3 – 1330 mV/m). This is very close to the RMS value used as the basis of the IEEE standard.

Peripheral neural stimulation

Some recent work on human perception and of associated mathematical modelling of neural stimulation allows limits to be estimated for this phenomenon. Most of this refers to work on the fields associated with the switching of gradient fields in Magnetic Resonance Imaging, which induce currents in the body and have characteristic frequencies typically in the range 500 – 1,000 Hz. A threshold for perception of just over 2 V/m was identified by Nyenhuis (Nyenhuis et al 2001) but further analysis using more sophisticated models gives a rather higher value of around 4 V/m (So et al 2004). Other work (Liu & Crozier 2004; Liu et al 2003), tends to confirm that the threshold value for sensation is lower than the 6.15 V/m value which form the basis for peripheral nerve stimulation in the IEEE standard (and which was derived using a mathematical model of a long, 20 μm diameter myelinated nerve).

Safety margins

There is considerable debate on the margin that should exist between the thresholds just discussed and basic restrictions for a) occupational or 'controlled environment' and b) general public categories of exposure. ICNIRP uses margins of 10, 5 or 2 depending on the context, whereas IEEE uses margins of either 1 or 3. The justifications for the actual values uses are often not fully substantiated. Another area of debate is on whether the basic restriction should be related to a threshold for sensation or for harm/pain, and what the relationship between these two levels is. There is some useful information emerging on the distribution of thresholds within the general population.

Reference or Maximum Permissible Exposure Levels: relationship with Basic Restrictions

Both the IEEE and ICNIRP standards use simple homogeneous geometrical models of the human torso/head in order to derive equivalent external field limits. In recent years highly sophisticated, voxel-based, models of both the adult male and female have become available (Caputa et al 2002) (Dimbylow 2000; Dimbylow 2005; Dimbylow 1998). In addition, models of the child (Hirata et al 2001) and the pregnant female Dimbylow (Dimbylow 2006) have also been studied. Given tissue-specific Basic Restriction values, the corresponding external fields required to produce these can be found. Although most of this work is at power frequencies, other frequencies in the ELF range have also been studied (Dimbylow 2005; Dimbylow 1998). This allows reference levels to be calculated for both the avoidance of retinal and peripheral nerve stimulation effects, the latter becoming more of a concern above a few hundred Hz. For magnetic (*B*) fields reference levels can be derived fairly straightforwardly, but levels for electric (*E*) fields are a little more complicated.

Electric field limits: direct and indirect effects

Previous standards have assumed that E_{int} induced by external electric (rather than magnetic) fields are of the order of fractions of mV/m per kV/m external. Electric (*E*) field reference levels have been set to avoid indirect effects such as contact current and micro-shock. The former effectively limits *E* fields via the Deno formula (Deno 1975) since the magnitude of contact current is directly proportional to *E*. Contact current is in turn limited by considerations of annoyance thresholds for the general population. However, the voxel-based modelling studies just described predict much larger E_{int} values than previously supposed (up to 50 mV/m per kV/m in bone, for example). Consideration of E_{int} in excitable tissue gives more conservative values for external *E* than are given by the Deno formula. However, data on micro-shock still determine *E*-field reference levels for the range of frequencies less than 100 Hz (and including DC).

Giving protection below 0.1 Hz

Here, external *E*- and *B*-fields need to be considered separately: for E-fields the need to avoid the production of micro-shocks in DC fields gives similar reference levels to those at power frequencies. On the other hand, data on *B*-fields is much more sparse, but it would appear that the reference level at DC should be at least two orders of magnitude higher than at power frequencies.

Progress within the Australian Working Party for an ELF Standard

The Working Party has developed a draft, incorporating the considerations just outlined, which it hopes will be available for public comment before the end of the year. At power frequencies, analysis along the lines just described tend to the view that the ICNIRP *B*-field reference levels are too conservative and the *E*-field levels too lax. Other considerations include: whether in controlled circumstances or activities reference levels can be relaxed for both occupational and general public exposures; what precise tissues (and what volume) do the basic restrictions refer to; what the safety margins should be? A Regulatory Impact Statement, which will include cost-benefit analyses of a) regulatory adoption or b) voluntary compliance (with the standard as an educative document), is being prepared.

The author chairs the ELF Standard Working Group set up by the Radiation Health Committee of the Australian Radiation Protection and Nuclear Safety Agency (ARPANSA). The views presented are personal to the author and should not be taken as representing those of ARPANSA or of the Australian Government.

References

Caputa K, Dimbylow P, Dawson T, Stuchly M. 2002. Modelling fields induced in humans by 50/60 Hz magnetic fields: reliability of the results and effects of model variations. *Phys Med Biol*. 47:1391-8

Deno DW. 1975. Currents induced in the body by high voltage transmission line electric field - measurement and calculation of distribution and dose. *IEEE Trans Power App Syst* 96:1517-25

Dimbylow P. 2000. Current densities in a 2 mm resolution anatomically realistic model of the body induced by low frequency electric fields. *Phys Med Biol.* 45:1013-22

Dimbylow P. 2005. Development of the female voxel phantom, NAOMI, and its application to calculations of induced current densities and electric fields from applied low frequency magnetic and electric fields. *Phys Med Biol* 50:1047-70

Dimbylow P. 2006. Development of pregnant female, hybrid voxel-mathematical models and their application to the dosimetry of applied magnetic and electric fields at 50 Hz. *Phys Med Biol* 51:2383-94

Dimbylow PJ. 1998. Induced current densities from low-frequency magnetic fields in a 2 mm resolution, anatomically realistic model of the body. *Phys Med Biol* 43:221-30

Hirata A, Caputa K, Dawson TW, Stuchly MA. 2001. Dosimetry in models of child and adult for low-frequency electric field. *IEEE Trans Biomed Eng* 48:1007-12

ICNIRP. 1998. Guidelines on limits of exposure to time-varying electric, magnetic and electromagnetic fields (1 Hz - 300 GHz). *Health Phys* 74:494-522

IEEE. 2002. IEEE standard for safety levels with respect to human exposure to electromagnetic fields, 0-3 kHz. *Rep. IEEE Std C95.6*, IEEE, New York

Liu F, Crozier S. 2004. A distributed equivalent magnetic current based FDTD method for the calculation of E-fields induced by gradient coils. *J Magn Reson* 169:323-7

Liu F, Zhao H, Crozier S. 2003. On the induced electric field gradients in the human body for magnetic stimulation by gradient coils in MRI. *IEEE Trans Biomed Eng* 50:804-15

Nyenhuis J, Bourland J, Kildishev A, Schaefer D. 2001. Health effects and safety of intense gradient fields. In *Magnetic resonance procedures: health effects and safety*, ed. F Shellock, pp. 31-53. Boca Raton, FL: CRC Press

So PP, Stuchly MA, Nyenhuis JA. 2004. Peripheral nerve stimulation by gradient switching fields in magnetic resonance imaging. *IEEE Trans Biomed Eng* 51:1907-14

METHODOLOGICAL PROBLEMS IN THE ASSESSMENT OF THE CARDIOVASCULAR FUNCTION IN WORKERS EXPOSED TO ELECTROMAGNETIC FIELDS

BORTKIEWICZ A., GADZICKA E., ZMYSLONY M.,SZYMCZAK W.

NOFER INSTITUTE OF OCCUPATIONAL MEDICINE,
91-348 LODZ, 8 TERESY ST., POLAND, e-mail: alab@bg.p.lodz.pl

Abstract

The aim of the study was evaluation the effect of occupational exposure to electromagnetic fields (EMF) on the cardiovascular system.

The examinations covered all technical personnel employed at selected AM Broadcast Stations (738 -1503 kHz) - (I), radio services (150 - 170 MHz - (II), power substations (50 Hz) - (III), radio and TV broadcasting stations (VHF 30-300 MHz and UHF 0.3-3 GHz) - (IV), and Radio Link Stations (no EMF exposure) - (0). Maximum electric field strength (E_{max}) and magnetic flux density (B_{max}) were assessed and doses per work shift – E_{dose} and B_{dose} were calculated. 287 male workers aged 21-69, with employment duration 1- 42 years, underwent medical examination, resting and 24-h ECG, ambulatory blood pressure monitoring (ABPM). Risk of abnormalities (mostly ventricular arrhythmia) in resting and/or 24-h ECG was significantly higher for group I than for controls (OR= 6.6). In the group III, ABPM revealed a significantly higher risk of increased BP values, referred mainly to systolic BP at night-time (OR=12.5). Also in group IV, BP disturbances were significantly more frequent than in controls (OR=8.6). Cardiovascular abnormalities correlated with EMF maximum value as well as its dose. In all cases, the exposure levels were below Polish OEL values. Nevertheless, significant cardiac abnormalities, related to EMF frequency and intensity, were observed.

Introduction

The electromagnetic fields are commonly present both in the communal and work environments. The potential hazard they may pose to human health is a matter of dispute among scientists. The external electric and magnetic fields have a theoretical potential to affect the functions of different body systems through generating electric impulses within them. Most sensitive to EMF influence are the cardiovascular and nervous systems, particularly the autonomic nervous system responsible, among others, for neurovegetative regulation of the cardiovascular function. The experimental studies conducted thus far indicate that EMF within radio-, microwave and power frequencies can produce measurable biological effects. However, there is no simple relation between the biological and health effects. The biological effects detected at the cell or tissue level may not, and most often do not, translate into overt health effects, owing to the adaptation and repair mechanisms of the living organisms. Moreover, the findings of experimental animal studies can hardly be extrapolated to humans in view of the anatomic and functional differences between species.

Therefore, for evaluating health effects of EMF exposure, the most significant are experimental, clinical or epidemiological studies on humans. The experimental studies make it possible to assess immediate response but not the delayed effects. Consequently, they are of little use for the assessment of effects of occupational exposure that may last several years. Much more valuable are the clinical studies. However, these have been rather scarce so far. Although there are quite a few reports on such studies conducted in the former Soviet Union, they have been commonly criticized for several methodological drawbacks and deficiencies, including ad hoc selection of the study population, lack of control group, lack of accurate assessment of electromagnetic environment, and lack of adjustment for the confounding factors [1]. Further, the methods applied may not have been relevant to the study objectives. To assess the cardiovascular function, the authors most frequently used resting ECG and office BP measurements which are inadequate for detecting functional impairments or early subclinical signs of cardiac dysfunction.

Epidemiological studies can provide the best evidence on the possible health effects of EMF exposure. The studies performed thus far were intended mostly for the assessment of cancer risk from EMF exposure. The results of the first epidemiological study concerning the cardiovascular system were published in 1999. Savitz et al. [2] examined the mortality from cardiovascular diseases in relation to occupational exposure to 50 Hz EMF in a cohort of 138 903 male electric utility workers from five US companies over the period of 1950-88. Age-, race-, and social class-adjusted long-lasting exposure to high level EMF was associated with an increased risk of

death from arrhythmia-related conditions: (n=212) SMR=1.11-2.04 and acute myocardial infarction: (n=4238) SMR=1.07-1.66. These data suggest a possible association between occupational EMF exposure and arrhythmia-related heart disease.

Few epidemiological studies on non-carcinogenic effects of radio frequency and microwave EMF exposures have been published. It was only the questionnaire studies on subjective complaints among mobile phone users and physiotherapists [3-5].

Since 1993, in Nofer Institute of Occupational Medicine, has been conducting comprehensive studies on the neurovegetative regulation of the cardiovascular function in workers exposed to different frequency EMFs [6-9]. The aim of these studies is to investigate the influence of EMF exposure on the cardiac function and find out whether and to what extent the EMF frequency and exposure level can determine the type of cardiovascular abnormalities and neurovegetative function affected.

Methods

For the study, the non-invasive methods of 24-h ECG (Holter) and blood pressure monitoring (ABPM) have been applied which are useful for the examinations of healthy individuals during their normal professional and daily activities. These methods are helpful in detecting not only the clinical manifestations of the disease, but also in early diagnostics of a dysfunction of the cardiovascular system. The examinations were carried out in compliance with the standards of the International Society for Holter and Noninvasive Electrocardiology [10]. The protocol was approved by the Regional Biomedical Ethics Committee.

In all workers the following examination were performed:

- *anamnesis*, with an interview on the risk factors of cardiovascular diseases: family history of metabolic and cardiovascular diseases, lifestyle, nutritional habits and physical activity,
- *routine physical examination*, with office blood pressure measurement (according to WHO guidelines),
- *routine ECG* during rest in the supine position, using Medea system (Gliwice, Poland) from 12 typical leads. The results obtained were evaluated based on generally adopted standards,
- *24 h ECG monitoring* on normal workday, using Medilog Suprima (Oxford, England) set from three bipolar leads. This method is thought to ensure the most accurate diagnostics of cardiac rhythm disturbances, conduction impairments and ischemia, especially silent ischemia. Final results, including heart rate, symptoms of ischemia, arrhythmia and conduction disturbances were related to the international standards for Holter ECG [10],
- *Blood pressure monitoring (ABPM)* - 24-h ambulatory blood pressure monitoring was performed during everyday professional and other activities using DX-Medilog Systems. The measurements were carried out automatically, every half hour during daily activities and every hour during sleep. Mean, systolic (BPS) and diastolic (BPD) blood pressure and heart rate (HR) for 24 hours (O), day-time activity (D) and night-time rest (N) were calculated and related to the Staessen's standards of arterial blood pressure as the reference values [11]. The day-night ratios were determined for systolic and diastolic blood pressure (BPSD/BPSN, BPDD/BPDN). Subjects with BP ratio lower than 1.1 are called the 'non-deepers' (subjects without a physiological nocturnal decrease in systolic and/or diastolic blood pressure).
- *Exposure evaluation:* To assess the worker's individual exposure to EMF, the following parameters were measured:
  I. in workers at AM broadcasting stations: maximum value of electric field strength (E_{max}) and dose per workshift (E_{Dose}),
  II. in workers of radioservices, who were periodically exposed to EMF emitted by the repaired equipment only (E_{max}) were measured, because it was impossible to calculate (E_{Dose}),
  III. in workers at substations: maximum value of electric field strength (E_{max}), maximum value of magnetic flux density (B_{max}) and doses per workshift - E_{Dose} and B_{Dose},
  IV. in workers at broadcasting stations: maximum value electric field strength (E_{max}), mean value of E (E_{mean}) and lifetime dose of E (E_{dose}) separately for VHF, UHF and VHF+UHF. Our assessment of exposure was based on the spectrum analysis of a typical station broadcasting in UHF and VHF bands and on the specifications of the apparatus installed there.

The EMF dose was determined using quasi-dosimetric method. The following procedures had to be completed prior to final exposure assessment:

1. Assessment of the average time the workers spent in particular functional units of the object within a workshift. This was based on an interview and work timing of each worker.
2. Calculation of the mean intensity of electric and magnetic field (if it was measureable) This was done by carrying measurements in several-several dozen locations all over each unit where the workers were

staying. The results of these partial measurements were then averaged for the whole area of the unit. In each of such areas, the maximum values were recorded of electric and magnetic field intensities that the workers had been exposed to.

3. For exposure assessment, the highest of the maximum value of EMF and the total E and H doses per workshift were considered. Lifetime dose was calculated for each worker from the history of employment and job timetable.

For electric field intensity measurement, the HOLADAY Ind. (USA) measuring set and broad-band MEH-1a meter (Technical University, Wroclaw, Poland) were applied
For measurements of magnetic field intensity, the MNP89 meter (Technical University of Wroclaw, Poland) was applied.

Subjects
The groups under study consisted of technical personnel and security service workers who were qualified by the occupational health practitioners as capable for work at permissible EMF levels. The subjects were randomly selected from the total number of such stations in Poland. All workers at each appointed station were examined. All subjects from the exposed and control groups gave their formal consent prior to inclusion in the study. Before the onset of the examinations, all the procedures were explained in detail to each participant.
The examinations were carried out in:

- AM broadcasting stations - exposed group I. The AM stations selected for the study operate at frequencies ranging from 738 kHz to 1503 kHz. These objects can be characterized by permanent exposure of their workers to electromagnetic fields (mostly electric). The main source of EM fields in the AM stations are the transmitting antennas (half-wave dipole), radio transmitters and feeders (which conduct radio signals from the transmitter to the antenna),
- Radio-services - exposed group II. Mobile radio-communication network requires permanent technical supervision by radio-service units. During the service operations, undesirable EM fields are generated by unscreened transmitters, improper tuning instruments and transmitting-receiving antennas installed in the service-rooms. The radio-service workers under study were exposed to EM fields with frequency varying from 150 to 170 MHz,
- Substations - exposed group III. Substations are the element of a power system, in which electric power is distributed and/or transformed. The substations under study work at high and extra high voltage (110 kV-400 kV). The substation equipment is a source of 50 Hz electric and magnetic field,Broadcasting stations that operate at frequencies ranging from 66 MHz to 727 MHz – exposed group IV,The operators of radio- and TV stations are exposed to different EMF levels, depending on various factors such as transmitter technological characteristics, feeder quality, distance from the antenna, etc. These factors differ considerably between the individual broadcast stations.Radio Link Stations - the control group (0). Radio Link Stations are the elements of a telecommunication system in which signals are transmitted using EM waves focused into very row beams by directional (mostly parabolic) antennas. As the antennas are installed in highly inaccessible locations and the radiation beams run high above the ground, the workers of the Radio Link Stations are free from being exposed.

Table 1. Characteristics of the study population

	Exposed groups				**Control group**
	AM Broadcasting Stations (I)	Radioservices (II)	Substations (III)	Broadcasting stations (IV)	Radio Link Stations (0)
Number of subjects	71	40	63	71	42
Age (years)	46.9±13.1*	36.9±11.5	39.0±10.0	45.3±9.4	40.7±2.2
Employment (years)	18.6±12.1	12.5±9.5	15.0±10.0	19.1±8.8	17±13
Diseases diagnosed: hypertension diabetes, type II Subjective symptoms	 12 (17%) 1 31 (44%)	 6 (15%) 0 26 (65%)	 11 (17%) 0 30 (46%)	 11 (15%) 1 36 (51%)	 8 (19%) 1 15 (29%)
BMI	26.0±3.0	25.0±3.0	26.0±4.0	26.9±3.8	25.4±4.0
No. of smokers (more than 10 cigarettes/day)	33 (47%)*	15 (37.5%)	21 (33%)	17 (24%)	17 (40%)

BMI (body mass index) = body mass/height^2 (kg/m^2)

* statistically significant difference ($p \leq 0.05$)

The exposed groups were similar with respect to the level of leisure time physical activity, and dietary and smoking habits. They differed only with regard to the age. The possible influence of this difference on the study results was eliminated using statistical methods.

Results

In all the exposed groups, the assessment of EMF exposure revealed levels not higher than those attributed to the hazard area according to Polish OEL values.

Table 2. EMF exposure in the study groups

Groups	**Exposed** AM Broadcast Stations (I)	Radio-services (II)	Substations (III)	Broadcasting stations (IV)	**Non-exposed** Radio Link Stations (0)
EMF frequency	738-1503 kHz	150-170 MHz	50 Hz	66-727 MHz	0
E_{max}	50-550 [V/m]	2-55 [V/m]	4.3-6.7 [kV/m]	7.9-16.7 [V/m]	0
B_{max}	negligible	negligible	26.1-37.3 [mT]	negligible	0
E_{dose}	50-260 [(V/m)h]	irregular exposure	0.2-15.2 [(kV/m)h]	50-260 [(V/m)h]	0
B_{dose}	negligible	negligible	1.4-38.9 [mTh]	negligible	0

Our studies did not reveal any significant differences between the exposed and non-exposed groups with respect to the frequency of abnormalities in resting ECG. Significant differences between group (I) and other groups, were found in Holter 24-h ECG and when the resting and Holter ECGs were regarded as complementary (table 3) In group (II-IV) the abnormalities in 24-h and/or resting ECG were more frequent than in non-exposed group, but the differences were insignificant. In group (I) among the abnormalities in Holter ECG records dominated the ventricular heart rhythm disturbances, in others repolarization impairments. In switch-yard substation workers (group III) exposed to high and extremely high voltages ranging from 110 kV to 400 kV blood pressure changes prevailed among the recorded cardiovascular impairments and were significantly more frequent in the exposed group than in controls (table 3). The ambulatory blood pressure monitoring revealed an increased frequency of subjects with elevated BP in substation workers (38%), and Broadcasting Stations workers (32%) as compared with the non-exposed subjects (23%).

Table 3. Percentage of subjects with ECG and blood pressure abnormalities

Groups	A: resting ECG	B: Holter monitoring	A and/or B	ABPM	Office BP
AM broadcasting stations (I)	34	56	83	6	20
Radioservices (II)	30	32.5	55	20	22.5
Substations (III)	29	40	48	38	19
Broadcasting stations (IV)	34	44	59	70	34
Radio Link Stations (0)	26	31	40	23	19
p	ns	I vs. 0 (p=0.02)	I vs. 0 (p=0.001)	III vs. 0, IV vs. 0 (p=0.04)	ns

In group (III) and (IV) the mean systolic blood pressure for 24 hours, day-time activity and night-time rest were significantly higher than in the controls. Mean values of diastolic blood pressure for 24 hours (24-h) and night-time rest were significantly higher in the group IV (Fig. 1). In groups I and II in comparison with control group it has been found that mean blood pressure, both 24-h and that recorded during daytime and at night, did not show statistically significant differences. Only the diastolic blood pressure recorded during the night hours was higher in group I, II and IV than in the control, but the difference was on the border of the statistical significance ($p = 0.0512$).

Number of non-dippers was significantly higher in group I (37%) and III (48%) and IV (61%) in comparison with control group (23%) and group II (28%). HRD was found to be significantly lower in the groups I and III than in the

control group, despite the fact that physical and mental load during work and leisure time were similar. HRD/HRN was significantly lower in the groups I, II and III than in the control group. The decreased value of this parameter may indicate a dysfunction of the neurovegetative regulation.

In the group IV it was a significantly higher percentage of subjects with impaired BP regulation, expressed as the absence of physiological nocturnal systolic and diastolic BP drop.

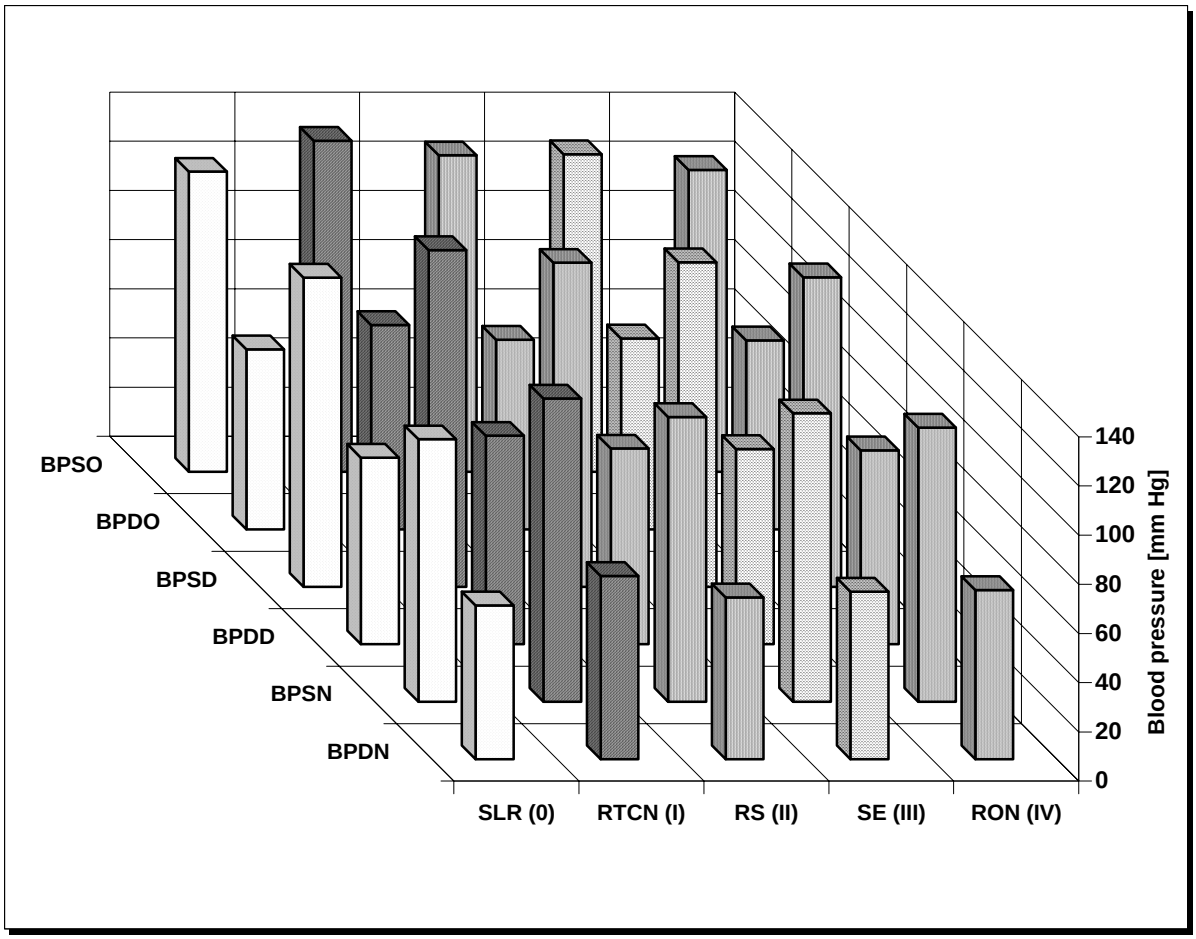


Fig. 1. Blood pressure in the study groups (ABPM results)

The risk analysis revealed that the probability (odds ratio) of abnormalities in resting and/or 24h ECG was 6.6 for group I, 2.0 for group II, 1.4 for group III and 4.5 for group IV, as compared with the control group. On the other hand, the ABPM monitoring revealed that when compared to the values found for controls, the risk of elevated blood pressure was lower in group I, comparable in group II, and significantly higher in group III and IV. The increased BP values referred mainly to systolic pressure at night (odds ratio=12.5). In group IV, the risk of elevated arterial blood pressure was 8.6.

Relationship between cardiovascular disturbances and parameters characterizing the level of exposure.

The disturbances in ECG and blood pressure regulation were dependent on EMF exposure level. In group I, a significant relationship was found between mean BPSN and E_{dose} (p=0.004) as well as between BPSN and E_{max} (p = 0.03). In group II, the relationship between BP level and exposure parameters was not analysed. Such an analysis could not be performed due to the specific job characteristics in this group - the workers were periodically exposed to EMF emitted by the repaired equipment and it was impossible to determine the level of their exposure. In group III, BP disturbances significantly correlated with exposure parameters. BPDO, BPDD, and BPDN were found to depend on the period of employment (p=0.023, p=0,05, p=0.001 respectively). A significant correlation was found between BPSN and BPDN and the maximum values of electric and magnetic fields (p=0.043 and p=0.026). In group IV, the disturbances in blood pressure regulation were dependent on EMF

exposure parameters. The risk of BP changes increased with higher lifetime dose in the UHF-VHF bands (OR=2.3) as well as higher E_{mean} in the UHF and VHF bands (OR=2.3, OR=2.5, respectively). The risk of impaired BP regulation (no nocturnal blood pressure drop) significantly increased with lifetime dose in the UHF range (OR=2.6) and with a growing E_{mean} in the VHF range (OR=2.1).

Summary

Although the occupational exposure limits, as laid down in respective Polish regulations, were not exceeded, the different impairments in circulatory system were observed in exposed workers. In workers at AM broadcasting stations, heart rhythm disturbances, detected by 24-h ECG monitoring, were more frequent than in the non-exposed workers as well as workers exposed to 50 Hz EMF. On the other hand, in workers at substations and broadcasting stations, an increased frequency of elevated BP (detected with ABPM) was found, compared with other groups. Our results suggest that the frequency of EMF determines the type of the observed cardiovascular disturbances.

Significant BP disturbances occurred mainly at night; therefore, the office BP measurement is inadequate to detect them. It is also worth noting that in EMF-exposed workers, increased BP levels in ABPM could be found both in the persons showing normal and increased BP values in a single office measurement. Therefore, the present scope of prophylactic examinations seems to be inadequate for workers occupationally exposed to EMF and it should be extended with 24h monitoring of the ECG and blood pressure.

References

[1] M.H. Repacholi, "Low level exposure to radiofrequency electromagnetic fields. Health effects and research needs," *Bioelectromagnetics*, vol. 19, pp. 1-19, January 1998.

[2] D.A. Savitz, L. Duanping, A. Sastre, R.C. Kieckner, and R. Knave, "Magnetic field exposure and cardiovascular disease mortality among electric utility workers," *Am J Epidemiol*, vol. 149, pp. 135-142, January 1999.

[3] B. Hocking, "Preliminary report: Symptoms associated with mobile phone use," Occup. Med., vol. 48, pp. 357-360, October 1998.

[4] G. Oftedal, J. Wilen, M. Sandstrom, and K.H. Mild, "Symptoms experienced in connection with mobile phone," *Occup. Med.*, vol. 50, pp. 237-245, May 2000.

[5] Hamburger S., Logue J.N., and Silverman P.M., "Occupational exposure to non-ionizing radiation and an association with heart disease: An exploratory study," *J.Chron.Dis*., vol. 36, pp. 791-802, November 1983.

[6] A. Bortkiewicz, M. Zmyslony, C. Palczynski, E. Gadzicka, and St. Szmigielski, "Dysregulation of Autonomic Control of Cardiac Function in Workers at AM Broadcast Stations (0.738-1.503 MHz)," *Electro-and Magnetobiology*, vol.14, pp. 177-191, November 1995.

[7] A. Bortkiewicz, E. Gadzicka, and M. Zmyslony, "Heart rate variability in workers exposed to medium-frequency electromagnetic fields," *J Auton Nerv Syst*., vol. 59, pp. 90-97, July 1996.

[8] St. Szmigielski, A. Bortkiewicz, E. Gadzicka, M. Zmyslony, and R. Kubacki, "Alteration of diurnal rhythms of blood pressure and heart rate in workers exposed to radiofrequency electromagnetic fields," *Blood Press Monit*, vol. 3, pp. 323-330, June 1998.

[9] A. Bortkiewicz, E. Gadzicka, M. Zmyslony, and W. Szymczak, "Neurovegetative disturbances in workers exposed to elektromagnetic fields, " in *Proceedings of the International Federation for Medical & Biological Engineering IX Mediterranean Conference on Medical and Biological Engineering and Computing Medicon 2001*, ed.: R. Magjarević, S. Tonković, V. Bilas, and I. Lacković., Pula, Croatia 2001, pp. 769-772., June 2001.

[10] ACC/AHA Clinical Competence Statement on Electrocardiography and Ambulatory Electrocardiography. *Circulation*, 104, pp. 3169-3178, December 2001

[11] J. Staessen, R. Fagard, P. Lijnen, L. Thijs, R. Van Hoof, and A. Amery, "Reference values for ambulatory blood pressure: a meta- analysis," *J. Hypertension*, vol. 8 (suppl 6), pp. S57-S64, December 1990.

EXTERNAL ELECTRIC & MAGNETIC FIELD ASSESSMENT ON THE GENERAL PUBLIC NEAR A 132 KV TRANSMISSION LINE RIGHT OF WAY

M. M. Dawoud, *Fellow IEE*, *Senior Member*, *IEEE*, C. A. Belhadj, *Member*, *IEEE*, I.O. Habiballah, *Member*, *IEEE*, T. K. Abdel-Galil, *Member*, *IEEE*, and M. Arif Abdul-Majeed.

King Fahd University of Petroleum and Minerals, Dhahran 31261, Saudi-Arabia.
(e-mail: mmdawoud@kfupm.edu.sa)

Abstract

The external electric and magnetic fields have been evaluated near a 132 kV transmission line, where members of the general public are likely to be exposed. A double circuit existing transmission line is used for the assessment. The fields have been generated using EPRI's EMF workstation software. The field calculations are based on the charge simulation method for the electric field, and Biot-Savart law for the magnetic field. The predicted electric field at the right of way was found to be 0.165 kV/m and the magnetic field was 21.4 mGauss. The results are presented in the form of field profiles at ground level around one span for both sides of the transmission line, and up to 250 ft. from the centre of the transmission line. The results for both the electric and magnetic fields have been compared with the international standards for the maximum allowable level. The comparison shows that members of the general public are exposed to field levels below those set by the standards.

Introduction

Exposure of the general public to electric and magnetic fields resulting from high voltage power transmission lines has been of prime concern for many years among electric power establishments as well as the general public. Field assessment and epidemiological studies drew a lot of attention to this during the past few decades. The aim of these studies has been to establish the safe exposure levels to power frequency electric and magnetic fields for the general public as well as line workers. Limited knowledge and information available regarding the general public exposure to these fields tends to magnify intensively the risk of exposure to extremely low frequency fields. The SEC transmission networks above 110 kV spans a total length of 33,685 circuit-km (ckm). This consists of 7,490 ckm for 110 – 115 kV, 14,451 ckm for 132 kV, 3,850 ckm for 230 kV and 7,894 ckm for 380 kV of transmission networks [1]. These figures indicate the proximity of high voltage transmission lines and locations of residential areas occupied by the general public. They also justify the need for the assessment of the electric and magnetic fields at and beyond the right of way (ROW) of the high voltage transmission lines.

There has been rising interest over the years in determining the safe exposure levels of people, mainly workers, and the general public, to power frequency electric and magnetic fields [2]-[8]. Several organizations have developed standards and guidelines for such permissible exposure levels. By far, the most important organizations that have contributed to the establishment of these standards and guidelines are the Institute of Electronic and Electrical Engineers (IEEE) [2], and the International Commission on Non-Ionizing Radiation Protection (ICNIRP) [3]. There are other organizations such as the American Conference of Governmental Industrial Hygienists (ACGIH) [4], and the National Radiological Protection Board (NRPB) that have made a major contribution [5],[6]. There are many government agencies and organizations that have published articled on this subject [7],[8].

The permissible levels quoted in many countries refer to the permissible levels set by the IEEE standard, and the ICNIRP guideline. Table 1 lists a summary of the external exposure limits for 60 Hz for the IEEE, ICNIRP, NRPB, and ACGIH for the general public.

TABLE 1
SUMMARY OF EXTERNAL EXPOSURE LIMITS FOR THE GENERAL PUBLIC.

Organization	E (kV/m)	Bx10^4 (mG)
IEEE	5	0.833
ICNIRP	4.2	0.1
NRPB	12	1.3
ACGIH	No specific standard for general public.	

This paper presents an exposure assessment study for the general public exposed to a practical double circuit HV transmission line. The selected line spans from substation 8114 (Qortoba Area) to substation 8079 (Alhamra Area-Khorais) in the Riyadh region of Saudi Arabia. Its nominal voltage and power ratings are 132 kV and 293 MVA respectively. This paper introduces detailed system data after this introduction. A description of the charge simulation method and Biot-Savart law used in the evaluation of the electric and magnetic fields follow the data section. The results of the external fields, with emphasis on the right of way and beyond are then presented. The following section introduces a comparison between the evaluated fields and the standards set by the IEEE, ICNIRP, ACGIH, and the limits recognized and used by several countries all over the world. The paper terminates with a conclusion, acknowledgment, and references.

System Data

A real double circuit transmission line is selected by SEC for the study of the exposure to electric and magnetic fields. The selected line spans from substation 8114 (Qortoba Area) to substation 8079 (Alhamra Area-Khorais) in Riyadh region. The nominal voltage and power ratings are 132 kV and 293 MVA respectively. Detailed line data and tower dimension are presented in Fig.1. and line details is delineated in Table 2.

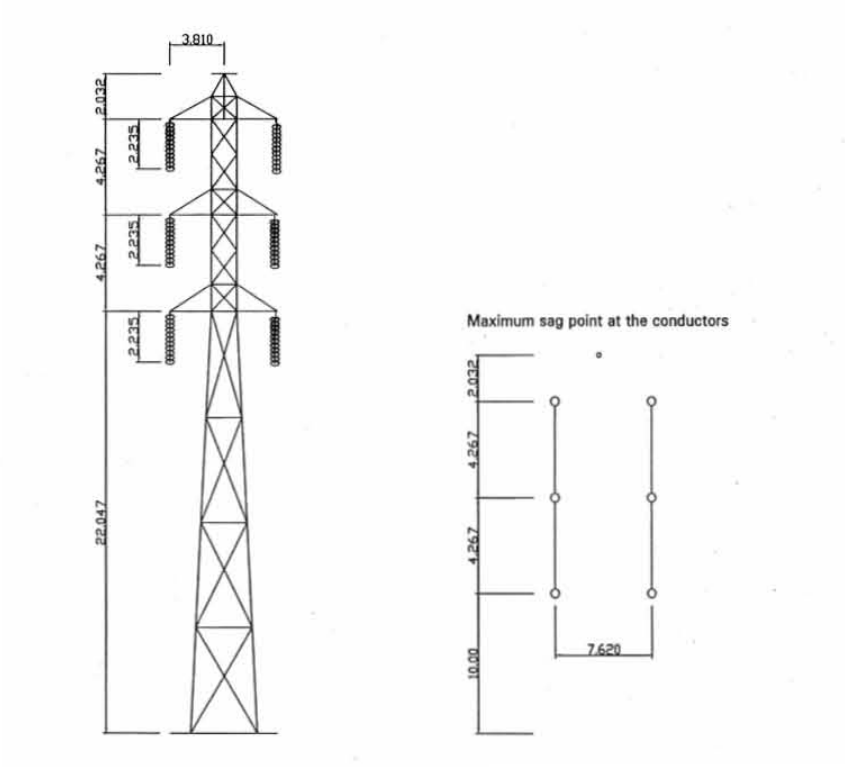


Fig. 1. Tower dimension for the 132 kV transmission line.

TABLE 2
TRANSMISSION LINE DATA FOR THE 132 KV LINE.

Line Ratings		
Rating (MVA)	293 MVA	
Nominal Line Voltage (kVL-L)	132 kV	
Actual Line Voltage (kVL-L)	132 kV	
Nominal Line Current (kA)	1.284 kA	
Peak Load Current (kA), for Both Circuits	Circuit 1	Circuit 2
	603 A	603 A
Line Conductor And Overhead Ground Wire Parameters		
Conductor/Ground Wire	Conductor	Ground Wire
Diameter (cm)	2.773 cm	1.03 cm
Number of Sub-conductors	SINGLE	
Phase Relation of Conductors	VERTICAL (R-Y-B)	
Right of Way	40 m	
Full span (m)	305 m	
Mid Span height (m) or Sag (m) (lowest point)	10 m	

The external field evaluation has been carried out at ground level and for distances up to ± 250 ft from the centre of the transmission line. This range encompasses the right of way of the transmission line and beyond and gives a good indication of the level of exposure of the general public to the electric and magnetic fields resulting from the near by transmission line. Similar results concerning line workers have been reported in [15].

External Electric and Magnetic Field Calculations

The basic physics of quasi-static fields allow separate discussion of power frequency electric and magnetic fields [9]. The solution methodology for both the electric and magnetic fields are highlighted in this section.

A. Charge Simulation Method

The solution methodology for electric field is based on the two-dimensional charge simulation method. This commonly used approach consists essentially of two stages: (l) calculation of the equivalent charges per unit length of conductor and (2) calculation of the electric field produced by these charges. A detailed treatment of the calculations is given in [10]-[13] and summarized here. The general relationship used to calculate the charges on a multi conductor system is presented in matrix form in (l).

$$[Q] = [P]^{-1} [V] \quad (1)$$

Where: [Q] is a column vector of the linear charge on each conductor; [V] is a column vector of the potentials of the conductors; $[P]^{-1}$ is the inverted matrix of the Maxwell potential coefficients of the conductors. A set of image conductors is used with charges opposite to those of the transmission line. The actual conductors and their images are characterized by real and imaginary voltages and diameters. Overhead shield wires are also included in this method (and assumed to be at zero potential). For bundled conductors, a single conductor with an equivalent diameter is used, on the basis of the following formula:

$$d_{eq} = D \sqrt[n]{\frac{nd}{D}} \quad (2)$$

where

d_{eq} is equivalent single conductor diameter; n is number of sub conductors; d is diameter of individual sub conductor ; D is geometric diameter of the bundle. The self and mutual Maxwell potential coefficients are calculated for the conductor system on the basis of line geometry and conductor diameter using the following equations.

Self:

$$P_{ii} = \frac{1}{2\pi\varepsilon} \ln\left(\frac{2y_i}{d_i}\right) \quad (3)$$

Mutual:

$$P_{ij} = \frac{1}{2\pi\varepsilon} \ln\left(\frac{(x_i - x_j)^2 + (y_i + y_j)^2}{(x_i - x_j)^2 + (y_i - y_j)^2}\right)^{1/2} \quad (4)$$

where

$\varepsilon = 8.85 * 10^{-12}$ F/m (Dielectric constant of air); di is conductor diameter or equivalent bundle diameter of conductor i ; yi, yj = heights of conductors i and j above ground; xi, xj = horizontal coordinates of conductors i and j with respect to a reference. The inverted potential coefficient matrix $[P]^{-1}$ is multiplied by the column matrix of line-ground conductor voltages to yield the charges per unit length of the conductor, as shown in (l). These charges are then used to calculate the real and imaginary parts of the horizontal and vertical components of the electric field [13].

B. BIOT-SAVART Law

The basic equation for calculating the magnetic field of a long, straight wire is derived from Ampere's Law [11,14] and given in (5):

$$H = \frac{i}{2\pi r} \quad (5)$$

Where: H is the magnetic field intensity (A/m); i is the electric current in the wire (Amperes); r is the distance between the wire and the point of interest (meters)

The fundamental unit for the magnetic field intensity, *H*, is the Ampere per meter (A/m). However, magnetic field exposure technology often uses the magnetic flux density, *B*. The relationship between H and B is given by

$$B = \mu H \quad (6)$$

where:; B is the magnetic flux density (Gauss); μ = Permeability constant used for both air and ground ($4\pi * 10^{-7}$ Henry/m)

The magnetic field is a vector field with both vertical and horizontal components. The field, as computed in Eq. 6, is separated into vertical and horizontal components by multiplying by $\sin(\theta)$ and $\cos(\theta)$. In general, both components must be retained. For three-phase ac fields, the vertical and horizontal components must be combined individually as phasors, regarding the angles of the different currents. The total magnetic field is the sum of all the contributions from the line currents as given in (7).

$$B_{i,j} = \sum \left[\frac{\mu I_i}{(2\pi r_{i,j})}\right] \varphi_{i,j} * 10^4 \quad (7)$$

Where: $r_{i,j}$ is the distance between point and conductors and $\varphi_{i,j}$ is the unit vector in the vector cross-product direction of the current vector and the vector segment $r_{i,j}$. For a three phase ac transmission line, the field at any point can be described by the field ellipse (similar to the electric field).

Evaluation of the External Electric & Magnetic Fields

In this study the electric and magnetic fields produced by the transmission line at ground level, have been modelled using the subroutine EXPOCALC of the EPRI's software EMF Workstation, Version 2.51 [14]. The software package used, starts by setting the general required parameters such as the designated area of concern parameters, the structure position, boundary area, as well as the field calculation height. The line design parameters are entered in a detailed manner and that includes phase structure of the line, conductor size, applied voltage and the operating current. The span specifications are then taken into consideration.

EMFW software provides the calculated field values in a 3-D volume around the transmission line space. Fig. 2 shows the 3-D calculated electric field around the transmission line between the mid-span point and the tower location.

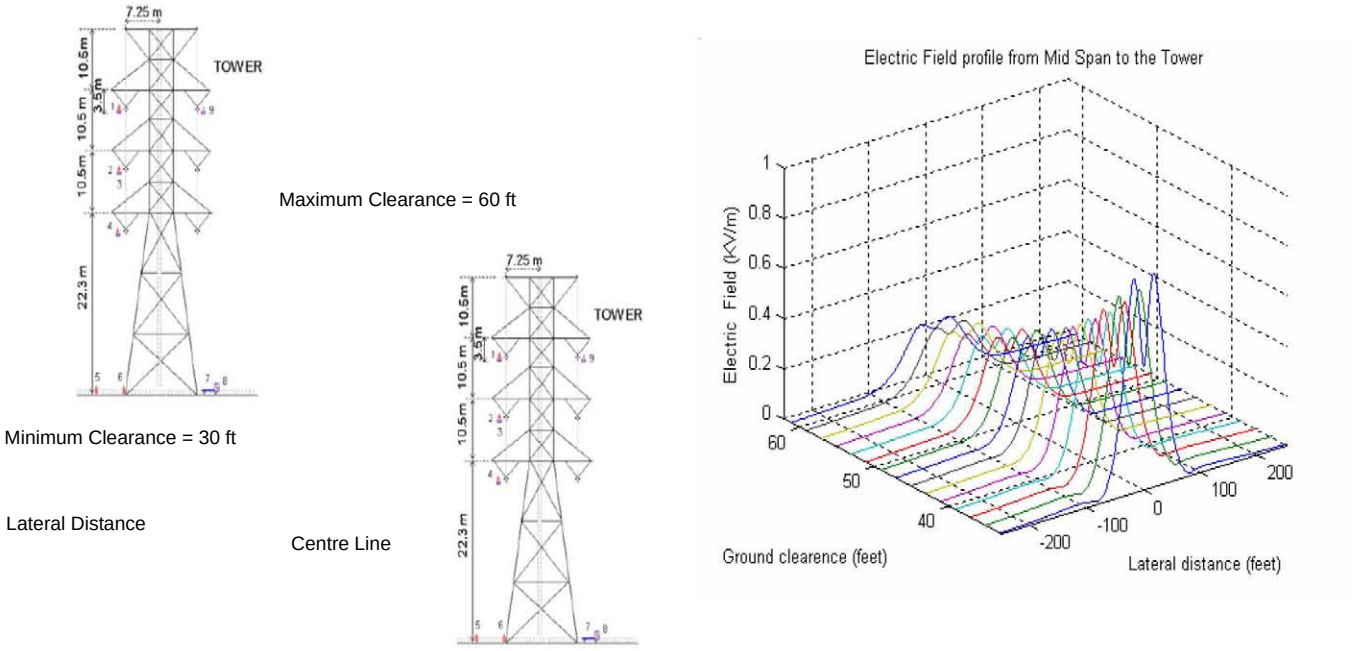
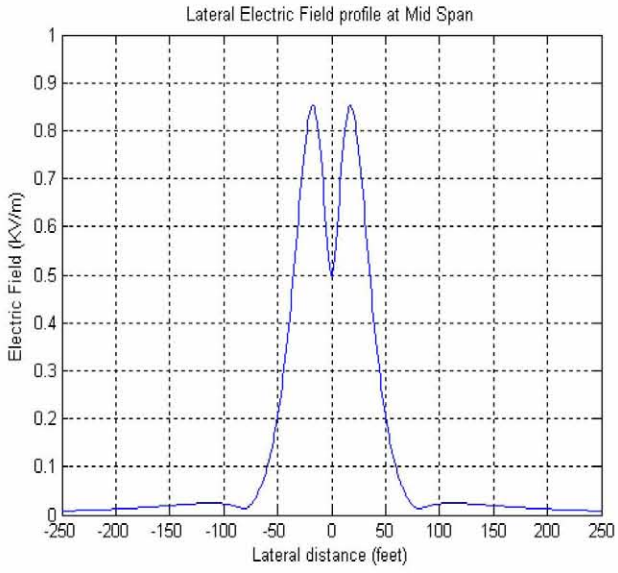


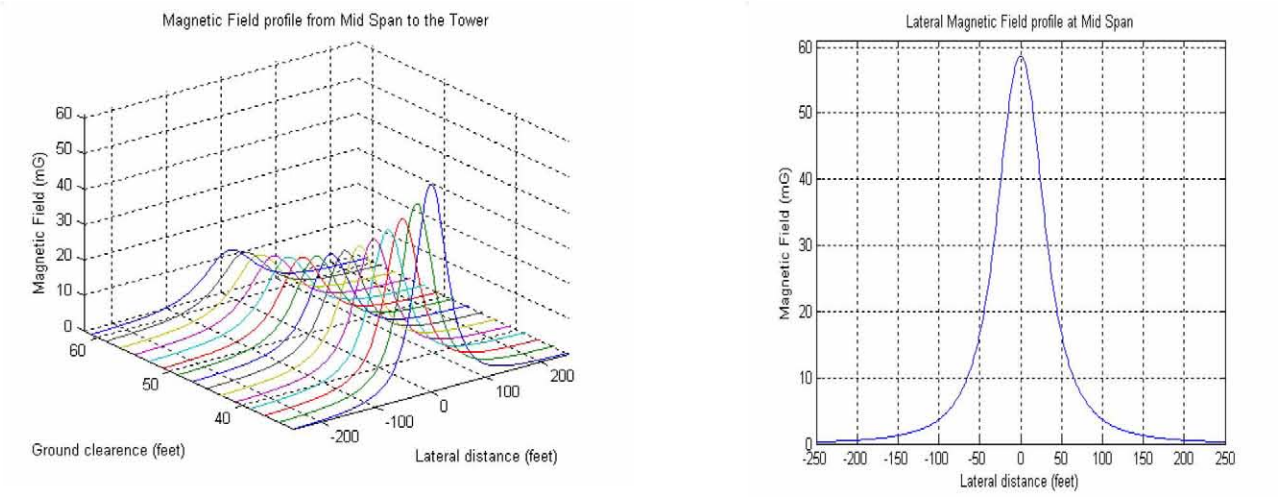
Fig. 2 Calculated External Electric Field Around the Transmission Line between Mid-Span and the Tower Location.

(a) Tower-to-tower geometry, showing mid-span between two towers.
(b) 3-D Electric field profile from mid-span to the tower for a lateral distance ranging between ± 250 ft. from the centre line.
(c) 2-D Electric field profile at mid-span.



The 2-D electric field profile shows that the calculated E field at the right of way is 0.165 kV/m. The E field decreases with increased distance from the centre line of the transmission line.

Similar behaviour is observed for the calculated magnetic field. This is shown in Fig. 3 (a and b).



(a) (b)

Fig. 3 (a) 3-D Magnetic field profile from mid-span to the tower for a lateral distance between ± 250 ft.
(b) 2-D Magnetic field profile at mid-span.

The results shown in the 2-D profile indicate that the magnetic field value at the right of way is 10 mG, which is far below the standards set by the IEEE, ICNIRP and NRPB. The maximum calculated magnetic field at the right of way is 21.4 mG, which is still far lower than all the standards set for the general public exposure.

Comparison to the International Standards

The calculated electric and magnetic field exposure levels are compared to the universal standards such as IEEE Standard C95.6 [2], ICNIRP guidelines [3], and NRPB [4]. The comparison is given in table 3. The IEEE Standard C95.6 recommends limits on exposures to electric and magnetic fields in the frequency range of 0 to 3000 hertz (Hz).

TABLE 3
COMPARISON OF THE CALCULATED FIELDS AT THE RIGHT OF WAY TO THE INTERNATIONAL STANDARDS

Organization	E (kV/m)	$Bx10^4$ (mG)
IEEE	5	0.833
ICNIRP	4.2	0.1
NRPB	12	1.3
ACGIH	No specific standard for general public.	
At ground level(ROW)	0.165	0.00214

The highest electric field exposure level computed at the right of way (ROW) is 0.165 kV/m. However, the Maximum Permissible Exposure (MPE) for the power frequency electric field as per the IEEE Standard C95.6 is 5 kV/m for a controlled (occupational) environment. The maximum permissible level according to the ICNIRP guidelines for occupational exposure is 4.2 kV/m. The limit according to the NRPB Guidelines for Exposure to 60 Hz EMF is 12 kV/m.

The maximum magnetic field computed at the right of way is 21.4 mG. However, the Maximum Permissible Exposure for the power frequency magnetic field by the general public as per the IEEE Standard is 0.833×10^4 mG. The maximum permissible level according to the conservative standard ICNIRP guidelines is 0.1×10^4 mG. The limit according to the NRPB for Exposure to 60 Hz EMF is 1.3×10^4 mG. There are no limits set by the ACGIH for the general public.

The highest electric and magnetic fields exposure level for the SEC 132 kV transmission line, therefore, is well below the limits set by the different standards for general public exposure.

Conclusion

The exposure of the general public to the electric and magnetic fields associated with a 132 kV HV transmission line has been evaluated. The EPRI's EMF Workstation software has been used to calculate the external electric and magnetic fields due to the 132 kV high voltage transmission line at ground level and for distances starting from the right of way of the transmission line. Comparison of the values of external electric and magnetic fields, with the allowable limits set by international standards reveals that the level of exposure of the general public to extremely low frequency electric and magnetic fields are well below the limits recommended by these international standards.

Acknowledgment

The authors acknowledge the support of King Fahd University of Petroleum & Minerals in conducting this research.

References

[1] Saudi Electricity Company, "Annual Report", Saudi Arabia, 2004.

[2] IEEE Std C95.6., "IEEE Standard for Safety Levels with Respect to Human Exposure to Electromagnetic Fields, 0–3 kHz", 2002.

[3] International Commission on Non-Ionizing Radiation Protection:, "Guidelines limiting exposure to time-varying electric, magnetic, and electromagnetic fields (up to 300 GHz)", Health Physics, Vol. 74, No. 3, pp. 494-522, 1998.

[4] American Conference of Governmental Industrial Hygienists, TLVs and BEIs, Cincinnati: ACGIH, 2001

[5] Advisory Group on Non-Ionizing Radiation (AGNIR) of the UK National Radiological Protection Board (NRPB), "Limiting Exposure to Electromagnetic Fields (0 300 GHz)", Doc. NRPB, Vol. 15, No. 2, 2004.

[6] National Radiological Protection Board, "Restrictions on human exposure to static and time varying electromagnetic fields and radiation: scientific basis and recommendation for implementation of the Board's statement", Doc. NRPB, Vol. 4, pp. 8–69, 1993.

[7] Olden, K. O., "Health Effects from Exposure to Power-Line Frequency Electric and Magnetic Fields", National Institute of Environmental Health Sciences, NIH Publication 99-4493, 1999.

[8] International Agency for Research on Cancer (IARC), Non-Ionizing Radiation, Part 1: "Static and Extremely Low Frequency Electric and Magnetic Fields", Publication 80, 2002.

[9] Electric Power Research Institute, "Transmission Line Reference Book 345 kV and Above", Fred Weidner and Sons, New York. NY., 1975.

[10] Singer, H., H. Steinbigler, and P. Weiss, "A charge simulation method for the calculation of high voltage fields", IEEE Trans. PAS, v. 93, pp. 1660-1668, 1974.

[11] Shen, L., and J. Kong, "Applied Electromagnetics", Brooks/Cole. Engineering Division, 1983.

[12] Foe, P. Y., and S. Y. King, "Bundle Conductors Electric Field by Integral Equations Method", Proc. IEE, Vol. 123, No. 7, pp. 702-706, 1976.

[13] Singer, H., H. Steinbigler, and P. Weiss, "A charge simulation method for the calculation of high voltage fields", IEEE Trans. PAS, Vol. 93, pp. 1660-1668, 1974.

[14] Electric Power Research Institute (EPRI), "Electric and Magnetic Fields Workstation (EMF WORKSTATION)", Users Manual Version 2.51.

[15] I.O. Habiballah, T. K. Abdel-Galil, M. M. Dawoud, C. A. Belhadj, M. Arif Abdul-Majeed, and T.A. Al-Betairi, "ELF Electric and Magnetic Fields Exposure Assessment of Live-Line Workers for 132 kV Transmission Line of SEC", 2006 IEEE PES Transmission and Distribution Conference and Exposition: Latin America, August 15-18, 2006, Caracas, Venezuela, Accepted.

TINNITUS AND MOBILE PHONE USE: IS THERE A CONNECTION?

HANS-PETER HUTTER[1], HANNS MOSHAMMER[1], PETER WALLNER[2], MONIKA CARTELLIERI[3], DORIS-MARIA DENK-LINNERT[4], MICHAELA KATZINGER[4], KLAUS EHRENBERGER[4], MICHAEL KUNDI[1]

[1]INSTITUTE OF ENVIRONMENTAL HEALTH, MEDICAL UNIVERSITY OF VIENNA, AUSTRIA
[2]MEDICINE AND ENVIRONMENTAL PROTECTION [MUS], VIENNA, AUSTRIA
[3]EAR NOSE AND THROAT DEPARTMENT, KAISER-FRANZ-JOSEF-SPITAL, VIENNA, AUSTRIA
[4]EAR NOSE AND THROAT DEPARTMENT, MEDICAL UNIVERSITY OF VIENNA, AUSTRIA

Abstract

Background: Recent studies suggest that about 10-15% of the adult population experiences tinnitus. As there are indications that mobile phone use could be a risk factor for the occurrence of tinnitus, we performed a case-control study on this issue.

Methods: One hundred patients presenting with tinnitus at the Ear-Nose-Throat (ENT) Department of the Medical University of Vienna were enrolled into the study. For each case a control subject was randomly selected matched for sex and age with various diagnoses not related to tinnitus. A standardized questionnaire (based on the protocol of the Interphone study) was answered by study participants. Patients' history was obtained and clinical examinations were conducted to exclude known underlying causes of tinnitus. Only patients were included that were negative in this respect and therefore suffered from “idiopathic” tinnitus. Odds ratios were computed based on conditional logistic regression with age, sex, years of education, and living in an urban area as covariates.

Results: Mobile phone use was highly prevalent in cases as well as controls (>90%). Concerning mobile phone use up to the index date (onset of tinnitus) neither regular use nor intensity or cumulative hours of use had a significant effect. However, prolonged use (four years or more) of a mobile phone was associated with a significant odds ratio of 1.95 (CI 1.003-3.80).

Conclusions: There could be an association between mobile phone use and the occurrence of tinnitus with a latency of several years.

Introduction

Subjective tinnitus (tinnitus aurium) is defined as a sound sensation that cannot be attributed to an external sound source. It is a symptom of different underlying diseases, not a disease itself. The numerous mechanisms that produce tinnitus are not fully known and associated with nearly all diseases and disorders of the ear (middle ear, inner ear) and retrocochlear disease also causing hearing loss. Different hypotheses explain the various pathophysiological aspects of tinnitus [1]. Tinnitus seems to be generated predominantly in the primary afferent synapses of the cochlea [2,3], but leads to a cortical reorganisation [3]. Tinnitus is experienced by the patients either uni- or bilateral as a sound in the ear/head of varying quality (e.g. roaring, hissing, ringing); it may occur of non-pulsatile or pulsatile character, the latter may be due to vascular pathology.

Most often tinnitus sensation is intermittent and sometimes associated with specific conditions - such as listening to loud music, fever, use of aspirin or quinine, or transient perturbations of the middle ear - and subsides over a period of time ranging from a few seconds to a few days. Studies indicate that the prevalence of tinnitus in adults falls in the range of 10-15% [4-6].

At least in 1-3% of the general population tinnitus affects the quality of life, involving sleep disturbance, work impairment and psychic distress [7].

Tinnitus is more common in the elderly but may also occur in children. It could become more common in the future as a direct consequence of the rise in recreational-noise-induced hearing loss (i.e. from overly loud music) combined with an increased life span. Due to the various pathophysiological mechanisms of tinnitus, therapy is problematic, and evidence-based therapeutic interventions are rare. There currently are very few interventions available that reduce tinnitus loudness and annoyance effectively [8]. Therefore it is important to focus research on possible (environmental) risk factors.

During the last years the habit to extensively use mobile telephones has emerged, such that the majority of the population of Western and Middle-European countries are regularly using these phones. There are concerns that mobile telecommunication could be a possible risk factor for the occurrence of tinnitus (complaints of patients to environmental out-patient departments, neighbours of basestations [e.g.9]). However, up to now there have been no systematic investigations of this problem.

Our study should provide first answers to the question whether or not intensive use of mobile phones increases the risk of tinnitus occurrence.

Methods

Study design and participants

The study was carried out as a hospital-based case-control study at the Ear-Nose-Throat (ENT) Department Medical University of Vienna, Austria. Cases were enrolled consecutively as they presented at the out-patient unit. For each case a control was selected from the same department, of the same age group (±2,5 years < 55 years; ±5 years > 55 years), the same sex and ethnic group. Exclusion criteria were diseases of the middle ear, status post middle ear surgery, retrocochlear disease, severe psychiatric and systemic diseases and medication with drugs that can influence tinnitus (ototoxic or psychopharmacological drugs). Patients with acute and chronic tinnitus who attended the ENT department (age 16 to 80 years) were included.

Controls were patients without any concomitant condition that is related to tinnitus (except for unspecific causes such as hypertension).

Diagnostics/investigation procedure

For the selection of patients, the diagnostic test battery contained the following procedures

- careful history with special regard to tinnitus and its risk factors
- clinical ENT examination with otomicroscopy
- pure-tone and speech audiogram
- tympanogram and testing of the stapedius reflex
- subjective rating of the tinnitus
- tinnitus matching
- MRI (if indicated, to exclude retrocochlear pathology)

Each case that was enrolled received a standardized questionnaire (Structured Tinnitus Interview, STI [8]). Items refer to central characteristics of tinnitus history, etiological factors and tinnitus-related psychological complaints. In addition, a medical interview was conducted. Patients' history and clinical examination concerning possible underlying causes of tinnitus were obtained by usual clinical procedures. For each patient a CRF (Case Report Form) was compiled that was maintained according to GCP (Good Clinical Practice) guidelines.

Pure-tone and speech audiometry (Clinical Audiometer AC 40, Interacoustics©) were applied in order to exclude tinnitus related to sudden deafness and Morbus Menière. Tympanometry and stapedius reflex measurements (Impedanz Audiometer AZ 26, Interacoustics©) were carried out in order to exclude tinnitus related to conductive hearing loss. If retrocochlear hearing loss was suspected, cranial MRI was applied.

For the evaluation of tinnitus, both a subjective rating of the tinnitus on a five-point scale (0 = no tinnitus; 1 = slight; 2 = moderate; 3 = severe; 4 = tormenting tinnitus) and a tinnitus matching as a psychoacoustic measurement of tinnitus were carried out.

The audiometric tinnitus simulation test (= tinnitus matching) (Clinical Audiometer AC 40, Interacoustics©) determined character (pure-tone, narrow and wide band), frequency and intensity of the tinnitus. Tinnitus matching was performed contralaterally.

With the help of this procedure tinnitus subtypes (esp. temporo-mandibular joint dysfunction related tinnitus, cervical tinnitus, acute tinnitus/sudden deafness/noise trauma, suspected cochlear-synaptic tinnitus) could be identified. This information was used to exclude patients with known underlying pathophysiology.

For the exploration of the mobile phone habits we used a standardized questionnaire (based on the protocol of the Interphone Study of the WHO). In short, for each mobile phone the subject used or has used, the type of phone, duration and intensity of use, side of the head the phone was predominantly held, use of head sets, use in urban/rural areas and in cars was assessed. In addition, to assess individual microwave exposure for future investigations we took two photos of the participants while using a mobile phone in typical position. Furthermore, somatometry of the head was performed on specific anthropogenic diameters (e.g. tragus - tragus, biauricular diameter) with a calliper.

Statistical Methods

Data on mobile phone use were censored at the date of first occurrence of tinnitus. Index date of controls was the occurrence of tinnitus in the matched case. Intensity of use, cumulative number and duration of calls were categorized based on the distribution of these variables in controls: The median (excluding never users) was chosen as cut-off. Reference category was never use of a mobile phone (prior to index date). In all cases data on mobile phone use were adjusted for the use of hands-free devices. Further adjustments were applied for the side of the head of predominant use. Mobile phone use was only counted if it occurred on the same side of the head as the tinnitus (controls were assigned the side of the matched case). Duration of mobile phone use was categorized into three groups: never use or use for less than one year (reference), 1 to 4 years, and longer than 4 years.

Conditional logistic regression analyses for individually-matched data were used to estimate odds ratios and 95% confidence intervals. All analyses were adjusted for gender, age, years of education (less than and 12 years or more) and living in an urban area.

Results

Subjects' characteristics were comparable in cases and controls (table 1). Due to matching for gender and age these variables were in agreement, but also other personal characteristics did not differ significantly between cases and controls. There was a slight tendency for a somewhat higher socio-economic status (SES) implied by the higher education, higher rate of white collar workers and urban residents in controls.

Table 1. Demographic characteristics of cases and controls[+)]. p-value for comparison of non-matching variables.

	Cases	Controls	p-value
Gender			
male	54	54	
female	46	46	
Age (mean±SD)	42.5±14.4	42.5±14.5	
Partner			
with	66	69	0.742
without	28	28	
Education			
<12 years	36	29	0.371
≥12 years	63	69	
Occupation			
unemployed	6	6	0.624
retired	16	16	
in education	15	10	
blue collar	9	10	
white collar	48	53	
City resident			
yes	70	76	0.361
no	23	18	

[+)] Percentages not summing up to 100 due to missing values

Almost all subjects at time of inquiry used a mobile phone (92% and 93% for cases and controls, respectively), however, at the time of first occurrence of tinnitus (and the respective index date in controls) only 73% of cases and 67% of controls were using a mobile. Another 7% of cases and 8% of controls used the mobile at that time for less than one year. For ever users prior to occurrence of tinnitus there was a slightly but not significantly increased odds-ratio of 1.37 (95% CI: 0.73-2.57). Moderate increases of odds-ratios were noted for all variables of intensity of use: average daily duration of use for 10 minutes or more was associated with an odds-ratio of 1.71 (95% CI: 0.85-3.45), cumulative hours of use of 160 or more gave an odds ratio of 1.57 (95% CI: 0.78-3.19), cumulative number of calls in excess of 4000 an odds-ratio of 1.28 that was less than for lower number of calls (odds-ratio 1.46) possibly indicating greater importance of duration as compared to number of calls. A borderline significant result was obtained for duration of use of 4 or more years: odds-ratio 1.95 (95% CI: 1.003-3.80). Test of trend for duration of use was also significant (p=0.046).

Table 2. Mobile phone use and risk of tinnitus.

	No. of cases	No. of controls	OR	95% CI
Mobile phone use				
never	27	33	1.00	
ever	73	67	1.37	0.73-2.57
Average duration				
never	27	33	1.00	
<10 min/day	39	34	1.02	0.48-2.16
≥10 min/day	43	33	1.71	0.85-3.45
Cumulative hours of use				
never	27	33	1.00	
<160 h	31	34	1.17	0.56-2.42
≥160 h	42	33	1.57	0.78-3.19
Cumulative number of calls				
never	27	33	1.00	
<4000 calls	37	33	1.46	0.71-3.00
≥4000 calls	36	34	1.28	0.62-2.63
Years of mobile phone use				
never, <1	34	41	1.00	
1-3	33	36	1.23	0.61-2.47
≥4	33	23	1.95	1.003-3.80

Discussion

The prevalence of tinnitus has increased over the past decade and is currently 10-15% in industrialized countries [7]. Increase in incidence may be due to better diagnostic tools and increased awareness of the disease; however, a number of environmental factors have been implicated to increase the risk of tinnitus. The suspected factors include electromagnetic fields emitted by hand-held cellular telephones.

Since the majority of the population is using mobile phones more or less intensively people were concerned about effects on wellbeing [11,12]. Practitioners are confronted with reports of sensation of tinnitus related to mobile phone use by their patients [13].

In our study slight increases in risk were noted for all variables of intensity of use. The study was designed to detect a twofold increase of risk with 80 percent power. Further investigations esp. multicenter designs will be more efficient to detect these moderately increased risks. Because of the high prevalence of tinnitus and the widespread use of mobile phones even a small enhancement of the risk could be of public health importance.

From a theoretical point of view this possible association of mobile phone use and occurrence of tinnitus has some plausibility, because the cochlea is located in an anatomic region where a considerable amount of the power emitted by cell phones is absorbed [14]. One etiologic factor for tinnitus is calcium imbalance in the neural acoustic pathway. It is well known that exposure to modulated high-frequency electromagnetic fields (HF-EMF) has the potential to affect calcium homeostasis especially in neural tissue [15].

Because some mobile telephones (especially newer types) cause rather high exposure of the cochlea [14] and along the acoustic pathway it is possible that tinnitus could be caused by calcium efflux. Effects of exposure on calcium homeostasis was also implied as one factors in the development of acoustic neuroma. Ten studies [16-25] investigating the association between mobile phone use and acoustic neuroma have been published so far.

Half of theses studies found indications of an association [21-25], the other 5 were those with shorter duration of mobile phone use and/or smaller number of long-term users of a mobile [16-20].

Tinnitus strongly interferes with the daily lives of people. In industrialized countries, 10-15% of the adult population currently experience tinnitus. There are very few interventions available that effectively reduce tinnitus loudness and annoyance. Therefore, all measures should be taken to avoid further increase of tinnitus prevalence.

Results indicate that high intensity and long duration of mobile phone use might be associated with occurrence of tinnitus. As more persons start using mobile phones at younger age, this indeed may become a public health problem.

Acknowledgements

We thank Elisabeth Cardis, International Agency for Research on Cancer, Lyon, for permitting use of the Interphone Questionnaire. Furthermore the assistance of Brigitte Piegler is gratefully acknowledged.

References

[1] Eggermont J (2005): Tinnitus: neurobiological substrates. Drug Discovery Today 10:1283-1290.
[2] Ehrenberger K, Brix R (1983): Glutamic acid and glutamic acid diethyl ester in tinnitus treatment. Acta Otolaryngol (Stockholm) 95:599-605.
[3] Eggermont J (1990): On the pathophysiology of tinnitus; a review and a peripheral model. Hear Res 48:111-23.
[4] Heller AJ (2003): Classification and epidemiology of tinnitus. Otolaryngol Clin North Am 36:239-248.
[5] Marsot-Dupuch K (2001). Pulsatile and nonpulsatile tinnitus: a systemic approach. Semin-Ultrasound-CT-MR 22:250-270.
[6] Henry JA, Dennis KC, Schechter MA (2005): General Review of Tinnitus: Prevalence, Mechanisms, Effects, and Management. Journal of Speech, Language, and Hearing Research 48:1204-1235.
[7] Dobie RA (2003): Depression and tinnitus. Otolaryngol Clin North Am 36, 383-388.
[8] Denk D-M, Heinzl H, Franz P, Ehrenberger K (1997): Caroverine in tinnitus treatment: a placebo-controlled blind study. Acta Otolaryngol (Stockholm) 117:825-830.
[9] Navarro EA, Segura J, Portosolés M, Gómez-Perretta de Mateo C (2003): The microwave syndrome: a preliminary study in spain. Electromagnetic Biology and Medicine 22:161-169.
[10] Hiller W, Goebel G, Schindelmann U (2000): Systematische Fremdbeurteilung von Patienten mit chronischem Tinnitus (Strukturiertes Tinnitus-Interview). Diagnostica 46:93-102.
[11] Hutter HP, Moshammer H, Wallner P, Kundi M (2004): Public perception of risk concerning celltowers and mobile phones. Sozial- und Präventivmedizin 49:62-66.
[12] Siegrist M, Earle TC, Gutscher H, Keller C (2005): Perception of Mobile Phone and Base Station Risks. Risk Analysis 25:1253-1264.
[13] Huss A, Röösli M (2005): Befragung von Ärztinnen und Ärzten zum Thema elektromagnetischer Felder in der hausärztlichen Praxis. Studie im Auftrag des Bundesamtes für Gesundheit (BAG). Institut für Sozial- und Präventivmedizin, Universität Bern, September 2005.
[14] Überbacher R, Schmid G, Tschabitscher M (2006): New high resolution numerical model of inner ear organs for RF-dosimetriy – preliminary results in the 900 MHz – 10 GHz range. The Bioelectromagnetics Society`s 28th Annual Meeting (June 11-15, 2006; Cancun, Mexico).
[15] Blackman CF (1992): Calcium release from neural tissue: experimental results and possible mechanisms. In Norden B, Ramel C (eds): "Interaction Mechanisms of Low-Level Electromagnetic Fields in Living Systems." Oxford: Oxford University Press, pp. 107-129.
[16] Hardell L, Nasman A, Pahlson A, Hallquist A, Hansson Mild K (1999): Use of cellular telephones and the risk for brain tumours: A case- control study. International Journal of Oncology 15:113-116.
[17] Johansen C, Boice J, Jr., McLaughlin J, Olsen J (2001): Cellular telephones and cancer—a nationwide cohort study in Denmark. J Natl Cancer Inst 93:203-720.
[18] Inskip PD, Tarone RE, Hatch EE, Wilcosky TC, Shapiro WR, Selker RG, Fine HA, Black PM, Loeffler JS, Linet MS (2001): Cellular-telephone use and brain tumors. N Engl J Med 344:79-86.
[19] Muscat JE, Malkin MG, Shore RE, Thompson S, Neugut AI, Stellman SD, Bruce J (2002): Handheld cellular telephones and risk of acoustic neuroma. Neurology 58:1304-1306.
[20] Warren HG, Prevatt AA, Daly KA, Antonelli PJ (2003): Cellular telephone use and risk of intratemporal facial nerve tumor. Laryngoscope 113:663-667.

[21] Hardell L, Hansson Mild K, Carlberg M (2003): Further aspects on cellular and cordless telephones and brain tumours. International Journal of Oncology 22:399-407.
[22] Christensen HC, Schuez J, Kosteljanetz M, Poulsen HS, Thomsen J, Johansen C (2004): Cellular telephone use and risk of acoustic neuroma. American Journal of Epidemiology 159:277-283.
[23] Loenn S, Ahlbom A, Hall P, Feychting M (2004): Mobile Phone Use and the Risk of Acoustic Neuroma. Epidemiology 15:653-659.
[24] Hardell L, Carlberg M, Hansson Mild K (2005): Case-Control Study on Cellular and Cordless Telephones and the Risk for Acoustic Neuroma or Meningioma in Patients Diagnosed 2000-2003. Neuroepidemiology 25:120-128.
[25] Schoemaker MJ, Swerdlow AJ, Ahlbom A, Auvinen A, Blaasaas KG, Cardis E, Christensen HC, Feychting M, Hepworth SJ, Johansen C, Klaeboe L, Loenn S et al. (2005): Mobile phone use and risk of acoustic neuroma: results of the Interphone casecontrol study in five North European countries. British Journal of Cancer 93:842-848.

EFFECTS OF 2.45 GHz ELECTROMAGNETIC FIELDS WITH A WIDE RANGE OF SAR ON CELLULAR GENOTOXICITY IN CULTURED CELLS

JUNJI MIYAKOSHI, SHIN KOYAMA, YOSHIKI KOMATSUBARA, JIN WANG, TOMONORI SAKURAI

GRADUATE SCHOOL OF HEALTH SCIENCES, FACULTY OF MEDICINE, HIROSAKI UNIVERSITY, HIROSAKI, AOMORI, 036-8564, JAPAN

Abstract

High-frequency electromagnetic fields (HFEMF) used for mobile phones may be of great concern for human health. In order to investigate the properties of HFEMF, we have examined the genotoxic effects of 2.45 GHz EMF on micronucleus (MN) formation, DNA strand breaks, and chromosomal aberrations in cultured cells. Chinese hamster ovary (CHO)-K1, human glioma MO54, and mouse m5S cells, respectively, were used in these experiments for MN formation, DNA strand breaks, and chromosomal aberration. The DNA strand breaks were detected using an alkaline comet assay. Cells were exposed to HFEMF for 2 h at average specific absorption rates (SARs) from 5 to 200 W/kg, and the effects on these cells were compared with those in sham-exposed cells. Heat treatment as a heat control was performed at temperatures of 37 to 44°C. MN frequency at SAR of lower than 50 W/kg did not differ from the sham-exposed controls, while MN frequency at SARs of 100 and 200 W/kg was significantly higher. No significant differences in the DNA strand breaks and the chromosomal aberrations were observed following exposure to HFEMF from 5 to 200 W/kg, compared with sham-exposed control. In summary, HFEMF exposure at 2.45 GHz for 2 h up to SAR of 50 W/kg does not induce MN formation, DNA strand breaks and chromosomal aberrations.

Introduction

In recent years there has been a rapid increase in the use of devices and systems employing high-frequency electromagnetic fields (HFEMF) in our lives, including radio and TV transmitters, microwave ovens, telecommunication links, and satellite communications, as well as mobile phones and their supporting transmitters (base stations). Thus exposure to HFEMF in the environment is greater than any of the former ages of human. A consequent result of this has been increased concern about the association between environmental exposure to HFEMF and cancer. Although several theoretical models have been proposed [1-3], the association between HFEMF and cancer remains unclear.

General concerns regarding the potential hazards of exposure to HFEMF have led to many epidemiological investigations [4-6]. Several studies have suggested that exposure to HFEMF can interact with behavior [7, 8]. *In vitro* studies have reported the effects of HFEMF on several end-points, including effects on DNA damage [9], chromosome aberrations [10], mutation [11], cell transformation [12] and gene expression [13]. In these studies, cells were typically subjected to exposures as low as specific absorption rates (SARs) of 10 W/kg to estimate the

---

Effects of 2.45 GHz Electromagnetic Fields with a Wide Range of SAR on Cellular Genotoxicity in Cultured Cells

Junji Miyakoshi, Shin Koyama, Yoshiki Komatsubara, Jin Wang, Tomonori Sakurai

Graduate School of Health Sciences, Faculty of Medicine, Hirosaki University, Hirosaki, Aomori, 036-8564, Japan

risk of weak HFEMF that we are actually exposed to daily, since this is the final goal of these studies. However, exposures to a higher intensity are also necessary to explore the effects of HFEMF for safety evaluation. We have previously reported that exposure to 2.45 GHz electromagnetic fields for 2-16 h induced Hsp70 in human glioma MO54 cells [14], and exposure to HFEMF at 100 W/kg did not cause any DNA damage according to the comet assay system [15]. HFEMF at high SAR mainly results in heating of the cells. Heat is known to cause many biological changes and the heating effect of HFEMF is well established [16]. However, there have been claims that HFEMF could exert non-thermal effects on biological systems. Hence, with exposure conditions used in these experiments it becomes very important to establish the differences between thermal and non-thermal effects.

Considering these previous data, we have examined the frequency of micronucleus (MN) formation in Chinese hamster ovary (CHO)-K1 cells following HFEMF exposure. MN formation is derived from clastogenic activity arising from chromosomal fragments that are not incorporated into daughter nuclei at mitosis. This occurs because of the lack of a kinetochore. MN formation is also derived from an aneugenic process when the whole chromosome is not correctly integrated into the two daughter nuclei at the time of cell division [17-20]. In the present study, we also examined the presence or absence of single-strand DNA breaks and chromosomal aberrations in mammalian cells exposed to 2.45 GHz HFEMFs with a wide range of SAR (5 W/kg to 200 W/kg) in human glioma MO54 and mouse m5S cells, respectively.

Materials and methods

1. Exposure system

The exposure system of HFEMF was described elsewhere [21-23]. In brief, the applicator is based on a rectangular waveguide, with its size determined to be 110 mm (wide) × 55 mm (high) × 310 mm (deep). The electromagnetic waves are propagated along the waveguide in TE_{10} mode. One end of the applicator is terminated with a short-circuiting plate to generate standing waves in the waveguide.

A rectangular culture dish is placed on two slits, which were bored into the wider wall of the waveguide. The cells in the dish are exposed to the HFEMF through these slits. The two slits are pinch shaped, which enhances the coupling of the electromagnetic field to increase the effective exposure area. The culture dish is divided into four compartments. The distribution of the electric field in the medium depends on the thickness of the medium. Therefore, it is preferable to choose a thickness that maximizes the SAR at the bottom of the well, where the cells are present. Numerical analysis indicates that the appropriate thickness is 8 mm, which corresponds to a half wavelength in the medium.

The SAR distribution in the exposure apparatus was calculated using the Finite Difference Time Domain (FDTD) method. An each compartment has a different value of SAR. The maximum SAR appears in compartment 3. The maximum SAR values in compartment 2 and 4 are 80% and 85% of the maximum SAR value in compartment 3. The minimum SAR in compartment 1 is 1% of the maximum value.

2. Cells and culture conditions

CHO-K1 cells were obtained from the Japanese Cancer Research Bank, Tokyo. Cells were maintained in Ham's F-12 medium (Nikken Bio Medical Laboratory, Kyoto, Japan) supplemented with 10% fetal bovine serum (Gibco, BRL) at 37°C in 95% air and 5% CO_2 [21].

MO54 cells, derived from a human malignant glioma, were used in this study. Cells were cultured in Dulbecco's modified Eagle's medium (Nikkenn Bio Medical Laboratory) supplemented with 10% fetal bovine serum (GIBCO, BRL) at 37°C in an atmosphere of 95% air and 5% CO_2 [22].

Mouse m5S cells are a near-diploid cell line established from embryonic skin; they are immortalized but non-tumorigenic [24]. The cells were grown as monolayers in Dulbecco's modified Eagle's medium supplemented with 10% fetal bovine serum (BioWest, Rue de la Caille 49340 Nuaill, br, France) at 37°C in an atmosphere of 95% air and 5% CO_2 [23].

3. MN analysis

After a 2 h exposure to HEFMF, the cells were trypsinized and seeded in 10 cm culture dishes in medium containing cytochalasin B at a final concentration of 3 μg/ml for 18 h, in order to prevent cell division. A sham-exposure experiment was performed as a negative control. Cells were treated in the same way to those that underwent HFEMF exposure, except that HFEMF exposure itself was omitted. Instead, the cells were incubated for 2 h in a conventional incubator. In addition, the cells were treated with bleomycin alone as a positive control, using the same conditions as those used for sham exposure.

The cells were collected at a concentration of 2.7×10^4 cells/ml, and samples of 0.2 ml were centrifuged onto slides, using a Cytospin centrifuge (Shandon Southern Ltd.) at 100 × g for 5 min. The cells were then fixed with 80% cold ethanol for 30 min. The slides were washed gently with PBS and soaked in new PBS for 5 min to

completely remove the ethanol.

The cells on the slides were stained with 20 µl of propidium iodide (PI) diluted in glycerol (to a concentration of 0.2 µg/ml), and kept in the dark until counting was performed. A total of 1000 binucleated cells were scored for evaluation of the frequency of induction of MN, using fluorescence microscopy (Olympus). Cells were counted as having MN formation when they contained at least one micronucleus. The procedure was performed in a double-blind manner, and followed the method described by Countryman and Heddle [20]. Statistical analysis of the data in the control and experimental groups was conducted using ANOVA (analysis of variance) followed by Fisher's Protected Least Significant Difference (PLSD) test.

4. Comet assay

To detect DNA damage at the single-cell level, an alkaline comet assay was performed. The method of the comet assay has been described previously [25]. In brief, we used a Trevigen Comet Assay system (Trevigen, Inc., Gaithersburg, MD). After the treatments, the cells were rinsed with phosphate-buffered saline (Ca^{++} and Mg^{++} free; PBS) and treated with trypsin. Cell suspension in 1×PBS on ice was mixed with low melting agarose at 37 °C (cell suspension : agarose = 1 : 8). The mixture of cell suspension and agarose was kept on a slide in the dark at 4 °C, underwent 5 minutes of fixation, and was then immersed in a lysis solution at 4°C for 40 min. The slide was placed in the alkali buffer for 15 minutes. Electrophoresis was performed as reported previously [26]. After the electrophoresis, the samples were fixed in ethanol for 5min and then dried. DNA in agarose was stained with SYBR Green according to the manufacturer's recommended procedure.

DNA Strand breaks were analyzed by using IDL Comet 6.0 (Adamnet, Tokyo, Japan). Tail length is the destance from the first non-zero element to the last non-zero elements in tail content. Tail content was calculated as the integrated value of the fluorescent brightness of the total comet minus the integrated value of the fluorescant brightness of the comet head. The unit of the parameter is given as "pixels". The tail length is the distance between the first and last non-zero elements in the tail content. The tail moment was calculated according to the following equation:

Tail moment = Differential between means ×% in tail.

For a statistical evaluation of the tail moment, tail length, and tail percent, An analysis of variance (ANOVA) test was used to determine any inte-group differences. When a significant *F* value was found ($p<0.05$), the Bonferroni/Dunn test was used for a multiple comparison. *P*-value that were less than 0.05 were considered statistically significant.

5. Chromosomal aberrations

After exposure, the cells were removed and cultured in a conventional incubator for 24 h. Colcemid (0.1µg/mL, Sigma) was added during the last 4 h. Unexposed control cells were incubated for the same period in a conventional incubator. Chromosome preparations were made according to the standard air-drying method and stained with 3% Giemsa solution (pH 6.4). For each culture, a minimum of 200 cells was assesed for the types and frequencies of chromosomal aberrations; all structural chromatid-type and chromosome-type changes, including gaps, were recorded. The scoring was conducted in a double-blind manner.

The experimental data are presented as the mean ± S.E.M. *Chi* square tests were performed to determine whether there was a significant difference in the proportion of cells with aberrations between the cells exposed to HFEMF and unexposed cells. The statistics were calculated either including or excluding gaps.

Results

1. MN formation

There was no increase in MN formation in cells exposed to HFEMF at SAR from 5 to 50 W/kg. However, the frequency of MN formation in cells exposed to HFEMF at SAR of 100 and 200 W/kg was statistically significantly different to that observed following sham-exposure (Fig. 1). The frequency of MN formation following treatment with bleomycin alone was statistically higher, compared with the sham-exposed control (Fig. 1). Although there was no increase in MN formation in cells treated with a combination of bleomycin and HFEMF exposure at SAR from 5 to 100 W/kg, there was a statistically significant difference in MN formation between treatment with bleomycin alone and combined treatment with bleomycin and HFEMF exposure at a SAR of 200 W/kg.

The frequency of MN formation with heat treatment increased in a temperature-dependent manner. However, there was no difference between bleomycin-treated cells and cells treated with a combination of heat and bleomycin for temperatures from 38 to 41°C (data not shown).

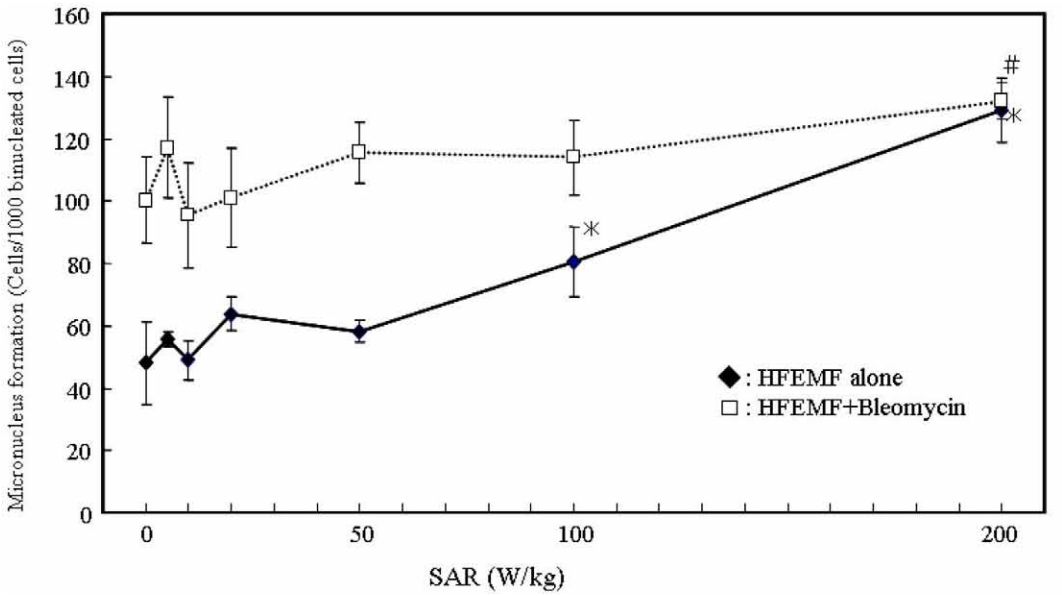


Figure 1. The frequency of MN formation in CHO-K1 cells exposed to HFEMF with or without bleomycin, compared to that following sham-exposure. The bars show standard deviations, based on three experiments. An asterisk indicates a statistically significant difference between sham- exposure and HFEMF exposure (p<0.01). A sharp indicates a statistically significant difference between treatment with bleomycin alone and combined treatment with HFEMF exposure and bleomycin (p<0.01).

2. DNA strand breaks

No significant difference in tail moment was seen for each exposure condition at SAR levels from 5 W/kg to 200 W/kg (Table 1).

Table 1 Comparison of Comet Parameters in MO54 Cells Exposed to 2.45GHz Continuous-Wave HFEMF, Sham and 100μg/mL bleomycin

Exposure Condition	Sham	5 W/kg	10 W/kg	20 W/kg	50 W/kg	100 W/kg	200 W/kg	Bleomycin
Tail Moment	406.6 ± 113.2	365.1 ± 13.9	425.1 ± 30.5	353.2 ± 44.0	372.3 ± 83.7	335.6 ± 53.9	432.6 ± 70.4	2071.9 ± 419.8*
Tail Length	54.7 ± 23.6	76.0 ± 8.5	80.3 ± 13.8	68.6 ± 25.4	61.2 ± 18.5	48.5 ± 3.9	53.9 ± 3.6	118.9 ± 41.1*
Tail Percent	24.5 ± 5.1	24.6 ± 1.1	25.2 ± 5.2	24.8 ± 0.8	24.3 ± 2.6	22.7 ± 3.2	25.0 ± 3.2	40.1 ± 9.7*

Data are presented as the mean ± standard deviation, based on three experiment.
The units of each parameter are Tail moment = arbitrary unit, Tail length – pixel, and Tail percent - %.
*Significantly different (at p<0.01) from Sham, HFEMF exposure and heat treatment groups.

No significant differences were observed in tail moment for each of the treatment conditions with sham and heating at 39 - 44°C. No cell killing was observed after the HFEMF exposure at the SARs of 5, 10, 20, 50 and 100 W/kg, while cell viability was slightly decreased at 200 W/kg (83.4 ± 4.9% (data not shown), No significant difference vs Control). No cell killing was also observed immediately after heat treatment at 39 and 41°C and the treatment with bleomycin. The cell viability at 44℃ was decreased (77.1 ± 2.5%, $p < 0.01$, Significantly different vs Control).

3. Chromosomal aberrations

A summary of chromosomal aberration data is showed in Table 2.

Table 2 Chromosomal aberration in m5S cells after treatment with HFEMF, MMC, or X-rays

Treatment	No. of cells analysed	Chromatid-type				Chromosome type				Aberrations/100 cells		%Aberrant Cells	
		ctg	csg	ctb	cte	Frag	Min	Dic	Ring	Total	Excl	Total	Excl
Sham	200	3	0	0	0	1	1	0	0	2.5	1	2.5	1
5 W/kg	200	2	0	2	0	0	0	0	0	2	1	2	1
10 W/kg	200	0	0	0	0	0	0	1	0	0.5	0.5	0.5	0.5
20 W/kg	200	1	0	0	0	0	0	0	0	0.5	0	0.5	0
50 W/kg	200	1	1	0	2	0	0	0	0	2	0.5	2	1
100 W/kg	200	1	0	1	1	0	2	0	0	2.5	1	2.5	2
MMC (0.1 μg/mL)	200	4	0	11	78	2	3	1	1	50	43.5	44.5	43.5
X-rays (3 Gy)	200	4	1	5	14	4	18	4	0	25	19	21.5	19

ctb= chromatid breaks, csg= isochromatid gaps, cte= chromatid exchanges.
Isochromatid breaks (csb) were included in acentric fragments (Frag).
Min=minute chromosomes, Dic dicentrics. Excl=excluding gaps.

The rate of incidence of chromosomal aberrations was less than 0.02. No differences were observed between control and HFEMF exposure. The frequency of chromosomal aberration appearance is less than 2.5% between 5 W/kg to 100 W/kg HFEMF exposures. In contrast, X-rays and MMC treatment resulted in chromosomal aberrations in 45% and 20% of the cells, respectively. Results obtained by chromatid and chromosome aberration analysis did not exhibit any statistically significant differences between sham control and HFEMF exposure conditions from 5 W/kg to 100 W/kg. As expected, MMC and X-ray treatment significantly increased ($p < 0.001$) the frequency of chromosomal aberration, chromatid aberration and total chromosomal aberration compared with sham controls.

Conclusions

In conclusion, HFEMF exposure at 2.45 GHz for 2 h up to SAR of 50 W/kg does not induce MN formation. We did not detect the increase in DNA strand breaks and chromosomal aberrations, even at 100 W/kg. For the MN formation, there were statistically significant increases at SARs of 100 and 200 W/kg, compared with the sham-exposed control. However, we also observed that the temperature elevation induced the increased MN formation. Although more research is required, the present study has shown that MN formation at SAR from 5-200 W/kg is connected to temperature raise caused by HFEMF.

In addition, we have reported the effect of HFEMF on cell growth rate, cell cycle distribution, Transformation, and heat-shock protein (hsp) expression. Cell growth rate and cell cycle distribution were not affected by exposure to HFEMF at SAR of lower than 100 W/kg for 2 h [27], No significant differences were observed in the malignant transformation (Type II + Type III) frequency between the sham-control and the HFEMF at SARs of 5 to 200 W/kg for 2 h [28]. The expression of hsp70 increased in a time and dose-dependent manner at SAR of over 50 W/kg for 1-3 h [29]. However, a similar effect was also observed in corresponding heat controls.

From these results, we considered that HFEMF exposure at 2.45 GHz for 2 h did not affect cell growth, cellular genotoxicity, cell transformation, and hsp70 expression, even at exposure level of 5 to 50 W/kg. Therefore, we can conclude that our investigations have indicate the absence of any relationship between

exposure to the HFEMF at an environmental level and adverse health effect. However, experiments should still be performed to evaluate the safety of the HFEMF exposures.

Acknowledgments

We thank Drs. M. Taki and Y. Suzuki (Tokyo Metropolitan University, Japan) for the supply of HFEMF exposure system. This work was supported in part by the committee to Promote Research on the Possible Biological Effects of Electromagnetic Fields, Ministry of Public Management, Ministry of Internal Affairs and Communications, Japan.

References

1. R Glaser (1992) Current concepts of the interaction of weak electromagnetiv fields with cells. Bioelectrochemistry and Bioenergetics, 27: 255-268.
2. PS Liburdy (1992) Calcium signaling in lymphocytes and ELF fields: evidence for an electric field metric and a site of interaction involving calcium ion channels. FEBS Lett., 301: 53-59.
3. PS Barnes (1996) Effect of electromagnetic field on the rate of chemical reactions. Biophysics., 41: 801-807.
4. L Hardell, A Nasman, A Pahlson, A Hallquist and K Hansson Mild (1999) Use of cellular telephones and the risk for brain tumours: a case-control study. Int J Oncol., 15: 113-116.
5. A Ahlbom, A Green, L Kheifets, D Savitz and A Swerdlow (2004) International Committee for Non-Ionizing Radiation Protection (ICNIRP) Standing Committee on Epidemiology. Epidemiology of health effects of raiofrequency exposure. Environ Health Perspect, 112: 1741-1754 .
6. A Lahkola K Tokola and A Auvinen (2006) Meta-analysis of mobile phone use and intracranial tumors. Scand J Woork Environ Health, 32: 171-177.
7. JA D'Andrea, ER Adair and JO de Lorge (2003) Behavioral and cognitive effects of microwave exposure. Bioelectromagnetics, 6: S39-S62.
8. LN Heynick, SA Johnston and PA Mason (2003) Radio frequency electromagnetic fields. Cancer, mutagenesis, and genotoxicity. Bioelectromagnetics, 6: S74-S100.
9. H Lai and NP Singh (1995) Acute low-intensity microwave exposure increases DNA single-strand breaks in rat brain cells. Bioelectromagneitcs, 16: 207-210.
10. Vijayalaxmi, KS Bisht, WF Pickard, ML Meltz, JL Roti Roti and EG Moros (2001) Links chromosome damage and micronucleus formation in human blood lymphocytes exposed in vitro to radiofrequency radiation at a cellular telephone frequency (847.74 MHz, CDMA). Radiat Res., 156: 430-432.
11. P Gos, B Eicher, J Kohli and WE Heyer (2000) No mutagenic or recombinogenic effects of mobile phone fields at 900 MHz detected in the yeast Saccharomyces cerevisiae. Bioelectromagnetics, 21: 515-523.
12. JL Riti Roti, RS Malyapa, KS Bisht, EW Ahern, EG Moros, WF Pickard and WL Straube (2001) Neoplastic transformation in C3H 10T(1/2) cells after exposure to 835.62 MHz FDMA and 847.74 MHz CDMA radiations. Radiat Res., 155: 239-247.
13. D Leszczynski, S Joenvaara, Reivinen and R Kuokka (2002) Non-thermal activation of the hsp27/p38MAPK stress pathway by mobile phone radiation in human endothelial cells: molecular mechanisim for cancer- and blood-brain barrier-related effects. Dfferentiation, 70: 120-129.
14. F Tian, T Nakahara, K Wake, M Taki and J Miyakoshi (2002) Exposure to 2.45 GHz electromagnetic fields induces hsp70 at a high SAR of more than 20 W/kg but not at 5W/kg in human glioma MO54 cells. Int J Radiat Biol., 78: 433-40.
15. J Miyakoshi, M Yoshida, Y Tarusawa, T Nojima, K Wake and M Taki (2002) Effects of High-Frequency Electromagnetic fields on DNA strand breaks using comet assay method. Elecrical Engineering in Japan, 141: 9-15.
16. GM Van Leeuwen, AN Kotte, BW Raaymakers and JJ Lagendijk (2000) Temperature simulations in tissue with a realistic computer generated vessel network. Phys. Med. Biol., 45: 1035-1049.
17. R Gudi, SS Sandhu, and RS Athwal, (1990) Kinetochore identification in micronuclei in mouse bone-marrow erythrocytes: an assay for the detection of aneuplodity-inducing agents. Mutat. Res., 234: 263-268.
18. GM Krishna, R Fiedler and JC Theiss (1992) Simultaneous evaluation of clastogenicity, aneugenicity and toxicity in the mouse micronucleus assay using immunofluorescence. Mutat. Res., 282: 159-167.
19. M Fenech and AA Morley (1989) Kinetochore detection in micronuclei: an alternative method for measuring chromosome loss. Mutagenesis, 4: 98-104.
20. PI Coutryman and JA Heddle (1976) The production of micronuclei from chromosome aberrations in irradiated cultures of human lymphocytes. Mutat. Res., 41: 321-332.

21. S Koyama, Y Isozumi, Y Suzuki, M Taki and J Miyakoshi (2004) Effects of 2.45 GHz electromagnetic fields with a wide range of SARs on micronucleus formation in CHO-K1 cells, Scientific World Journal, 4: 29-40.
22. Y Komatsubara, H Hirose, T Sakurai, S Koyama, Y Suzuki, M Taki and J Miyakoshi (2005) Effect of 2.45GHz electromagnetic fields with a wide range of SARs on DNA damage in MO54 cells. European Biology and Bioelectromagnetics, 1: 148-170
23. Y Komatsubara, H Hirose, T Sakurai, S Koyama, Y Suzuki, M Taki and J Miyakoshi (2005) Effect of high-frequency electromagnetic fields with a wide range of SARs on chromosomal aberrations in murine m5S cells. Mutat. Res., 587: 114-119
24. MS Sasaki and S Kodama (1987) Establishment and some mutational characteristics of 3T3-like near-diplold mouse cell line, J. Cell Phys., 131: 114-122.
25. J Miyakoshi, M Yoshida, K Shibuya and M Hiraoka (2000) Exposure to strong magnetic fields at power frequency potentiates X-ray-induced DNA strand breaks. J. Radiat. Res., 41: 293-302.
26. PL Olive, D Wlodek, RE Durand and JP Banath (1992) Factors influencing DNA migration from individual cells subjected to gel electrophoresis. Exp vell Res., 198: 259-267.
27. Y Takashima, H Hirose, S Koyama, Y Suzuki, M Taki and J Miyakoshi (2006) Effects of continuous and intermittent exposure to RF-fields with a wide range of SARs on cell growth, survival and cell cycle distribution. Bioelectromagnetics, 27: 392-400.
28. J Wang, T Sakurai, S Koyama, Y Komatubara, Y Suzuki, M Taki and J Miyakoshi (2005) Effects of 2450 MHz Electromagnetic fields with a Wide Range of SARs on Methylcholanthrene-induced Transformation in C3H10T1/2 Cells. J. Radiat. Res., 46: 351-361
29. J Wang, S Koyama, Y Komatubara, Y Suzuki, M Taki and J Miyakoshi (2006) Effect of a 2450 MHz high-frequency electromagnetic field with a wide range of SARs on the induction of heat-shock proteins in A172 cells. Bioelectromagnetics, *(in press)*.

ELECTROMAGNETIC RADIATION EFFECTS ON ELECTRONIC PARTICLES TRANSFER IN DNA – APPLICATIONS TO MILLIMETER AND OPTICAL RANGES

Gérard DUBOST
Institut d'Electronique et de Télécommunications de Rennes
UMR CNRS 6164, Université de Rennes 1,
Avenue du Général Leclerc, Campus de Beaulieu, 35042 – Rennes Cedex – France

André BELLOSSI
Villa Gabrielle, Chemin du Goh Vras, 56730 – Saint Gildas de Rhuys – France

ABSTRACT

We justify the validity of the biexponential Debye relaxation model of the pure water extrapolated until the optical range by means of experiments results obtained on the human skin. The pure water attenuation per wavelength is maximum in the millimeter-wave range. We confirm the measurements which have shown appreciable AC conductivity of DNA due to relaxation losses of their surrounding water dipoles. We extend this property to the UV range showing the action of photons upon free electrons. Excited ions, by means of our external plasma device generator of solitary-waves is the object of photon emissions in the optical range. In particular in UV range the free electron alone is liable to be propeled by a photon with a kinetic energy with a some idea of the size to 10^{-23} Joules. In a large range until millimeter waves, the excited ions can attract electrons showing a kinetic energy of 10^{-21} Joules. They can be used to activate control and explain the division of fibroblasts and the cancer mechanisms of human skin, the main modification of DNA molecules by UV radiation being the formation of pyrimidine dimers. Finally we can conclude that the molecule of DNA has a conducting which is always increasing with the frequency, but can be considered as a real conductor only in the millimeter-wave range with an important absorption per wavelength. The "conduction quality" is the ratio of the conduction to the displacement currents.

INTRODUCTION

PRELIMINARY CLARIFICATION

The electronic conduction in DNA is a polemic subject always going on nowadays. Is DNA conductive or not ? DNA has been reported to be a metal, a semiconductor, an insulator and even a proximity effect induced superconductor. Above all it was advisable to go back to some reminders. In a recent paper [1] it as been shown that appreciable AC conductivity of DNA, measured in the millimeter wave range, is largely ascribed to relaxational losses of the surrounding water dipoles. So it was necessary from the theoretical complex dielectric constant $\tilde{\varepsilon}_r = \varepsilon_r - j\sigma/\omega\varepsilon_o$ of bulk pure water, described by a biexponential Debye relaxation model [2], to calculate its conductivity σ, and the coefficient of absorption A given by the classical expression :

$$A\ (\text{Neper}/\lambda_o) = 2\pi\left[-\frac{\varepsilon_r}{2}+\frac{1}{2}\sqrt{\varepsilon_r^2+(\sigma/\omega\varepsilon_o)^2}\right]^{1/2} = \frac{\lambda_o}{\delta} \quad (1)$$

δ is the thickness penetration and λ_o the free space wavelength.

We introduced the "conduction quality" C_p which is the ratio of the conduction to the displacement currents equal to : $C_p = \sigma / 2\pi f\, \varepsilon_o\, \varepsilon_r$ (2)

The **Table I** shows the various parameters in terms of the frequency for the pure water at 20 °C. We can conclude :

a) The conductivity σ is increasing with the frequency.
b) The absorption coefficient $A(N/\lambda_o)$ has a maximum in the millimeter range (N means Nepers : 1N = 8.69 dB).
c) The absorption per unit of length (dB/mm) is increasing with the frequency.
d) In the millimeter wave range the water can be considered as a "conductive medium" (C_p >1), and as an insulator medium (C_p <1) when f < 2.10^{10} Hz or f > 2.10^{11} Hz. Nevertheless its conductivity σ is always increasing with the frequency.
e) We can justify the values of the conductivity and the absorption in the UV range deduced from the experiments realized on the epidermis. The epidermis is composed, from the skin surface to the depth, by the stratum corneum, the stratum granulosum, the stratum spinosum and the stratum basale. Due to the water content of the cells we can put together the three later layers ; we call them mucus body.

The **Table II** shows the values extracted from measurements upon the human skin which must be compared with these given in **Table I**.
The range UV is separated into two ranges : UVA and UVB. For each of them, and from the measured transmission coefficient [18], we deduced the conductivity σ and the absorption related to the stratum corneum and the mucus body. We note that the bulk water theoretical conductivity is comprised between those of the stratum corneum and mucus body.

f(Hz)	λ_o	(2) C_p	$\sigma(S/m)$	(1) δ	v_p/c	ε_r	(1) $A(N/\lambda_o)$	A(dB/mm)
10^9	300 mm	0.05	0.22	0.21 m	0.11	80.0	1.4	0.04
5.10^9	60 mm	0.25	5.2	9 mm	0.11	75.2	6.7	0.97
10^{10}	30 mm	0.49	17.3	2.5 mm	0.12	63.6	12.0	3.5
2.10^{10}	15 mm	0.93	41.6	0.9 mm	0.145	40.2	17.1	9.9
5.10^{10}	6 mm	1.72	68.7	360 µm	0.22	14.4	16.7	24
7.10^{10}	4.3 mm	1.85	73.3	290 µm	0.25	10.2	14.9	30
10^{11}	3.0 mm	1.79	76.5	250 µm	0.29	7.7	12.0	35
5.10^{11}	600 µm	0.74	99.7	125 µm	0.43	4.9	4.8	70
10^{12}	300 µm	0.54	131	86 µm	0.47	4.2	3.5	100
5.10^{12}	60 µm	0.18	172	57 µm	0.54	3.4	1.06	150
10^{13}	30 µm	0.10	176	38 µm	0.55	3.3	0.80	230
10^{14}	3 µm	10^{-2}	177	38 µm	0.55	3.3	0.08	230
10^{15}	0.3 µm	10^{-3}	177	38 µm	0.55	3.3	0.008	230

Table I : Electrical parameters of pure bulk water at 20 °C in terms of frequency

Range (μm)	λ_m (μm) (mean)	Mean Transmission T [18]	T_{SC} (dB)	T_{MB} (dB)	A(dB/mm)	σ(S/m)	
UVA (0.315 – 0.390)	0.352	4.6 % - 13.4 dB	-9	-4.4	529 67	588 74	SC MB
UVB (0.280 – 0.315)	0.298	0.9 % - 20 dB	-14	-6	823 92	914 102	SC MB
UV (0.280 – 0.390)	0.335	3.5 % - 14.6 dB	-10	-4.6	588 70	653 78	SC MB

Table II (valid for $\varepsilon_r = 3.3$ and $\sigma/\omega\varepsilon_o << \varepsilon_r$)

SC : Stratum corneum : thickness : 17 μm Transmission : T_{SC}

MB : Mucus body thickness : 65 μm Transmission : T_{MB}

$$\text{With : } T = T_{SC} + T_{MB} \quad \text{and} \quad \sigma(S/m) = \frac{A(dB/mm)}{0.9}$$

CHARGE TRANSPORT IN SYNTHETIC DNA

The denaturation of the DNA is due to the breaking of the hydrogen bonds, which keep in position the two strands (fig. 1).
In the course of the DNA duplication, two complementary strands give birth to two new DNA molecules. The DNA macromolecule structure was introduced in 1953 by Watson and Crick.

Electronic transport along DNA is crucial for the repair mechanism after radiation damage and biosynthesis [3]. In 1989 Peyrard-Bishop study the structure by means of global energies expressed with a Lagrangian.

The various parameters used are :

- the relative displacements of the nucleotidic bases at different sites of each DNA strand,
- the equivalent mass m of a nucleotide pair equal to 300 amu ($m = 5.10^{-25}$ Kg),
- the Morse potential which is the energy of a hydrogen bond between a pair of nucleotides,
- the average of the energy values for the guanine-cytosine basis (G-C) and for the thymine-adenine basis (A-T), which is called the well depth or Morse depth. It corresponds to the dissociation energy of a base pair and is equal do D = 0.04 eV let us be $0.64\ 10^{-20}$ J,
- the width of the well equal to : w = 0.224 Å,
- the stacking energy between neighboring bonds,
- the energy of the dipole-dipole interaction,
- the dipole parameter expressed in terms of electric charge transfer and of the distance between neighboring base pairs,
- the potential energy between two consecutives bases along a strand V_o = 0.1eV in an equilibrum state,
- the linear frequency of the isolated oscillator which is equal to :

$$f_o = (1/2\pi)\left(2D/mw^2\right)^{1/2} = 1.14\,10^{12} \text{ Hertz} \qquad (3)$$

One considers the radial displacement of the base unit and the angular rotation between two adjacent base pairs from their equilibrium state. The lattice oscillations are designed by pulsation Ω_r for the radial displacement and Ω_p for the twist one.

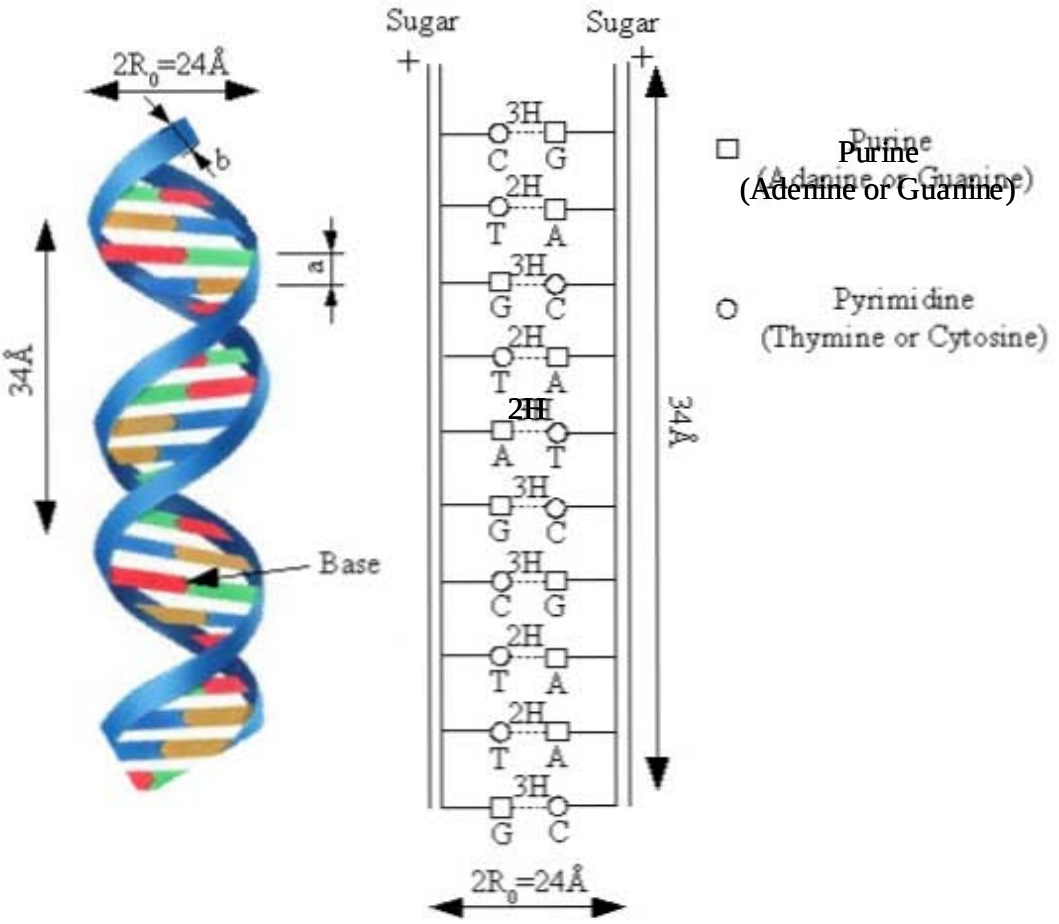


Fig. 1.

The adiabaticity parameter $(h/2\pi)(\Omega_r / V_o)$ (4) equal to : 0.041 proves the adiabatic right hypothesis during a quasi instantaneous displacements. From the fixed parameters at an equilibrium state : a = 3.4 Å, $\theta_o = 36°$, $R_o = 12$ Å, we deduced the distance ℓ_o between two consecutive bases along a strand :

$$\ell_o = \sqrt{a^2 + 4R_o^2 \sin^2(\theta_o/2)} = 8.16 \text{ Å}$$

The potential energy V_o is equal to :

$$V_o = p_o.q \ / \ 4\pi\varepsilon_o \ell_o^2 \qquad (5)$$

where p_o is the moment of the charge. With $V_o = 0.1\text{eV}$ we deduced : $q.p_o = 1.18\,10^{-48}$. Taking $p_o = q.1$ Å, gives : $q = 1.08\,10^{-19}$C which is approximately the electron charge. The mobility of the charge is possible in the presence of random parametrical and structural disorders inherent to DNA molecules [3].

Recently some authors [4] have considered the charge q when hydrogen bonds stretch using quantum chemical methods taking into account the nucleoside pairs (sugar linked to base). The value of the dipole parameter $J = q^2 \ / \ 4\pi\varepsilon_o a^3$ (6) is equal to : $3.3\,10^{-3}\text{eV}/\text{Å}^2$ let us be $0.053\,\text{J}/\text{m}^2$ with q = - 0.095 e, which is the charge transfer intermediate between the A-T and G-C base pairs [1].

The stacking parameter is given by some authors [5] equal to 0.96 J/m^2 (let us be 0.06 eV/ Å^2), and by others [6] comprised between 0.01 and 10 eV/ Å^2. It has been then considered as adjustable parameter [4]. In short we can report according [4] that solitons or "discrete breathers" can be also generated from or exist among random thermal fluctuations. Moving breathers with speed comprised between 4 and 24 m/s, behave as quasiparticles, having an effective mass between 30 and 46 amu and a kinetic energy comprised between $6.5\,10^{-25}$J and

2.10^{-23}J, which is able to pass over a bending point in function of the strand curvature. For T = 310° K the thermal energy is $KT = 4.310^{-21}$J or 2.710^{-2}eV. The conduction mechanism in DNA was recently studied [7], showing the impact of disorder. Evidently the charge motion is influenced by the vibrational modes of the double helix. Results concerning the electron transport in synthetic DNA polymers had been recently published [8]. For many organs we know that beyond a frequency of 2.10^{10} Hertz, the conductivity trends upward very quickly [Gabriel King's College, London, June 1996]. To establish the theory of the cell division Popp [8] supposed a high conductivity for the cell membrane without indication of its value. Albrecht-Buehler [9] thinks that centriolar "blades" have a high conductivity. Centrosome is an intracellular organelle composed of 2 centrioles and pericentriolar material. The centrioles are a pair of cylinder-like structures. (0.8 × 0.15 µm) often disposed in an orthogonal way to each other. Each centriole is composed of 9 separate protofilaments (0.8 µm × 40 nm). Electrons of very low energies can induce substantial yields of single and double strand breaks of DNA in near infrared spectrum [10] and [11]. To be in a good agreement with numerous experimental results in near infrared, visible and near ultraviolet spectra we must choose a conductivity of 10^5S/m for the membrane medium [12].

The figure 2 gives the theoretical velocity v of the moving electron along the DNA chain, as a function of the amplitude E_o of the periodic field parallel to the double helix axis, for different frequencies in the millimeter wave ranges. It is taken out from [3] but expressed now with more convenient parameters. The normalized frequency given in [4] is related to the frequency f_o (3), with D = 0.04 eV, w= 0.224Å and $m = 5.10^{-25}$Kg. Coherent electron transfer can be stimulated when the frequency of the applied field is such that : $10^{11} < f < 3.10^{12}$ Hz .To be efficient the applied external electric energy $eE_o\ell_o$ has to be higher than V_o let us be : $E_o\ell_o > 0.1V$ with $\ell_o = 8.16$ Å that is $E_o > 10^8$ V/m.

Moreover the electron kinetic energy comprised between 4.10^{-26} and , 610^{-26}J, is very weak compared with the thermal fluctuation kT.

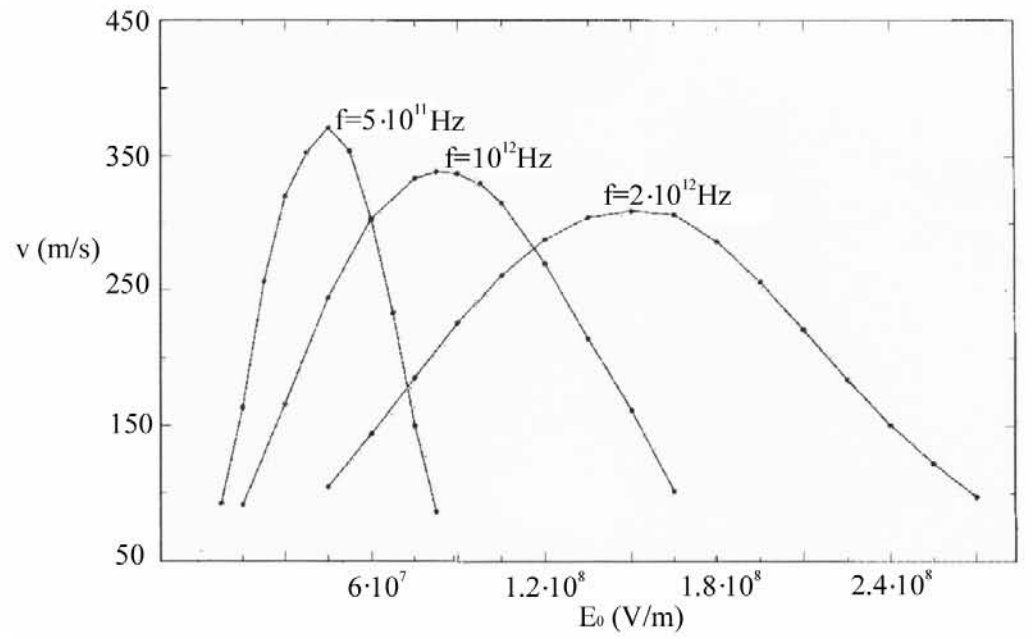


Fig. 2

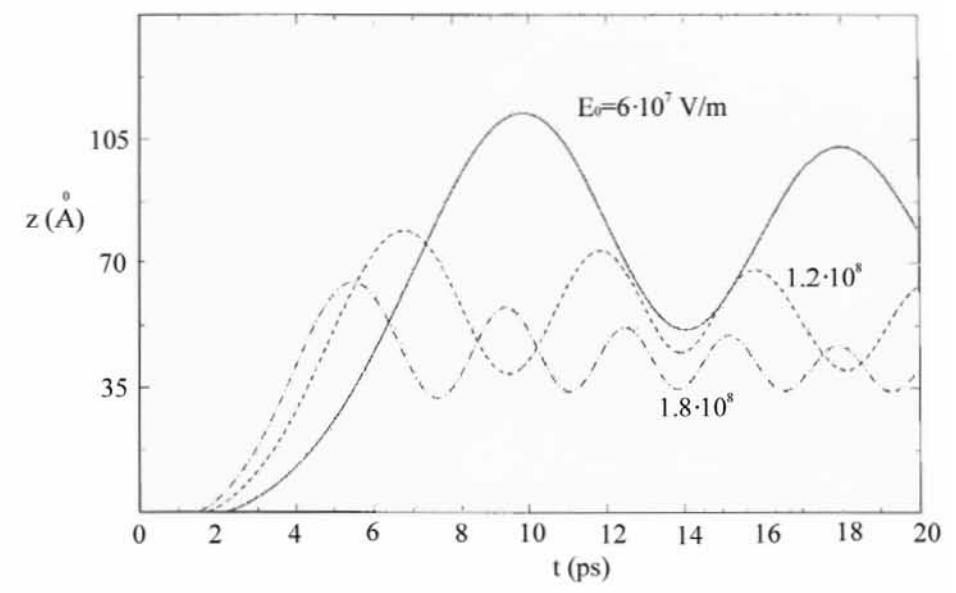


Fig. 3 : Temporal electronic occupation probability

The figure 3 shows the temporal behavior of the electronic occupation probability of the electron along the DNA axis in the presence of the external field at $f = 10^{11}$ Hz for different amplitudes E_o and a disorder of 0.02 eV. The position $z(\text{Å})$ corresponds to the electronic occupation probability after a propagation from a starting one for t = 0. When the field amplitude is enlarged the dynamic of the electron and the amplitude of the oscillations become weaker. The oscillation frequencies f_{osc} are higher than the electronic one equal to 10^{11} Hz as indicated in Table III.

$E_o\,(V/m)$	6.10^7	$1.2\,10^8$	$1.8\,10^8$
f_{osc} (Hertz)	$1.25\,10^{11}$	2.10^{11}	$2.8\,10^{11}$

Table III (valid for $f = 10^{11}$ Hz)

Whatever E_o, the maximum velocity v_M at $f = 10^{11}$Hz is equal to $2.3\,10^3\,m/s$. All these results, valid for a relative strong disorder ΔE on site electronic energy equal to 0.02 eV, are due to the nonlinear physics applied to DNA.

COMPARISON BETWEEN THEORY AND EXPERIMENTS IN MILLIMETER RANGE

AC conducting DNA in the millimeter range has been measured. Several authors have shown an appreciable conducting which approaches that of a well-doped semiconductor. Nevertheless it has been found that the high AC conductivity of DNA can be attributed largely to relaxational losses of the dipoles of the water molecules in surrounding hydratation layers [1]. The total number of water molecules per nucleotide has to be correlated with the relative humidity [13]. For instance the adsorption of water molecules per nucleotide is equal to 13 for a rate of humidity (R.H) equal to 84 % and 4 for a R.H of 60 %. For an R.H of 0 %, there are 2.5-3 water molecules

per nucleotide which cannot be removed from the helix. The table IV shows the AC conductivity of calf thymus DNA measured in terms of the frequency [1].

f(Hz)		10^{11}	$2\,10^{11}$	$5\,10^{11}$	10^{12}
RH : 0 % σ (S/m) [1]		1	12	35	100
RH : 84%	σ(S/m) [1]	25	50	70	110
	A(N/λ_o) (1)	4.9	5.4	3.5	3.0
	C_p (2)	0.60	0.75	0.40	0.50

Table IV : conductivity σ measurements of calf thymus DNA

The conductivity σ, which is increasing with the frequency and the rate of humidity, can be attributed largely to the water layer surrounding the DNA blackbone. In effect, for a R.H equal to 84 % the absorption A(N/λ_o) and C_p were calculated with the relations (1) and (2) using the experimental conducting σ [1] and ε_r given in **Table I**. The experimental values σ [1] and the deduced absorption A(N/λ_o) shown in **Table IV** are normally as should be weaker than these shown in **Table I** valid for the bulk pure water. The measured conductivities of the single and double strands have been found identical [1]. Considering the weak values of C_p we can say that the DNA can be reported to a dielectric medium in spite of its important conductivity. Previously reported conductivity value of 240 S/m was evaluated from the measured loss of highly sensitive resonant cavities operating at 12 and 100 GHz [14].

SOLITARY-WAVE EMISSIONS

The emission are due to solitary-waves or solitons issued from an external confined plasma device [15]. The induced emission lifetime of the ion in vivo medium is given [17] :

$$\tau_B = \frac{78}{\pi^2}.\left(\frac{c}{f_r}\right)^3.\frac{h^2}{Z^2}.\sqrt{\frac{\varepsilon_o}{\mu_o}}.\frac{\varepsilon_o}{P_t^2}\left[2\pi e(\Delta n_i)V_p\frac{L}{r}\right]^{-2}.|\tilde{n}|^2 \qquad (7)$$

$\tilde{n}$ is the mean complex, index of refraction at f_r in the vivo medium.
The parameters inserted between brackets are related to the plasma device.
P_t is the electric moment of the dipolar transition. Z is the atomic number of the ion. f_r is the square signal modulation frequency of a high RF frequency used to light the discharge inside the plasma tube. The density of the ions at the fundamental state in a strong electrolyte, equivalent to the interstitial liquid, which has been carried is equal to : $N_1 = 1.85\,10^{26}/m^3$: [16].
From [17] we deduced in the vivo medium :

$$N_2 = N_1\,3.7\,10^{16}\left(\frac{f_r}{\nu}\right)^3.\frac{1}{|\tilde{n}|^2} \qquad (8) \qquad\qquad \tau_B = 4.10^{20}\,f_r^{-3}.|\tilde{n}|^2 \qquad (9)$$

N_2 is the density of excited ions per unit of volume and ν the frequency of their photonic emission. From N_2 we deduced the mean distance between sollicitaded ions by the expression : $d = (N_2)^{-1/3}$ (10)

We showed that a low frequency f_r acting upon ion produce an ionizing radiation in the optical range [17]. The **Table V** shows the calculated values related to the ion induced emissions in terms of the free wavelengths for a higher modulation frequency f_r and a weak lifetime.

λ_o	0.25 µm	1µm	10 µm	100 µm	1 mm	1.78 mm
d	16 µm	4 µm	0.4 µm	400 Å	40 Å	22 Å
$n = N_2 / N_1$	$1.3\,10^{-12}$	$8.8\,10^{-11}$	$8.8\,10^{-8}$	$8.8\,10^{-5}$	$8.8\,10^{-2}$	0.5
N_2 / m^3	$2.4\,10^{14}$	$1.6\,10^{16}$	$1.6\,10^{19}$	$1.6\,10^{22}$	$1.6\,10^{25}$	$9.2\,10^{25}$
ν(Hz)	$1.2\,10^{15}$	3.10^{14}	3.10^{13}	3.10^{12}	3.10^{11}	$1.69\,10^{11}$
$W = h\nu$ (J)	8.10^{-19}	2.10^{-19}	2.10^{-20}	210^{-21}	2.10^{-22}	$1.1\,10^{-22}$
d / λ_o	64	4	0.04	4.10^{-4}	4.10^{-6}	$1.2\,10^{-6}$

Table V : Ion induced emission

valid for $f_r = 4.10^6$ Hz, $\tau_B = 6.10^3$ s (9), $N_1 = 1.85\,10^{26} / m^3$, $|\tilde{n}|^2 = 10^3$,

When the wavelength is enlarged the mean distance d between the sollicited ions and the energy of the quantic oscillator W are decreasing, while their density N_2 increases. We have shown in [17] that when $d / \lambda_o < 1/\pi$ two adjacent dipoles have a strong mutual coupling such that the radiation of the array due to the whole excited ions was suppressed. Nevertheless the electric field amplitude E_o due to one ion is given by :

$$E_o = P_t / 4\pi\varepsilon_o r^3 \qquad (11)$$

P_t is the electric moment of the dipolar transition approximately equal to :

$$P_t = e.1\,Å = 1.6\ 10^{-29}\ (C.m)$$

For r = 10Å, we obtain from (11) : $E_o = 1.4\,10^8$ V / m . Let us consider the electrostatic attraction of an electron by the ion when the viscosity strength is taken into account. We calculate for r = 10 Å a speed of $5.510^4 m/s$, that is a kinetic energy equal to 10^{-2} eV. Let be a free electron motionless knocked by a photon of $W = h\nu$ energy. We suppose a perfectly elastic shock. Before and after the shock the whole impulse is unchanged. If we neglect the Compton effect, that is the frequency variation of the photon, we can write :

$$\frac{2h\nu}{c} = m_e v_e \qquad (12),$$

With : $h\nu = 5.1\,eV$, $m_e = 0.91\,10^{-30}$ Kg, we deduced from (12) the electron speed : $v_e = 6.10^3 m/s$. So the electron kinetic energy is equal to : 1.610^{-23} J, that is 10^{-4} eV. The photon which is associated with an electromagnetic wave is moving along the DNA with a speed equal to : $v_p = 1.65\,10^8$ m / s (see Table I). The photon can be also absorbed by the particle. Then the photo-ionization principle may give birth to an electron, with an energy higher than 10^{-4} e V .

SUMMARY

a) We introduced the ratio of the conduction to the displacement currents to express the conduction quality C_p (2) of a medium. Thus the pure water has a conduction σ which is always increasing all along the frequency range, while the conduction quality C_p is the highest in the millimeter wave range (**Table I**).

b) We justify the validity of the biexponential Debye relaxation model of the pure water extrapolated until the U.V range, by means of experimental results obtained on the human skin.

c) **Table I** shows the attenuation per wavelength which is maximum in the millimeter-wave range. Recent measurements in that range have shown appreciable AC conductivity of DNA which is largely ascribed to relaxational losses of the surrounding water dipoles [1]. We have extended this property to the UV range **(Table II),** showing further the action of photons upon free electrons.

d) Excited ions, by means of our external plasma device generator of solitary waves, is the object of photon emissions where an example is given in the Table V. An electron can be shocked by a photon in UV, showing a kinetic energy equal to 10^{-4} eV. What's more by means of the electrostatic attraction of one ion, an electron can show a kinetic energy equal to 10^{-2} eV. They can be used to activate, control and explain the division of fibroblasts and the cancer mechanisms of human skin, the main modification of DNA molecules by U.V radiation being the formation of pyrimidine dimers [11].

REFERENCES

[1] **M. BRIMAN, N.P. ARMITAGE et all**, *Dipole relaxation losses in DNA*. Depart. of Physics and Astronomy, University of California, Los Angeles, CA 90095, 8 Nov. 2005.

[2] **C. RONNE et al**, J. Chem. Phys. 107, 5319 (1997).

[3] **D. HENNING, J.F.R. ARCHILLA** , *Polaronic charge transport mecanism in DNA*. Elsevier Preprint, May 18, 2005.

[4] **J. CUEVAS, E.B. STARICOV et all**, *Moving breathers in bent DNA with realistic parameters* ar Xiv : nlin.PS/0404029V3,4, Nov. 2004.

[5] **T. DAUXOIS, M. PEYRARD, A.R. BISHOP**, Phys. Rev. E 47, 684 (1993).

[6] **J. CUEVAS, J.F.R. ARCHILLA et all,** *Moving breathers in a DNA with competing short and long-range dispersive interactions*, Physica D 163 : 106, 2002.

[7] **P. CARPENA, P. BERNAOLA-GALVAN et all**, Nature 418, 955 (2002).

[8] **F.A. POPP,** *Basic theory of cancer development and defense*, Intern. Conf. Biological Cancer Defense in Heidelberg, May 3-5, 2002.

[9] **G. ALBERCHT BUEHLER,** *Altered drug resistance of microtubules in cells exposed to infrared light pulses*. Cell mobility and cytoskeleton, 1998, vol. 40, pp. 183-192.

[10] **A. BOUDAFFA, P. CLOUTIER et all**, *Resonant formation of DNA strands breaks by low energy electrons*, Science 3 March, 2000, vol. 287.

[11] **J. HUGO, NIGGLI**, *Ultra weak photon emission in differentiated fibroblasts.* Conference on biophotons, 1999.

[12] **G. DUBOST, A. BELLOSSI**, *Cell membrane physical model in near infrared, visible, and near ultraviolet spectra*. Biological Effects of EMFS, 3rd Intern. Workshop Kos, Greece, 4-8 October, 2004, p. 492 to 500.

[13] **S. BRAUNAUER, P. EMMETT et all**, J. Am. Chem. Soc., 80, 309 (1938).

[14] **K.H. YOO, D.H. HA et all**, Phys. Rev. Lett. 87, 198102 (2001).

[15] **G. DUBOST, A. BELLOSSI, J. BARE**, *Efficiency of solitary-waves radiated by the discharge in a confined plasma column*. Biological Effects of EMFS, 3rd Intern. Workshop Kos, Greece, 2004, p.473 to 481.

[16] **G. DUBOST, A. BELLOSSI**, *Electromagnetic field diffracted by a nervous fiber excited by an external electric field.* Biological Effects of EMFS, 3rd Intern. Workshop Kos, Greece, 2004, p. 482 to 491.

[17] **G. DUBOST, A. BELLOSSI, J. BARE**, *Solitary waves effects on Ions Emissions in the living matter.* MMS Proceedings : MSA6, pp. 210-215, sept. 6-8, 2005, Athens, Greece.

[18] **K. HOFFMANN, K. KASPAR, P. ALTMEYER, T. GAMBICHLER**, *UV Transmission Measurements of Small Skin Specimens with Special Quartz Cuvettes*. Dermatology 2000; 201; 307-311, Ruhr University, Bochum, Germany.

PARAMETERIZATION OF ALTERED HUMAN ERYTHROCYTE SHAPES. APPLICATION TO THE CALCULATION OF THE INDUCED TMP AND STRESS FORCES

J.L. SEBASTIÁN

S. MUÑOZ

M. SANCHO

J.M. MIRANDA

DPT. DE FÍSICA APLICADA III, FACULTAD DE CIENCIAS FÍSICAS
UNIVERSIDAD COMPLUTENSE, 28040 MADRID, SPAIN

Abstract
Simple parametric equations are presented in terms of Jacobi elliptic functions that provide a realistic model of abnormal variations in size which maintain the biconcave shape of a normal erythrocyte (anisocytosis), and abnormal variations in shape which maintain the original volume of the erythrocyte (poikilocytosis), as well as continuous deformations from the normal to the altered shapes. We illustrate our results with parameterizations of spherocytes, ellipsoids, microcytes, macrocytes and stomatocytes, and apply these parameterizations to the numerical calculation of the induced transmembrane potential in stomatocytes and the induced electric stress on the membrane of erythrocytes when both cells are exposed to an external electromagnetic field of 1800 MHz.

Introduction
Erythrocytes are the most numerous cells in the blood and their complete characterization has attracted much effort. In particular it has been known experimentally for more than fifty years that a variety of agents can modify systematically and reversibly the normal erythrocyte shape and size [Ponder 1948]. From a biophysical point of view changes in shape have been related to different mechanisms, such as variations of the membrane potential and temperature [Glaser 1979], to anion-exchange protein band 3 [Wong 1994, Gimsa 1998] or to the influence of the cytoplasmatic pH [Gedde et al. 1995]. From a complementary point of view, the increasing use of numerical techniques in the calculation of multiple-cell phenomena has prompted the development of realistic mathematical models for the shape of normal erythrocytes [Gray 1998, Bloor and Wilson 2000, Oroz 2004]. In fact, we have shown in previous work the crucial role played by an accurate geometry of the cell in the study of the response of normal erythrocytes to electromagnetic fields [Sebastian et al. 2001, 2004, Muñoz et al. 2003]. However, we are not aware of any simple geometrical model for altered erythrocyte shapes.

In this paper we address the modeling of abnormal variations in size which maintain the basic biconcave shape of the normal erythrocyte (anisocytosis), and abnormal variations in shape which maintain the original volume of the erythrocyte (poikilocytosis).

Anisocytosis is the generic term used to describe an abnormally wide distribution of the sizes of the erythrocytes in the blood, be it due to the presence of young red blood cells such as macrocytes which are larger than mature normal red blood cells, or to the presence of smaller red blood cells such as microcytes. Although anisocytosis by itself is not diagnostic, an improved anemia classification might be available by combining measures of red blood cell size variability with mean corpuscular volume [Simel et al. 1988]. Microcytic cells occur in immune-

mediated hemolytic anemia, microvascular constriction, early Heinz-body anemia and iron-deficiency anemia. Macrocytic cells occur with regenerative anemia and rarely with erythrocytic leukemia.

The rather non-specific term poikilocytosis is used to describe an unusually high (greater than 10%) population of abnormally shaped erythrocytes in peripheral blood [Harvey 2001]. These morphologically abnormal erythrocytes (poikilocytes) may be caused by a variety of conditions, including fragmentation of erythrocytes, oxidative injury, immune-mediated damage, and congenital abnormalities [Cowell et al.1999]. Among these morphologically abnormal cells are the spherocytes and stomatocytes. Spherocytes are red blood cells that are almost spherical in shape. They have no area of central pallor like a normal red blood cell. Large spherocytes (macrospherocytes) are seen in hemolytic anemia, whereas small spherocytes (microspherocytes) are sometimes seen in severe burn cases. Stomatocytes are characterized by a slit-like zone of central pallor. Stomatocytes are usually the result of a water content increase, an alteration of cation content and flux or and amphipathic drug use [Lim et al. 2002, Fujii et al. 1979, Elgsaeter and Mikkelsen 1991, Isomaa et al. 1987]. This altered erythrocyte shape is particularly interesting because of its abnormal increase in osmotic fragility which could lead to mechanical damage in turbulent blood flow circulation.

Considering the essential role played by the shape and size of the red blood cells in all the processes mentioned above, realistic cell models for spherocytes, macrocytes, microcytes and stomatocytes (as typical representatives of poikilocytes) must be used in any morphological cell analysis. In particular, the variation of the transmembrane potential when the cell is exposed to an electromagnetic (EM) field is a good probe of the interaction mechanism between biological cells and external radiation.

The layout of this paper is as follows: in the next section we briefly review existing mathematical models for the normal erythrocyte shape, and then present a new set of simple parametric equations that by means of free parameters model accurately continuous deformations from a simple sphere to the final erythrocyte altered shapes; then, as applications of these equations, we determine the transmembrane potential and the electric stress forces induced in the membrane of different cell shapes when they are exposed to an external EM field; the paper ends with a brief summary.

Parameterizations of erythrocyte shape abnormalities

Among the methods frequently used to model the erythrocyte normal shape [Sebastian et al. 2004, Moon and Spencer 1998] we mention the surface of revolution generated by a Cassini curve [Gray 1998]. Its main advantage is that Cassini curves have simple parametric representations in terms of trigonometric functions; its main limitations are that Cassini curves are determined by only two parameters (which can be used to fix only the length and the height of a real erythrocyte), and that the implementation of anisotropic deformations is not straightforward (in particular poikilocytosis and the changes in the shape of membranes which occur spontaneously when the cells are immersed in an aqueous environment under appropriate conditions [Jie et al. 1998]).

At the other end in complexity is the approach proposed by [Bloor and Wilson 2000], who use an elliptic partial differential equation in combination with an expression for the membrane surface energy to give a most realistic representation of the shape of the membrane surface. This approach, however, lacks the advantages of a simple parametric representation.

To find a reasonably simple parametric representation that allows for the modeling of the deformations we finally recall the parametric representation of the normal biconcave erythrocyte in terms of the $\mathrm{sn}(u|m)$, $\mathrm{cn}(u|m)$ and $\mathrm{dn}(u|m)$ Jacobi elliptic functions with three free parameters [Kuchel and Fackerell 1999], which we prefer to write directly in terms of as many physically measurable parameters as possible:

$$\mathbf{r}(u,\phi)=\left(\frac{\ell}{2}\mathrm{cn}(u|m)\cos\phi,\frac{\ell}{2}\mathrm{cn}(u|m)\sin\phi,\pm h_0\,\mathrm{sn}(u|m)\frac{\mathrm{dn}(u|m)}{\mathrm{dn}(U|m)}\right), \tag{1}$$

where ℓ is the diameter of the erythrocyte, $2h_0$ is the height of the erythrocyte at its center, $U=K(m)$ is the corresponding complete elliptic integral of the first kind (which satisfies $\mathrm{cn}(U|m)=0$, $\mathrm{sn}(U|m)=1$ and

$\mathrm{dn}(U|m)=\sqrt{1-m}$, although for clarity we keep the functional form of this last expression in the parametric equations), $u\in[0,U]$, $\phi\in[0,2\pi]$, and the plus and minus signs correspond to the upper and lower half of the cell respectively. The only remaining parameter is $m\in[0,1)$, which can be used to fix for example $2h_{\max}$, the maximum height of the erythrocyte. Equation (1) is obviously suitable to model not only normal erythrocytes but also macrocytes and microcytes, because they essentially keep the normal erythrocyte shape and only differ in that they have different values for the diameter and height of the cell (and therefore different volumes).

To discuss the parameterization of altered shapes we first proceed by example: our model of the stomatocyte is generated by the equations

$$\mathbf{r}_{+}(u,\phi)=\left(\frac{\ell}{2}\mathrm{cn}(u|m_{+})\cos\phi,\frac{\ell}{2}\mathrm{cn}(u|m_{+})\sin\phi,h_{+}\,\mathrm{sn}(u|m_{+})\left(\frac{\mathrm{dn}(u|m_{+})}{\mathrm{dn}(U_{+}|m_{+})}\right)^{3}\right), \tag{2a}$$

$$\mathbf{r}_{-}(u,\phi)=\left(\frac{\ell}{2}\mathrm{cn}(u|m_{-})\cos\phi,\frac{\ell}{2}\mathrm{cn}(u|m_{-})\sin\phi,-h_{-}\,\mathrm{sn}(u|m_{-})\left(\frac{\mathrm{dn}(u|m_{-})}{\mathrm{dn}(U_{-}|m_{-})}\right)^{2}\right), \tag{2b}$$

for the upper and lower parts of the cell respectively. Note that in addition to the different powers (cube and square respectively) of the Jacobi $\mathrm{dn}(u|m)$ function in the third component of $\mathbf{r}_{\pm}(u,\phi)$, we also use independent values of the parameters $h_{\pm}$ and $m_{\pm}$ (and the ensuing $U_{\pm}=K(m_{\pm})$) for the upper and lower part of the cell.

Figure 1 shows the parameters and 2D generating curves for the sphere, ellipsoid, basic discocyte and a stomatocyte of the same volume obtained from Eqs. 1 and 2 respectively. Similarly, Figure 2 shows the 3D

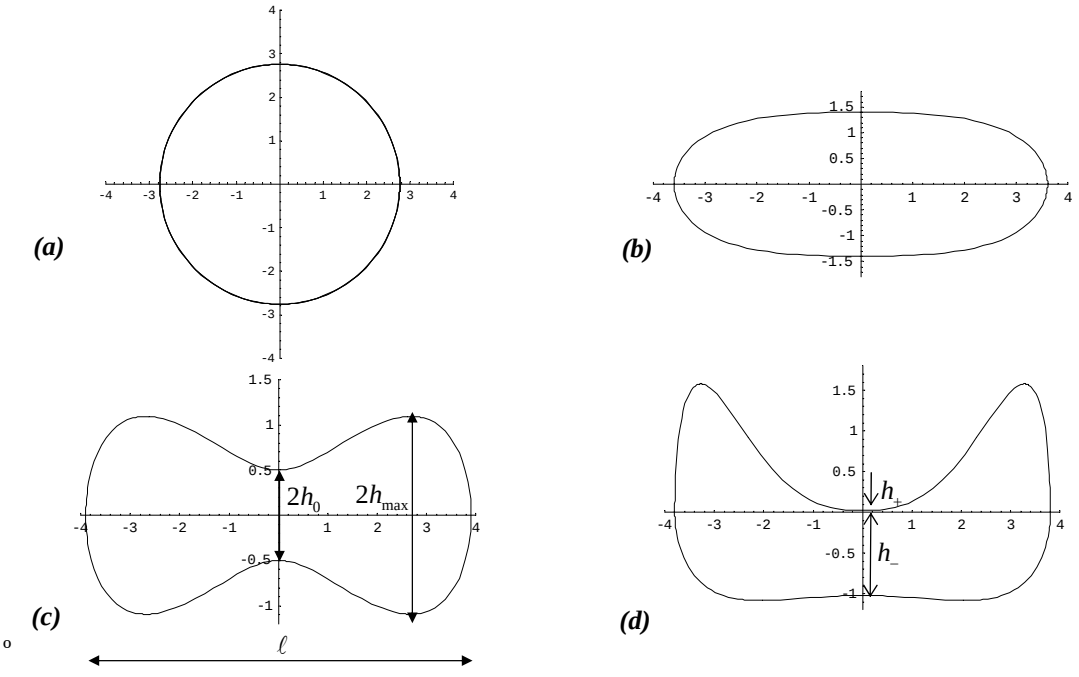


Fig. 1 2D generating curves obtained from equations 1 and 2 for a) spherocyte b) ellipsoid c) normal biconcave erythrocyte and d) Stomatocyte. The different modeling parameters used in the equations are shown in Table 1.

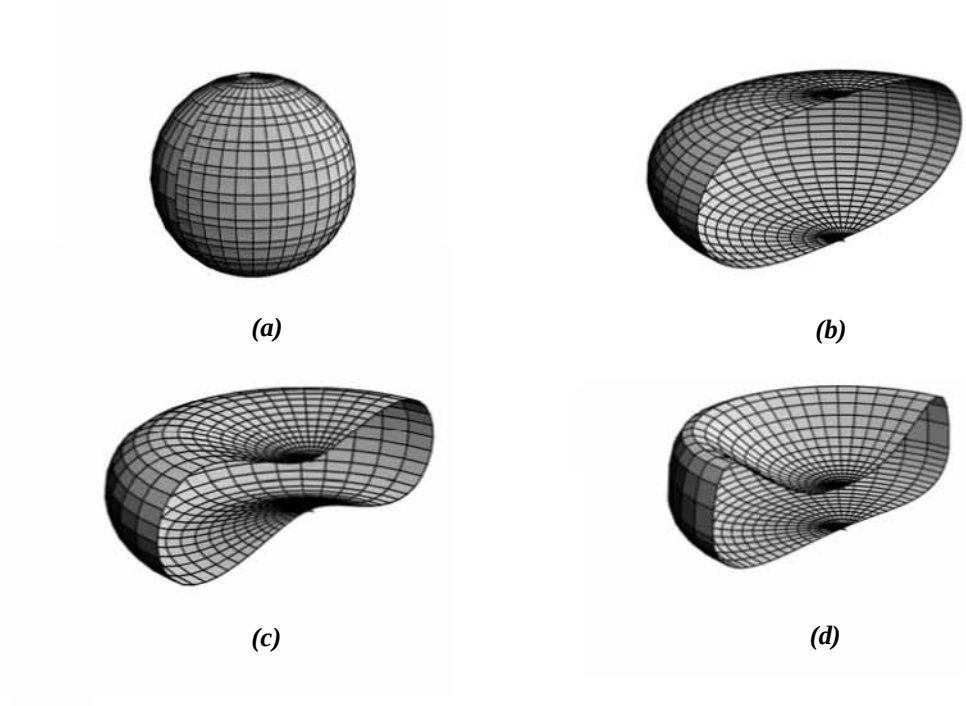


Fig. 2 3D view of the spherocyte, ellipsoid, erythrocyte and stomatocyte models generated using *Mathematica*.

cell geometries generated in *Mathematica* [Wolfram 2003] by rotation of these curves around the vertical axis. As it can be easily seen in both the 2D and the 3D figures, our stomatocyte model has a deep dimple. This degree of severity of the invagination determines that it belongs to subclass II [Bessis 1977] and is perfectly modeled by the modified Eq. 2. In Table 1 we present the numerical values of the parameters of these cells as well as of the parameters of the macrocyte and microcyte. Note that the maximum height of the stomatocyte has to be determined by using the inverse functions $u_{\pm} = \mathrm{sn}^{-1}(x, m_{\pm})$, and that the volumes of the upper and lower parts of the cells can be readily calculated thanks again to the parametric equations:

$$V_{\pm} = -2\pi \int_0^{U_{\pm}} x'(u, m_{\pm}) x(u, m_{\pm}) z(u, m_{\pm}) du \,, \tag{3}$$

where the prime denotes derivation with respect to *u*.

Cell	$\ell\,(\mu\mathrm{m})$	$h\,(\mu\mathrm{m})$	m	$V\,(\mu\mathrm{m}^3)$	$2h_{\max}\,(\mu\mathrm{m})$	$\delta\,(\mathrm{nm})$
Spherocyte	5.46	2.73	0	85.29	5.46	8
Ellipsoid	7.2	1.4	0.3954	85.17	2.8	8
Normal erythrocyte	7.8	0.5	0.9447	85.1	2.19	8
Microcyte	5	0.4	0.9520	29.8	1.87	8
Macrocyte	10	0.65	0.8446	118.1	1.79	8
Stomatocyte II $(+,-)$	7.6	(0.1242,1.4037)	(0.9741,0.4720)	85.02	2.19	8

Table 1. Parameters used in Eqs. 1 and 2 to model the different cell shapes: ℓ is the diameter of the cell, $2h$ ($h_+ + h_-$ for the stomatocyte) is the height at the centre, m (m_+ and m_- for the stomatocyte) is the parameter in the Jacobi elliptic functions, V is the volume, $2h_{\max}$ the maximum height and δ the thickness of the membrane.

We now proceed to discuss the rationale behind and the generalization of the parameterization given by Eq. 2. Note that the common structure of Eqs. 2a and 2b is

$$\mathbf{r}(u,\phi)=\left(\frac{\ell}{2}\mathrm{cn}(u|m)\cos\phi,\frac{\ell}{2}\mathrm{cn}(u|m)\sin\phi,h\,\mathrm{sn}(u|m)\left(\frac{\mathrm{dn}(u|m)}{\mathrm{dn}(U|m)}\right)^{p}\right) \tag{4}$$

where the exponent p (here equal to 3 and 2 respectively) is a new parameter which in effect controls the gross features of the shape. Note also that the original parameterization of the normal erythrocyte shape of Kuchel and Fackerell is the particular case $p=1$ of our Eq. 4. In fact, taking into account that the Jacobi elliptic functions can be considered as deformations of the familiar trigonometric functions to which they reduce for $m=0$ ($\mathrm{sn}(u|0)=\sin u$, $\mathrm{cn}(u|0)=\cos u$ and $\mathrm{dn}(u|0)=1$, in which case the parametric Eq. 4 represents a revolution ellipsoid) and taking into account also the elementary properties of these Jacobi functions [Abramowitz and Stegun 1972], it can be seen that the essential features of the parameterization (4) are maintained for positive (not necessarily integer) values of p. This new, continuous parameter can be used to advantage in the modeling not only of altered shapes, but of continuous deformations of the normal erythrocyte into these deformed shapes.

Finally, we have insisted on the advantages of an explicit parametric representation: in particular we can easily generate the uniform shell representing the membrane by shifting any parametric surface given by Eq. 4 by a constant distance δ along the outer normal at each point, i.e., the outer layer of the membrane is given by

$$\mathbf{r}_{\delta}(u,\phi)=\mathbf{r}(u,\phi)+\delta\,\mathbf{n}(u,\phi) \tag{5}$$

where

$$\mathbf{n}(u,\phi)=\frac{(\partial\mathbf{r}/\partial\phi)\times(\partial\mathbf{r}/\partial u)}{\left\|(\partial\mathbf{r}/\partial\phi)\times(\partial\mathbf{r}/\partial u)\right\|}\,. \tag{6}$$

Eqs. 4, 5 and 6 summarize our rather general model of normal or altered erythrocytes.

Applications

To illustrate the practical use of these parameterizations, we present (1) the numerical calculation of the induced transmembrane potential in stomatocytes and (2) the induced electric force (electrical stress tensor) on the interface between the realistic curved membrane and the external medium in normal erythrocytes. Both cells are exposed to an 1800 MHz plane wave, a typical carrier frequency in cellular phones and in wireless surveillance systems.

The resting transmembrane potential is a basic magnitude to the physiological state of the cell [Gedde and Huestis 1997, Glaser 1998, Bifano et al.1984], and therefore the determination of induced field strengths and transmembrane potentials can provide a good insight on the relation between the exposition to radiofrequency fields and subsequent cell changes. The relevance of the induced transmembrane potential can be inferred from the numerous papers previously published by different authors [Grosse and Schwan 1992, Kotnik and Miklavcic 2000a, 2000b and therein]. However, these former studies have generally used simplified spherical or spheroidal cell geometries (also a particular case of Eq. 4), or at most the more realistic parameterization of the normal erythrocyte by a Cassini curve. Given the numerical precision that can be attained in these calculations we do not expect a significant difference between the results for a normal erythrocyte parameterized by a Cassini curve and a normal erythrocyte parameterized by Eq. 1. However, Eqs. 4-6 permit us to perform the corresponding calculations for abnormal erythrocytes, which to our knowledge has not been carried out before.

Our model of cell (stomatocyte and erythrocyte) is formed by two media: the membrane and the cytoplasm. The cytoplasm is a physiological saline solution with a protein volume fraction of 0.26. The membrane will be represented by a shell of constant thickness $\delta=8\mathrm{nm}$ that has a very low conductivity and a frequency-independent relative permittivity [Gimsa et al. 2001]. The cell is immersed in an external continuous medium - the radiation region - formed by an electrolyte with the dielectric properties of physiological saline. Table 2 shows the electrical parameters for the membrane, cytoplasm and external medium. These values are typical for the erythrocyte structure and have been extensively used in the literature [Simeonova et al. 2002].

As the cell dimensions (≈ 8 μm) are much smaller than the wavelength at the working frequency (≈ 2 cm), we can assume that the cell is exposed to a uniform field. Therefore a quasistatic approximation holds and we can calculate the field distribution by solving directly the full Maxwell equations using a discretization of the cell model geometry into tetrahedral elements with an adaptive mesh.

Cell	$\varepsilon/\varepsilon_0$	$\sigma\ (S/m)$	Loss tangent
Cytoplasm	50	0.53	0.10590
Membrane	9.04	$1x10^{-6}$	$1.1052x10^{-6}$
External medium	80	0.12	0.014986

Table 2. Relative permittivity $\varepsilon/\varepsilon_0$, conductivity $\sigma\ (S/m)$, and loss tangent for the cytoplasm, membrane and external continuous medium at 1.8 GHz.

In this paper we use a finite element (FE) technique [Jin 1993, Douglas et al. 2000] with a variable density mesh to determine the electric field intensity within the different layers of the cell. The cells are exposed to a linearly polarized EM plane wave of frequency 1.8 GHz propagating along the *y* axis, with the **E** and **H** field vectors parallel to the *z* and *x* axes. The radiation region is taken to be a cube in which the cells are immersed. This region is filled with the external medium and surrounded by perfectly matched layers (PML). This setup provides a reflectionless interface between the region of interest and the PML layers at all incident angles [Becache and Joly 2001]. We achieve a good compromise between accuracy and computing resources by extending the dimensions of the radiation region to the order of four wavelengths in the external medium. This FE numerical technique has already been validated by the authors in previous works with simpler [Sebastian et al. 2001, Muñoz et al. 2003] and more complex geometries [Muñoz et al. 2004, Sebastian et al. 2005]. For normalizing purposes the electric field intensity is set to 1 V/m.

a) Determination of the induced transmembrane voltage in stomatocytes

In contrast to the symmetrical erythrocyte shapes, the asymmetry of the stomatocyte around the major axis leads to different values of the induced transmembrane potential in the upper and in the lower parts of the cell. Figure 3 shows this induced transmembrane potential both in the upper and in the lower parts of a stomatocyte as a

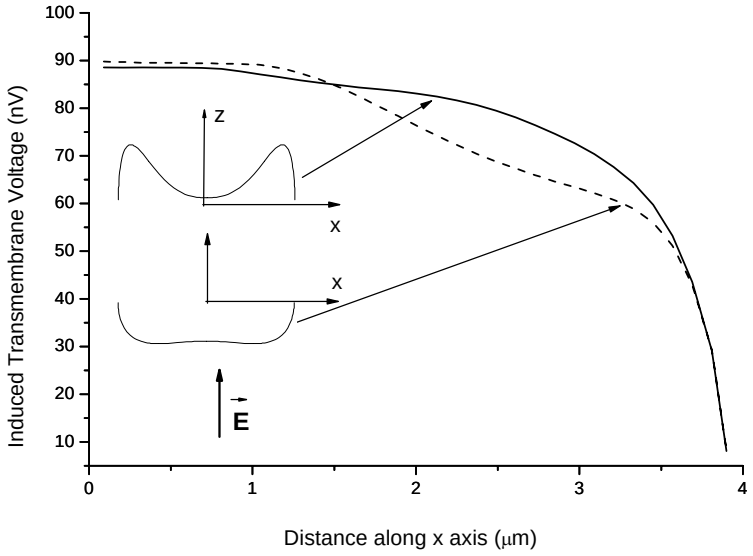


Fig. 3 Induced transmembrane potential in the upper and lower parts of a stomatocyte as a function of the distance *x* along the major axis of the cell. The cells are exposed to an RF field of frequency 1800 MHz. The electric field has an intensity of 1 V/m and is linearly polarized parallel to the vertical axis.

function of the distance *x* along the major axis. Again, the incident external electric field is parallel to the vertical axis. Note that in the flattest regions of the lower and upper parts of the stomatocyte the applied external field is perpendicular to the membrane surface. As the values of the conductivities of both the external medium and the

membrane are very low, the induced transmembrane voltage in these regions is, as expected, mainly governed by the ratio of the respective permittivities.

b) Determination of the induced electric stress forces on the membrane of erythrocytes

An obvious assumption concerning the field **E** in the membrane is that it generates a Maxwell stress which will compress the membrane. This electrical stress plays a fundamental role in electroporation processes. In the quasistatic case, the forces exerted on a finite volume of material by the electric field can then be expressed as a result of forces acting on the surface limiting this volume by (Giner *et al* 1995)

$$f_i = \int_S T_{ij} dS_j \tag{7}$$

with the stress tensor for the electric field in a material medium defined by

$$T_{ij} = \varepsilon E_i E_j - \frac{1}{2}\delta_{ij} E^2 (\varepsilon - \eta \frac{d\varepsilon}{d\eta}) \tag{8}$$

In this work, we have not considered any variations of the electric permittivity of both media with their respective mass densities, i.e. $d\varepsilon_i \;\; d\eta_i = 0$, and therefore Eq. 8 is greatly simplified.

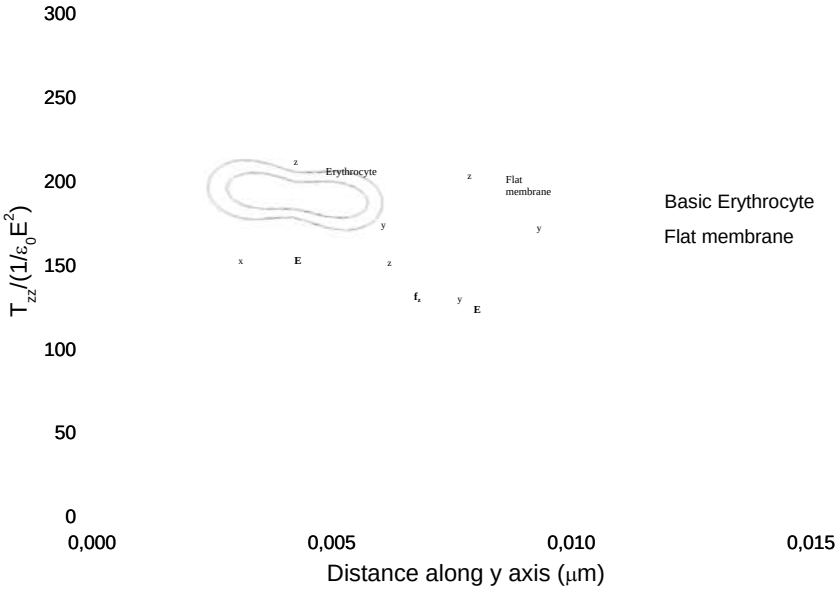


Figure 4 Stress force density (T_{zz}) exerted on the centre of the curved erythrocyte membrane (solid line) and on a flat membrane (dashed line). The force density is directed inward the membrane (along the negative *z* axis as shown in the inset) and is normalized with respect to the external field ($\varepsilon_0 E^2$).

Although our analysis has only been limited to electrical stress and to a very short radius around the *z* axis of the erythrocyte (as it would be the case of a pore), the results clearly show that the electrical forces favour deforming of the membrane. The shape and size evolution of the cell will eventually be determined by a combination of electrical and mechanical forces. A comparison of the force densities obtained for an unstretched flat membrane and for the realistic erythrocyte model shows that the curvature of the membrane cannot be neglected.

Summary

We have given a simple parameterization of erythrocyte shapes which includes as a special case the normal biconcave erythrocyte of Kuchel and Facherell (and consequently spherical or ellipsoidal models), but allows for continuous deformations from this normal shape to rather general altered shapes (like stomatocytes). As an

added advantage of having a simple, explicit parameterization, we can generate a realistic three dimensional model of these erythrocytes by shifting the inner surface a constant distance along the outer normal.

As an application of this parameterization we have performed numerical calculations of the transmembrane potential induced by an electromagnetic field of 1800 MHz and 1 V/m in stomatocytes and normal erythrocytes. The results for the unsymmetrical stomatocyte depend essentially on the new parameterization, and have to be given separately for the upper and the lower parts of the cell.

Our calculations give insight into electrical stresses on realistic curve membranes of cells immersed in an electric field. This work can be applied to different cell shapes and the refinements thereof may be of potential value in understanding the kinetics of the rupture of membranes and related phenomena such as electrorotation and dielectrophoresis.

Finally, we point out that this analysis is purely theoretical and has been performed for a particular orientation of the external RF field, and as such necessarily calls for further investigations.

Acknowledgements
This work was supported by the Comunidad de Madrid under Grant number: PR45/ 05 - 4166

References

Abramowitz M., and Stegun I.A. Eds., Handbook of Mathematical Functions (Dover, New York, 1972).

Becache E. and Joly P., Tech. Rep. 4164, INRIA, 2001.

Bessis M., Blood Smears Reinterpreted (translated by George Brecher) (Springer-Verlag, Berlin, 1977) pp. 68-70.

Bifano T., Novak S. and Friedman J.C., Relationship between the Shape and the Membrane Potential of Human Red Blood Cells, J. Membr. Biol. 82 (1984): 1-13.

Bloor M.I.G and Wilson M.J., Method for Efficient Shape parametrization of Fluid Membranes and Vesicles, Phys. Rev. E, 61(4) (2000): 4218-4229.

Cowell R.L, Tyler R.D. and Meinkoth J.H., Diagnostic Cytology and Hematology of the Dog and Cat, 2nd ed. (Mosby, St. Louis, 1999).

Douglas J. Jr., Santos, J. E. and Sheen D., A Nonconforming Mixed Finite Element Method for Maxwell's Equations, Math. Models Meth. in Appl. Sci. (M3AS),10 (2000): 593-613.

Elgsaeter A. and Mikkelsen A., Shape and Cell Changes in Vitro in Normal Red Blood Cells, Biochimica et Biophysica Acta 1071 (1991): 273-290.

Fujii T., Sato T., Tamura A., Wakatsuki M. and Kanaho Y., Shape Changes of Human Erythrocyte Induced by Various Amphipathic Drugs Acting on the Membrane of the Intact Cell, Biochem. Farma. 28 (1979): 613-620.

Gedde M., Yang E. and Huestis W.H., Shape Response of Human Erythrocytes to Altered Cell pH, Blood 86 (1995): 1595-1599.

Gedde M. and Huestis W.H., Membrane Potential and Human Erythrocyte Shape, Biophys. J. 72 (1997): 1220-1233.

Gimsa J., A Possible Molecular Mechanism Governing Human Erythrocyte Shape, Biophys J. 75 (1998): 568-570.

Gimsa J.and Wachner D., Analytical description of the transmembrane voltage induced on arbitrarily oriented ellipsoidal and cylindrical cells *Biophys J.* 81 (2001): 1888-96.

Giner V, Sancho M and Martinez G Electromagnetic forces in dissipative dielectric media *Am. J. Phys*. 63 (8) (1995): 749-53.

Glaser R., The Shape of Red Blood Cells as a Function of Membrane Potential and Temperature, J. Membrane Biol. 51 (1979): 217-228.

Glaser R., Does the Transmembrane Potential or the Intracellular pH Control the Shape of Human Erythrocyte? Biophys. J. 75 (1998): 569-570.

Gray A., Modern Differential Geometry of Curves and Surfaces with Mathematica, 2nd Ed. (CRC Press, Boca Raton, 1998).

Grosse C. and Schwan H.P., Cellular Membrane Potentials Induced by Alternating Fields, Biophys. J. 63 (1992): 1632-1642.

Harvey J.W., Atlas of Veterinary Hematology: Blood and Bone Marrow of Domestic Animals, (WB Saunders, Philadelphia, 2001).
Isomaa D., Hagerstrand H. and Paatero G., Shape Transformations Induced by Amphiphiles in Erythrocytes, Biochimica et Biophysica Acta 899 (1987): 93-103.
Jie Y., Quanhui L., Jixing L, and Ou-Yang Zhong-Can, Numerical Observation of Nonaxisymmetric Vesicles in Fluid Membranes, Phys. Rev. E 58 (1998): 4730-4736.
Jin J., The Finite Element Method in Electromagnetics (Wiley, New York, 1993).

Kotnik T. and Miklavcic D., Second Order Model of Membrane Electric Field Induced by Alternating External Electric Fields, IEEE Trans on Biomed. Eng. 47 (2000)a: 1074-1081.
Kotnik T. and Miklavcic D., Analytical Description of Transmembrane Voltage Induced by Electric Fields on Spheroidal Cells, Biophys. J. 79 (2000)b: 670-679.
Kotnik T. and Miklavcic D., Theoretical Evaluation of the Distributed Power Dissipation in Biological Cells Exposed to Electric Fields, Bioelectromagnetics 21 (2000)c: 385-394.
Kuchel P. and Fackerell E., Parametric Equation Representative of Biconcave Erythrocytes, Bulletin of Mathematical Biology 61 (1999): 209-220.
Lim H.W.G., Wortis M. and Mukhopadhyay R., Stomatocyte-discocyte-echinocyte Sequence of the Human Red Blood: Evidence for the Bilayer Couple Hypothesis from Membrane Mechanics., Pnas 99 (26) (2002): 16766-16769.
Moon P. and Spencer D.E., Field Theory Handbook: Including Coordinate Systems, Differential Equations and Their Solutions (Springer, Berlin, 1998).
Muñoz S., Sebastián J.L, Sancho M. and Miranda J.M., A Study of the Electric Field Distribution in Erythrocyte and Rod Shape Cells from Direct RF Exposure, Phys. Med. Biol. 48 (2003): 1649-1659.
Muñoz S., Sebastian J.L., Sancho M., and Miranda J.M., Transmembrane Voltage Induced on Altered Erythrocyte Shapes Exposed to RF Fields, Bioelectromagnetics 25 (2004): 631-634.
Oroz L.M.A., Morphologie Mathematique en Coordonnees Logarithmique-polaires et Methodes Geometriques de Classification. Application a L´etude des Erythocytes, (Master Thesis, Ecole des Mines de Paris, 2004).
Ponder E., Hemolysis and Related Phenomena (Grune & Stratton, New York, 1948).

Sebastian J.L., Muñoz S, Sancho M. and Miranda J.M., Analysis of the Influence of the Cell Geometry, Orientation and Cell Proximity on the Electric Field Distribution from Direct RF Exposure, Phys. Med. Biol. 46 (2001): 213-225.
Sebastian J.L., Muñoz S, Sancho M. and Miranda J.M., Modeling the Internal Field Distribution in Human Erythrocytes Exposed to MW Radiation, Bioelectrochemistry 64 (2004): 39-45.
Sebastian J.L., Muñoz S., Sancho M., Miranda J.M. and Álvarez G., Erythrocyte Rouleau Formation under Polarized Electromagnetic Fields, Phys. Rev. E 72 (2005): 31913(9).
Simel D.L., DeLong E. R., Feussner J.R., Weinberg J.B. and Crawford J., Erythrocyte Anisocytosis. Visual Inspection of Blood Films vs Automated Analysis of Red Blood Cell Distribution Width, Arch Intern Med. 148(4) (1998): 822-824.
Simeonova M., Wachner D. and Gimsa J., Cellular Absorption of Electric Field Energy: Influence of Molecular Properties of the Cytoplasm, Bioelectrochemistry 56 (2002): 215-218.
Wolfram S., The Mathematica Book (Wolfram Media, Champaing 2003).

THE DEPENDENCE OF BIOLOGICAL EFFECTS ON THE AMPLITUDE OF EXTREMELY WEAK POWER - FREQUENCY MAGNETIC FIELD

N.A. BELOVA, O.N. ERMAKOVA, A.M. ERMAKOV[1], V.V. LEDNEV

INSTITUE OF THEORETICAL AND EXPERIMENTAL BIOPHYSICS RAS

[1]PUSHCHINO STATE UNIVERSITY

E-MAIL: belova@iteb.ru

Abstract.

We report the results of a study on the influence of extremely-weak power frequency (60 Hz) magnetic field on the rate of regeneration in planarians Girardia tigrina and on the rate of gravitropic curvature development in the segments of the line stems. The data presented here demonstrate that the dependence of biological effects on the field's amplitude in the range from 0.5 to 8 μT is polyextremal. In particular, the maxima of effects (activation of regeneration) is observed at B_{AC} = 1.3 and 3.9 μT, while at B_{AC} = 2.5 and 5.4 μT the value of bioeffects are close to zero. The experimentally observed dependence of bioeffects on the field's amplitude can be reasonably well approximated by the theoretical expression, which we obtained earlier. At the values of B_{AC} >8-10 μT the bioeffect changes its sign – activation of planarian's regeneration starts to be replaced by its inhibition. The inhibition takes place for the range of the amplitudes from 10 to 140 μT. Simple theoretical estimates indicate, that the observed change in the sign of the effect may result due to the prevalence of the effects caused by the induction of the alternating currents in the test-system at relatively high B_{AC} – amplitudes. These results provide additional evidences for the model, explaining the interaction of weak and extremely weak alternating magnetic fields with biosystems, suggested earlier and provide the basis for planning of the epidemiological studies and interpretation of the corresponding results.

1. Introduction.

At present time it is generally accepted, that low-frequency alternating magnetic fields (AMF) with amplitudes (magnetic induction values, B_{AC}) equal or exceeding 10 μT are capable to induce the biological effects in a number of biosystems. This kind of magnetic fields are widely used in medicine, in particular, to stimulate regeneration of bones and soft tissues. However, humans in living and working places are exposed to the influence of rather weak or exteremely weak alternating magnetic fields (EW AMF), originating from technogenic and natural sourses. The amplitudes of the power-frequency magnetic fields in most of the living places range from 0.01 to 1-2 μT, while at some working places it may reach 5-6 μT [1]. Some experimental studies indicate that EW AMF may substantially influence some biological systems [1-16]. It should be noted, that in most cases the experiments with AMF are usually performed on the background of the static Earth's magnetic field, B_{DC}, with the value of magnetic induction of about 50 μT. Correspondingly, in a general case the term EW AMF means, that one is using the combined magnetic field, which contains both static and exteremely weak alternating components. This circumstance is important for understanding of the physical mechanism the of influence of EW AMF on biological systems. Nevertheless, the term " bioeffects of EW AMF " is often used for brevity and also to emphasize the specificity of the mechanism of action of such fields.

It is necessary to note, that reports on the bioeffects of AMF with the amplitudes higher than 10 μT, as a rule, do not cause any doubts. At the same time some authors deny even a mere possibility of bioeffects of AMF with the amplitudes less than 10 μT. Contrary to the claims denying the possible existence of biological effects of low-frequency magnetic fields with the amplitudes ≤ 2 μT in the frame of traditional physics and biology [8, 17], there is a considerable number of experimental evidence confirming this kind of effects. It is remarkable, that the

important data demonstrating the inhibiting influence of sinusoidal magnetic field (B_{AC} =1.7 μT, f_{AC} = 60 Hz) on the oncostatic action of melatonin in a culture of human breast cancer cells have been obtained independently by several laboratories [5, 6, 7, 14, 15].

Despite of a certain, although quite slow, progress in the experimental proof of biological efficiency of some types of EW AMF, there is still no clear understanding of the corresponding mechanisms. In order to develope the possible theoretical models for the interaction of EW AMF with biosystems it is necessary to have the thorough experimental data on the dependence of bioeffect's value on the parameters of the magnetic field.

We have shown recently, that EW AMF with the values of amplitudes in the microtesla, nanotesla and even picotesla range substantially influence the properties of biological test-systems prepared from animal and plant sourses [18, 19]. In particular, such fields were found to affect the rate of regeneration in planarians (*Girardia tigrina*) and also the rate of gravitropic response in the stem segments of flax (*Linum bienne*). We have found that the maximal and minimal values of the bioeffects were observed at certain (identical for the different test-systems) values of the amplitude/frequency - ratio of the AMF; the values of the bioeffects did not change with a simultaneous proportional change of the amplitude and the frequency of AMF.

The theoretical analysis of the obtained experimental data has shown, that in the range of frequencies and amplitudes used in our experiments, the value of bioeffects of EW AMF strongly depends on the parameter $\gamma B_{AC} / f$, where γ - gyromagnetic ratio for the particular type of magnetic moment, and B_{AC} - and f_{AC} – correspond to magnetic induction and frequency of the alternating magnetic component [19]. We have shown, that experimental dependence of the value of bioeffects on the frequency of alternating component (in a range from 10 to 320 Hz) at constant amplitude (B_{AC} = 1.6 μT) may be approximated by a theoretical curve with γ = 42.578 Hz/μT, corresponding to the gyromagnetic ratio of the nuclear spins of hydrogen atoms. The dependence of bioeffect's value on $\gamma B_{AC} / f$ - parameter is polyextremal: well expressed maxima are observed at $\gamma B_{AC} / f$ = 0.9; 2.75 and minor maxima – at $\gamma B_{AC} / f$ = 4.5; 6.1. The bioeffects are absent at $\gamma B_{AC} / f$ = 1.8; 3.8; 5.3; 6.7 [19].

In order to estimate the biotropic action of the particular exteremely weak power-frequency magnetic field (on the background of the geomagnetic field), it is nessesary to obtain the dependence of the bioeffect's value on the amlitude of the field at fixed frequency. Here we present the corresponding experimental data, indicating that at rather small amplitudes (0< B_{AC} <10 μT) of 60 Hz magnetic field the maxima and minima of the corresponding bioeffects are observed at exactly the same values of the $\gamma B_{AC} / f$ - parameter, which were found earlier [19] in the frequency- dependence studies (as it was expected).

2. Experimental section.

2.1. Magnetic fields.

The exposure of the test-systems to the power – frequency magnetic field (60 Hz) with the value of magnetic induction, B_{AC}, was carried out on a background of an ambient static magnetic field, $B_{DC} \cong 42.0$ μT. The alternating (sinusoidal) magnetic field, generated with the use of Helmholtz coils (39 cm in diameter) was oriented co-linear with a vector of the Earth's magnetic field. The Helmholtz coils have been fed by standard signal generators G4-153 or G6-28. The control test-systems were exposed to the static Earth's magnetic field. The necessary values of alternating magnetic field were established taking into account the transmission coefficient for a Helmholtz coil, equal to 10 μT/1V.

The experiments were performed using EW AMF with the following parameters:

f_{AC} = 60 Hz; 0.1 μT < B_{AC} < 140 μT; B_{DC} = 42.0 μT.

The value of magnetic induction of the background alternating (50 Hz) magnetic field at the position of experimental test-systems inside of the Helmholtz coils was 15 nT. Experiments were conducted at room temperatures of about 20-22 ^{0}C.

2.2. Test-systems.

2.2.1. Regnerating planarians. Preparation, computer morphometry, data analysis.

The flat worms (planarians *Girardia tigrina*), asexual laboratory race were reared in pond water at room temperature and were fed once a week with the Diptera larvae. For the experiments the animals of about 7-8 mm in length were selected. The feeding of the selected planarians was stopped one week prior to the start of the experiment. The head portions of planarians were amputated with an eye scalpel under a binocular microscope: approximately 1/5 part of a body containing head ganglion was dessected. Then regenerants were placed in two glass vessels filled with 50 ml of pond water (30 regenerating planarians per vessel).

The rate of regeneration in experimental and control animals was estimated with the use of computer morthometry method, based on of photocontrast between old (pigmented) and new (transparent) parts of a planarian's body.Each planarian has been photographed with the use of binocular microscope and videocamera in 3 days after amputation. It takes about 30 minutes to get photo pictures of a groop of 30 animals. The video images of rgenerating planarian were introduced into computer. Using the special program for image analysis, we determined the area, S, of whole planarian and the area, s, of the newly formed (transparent) blastema (Fig.1). The results of these measurements were used in calculations of the regeneration index, $R = s / S$, averaged over 30 planarians in control and experimental animals. The values of the EW AMF bioeffect was determined according to the expression:

$\Delta R\ (\%) = \dfrac{(R_{\exp} - R_{con}) \pm (\delta_{\exp} + \delta_{con})}{R_{con}} \times 100\%$, where $\delta_{\exp}$ and δ_{con} - standard errors of the average values, obtained for the experimental and control animals.

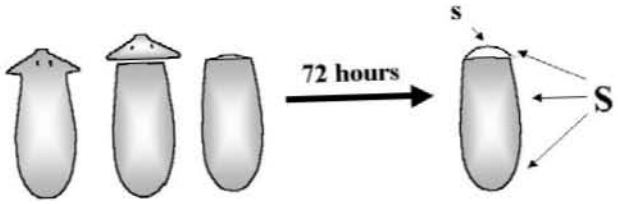


Figure 1. The scheme of measurements of the planarian's regeneration index; *s* - the area of newly formed tissue (blastema), *S* – the area of the whole body of planarian; *s/S* – regeneration index

2.2.2. Segments of flax stems. Preparation, stimulation of gravitropic bending, data analysis.

Seedlings of flax (*Linum bienne*) were grown from the seeds at thermostat at 26 ^{0}C in complete darkness during 4 days. In 4 days the stems seedlings were about 3-4 cm long. The apical parts (2.5 cm in length of stems) were excised and the leaves were removed from the obtained segments. The segments were placed horizontally in the Petri dishes (90mm in diameter) on the filter paper moistened with 2 ml of distilled water. The basal ends of the segments were fixed by the rings cut off from the silicon tube. Two dishes (with 20 segments per dish) were exposed to magnetic field and two dishes were used as a control. The gravitropic upward bending in segments begins in about 30 min after placing them in horizontal position and in about 3 hours the apical ends of segments attain the vertical positions with the tips directed against the gravity force vector. The value of the gravitropic bending in segments was defined as an averaged (over the number of 40 segments) angle formed between the apical end of a segment and the horizontal plane, $\alpha \pm \delta$, where δ -standard deviation of the mean (Fig. 2).

The measurements were performed with a protractor in 2 hours after beginning of the experiment. The collection of data on bending angles for 20 segments in one dish takes 3-4 minutes. All experiments were performed at 25 $\pm$ 0.5 ^{0}C.

The value of the bioeffect induced by 60 Hz magnetic field was expressed as the relative difference between the average angle of bending in the experiment, $\alpha_{\exp}$, and in the control, α_{con}, according to the equation: $\frac{(\alpha_{\exp} - \alpha_{con}) \pm (\delta_{\exp} + \delta_{con})}{\alpha_{con}} 100\%$, where $\delta_{\exp}$ and δ_{con} - standard errors of the means.

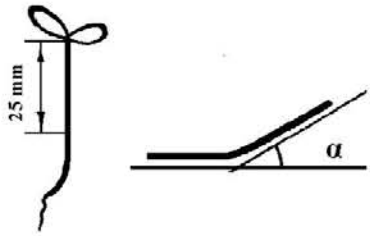


Figure 2. The scheme of measurements of the gravitropic bending angle in a segment of flax stem.

3. Results and discussion.

Earlier we have shown, that the value of bioeffects, ***I***, induced by EW AMF can be described by the expression:

$$I = kJ_1(\gamma B_{AC} \quad f) \times [J_2(\gamma B_{AC} \quad f) - J_0(\gamma B_{AC} \quad f)] \qquad (1),$$

where k - constant, $\gamma B_{AC} \quad f$ - argument of Bessel's functions, γ = 42.578 Hz/μT – gyromagnetic ratio of the nuclear spin of hydrogen atom, B_{AC} and f_{AC} - magnetic induction and a frequency of an alternating component of the EW AMF [19]. As it may be seen (Fig. 3 and Fig. 4), the expression (1) reasonably well approximates the experimentally observed dependence of bioeffects on the amplitude of the 60 Hz magnetic field: the maximal values of bioeffects (i.e. activation of the rate of regeneration in planarians and activation of the gravitropic bending in the stem segments of flax) appear at the values of $\gamma B_{AC} \quad f$ equal to 0.9 and 2.75, while at $\gamma B_{AC} \quad f$ equal to 1.8 and 3.8 the effect of the field is absent. These results confirm our earlier conclusion, according to which the nuclear spins of hydrogen atoms are the primary targets in the the interaction of EW AMF with biosystems [19]. It should be noticed, that according to expression (1) at standart experimental conditions the value of bioeffects of EW AMF for the particular type of magnetic moment is completely defined by the amplitude/frequency - ratio of the alternating component and practically does not depend on the exact value of a static magnetic field.

An increase of the amplitude of the 60 Hz magnetic field up to 8-10 μT is accompanied by a change in a sign of the bioeffect - activation of planarian's regeneration is replaced by its inhibition. In Fig. 3 we have given only one experimental point. In fact, the inhibition of regeneration, characterized by a decrease in the regeneration index, s/S, by 20-30 % was observed with an increase of the amplitude in the range from 10 μT to at least 140 μT. Apparently a change of a sign of effect is caused by the induction of eddy currents in the vessels with planarians at relatively high amplitudes of the 60 Hz magnetic field.

It seems quite instructive to compare the results and conclusions represented in this paper with those of another study devoted to the influence of sinusoidal 60 Hz magnetic fields with amplitude ranging from 1 μT to 20 μT on the enzymatic activity of ornithine decarboxylase (ODC) in cultured fibroblast cells, exposed to the field during 4 hours [20]. The authors came to the following conclusions: 1) the enchancement of ODC activity induced by exposure of culture cells to a 60 Hz magnetic field suggested a sigmoidal relationship to magnetic field amplitude; an approximate doubling of the ODC activity was observed at field amplitude of 7 μT or higher; 2) the observed bioeffects are caused by the induced electric fields in a test-system, which is a function of the orientation of the magnetic field relative to the exposed sample, and the geometry and electrical properties of the sample; therefore, the threshold amplitude - value of the 60 Hz magnetic field may substantially differ for the different test-systems.

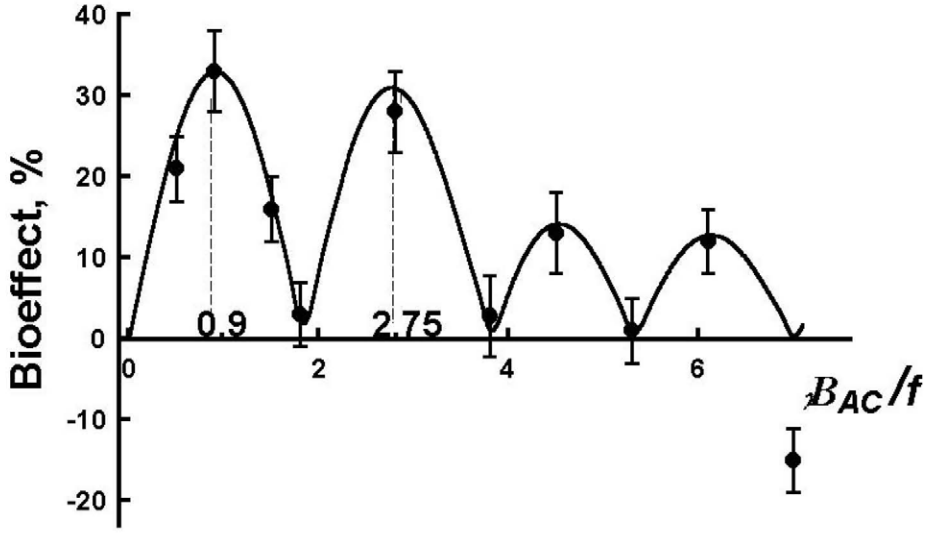


Figure 3. The dependence of the rate of planarian regeneration on value of γB_{AC} f - parameter. The solid curve represents theoretically expected dependence. The parameters of combined magnetic field: B_{DC} = 42 μT, f_{AC} = 60 Hz B_{AC} = 0.7; 1.3; 2.1; 2.5; 3.9; 5.4; 6.3; 7.4; 8.6; 9.8 μT corresponding to γB_{AC} f = 0.5; 0.9; 1.5; 1.8; 2.75; 3.8; 4.5; 5.3; 6.1; 7.0.

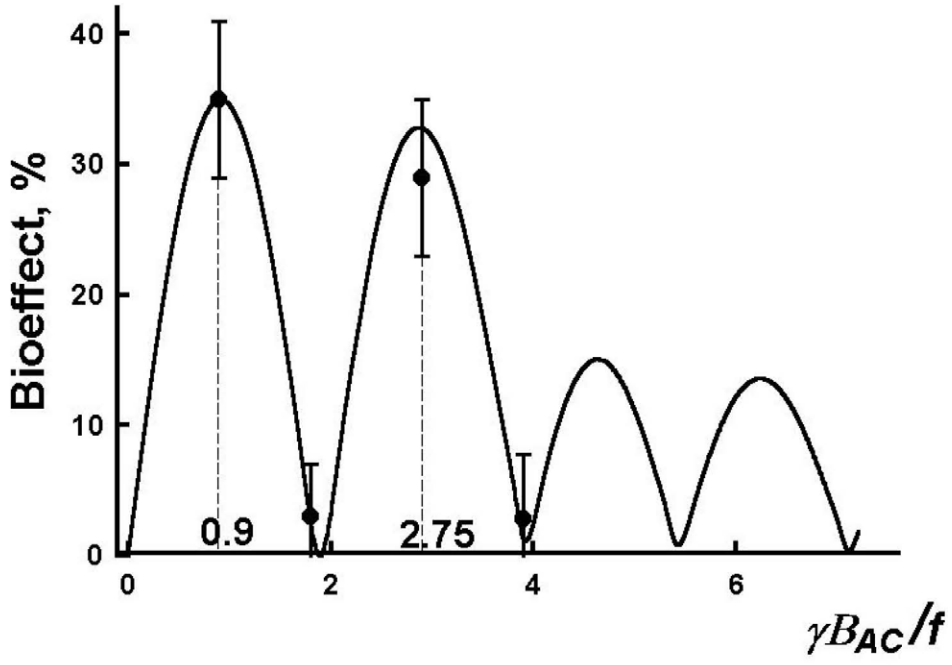


Figure 4. The dependence of the value of gravitropic bending in the segments of flax stem on value γB_{AC} f - parameter. The solid curve represents theoretically expected dependence. The parameters of the combined magnetic field: B_{DC} = 42 μT, f_{AC} = 60 Hz B_{AC} = 1.3; 2.5; 3.9; 5.4 μT corresponding to the values γB_{AC} f = 0.9; 1.8; 2.75; 3.8.

As it can be seen, the experimental results and conclusions presented by Mullins et al. [20] seem to be drastically different from those obtained in this paper. However, it is nesessary to point out that the experimental results published by Mullins et al. [20] and by some other groops [6, 7, 14, 15] were obtained with the use of μ - metal shielded Helmholtz coil pairs, so that the amplitude of a residual static Earth's magnetic field at the location of the test-systems was not exceeding 0.1-0.2 μT. It means that in these studies the test-systems were exposed to very weak sinusoidal 60 Hz magnetic field in the practical absence of a static magnetic field. It is known, the effects of AMF in the presence and in the absence of a static magnetic component may be essentially different [21, 22]. Obviously, in the real enviroument and work places both EW AMF and geomagnetic static field are pesent. Therefore, the experimental data obtained with a shielded Earth's magnetic field do not seem to be directly related to the effects of power – frequency magnetic fields, which may occur at real environmental conditions.

4. Conclusions.

The experimental results presented in this paper and earlier [18, 19] show, that the combined magnetic fields with the extremely weak amplitudes of the alternating component are capable to influence substantially the properties of biological test-systems derived from the animal's and plant's sourses (regenerating planarians and gravitropically responding stems of flax). Our data clearly show that the dependence of biological effects on the amplitude of the 60 Hz magnetic field ranging from 0.5 to 8 μT is polyextremal. In particular, the maxima of effects is observed at B_{AC} = 1.3 and 3.9 μT, while at B_{AC} = 2.5 and 5.4 μT the value of bioeffects are close to zero. The experimental points can be reasonably well approximated by the theoretical expression, which we obtained earlier [19]. These results confirm our earlier conclusion, according to which the nuclear spins of hydrogen atoms are the primary targets in the the interaction of some types of EW AMF with biosystems. At the values of B_{AC} >8-10 μT the bioeffect changes its sign – in particular an activation of planarian's regeneration starts to be replaced by its inhibition. The inhibition takes place for the range of the amplitudes from 10 to 140 μT. The change in the sign of the effect may appear due to the prevalence of the effect caused by the induction of the alternating currents in the test-system at relatively high B_{AC} – amplitudes. These results allow to clarify the interaction mechanism of the weak power-frequency magnetic fields with biosystems and provide the basis for planning of the epidemiological studies and interpretation of the corresponding results.

This study was supported by the Russian Foundation for Basic Research (grant № 04-04-97324) and by the Programm " Fundamental sciences in medicine".

5. References.

1. Hansson Mild K. IEEE Transactions on Instrumentation and Measurement. 1996, Vol. 45, №3, 710-714.
2. Juutilainen J., Laara E., Saali K. // International Journal Radiation Biology & Relat. Stud. Physical Chemistry Medicine 1987. Vol. 52, № 5, 787-793.
3. Berman E., Chacon L., House D. // Bioelectromagnetics. 1990. Vol. 11, №2. P. 169-187.
4. Martin A.H. // Bioelectromagnetics. 1992. Vol. 13, №3, 223-230.
5. Liburdy R.P., Sloma T.R., Sokolic R., Yaswen P. // Journal Pineal Research 1993. Vol. 14, 89-97.
6. Luben R.A., Saraiya S., Morgan A.P. // Abstract A-1. Annual Review of Research on Biological Effects of Electric and Magnetic Fields from the Generation, Delivery & Use of Electricity. San Antonio, TX, 1996, Nov. 19-21.
7. Harland J.D., Liburdy R.P. // Bioelectromagnetics. 1997. Vol. 18, №8, 555-562.
8. Valberg P.A., Kavet R., Rafferty C.N. // Radiation Research. 1997. Vol. 148, №1, 2-21.
9. Harland J., Eugstrom S., Liburdy R. // Cell Biochemistry and Biophysics 1999. Vol. 31, №3 295-306.
10. Persinger M.A., Cook L.L., Koren S.A. // International Journal of Neuroscience. 1999. Vol. 100, №1/4, 107-116.
11. Cook L.L., Persinger M.A. // Neuroscience Letters. 2000. 13/292, №3, 171-174.
12. Belova N.A. & Lednev V.V. // Biofizika 2001, v. 46, № 1, 122-125 (in Russian).
13. Novoselova E.G., Ogay V.B., Sorokina O.B. et al. // Biofizika. 2001. Vol. 46, № 1, 131-135 (in Russian).
14. Blackman C.F., Benane S.G., House D.E. // Bioelectromagnetics. 2001. Vol. 22, №2, 122-128.
15. Ishido M., Kabuto M. // Carciogenesis. 2001. Vol. 22, №7, 1043-1048.

16. Lednev V.V. & Malyshev S.L. // Abstract Collection Bioelectromagnetics Society Annual Meeting, St Paul, Minnesota, USA. 2001, 3-4.
17. Adair R.K. // Physical Review. A. 1991. Vol. 43, 1039-1040.
18. Lednev V.V., Belova N.A., Rojdestvenskaya Z. Ye., Tiras Kh. P. // Geophysical processes and biosphere. 2003. Vol. 2, № 1, 3-11 (in Russian).
19. Lednev V.V. // In a book "Modelling of geophysical processis. 2003, 130-136 (in Russian)
20. Mullins J.M., Penafiel L.M., Juutilainen J., Litovitz T.A. // Bioelectrochemistry and Bioenergetics. 1999. Vol. 48, 193-199.
21. Alexandrov Ye.B., Konstantinov O.B., Perel V.I., Khodovoy V.A. // Journal experimental and theoretical physics. 1963. Vol. 45, iss. 3. № 9, 503-510 (in Russian).
22. Lednev V.V. // Biofizika. 1996., Vol. 41, № 1, 224-232 (in Russian).

MAGNETIC FIELD ZONING IN THE FRAMEWORK OF THE DUTCH POWER LINE POLICY

GERT KELFKENS, MATHIEU PRUPPERS

RIVM, NATIONAL INSTITUTE FOR PUBLIC HEALTH AND THE ENVIRONMENT, P.O. BOX 1, 3720 BA BILTHOVEN, THE NETHERLANDS, E-MAIL: GERT.KELFKENS@RIVM.NL

Abstract

The possibility of a greater risk of childhood leukaemia due to magnetic fields caused by overhead power lines is currently a matter of scientific and public debate. However, a causal relationship has not been proven and it is not obvious whether the magnetic fields are the cause. In October 2005 the Dutch government issued a power-line policy based on the precautionary principle aimed at avoiding new situations in which children undergo prolonged exposure to magnetic fields exceeding 0.4 microtesla. For this purpose, a 0.4 microtesla magnetic field zone in the vicinity of overhead power lines would have to be established. However, defining such a zone is complicated, firstly, because the width of the zone varies continuously with the actual line load and, secondly, because the width of the magnetic field zone should account for future growth in the use of electricity.

The Ministry of Housing, Spatial Planning and the Environment has succeeded, nevertheless, in developing magnetic field zoning in consultation with the grid companies. This paper describes the choices made in establishing the 0.4 microtesla zone. The approach used has led to a guideline for calculating the width of the 0.4 microtesla zone. The calculations are based on a line load equivalent to a fixed fraction of the maximum allowable line load, where the fixed fraction is deduced from an analysis of the line loads during 2003.

Introduction

Modern society benefits greatly from electricity, but generation, transport and use of electricity create electric and magnetic fields with extremely low frequencies (ELF-fields). In 1979 Wertheimer and Leeper [1] demonstrated an increased cancer risk for children living near electric wiring configurations. Since then the adverse health effects possibly induced by ELF-fields have been a matter of scientific and social debate. The scientific investigations focused on the possibility of an increased risk for childhood leukaemia associated with transport and distribution of electricity. Initially, not all studies met solid scientific standards and the scientific evidence was inconclusive and contradictory, but over the years the number and quality of the investigations improved. From the aggregate of the epidemiological evidence in the year 2000, the Health Council of the Netherlands – an advisory council to the Dutch government - inferred a consistent statistical association between the occurrence of childhood leukaemia and living near overhead power lines, although a causal relationship between childhood leukaemia and ELF-fields could not be proven [2]. Two pooled analyses published in 2000 (Ahlbom *et al.* [3] and Greenland *et al.* [4]) support the statistical association between childhood leukaemia and exposure to ELF magnetic fields. From these pooled analyses the Netherlands National Institute for Public Health and the Environment (RIVM) concluded that there is a possibly elevated risk of childhood leukaemia at magnetic field strengths above a value somewhere between 0.2 and 0.5 microtesla [5]. On the assumption of a causal relationship between exposure to magnetic fields and development of childhood leukaemia, which is not proven, and the relative risks observed by both Ahlbom and Greenland, RIVM calculated the number of additional cases of childhood leukaemia due to overhead power lines [6]. In the Netherlands, with a childhood leukaemia incidence of 110 new cases every year, approximately 0.5 cases may be attributable to the magnetic fields due to overhead

power lines. In 2002 the International Agency on the Research of Cancer (IARC), which is related to the World Health Organisation, also concluded a consistent statistical association between ELF magnetic fields and childhood leukaemia, and designated the ELF magnetic fields as 'possibly carcinogenic to humans' [7]. A recent investigation yielded a statistical association between childhood leukaemia and living in the vicinity of overhead power lines in Great Britain [8].

Because of the public concern and the inconclusive scientific evidence the Dutch government indicated, in the Fourth National Environmental Policy Plan (NMP4), that the present evidence formed sufficient reason for further research and for taking appropriate precautionary measures in relation to social costs and benefits [9]. Studies were started into the actual number of dwellings in the vicinity of the overhead power lines [10], into the expected rise in the number of 'exposed' dwellings during the next 25 years due to realisation of plans for new dwellings [11, 12] and into the costs of the reduction of magnetic field strengths [13].

Finally, in 2004 the State Secretary of Housing, Spatial Planning and the Environment, P.L.B.A. van Geel, stated his policy aim with respect to overhead power lines in the policy document 'Nuchter omgaan met risico's' [1] [14]. The objective of this policy is to prevent the development of new situations in which children are exposed to magnetic fields near overhead power lines whenever possible. The policy to achieve this goal was designed in consultation with stakeholders (municipalities, provinces, grid companies). On October 3, 2005 this policy was issued in a policy letter [15]. The policy letter is addressed to stakeholders with 'recommendations with regard to overhead high-voltage power lines'.

Overhead power lines

In the Netherlands overhead high-voltage power lines have five voltage levels: 380, 220, 150, 110 and 50 kilovolts (kV). Occasionally circuits of different voltages are attached to the same pylon, the so-called combi-lines (380 and 220 kV circuits, 380 and 110 kV circuits, 220 and 110 kV circuits). In the framework of a previous study [10] the Dutch network of overhead power lines was digitised from topographic maps (1:25,000) by KEMA (a technical consultancy with expertise in the energy sector). The map of the high-voltage power grid in the Netherlands is depicted in Figure 1.

The total length of overhead high-voltage power lines amounts to nearly 4000 km (Table 1). The regional grid of 150 kV has the highest share in this total, approximately 45%.

Table 1 Summary of the overhead power lines in the Netherlands

voltage level (kV)	total line length (km)
50	164
110	778
150	1781
220	249
380	840
combi	159
total	3971

[1] English translation: Coping Rationally with Risks

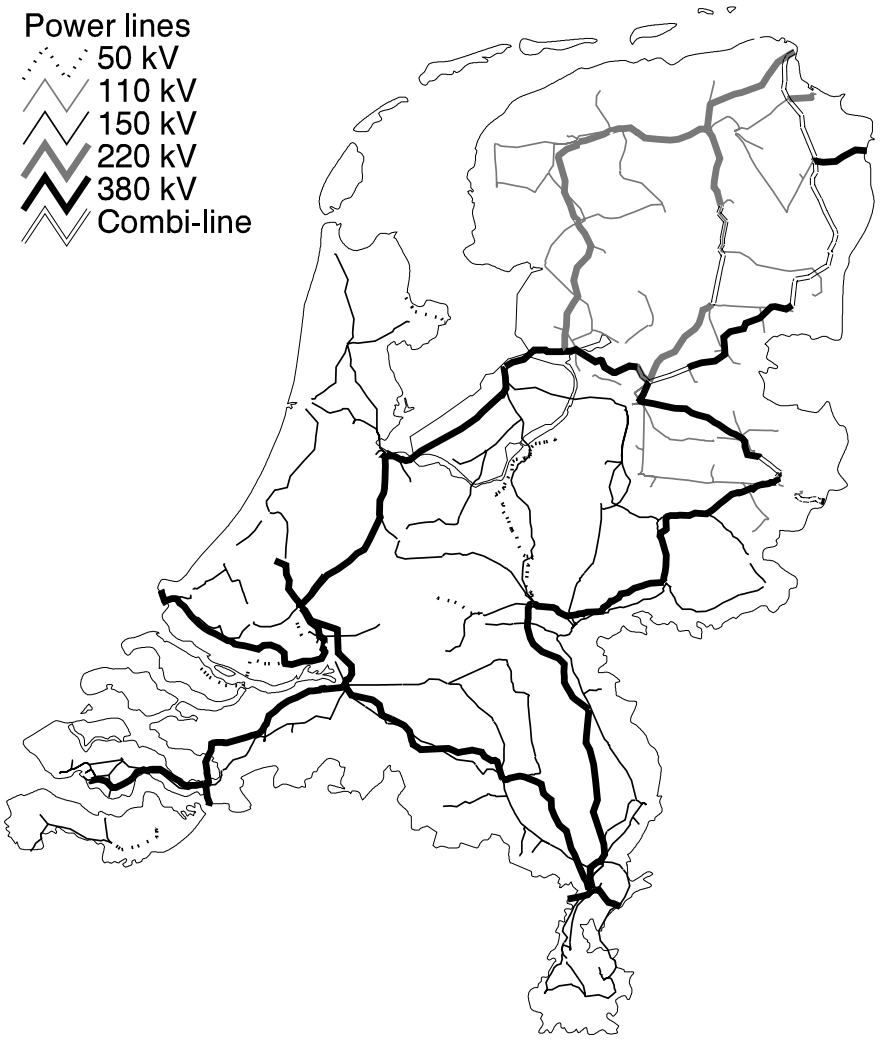


Figure 1 Overhead power lines in the Netherlands (2002)

Children living near overhead power lines

As a first step to calculating the number of children living in the vicinity of overhead power lines RIVM analysed the number of dwellings close to overhead power lines [11, 12]. A total number of 45,000 dwellings are located within 100 m (on both sides) of the overhead power lines. About 23,000 dwellings are situated within the 0.4 microtesla zone.

The average Dutch dwelling is inhabited by 2.6 persons, including 0.49 children aged 0-15 years [6]. As a result the number of children living within the 0.4 microtesla zone is estimated at 11,000.

For the next 25 years 800,000 new dwellings have been planned for the Netherlands. In a 'business-as-usual' scenario 10,000 of these dwellings will be built within the 0.4 microtesla zone. Consequently the number of children living within this zone may increase by 5,000 over the next 25 years.

Outline of the Dutch power line policy

Legal status

The Dutch power line policy was sent on October 3, 2005 as a policy letter by the State Secretary. The policy letter is addressed to stakeholders (municipalities, provinces, grid companies) with 'recommendations with regard to overhead high-voltage power lines'. Stakeholders are advised to act in accordance with this advice whenever this is reasonably possible, but the recommendations have no force of law. As a consequence stakeholders have no obligation to act according to the proposed policy.

New situations versus old situations

The Dutch power line policy is based on the observed statistical association between ELF magnetic fields and childhood leukaemia and the social concern on possible health effects, and follows the precautionary principle. The State Secretary has limited his policy to new situations, because the effects on health are unclear and because measures in existing situations often have substantial social consequences, and are expensive. In new situations prevention is possible at lower costs. With regard to the power line policy there are two types of 'new situations':

- new spatial plans (or changes in existing ones) in the vicinity of an existing overhead power line
- new overhead power lines (or changes in existing ones) in the vicinity of existing buildings

Sensitive designated uses

The statistical association between ELF magnetic fields and childhood leukaemia is observed in children living near overhead power lines. As a precaution the Dutch power line policy is not restricted to dwellings only. Some other places where children may undergo long-term exposure to the ELF magnetic field are indicated as 'sensitive uses'. The Dutch policy defines dwellings, schools, crèches and day-care centres as sensitive uses. The restrictions formulated in the Dutch overhead power line policy only apply to these sensitive uses. Other locations where children spend shorter periods in comparison to how long they spend at home, like sports centres, playgrounds, swimming pools etc. are not indicated as sensitive use. The Dutch policy does not apply to these locations. The purpose of the policy is to prevent the realisation of new sensitive uses within the magnetic field zone.

Magnetic field zones

Specific zone

In an Annex to the recommendations by the State Secretary the magnetic field zone is characterised as being:

… the area which extends along both sides of the overhead high-voltage power line and within which the magnetic field is, on average over a year, higher than 0.4 microtesla or can become so in the future.

This magnetic field zone is referred to as 'specific zone'. The value of 0.4 microtesla is a somewhat arbitrary choice in the range of 0.2 – 0.5 microtesla, the range where the childhood leukaemia risk possibly begins to be elevated [5]. The value of 0.4 was firstly mentioned with respect to overhead power lines in a letter from the former Minister of Housing, Spatial Planning and the Environment, J.P. Pronk, in 2001 [16]. The value of 0.4 microtesla was advocated by the Ministry and acceptable to the grid companies. The specific zone is calculated at a given location with the actual parameters (representative line load, pylon type, number of circuits, phase conductor geometry and earthing) for the specific section of the power line. RIVM has developed 'Guidelines for the calculation of the specific 0.4 microtesla zone in the vicinity of overhead high-voltage power lines'.

At the launching of the Dutch power line policy in 2005 no specific zones were known. To facilitate municipalities in the implementation of the policy the indicative zone was introduced in addition to the specific zone.

Indicative zone

Prior to the launching of the power line policy the indicative zone was established for all overhead power lines in the Netherlands [17]. The indicative zone is meant as an indication of the width of the specific 0.4 microtesla zone. In establishing the indicative zone, typical parameters for power lines at a given high-voltage level were used. Based on these typical parameters, zone widths were calculated for all power lines with the same voltage level. The 90th percentile of these zone widths was chosen as the indicative zone for that voltage level. Table 2 gives the values calculated for the indicative zone widths. The width of the indicative zone is not location-specific. Because the choice for the 90th percentile and due to the fact that for some of the parameters the 'worst-case' value was chosen, the specific zone is expected to be smaller than the indicative zone in most cases.

Table 2 Indicative 0.4 microtesla zone widths used in the Dutch power line policy: zone widths are rounded off to the nearest multiple of five

voltage level (kV)	zone width (m)
50	2 x 40
110	2 x 50
150	2 x 80
220	2 x 150
380	2 x 125
combi	2 x 200

TenneT, the operator of the national grid of 220 kV and 380 kV lines, was not satisfied with the established indicative zone in [17], because it gave only a rough indication of the specific zone. Consequently, TenneT recalculated the magnetic field zones for all 220 kV and 380 kV power lines. For line load, number of circuits, phase conductor geometry and earthing, TenneT used power line specific values in the calculation. One type of pylon was chosen for the entire power line. The zone from this recalculation is referred to as the 'improved indicative zone'.

The indicative (or the improved indicative) zone is used as a first check for a new spatial plan. If the plan does not overlap the indicative zone, the power line policy has no further consequences for the planning procedure. If the new spatial plan and the indicative zone overlap, it is advised to calculate the specific zone.

As a service to municipalities and provinces the indicative zone for every power line is given on a clickable Gridmap. This Gridmap is part of an internet site [18], developed by RIVM, to support implementation of the power line policy.

Establishing the specific zone

The definition of the specific zone is the result of a series of discussions between the Ministry and the grid companies. The discussions focused on two aspects of the calculation of the specific zone. The first problem to tackle was establishing which load of the power line best accounted for the actual line loads and for the expected future growth in electricity use. The second topic was how to average the magnetic field over time.

Estimating power line load

Power line loads during 2003

As a first step to estimating the line loads RIVM analysed the load of the power lines during the year 2003. Because not enough detailed information is available for the regional grid (150 kV, 110 kV, 50 kV) analyses had to be restricted to the 220 kV and 380 kV lines. The grid operator (TenneT) kindly provided RIVM with measurements of the 5-minute averaged current flowing through the circuits during 2003. Line loads vary over the day, over the days of the week and during the seasons. Figure 2 shows the variation of the line load over the day and Figure 3 over the year for a typical 380 kV power line. As the current through the power line changes the width of the actual 0.4 microtesla zone will change too. Figure 4 shows the variations of the distance of the 0.4 microtesla contour to the heart of this typical power line.

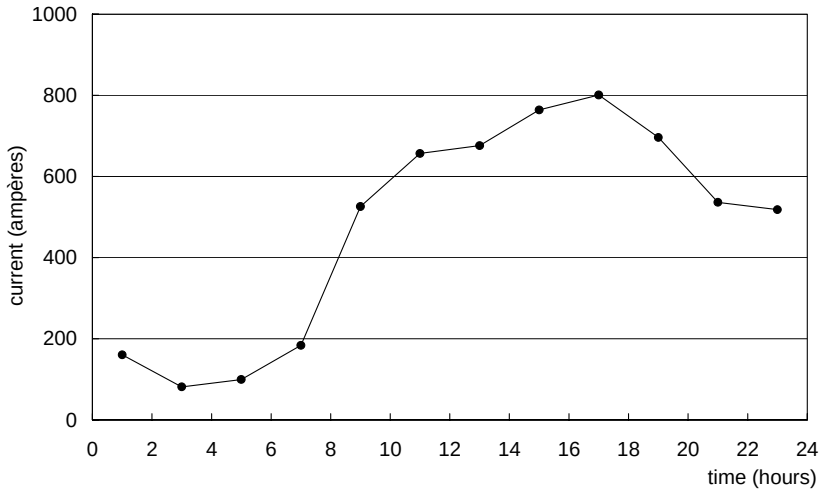


Figure 2 *Line load (two-hourly averaged current) of a typical 380 kV circuit on a typical day (July 7, 2003)*

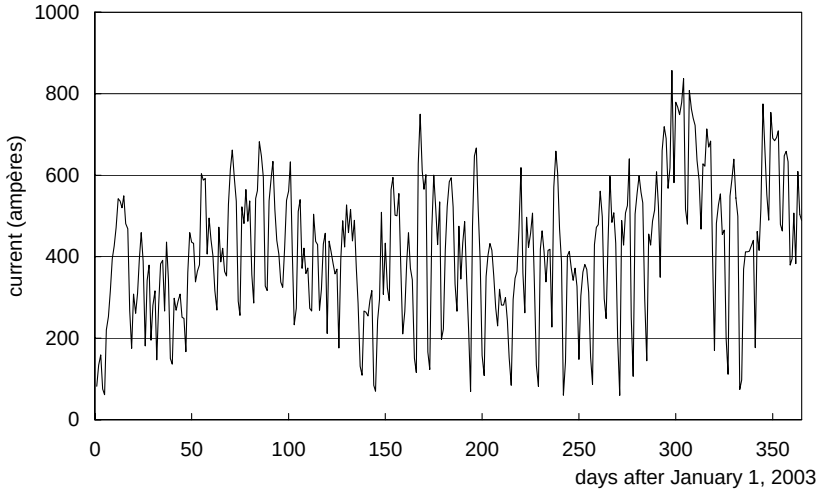


Figure 3 *Line load (daily averaged current) of a typical 380 kV circuit during 2003*

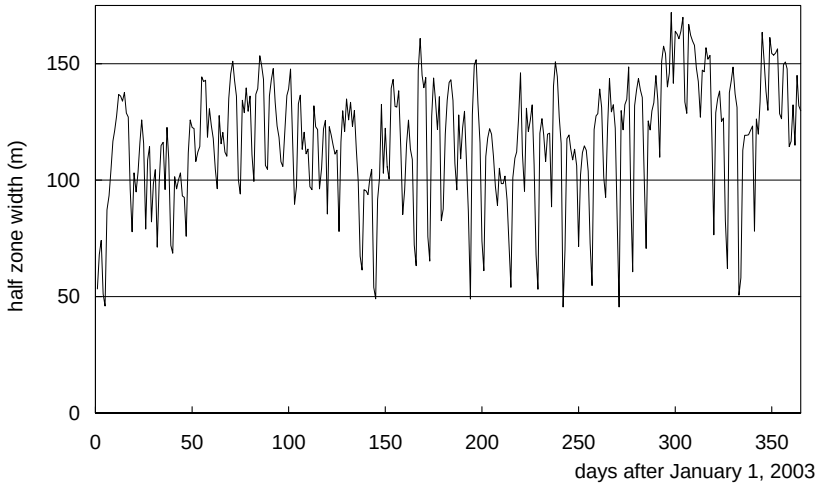


Figure 4 *Variation of the zone width for a typical 380 kV power line over the year 2003; the distance of the 0.4 microtesla contour to the heart of the power line was calculated based on the daily averaged current*

Estimating the representative current

A last, but crucial step, is to estimate the current used for the calculations of the magnetic field zone. In principle the actual yearly averaged current over the year 2003 could be used in this calculation for every power line. However, this approach does not account for the growing use of electricity, and the heavier line loads for the power lines expected in the coming decades. Calculating the width of the 0.4 microtesla zone on basis of the 2003 line load data would underestimate the width of the zone in the near future. Accounting for this growing use of electricity is one of the explicit requirements, as can be judged from the wording 'can become so in the future' added to the definition of the specific zone. In fact most power lines in the Netherlands are designed for heavier line loads than observed in 2003, and are likely to get loaded more heavily in the near future. All power lines have been designed for a maximum allowable line load, the so-called 'maximum design load'. This maximum design load is mainly determined by the cross-section of the conductors, the material (aluminium, copper) of the conductors, the surface treatment of the conductors, the ambient temperature and the wind speed. The maximum design load for a power line sets an absolute maximum to the width of the 0.4 microtesla zone. However, deriving the 0.4 microtesla zone directly from this maximum design load places a strain on the available land. Moreover, from the viewpoint of operational safety the maximum allowable yearly averaged load must be below the maximum design load.

To get an insight into the relationship between the yearly averaged load and the maximum design load the 'load fraction', defined as the yearly averaged line load divided by the maximum design load, was calculated for the year 2003. Load fractions for the 220 kV and 380 kV lines are plotted in Figure 5.

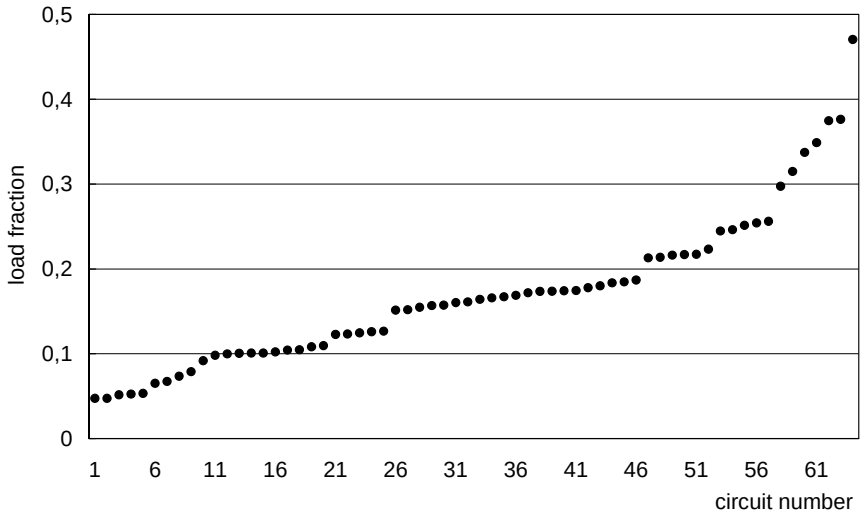


Figure 5 *Relative load of all 380 kV and 220 kV power lines: the load fraction is defined as the yearly averaged load (over 2003) divided by the maximum design load*

From Figure 5 it is evident that in 2003 these power lines were not heavily loaded. Averaged over all the 220 kV and 380 kV circuits the relative load is 0.17, and 90% of the circuits have a load fraction below 0.3. Based on this analysis the grid companies and the Ministry agreed to use a fraction of 30% of the maximum design load for the 220 kV and 380 kV power lines as yearly averaged load for the calculation of the specific 0.4 microtesla zone. For most power lines a load fraction of 30% will not be reached in the near future, and the calculated specific zone will maintain its validity during the next decades.

For the regional power lines (150 kV, 110 kV, 50 kV) a similar analysis could not be done because of the lack of sufficient data. For these lines a load fraction of 50% of the maximum design load was chosen as a 'worst case' estimate.

Time averaging the magnetic field

The epidemiological studies showing an association between the magnetic field and an increased risk for childhood leukaemia relate the leukaemia risk to magnetic field strength averaged over relatively long periods of time [3, 4]. Most studies measure the magnetic field in the dwelling, typically over a period of 24 hours. Other studies calculate the magnetic field in the dwelling, based on the yearly averaged current. From Figure 4, it can be concluded that averaging over a relatively short period may

lead to erroneous and divergent values for the magnetic field zone. For instance, averaging over a twenty-four-hour period in the beginning of January would result in a full zone width of 2 x 50 metres, whereas averaging over the same period in the beginning of November would yield a full zone width of 2 x 160 metres. In view of the epidemiological studies and the strong variation of the line load and zone width over the year the Ministry decided to base the power line policy on the yearly averaged magnetic field.

For practical purposes in calculating the width of the 0.4 microtesla zone, the yearly averaged current through the power line is estimated and with this current the width of the specific zone is calculated with one of the available software packages. For this calculation commercially-available software packages may be used. Although no comparative research into these software packages has been carried out yet, the packages used in the Netherlands[2] are regarded to yield equivalent results.

Comparison with the Swiss situation

In Switzerland precautionary emission limitations, so-called installation-limit values must be respected at places of sensitive use. For high-voltage power lines the installation limit value is 1 microtesla at the maximum rated current for the power line. In practical terms the 0.4 microtesla zone calculated at 30% of the maximum load (380 kV, 220 kV) or at 50% of the maximum load (150 kV, 110 kV, 50 kV) according to the Dutch guidelines leads to widths for the magnetic field zone that are nearly the same. For a typical 380 kV power line the 'Swiss' 1 microtesla zone is 2 x 77 metres, whereas the 'Dutch' 0.4 microtesla is 2 x 70 metres. For a typical 150 kV the 'Swiss'1 microtesla zone is 2 x 57 metres and the 'Dutch' 0.4 microtesla zone 2 x 65 metres. Starting from quite different viewpoints the Dutch and the Swiss policies lead to comparable magnetic-field zoning. Apart from this similarity there are a number of differences between the Swiss and the Dutch policies. The most striking are:

- the Swiss installation limit values have power of law and must be respected[3], whereas the Dutch policy only advises stakeholders to abandon certain activities in the 0.4 microtesla zone;
- the Dutch policy only applies to overhead power lines as sources of magnetic fields; in Switzerland the installation limit value of 1 microtesla also applies to magnetic fields generated by transformer stations, substations and switchyards; and
- the Swiss policy applies to a larger number of sensitive uses; in the Netherlands only dwellings, schools, crèches and day-care centres are designated as sensitive uses. The Swiss list of 'places of sensitive use' encompasses dwellings, schools, hospitals, playgrounds and permanent workplaces.

Discussion

Several European countries are considering a precautionary policy for overhead power lines. The basis for such a policy is the observed statistical association between childhood leukaemia and living near overhead power lines. The epidemiological studies suggest that the association holds for childhood leukaemia and long-term exposure to magnetic fields, although a causal relationship between leukaemia and magnetic fields has not been proven. According to the epidemiological data, a possibly elevated risk is observed at magnetic field strengths above a value somewhere between 0.2 and 0.5 microtesla. The Ministry of developed a precautionary power line policy. This policy is founded on a 0.4 microtesla zone, the value of 0.4 microtesla being a somewhat arbitrary choice within this 0.2 - 0.5 range. This value of 0.4 microtesla is often compared to the exposure limit of 100 microtesla for 50 Hz recommended by the European Union [19]. But in fact these two magnetic-field strengths are incommensurable. The recommendations of the European Union are derived from the International Commission on Non-Ionizing Radiation Protection and based on well-established short-term effects.

[2] In the Netherlands magnetic field calculations are based on EFC-400 (Program package developed by Forschungsgesellschaft für Energie und Umwelttechnologie: FGEU, GmbH, Berlin, Germany), CDEGS (Current Distribution, Electromagnetic Fields, Grounding and Soil Structure Analysis Program package developed by Safe Engineering Services & technologies ltd., Quebec, Canada) and ATP (Alternative Transient Program European EMTP-ATP Users Group (EEUG), Osnabrück, Germany). These software packages cannot directly calculate the width of the 0.4 microtesla zone, but calculate profiles for the magnetic field as a function of distance to the heart of the power line. To calculate the actual zone width these profiles need to be exported for further processing.

[3] Exemptions are granted if the line operator shows that all measures to limit radiation that are technically and operationally possible and economically acceptable have been taken.

The 0.4 microtesla, on the other hand comes from epidemiological evidence for a possible long-term effect.

Summary

In the Netherlands, a policy has been implemented to prevent new situations where children are exposed to magnetic fields due to overhead power lines. To achieve this goal municipalities and provinces are advised to avoid realisation of new sensitive uses (dwellings, schools, crèches and day-care centres) within the specific 0.4 microtesla zone. RIVM developed guidelines for the calculation of the 0.4 microtesla zone. This paper describes the choices that have been made in dialogue between the Ministry of Housing, Spatial Planning and the Environment, and the grid companies for the calculations of this specific 0.4 microtesla zone.

In accordance with the epidemiological studies, the specific 0.4 microtesla zone is based on a yearly averaged magnetic field. To calculate this yearly averaged magnetic field a ‘representative’ yearly averaged current through the power line has to be estimated. This representative current should reflect the present load of the power lines as well as the growth of the load expected during the coming decades. The growth potential for the load of a power line is set by the maximum design load and operational safety criteria. Analysis of the line loads during 2003 led, after careful consideration between the Ministry and the grid companies, to a choice for the representative load. For 380 kV and 220 kV the yearly averaged load is estimated as 30% of the maximum design load. For lack of data on the 150 kV, 110 kV and 50 kV overhead power lines, a ‘worst case’ estimate of the yearly averaged load is used: 50% of the maximum design load. Based on this representative load and location specific data on the power line section (type of pylons, number of circuits, phase conductor geometry and earthing) the specific 0.4 microtesla zone at a specific location can be calculated with commercially-available software.

References

1 Wertheimer N and Leeper E. Electrical wiring configurations and childhood cancer. Am. J. Epidemiol. 1979; 109(3):273-84.

2 Health Council of the Netherlands. ELF Electromagnetic Fields Committee. Exposure to electromagnetic fields (0 Hz - 10 MHz). The Hague: Health Council of the Netherlands. 2000; publication no. 2000/6 (in Dutch).

3 Ahlbom A, Day N, Feychting M et al. A pooled analysis of magnetic fields and childhood leukaemia. Br. J. Cancer. 2000; 83(5):692-8.

4 Greenland S, Sheppard AR, Kaune WT, Poole C, Kelsh MA. A pooled analysis of magnetic fields, wire codes, and childhood leukemia. Epidemiology. 2000; 11(6):624-34.

5 Van der Plas M, Houthuijs DJM, Dusseldorp A, Pennders RMJ and Pruppers MJM. Magnetic fields due to overhead power lines and leukaemia in children. RIVM report 610050007. RIVM, Bilthoven, 2001 (in Dutch with English abstract).

6 Pruppers MJM. 'Blootstelling aan extreem laag frequente elektromagnetische velden van hoogspanningslijnen' - Herberekening naar aanleiding van het KEMA/RIVM-onderzoek naar de kosten en baten van maatregelen ter beperking van magnetische velden bij hoogspanningslijnen. RIVM-briefrapport 032/2003. RIVM, Bilthoven, 2003 (in Dutch).

7 IARC Monographs on the Evaluation of Carcinogenic Risks to Humans Static and Extremely Low-Frequency Electric and Magnetic Fields, Vol. 80. IARC Press, Lyon, France 2002.

8 Draper G, Vincent T, Kroll ME and Swanson J. Childhood cancer in relation to distance from high voltage power lines in England and Wales: a case-control study. British Medical Journal. June 2005. Vol. 330 (7503): 1290-1295.

9 National environmental policy plan (NMP4). Chapter 10.1. Ministry of Housing, Spatial Planning and the Environment (VROM). The Hague, 2001 (in Dutch).

10 Kelfkens G, Pennders RMJ and Pruppers MJM. Dwellings near overhead power lines in the Netherlands. RIVM report 610150001. RIVM, Bilthoven, 2002 (in Dutch with English abstract).

11 Kelfkens G, Pennders R and Pruppers MJM. Planning new dwellings near overhead power lines, presented at the 6th International Congress of the European Bioelectromagnetics Association (EBEA), November 13-15 2003, Budapest, Hungary.

12 Kelfkens G, Pennders RMJ and Pruppers MJM. Planning new dwellings near overhead power lines. RIVM report 610150004 RIVM, Bilthoven, 2003 (in Dutch with English abstract).

13 Kelfkens G, Van Wolven J, Pennders RMJ, Stuurman C, Van Aernsbergen L, Delfini G and Pruppers M. Costs and benefits of the reduction of magnetic fields due to overhead power lines. Proceedings of the 2nd International Workshop on Biological Effects of Electromagnetic Fields, October 7 - 11 2002, Aldemar Paradise Royal Mare Hotel, Rhodes, Greece.

14 Ministry of Housing, Spatial Planning and the Environment (VROM). Nuchter omgaan met risico's. Beslissen met gevoel voor onzekerheden. (Coping Rationally with Risks) Document number 4016. The Hague, 2004 (in Dutch).

15 Policy letter with annexes sent by State Secretary of Housing, Spatial Planning and the Environment, P.L.B.A. van Geel, to Provincial and Municipal Executives and grid companies, October 3, 2005, reference SAS/2005183118

16 Letter from the Minister of Housing, Spatial Planning and the Environment, J.P. Pronk, to Mayor and Alderman of the city of Utrecht, November 13, 2001, reference SAS/2001140036.

17 Stuurman CS and Van Wolven JF. Kostenanalyse van de technische maatregelen ter beperking magnetische velden nabij bovengrondse hoogspanningslijnen (vooronderzoek), Deel 1: samenvatting, KEMA T&D consulting report no. 40130074-TDC 02-25766A, October 2002 (in Dutch).

18 Internet site: www.rivm.nl/hoogspanningslijnen (general site in Dutch) and http://milntj34.rivm.nl/website/lso/hoogspanningsnet/viewer.htm (Gridmap, with Dutch annotation).

19 Council Recommendation 1999/519/EC of 12 July 1999 on the limitation of exposure of the general public to electromagnetic fields (0 Hz to 300 GHz). Official Journal of the European Communities, L 197 of 30 July 1999; 59-70.

IMPLICATIONS OF THE NEW POLICY ON MAGNETIC FIELDS IN THE VICINITY OF HIGH-VOLTAGE POWER LINES IN THE NETHERLANDS

M.A.M. Beerlage, e-mail: monique.beerlage@kema.com
C.S. Stuurman, e-mail: claudi.stuurman@kema.com
J.F. van Wolven, e-mail: jos.vanwolven@kema.com

KEMA Nederland BV, PO Box 9035, 6800 ET, Arnhem, The Netherlands

ABSTRACT

The Council of the European Union has made recommendations to its member states regarding specific actions on magnetic field exposure of the general public [1]. These recommendations are based on the reference values by ICNIRP, published in 1998 [2].

In the year 2000 two pooled analyses were published, both dedicated to epidemiological studies on the incidence of leukaemia among children living in the vicinity of overhead power lines. Especially the paper by Ahlbom c.s. [3] was and still is giving rise to a lot of concern for governments, as well as for many people living close to overhead power lines.

In the past few years, the Dutch government has initiated additional research, based on the assumption (consistent with the conclusion of Ahlbom c.s. [3]) that the leukaemia risk indeed increases twofold for children with a long-term mean exposure to magnetic field strengths higher than 0,4 μT, originating from overhead high-voltage power lines [4]. This research contained investigations of e.g.:

- the number of "extra" children that may develop leukaemia due to the presence of overhead high-voltage power lines each year in The Netherlands (i.e. 0.5 per year)
- the number of Dutch dwellings situated within the zones around high-voltage power lines with long-term magnetic field strengths > 0,4 μT, at present (i.e. 23.000 in 2003) and in the future (i.e. 33.000 in 2028)
- implementation costs of field reducing measures, on a national scale.

Consequentially, the Dutch government has published new recommendations for municipal executives, other local authorities and grid operators in October 2005 [5]. This advice is based on the recommendations of the European Council as mentioned above, but with the addition of some important precautionary measures: for new situations in the vicinity of overhead high-voltage power lines the government recommends to prevent that children experience long-term exposure to magnetic fields, with annually averaged field strengths higher than 0,4 μT.

As an aid to local authorities and grid operators, magnetic field zoning around high-voltage power lines has been introduced. Two types of zones have been defined:

- an indicative magnetic field zone: a rough estimate of the zone, based on known indicators for Dutch high-voltage power lines in general
- a specific zone: a more accurate calculated estimate of the zone, based on actual phase configurations and electrical current of the high-voltage power line.

The recommendations are accompanied by a set of guidelines to calculate the specific magnetic field zone, as a surrogate for the "long-term mean magnetic field" of a Dutch high-voltage power line [6].

During the past few months, municipal executives, local authorities and grid operators have been managing this new Dutch policy on power lines. They have initiated or already performed several practical solutions to meet the recommendations. These solutions can be based mainly on two principles:

- reduction of the magnetic field by technical measures
- reduction of the exposure by revision of new housing development plans.

During the presentation, several implications and consequences of the Dutch recommendations for local authorities, grid operators, as well as for the general public will be discussed. This will be illustrated by presenting some examples of practical solutions.

References

[1] The Council of the European Union (1999). Council recommendation of 12 july 1999 on the limitation of exposure of the general public to electromagnetic fields (0 Hz to 300 GHz). In: Official Journal of the European Communities, L 199/59 (1999/519/EC)

[2] ICNIRP (1998). Guidelines for Limiting Exposure to Time-Varying Electric, Magnetic, and Electromagnetic Fields (up to 300 GHz). In: Health Physics, vol. 74, pp. 494-522

[3] A. Ahlbom et al (2000). A pooled analysis of magnetic fields and childhood leukaemia. In: British Journal of Cancer, vol. 83, pp. 692-698

[4] Several reports are available (in Dutch language) on the website of the Dutch Ministry of Spatial Planning, Housing and the Environment: www.vrom.nl

[5] P.B.L.A. van Geel (State Secretary of Housing, Spatial Planning and the Environment) (2005). Recommendations with regard to overhead high-voltage power lines. Letter dated on October 3rd, SAS/2005183118 (also on www.vrom.nl)

[6] G. Kelfkens and M.J.M. Pruppers (2005). Guidelines for the calculation of the specific 0.4 microtesla zone in the vicinity of overhead high-voltage power lines. RIVM, appendix to [5] (also on www.vrom.nl)

The German Mobile Telecommunication Research Programme (DMF)

Cornelia Baldermann [(1)], Gunde Ziegelberger [(1)] , Blanka Pophof [(1)]

[(1)] Federal Office for Radiation Protection
Ingolstädter Landstraße 1, D-85764 Oberschleißheim, Germany, cbaldermann@bfs.de

Abstract

The purpose of this paper is to introduce the current state of the German Mobile Telecommunication Research Programme (DMF). The Programme was initiated by the German Federal Ministry for the Environment, Nature Conservation and Nuclear Safety (BMU) and is performed by the Federal Office for Radiation Protection (BfS). In the period from 2002 to 2007 a total of 51 research projects in mobile telecommunications are proceeded in four fields: biology, dosimetry, epidemiology and risk communication. The total financial volume of the program is 17 million €. Final results of the programme are expected at the end of 2007.

Keywords: high frequency electromagnetic fields; mobile communication, health impact, research programme, Germany

1 Introduction

High frequency electromagnetic fields such as those found, for example, near transmitters (e.g. radio frequency towers and mobile telephone base stations) or when using mobile end devices (cell phones) are often suspected by the public of having adverse health effects on human. There is some indication that such electromagnetic fields can cause biological or physiological effects at levels below international limit values. In which extent they pose a health risk to the general public can´t be completely determined at this time.
The German Mobile Telecommunication Research Programme (DMF) was initiated by the German Federal Ministry for the Environment, Nature Conservation and Nuclear Safety (BMU) and the Federal Office for Radiation Protection (BfS) to take part in the international efforts clarifying the above question. The total financial volume of the program is 17 million €, appropriated half by half by the BMU and the network providers. Coordination and implementation is carried out by the BfS. The research projects chosen for the program are based on the findings of two expert workshops in 2001 and 2003 in Berlin and additional comments expressed by the general public. The first preliminary results were presented in April 2005 at a public expert workshop.
Detailed information on the single projects can be found on the DMF website http://www.emf-forschungsprogramm.de/. Project descriptions, current results and workshop results are presented. Regular reports on the state of the research projects can be found on this web-site. The researcher's Final Report together with an evaluative statement by the BfS will be made available to the public at the conclusion of every project. Further general information on electromagnetic fields and cellular telecommunication can be found on the BfS websites under http://www.bfs.de/.

2 Research Projects

In the period from 2002 to 2007 51 research projects in mobile telecommunications are realized in four scientific fields: biology, dosimetry, epidemiology and risk communication. With state of Oktober 2006 23 of them are already finished, the remaining will be completed within 2006 and 2007. The topics cover a broad spectrum, reaching beyond current GSM and UMTS standards. One objective, among others, is to clarify fundamental effects and mechanisms. Another will be to delve into the possible causes of electromagnetic sensitivity. The programme will seek results pertinent not only to existing mobile telecommunications but in order to make statements on future developments as well.

2.1 Biology

The 23 projects investigating possible biological and effect and health consequences of high frequency electromagnetic fields cover about 56 % of the financial volume of the DMF. Four projects are already completed. It could be shown, that a life-long exposure with GSM and UMTS signals does not influence the survival and the incidence of lymphoma in a genetically modified mice stock especially susceptible to lymphoma (AKR-mice). Though, the hypothesis, that chronic exposure to high frequency electromagnetic fields promote neoplastic development in the hematopoietic system in genetically predisposed mice was not supported. The "melatonin hypothesis", claiming that ELF as well as HF electromagnetic fields result in decreased melatonin levels, could not be confirmed during investigations on explanted pineal organs of hamster. A feasibility studies was successfully finished and made it possible to start investigations on the age dependence of the action of HF EMF. A study on the sleep quality of population living close to mobile phone base stations started as well.

2.2 Dosimetry

13 projects, covering about 14 % of the total financial volume of the DMF, are concerned with dosimetry and exposure assessment, eleven of them are already finished. The topics cover on the one hand the field distribution around transmitters and far-field exposure of the population by mobile phone base stations, WLAN transmitters, transmitters of the digital TV, etc. On the other hand, near-field scenarios are investigated predominantly by modelling the indoor field distribution in homes, offices, shielded rooms, etc. SAR and temperature variations in the heads and trunks of persons using mobile communication devices are determined. The SAR distribution in experimental animals was investigated as well. Investigations of the real exposure due to daily use of mobile phones have shown, that GSM-mobile phones regulate quite often to the maximum transmission power, predominantly as a result of frequent handovers and poor signal quality, and cause therefore correspondingly high SAR-values in the heads of the user. The different regulatory mode of UMTS-mobiles results in drastically reduced exposure of the user by a factor of about 1000. Determination of human exposure caused by indoor wireless communication technologies applied in homes and offices showed that in general the exposure values lay far below the prescriptive limits. Another study analysed the exposure from transmitters worn near the trunk of the body. In generic and anatomical models was revealed that under far-field-like conditions standing waves can develop, and a rise of the SAR value specifically in the skin was determined. The limit values were not exceeded. In near-field-like conditions standing waves do not arise. Although the temperature rise due to HF exposure was calculated. With free convection a maximum of 0.8 ^{o}C was determined. Using anatomical models the values determined are up to 0.31 ^{o}C at the body surface. The temperature rise determined under these conditions for the internal organs is negligible as long as the SAR limit values are kept. A project concerning the exposure of the head has shown that the temperature increase in the skin. This is caused more by the heat accumulation under the phone than by the radiation. The temperature increase within the skull (brain, pineal, inner ear) was up to 0.01 °C. One project concerned determination of exposure to the population living near digital radio and television transmitters. The measurements in Bavaria before and after introduction of the digital transmitters showed an increasing of mean exposure in the areas with "portable indoor" coverage around the transmitter sites caused by the introduction of DVB-T.

2.3 Epidemiology

Eight epidemiological projects are performed covering about 19 % of the financial volume of the DMF. Four projects are already finished. A feasibility study has shown, that an occupational cohort study on persons highly exposed to HF EMFs cannot be performed due to a lack of a highly exposed cohort of an acceptable size and without conflicting confounders. Furthermore, the feasibility of a prospective cohort study on handy users failed because of a response rate of only 5 %. The effort necessary to recruit a sufficient number of participants would be enormous and is not practicable within the DMF. The German part of INTERPHONE study is finished, the results of the evaluation of the internationally pooled data are expected in 2006. According to preliminary national results, there seems to be no increased risk for brain cancer due to a regular handy usage for up to 10 years. Two epidemiological studies on children are just starting – one investigating childhood leukemia around powerful radio and TV transmitters, another concentrating on health effects in the vicinity of mobile phone base stations. In the later one, personal dosimeters will be used to assess the exposure.

2.4 Risk Communication

Seven projects are concerned with risk perception and some other social aspects of mobile communications, covering about 9 % of the financial volume of the DMF. Yet, four projects are already finished. The analysis of target groups for differentiated information showed, that different population groups are differentially worried about possible health effects of electromagnetic fields. The results of the project “Examination of the knowledge and effects of information activities in the field of mobile telecommunications and determination of further approaches to improve information of different population groups” gained from the focus groups and the mobile phone survey in 2005 illustrate the importance of differentiating between target groups. The essential differences but also potential similarities between the views of the different citizens’ groups and the experts have become apparent. The quantitative and qualitative survey performed in the framework of the project “Supplementary information about electromagnetic hypersensitive persons” provide more detailed findings of persons who see the origin of certain physical disorders in the existence of electric, magnetic or electromagnetic fields (EMF). According to the working definition, this group is considered as electrosensitive persons. The study also reveals, however, that only a small part of this group declares themselves to be "electrosensitive". The important factor is rather their handling and/or the significance of "radiation" in the context of their everyday lives, irrespective of terms and definitions. The findings obtained are an important basis for improving the communication with people who feel impaired. They also help to adapt the way information is offered to the particular needs of this group of people.

3 Summery

A large portion of the projects will be finished in 2006 and 2007. To provide a scientific evaluation of all results of the German Mobile Telecommunication Research Programme (DMF) in the international context, single thematic topics will be presented internationally in scientific workshops and discussed with national and international experts. First, the workshop with the topic “dosimetry” was proceeded in July 2006. The next workshop with the topic “risk communication” will take place at October 2006. The biological and epidemiological projects are combined in three workshops with the topics “Acute health effects” (December 2006) as well as “Action mechanism” and “Long-time health effects” in 2007.
A final evaluation of the combined national and international research on the health effects of high frequency electromagnetic fields within and outside of DMF is planned in the form of an international scientific conference, together with international experts and the WHO. The results will be presented in a final national expert workshop at the end of 2007 and will be the base for a re-evaluation of the limits.

4 Appendix: Projects of the DMF

4.1 Biology

Completed

- Feasibility study on age dependent effects of RF electromagnetic fields on the basis of relevant biophysical and biological parameters
- Investigation of mechanisms of action in cells exposed to the high frequency electromagnetic fields of mobile telephone technology. B. Pineal gland
- Influence of low and high frequency electromagnetic fields on spontaneous leukaemia in AKR/J mice
- *in vivo* experiments on exposure to the high frequency electromagnetic fields of mobile telecommunication. B. carcinogenesis

Assigned – results in 2006 and 2007

- Investigation of mechanisms of action in cells exposed to the high frequency electromagnetic fields of mobile telephone technology. A. Demodulation / communication
- Investigation of mechanisms of action in cells exposed to the high frequency electromagnetic fields of mobile telephone technology. C. Functions
- *in vivo* experiments on exposure to the high frequency fields of mobile telecommunication. A. Long-term study
- *in vitro* experiments on exposure to the high frequency fields of mobile telecommunications. C. Blood-brain barrier
- Influence of mobile telecommunication fields on the permeability of the blood-brain barrier in laboratory rodents (*in vivo*)
- Influence of high frequency electromagnetic fields of mobile telecommunications on sensory organs. A. The auditory system
- Possible influence of high frequency electromagnetic fields of mobile communication systems on the induction and course of phantom auditory experience (tinnitus)
- Influence of high frequency electromagnetic fields of mobile telecommunications on sensory organs. B. The visual system
- Possible genotoxic effects of GSM signals on isolated human blood
- Influence of GSM signals on isolated human blood. B. differential gene expression
- Long-term study on the effects of UMTS signals on laboratory rodents
- Influence of high frequency electromagnetic fields of mobile telecommunications on the metabolic rate in laboratory rodents
- Investigation of age-dependent effects of high frequency electromagnetic fields based on relevant biophysical and biological parameters
- Investigation of sleep quality in persons living near a mobile base station - Experimental study on the evaluation of possible psychological and physiological effects under residential conditions
- Investigation of sleep quality of electrohypersensitive persons living near base stations under residential conditions
- Studies of the effects of exposure to electromagnetic fields emitted from mobile phones on volunteers
- Investigation of the phenomenon of 'electromagnetic hypersensitivity' using an epidemiological study on 'electrosensitive' patients including the determination of clinical parameters
- Investigation of electrosensitive persons with regard to accompanying factors or diseases, such as allergies and increased exposure or sensitivity to heavy metals and chemicals
- Influence of HF-EMF of mobile communications on the metabolic rate in an animal model (laboratory rodents)

4.2 Dosimetry

Completed

- Investigation of SAR distribution in laboratory animals exposed to electromagnetic fields
- Development of measurement and calculation methods for the determination of the public exposure due to electromagnetic fields in the vicinity of mobile phone base stations
- Determination of the exposure of groups of people that will be investigated within the scope of the project 'Cross-sectional study for ascertainment and assessment of possible adverse effects by the fields of mobile phone base stations'
- Determination of human exposure caused by indoor wireless communication technologies applied in homes and offices
- Determination of the specific absorption rate (SAR values) occurring during day-to-day mobile phone use
- Exposure from transmitters worn near the trunk of the body
- Determination of exposure distribution from high frequency fields in the human body with regard to small structures and relevant thermo-physiological parameters
- Determination of the real field distribution of high frequency electromagnetic fields near wireless LAN installations (WLAN) in inner cities
- Determination of the real field distribution from high frequency electromagnetic fields near UMTS transmitters
- Determination of the real exposure from using mobile phones in partially shielded rooms as compared to exposure under optimal conditions outdoors
- Determination of exposure to the population living near digital radio and television transmitters

Assigned – results in 2006

- Investigation of the validity of macroscopic dielectric tissue properties at cellular and subcellular level
- Determination of exposure by ultra-wideband-technolgies

4.3 Epidemiology

Completed

- Feasibility study for a cohort study: the cohort study should investigate highly exposed (occupational) groups to estimate the risk associated with high frequency electromagnetic fields.
- Feasibility study for a prospective cohort study on mobile phone users
- Extension of an international epidemiological study on the association between high-frequency electromagnetic fields and the risk of brain cancer (INTERPHONE)
- Addendum to a case control study on uveal melanoma and radio frequency radiation (RIFA Study)

Assigned – results in 2006 and 2007

- Cross-sectional study to record and evaluate possible adverse health effects due to electromagnetic fields from cell-phone base stations
- Addendum to the cross-sectional study on acute health effects caused by fields of mobile phone base stations
- Epidemiological study on childhood cancer and proximity to radio and television transmitters
- Acute health effects by mobile telecommunication among children

4.4 Risk Communication

Completed

- Knowledge-based database of literature describing the effects of electromagnetic fields on the organism and implants
- Analysis of target groups for differentiated information
- Supplementary information about electromagnetic hypersensitive persons
- Examination of the knowledge and effects of information activities in the field of mobile telecommunications and determination of further approaches to improve information of different population groups

Assigned – results in 2006

- Identifying the general public's fears and anxieties with regard to the possible risks of high frequency electromagnetic fields of mobile telecommunications (annual survey)
- Innovative methods of conflict mediation when determining the location for mobile phone base stations
- Support of the cooperation of the mobile telecommunication players by the local agenda 21

Reflection and Absorption Characteristics of Human body at Millimeter Wave

Naoyuki YAMADA[†] **Masahiro HANAZAWA**[††] **Soichi WATANABE**[††]

Koji SUZUKI[†††] **Setsuo TOKORO**[†††]

[†]*Toyota Central Research and Development Laboratories, Inc.*
[††]*National Institute of Information and Communications Technology*
[†††]*Toyota Motor Corporation*

E-mail: [†]yamada@mosk.tytlabs.co.jp, [††]hana@nict.go.jp, [††]wata@nict.go.jp,
[†††]koji@suzuki.tec.toyota.co.jp, [†††]tokoro@setsuo.tec.toyota.co.jp

Abstract

A traffic accident by a car becomes a social problem all over the world. Therefore, the requirement for safety system of a car is increasing. In Japan, there are many car accidents with pedestrian, a performance enhancement of the pedestrian detection with an in-vehicle sensor such as millimeter wave radars is demanded. In this report, we were aimed for construction of a human body electromagnetic phantom for millimeter wave, we derived a reflection and an absorption characteristic in the human body by an experiment. As a result, the reflection coefficient (S11) when we irradiated a millimeter wave on the human body surface was about -5dB. In addition, we measured a transmission coefficient (S21) of meat for the purpose of evaluating an absorption characteristic in the human body of millimeter wave. As a result, we understood that most of electricity was absorbed within around 2mm by the surface. Based on these results, we developed a human body phantom for automotive radar designs.

1. Introduction

A traffic accident by a car becomes a social problem all over the world. Therefore, the requirement for safety system, such as the Forward Collision Avoidance Assistance System (FCAAS), has been increasing. The radar sensor of such a safety system has to be capable of detecting not only other vehicles but also pedestrians, bicycles, and roadside objects [1]. Furthermore, such a safety system should be able to make a decision without any mistake as to whether a collision occurs. Therefore, the radar sensor must be capable of detecting objects immediately before a collision would otherwise occur. The development of a radar sensor for safety system requires that we know the radio wave reflection characteristics, such as the average value of the radio wave reflection intensity, of an object relatively close to the sensor, as well as the range of fluctuation. That is, if the radio wave reflection characteristics of objects are known, the performance of a safety system using a radar sensor can be refined.

In this paper, we evaluated a reflection and an absorption characteristic when a millimeter wave was irradiated by the human body by an experiment. In addition, we evaluated a reflection and an absorption characteristic for the wearing cloths quantitatively.

2. Measurement method

2.1 Reflection characteristic

We measured a millimeter wave reflection characteristic in the human body surface by free space method (figure 1). In this method, we set a calibration plane in the back side of the acrylic board which is fixed at a position of 0.27m by a lens antenna. Then, a reflection characteristic of a forearm part is measured by a network

analyzer accurately. When it measures a millimeter wave reflection from the human body, it is a problem to suppress a fluctuation of the reflection depended on movement of a body. However, the high precision measurement is possible by pushing an arm to an acrylic board. This measurement frequency range is 75GHz - 110GHz.

2.2 Absorption characteristic

It is difficult to measure a millimeter wave absorption characteristic in a body tissue directly, so we measured it by the following method. At first, we measure a complex permittivity of the human body surface by a coaxial probe method. Then, we measure the complex permittivity of meat (chicken, a chicken cuticle, pork, etc.) of some thickness. We measure a transmission characteristic of meat by free space method. So, the absorption characteristic of millimeter wave in the human body is derived equivalently.

3. Measurement result

3.1 Reflection characteristic

Figure 2 shows a millimeter wave reflection characteristic of a forearm part of four persons (30-40 generations). Although there was some difference in a value by frequency, the reflection characteristic was almost -5dB to -4dB. The difference by a person was small with less than 1dB. From this result, It understand that 30% of millimeter wave incidence energy reflect in an incidence direction in the human body surface

3.2 Absorption characteristic

Figure 3 shows the complex permittivity of the human body surface by a coaxial probe method. In this coaxial probe method, only a characteristic up to 50GHz is provided precisely, so the complex permittivity more than 50GHz estimated by extrapolation. As a result, the complex permittivity (real part) of the human body surface at 70GHz was 3 to 4. Figure 4 shows the complex permittivity of the meat (pork) by a coaxial probe method. The complex permittivity of a fat and a muscle at 70GHz was 4 and 7 respectively. In addition, compare with the complex permittivity of the human body surface, fat characteristic was near to the human body surface one. Transmission characteristics of several kinds of meat are shown in figure 5. The transmission characteristic was about -10dB at thickness 0.3mm, and it was about -60dB more than thickness 3mm. When a millimeter wave was irradiated by the human body, about 30% of electric power was reflected and other electric power was absorbed at less than 2mm by the surface of human body. From these results, it is thought that a millimeter wave reflection in the human body has little influence of inside composition. In addition, this experiment result accords with an analysis result by FD-TD method very well.

4. Reflection and transmission characteristic of clothes

It is thought that a millimeter wave reflection and absorption characteristic of the person who wore clothes is different from the state that does not wear clothes. In this chapter, we evaluated a millimeter wave reflection and transmission characteristic of clothes by an experiment. Same as the measurement of a reflection and transmission characteristic of the human body and meat, we applied free space method. Table 1 shows measurement results. Average values of reflection and transmission characteristics from 75GHz to 110GHz are shown in this table. From these results, the reflection characteristics were -13dB to -30dB, and the transmission characteristics were -0.1dB to -0.8dB. The transmission losses in one piece of cloth were less than 1dB. There were less transmission losses of chemical fiber materials such as polyester than a loss of cotton materials.

Furthermore, we performed the measurement that assumed wearing clothes one over another. As a result of three pieces of cloth (No.2, No.3 and No.4), the reflection and transmission characteristics were -13.2dB, -1.51dB respectively. A reflection characteristic depends on cloth of large reflectance, and a transmission characteristic is almost a total of each transmission characteristic. When we examine a millimeter wave reflection and absorption characteristic of pedestrian of a wearing clothes, we have to consider these influence.

5. Conclusion

We evaluated a reflection and absorption characteristic experimentally when a millimeter wave was irradiated by the human body. In addition, we evaluated a reflection and transmission characteristic of cloth used for

wearing clothes in the same way.

When a millimeter wave was irradiated by the human body, about 30% of electric power was reflected and other electric power was absorbed at less than 2mm by the surface of human body. Furthermore, the reflection characteristics of clothes were -13dB to -30dB, and the transmission characteristics were -0.1dB to -0.8dB.
Based on these results, we developed a human body phantom for automotive radar designs and development of millimeter wave radar for pedestrian detection.

REFERENCES

[1] S. Ohshima, Y. Asano and K. Nishikawa, "A Method for Accomplishing Accurate RCS Image in Compact Range", IEICE Trans. Commun., E79-B-12(1996), 1799-1805

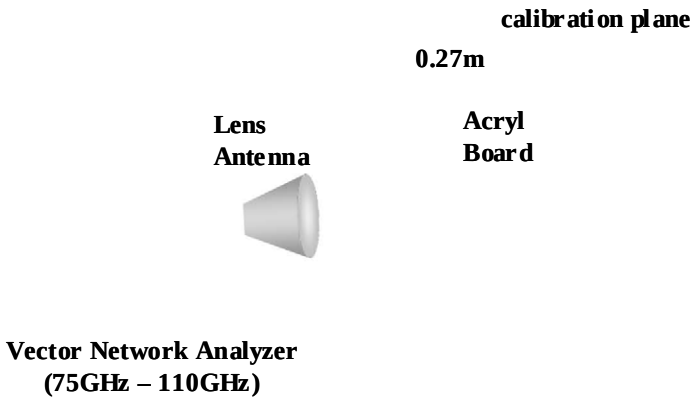


Fig. 1 reflection characteristic measurement method (A human body forearm part)

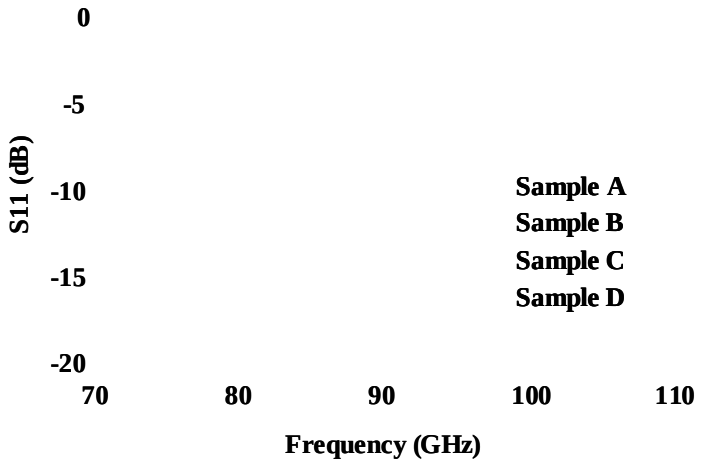


Fig. 2 reflection characteristic measurement result (A human body forearm part)

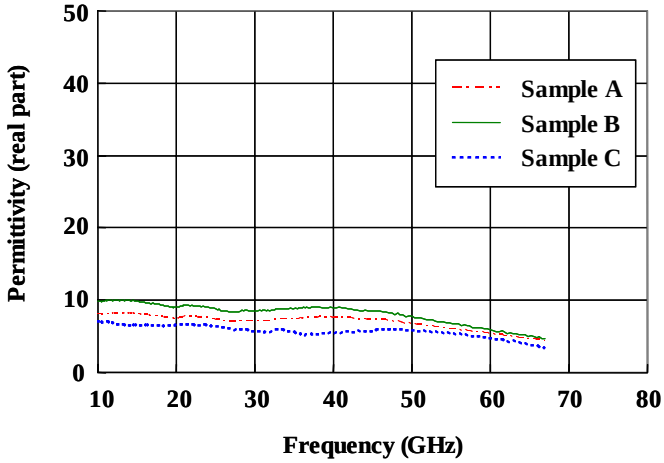


Fig. 3 permittivity of the human body surface

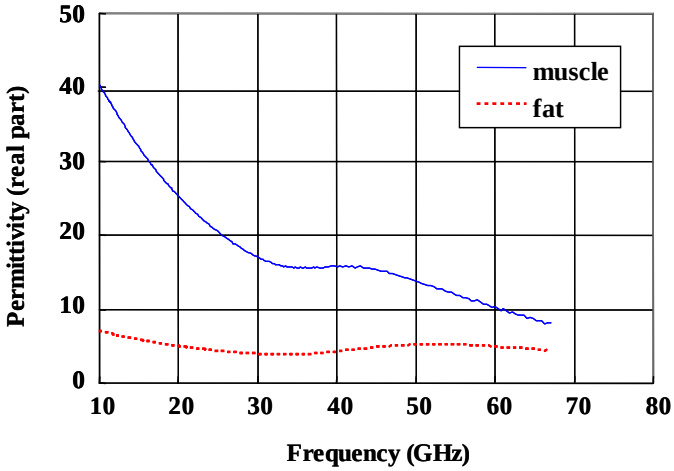


Fig. 4 permittivity of the pork

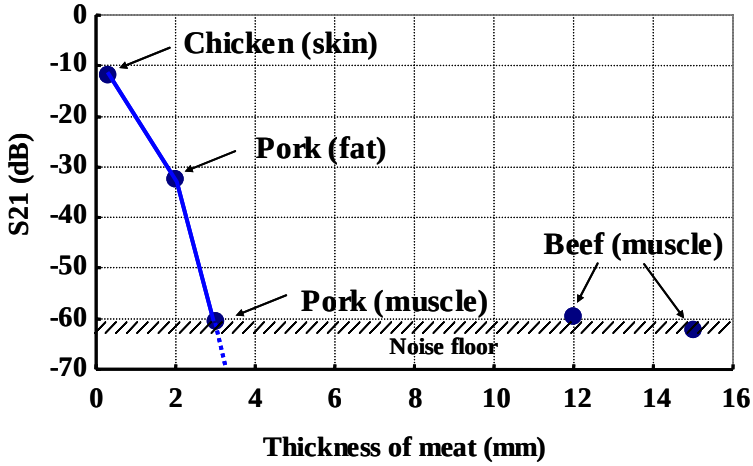


Fig. 5 transmission characteristic for thickness of meat

Table.1 reflection and transmission characteristic measurement result of various cloth

	material	s11(dB)	s21(dB)
No.1	polyester:50%, acryl:30%, cotton:20%	-26.5	-0.18
No.2	polyester:65%, cotton:35%	-18.3	-0.36
No.3	cotton:100%	-17.2	-0.77
No.4	cotton:95%, polyurethane:5%	-13.8	-0.79
No.5	polyester:100%	-27.4	-0.46
No.6	acryl:80%, nylon:20%	-30.1	-0.28
No.7	polyester:100%	-22.9	-0.21
No.8	polyester:100%	-17.8	-0.26
No.9	polyester:100%	-23.7	-0.11
No.10	acryl:85%, wool:15%	-23.3	-0.3
No.11	cotton:98%, polyurethane:2%	-19.4	-0.79

ELECTROMAGNETIC INDUCTION THROUGH THE BIOLOGICAL TISSUE

N. M. SALEM

DEPT. OF ENGINEERING PHYSICS, FACULTY OF ENGINEERING, CAIRO UNIVERSITY, EGYPT

Abstract

The study of the BIA has firstly been introduced as an effective tool to assess many of the biological and biochemical activities of the body. Due to the ubiquitous exposure to electromagnetic waves in our environment and the recent extensive use of mobile handsets, another trend appeared to exploit the BIA, namely its relation to electromagnetic absorption of the body especially in terms of its frequency dependence and the possible ability of power attenuation. In the present study we concentrate on the biological impedance of the body when subjected to high frequency and low energy microwaves. Full mathematical analysis is introduced to examine the fraction of power transmitted via the body impedance and the possible wave shape delay or distortion of the incident wave.

Introduction

Perhaps the term bioelectrical impedance analysis (BIA) was first introduced in 1940's [1], to assess the induced changes in hydration status as it is related to the total body changes in resistance and capacitive reactance. BIA was also associated with the dynamic changes in pulsatile blood flow to organs, arterial pulse waveforms and respiration [2]. The applications of impedance plethysmography, to detect dynamic blood volume changes, have been widely confirmed by numerous research workers [3-6].

The significant correlation between total body water (TBW) and the BIA has been reported by hundreds of peer reviewed papers [4,7,8].

Measurement of the electrical impedance of biological tissue in vitro and in vivo has entered into several prominent classes of biological research and biomedical applications. More than half a century ago, Fricke [9], then followed by Cole and Curtis [10], have measured the electrical self-impedance of a variety of cell and tissue systems; these measurements were made across a large spectrum of frequencies ranging from the audio to the high radio frequencies. Their results were studied in the usual impedance domain of resistance and reactance rather than in the electrically equivalent admittance domain of conductance and susceptance, thus a series of organized circuit models were obtained.

Most of the body tissue contains large amounts of water and conducting electrolytes, and represents a low resistance electrical pathway; hence the resistance is indirectly related to the extracellular mass. This equivalent electric resistance has conductivity σ. Also the body tissue has an equivalent electric capacitance which reflects the ability of the tissue to store electrical energy. This reactance originates from the cell membrane that consists of two conductive layers of protein molecules having a nonconductive lipid material of relative permittivity ε_r . The dielectric constant of the biological tissue is anisotropic and frequency dependent. The reactance is a measure of the volume of cell membrane capacitance and an indirect measure of the intracellular volume or body cell mass.

In the present work the emphasis is on the dependence of the BIA on the frequency particularly in the microwave region. Moreover, the power attenuation through a biological tissue is examined.

Models for the equivalent biological circuit

Different models have been put forward to describe the human body. As of yet, there is no consensus on the equivalent biological circuit that will serve all purposes.

The basic concept of the proposed models depends on the assumption that human tissues can be treated as a set of resistors and capacitors connected together in series or in parallel. Two effective simple models of the skin barrier will be assumed. Firstly, Model A consists of a capacitor and resistor connected together in series, where the resistor represents the input ohmic impedance of the rest of the body. Secondly, Model B consists of a capacitor and a resistor connected in parallel, and all the rest of the human body may be represented by an ohmic resistor, R_2, which represents the input impedance of the body. The electromagnetic wave enters as V_{in} and the induced wave is represented by V_{out}. The capacitor in Model A, and the parallel combination in Model B represent the skin barrier.

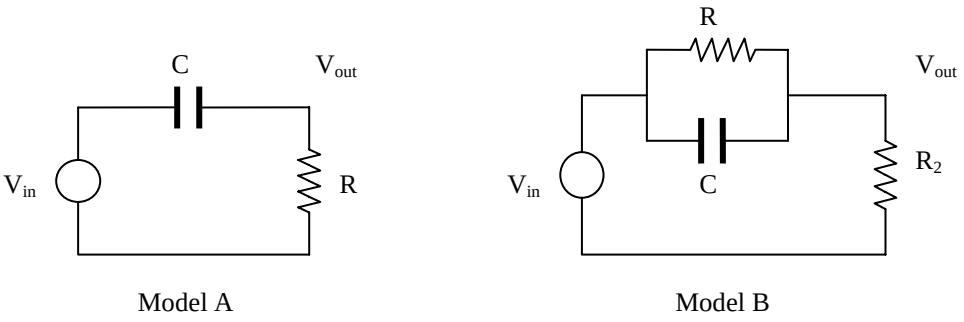


Fig. 1. Two bioelectric equivalent circuits, Models A and B, respectively.

We investigate two assumptions: firstly that the dielectric constant of either model is frequency independent and secondly, as it should, a function of the incident frequency. The particular treatment in the present work considers that the tissue is subjected to pulsating microwaves that are emitted from sources like mobile network antenna or mobile handsets.

Mathematical Analysis

Typically, for mobile communication, the incident wave comprises pulses of sinusoidal waves. The frequency of the pulses is around 100 KHz, while that of the sinusoidal waves is of the order of GHz. The pulses may be considered as square waves of periodic time *T*. For the first period the square wave is nonzero in the region $-T_1 \le t \le T_1$ where its value is unity. The sinusoidal wave may be simply represented by $V_o \cos(m\omega_o t)$, where $\omega_0 = \dfrac{2\pi}{T}$ is the angular frequency of the square wave, while $m\omega_0$ is the angular frequency of the sinusoidal wave; V_o is the amplitude of the incident signal. Therefore the input signal may be considered as the direct multiplication of the square and sinusoidal functions and is given by

$$V_{in}(t) = \begin{cases} V_o \cos(m\omega_o t) & -T_1 \le t \le T_1 \\ 0 & T_1 \le t \le T - T_1 \end{cases}$$

The input signal is illustrated in Fig. 2. $V_{\text{in}}(t)$ is then represented as a Fourier series [11] such that

$$V_{\text{in}}(t) = \sum_{k=-\infty}^{\infty} c_k \, \mathrm{e}^{jk\omega_0 t}$$

The Fourier coefficients c_k are evaluated; to elaborate

$$c_k = \frac{1}{T}\int_T V_{in}(t)\mathrm{e}^{-jk\omega_0 t}dt = \frac{V_0}{T\omega_0}\left\{\frac{\sin(k+m)\omega_0 T_1}{(k+m)} + \frac{\sin(k-m)\omega_0 T_1}{(k-m)}\right\}$$

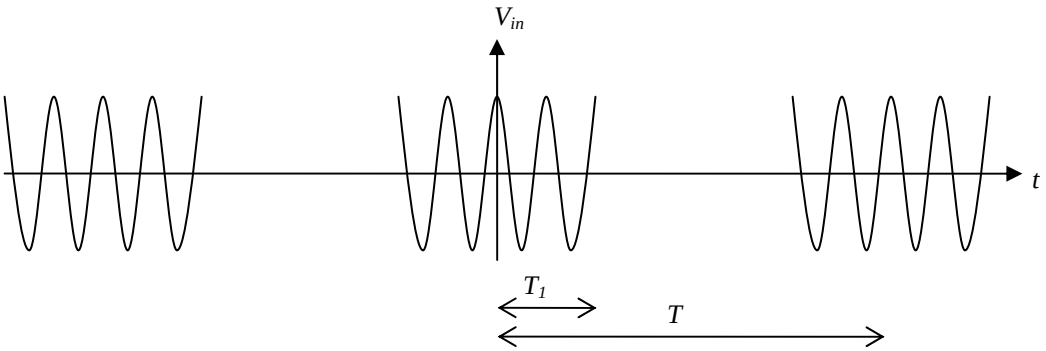


Fig. 2. The input singnal.

As soon as the signal is converted into its Fourier series and the coefficients are obtained for each harmonic component, each frequency may be treated separately such that $V_{\text{in}}(k\,\omega_0) = c_k$. The output signal, V_{out}, is calculated by standard circuit analysis; namely

$$V_{\text{out}}(\omega) = \frac{R}{Z(\omega)} V_{\text{in}}(\omega); \qquad Z(\omega) = R + \frac{1}{j\,\omega C} \qquad \text{(Model A)}$$

$$V_{\text{out}}(\omega) = \frac{R_2}{Z(\omega)} V_{\text{in}}(\omega); \qquad Z(\omega) = \frac{R}{1 + j\,\omega CR} + R_2 \qquad \text{(Model B)}$$

where $\omega = k\,\omega_0$. The total output signal as a function of time is given by

$$V_{\text{out}}(t) = \sum_{k=-\infty}^{\infty} V_{\text{out}}(k\,\omega_0) \mathrm{e}^{jk\,\omega_0 t} = \sum_{k=-\infty}^{\infty} d_k\, \mathrm{e}^{jk\,\omega_0 t}$$

The average power of a signal that is dissipated in a resistor is given by Parseval's relation and is proportional to

$$V_{\text{rms}}^2 = \frac{1}{T} \int_T |V(t)|^2\, dt = \sum_{k=-\infty}^{\infty} |a_k|^2$$

where a_k are the Fourier series coefficients of $V(t)$.

Results

The dielectric characteristics, permittivity and conductivity, of the human tissues have been subject to a great research [12,13]. As of yet there is no agreement among research workers regarding their values. In this work the values used for the specific absorption rate (SAR) calculations according to the IEEE 1528-200x [14] are used as a guideline. A summary of these values is given in Table 1. The extrapolated values [13] from Hartsgrove's *et al.* [15] formula for simulating body tissues at higher frequencies are supplied as well

Table 1. The permittivity and conductivity as a function of frequency.

Frequency MHz	ε_r	σ S/m	Reference
900	41.5	0.97	IEEE 1528-200x [14]
1800	40	1.4	
2100	39.8	1.49	
2450	39.2	1.8	
3000	38.5	2.4	
8000	26	9	Hartsgrove *et al.* [15]
10000	23	11	

Two calculations for each of Models A and B were conducted. The first one explicitly considers the frequency dependence of the permittivity and conductivity and, by curve fitting, relations are obtained that satisfy the above data. The fitted relation for the permittivity as a function of frequency is:

$$\varepsilon_r(f) = 10^4 \times \left(0.8871f^{-8} - 4.5381f^{-6} + 6.544f^{-5} - 3.9988f^{-4} + 1.2852f^{-3} - 0.2507f^{-2} + 0.0376f^{-1} + 0.0001\right)$$

Whereas the fitted relation for the conductivity as a function of frequency is:

$$\sigma(f) = \left(0.0002f^{8} - 0.01f^{7} + 0.163f^{6} - 1.2121f^{5} + 4.2548f^{4} - 6.1646f^{3} + 8.1443f - 4.0236\right)$$

For the sake of simplicity and the lack of experimental data, it is assumed that the above equations hold for the other frequency values that are not included in the table. In the second approach constant average values were taken, namely $\varepsilon_r = 40$ and $\sigma = 2$ S/m. As usual, $C = \frac{\varepsilon_0 \varepsilon_r A}{d}$ and $R = \frac{d}{\sigma A}$. The length d and area A are taken to be unity in SI units, thus our results are for unit length and unit area. The obtained results are summarized in Tables 2 and 3.

Table 2. Summary of the results for Model A.

Frequency	Frequency dependent dielectric parameters		Frequency independent dielectric parameters	
	$\frac{V^2_{\text{out, rms}}}{V^2_{\text{in, rms}}}$	$20\log\frac{V_{\text{out, rms}}}{V_{\text{in, rms}}}$ dB	$\frac{V^2_{\text{out, rms}}}{V^2_{\text{in, rms}}}$	$20\log\frac{V_{\text{out, rms}}}{V_{\text{in, rms}}}$ dB
10^7	0.999986	-0.00006	0.000219	-36.6
10^8	0.999981	-0.00008	0.0123	-19.1
10^9	0.99617	-0.0167	0.553	-2.57
2×10^9	0.9053	-0.432	0.832	-0.799
5×10^9	0.1925	-0.716	0.969	-0.138
8×10^9	0.001803	-27.4	0.988	-0.0545
10^{10}	0.000054	-42.7	0.992	-0.0349

Table 3. Summary of the results for Model B. $R_2 = 100\ \Omega$.

Frequency	Frequency dependent dielectric parameters		Frequency independent dielectric parameters	
	$\frac{V^2_{\text{out, rms}}}{V^2_{\text{in, rms}}}$	$20\log\frac{V_{\text{out, rms}}}{V_{\text{in, rms}}}$ dB	$\frac{V^2_{\text{out, rms}}}{V^2_{\text{in, rms}}}$	$20\log\frac{V_{\text{out, rms}}}{V_{\text{in, rms}}}$ dB
10^7	0.99993	-0.00029	0.99008	-0.0433
10^8	1	0	0.9902	-0.0428
10^9	1	0	0.996	-0.0194
10^{10}	1	0	0.9999	-0.000349

Conclusion

The main objective of the present work is to demonstrate the behaviour of the BIA as a power attenuator at different values of modulated high frequency. Comparison was set out between two simplified models of the skin barrier of a body. This is considered under the two assumptions that firstly the dielectric constant is sensitively dependent on the frequency or, secondly, its variation with the frequency is insignificantly small within the given frequency range.

Regarding the frequency dependent assumption, the results show that for both models the input induced voltage is slowly attenuated at frequencies below 10^7 Hz, but over this frequency Model B shows no attenuation while Model A indicates that as the frequency increases a considerable amount of energy is absorbed within the skin.

On the other hand when the dielectric constant is insensitive to frequency variation, Model A shows large attenuation at low frequencies which decreases gradually as the frequency increases, whereas Model B displays an opposite behaviour such that the attenuation is very poor almost at all frequencies in the range from 10^7 to 10^{10} Hz. This seems reasonable since according to the first model the skin behaves as a high pass filter, while the second model shows insensitivity to the variation of frequency.

We believe that the problem is more sophisticated than the proposed two models, which can only be considered as a first order approximation of the problem. There are other important factors that should be considered such as the multilayered structure of biological tissues, the effect of blood circulation, as well as the active elements incorporated in living tissues.

References

[1] Barnett, A., *Electrical method for studying water metabolism and translocation in body segments.* Proc. Soc. Exp. Biol. Med., 44: 142, 1940.

[2] Nyboer, J., Bango, S., Barnett, A. and Halsey, R.H.: *Radiocardiograms - the electrical impedance changes of the heart in relation to electrocardiograms and heart sounds.* J. Clin. Invest., 19: 963, 1940.

[3] Kubicek, W.G.: *Development and Evaluation of an Impedance Cardiographic System to Measure Cardiac Output and Other Cardiac Parameters*. National Aeronautics and Space Administration (NASA). July 1, 1968 to June 30, 1969. Contract No. NAS 9-4500.

[4] Nyboer, J.: *Electrical Impedance Plethysmography.* Second Edition. Charles C. Thomas, Springfield, IL, 1970.

[5] Nyboer, J.: *Workable volume and flow concepts of biosegments by electrical impedance plethysmography.* T.I.T. Journal of Life Sciences (2): 1-13, 1972.

[6] Thomasett, A.: *Bioelectrical properties of tissue impedance.* Lyon Med. 207: 107-118, 1962.

[7] Hoffer, E.C., Meador, C.K. and Simpson, D.C.: *Correlation of whole body impedance with total body water volume.* J. Appl. Physiol., **27**, 531, 1969.

[8] Nyboer, J., Liedtke, R.J., Reid, K.A. and Gessert, W.A.: *Nontraumatic electrical detection of total body water and density in man.* Proceedings of VIth ICEBI, 381-384, 1983.

[9] Fricke, H., *The theory of electrolyte polarization*, Phil. Mag., **14**, 310-318, 1931.

[10] Cole, K. S. and Curtis,H. J., Electric impedance of the giant squid axon during activity. Journal of general Physiology, **22**, 649–670, 1939.

[11] V. Oppenheim, A. S. Willsky, and S. Hamid Nawab, *Signals and Systems*, Second Edition, Prentice-Hall International, Inc., 1997.

[12] Martinsen, Ø. G., Grimnes, S., Schwan, H. P., Interface phenomena and dielectric properties of biological tissues, Encyclopedia Surface and Colloid Science, Marcel Dekker, New York, pp. 2643-2652, 2002.

[13] Ping Liu, Rappaport, C.M., Yan-zhen Wei, and Sridhar, S**.,** *Simulated Biological Materials at Microwave Frequencies for the Study of Electromagnetic Hyperthermia***,** Engineering in Medicine and Biology Society, Proceedings of the Annual International Conference of the IEEE**, 14**, 1992.

[14] IEEE Standard P1528-200x. Recommended Practice for Determining the Spatial-Peak Specific Absorption Rate (SAR) I the Human Body Due to Wireless Communications Devices: Experimental Techniques.

[15] G.Hartsgrove, A. Kraszewski, and A. Surowiec, *Simulated Biological Materials for Electromagnetic Radiation Absorption Studies*, Bioelectromagnetics, **8**, pp. 29-36, 1987

ARTIFICIAL AND NATURAL NEAR-INFRARED RADIATION EFFECTS UPON THE CELL MOTILITY. BIOLOGICAL HYPOTHESE

Gérard DUBOST
Institut d'Electronique et de Télécommunications de Rennes
UMR CNRS 6164, UNIVERSITE DE RENNES 1
Avenue du Général Leclerc, Campus de Beaulieu, 35042 – Rennes Cedex – France

André BELLOSSI
Villa Gabrielle, Chemin du Goh Vras, 56730 – Saint Gildas de Rhuys – France

ABSTRACT

We proved that the centrioles were the device used for the detection of an artificial infrared source external to 3T3 fibroblast and epithelial CV1 cells. The fundamental contribution of the cytoskeleton explains the cell motility. In effect the strain due to the physical pressure on the plasma cell membrane is a sufficient stress to activate Hsp 27 which results in actin polymerization and motility of the cell. We calculate the diffracted field inside the cell due to the current induced along the centriole equivalent to a cylindrical dipole. We deduced the centriole bistatic area function of the directions of the incident and diffracted fields. Some idea of the theoretical pressure equal to several $nN/\mu m^2$ is in good agreement with recent experiments. About the two centrioles in orthogonal positions 100 % of the space is covered, while during the experiments 88 % of 3T3 and 50 % of CV1 cells were put in motion in presence of a near infrared source. So we must consider than the strain due to the pressure on the membrane can be transmitted to the side facing the light source throughout the actin cyto-skeleton. The stress fibers serve as force transmitters in fast mecanotransduction and act as mechano-sensors with direction sensitivity on slow mechanotransduction. We determine the spectral emission power of a single cell from the black-body one. Finally a cell scatters a weak ambient black-body theoretical power radiation. The cellular agregate radiation is able to be detected by one cell located at a certain distance following recent measurements.

INTRODUCTION

Albrecht-Buehler showed that 3T3 mouse fibroblast cells and epithelial CV1 cells could react to a near-infrared light by moving either towards or away from the light source. The type of response depended on the cell type and on the temporal pattern of the emission of the light. He also proved that the centrioles were the detection device for the direction of the infrared source [1] - [4].

CONTRIBUTION OF THE CYTOSKELETON CONCERNING THE CELL MOTILITY (fig. 1)

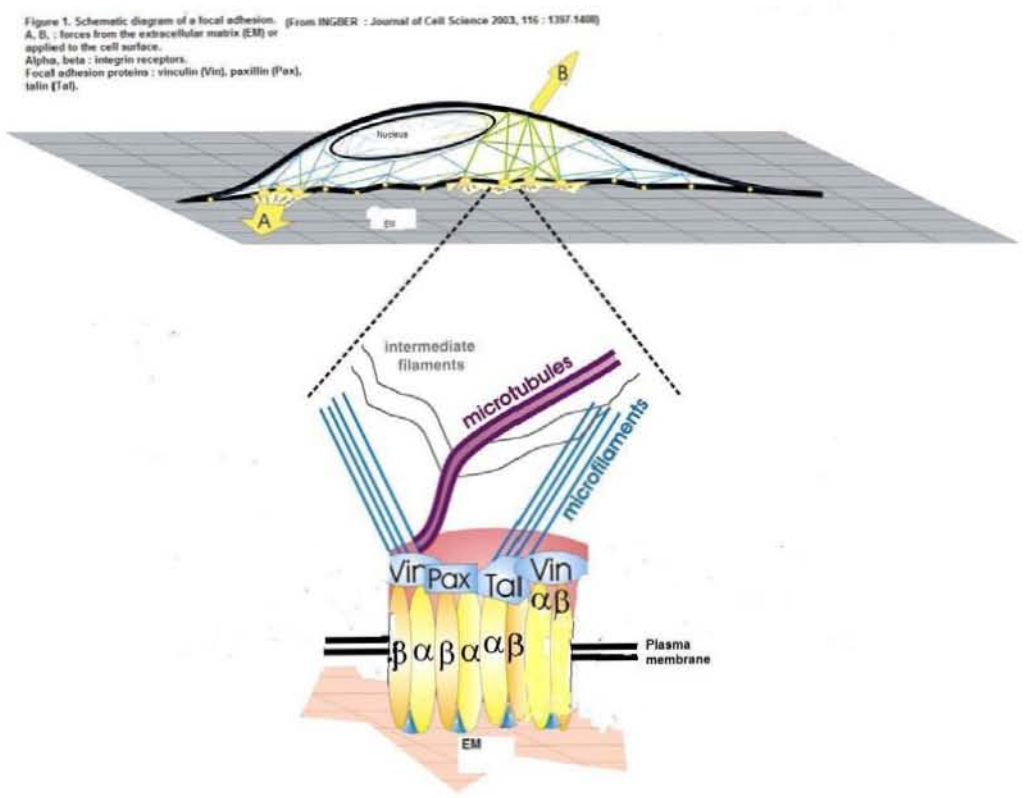


Fig. 1 : Schematic diagram of a focal adhesion.
(From INGBER : Journal of Cell Science 2003, 116 : 1397-1408)
A, B : forces from the extracellular matrix (EM) or applied to the cell surface
Alpha, beta : integrin receptors.
Focal adhesion proteins : vinculin (Vin), paxillin (Pax), talin (Tal).

The plasma membrane is an assembling of various proteins inserted in the fluid matrix of a lipid bilayer. In non muscle cells integrins receptors are membrane spanning proteins that ligate extracellular matrix proteins and link to actin skeleton on the inside of the cells [5] providing a great degree of mechanical coupling across the cell surface. The cytoskeleton is composed of microtubules, actin microfilaments and intermediate filaments. Application of forces to integrins receptors and associated focal adhesion proteins results in physical distorsion of the membrane surface and repositionning of the cytoskeletal filaments along applied field lines within the cytoplasm [6]. Among the three filament systems that form the cytoskeleton, the actin network plays the principal role in determining the cell dynamic response [7]. The cell motility is driven by the sum of asymmetric traction forces exerted on the substrate through adhesion foci that interface with the actin skeleton [8] stimulating polymerization of monomeric globular actin to filamentous actin [9]. Polymerization of actin filaments is necessary for the extension of membrane structures, creating a propulsive force that pushes forward the lamellipodia at the front of migrating cell [10], [11]. Stress proteins, called heat shock proteins (Hsps), are synthesized by cells in case of stress. In the small heat shock protein family, Hsp27 participed in regulating the organization of the actin cytoskeleton in both control and stress conditions. When Hsp27 is phosphorylated, its stimulates actin polymerization and modulates the rate of polymerization, therefore determining the motility of the cell [10], [12], [13], [14], [15]. So we could assume that the strain due to the pressure on the plasma

membrane, resulting from the near infrared radiation, constituted a sufficient stress to activate Hsp27 which resulted in actin polymerization and motility of the cell.

INFLUENCE OF A FLUCTUATING NEAR-INFRARED EXTERNAL SOURCE ABOUT THE CENTRIOLE DIFFRACTION INSIDE THE CELL

Albrecht-Buehler G. showed [1], [4], that a pair of centrioles is able to detect the direction of a near-infrared pulsed source of a 0.8 µm wavelength. Recently [16] we introduced the theoretical selective transparence of the cell membrane deduced from experimental results in the range stretched from 0.2 to 1µm. It was called the transmission coefficient T_{13} . Then from an isotropic radiated power of 4 µW of the light source located at 60 µm, we calculated, inside the cell, an electric field E_i equal to 40 V/m. The wave attenuation along the path and the transmission through the membrane (T_{13}) were taken into account. Inside the cell the mean incident power per unit of area is equal to :

$$p_i = \frac{1}{2}\sqrt{\frac{\varepsilon_o}{\mu_o}}\left|\vec{E}_i\right|^2 \qquad (1)$$

We compare each protofilament of the centriole to a cylindrical dipole of length 2h and diameter 2a, which is equivalent to an opened transmission line of characteristic impedance Z_c and linear propagation constant : $\gamma = \alpha + jk$ [17].
We use the following parameters without dimension :

$$\left.\begin{aligned} K = kh = 2\pi h/\lambda, \qquad \Omega = 2\log_e(2h/a), \\ A = \alpha h = (kh)^2 \big/ 2(\Omega - 3.4) \end{aligned}\right\} \qquad (2)$$

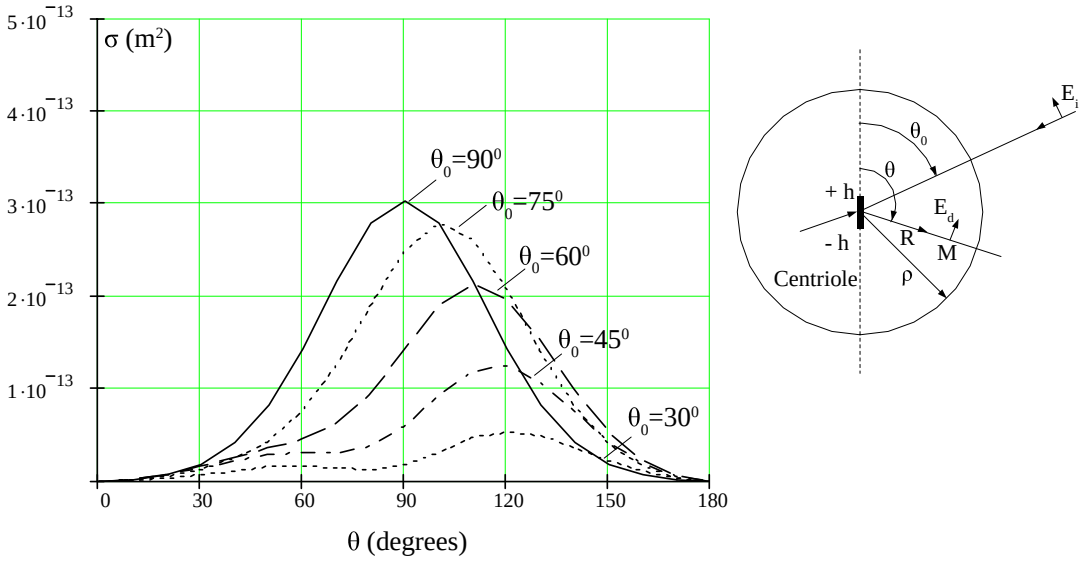


Fig. 2. Cell bistatic area σ (θ, θ_0)

The figure 2 shows the centriole lighted by a plane-wave from the θ_o direction with an electric field $\vec{E}_i(\theta_o)$. The diffracted field at point M : $\vec{E}_d(\theta,\phi,\theta_o,R)$ $(0 \le \phi \le 2\pi)$, inside the cell is due to the current $I(z,\theta_o)$ induced along the centriole. The distance between the center of the centriole and M is R. The bistatic area of the centriole related to the two directions θ_o and θ is given by the following expression :

$$\sigma(\theta,\theta_o) = \frac{\lambda^2}{\pi}|S(\theta,\theta_o)|^2 \qquad (3)$$

$$\text{with :} \quad \left|\frac{\vec{E}_d(\theta,\theta_o,R)}{\vec{E}_i(\theta_o)}\right|^2 = \frac{|S(\theta,\theta_o)|^2}{(kR)^2} = \frac{\sigma(\theta,\theta_o)}{4\pi R^2} \qquad (4)$$

The expressions (3) and (4) are valid when $R \ge 8h^2/\lambda$ (5), that is when the diffracted field is associated with an electromagnetic plane-wave.

$I(z,\theta_o)$ and $S(\theta,\theta_o)$, which depend on A, K and Ω parameters are given in the annex of calculation.
The whole power P_d diffracted inside the cell by the centriole is :

$$P_d(\theta_o) = \frac{1}{2}\sqrt{\frac{\varepsilon_o}{\mu_o}}\int|\vec{E}_d|^2 ds = \frac{1}{2}\sqrt{\frac{\varepsilon_o}{\mu_o}}|\vec{E}_i|^2 \int\frac{\sigma(\theta,\theta_o)\,ds}{4\pi R^2} = \frac{p_i}{2}\int_o^\pi \sigma(\theta,\theta_o)\sin\theta\, d\theta \qquad (6)$$

with $ds = R^2 \sin\theta\, d\theta\, d\phi$.

For the pulse light emission the form factor is the product of the length of time τ by the frequency f_r.
In a corresponding stochastic way the energy is stored inside the cell of radius ρ, where it is trapped because its transmission through the membrane is lower than 10 percent [16].

The stored energy during a length of time Δt will be equal to :

$$W_S = P_d(\theta_o)\Delta t\, \tau\, f_r \qquad (7)$$

The density of energy u_S and the mean pressure P applied on the membrane are then :

$$u_S = \frac{W_S}{(4/3)\pi\rho^3} \qquad (8) \qquad\qquad P = \frac{u_S}{3} \qquad (9)$$

In the fig. 2 we present the bistatic area (3) in terms of θ for several θ_o values with the following parameters given in (2) :

$$2h = \lambda = 0.8\,\mu m, \quad 2a = 40\,nm, \quad \Omega = 7.38, \quad K = \pi, \quad A = 1.24$$

The validity condition (5) is fulfiled when : $R \ge 1.6\,\mu m$. Whatever, the chosen incident angle θ_o, the max of σ and P_d occur for $\theta \ge 90°$. The active diffracted beam draws an asymmetrical cone-shaped zone around the centriole axis so that the diffracted light propagation goes away from the light source.
The Table I shows P_d, W_S, u_S and P with $p_i = 2W/m^2$ (1), $\tau f_r = 1/2$,

$\rho = 11\mu m$ and $\Delta t = 600\,s$.

θ_o (degrees)	90	75	60	45	30
P_d (watts) (6)	3.10^{-13}	3.10^{-13}	$2.6\,10^{-13}$	$1.4\,10^{-13}$	$7\,10^{-14}$
W_S (Joules) (7)	9.10^{-11}	9.10^{-11}	8.10^{-11}	4.10^{-11}	2.10^{-11}
u_S (Joules/m^3) (8)	$1.6\,10^4$	$1.6\,10^4$	$1.4\,10^4$	$7.4\,10^3$	$4\,10^3$
P(nN/μm^2)	5.0	5.0	4.6	2.3	1.2

Table I : Power and energy diffracted by a 3T3 cell.
Pressure applied on the membrane

Some idea of the size of the pressure P has been obtained in recent experiments [18]. In the abstract we can read: "we measure dynamic traction forces applied by epithelial cells (monolayer) on a substrate. The force sensor is a high-density array of elastomeric microfabricated pillars that supports the cells. Traction forces induced by cell migration are deduced from the measurements of the bending of these pillars and are correlated with actin localization by fluorescence microscopy". Each post or pillar is a cylinder of radius r and length L. The deflection Δx of the free end of the post is due to a force F exerted by the cell on its underlying substrate given by :

$$F = \left(\frac{3}{4}\pi E \frac{r^4}{L^3}\right)\Delta x \qquad (10)$$

E is the Young's modulus of the pillar.

With $\Delta x = 0.1\mu m$, $r = 1.5\ \mu m$, $L = 5\ \mu m$, $E = 2\ 10^6\ P_a$, we find : F = 19 nN.

This force applied to the area of the pillar $\pi r^2 = 7.07\ \mu m^2$ corresponds to a pressure of 2.7 nN/μm^2.
This pressure is in good agreement with our theoretical results shown in Table I.
Previous analysis (2001, 1999), related in [18], have indicated a 5.5 nN/μm^2 value relating force and contact area.

Note : Albrecht-Buehler said (April 23, 2003) : *"The cells used were always moving. The first sign of changing direction, i.e the extension of a new lamellipodium in the direction of the light source, was usually visible after 5-10 min (factor 2) since the beginning of the lighting"*. This explains the choice of $\Delta t = 600$ s in W_S (7).

Then the radiation by one centriole is the most efficient when $45° \le \theta_o \le 135°$ which correspond to a diffraction zone : $60° \le \theta \le 120°$ (fig 2) for a variation of σ and P_d by a same factor 2. If the two centrioles are in orthogonal positions 100 % of the space is covered. According to Albrecht-Buehler about 88 % of 3T3 cells and 50 % of CV1 cells were put in motion in presence of near-infrared source. This information is related in [19].

CELL SCATTERING OF A NEAR-INFRARED FRACTION OF THE BLACK-BODY RADIATION

Recently Albrecht-Buehler G. explains that a cell can scatter the near-infrared portion of the ambiant black-body radiation to become a light source, as a result of the experiments [20]. The present purpose is to justify a

such hypothesis giving some theoretical development. We are sure that the scattered light of the black-body radiation for one cell in the near-infrared range is very small and cannot be detected, but may be by a group of aggregated cells.

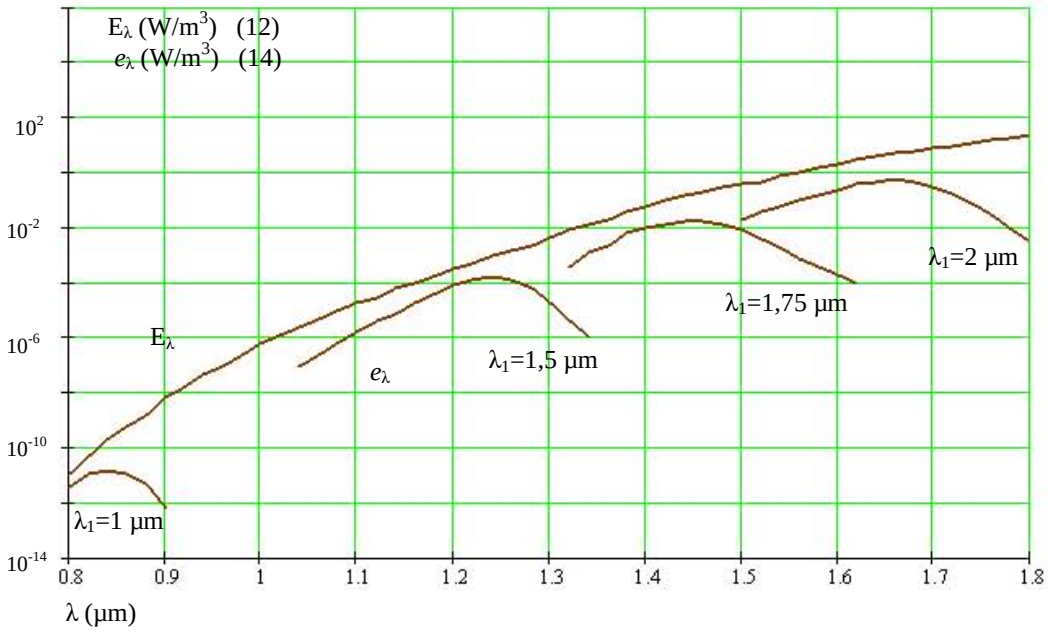


Fig. 3. Spectral emission powers E_λ and e_λ (for T=310°K).

The spectral-emission power E_λ is given by :

$$E_\lambda = \frac{2hc^2}{\lambda^5} \cdot \frac{1}{\exp\left(\frac{h\nu}{kT}\right)-1} \qquad (11)$$

In international units it is expressed in W/m^3 :

$$E_\lambda = \frac{1.19\,10^{-16}}{\lambda^5} \cdot \frac{1}{\exp\left(\frac{14.4\,10^{-3}}{\lambda T}\right)-1} \qquad (12)$$

The whole specific intensity E_T of the black-body expressed in W/m^2 is :

$$E_T(\lambda, T) = \int_0^\infty E_\lambda \, d\lambda \qquad (13)$$

The spectral-emission power of one cell is equal to :

$$e_\lambda = \alpha_\lambda E_\lambda = T_{13}{}^2 . E_\lambda \qquad (14)$$

$\alpha_\lambda < 1$ is the absorption coefficient, and T_{13} the transmission coefficient through the cell membrane given in [16] by :

$$T_{13}{}^2 = 1 \left[ch^2(\Gamma_2 d) + k_2^2 sh^2(\Gamma_2 d) \;\; 4n_1^2 \right] \qquad (15)$$

d is the membrane thickness and $\Gamma_2 d = 2\pi k_2 d/\lambda$. k_2 is the index of absorption of the membrane and n_1 is the index of refraction of the interstitial medium. We present in fig. 3 the spectral-emission powers E_λ and e_λ in terms of λ for T = 310° K. The parameter λ_1 is the maximal wavelength which limits the near-infrared absorption range. The max of E_λ is equal to $10^7\,W/m^3$ for $\lambda = 9.3\,\mu m$.
The whole specific intensity e_T of the cell is then given by :

$$e_T = \int_0^{\lambda_1} e_\lambda d\lambda \qquad (16)$$

It appears in the table II :

$\lambda_1(\mu m)$	1	1.5	1.75	2
$e_T\left(\mu W/cm^2\right)$ (16)	10^{-16}	10^{-9}	2.10^{-7}	8.10^{-6}

Table II (valid for T = 310 °K)

According to the second principle of thermodynamics, at $T = 310°K$, the power radiated by a cell of radius ρ is : $P_d = 4\pi\rho^2 e_T$ (17)

For a 3T3 cell with : $\rho = 11\,\mu m$, P_d is shown in Table III.

$\lambda_1(\mu m)$	1	1.5	1.75	2
P_d (watts) (17)	$1.5\,10^{-27}$	$1.5\,10^{-20}$	3.10^{-18}	$1.2\,10^{-16}$

Table III – Power radiation by a 3T3 cell

We note the great importance of the limit of the membrane cell transparence upon its natural radiation power. So a cell scatters a weak ambient black-body radiation. Only aggregate cells is able to be detected by one cell located at a certain distance as recently measured [20].

BIOLOGICAL HYPOTHESE

Could the pressure P calculated in (9) be the cause of the displacement of the cell to protect the overall integrity of the membrane ?

The strain (fig. 1, A) due to the pressure P, is received in focal adhesion proteins and integrins activate the signaling pathway leading to actin polymerization and motility of the cell towards the light source. However Albrecht-Buehler observed more cells were going forward than backward. So we must consider that the strain on the membrane can be transmitted to the side facing the light source. Externally applied forces (fig. 1, A) are transmitted throughout the actin cytoskeleton and result in immediate repositionning of cytoskeletal filaments along applied tension field lines within the cytoplasm [6], [21]. Stress fibers, composed of actin filaments, myosin and α-actinin, are anchored at focal adhesions at one side of the cell, and at focal adhesions on the other side of the cell. They serve as force transmitters in fast mechanotransduction and act as mechanosensors with direction sensitivity on slow mechanotransduction [22]. So the strain due to the pressure could be transmitted to the opposite side of the cell where it would determine the moving of the cell away the light source. This can be akin to the transmission of tension due to fluid shear stress from the apical surface of endothelial cells through the cytoskeleton to the integrins which then change in tension (23). Moreover, in the Albrecht-Buehler's experiments, the percentages of cells that were either attracted or pushed away from the light source depended on the pulsing frequencies of the light source. Were the threshold between a fast and a slow mechanotransduction linked to the difference in frequency ?

SUMMARY

The 3T3 fibroblast and epithelial CV1 cells motility has been explained :

- firstly by their centrioles diffraction under the influence of a fluctuating near-infrared artificial external pulsed source. The diffraction light propagation is such that, due to the physical pressure on the plasma cell membrane, the cell goes towards the light source.
- secondly when a sufficient strain, transmitted along the cytoskeleton, can move the cell away the light pulsed source.

On the other hand, we show that a cell scatters a weak part of the natural near infrared ambient black body radiation.
All these theoretical results are in good agreement with recent published measurements.

REFERENCES

[1] Albrecht-Buehler G., Surface extension of 3T3 cells towards distant infrared sources. J. Cell. Biol. 1991, 114 : 493-502.
[2] Albrecht-Buehler G., Changes of cell behavior by near-infrared signals. Cell Mobility and the Cytoskeleton 1995, 32 : 299-304.
[3] Albrecht-Buehler G., Does the geometric design of centrioles imply their function ? Cell Motility 1981, 1 : 237-265.
[4] Albrecht-Buehler G., The cellular infrared detector appears to be contained in the centrosome. Cell Motility and the Cytosketelon 1994, 27 : 262-271.
[5] W.T. Gerthoffer, S.J. Gunst, Signal transduction in smooth muscle. Invited review : focal adhesion and small heat shock proteins in the regulation of actin remodeling and contractility in smooth muscle. J. Appl. Physiol. 2001, 91 : 963-972.
[6] D.E. Ingber Tensegrity I., Cell structure and hierarchical system biology. Journal of Cell Science 2003, 116 : 1157-1173.
[7] D. Stamenovic, Z. Liang, J. Chen, N. Wang, Effect of the cytoskeleton prestress on the mechanical impedance of culture airway smooth muscle cells. J. Appl. Physiol. 2002, 92 : 1443-1450.
[8] I. Kaverina, O. Kryliskina, K. Beningo, K. Anderson, Y-L Wang, J.V. Small : Tensile stress stimulates microtubule outgrowth in living cells. Journal of Cell Science 2002, 115 : 2283-2291.

[9] D. Mehta, S.T. Gunst, Actin polymerization stimulates by contractil activation regulates force development in canine tracheal smooth muscle. The Journal of Physiology, 1999, 519, 3 : 820-840.
[10] D.A. Schafer, M.T. Welch, L.M. Machessky, P.C. Bridgman, S.M. Meyer, J.A. Cooper, Vizualisation and molecular analysis of actin assembly in living cells. J. Cell Biol. 1998, 143, 7 : 1919-1930.
[11] Dynamique de la membrane et du cytosquelette. Compartimentation et dynamique cellulaire. UMR 144 CNRS/IC. Avril 2004.
[12] Histologie de la peau. Collection Mémoires et thèses électroniques, R. Benndorf., Université de Laval (Québec).
[13] J. Landry, J. Huot, Modulation of actin dynamics during stress and physiological stimulation by a signaling pathway involving p38MAP kinase and heat shock protein 27. Biochem. Cell Biol. 1995, 73, 9-10 : 703-707.
[14] C. Schäfer, P. Clapp, M.J. Welsh, J.A. Williams HSP 27 expression regulates CCK-induced changes of the actin cytoskeleton in CHO-CCK-A cells. Am. J. Physiol. Cell. Physiol. 1999, 227 : 1032-1043.
[15] S. Hirano, E.A. Shelden, R.R. Glimont Hsp 27 regulates fibroblast adhesion, motility and matrix contraction. Cell Stress and Chaperones 2004, 9, 1 : 29-37.
[16] G. Dubost, A. Bellossi, Cell membrane physical model in near-infrared, visible and near-ultraviolet spectra. Biological Effects of EMFS, 3rd International Workshop KOS, Greece 2004, October : 492-500.
[17] G. Dubost, S. Desclos, Y. Commault, G. Debionne, Calcul en mode TEM du courant et de la section efficace bistatique d'une antenne filaire chargée éclairée par une onde plane. Ann. Télécommun. 44, n°7-8, 1989, pages 374 to 380.
[18] O. du Roure, A. Saez and all, communicated by Pierre-Gilles de Gennes, Collège de France. Force mapping in epithelial cell migration. PNAS, February 15, 2005, vol. 102, n° 7, 2390-2395.
[19] C. Lowry, Comment les cellules se voient-elles ? Fusion 2001, 87 : 20-25.
[20] G. Albrecht-Buehler, A long-range attraction between aggregating 3T3 cells irrediated by near-infrared light scattering. PNAS 2005, 102, 14, 5050-5055.
[21] M.F. Coughlin, D. Stamenovic, A prestress cable network model of the adherent cytoskeleton. Biophysical Journal 2003, 84 : 1328-1336.
[22] M. Sokabe, K. Hayakawa, H. Tatsumi, Varieties of mechanotransduction : the cytoskeletal stress fiber as a force transmitter and mechanosensor. http://www.aups.org.au/Proceedings/36/95P.
[23] A. Katsumi, A.W. Orr, E. Tzima, M.A. Schwartz, Integrins in mechanotransduction. J. Biol. Chem. 2004, 279, 3 : 12001-12004.

APPENDIX

Induced current along the centriole due to the incident electric field $\vec{E}_i(\theta_o)$ (figure 1)

It is given by the following equation [17] :

$$I(z,\theta_o) = C\left\{-j\frac{\sin(K\cos\theta_o)}{sh(A+jK)}sh\left[\frac{z}{h}(A+jK)\right]-\right.$$

$$\left.-\frac{\cos(K\cos\theta_o)}{ch(A+jK)}ch\left[\frac{z}{h}(A+jK)\right]+\exp(jKz\cos\theta_o)\right\}$$

$$\text{with :} \quad C = \frac{2hE_i}{Z_c} \frac{(A + jK)\sin\theta_o}{\left[(A + jK)^2 + K^2\cos^2\theta_o\right]}, \qquad Z_c = \frac{Z_o}{2\pi}\left(1 - j\,2\frac{A}{K}\right)^{1/2} \quad (\Omega - 3,4)$$

With the previous parameters, $E_i = 40\,V/m,$ and $Z_o = 377$ ohms , the module of the current $\frac{2\,h\,E_i}{Z_c}$ is equal to 0.12 µA.

Bistatic area of the centriole

The function $S(\theta,\theta_o)$ is extracted from [17] : $S(\theta,\theta_o) = j\frac{K\,Z_o}{2\pi\,Z_c}F(\theta,\theta_o)$

$$\text{with} \qquad F(\theta,\theta_o) = (p + q + r).\frac{s}{u}$$

$$\text{and} \quad p = K\frac{shx}{x}\left[\frac{-z}{ch(A + jK)} + j\frac{t}{sh(A + jK)}\right] \qquad q = -\left(K\frac{sh\,y}{y}\right)\left[\frac{z}{ch(A + jK)} + j\frac{t}{sh(A + jK)}\right]$$

$$r = 2\frac{\sin(Kv)}{v} \qquad s = (A + jK)\sin\theta\sin\theta_o$$

$$u = (A + jK)^2 + K^2\cos^2\theta_o \qquad x = A + jK(1 - \cos\theta)$$

$$y = A + jK(1 + \cos\theta), \qquad z = \cos(K\cos\theta_o), \qquad t = \sin(K\cos\theta_o), \qquad v = \cos\theta + \cos\theta_o$$

Hypersensitivity to Electricity: The effect of the current waveform on the perception level.

B. Mattivi, V. Beauvois, P. Dular, J.L. Lilien, R. Lorphèvre, R. V. Sabariego

University of Liège - Dept. of Electrical Engineering and Computer Science
Institut Montefiore – Sart Tilman Bât 28 – B-4000 Liège (Belgium)
Contact email : JL.Lilien@ulg.ac.be

Abstract - Hypersensitivity to electricity has been reported many times in the literature. From another point of view, numerous measurements have been performed on perception level. Even if it appears that part of the population has a lower perception level of current, there is no clear link with the so called "hypersensitivity to electricity" which is more related to declared physiological disorders in part of the population (sleeping problem, headache …). Such declared hypersensitivity is currently not yet related to any biological parameter.

Our research team is currently trying to determine a relationship between hypersensitive declared people and the perception level when injecting current in the low frequency range 50-1000 Hz.
We have performed current perception tests with individuals under different conditions (different wave shapes, frequencies, influence of external electric field, male and female…) using a particular protocol and our own designed system for current injection.

This paper will present our test system design (current injector, wave shape converter, safety aspects) and our first results based on both sine wave (different frequencies) and wideband signal.

I. Introduction

Hypersensitivity to electricity, i.e. non-specific health symptoms such as headache, sleep disturbance, nervousness, concentration disturbances or skin arousal, attributed by the patient to the "electromagnetic pollution", has been frequently reported in the literature (Hilert et al, 2002, Leitgeb, 1998) but until now, no clear link has been shown between the electromagnetic field and the symptoms of these persons.

In (Leitgeb and Schrötner, 2003), a subgroup of people with significantly increased electrosensibility was detected. Herein, the electromagnetic sensibility is described as the ability to perceive electric and electromagnetic exposure, and electromagnetic hypersensitivity, developing health symptoms due to exposure to environmental field. The measurements showed a clear difference between men and women. A log-normal law was proved to fit fairy well to their results (see fig 1).

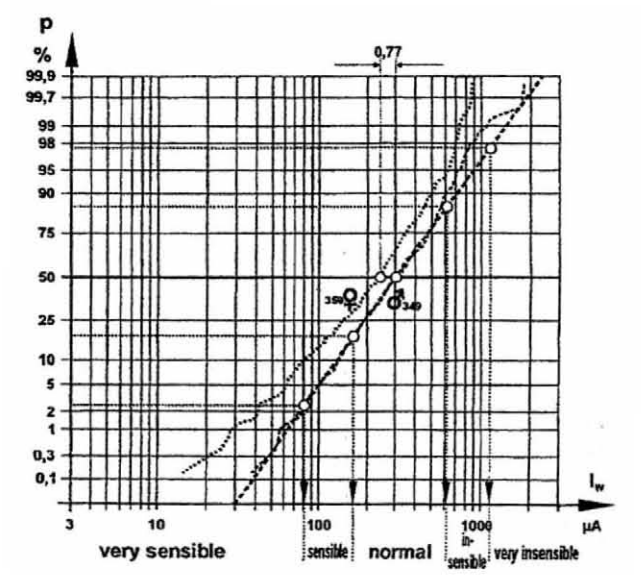


Fig1: Distribution of the cumulative probability perception Threshold current I_w (following Leitgeb-2003)

The existence of the very "electrosensible" subgroup can be seen as the second log-normal distribution on the fig 2.

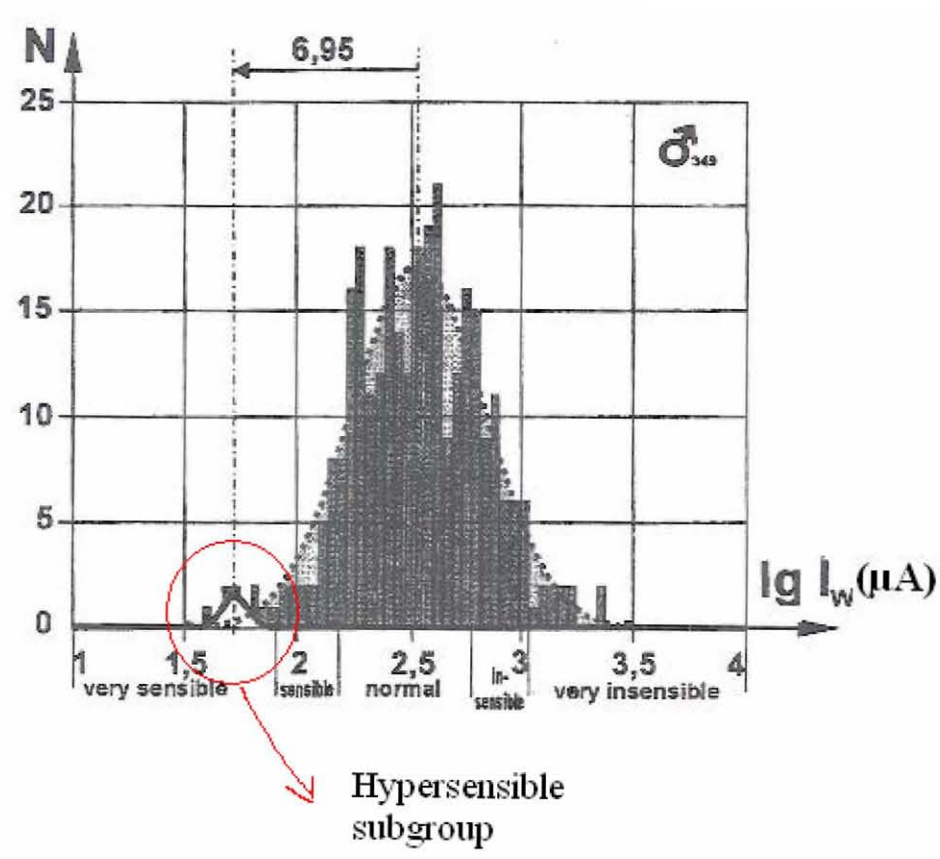


Fig 2: Best least square fit of two ideal log-normal distributions with the frequency distribution of measured electric current perception thresholds of men (following Leitgeb-2003.

Similarly to the work in (Leitgeb and Schrötner, 2003), but in a wide band of frequency, and signal shape, we try to determine a link between the "hypersensitivity to electromagnetism" and the sensibility to electricity. Our aim is to measure the smallest current intensity that a given person can feel when electrical current is flowing between two electrodes placed on the forearm of this person.

A home-made device, that allows injecting any waveform current within the frequency range 50Hz-1kHz, has been designed. This injector will be described in detail hereafter.

This paper will be focused on the sensitivity to electricity of a person according to the frequency. The first results of measurements will be shown for two different frequencies (50Hz and 1 kHz).

II. Measurements method

The developed experimental system is composed of a computer, a current injector and an external supply (see fig 3).

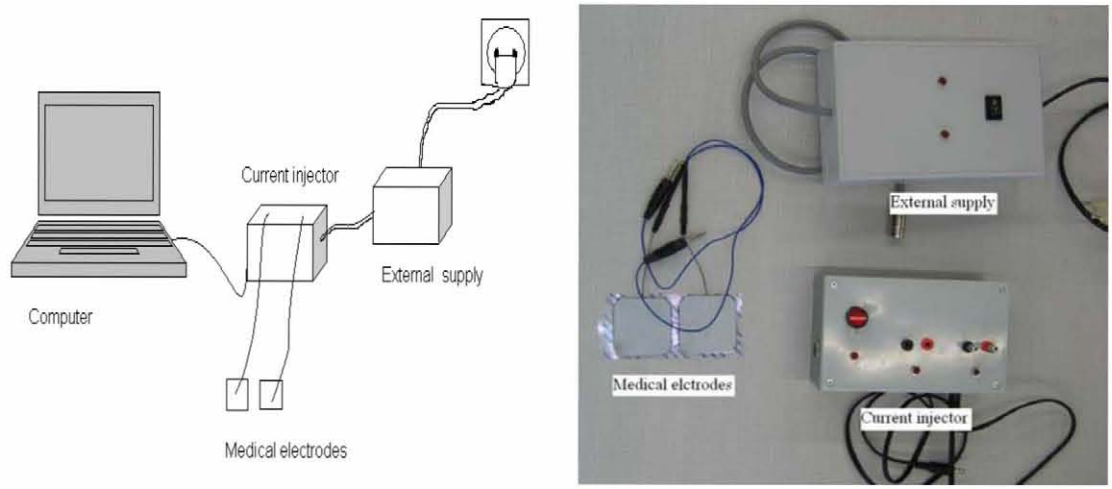


Fig3: Experimental System

A home-made program creates an audio signal (wave file) which is transmitted via the sound card to the current injector. The latter converts the voltage in a stable current flowing between the two electrodes through the body of the volunteer. For safety reasons and to prevent any electric current pathways across the heart, the investigations were done on the forearms on the volunteers. The complete description of the current injector can be found on the Section 3.

The sinusoidal current is applied by trains of constant rms (root mean square) value with dead time of 5 ms between each of them. Between two sequences, the rms current level is increased following a given law, which has been chosen in these experiments as exponential. Our system can easily handle any dead time or increasing law at a given frequency. Currents were increased by step until the program was interrupted by the volunteer's push of the computer's space bar (or any other computer's button) when perceiving the current flow. To minimize random influences, measurements were performed six times with 5 seconds break between each. The mean value of this first test was considered as the first evaluation of the perception level. After 30 sec, the measurements were performed six more times, but with a more precise range of current, according to the first evaluation. The tests evaluated the sensitivity to a 50 Hz sinusoidal wave and 1 kHz sinusoidal wave. The value of 1 kHz was arbitrary chosen to compare the sensibility at two different frequencies. Recruitment method of volunteer was done essentially on the student of the University of Liège; they were informed about the procedure and explicitly expressed their consent to the measurements.

III. Technical specification and safety aspect

The electronic scheme of the current injector is shown on the Fig.4. It is composed of seven "blocks".

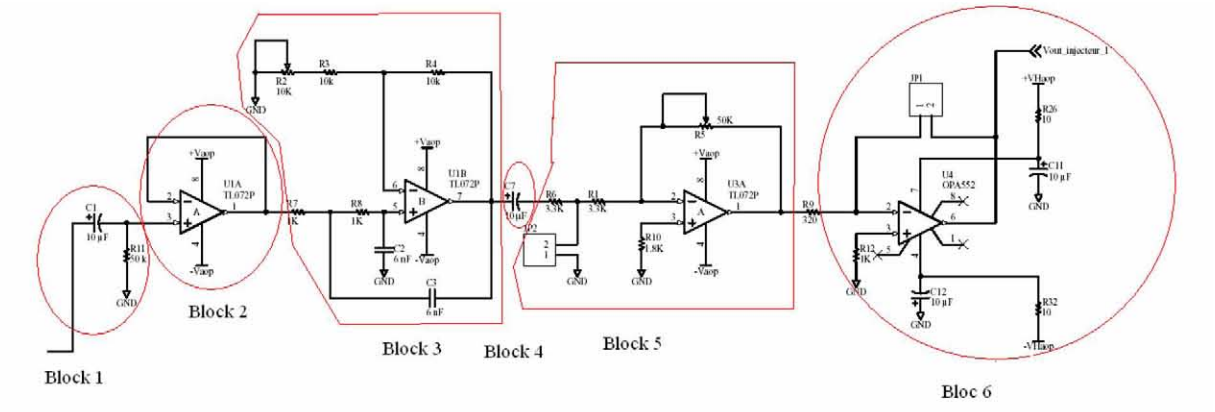


Fig4: Scheme of the current injector

- *Block 1: RC high pass filter:*

Its role is to eliminate the DC component of the signal. The value of the cut down frequency is 0.3 Hz. The DC part has to be eliminated because it could damage the tissues of the volunteer.

- *Block 2:Follower circuit*

It makes sure that there is no interference between the part one and the part three of the circuit.

- *Block 3: Butterworth low pass filter*,

This block eliminates the high frequency parasites. Its cut down frequency is 25 kHz

- *Block 4: RC high pass filter*:

It serves to eliminate the DC component of the signal. Indeed, the signal can have been perturbed by the precedent part of the circuit and have again a DC component. Its cut down frequency is the same than the block 1's : 0.3 Hz.

- *Block 5:Amplifier with variable gain*:

This part of the circuit is used to adjust the output (calibration) of the device.

- *Block 6: Current injector circuit* :

This part of the circuit is the current injector itself; it uses the human body resistance as feedback resistance.

We have characterized the bandwidth of the device in order to be sure that our signals are not altered (attenuated). The results are shown on the following figure (voltage peak to peak taken on the output of the device in function of frequency). The results measurements showed that in the range of our experiment, i.e. 50 Hz to 1 kHz, the signals are not altered.

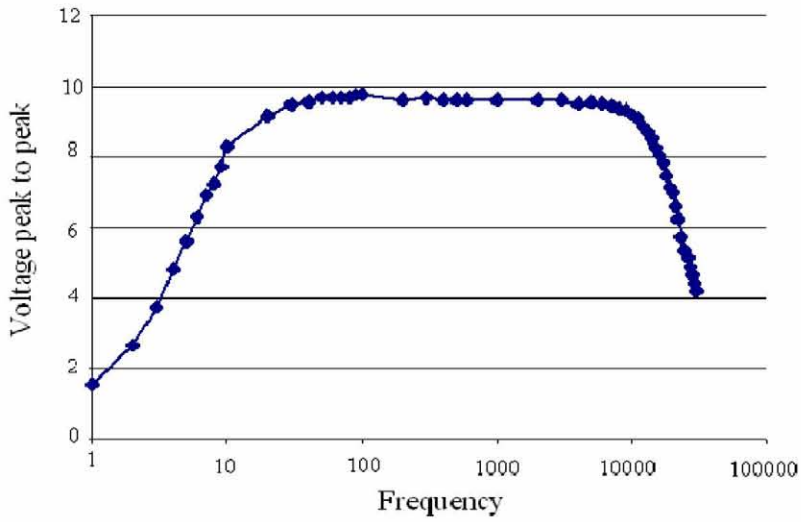


Fig 5: Frequency response of the current injector

On such a kind of device, the safety aspect is crucial. In order to be sure that any perturbation of the electric network is rejected, a system of low pass filter, in the external supply, has been designed to eliminate the high frequency component, as the perturbation can be seen as a high frequency signal, it is thus eliminated. The device is also limited with a maximum output current of 5mA.

As already mentioned, we have ensured, by a system of high pass filter, that the signal injected in the body does not have a continuous (DC) component, as a DC component would be dangerous for the tissues.

The last feature that guarantees the security of the person tested is a stop button that disconnects immediately the person from the current injector. When the user pushes the button, the entry of the amplifier (Block 5) is forced to the mass, so the entry of the amplifier is zero.

IV Results and discussion

It was possible to perform measurement on 150 persons. These persons were aged between 17 and 60 years, in order to avoid bias by including possibly more sensitive children or less sensitive elderly. As the persons were generally students of the university, almost all of them were under 25 years old.

Our first data clearly show a difference to the perception level at 50 Hz and 1 kHz. It has already been shown that the sensitivity to electricity varies according with the frequency (Dalziel & Manfield, 1950) of the signal; but our study is focused on the low frequency range.

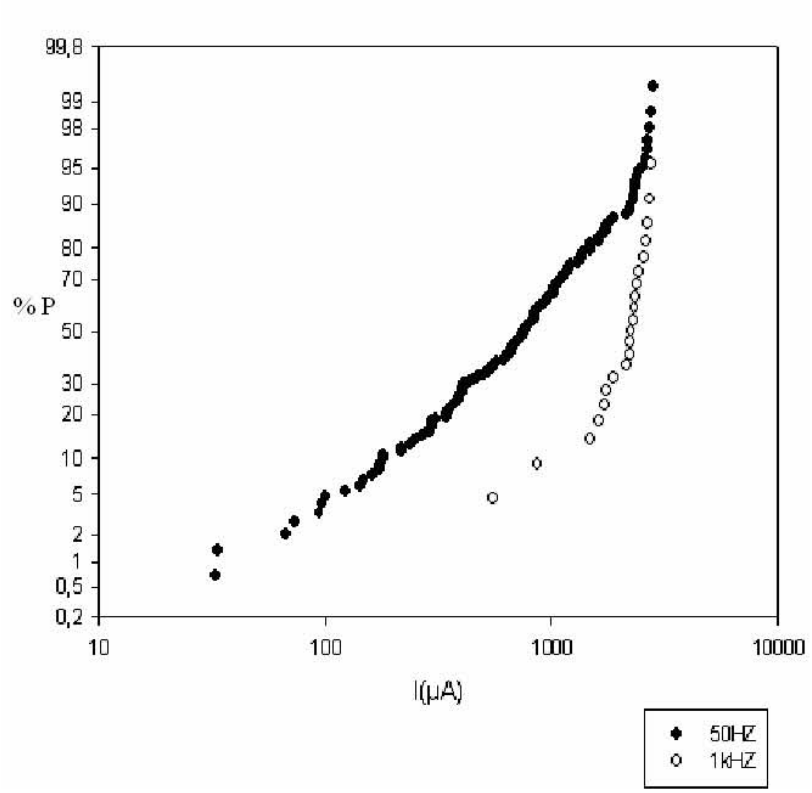


Fig 6: distribution of the cumulative frequency

We have compared our data concerning the 50Hz sinusoidal current to Leitgeb's results (Leitgeb and Schrötner, 2003). Our results superpose to their results are shown on the Fig 7. The mean value of the perception threshold in our study (760.23 µA) is higher than the mean value they found (for men, near 300µA). Nevertheless the mean value we found is still lower than the related mean value (Reilly, 1998). It seems also that the mathematical law is different; the kind of frequency distribution of perception level was analyzed by Kolmogorov-Smirnov testing. The null hypothesis of log-normal distribution data was rejected by a significance $P<0.01$. Until now, we hadn't found a proper law to fit our results. The histogram of the frequency distribution of measured electric current perception threshold is shown on the Fig 7

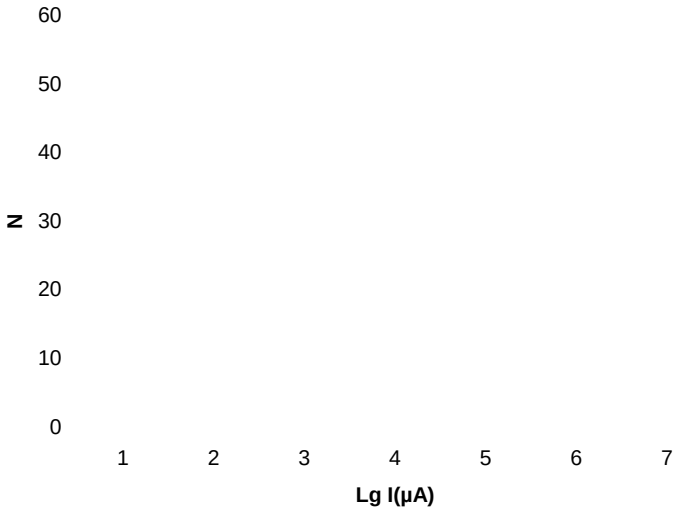


Fig 7: histogram of the frequency distribution of measured electric current perception threshold

It is possible that the observed differences are due to the differences in the measurements protocol, Leitgeb (Leitgeb and Schrötner, 2003) increased their current linearly, but we increased it exponentially, they also took six measurements, but did not proceed to a refining like us and take a break of 3min after each measurement whereas we took only 5sec. Two other differences are the facts that our volunteers were almost all under 25 years old. The results are not separated between male and female because we had only 19 percent of female volunteers. It has to be said that the two "weak perception volunteers" were male.

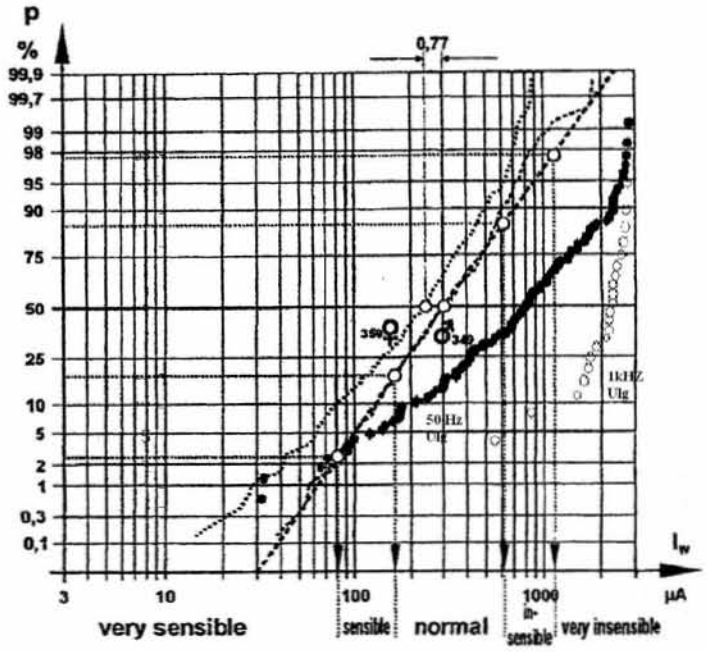


Fig 8: Our results superposed to Leitgeb's data

The current injector and its program can be used to generate a more complex waveform than a sinus. The Fig 8 and 9 show a typical waveform used during the last year in our study. Even if our device is now able to generate any whished waveform, the problem is to have a comparison point between two waveforms. Up to now, we have chosen to compare the RMS (Root Mean Square) value, but we have doubts about the validity of this approach. A value linked to a biological characteristic such as the Action Potential of the nervous cells would certainly be more suitable.

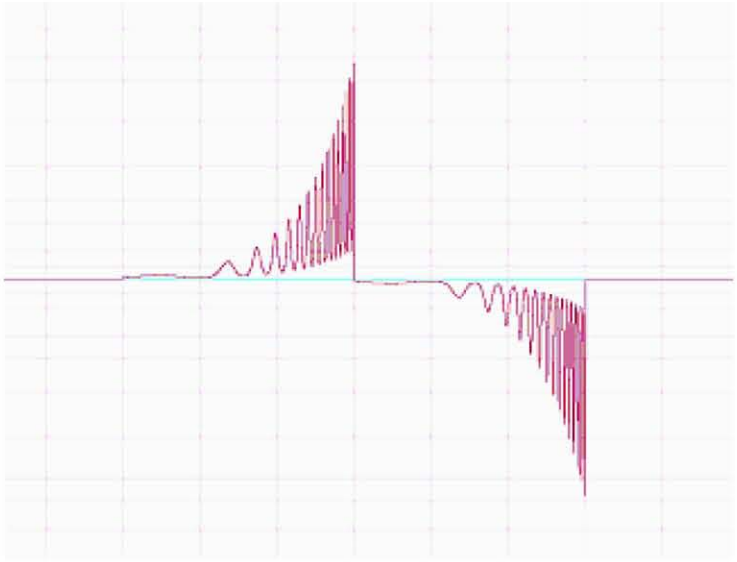


Fig 9: Wideband signal

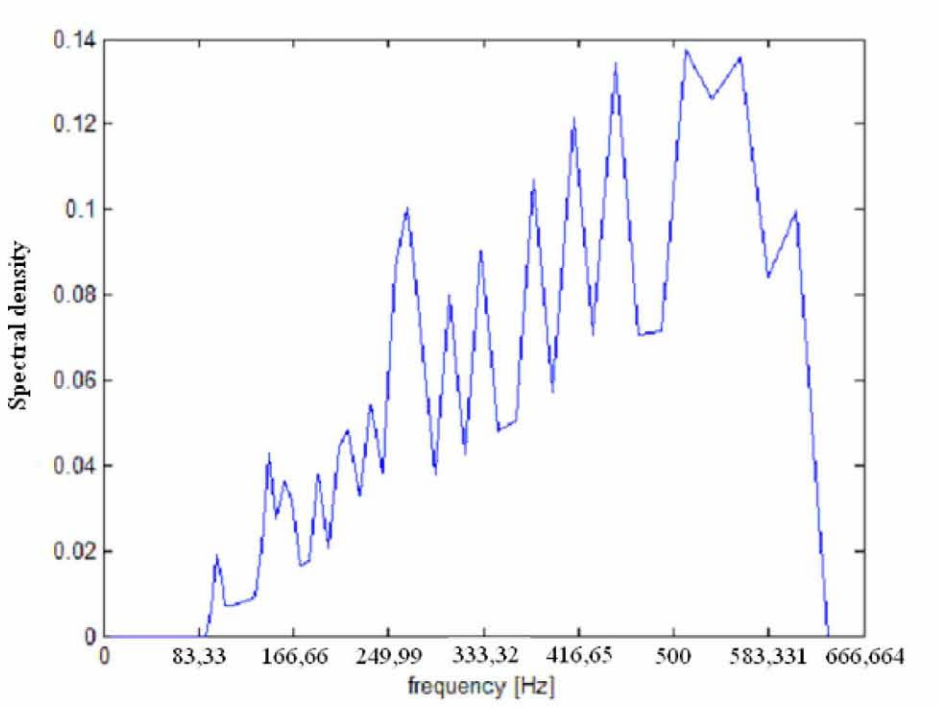


Fig10. Frequential analysis by the wavelet method of the wideband signal.

V. Conclusion

We have designed a device that has shown to be a useful tool to study the human sensibility to electricity. One of our priorities was to ensure the security of the volunteers.

The measurements obtained with our device were quite different from those published in a similar work. We concluded that the protocol chosen influences considerably the results.

A study on the effects of the frequency and the waveform on the perception level has begun. The first results, even if few measurements have been done, clearly show that the human sensibility decreases with the frequency. This effect is maybe due to a “relaxation effect” of the neurons. Our device is able to generate any waveform, but the problem is to have or select a comparison magnitude between two waveforms. This magnitude could maybe be linked to a biological characteristic like the Action Potential of the nervous cell.

Acknowledgments

This research has been supported by Elia, the Belgium's transmission system operator. We would like to thanks Pascal Harmeling for the realisation of the electronic part of this work and David Lilien for the implementation of the wave-generating software.

References

Hillert L, Berglind N, Arnetz BB, Bellander T. Prevalence of self-reported hypersensitivity to electric or magnetic field in a population based questionnary survey. Scand J work Environ Health. 2002; 28:33-41.

Leitgeb N, Schrötner J, Electrosensibility and Electromagnetic hypersensitivity, Bioelectromagnetics 2003;24: 387-394.

Lyskov E, Sandström M, Hansson Mild K. 2001.b, Neurophysiology study of patients with perceived hypersensitivity. Int J. Psychophysiol 42: 223-241.

Reilly JP. 1998. From electrical stimulation to electropathology. New York: Springer Verlag.

Appendix I: Results (table)

Person number	Sensibility(µA)	Person number	Sensibility(µA)	Person number	Sensibility (µA)	Person number	Sensibility (µA)	Person number	Sensibility (µA)
1	32,98	31	348,03	61	644,38	91	918,47	121	1496,1
2	33,76	32	349,17	62	665,58	92	952,13	122	1501,41
3	67,68	33	358,22	63	669,33	93	957,31	123	1633,51
4	74,22	34	372,24	64	672,67	94	963,44	124	1641,22
5	94,8	35	379,69	65	673,03	95	969,53	125	1658,06
6	96,79	36	382,21	66	680,98	96	996,15	126	1716,69
7	101,82	37	388,82	67	689,03	97	1031,19	127	1741,75
8	124,12	38	392,52	68	696,02	98	1033,52	128	1761,12
9	143,2	39	402,25	69	699,17	99	1036,11	129	1766,01
10	147,57	40	404,86	70	717,8	100	1037,6	130	1838,65
11	162,86	41	409,32	71	723,5	101	1044,95	131	1895,77
12	174,75	42	410,17	72	738,21	102	1047,75	132	2141
13	176,58	43	413,25	73	744,01	103	1081,14	133	2219,56
14	177,48	44	415	74	760,14	104	1097,02	134	2230,09
15	181,05	45	416,23	75	760,23	105	1109,5	135	2251,5
16	181,35	46	438,42	76	765,18	106	1125,08	136	2323,71
17	216,51	47	451,58	77	774,43	107	1136,47	137	2328,3
18	218,93	48	471,99	78	781,19	108	1158,31	138	2332,96
19	240,99	49	477,37	79	805,99	109	1178,81	139	2336,15
20	248,03	50	502,34	80	813,27	110	1185,21	140	2360,27
21	258,5	51	529,54	81	823,39	111	1200,55	141	2401,14
22	270,14	52	532,75	82	837,5	112	1207,93	142	2432,56
23	292,25	53	538,85	83	840,67	113	1320,73	143	2578,9
24	293,9	54	552,89	84	840,67	114	1331,47	144	2642,4
25	295,99	55	553,71	85	848,9	115	1341,86	145	2664,78
26	298,27	56	562,55	86	850,2	116	1354,68	146	2700
27	298,71	57	579,62	87	853,4	117	1361,42	147	2743,05
28	309,97	58	615,64	88	855,8	118	1381,65	148	2783,27
29	345,11	59	636,58	89	870	119	1489,26	149	2820,93
30	345,55	60	637,53	90	895,29	120	1495,92	150	3000

Table1: electrical sensibility to a 50Hz sinusoidal current.

Person number	Sensibility (µA)	Person number	Sensibility
1	552,89	12	2328,3
2	870	13	2332,96
3	1495,92	14	2336,15
4	1633,51	15	2401,14
5	1716,69	16	2432,56
6	1761,12	17	2578,9
7	1895,77	18	2642,4
8	2141	19	2700
9	2219,56	20	2743,05
10	2230,09	21	2783,27
11	2251,5	22	3000

Table 2: Electrical sensibility to a 1 kHz current.

MOBILE TELECOMMUNICATIONS RISK PERCEPTION AND COMMUNICATION IN EGYPT

HAMDY ELLAITHY, EBI ELOMBI

VODAFONE EGYPT

Abstract

Health concern of mobile telecommunications is widespread and found in all countries with the technology. The level of perceived risk varies among countries depending on a number of factors. In developing countries such as Egypt, the level of concern and perceived risk is heightened mainly due to the overall average lower level of education, lack of understanding of the technology as well as the natural fears of an invading and extensively used technology.

This paper discusses the current level of concern and risk perception in Egypt and how various factors have contributed to their changes over the past three years. Various risk communication strategies are discussed; in particular a project to address the public's concerns regarding emissions from mobile telecommunications base stations.

This project, called HORUS, continuously measures the electric field levels from GSM base stations across Egypt with the use of solar-powered GSM EMF monitoring stations. The 24-hour a day measured field readings are compared with national and international limits and published on a dedicated website.

Introduction

In 2003, an EMF perception survey, commissioned by Vodafone, was carried out in several countries including Egypt by an independent marketing research company - MORI. The main aim of the survey was to assess the level of concern among the public and to assess how this could be addressed. This survey provided Vodafone with an objective view of how the mobile telecommunications industry and technology is perceived in terms of health concerns and how this public concern differs from that in other countries [1, 2]. The results of this survey guided communication strategies to address the public's concern and attempt to reduce the level of concern.

Another survey carried out by the same company in 2005 in Egypt, showed the current level of public concern and highlighted areas where there have been significant changes. It is clear that several factors including communications programs put in place after the 2003 EMF perception survey may have had an impact in the way the public perceives the technology.

I. The Ipsos-MORI EMF Perception survey

A total of 1,000 interviews were conducted in Egypt, among the general public, using CATI (Computer Assisted Telephone Interviewing). This was in contrast to the 2003 survey when the interviews were conducted face-to-face [2]. Respondents were aged 18+ and were from across the whole of Egypt. Quotas were set on age, gender and region. The results are weighted to reflect the population of Egypt.

The main aim of the survey was to assess the nature and level of concern among the Egyptian public and to determine what impact this concern may have for the telecommunications business.

II. Key Findings of the 2005 EMF survey in Egypt

The results of the 2005 survey summarised below is taken from the independent Ipsos-MORI report [3].

Mobile phones, masts and health were not a major top-of-mind concern; ranking 8th amongst the issues mentioned such as air pollution, smoking or cancer. On prompting, mobile phones and masts rose in importance to 4th place.

Concern appeared to be caused largely by the respondent having read or heard information on this issue, as opposed to direct personal experience. Only 10% of all respondents were concerned about mobile phones and masts with 79% of those concerned (8% of the population) because of information read or heard, see Figure 1.

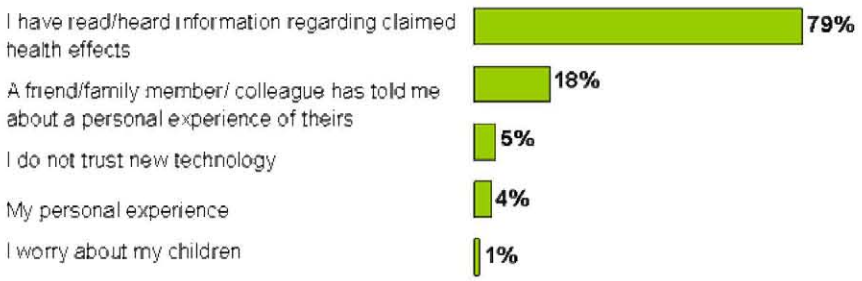


Figure 1: Causes of Concern

Despite this initial low level of concern, 36% of the Egyptian population surveyed, thought that mobile phones were not safe to use, with about 50% believing that masts were worse for health than mobile phones. However, the majority (90%) agreed that they have more important things to worry about. This reiterates the observation obtained from the initial concern result, that is that mobile phones, masts and health are an issue for some, but when put in context other health problems are of a greater priority.

Many believed that mobile phones cause some kind of physical effect, whether that be headaches, a warming of the ear or, more seriously, cancer – Figure 2.

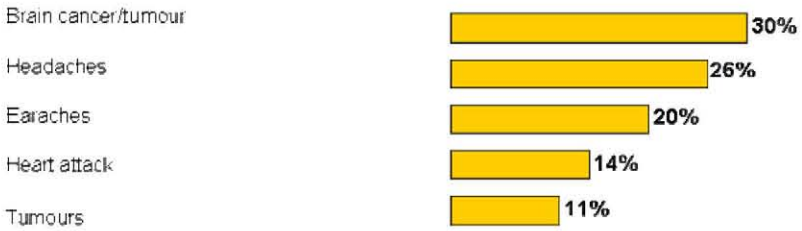


Figure 2: Claimed health problems

Knowledge of the role of masts in mobile operation was still an issue. 17% did not understand the necessity for masts in the operation of mobile phones, stating that they believed a mobile phone could work without being near to a mast.

49% of respondents were aware of a mast anywhere e.g. neighbourhood, work, other locality. However, the majority of mobile phone users were indifferent, with a small minority (6%) actively objecting.

62% of respondents believed that there was no conclusive information on mobile phones, masts and health, whilst 81% stated that they did not know whom to believe. Despite this reservation, 77% believed the benefits of using a mobile phone outweighed any potential risks involved.

13% stated on an unprompted basis that they required information on how mobile masts work. On prompting, the information sought ranged from information on how mobile phones work through to the relative safety of a mobile phone in comparison to other items.

The study revealed a lack of trust, with 72% of the public believing that the industry was withholding

information on this issue, whilst large numbers did not know whether the industry takes this issue seriously or not.

40% would speak more highly of an operator who supplied information on this issue. 3% would be less inclined to trust their operator should they do this.

III. Changes in attitude and concern between 2003 and 2005

The most significant changes in the attitude of the Egyptian public has been in the level of concern and the understanding of the role of masts or base stations in the operation of mobile phones. Some of the key changes are illustrated in Figure 3.

Issue	2003	2005
Prompted concern on Mobile Phones/Masts	43%	10%
Percentages who do not believe mobile phones are safe to use.	71%	36%
Percentages who believe benefits outweigh the risk	68%	77%
Percentages who do not understand the necessity of masts in the operation of mobile phones.	41%	17%

Figure 3: Comparison of attitudes between 2003 and 2005

The general level of concern dropped by more than 70% to 10% in 2005 while concern regarding the safety of mobile phones was halved to 36% in 2005. The level of knowledge and understanding of the technology has also increased with significantly more people understanding the relationship between masts and mobile phone operation.

These changes could be attributed to some communication initiatives implemented by Vodafone after the 2003 survey as well as to changes in the technological environment.

Over this period, Vodafone organised and sponsored several seminars on mobile phones, masts and health across Egypt, targeting various segments of the public. Providing material for and speaking to local councils, landlords and the press as well as leaflets made available to customers. One of Vodafone Egypt's key initiatives has been the implementation of a project called Project HORUS, which continuously monitors field levels from GSM base stations in selected locations across the country and makes the readings available to the public through a dedicated website.

Other influencing factors include the fact that the penetration level moved from 8% in 2003 to 18% in 2005; increased familiarity with the technology over time; government support for a third operator into the market as well as ongoing coverage campaigns by the existing operators.

IV. The project HORUS

This project was an initiative to inform the general public about Radio Frequency (RF) Radiation, through the continuous (24-hour) monitoring of RF field levels in selected locations. Through Project HORUS the public are able to monitor RF radiation levels in several locations across Egypt 24 hours a day.

Vodafone Egypt has deployed over 54 electro-magnetic radiation probes across Egypt. The probes measure radio frequency field levels emitted in the GSM frequency bands at 900 MHz and 1800 MHz, and are powered by solar cells Figure 4. This makes it easy to relocate the units to monitor new areas where there is public concern.



Figure 4: A PMM8055S EMF monitoring station deployed on a rooftop

The readings from each probe are downloaded daily to a web server, which then displays readings on a dedicated website. These readings are displayed on graphs, which can be viewed in comparison with the maximum allowable levels set by the Egyptian authorities and the ICNIRP (International Commission on Non-Ionizing Radiation Protection). Typical readings are hundreds of times below standards as illustrated in Figure 5. More details on the project can be found on the project's website www.projecthorus.com.

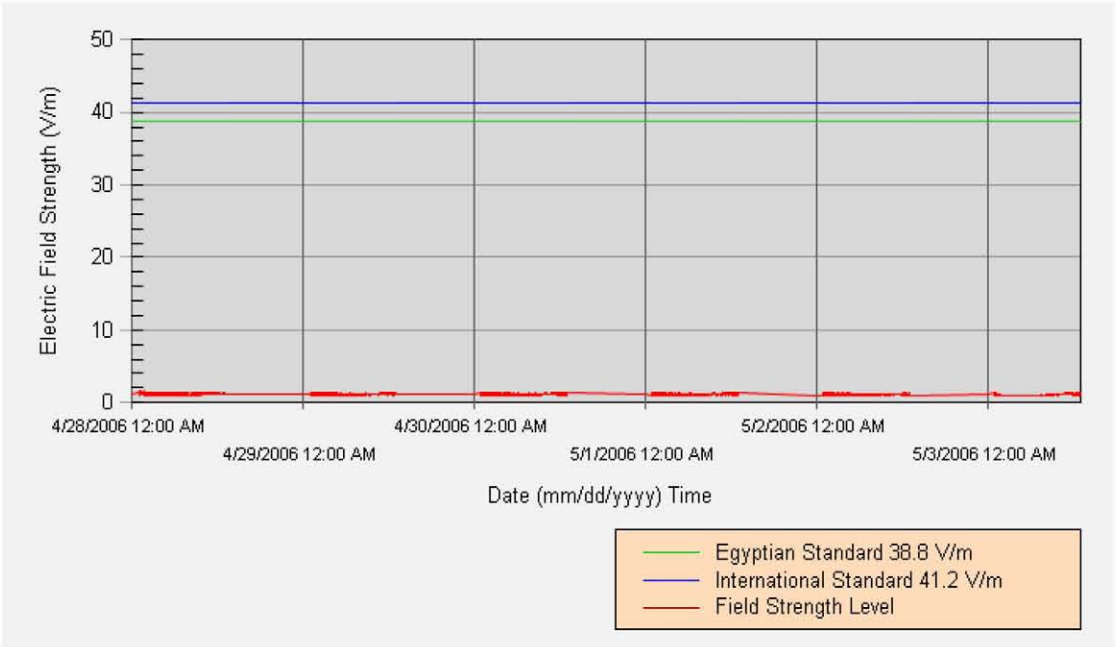


Figure 5: Readings from a monitoring station in the Alexandria governorate

The average reading during this period was 1.15V/m, which is less than 3% of national or international safety limits.

The project was a direct result of the 2003 survey which showed that a significant proportion of the public was concerned about emissions from base stations. Vodafone Egypt first launched Project HORUS in early 2005 across 13 governorates and has expanded the project to cover all 27 governorates. The project has been a useful tool in communication with the public as it demonstrates compliance with standards and an openness and transparency on Vodafone's part which seems to have a positive impact on the public's level of concern.

V. Conclusion

Mobile phones, masts and health is an important issue, but not a primary health concern. This low level of concern mirrors the findings of MORI's research for Vodafone in 2003. The majority of the population are more concerned about other health issues. However, the industry as a whole needs to respond to concerns that important information is being withheld.

The principal trigger leading to concern is information on health effects that people have heard or read, not their personal experience. Lack of understanding, especially on the need for masts, is also fuelling concern. Many people would like to receive more information, including explanations of how the technology works. Communication material will need to be tailored to specific requirements, as different people would like to receive information on a variety of topics.

Open and transparent communication on the issue seems to have an effect on reducing concern, with the continuos EMF monitoring project HORUS, serving to reduce both concern and build operator trust and confidence.

References

1. H. Ellaithy, "Microwave Risk Perception In Egypt", 3rd International Workshop on Biological Effects of EMF, Oct. 4-8, 2004, Kos, Greece.
2. H. Ellaithy, "RF Exposure Health Risk Perception – A Field Study On The Egyptian Public", The Environmentalist, November 2005.
3. Ipsos MORI report, "Understanding Public Perceptions of Mobile Phones, Masts and Health", 2006.

DESIGN, DEVELOPMENT AND OPERATION OF AN ELECTROMAGNETIC RADIATION MONITORING NETWORK IN GREECE: "HERMES" PROJECT

D. KOMNAKOS, A. GOTSIS, N. KOUTSIANAS, A. YALOFAS, P. CONSTANTINOU

NATIONAL TECHNICAL UNIVERSITY OF ATHENS
MOBILE RADIO-COMMUNICATIONS LABORATORY
9, HEROON POLYTECHNEIOU ST., 15773, ATHENS, GREECE
Tel: +30 210 7724196, Fax: +30 210 7723851
E-mail: {dkomna, gotsis, nkout, yalofas, fkonst}@mobile.ntua.gr

T. GANATSOS, A. BOURSIANIS, G. TSANIDIS, T. SAMARAS, J. SAHALOS

ARISTOTLE UNIVERSITY OF THESSALONIKI
RADIOCOMMUNICATIONS LABORATORY, DEPT. of PHYSICS,
GR-54124 THESSALONIKI, GREECE
E-mail: {teogan, ampoursi, theosama, sahalos}@auth.gr

E.CHERA, C.TYRAKIS, G. BELESIOTIS, M. PETKARIS, K.VASILIOU

VODAFONE-PANAFON S.A.
1 – 3 TZAVELA ST., GR-15231, HALANDRI, GREECE
E–mail: { Charilaos.Tyrakis, georgios.belesiotis, marios.petkaris }@vodafone.com

Abstract

A network for the monitoring of the non-ionizing electromagnetic radiation levels in several areas of Greece is presented in this paper. During its 4-year operation more than 4,000,000 measurements of the electric field strength have been performed and recorded. The results aided by useful scientific information are open to the public through a devoted web site. The network measurement results have shown that the field values are several times below the EC recommended and Greek law safety values.

I. Introduction

During the last decade, the installation and operation of several wireless networks, such as the GSM, UMTS and TETRA system has led to increasing public concerns about the exposure to electromagnetic radiation emitted from these sources. In conjunction with traditional broadcasting systems such as FM Radio and TV services, RADAR systems etc. these concerns call for the continuous information of the public regarding their exposure to EM radiation levels. The conduction of repetitive, on site, "ad-hoc" measurements is a first step for estimating the exposure levels. Nevertheless, ad-hoc measurements refer to a specific time period (usually 1-2 hours). On the other hand the notion of continuous measurement of EM radiation levels on a 24-hour basis is more appealing to the concerned public. This is due to the fact that the recorded values can be compared to the public exposure safety values, called reference levels, which are set by the relevant organisations, such as the EC [5] and government authorities [6].

Therefore, a network for the measurement and recording of non-ionizing Electromagnetic Radiation (EMR) emissions on several sites and on a 24-hour basis is one of the best solutions for keeping the public informed. Another important parameter of such a network is the possibility to present the results via a public accessible and user-friendly web site.

As described above, monitoring networks are a valuable tool in attempting to deal with public concerns about the

potential health effects of non-ionizing radiation of electromagnetic radiation. As a result, several monitoring networks are implemented all over Europe and Africa (Italy, Spain, Portugal, United Kingdom, Malta, Egypt etc.) [1]-[4]. Moreover network deployment entails a number of challenges, in terms of hardware certification, network control and daily maintenance. With all the above considerations in mind an Electromagnetic Radiation Monitoring System was developed in Greece. It is known as the "Hermes" project [7], and it is fully operational since November 2002 and currently expanding in several areas around the country.

The paper below is structured as follows: Section II gives a general technical description of a monitoring network, as well as a framework which may be applied in any similar system. Section III presents the system developed for the "Project Hermes" and the measurement results to date. Finally, Section IV presents the current project phase and future planning.

II. Design Aspects of the Monitoring Network

The system architecture is depicted in Figure 1.

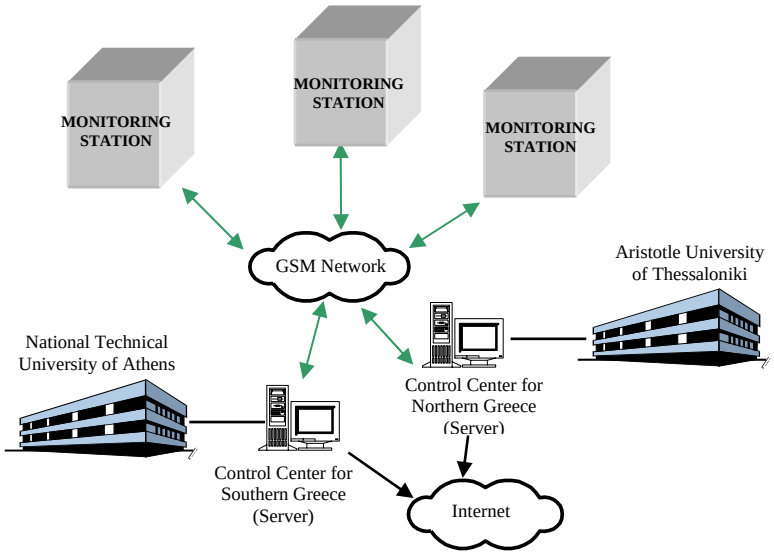


Figure 1: *Block diagram of the monitoring network.*

The system consists of:

(a) The remote monitoring stations, which are located on the desired sites and perform continuous measurements of the Radio frequency (RF) radiation levels and,

(b) The two central control stations (one for Southern and one for Northern Greece), which are located at the corresponding administrative authorities. The control units are responsible for the control of the monitoring stations and the publication of the measurement results on the web site.

a. The Measuring Equipment

The Measuring Equipment must be able to: (a) operate continuously (24 hours per day) (b) perform Electromagnetic Radiation measurements in the frequency range of interest covering the main sources that contribute to the total electromagnetic pollution, (c) store the measurements in its internal memory and transmit them to the Control Centre via a wireless interface for further elaborations, (d) supplied either by the main power supply or a solar panel (preferable), (e) be fully remotely controlled, which means that after their installation no human presence is needed on site and (f) detect abnormal operation of any kind (self diagnostics such as power loss and overheating problems) and inform the central control stations of the problem. To fulfil these requirements, the remote monitoring station consists of a broadband isotropic and triaxial electric field sensor, a module containing the necessary electronics, a GSM modem, as well as temperature and humidity sensors. A major problem encountered in this system is the periodic calibration of the monitoring stations. The calibration procedure requires the deinstallation of the stations, which means the interruption of the measurements, unless a spare station is available for the replacement.

Regarding the measurement quantities, either broadband or narrow-band measurements can be conducted. Broadband Measuring Stations record the Electric Field Strength for a given frequency range. A range of 100 KHz - 3 GHz is usually enough in order to take into account the multitude of the sources. Other possible ranges are for example 880 - 960 MHz (the GSM900 band), 1880 - 2100 MHz (GSM-1800 + UMTS bands), etc. In [8], [9] and [10] the interested reader could find a plethora of such monitoring units. Recently, selective (spectrum analysers) monitoring systems became commercially available. The referred stations are fully autonomous and can be remotely controlled via the GSM/GPRS protocol.

The main drawback of broadband stations is that they cannot estimate the radiation level from each source; rather they estimate the total exposure. Equipment such as a spectrum analyser is capable of measuring and quantifying the contribution of each electromagnetic radiation source to the total exposure level. Nevertheless, this equipment is not designed for continuous operation. If selective monitoring stations are not installed, the best solution is the use of a continuous broadband monitoring station for 24-hour recording and conducting "ad-hoc" narrow band measurements with a period of 3 - 6 months for every measurement site.

b. The Control Centre

The Control Centre is equipped with a Server Station, a wireless modem and the necessary software applications and it is responsible for: (a) controlling the remote monitoring stations and configuring the operational parameters, (b) downloading the measurement data via the wireless interface (e.g. GSM network), (c) storing the data in its hard disk and (d) processing the measurement results and publishing them to the corresponding web site.

The measurement data is stored in a Database (such as MS Access, SQL Server or MySQL) after their checking and processing. Therefore the full historical record for every measurement site is kept on the Server. In addition, a Web Server (such as MS IIS or Apache) hosts the web site.

c. The Web Site

The Web Site contains both static and dynamic pages and it aims at presenting the measurement results for every monitored site. It also provides thorough information concerning the electromagnetic radiation issue. Through the web site the user may view electric field strength graphs with custom time interval selection and statistical quantities about the measurements. Furthermore, a comparison of the measured quantity with the Greek legislation reference levels is presented. A feedback form can be also available to the public in order for them to express questions or comments to the administrators of the system.

III. The "Hermes" Monitoring Network

a. General Description

A monitoring network based on the principles described above has been developed and operating since November 2002. The system at its present state (April 2006) comprises 27 remote monitoring stations spread all over Greece (23 active and 4 inactive) and two control units located in two University laboratories (National Technical University of Athens – NTUA and Aristotle University of Thessaloniki – AUTH). The stations are located at schools, universities, public authorities' buildings and private flats. The following figure depicts the spreading of the monitoring stations.

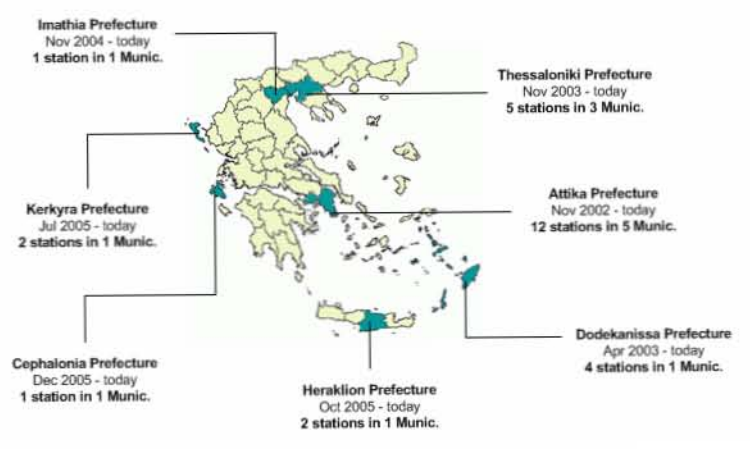


Figure 2 : *"Hermes" Monitoring Network*

The measuring devices record the broadband electric field strength quantity for the range 100 KHz - 3 GHz [10]. Three slightly different monitoring units' models are used.

- EE4070 - WB model which records the Electromagnetic Field Strength in the band 100 KHz - 3 GHz
- EE4070 - SL which records the field strength for three bands: 100 KHz - 3 GHz, GSM-900 Band and GSM1800 + UMTS band.
- MCE410 - SL, which records the field strength for two bands: 100 KHz - 3 GHz and 900 MHz - 3 GHz.

A detailed description of the specific units and the measurement procedure can be found in [11]. In the following figures several measurement sites are presented.



Figure 3: *EE4070-WB Station at Koskinou, Rhodes*



Figure 4: *EE4070-SL Station at Menemeni, Thessaloniki*



Figure 5: *MCE410-SL station at Heraklion, Crete*

Regarding the "ad-hoc" measurements, the guidelines proposed in the ECC recommendation [12] serve as the basis for our measurement procedure. A set of directional antennas covering the frequency range of 20 MHz – 3 GHz and a Spectrum Analyzer for measuring the received RF Power comprise the measurement apparatus (see Figure 6*).* Each frequency band is scanned and the power of each RF source, such as a FM or TV radio stations, a GSM channel etc is recorded. After the needed processing the total exposure levels and the contribution of each frequency band are estimated. A similar procedure is performed if we substitute the Spectrum Analyser with a Selective Radiation Meter such as the one presented in [13] and the directional antennas with broadband isotropic triaxial E-field probes (see Figure 7).



Figure 6: *"Ad-Hoc" Measurement Apparatus (Spectrum Analyser based)*



Figure 7: *"Ad-Hoc" Measurement Apparatus (SRM based)*

b. Measurement results

On the Web Site, both broadband and narrow-band measurement results are presented. The broadband measurements are updated on a daily base. Below, at first a table containing the most significant information about the monitoring stations is given. Afterwards in the following figures sample diagrams from the web site are drawn (Figure 8 - Figure 11). Finally, cumulative results regarding all the stations are presented (Figure 12 - Figure 13).

Table 1 *: Stations informative table*

Station ID	Site Name	Activation date	Mean 6-min Average value of electric field	Standard deviation of electric field	Maximum 6-min Average value of electric field	Number of recorded measurements	Status
1	1st & 6th Pr. Schools at Holargos	November 18, 2002	1.6	0.1	2.7	77,603	Inactive
2	2nd & 3rd Pr. Schools at Holargos	November 18, 2002	1.9	0.1	2.3	77,609	Inactive
3	5th Primary School at Holargos	November 22, 2002	2.6	0.2	3.2	72,726	Inactive
4	1st Primary School at Zefiri	March 31, 2003	1.7	0.2	2.5	263,276	Active
5	High School at Zefiri	April 1, 2003	1.7	0.6	8.9	250,005	Active
6	Municipal Office of Psinthos	April 23, 2003	0.9	0.8	5.8	209,517	Active
7	Municipal Office of Koskinou	April 23, 2003	1.5	0.3	4.0	209,808	Active
8	First Aid Station of Faliraki	April 23, 2003	0.0	0.1	1.5	91,620	Inactive
9	Building of E.C.E. School	November 6, 2003	2.9	0.2	4.6	172,585	Active
10	5th Primary School at Renti	November 10, 2003	0.7	0.1	1.0	209,315	Active
11	Kindergarten at Renti	November 10, 2003	1.5	0.3	2.1	206,892	Active
12	1st Primary School at Renti	November 10, 2003	1.1	0.5	4.3	193,026	Active
13	Kalithies, DEYAK	May 11, 2004	0.1	0.2	1.1	155,210	Active
14	1st Primary School at N. Erithrea	July 7, 2004	2.5	0.3	3.5	129,941	Active
15	2nd & 3rd Pr. Schools at N. Erithrea	July 7, 2004	2.5	0.2	3.1	132,297	Active
16	Esperia Build. - Town Planning Build.	October 5, 2005	1.6	1.0	3.5	45,115	Active
17	Dimokratias Avenue	October 5, 2005	2.1	1.0	7.8	44,061	Active
18	1st Primary School at Ilion	November 21, 2005	2.2	0.1	2.9	33,872	Active
19	3rd High School of Argostoli	December 21, 2005	0.1	0.4	6.5	18,336	Active
20	A.U.TH., Building of School of Science	November 1, 2003	1.3	0.2	3.5	206,279	Active
21	A.U.TH., Rectorate Building	February 27, 2004	3.7	1.4	17.7	173,067	Active
22	City Hall of Menemeni	June 12, 2004	2.7	0.5	7.7	155,283	Active
23	City Hall of N. Michaniona	June 9, 2004	0.9	0.2	1.8	153,406	Active
24	High School of N. Michaniona	June 4, 2004	1.8	0.4	3.4	163,964	Active
25	1st and 2nd High Schools of Naoussa	November 16, 2004	0.7	0.2	2.1	123,851	Active
26	City Hall of Lefkimi	July 22, 2005	1.7	0.3	3.0	57,957	Active
27	2nd Primary School of Lefkimi	July 22, 2005	0.8	0.2	1.7	63,977	Active

In Figure 8 the measured points correspond to 6-minute average electric field (E-field) values as is proposed in [5]. An immediate comparison with the reference levels can be done based on this diagram. Moreover the

variation of the field during one day or a longer period is distinguishable. The time span can vary from 1 hour to the whole measurement period (several years). In Figure 9(a) and 9(b), the mean and the maximum of the total set of 6-min average E-field values are presented and compared with the corresponding reference levels, for both EE4070 – SL and MCE410 – SL models.

Sample measurement results from two "ad-hoc" measurements are depicted in Figure 10. Specifically, one can see how many times below the safety values were the measured field values, in terms of the Power Flux Density (Watt/m^2) (Figure 10(a)) and in terms of the Electric Field Strength (V/m) (Figure 10(b)), for each frequency band such as FM, TV, GSM900, UMTS etc. The total exposure level is also evaluated and presented. The comparison between the results of Figures 9(b) and 10(b) (which correspond to the same measurement site) shows that the values of the monitoring station measurements are close to the "ad-hoc" measurement values. In addition, Figure 11 illustrates the percentage contribution of each frequency band to the total EMR exposure level.

Finally, the last two diagrams (Figure 12 and Figure 13) present cumulative results regarding the mean 6-min average E-field strength (continuous measurements) and the exposure level in terms of the Power Flux Density extracted by "ad-hoc" measurements.

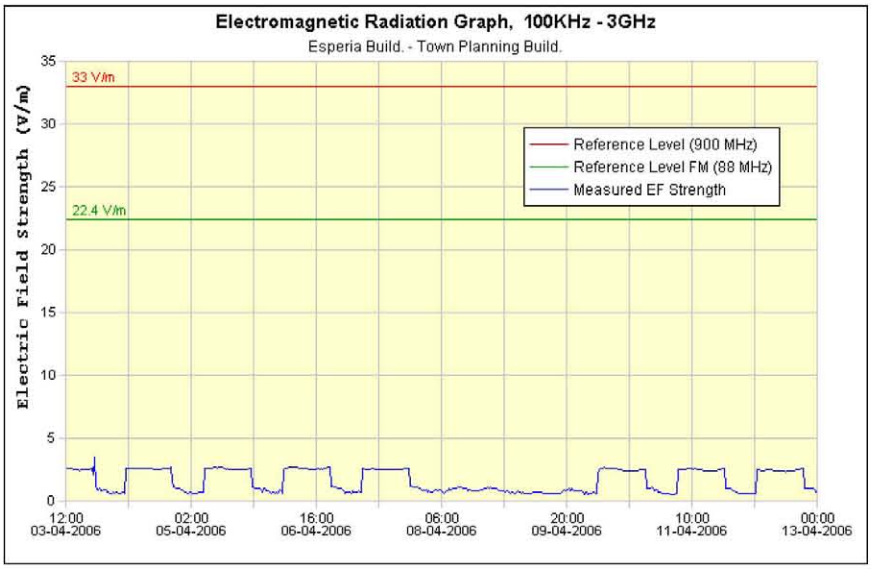
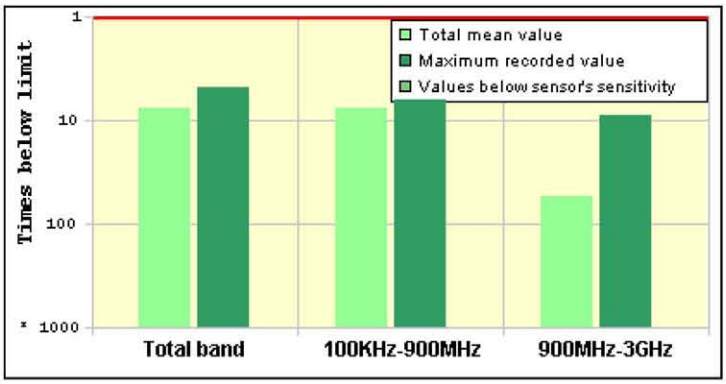
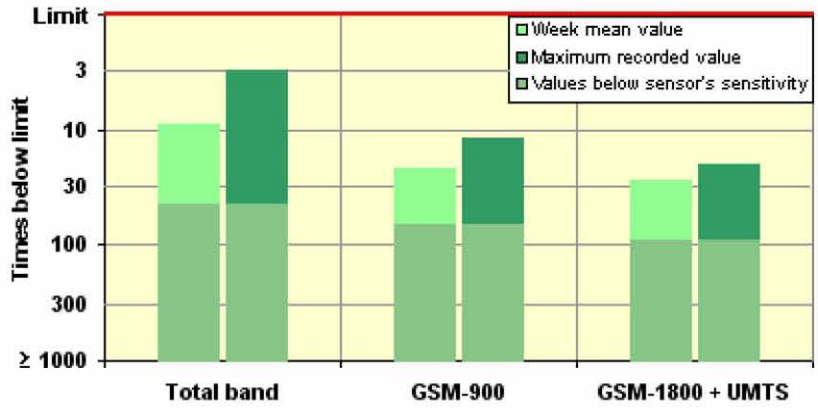


Figure 8: *Sample Electric Field Strength Diagram (Broadband)*

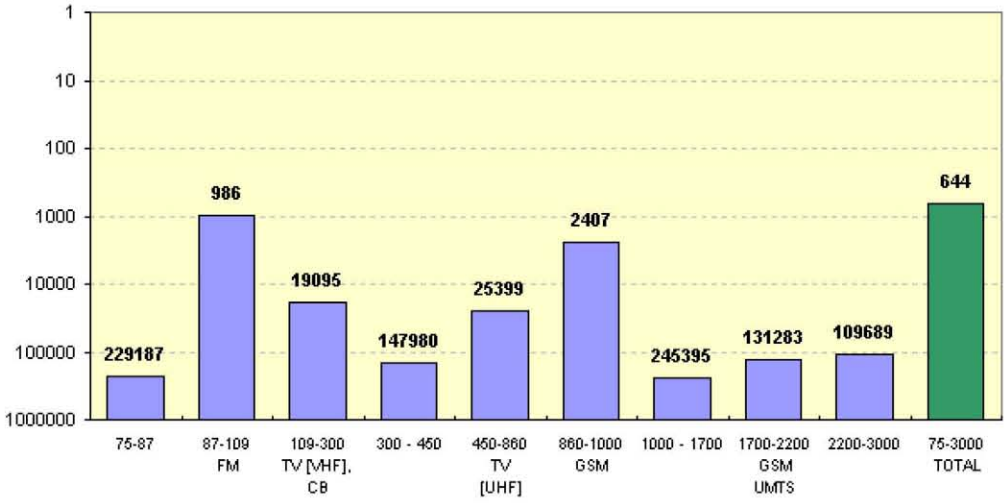


(a)

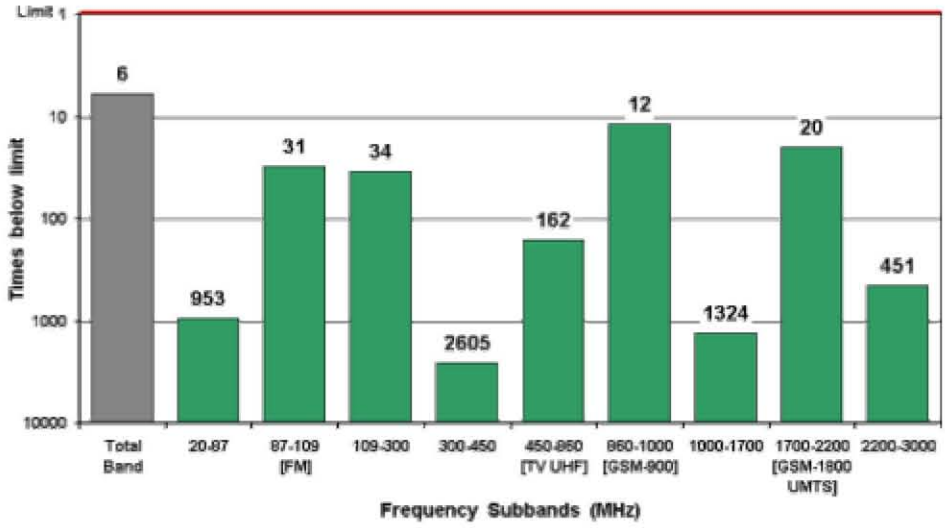


(b)

Figure 9. *(a) Sample Mean Electric Field Strength Diagram for Selective Stations (MCE410 – SL model). (b) Sample Mean Electric Field Strength Diagram for Selective Stations (EE4070 – SL model)*



(a)



(b)

Figure 10: *(a) Sample of Power Density Measurement Results conducted with SRM (Narrow-Band). (b) Sample Equivalent Electric Field Strength Measurement Results conducted with Spectrum Analyzer (Narrow-Band)*